

GEOMORPHOLOGY OF THE NORTH KARST  
SOUTH NAHANNI RIVER REGION  
NORTHWEST TERRITORIES  
CANADA

GEOMORPHOLOGY OF THE NORTH KARST  
SOUTH NAHANNI RIVER REGION  
NORTHWEST TERRITORIES  
CANADA

By

GEORGE ALBERT BROOK, B.Sc., M.Sc.

A Thesis

Submitted to the School of Graduate Studies  
in Partial Fulfilment of the Requirements

for the Degree

Doctor of Philosophy

McMaster University

August 1976

DOCTOR OF PHILOSOPHY (1976)  
(Geography)

McMASTER UNIVERSITY  
Hamilton, Ontario

TITLE: Geomorphology of the North Karst, South Nahanni River  
Region, Northwest Territories, Canada

AUTHOR: George Albert Brook, B.Sc. (Edinburgh University)  
M.Sc. (University of the  
Witwatersrand)

SUPERVISOR: Dr. D. C. Ford

NUMBER OF PAGES: xxi, 627

## Abstract

First investigated on the ground in June 1972, the Nahanni karst of northern Canada is the most complex karst terrain yet reported from high latitudes. It is centered at  $61^{\circ}28'$  N, longitude  $124^{\circ}05'$  W and lies within the zone of discontinuous permafrost. Mean annual temperature is  $24^{\circ}\text{F}$  and mean total precipitation 22.3 inches. Principal karst forms are fracture-located karst streets and irregularly-shaped closed depressions called karst platea which may be up to 600 feet in depth. Platea often contain karst towers which are residuals of wall recession. Vertical-walled pond dolines up to 120 feet deep are common in bare karst areas while subjacent karst collapse, subsidence and suffosion depressions occur on marginal shale- and drift-mantled surfaces. Three small poljes have been identified, two produced entirely by solution, the other a structural form. These are periodically inundated. There are several peripheral fluvial canyons up to 3,000 feet deep that are blocked by glacial drift and which presently drain underground. Similarity in the hydrogeological properties of Nahanni Formation limestones at a variety of scales has led to the development of morphologically-identical karst forms which range in size from inches up to hundreds of feet. Furthermore, many of these landforms are part of a developmental sequence that at one scale links vertical-walled dolines, karst streets, platea and poljes; and at another links solution pits, grikes and joint hollows on limestone pavements. The evidence suggests that poljes can form by the coalescence of dolines and uvalas just as Cvijić suggested in 1918. In attempting to explain the almost "tropical" nature of the sub-arctic Nahanni karst landform assemblage, a number of facts are of importance.

(a) The Nahanni Formation limestones have been highly warped and intensively fractured during the past one million years. Open fractures have encouraged karstification by allowing easy movement of water underground. Warping has provided the relief necessary for the development of solutional forms with a distinct vertical component.

(b) The karst can not be considered relict because it was glaciated during the Pleistocene. In addition the hydrological activity in it today is comparable with that in many humid tropical karst areas.

(c) Solutional denudation rates governed by aspects of surficial and bedrock geology may in some localized areas be equivalent to rates in humid tropical carbonate regions.

(d) At present rates, the most highly developed forms could have been produced within the last 200,000 years and because there is evidence to indicate that the karst may not have been glaciated for up to 250,000 years, such a period has been available for solutional development.

Because the Nahanni region has not been glaciated for an extremely long period, it may be one of only a few high-latitude carbonate terrains that have had time to develop fully. Its very existence questions the validity of the concept that the intensity and direction of karst development is climate-controlled. In the Nahanni at least, the structural and lithological properties of the host limestone appear to have been of greater importance. The labyrinth karst type present in regions of humid-tropical to sub-arctic climate, is an outstanding example of a structurally-controlled karst landscape. It may well be that the same controls also influence the distributions of other karst types.

## ACKNOWLEDGEMENTS

I would like to express my sincere gratitude to Dr. D.C. Ford who not only gave me the chance to conduct research in Canada's north, but has worked diligently on my behalf, and has given constant encouragement, advice, friendship, and consideration. Thanks must also go to Drs. S.B. McCann, P.J. Howarth, and P. Clifford for their aid as members of my supervisory committee; Drs. J.J. Drake, R.S. Harmon and J.G. Cogley for their free advice and useful discussions; many of my fellow graduate students; R. Bignall, R.Ewers, A. Jackson, N. Prout, L. Simpson and F. Weirich for their help and honor in the field; J. Glew who kindly drew Figure 3.45; and to V. Register for her efforts in typing this manuscript. Last but by no means least I would like to express my deep thanks to my wife, Diane, without whom I doubt that this thesis would be complete. Her help in the field and at all stages of work on this project was considerable and her constant encouragement through the trials and tribulations of graduate work was of inestimable value.

## TABLE OF CONTENTS

		<u>Page</u>
CHAPTER 1 INTRODUCTION		
1	The Nahanni Karst .....	1
	(a) The Discovery .....	1
	(b) The Area .....	2
	(i) Location and Physiography .....	2
	(ii) Climate .....	11
	(iii) Vegetation .....	13
	(iv) Bedrock Geology .....	14
	(v) Glaciation .....	15
2	The Problem Posed by the Nahanni Karst Assemblage .....	16
3	The Structure of the Answer .....	26
CHAPTER 2 GEOLOGY OF THE SOUTHERN MACKENZIE MOUNTAINS		
1	Introduction .....	32
2	Stratigraphy .....	33
	(a) Regional Stratigraphy of the Upper Mackenzie River Area .....	33
	(i) Lower Devonian .....	33
	(ii) Middle Devonian .....	35
	(iii) Upper Devonian .....	38
	(b) Stratigraphy of the Nahanni Region .....	38
	(i) The Map-Units and Stratigraphic Formations .....	38
	(ii) Facies and Faunal Relations in the Nahanni Area .....	49
	(iii) Observed Sections in the Karst .....	53
3	Structure .....	59
	(a) Major Orogenies .....	59
	(i) Columbian Orogeny .....	59
	(ii) Laramide Orogeny .....	60
	(iii) Cascadian Orogeny .....	62
	(b) Structural Geology of the Upper Mackenzie River Area .....	62
	(c) Patterns of Structural Deformation in the Southern Mackenzie Mountains as Suggested by Topographic Analysis .....	66
	(i) Structural Deformation in the Nahanni Karst Belt .....	71
	(ii) Structural Deformation in the South Nahanni River Region .....	73
	(d) Fault and Joint Patterns in the Nahanni Karst Belt .....	81

		<u>Page</u>
	(i) A Tentative Interpretation of Fracture Orientations .....	81
	(ii) Variations in Fracture Density .....	91
CHAPTER 3	THE KARST LANDFORM ASSEMBLAGE	
1	Introduction .....	93
2	Limestone Pavements .....	93
	(a) Characteristics of the Bedrock .....	96
	(i) Lithology .....	96
	(ii) Bedding .....	99
	(iii) Fracturing .....	103
	(b) Some Morphological Characteristics of Nahanni Pavements .....	105
	(i) Characteristics of Clint and Grike Systems .....	105
	(ii) Pit-and-Tunnel Networks .....	108
	(iii) Natural Rock Hollows .....	111
	(c) The Scale of the Solution Process .....	117
	(i) The Chemical Characteristics of Waters on Pavements .....	117
	(ii) Soil Carbon Dioxide and Variations in Solution Intensity Across a Pavement Surface .....	123
	(d) The Development and Evolution of Nahanni Pavements .....	127
3	Dolines .....	133
	(a) Structural Dolines .....	135
	(b) Solution Dolines .....	139
	(c) Collapse and Subjacent Karst Collapse Dolines .....	152
	(d) Subsidence, Suffosion and Alluvial Stream-sink Dolines .....	157
	(e) Characteristics of Solution in Nahanni Dolines .....	162
4	Labyrinth Karst .....	169
	(a) Karst Streets .....	170
	(b) Karst Platea .....	181
	(c) Characteristics of Solution in Karst Streets and Platea .....	189
5	Poljes .....	196
	(a) Morphological Characteristics of Nahanni Poljes .....	198
	(i) First Polje .....	198
	(ii) Second and Third Poljes .....	206
	(b) Characteristics of Solution in Nahanni Poljes .....	213
6	Blind Valleys and Closed Fluvial Canyon Systems .....	220
	(a) Stream Networks Disorganized Entirely by Karstic Processes .....	223
	(i) Networks with Headwaters, in Shale .....	223

	<u>Page</u>
(ii) Networks Entirely in Limestone .....	225
(iii) Networks Developed on Till-Covered Limestone .....	227
(b) Closed Fluvial Canyon Systems of Glaciokarstic Origin .....	228
(i) Morphological Characteristics .....	228
(ii) Characteristics of Solution .....	241
(iii) Origin of the Closed Fluvial Canyon Networks .....	250
7 Caves .....	251
(a) Cavern Morphology .....	251
(b) The Past and Present Microclimates of Na- hanni Caves .....	254
(c) Evolutionary History of Fossil Caves in the Nahanni Karst .....	264
8 Relationships Between the Karst Landforms of the Nahanni Region .....	268
(a) The Size Hierarchy of Karst Landforms .....	268
(b) The Sequential Development of Karst Land- forms in the Nahanni .....	271

#### CHAPTER 4 SURFACE AND GROUNDWATER HYDROLOGY

1 Climatology .....	283
(a) Mean Temperature and Precipitation .....	283
(i) Estimates from Climatological Data .....	283
(ii) Precipitation Estimates from Stream Dis- charge and Evapotranspiration Data ....	292
(b) Effective Snowfall in the Karst and the Geomorphic Significance of its Distribution	303
(c) Temperature and Precipitation Measurements During the Summers of 1972 and 1973 .....	314
(i) Precipitation .....	314
(ii) Temperature .....	319
(d) Seasonal Distribution of Precipitation .....	322
(i) The Storm of August 15th - 17th 1970 ....	324
(ii) The Storm of July 16th - 31st 1972 ...	324
2 General Patterns of Surface and Groundwater Flow in the Nahanni Karst .....	333
(a) Groundwater Recharge .....	333
(b) Groundwater Discharge .....	335
(c) Groundwater Flow Directions and Velocities as Determined by Dye Tracing Experiments ..	339
(d) Spring Catchment Areas and Possible Concen- trated Groundwater Flow in the Nahanni Karst .....	343
3 The Flooding and Draining of Depressions in the North Karst Region: An Account and an Explana- tion .....	350



	<u>Page</u>
(a) Flooding and Draining: The Evidence .....	350
(i) A Chronological Account of Flooding and Draining for the Period 1971-1975 Based upon Ground and Aerial Reconnaissance Observations .....	350
(ii) Data on the Flooding of North Karst De- pressions Obtained from Aerial Photo- graphs .....	362
(iii) Order, Frequency and Seasonality .....	365
(b) Flooding and Draining: An Explanation .....	367
(i) Flooding as a Result of Rapid Surface Runoff and the Ponding of Water in De- pressions .....	368
(ii) Flooding and Draining of North Karst Depressions due to Fluctuations .....	376
(iii) A Compromise Hydrologic Model for the North Karst .....	383

## CHAPTER 5 CHARACTERISTICS OF SOLUTION

1	Introduction .....	390
	(a) Karst Solution .....	390
	(b) Analytical Methods .....	398
2	Aspects of the Total Data Set .....	401
3	Hydrochemical Classification of Waters in the Nahanni Karst .....	412
4	Spatial Variations in the Biogenic Carbon Dioxide Content of Nahanni Soils .....	433
	(a) Importance of Biogenic Carbon Dioxide .....	433
	(b) Soil Carbon Dioxide Levels in the Nahanni .....	435
5	Carbon Dioxide and the Chemistries of Natural Waters in the Nahanni .....	444
	(a) The Chemistry of Hydrogeological Water Groups and Soil Carbon Dioxide Levels .....	446
	(i) Spring Waters .....	448
	(ii) Pool and Pond Waters .....	452
	(iii) Lake Waters .....	455
	(iv) Stream Waters .....	457
	(v) Soil Waters .....	459
	(vi) Seepage Waters on Limestone .....	459
	(b) Changes in the Chemistry of Tufa Spring Waters Under Atmospheric Conditions and Reasons for Tufa Deposition in this Cold Sub-arctic Spring .....	461
	(c) Spatial Variations in the Chemistry of the Mosquito Creek Drainage System .....	469
6	Models of Chemical Interaction Between Waters in Similar Geological Environments .....	476

		Page
	(a) The Drift-mantled Shale Environment .....	476
	(b) The Limestone Environment .....	478
7	Nahanni Solution Rates Placed in a Regional Context .....	482
	(a) Solution Potential and the Actual Intensity of Solution in Different Climatic Environ- ments .....	482
	(b) Karst Denudation Rates .....	496
CHAPTER 6	PLEISTOCENE GLACIATION IN THE SOUTHERN MACKENZIE MOUNTAINS N.W.T., CANADA	
1	Pleistocene Glaciation of the Western Cordillera, Yukon, and N.W.T.: An Examination of the Pub- lished Evidence .....	500
	(a) An Unglaciaded Area? .....	500
	(b) Laurentide and Cordilleran Ice Sheet Limits and Evidence of Multiple Glaciation in the Western Cordillera, Yukon, British Columbia and N.W.T. ....	501
	(c) Cirque and Valley Glaciation .....	512
	(d) Ice-dammed Lakes and Ice-marginal Drainage in the Easternmost Ranges of the Western Cordillera, Yukon and N.W.T. at the Front of a Laurentide Ice Sheet .....	518
2	Evidence of Glaciation in the Nahanni Karst Belt and in Surrounding Areas .....	525
	(a) An Unglaciaded Area? .....	526
	(b) Laurentide Ice Sheet Limits .....	526
	(i) The First Canyon Glaciation .....	526
	(ii) The Death Canyon Glaciation .....	528
	(iii) The Sundog Glaciation .....	534
	(iv) The Clausen Glaciation .....	535
	(v) The Jackfish Glaciation .....	536
	(c) Ice-Dammed Lakes .....	540
	(d) Cirque and Valley Glaciation .....	543
3	A Tentative Glacial Chronology for the South- eastern Mackenzie Mountains .....	544
CHAPTER 7	DISCUSSION	
1	The Natural Rock Labyrinth Phenomenon .....	555
	(a) Labyrinths in Karst Rocks .....	555
	(b) Labyrinths in Non-karst Rocks .....	562
	(i) The Wright Dry Valley Labyrinth .....	562
	(ii) The Channeled Scablands of Eastern Wash- ington .....	565

	<u>Page</u>
	(iii) Vallons de Gélivation ..... 567
2	The Age and Origin of Nahanni Karst Landforms and Relationships Between their Development and Glacial and Periglacial Events ..... 569
	(a) The Onset of Karstification: An Age Estimate ..... 569
	(b) Surface Karst Landforms. Their Age and Relationships to Glacial and Periglacial Events ..... 570
	(i) Surface Karst Development and Periods of Glacial Erosion ..... 570
	(ii) Relationships Between Ice-gammed Lakes in the Sundog Basin and the Development of the North Karst Labyrinth ..... 572
	(iii) Surface Karst Development and Phases of Intense Periglacial Climate ..... 574
	(c) The Karst-Glacial Meltwater Problem ..... 575
	(d) A Unique Sub-Arctic Karst? ..... 578
3	A Tentative Denudation Chronology for the Nahanni Karst Region ..... 580
	(a) Events 1 through 3 - The Columbian and Laramide Orogenies and the Cretaceous Surface of Erosion ..... 580
	(b) Events 4 and 5 - The Cascadian Orogeny? and Early Cavern Genesis ..... 582
	(c) Events 6 and 7 - The First Canyon Glaciation and the Grotte Valerie Interglacial I Period ..... 585
	(d) Events 8 and 9 - The Death Canyon Glaciation and the Grotte Valerie Interglacial II Period ..... 586
	(e) Events 10 and 11 - The Sundog Glaciation and the Sangamon Interglacial ..... 589
	(f) Events 12 and 13 - The Clausen Glaciation and the Wisconsin Interstadial ..... 590
	(g) Events 14 and 15 - The Jackfish Glaciation and the Post Glacial Period ..... 592
4	Significance of the Nahanni Karst Landform Assemblage to the Morphoclimatic Theory of Karst Landform Development ..... 593
5	A Structural-Lithological Model of Karst Landform Development ..... 595
6	Summary Remarks ..... 603
APPENDIX I	Selected Glossary of Karst Terms ..... 607
APPENDIX II	The Calculation of Saturation Indices and Log PCO <sub>2</sub> ..... 610
BIBLIOGRAPHY	..... 611

## LIST OF FIGURES

<u>Figure</u>		<u>Page</u>
1.1	Physiographic regions of the district of Mackenzie, N.W.T., Yukon, British Columbia, and Alberta (after Bostock 1970).....	3
1.2	Location and major topographic features of the Nahanni karst region.....	5
1.3	The karst cycle (after Grund 1914).....	17
1.4	Evolution of water circulation and development of karst relief (after Cvijic 1918).....	19
1.5	Topography of the Nahanni karst belt.....	27
1.6	The karst landform assemblage.....	28
2.1	Schematic cross section through the upper Mackenzie River area, N.W.T. (after Law 1971).....	34
2.2	Faunal zones of the Middle Devonian in the Liard-Nahanni area and correlation with the Norman Wells and northern Alberta regions (after Noble and Ferguson 1971).....	39
2.3	Geology of the Nahanni karst region (after Douglas and D.K. Norris 1960).....	41
2.4	Approximate stratigraphic relationships of Middle Devonian and older units in the Virginia Falls map area (after Douglas and D.K. Norris 1960).....	43
2.5	Correlation of Ordovician, Silurian and Devonian formations and map-units of Camsell Bend, Root River and Virginia Falls map-areas (after Douglas and D.K. Norris 1961).....	44
2.6	Correlation of Devonian formations of Dahadinni River, Wrigley, and adjacent map areas (after Douglas and D.K. Norris 1962).....	45
2.7	Cross section showing lithofacies changes across the shelf-basin transition, South Nahanni area, N.W.T. (after Noble and Ferguson 1971).....	50
2.8	Cross section showing biofacies changes across the shelf-basin transition, South Nahanni area, N.W.T. (after Noble and Ferguson 1971).....	51
2.9	Schematic geological section at Death Lake, North Karst....	54
2.10	Schematic geological section at Cenote-Col, North Karst....	55
2.11	Early upper Cretaceous tectonic elements of the Cordilleran Geosyncline and Interior Platform.....	61
2.12	Late upper Cretaceous and early Tertiary tectonic elements of the Cordilleran Orogen and Interior Plain.....	61
2.13	Schematic geological cross section through the upper Mackenzie River area (after Law 1971).....	61
2.14	Schematic geological cross section through the Nahanni Range, Yohin Syncline and Ram Plateau (after Douglas and D.K. Norris 1960).....	64
2.15	Schematic geological cross section through the Nahanni Range, Bluefish Syncline and Mattson Anticline (after Douglas and D.K. Norris 1960).....	64

	<u>Page</u>
2.16	Schematic geological cross section through the Ram Plateau (after Douglas and D.K. Norris 1960)..... 65
2.17	Schematic geological cross section through the Deadman Syncline and the Southern Nahanni Plateau (after Douglas and D.K. Norris 1960)..... 65
2.18	Grid filters used to extract summit altitude data from 1:50,000 topographic map sheets..... 69
2.19	Structural deformation of the South Nahanni River region: the area of study and the 1:50,000 topographic maps analyzed..... 70
2.20	Structural deformation of the Nahanni karst belt from topographic analysis (144 grid units in each 1:50,000 topographic map)..... 72
2.21	Structural deformation of the Mackenzie Mountains from topographic analysis (16 data points in each 1:50,000 map)..... 74
2.22	Structural deformation of the Mackenzie Mountains from topographic analysis (9 data points in each 1:50,000 map)..... 75
2.23	Structural deformation of the Mackenzie Mountains from topographic analysis (4 data points in each 1:50,000 map)..... 77
2.24	Cubic trend surface fitted to 84 data points in the South Nahanni River region..... 79
2.25	The pattern of fractures that might be expected in a moderately folded limestone (after de Sitter 1964)..... 82
2.26	Fractures and regions in the Nahanni karst belt..... 84
2.27	Fracture orientation histograms by region, Nahanni Karst... 85
2.28	Major sets of fractures in the Nahanni Karst and the postulated direction of the principal stress that produced them..... 86
3.1	The principal karren types on the dolomite pavements of the Niagara Escarpment in the Hamilton district of southern Ontario (after Pluhar and Ford 1970)..... 109
3.2	Calcium carbonate and pH of rock pools, County Clare, plotted on Trombe's graph (after Williams 1966)..... 121
3.3	SI <sub>c</sub> against log PCO <sub>2</sub> for pavement waters..... 126
3.4	Some stages in the evolution of limestone pavements (after Williams 1966)..... 128
3.5	The main categories of doline (after Jennings 1970)..... 136
3.6	Plan and schematic geological sections of Palsa Basin, a structural doline..... 138
3.7	Plan and section of Surprise and Hidden dolines, Cenote Col, North Karst..... 145
3.8	The solution dolines of Cenote Col, North karst labyrinth..... 147
3.9	Distribution of subjacent karst collapse dolines south of Mosquito Lake..... 154

	<u>Page</u>
3.10	Schematic geologic and topographic section through the subjacent karst collapse dolines south of Mosquito Lake..... 156
3.11	Map of suspected subsidence and suffosion dolines on the Sinkhole Plain, Nahanni North Karst..... 158
3.12	Graph of $SI_c$ against $\log PCO_2$ for pond and seepage waters in Nahanni North Karst dolines..... 166
3.13	The North Karst labyrinths..... 172
3.14	Networks of karst streets on residuals of the Nahanni Plateau, South Karst..... 173
3.15	Plan and sections of a small karst street on the Nahanni Plateau, south of Death Lake..... 176
3.16	Plan and sections of Stal Gorge, a large karst street..... 177
3.17	Longitudinal profile of Stal Gorge, North Karst..... 178
3.18	Shallow karst street on the Nahanni Plateau south of Death Lake..... 180
3.19	Polaski Plateau, North Karst..... 184
3.20	North Col Canyon, the largest karst plateau in the Nahanni karst region..... 186
3.21	Simpson Plateau, North Karst labyrinths, Nahanni..... 187
3.22	$SI_c$ and $\log PCO_2$ graph of stream, pond and lake waters in streets and plateaus in the North and Central karst regions..... 195
3.23	Geomorphic map of the northern section of the labyrinths showing the Nahanni poljes..... 199
3.24	First Polje..... 201
3.25	Second Polje..... 207
3.26	Third Polje..... 210
3.27	$SI_c - \log PCO_2$ relationships for waters in the three Nahanni poljes..... 219
3.28	Disorganized valley systems in the North Karst, Nahanni.... 224
3.29	Schematic plan and profiles of Lost Valley, a blind valley formed by an allogenic stream, North Karst, Nahanni..... 226
3.30	The closed fluvial canyons of the Nahanni Karst..... 229
3.31	Geomorphic map of Hiller and Texas closed canyons, Ram Plateau..... 231
3.32	Long profiles of Hiller and Texas Canyons, Ram Plateau..... 233
3.33	Long profiles of Canal and Death Canyons..... 235
3.34	Geomorphic map of Death Canyon..... 238
3.35	Sections across Death Canyon..... 239
3.36	$SI_c - \log PCO_2$ graphs for waters in the Hiller Canyon network and in the Death Canyon network..... 248
3.37	Raven Lake Pit, Nahanni North Karst..... 253
3.38	Igloo Cave, Death Canyon, Nahanni North Karst..... 255
3.39	Plan and sections of Ice Curtain Cave, Death Canyon..... 256
3.40	The summer microclimate of Ice Curtain Cave, Death Canyon, July 23, 1973..... 259
3.41	Tunnel Cave, Nahanni Karst..... 260

	<u>Page</u>
3.42	Three stages in the development of a natural rock labyrinth in a highly fractured limestone surface..... 273
3.43	Strings of ellipsoidal, vertical-walled dolines, Nahanni Plateau..... 274
3.44	Diane Cave, an early stage in the modification of a fracture into a karst street via the development of a vertical shaft..... 275
3.45	The development of Karst plateaus, towers and poljes from networks of karst streets..... 277
4.1	Location of Nahanni Karst and climatic stations in its vicinity..... 284
4.2	Monthly precipitation relationships between Cadillac Mine, Fort Simpson and Tungsten..... 287
4.3	Climograph for Cadillac Mine, N.W.T..... 297
4.4	Daily rainfall histograms, Nahanni karst belt 1972 and 1973..... 316
4.5	Maximum and minimum daily temperatures, Nahanni Karst 1973..... 321
4.6	Surface pressure characteristics, district of Mackenzie, T200Z, 1970..... 325
4.7	Rainfall in the southern Yukon, southwest district of Mackenzie and northern British Columbia August 14-19, 1970..... 326
4.8	Surface pressure characteristics, district of Mackenzie, 0000Z July 22, 1972..... 328
4.9	Rainfall in the southern Yukon, southwest district of Mackenzie and northern British Columbia July 16-27, 1972..... 329
4.10	Mass curves of rainfall July 20-27, 1972..... 330
4.11	Corridors of "primary" and "secondary" lows in the Mackenzie River basin (after Burns 1973)..... 332
4.12	The Nahanni Karst: surface and groundwater hydrology..... 336
4.13	Topographic and geologic section through the Nahanni Karst from Bubbling Spring to White Spray..... 345
4.14	Flooding characteristics of Nahanni North karst depressions as determined from aerial photographs and ground observations..... 364
4.15	Relationships between rainfall and groundwater and surface runoff, Nahanni Karst, June 1973..... 370
4.16	Rainfall-runoff relationships, Mosquito Creek, July and August 1973..... 374
4.17	Water levels in Nahanni North Karst depressions, July 1972 and August 1973..... 381
5.1	The chemistry of Nahanni waters: Calcium-magnesium..... 404
5.2	The chemistry of Nahanni waters: Log total hardness - pH. 405
5.3	The chemistry of Nahanni waters: Alkalinity - total hardness..... 407

	<u>Page</u>
5.4	The chemistry of Nahanni waters: $SI_C - SI_D$ ..... 409
5.5	The chemistry of Nahanni waters: $SI_C \sim \log PCO_2$ ..... 411
5.6	Temperature dependence of the solubilities of calcite and gypsum (after Drake 1974)..... 436
5.7	Frequency histograms of calculated $\log PCO_2$ in Nahanni waters and measured $\log PCO_2$ in Nahanni soils..... 445
5.8	Changes in the chemistry of Tufa Spring waters under atmospheric conditions..... 463
5.9	Spatial variations in water chemistry within the Mosquito Creek drainage basin..... 470
5.10	Chemical interaction between waters in the drift-mantled shale environment..... 477
5.11	Chemical interaction between waters in the limestone environment..... 479
5.12	Location of regions discussed in the text..... 487
5.13	Regional variation in $Ca^{2+}$ concentration and water temperature..... 489
5.14	Regional variations in $HCO_3^-$ concentration and water temperature..... 490
5.15	Regional variation in $SI_C$ and water temperature..... 491
5.16	Regional variation in $\log PCO_2$ and water temperature..... 493
5.17	Regional variation in groundwater aggressiveness and water temperature..... 494
6.1	Glaciation of the South Nahanni National Park, Mackenzie Mountains, N.W.T., Canada (after Ford 1976)..... 506
6.2	Glaciation of the Nahanni Karst, N.W.T., Canada..... 533
6.3	Altered stream course, Ram Plateau..... 537
6.4	Topographic section across Mackenzie Plain showing the bevel on sediments laid down in Lake Tetcela..... 538
6.5	Altered stream courses on the eastern edge of Ram Plateau... 537
6.6	East to west topographic sections across Sundog Basin showing bevels on sediments laid down in Lakes Sundog I and II..... 539
7.1	Three ways in which fractures in a limestone mass can be etched out by solution and simple waveforms which simu- late the resulting landscape profiles..... 600
7.2	A model of the susceptibility to solution of a limestone mass crossed by one set of equally-spaced fractures..... 601
7.3	A model of the susceptibility to solution of a limestone mass crossed by two sets of equally-spaced fractures which intersect at right angles..... 604
7.4	A three-dimensional model of the susceptibility to solu- tion of a limestone mass crossed by three sets of fractures..... 605



## LIST OF TABLES

		<u>Page</u>
1.1	Extreme Maximum Temperatures (°F) at Tungsten, N.W.T., 1966-1971.....	12
1.2	Extreme Minimum Temperatures (°F) at Tungsten, N.W.T., 1966-1971.....	12
2.1	Table of Geologic Formations in the South Nahanni Region (after Douglas and D. K. Norris 1960).....	42
2.2	Fracture Patterns in the Nahanni Karst.....	87
3.1	Chemical Characteristics of Waters in Pavement Areas of the Nahanni Plateau South of Death Lake.....	118
3.2	Mean Chemical Characteristics of Water Types on Nahanni Pavements.....	119
3.3	Carbon Dioxide Levels in Soils on Limestone Pavements in the Nahanni.....	124
3.4	Chemical Characteristics of Some Waters Associated with Solution Dolines in Bare Limestone Regions of the North Karst.....	163
3.5	Chemical Characteristics of Some Standing Waters in Subjacent Karst Collapse Dolines on Shales South of Mosquito Lake and in Solution Dolines in Mantled Karst Areas North of Death Lake.....	164
3.6	Mean Chemical Characteristics of Some Waters in Dolines in the Nahanni North Karst Region.....	165
3.7	Chemical Characteristics of Some Pond and Seepage Waters in the Karst Streets of the Central Karst Region, Nahanni.....	190
3.8	Chemical Characteristics of Some Stream, Pond, Lake and Seepage Waters in the North Karst Labyrinths, Nahanni.....	192
3.9	Chemical Means of Some Waters in Karst Streets and Platea of the Central and North Karst Regions, Nahanni.....	193
3.10	Chemical Characteristics of Some Stream and Spring Waters in Nahanni Poljes.....	214
3.11	Chemical Characteristics of Lake and Overflow Waters in Nahanni Poljes During Flood.....	216
3.12	Mean Chemical Characteristics of Waters in Nahanni Poljes.....	217
3.13	Chemical Characteristics of Some Waters in Hiller Canyon, Ram Plateau.....	242
3.14	Mean Chemical Characteristics of Some Waters in Hiller and Death Canyons, Nahanni Karst.....	244
3.15	Chemical Characteristics of Some Waters in the Death Canyon Area.....	246
3.16	Phases in the History of Grotte Valerie in the North Wall of First Canyon, South Nahanni River (after Ford 1973).....	265

	<u>Page</u>
4.1 Mean Temperature and Precipitation Data, Fort Simpson, N.W.T.....	285
4.2 Mean Temperature and Precipitation Data, Tungsten, N.W.T.....	288
4.3 Temperature and Precipitation at Cadillac Mine, N.W.T., 1970.....	290
4.4 Linear Regression Relationships between 1970 Temperature and Precipitation Values and Long Term Means for Fort Simpson and Tungsten.....	291
4.5 Long Term Mean Temperature and Precipitation Estimates at Cadillac Mine Using Fort Simpson Relationships.....	293
4.6 Long Term Mean Temperature and Precipitation Estimates at Cadillac Mine Using Tungsten Relationships.....	294
4.7 Tentative Estimates of Mean Temperature and Precipitation at Cadillac Mine Obtained by Averaging the Estimates from Fort Simpson and Tungsten Relationships.....	296
4.8 Evapotranspiration and Effective Precipitation Estimates for Fort Simpson, Tungsten and Cadillac Mine.....	301
4.9 Hourly Wind Speeds (m.p.h.) at Fort Simpson, N.W.T. (after Burns 1972(a)).....	305
4.10 Snow Retention Coefficients for Various Surfaces Relative to Virgin Soil (after Kuzmin 1960).....	305
4.11 Snow Accumulation in Clearings of Various Sizes for the Observation Period 1945-59 (after Kuzmin 1960).	308
4.12 Average Snowpack Densities (after Seligman 1962).....	308
4.13 Average Reserves of Moisture in the Different Elements of Karst Relief in the Ai-Petra Massif, Crimean Mountains, USSR (after Dubljanskij 1963).....	312
4.14 Daily Precipitation Summary, Nahanni Karst, Summers 1972 and 1973.....	315
4.15 Rainfall Intensities in the Nahanni Karst, Summer 1973.....	318
4.16 Mean Daily and Daily Maximum and Minimum Temperatures in the Nahanni Karst, Summer 1973.....	320
4.17 The Seasonal Distribution of Precipitation at Fort Simpson, Tungsten and Cadillac Mine.....	323
4.18 Altitudes of Important Levels in the North Karst as Determined by Altimeter Survey in 1973.....	380
5.1 Chemical Equations and Equilibrium Constant Relationships Pertinent to the Calculation of Saturation Indices (after Garrels and Christ 1965).....	395

	<u>Page</u>	
5.2	Mean Chemical Characteristics of All Water Samples Taken in the Nahanni Karst in 1972 and 1973.....	402
5.3	Hydrogeological Water Types in the Nahanni Karst.....	416
5.4	Correlation Matrix of 12 Chemical Variables from Analysis of 214 Water Samples, Nahanni Karst, 1972-1973.....	417
5.5	Stepwise Linear Discriminant Function Analysis of the Chemistries of Major Water Types in the Nahanni Karst.....	419
5.6	Stepwise Linear Discriminant Function Analysis of the Chemistries of Spring Water Types in the Nahanni Karst.....	421
5.7	Stepwise Linear Discriminant Function Analysis of the Chemistries of Pond Water Types in the Nahanni Karst.....	423
5.8	Stepwise Linear Discriminant Function Analysis of the Chemistries of Lake Water Types in the Nahanni Karst.....	424
5.9	Stepwise Linear Discriminant Function Analysis of the Chemistries of Stream Water Types in the Nahanni Karst.....	427
5.10	Stepwise Linear Discriminant Function Analysis of the Chemistries of Soil Water Types in the Nahanni Karst.....	428
5.11	Stepwise Linear Discriminant Function Analysis of the Chemistries of Some Water Types on Shales in the Nahanni Karst.....	430
5.12	Stepwise Linear Discriminant Function Analysis of the Chemistries of Some Water Types on Limestone in the Nahanni Karst.....	432
5.13	Mean Carbon Dioxide Levels in Nahanni Soils.....	438
5.14	Relationships Between Soil Log PCO <sub>2</sub> in the Source Area and Log PCO <sub>2</sub> in Natural Waters, Nahanni Karst, N.W.T.....	447
5.15	Mean Chemical Characteristics of Spring Water Types in the Nahanni Karst.....	450
5.16	Mean Chemical Characteristics of Pond Water Types in the Nahanni Karst.....	453
5.17	Mean Chemical Characteristics of Lake Water Types in the Nahanni Karst.....	456
5.18	Mean Chemical Characteristics of Stream Water Types in the Nahanni Karst.....	458
5.19	Mean Chemical Characteristics of Soil Water Types in the Nahanni Karst.....	460
5.20	Mean Chemical Characteristics of Seepage Water of Limestone in the Nahanni Karst.....	460
5.21	Mosquito Creek Sample Sites and Water Chemistry Data.	472

	<u>Page</u>
5.22	Calculated Rates of Karst Denudation (largely after Jennings 1971)..... 498
6.1	Laurentide Ice Sheet Limits in the Eastern Ranges of the Western Cordillera, North of Latitude 60°N..... 511
6.2	Evidence of Cirque and Valley Glaciation in the Eastern Ranges of the Western Cordillera, North of Latitude 60°N..... 515
6.3	Glacial Lakes Poned by Laurentide Ice in the Eastern Ranges of the Western Cordillera North of Latitude 60°N..... 524
6.4	230-Th/234-U Age Determinations of Speleothem from Caves in the Nahanni Karst..... 546
6.5	Interglacial Periods in the Nahanni Region Suggested by Periods of Enhanced Speleothem Growth..... 547
6.6	Comparison Between Periods of High Sea Level, Enhanced Speleothem Growth in the Nahanni Karst and Peaks in the Earth's Orbital Eccentricity (years B.P.)..... 548
6.7	Tentative Glacial Chronology and Correlations for the Southeastern Mackenzie Mountains..... 550
7.1	A Tentative Denudation Chronology for the Nahanni Region..... 581

## LIST OF PLATES

	<u>Page</u>
2.1	The stratigraphical section at Death Lake..... 57
2.2	A small thrust fault visible in the north wall of Canal Canyon..... 90
3.1	Limestone pavement on a spur in the north wall of Crash Canyon..... 94
3.2	Steeply dipping pavement on the Nahanni Plateau surface south of Death Lake..... 95
3.3	Field of rillenkarren on a little-jointed limestone pavement, Nahanni Plateau south of Crash Canyon.. 97
3.4	Ripple and step development on an almost unjointed limestone pavement, Nahanni Plateau..... 98
3.5	Solutionally etched current bedding structures and solution "tunnels" in a clint wall, Nahanni Plateau..... 100
3.6	Clint and grike hierarchies, Nahanni Plateau..... 101
3.7	Secondary clint and grike networks making up natural crazy paving, Nahanni Plateau..... 102
3.8	Elliptical solution pits developed in microfractures filled with secondary calcite..... 104
3.9	Relict vegetation hollow on a pavement surface.... 113
3.10	Large joint hollow on a limestone pavement surface, Nahanni Plateau..... 116
3.11	Destruction of a limestone pavement in the Nahanni Karst..... 132
3.12	Palsa Basin, a structural doline..... 137
3.13	Synclinal structure in Nahanni Formation lime- stones..... 140
3.14	Rappel Cenote, Cenote Col, North Karst..... 141
3.15	Vertical-walled solution doline in bare karst, Nahanni Plateau south of Crash Canyon..... 142
3.16	Solution doline on till-covered limestone..... 144
3.17	Aerial view of Cenote Col, North Karst labyrinths, showing the spectacular solution doline assem- blage..... 146
3.18	Suffosion doline in fluviolly-reworked glacial debris resting on limestone, Insel Tower region, North Karst..... 160
3.19	Funnel-shaped suffosion dolines developed in super- ficial glacial debris resting on limestone, Sink- hole Plain, North Karst..... 161
3.20	Stal Gorge, a moderately sized karst street 150- 250 feet deep..... 174

	<u>Page</u>	
3.21	Shallow karst platea in the surface of the Nahanni Plateau between Death and Crash Canyons..	182
3.22	North Col Canyon, the largest karst platea in the Nahanni Karst is approximately 900 yards long, 450 yards wide and more than 300 feet deep.....	183
3.23	The natural rock labyrinths of the Nahanni North Karst looking south towards the Nahanni Plateau..	188
3.24	Aerial view of First Polje, Nahanni North Karst....	202
3.25	Second Polje partially inundated.....	208
3.26	Hiller Canyon, a closed fluvial canyon dissecting the western edge of the Ram Plateau.....	232
3.27	Canal Canyon, a glacio-karstic depression.....	236
3.28	Tunnel Cave.....	257
3.29	Spectacular ice formations in Igloo Cave, Death Canyon.....	262
3.30	Moderate-scale labyrinth karst to the west of Raven Canyon.....	278
3.31	Insel Tower.....	280
3.32	Karst platea south of Insel Tower, North Karst.....	281
4.1	First Polje dry and in flood.....	351
4.2	Third Polje dry and in flood.....	352
4.3	Raven Lake at low and high levels.....	354
4.4	Second Polje in flood.....	356
4.5	Aerial view of Bubbling Spring, North Karst.....	358
4.6	Eyehole Doline, Nahanni Plateau north of Death Lake.....	377
6.1	Patterned ground at 4,800 feet, Nahanni Plateau between Death and Canal Canyons.....	527
6.2	Fresh limestone erratic at 3,700 feet elevation, Nahanni Plateau south of Death Lake.....	529
6.3	Highly disintegrated limestone erratic at 4,000 feet elevation, Nahanni Plateau north of Canal Canyon.....	530
6.4	The remains of a huge delta laid down in an ice-dammed lake, Ranger Canyon, Nahanni Plateau.....	532
6.5	Sundog Basin.....	541
7.1	Karst cockpit and mogotes, Puerto Rico.....	602

1. The Nahanni Karst.

(a) The Discovery.

In August 1971 a party led by Derek C. Ford<sup>1</sup> of McMaster University conducted a survey of caves and karst in the First Canyon area of the South Nahanni River, N.W.T., Canada (Ford 1971). As well as looking at a number of interesting caves the party examined networks of fracture-located solution streets or corridors on residual portions of the upland plateau surface. These highly developed solution forms appeared exotic to the surrounding bare tundra-covered terrain. Examination of aerial photographs of the region during the course of fieldwork led to the discovery of an extensively developed karst landscape to the north of First Canyon. A one-hour aerial reconnaissance of the area in late August allowed the writer, D. C. Ford and J. N. Jennings<sup>2</sup> a glimpse of the most complex high-latitude karst known. After the first ground explorations in early July of 1972 it became even more evident that the Nahanni karst was something special.

---

<sup>1</sup>Prof. Derek C. Ford, Department of Geography, McMaster University, Canada.

<sup>2</sup>Prof. Joseph N. Jennings, Department of Geography, Australian National University, Australia.

(b) The Area.

(i) Location and Physiography.

The broad physiography of the Canadian Cordillera has been outlined by Bostock (1948, 1970) who has divided this region on the basis of geology and topography into three longitudinal units, the Eastern, Interior and Western Systems. The Eastern System is composed almost entirely of folded sedimentary strata. The Interior System is built of folded sedimentary and volcanic strata, and massive metamorphic rocks which are all intruded by large or small bodies of igneous rocks. In the Western System, the largest unit, the Coast Mountains are composed mainly of plutonic rocks whereas other parts contain a mixture of folded volcanic and sedimentary strata intruded by scattered bodies of massive igneous rocks. Bostock (1970) also points out that the Cordillera is segmented east to west by belts of relatively low terrain. For instance north of 60°N latitude a belt of low land made up of Liard Plateau, Liard Plain and Yukon Plateau separates the Rocky and Cassiar Mountains in the south, from the Mackenzie, Selwyn and Ogilvie Mountains in the north. In addition this latter group of physiographic units is separated from the Richardson Mountains further to the north by Porcupine and Peel Plateaux (Figure 1.1).

North of 60°N latitude in the region of the South Nahanni River, Liard Plateau, Franklin Mountains, Mackenzie Plain and Mackenzie Mountains are part of the Eastern System. Yukon Plateau, Pelly Mountains, Hyland Plateau and Selwyn Mountains, on the other hand, are part of the Interior System (Figure 1.1). The Nahanni karst region



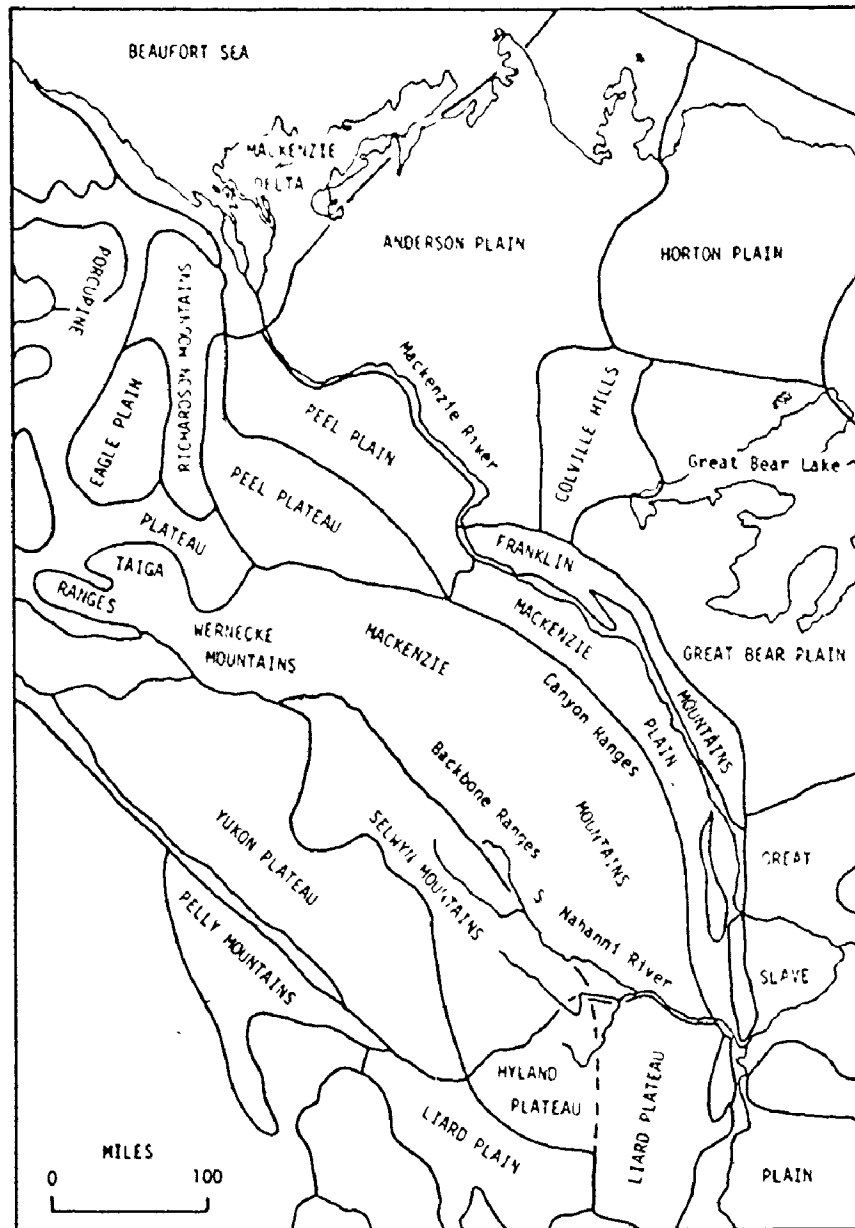


Figure 1.1. Physiographic regions of the District of Mackenzie, N.W.T., Yukon, British Columbia and Alberta (after Bostock 1970).

centered at latitude 61° 28'N, longitude 124° 05'W is located in the extreme southeastern portion of the Mackenzie Mountains. Solutional landforms have been identified within a narrow belt of country 308 square miles in area which extends for 28 miles north of First Canyon, South Nahanni River. The belt is 11 miles wide and is bounded by lines of latitude 61° 15'N and 61° 40'N and lines of longitude 123° 55'W and 124° 15'W. Intense karst development is even more localized in an extremely narrow zone 121 square miles in area which is 22 by 5.5 miles. It is bounded by lines of latitude 61° 17'N and 61° 36'N and lines of longitude 124° 00'W and 124° 10'W (Figure 1.2). East of the karst belt is the southern portion of the Mackenzie Plain; Nahanni Range, the southernmost range of the Franklin Mountains; and beyond the mountain belt the Interior Plains which in this vicinity is the Great Slave Plain. South of the karst, across the South Nahanni River, is the Liard Plateau (Figure 1.1).

East of the Franklin Mountains the Great Slave Plain is a surface of little relief cut across Paleozoic strata. In the west it is crossed by the Liard River which joins the Mackenzie at Fort Simpson. The settlement of Nahanni Butte is located where the South Nahanni River joins the Liard. The Plain is heavily wooded on a thick cover of glacial drift; exposures of bedrock are rare. East of the Nahanni Range the Great Slave Plain is at an altitude between 500-1000 ft. a.s.l. and is typically swampy and characterized by several large and small lakes and numerous ponds.

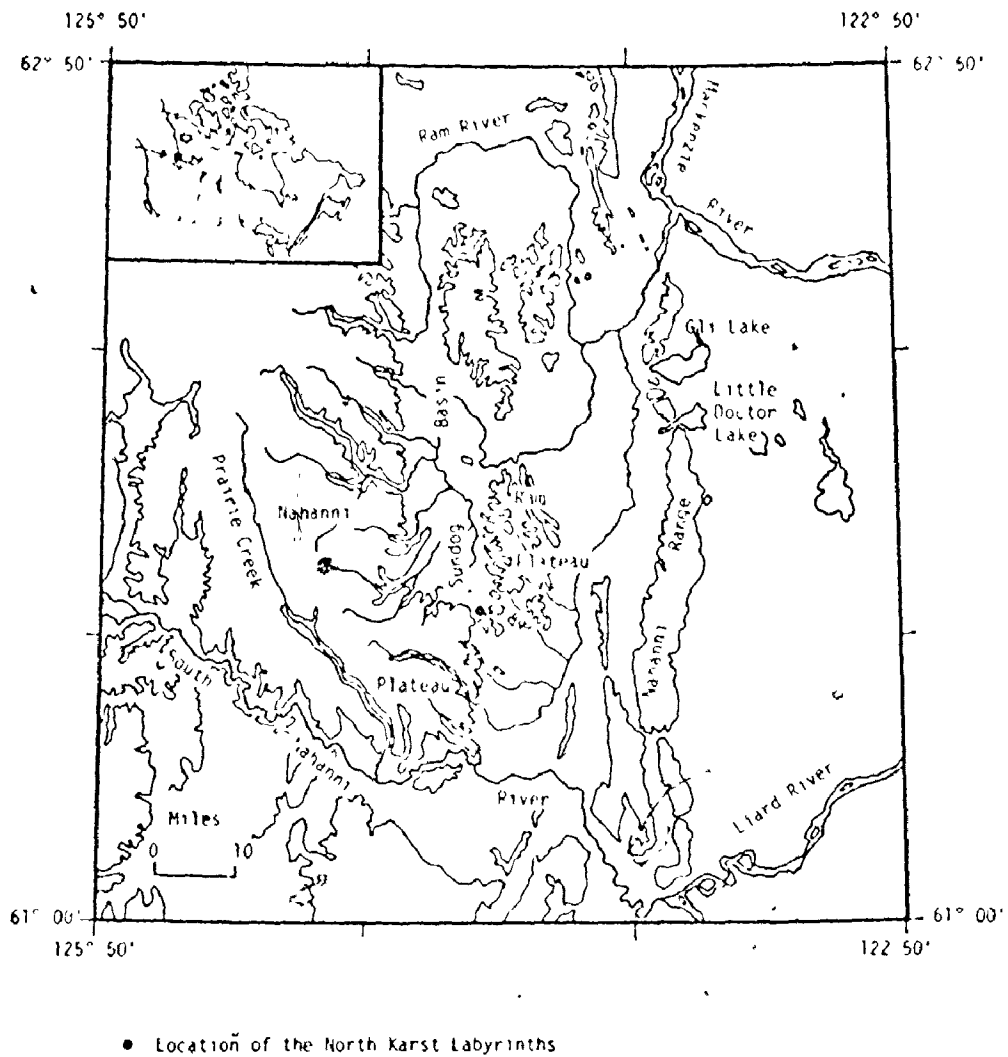


Figure 1.2. Location and major topographic features of the Nahanni karst region. The Franklin Mountains are depicted according to the 2,000 ft. contour, the Mackenzie Mountains in relation to the 3,000 ft. contour.

In the region of the South Nahanni River are the southernmost elements of the Franklin Mountains, namely Nahanni Range and Liard Range (Bostock 1948, p. 13). At Nahanni Butte, Nahanni Range rises from 680 ft. at the river, to an elevation of 4,579 ft. a.s.l. It extends north to Camsell Bend on Mackenzie River and forms a remarkably narrow rugged wall with a maximum width of 4 miles and with ridge crest elevations varying from 4,500-5,000 ft. Near its northern end, Nahanni Range is pierced by two deep narrow gaps, the southernmost occupied by Little Doctor Lake 6 miles long and the northernmost by Cli Lake 7 miles long (Figure 1.2). Nahanni Range is formed of hard, massive and resistant carbonates which support little vegetation.

West of Nahanni Range and part of the Franklin Mountain Chain are the Silent Hills which extend for 50 miles north of South Nahanni River. In the south, Silent Hills consists of two ridges; in the west The Twisted Mountain more than 4,000 ft. in elevation and in the east Bluefish Mountain more than 3,000 ft. high. The ridge of Silent Hills, which provides a second barrier between the southern Mackenzie Mountains and the Interior Plains, decreases in elevation from more than 4,000 ft. in the south to only a little more than 2,500 ft. where it is breached by Tetcela River. Still further to the west on the north banks of the South Nahanni River, is a third minor ridge 10 miles long and a little more than 2,500 ft. high which is a continuation of Yohin Ridge that is well developed to the south of the river.

To the west of the Franklin Mountains in the South Nahanni River area and to the east of the Mackenzie Mountains, is Mackenzie

Plain, a linear area of low relief. In the south it abuts against the Liard Plateau a few miles south of South Nahanni River. Immediately north of this river it is a little less than 10 miles wide between Mackenzie Mountains and Yohin Ridge. Northwards, in the vicinity of Ram Plateau, the Plain narrows to 5 miles bounded on the east by Silent Hills. Further north, as Silent Hills decrease in elevation, the Plain broadens to 15 miles west of Little Doctor and Cli Lakes. The Plain broadens northwards to 30 miles at North Nahanni River and throughout it is a broad rolling, drift- and tree-covered plain cut across soft shales and sandstones. Much of the rolling surface is elevated above the valleys of the main streams that run through it. Average elevations on the Plain vary between 1,000-1,500 ft. a.s.l.

West of the Mackenzie Plain are the Mackenzie Mountains in which Bostock (1948) recognized two physiographic provinces, namely the Backbone Ranges which he describes as "a sea of peaks and ridges reaching to 8,500 ft." (p. 24) and the Canyon Ranges which "are lower, divided by wide valleys or cut by deep canyons" (p. 24). Canyon Ranges may be as much as 400 miles long and form a front arc to the Mackenzie Mountains block and are composed of mountains of smooth profile, plateaux and widely separated low ranges. Bostock (1948) has expressed the opinion that the Canyon Ranges end a few miles south of North Nahanni River in an area of broken country indistinguishable from Backbone Ranges (p. 25). Douglas & D. K. Norris (1961) have noted, however, that in Camseil Bend and Root River



map-areas immediately to the north of the Nahanni karst region, Canyon Ranges have a distinct north to south grain and are characterized by sub-linear mountain ranges in which canyons have been cut by most of the major streams. Between these ranges and domes, linear valleys occur at elevations of about 1,500 ft. in contrast to the 4,000-5,000 ft. elevations of the Ranges.

The eastern front of the Mackenzie Mountains, west of Nahanni Range, also has a marked north to south grain with isolated domes separated by broad low-lying areas. The region of the Nahanni karst is therefore considered to be part of Bostock's Canyon Ranges of the Mackenzie Mountains. Prominent among the positive physiographic elements are Nahanni and Ram Plateaux, while separating north Nahanni Plateau from Ram Plateau is the low lying Sundog Basin which has an average elevation of 2,000-2,500 ft. and is 8 miles across and approximately 30 miles long. Ram Plateau is an elliptical dome 22 miles long and 15 miles wide. It has an elevation of more than 5,000 ft. at its crest (Figure 1.2). South Nahanni Plateau, like the Ram Plateau is a domical physiographic unit reaching elevations of more than 6,000 ft. in the western section. North Nahanni Plateau, on the other hand, is a flat-topped ridge with a steep eastern side. The upper surfaces of both Nahanni and Ram Plateaux are structural surfaces in resistant carbonates almost completely stripped bare of the more readily eroded overlying shales and characterized by a tundra vegetation. West of Nahanni Plateau in the Backbone Range province are several north-trending ranges reaching elevations of 5,000-6,000 ft.

including such ranges as Headless, Funeral and Manetoe and Tundra Ridge. The Nahanni karst is located principally on the eastern limb of southern Nahanni Plateau and in the southern section of the Ram Plateau with the accentuated forms occurring on the col which separates these two physiographic upland units.

South Nahanni and Flat Rivers form the boundary between Mackenzie Mountains and Liard Plateau according to Bostock (1948), although Douglas & D. K. Norris (1960) feel that the Nahanni Plateau extends for a short distance south of South Nahanni River. Liard Plateau lies between South Nahanni and Liard Rivers; Bostock (1948) describes it as a region of tree- and tundra-covered hills mostly less than 4,500 ft. in elevation and underlain mainly by shale and sandstone.

The region surrounding the Nahanni karst is drained by two important tributaries of the Mackenzie River, namely the North and South Nahanni Rivers. In the south, the South Nahanni River and its principal tributary, Flat River, have their headwaters in the Selwyn Mountains of the Yukon (Figure 1.1). South Nahanni River flows southeasterly for 250 miles and joins the Liard at Nahanni Butte. The Flat has a mean annual discharge of 4,190 c.f.s. with peak flows in June when the monthly mean flow is 11,400 c.f.s. and low flow being reached in March (591 c.f.s.). Mean annual discharge of the South Nahanni at the mouth of First Canyon is 16,600 c.f.s.; maximum flow occurs in June when the mean discharge is 52,800 c.f.s. and low flow is again in March with an average flow of 2,230 c.f.s. No figures are

available for the North Nahanni River. Where South Nahanni River crosses Funeral Range it has cut Third Canyon 12 miles long and far most of its length 3,000-4,000 ft. deep. Second Canyon, 4 miles long and 4,000 ft. deep has been cut through Headless Range, and First Canyon 12 miles long and up to 3,500 ft. deep is cut in the limestones and dolomites in the south-facing limb of the southern Nahanni Plateau.

In the north, North Nahanni River rises in the Backbone Ranges of the Mackenzie Mountains and drains in an eastward direction for 90 miles before joining the Mackenzie River at Camsell Bend. An important tributary of the North Nahanni, the Ram River, drains the northern Nahanni Plateau, Sundog Basin and then traverses the northern limb of Ram Plateau through a canyon 5 miles long and 1,500-2,000 ft. deep. It joins North Nahanni River in Mackenzie Plain. North and South Nahanni Rivers and Ram River all drain the region across the north-to-south grain of the Canyon Ranges of the Mackenzie Mountains. For most of their courses they flow against the structure. Elsewhere in the region subsequent streams dominate, following structural lines. Drainage on southern Nahanni Plateau and Ram Plateau is deeply incised in steep-walled canyons carved in massive grey and dark grey limestones and dolomites. The main canyons dissecting southern Nahanni Plateau are Canal Canyon, Lafferty Canyon and Ranger Canyon which are from 1,500-2,500 ft. in depth. The drainage elements on Ram Plateau are arranged in a distinctive radial pattern from the dome crest. Canyons are 1,500-3,000 ft. in depth. Between south



Nahanni and Ram Plateaux and Nahanni Range drainage is to the north via the Tetcela River, which has its headwaters in the southern limb of the Ram Plateau. In Bundog Basin, the drainage lines also flow north before joining the Ram River which funnels water through the front ranges. In the Nahanni karst itself, drainage is principally underground, ultimately reaching the South Nahanni and Ram Rivers via springs (Figure 1.2).

(ii) Climate.

The climate of the area is continental with short, warm summers and long cold winters. Estimated mean annual temperature is 24°F and mean annual precipitation 22.3 inches with 84 inches of snowfall characteristic (Table 4.7 & Figure 4.3). At Tungsten on Flat River (Figure 4.1) at an altitude of 4,250 ft. the coldest month of the year is January with a mean daily maximum temperature of -7.0°F, a mean daily minimum temperature of -25°F and a mean daily temperature of -16°F. The warmest month is July; it has a mean daily temperature of 51.1°F, a mean daily minimum of 40.7°F and a mean daily maximum of 61.5°F (Table 4.2). The extreme maximum temperature recorded at Tungsten is 83°F which was recorded in June (Table 1.1). At Fort Simpson (432 ft. a.s.l.), at the junction of the Liard and Mackenzie Rivers, where a record has been kept for a longer period, the extreme maximum is 97°F and this was recorded in July. The extreme minimum recorded at Tungsten is -52°F which occurred one January (Table 1.2); at Fort Simpson the extreme minimum is -69°F, a temperature recorded in the months of both February and December.

Table 1.1. Extreme Maximum Temperatures (°F) at Tungsten, N.W.T., 1966-1971.

	Jan	Feb	Mar	Apr	May	June	July	Aug	Sept	Oct	Nov	Dec
1966										42	34	24
1967	22	29		49	60	74	70	72	68	39	36	
1968	34	46	38		62	67	74			38	30	36*
1969	5	25	31		62*	83*	72*	68	56	51	35	28
1970	28	35	39			68	73		54	42	33	31
1971	29	37	29									

\*Incomplete data.

Table 1.2. Extreme Minimum Temperatures (°F) at Tungsten, N.W.T., 1966-1971.

	Jan	Feb	Mar	Apr	May	June	July	Aug	Sept	Oct	Nov	Dec
1966										-13	-33	-42
1967	-42	-38	-36	-6	19	28	32	31	19	6	-31	-32
1968	-47	-55	-14		12	29	34*	31*	18*	-6*	-20	-43
1969	-49	-37	-23		22	29*	34*	27*	17*	-5	-42	-16
1970	-44		-26			28			6		-35	-45
1971	-52	-44	-30									

\*Incomplete data.

The mean date of complete freeze over for lakes in the southeastern Mackenzie Mountain area is October 30th; the major streams do not freeze over, however, until early November. The Mackenzie River at Fort Simpson, for instance, freezes over on average close to November 15th. The mean date that rivers are clear of ice is approximately May 15th; for lakes the date is June 15th. According to Burns (1974) the mean maximum ice thickness on lakes is close to 60 inches, that on rivers 40 inches. Because the mean annual temperature is below freezing and the mean daily minimum temperature in the coldest month is  $-25^{\circ}\text{F}$  it is not surprising that the southern Mackenzie Mountains fall within the zone of discontinuous permafrost (Brown 1970). In addition, frozen ground phenomena are common, particularly at higher elevations where patterned and sorted ground forms are characteristic.

(iii) Vegetation.

The vegetation of the South Nahanni and Flat River areas is characterized by boreal and alpine plant species (Scotter et al. 1971). There is an altitudinal transition from closed forests in the lowlands to alpine tundra on the mountains. The tree line is at about 3,900 ft. on north- and east-facing slopes. In low-lying valley floors and on floodplains there is a dense growth of tall trees with white spruce and balsam poplar the dominant species. A dense shrub layer of alder, squashberry and wild rose is often present. Over much of Mackenzie Plain, Sundog Basin and in areas of Ram Plateau underlain by shales, a widely occurring forest type is open black spruce


and reindeer lichen forest. The soil is generally heavy and is covered by shallow peat.

The upland surfaces of Nahanni and Ram Plateaus as well as much of the bare limestone terrain at lower elevations in the karst belt, are characterized by outcrops of solid or fractured bedrock. It is a poor environment for plant growth and typical forest is scattered white and black spruce with some lodgepole and jack pine. At higher elevations alpine tundra is characteristic with mountain avens, ericaceous shrubs, sedges and grasses.

(iv) Bedrock Geology.

The broad topographical features of the southwestern district of Mackenzie are largely the result of folding and thrust faulting in Palaeozoic sediments. The principal structural elements, which are thought to have originated during the Laramide Orogeny, are north-trending and consist of homoclinal thrust sheets, faulted folds and broad elongate uplifts and depressions. The major thrust faults and the axial planes of the major folds dip either east or west.

Solutional landforms in the Nahanni karst belt are principally developed in the medium- to massively-bedded micritic limestones of the Middle Devonian Nahanni Formation and in the underlying argillaceous limestones and calcareous shales of the Headless Formation. At First Canyon, South Nahanni River these units are 350 ft. and 130 ft. thick respectively. Underlying the Headless unit at First Canyon are 2,675 ft. of dolomites, the upper 375 ft. belonging to the Manetoe Formation, the next 1,650 ft. belonging to the Arnica Formation; both



these units are of Middle Devonian age. The basal 650 ft. is Sombre Formation dolomites of Silurian/Devonian age. Because the dolomites are much less soluble than the overlying formations, surface depressions rarely penetrate into them although they do transmit groundwater. They appear to act as a base level for solution, restricting the vertical development of many of the landforms in the karst region. Overlying the Nahanni Formation are Upper Devonian shales of the Fort Simpson Formation which may attain thicknesses in some areas of up to 1,800 ft. In the Nahanni karst terrain they are rarely more than a few hundred feet in thickness but, where present, are a source of acid allogenic water to the bare limestone landscape.

(v) Glaciation.

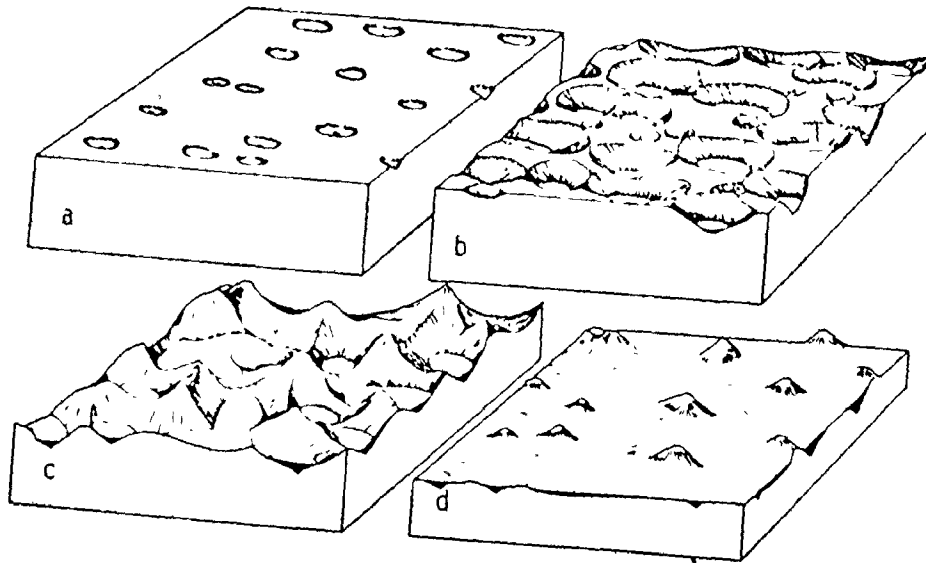
The Great Slave Plain, Franklin Mountains, Mackenzie Plain and the eastern ranges of Mackenzie Mountains have been covered by Laurentide ice from the east one or more times during the Pleistocene period. The Selwyn Mountains, Hyland Plateau, Liard Plateau and parts of the Mackenzie Mountain Backbone Ranges, on the other hand, have been covered one or more times by Cordilleran ice sheets and have also suffered Cordilleran valley glaciation. There is an increasing body of evidence to suggest, however, that a large portion of the southern Mackenzie Mountains was not glaciated by either Laurentide or Cordilleran ice during the Wisconsin and what is more, it now seems possible that some areas may not have been glaciated at any time during the Pleistocene.

## 2. The Problem Posed by the Nahanni Karst Assemblage.

Roglić (1972) points out that in 1899, A. Penck together with his students and in company of W. M. Davis, gave instruction on field trips in the karst of Bosnia and Hercegovina. Roglić notes that this meeting of Penck and Davis was of decisive importance for the further development of karst geomorphological concepts. Penck (1900) and Davis (1901) both pointed out the existence of plains in the karst of Heregovina and Dalmatia which they ascribed to denudation and fluvial erosion. They essentially introduced the concept that fluvial erosion occurred first and this was followed by 'karstification.' During karstification the landscape was believed to pass through a series of morphologic phases in a karst cycle of evolution.

In 1901 Cvijić, a student of Penck, accepted that karstification followed fluvial erosion and proposed a cycle of landform evolution whereby dolines coalesce to form uvalas and that by their coalescence, poljes, the final and largest karst features, are produced.

Like Cvijić, Grund (1914) believed that the doline was the basic feature of karst, as the valley is the basic form of fluvial relief. He felt that karst forms deepened and evolved in relation to the level of groundwater in the limestone which he felt was a base level for corrosion. Grund (1914) believed that the dolines of the Yugoslav karst were merely an early stage in the development of cockpit karst such as exists in Jamaica. The karst cycle proposed by Grund (1914) is illustrated in Figure 1.3. Karst development begins on a plane of corrosion and passes through young, adolescent, mature



- a 'Young' karst with extensive flat surfaces between dolines much of the original surface remaining.
- b 'Adolescent' karst with larger dolines and many coalescing.
- c 'Mature' karst: the original surface has disappeared; large dolines and uvalas lie between the hills.
- d 'Old' karst. Only isolated hills remain upon the plain.

Figure 1.3. The karst cycle (after Grund 1914).

and old stages. In the young stage of karstification extensive flat surfaces separate small dolines. In the adolescent stage dolines are much larger and deeper and are separated by residual ridges. Further karstification leads to the mature stage, at which time the ridges separating dolines have either been completely removed with the formation of uvalas, or alternatively they have been reduced to isolated steep-sided hills. Cockpit karst landscapes were believed by Grund to have reached the mature stage in his evolutionary cycle. In the old stage, plains form by corrosion and accumulation of residue with isolated hums which are eventually removed by solution. The final result is a 'corrosional peneplain.'

In 1918 Cvijić published a synthesis of his views on the evolution of karst relief in relation to hydrological zones in the rock mass. Cvijić suggested that a short fluvial phase preceded karstification with the formation of large plains. In the new cycle initiation of karst relief is by means of a series of normal valleys at the surface (Figure 1.4 (I)). At this stage according to Cvijić there is only one hydrographic zone, the fissures in the rock are little-opened by solution and dolines are few and of small dimensions. Neither uvalas nor poljes are characteristic of the karst relief in this initial phase. As the surface drainage is absorbed, the upper part of the limestone mass becomes dry so that two hydrographic zones are present in the rock mass, an upper dry zone and a lower saturated zone. The further enlargement of fissures causes a displacement of these zones to lower levels until eventually three hydrographic zones



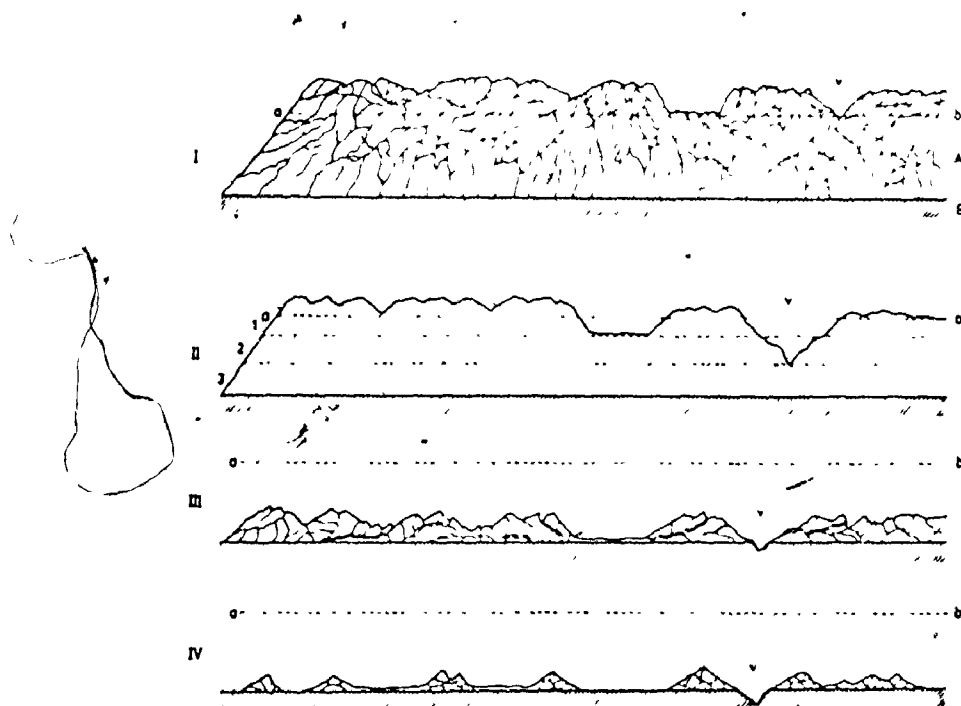


Figure 1.4. Evolution of water circulation and development of karst relief. I, II, III and IV are phases of karst development. A = calcareous cover; B = impervious base; a-b = lower limit of the first 'hydrographic' zone; v = allogenic river; 1 = dry zone; 2 = periodically inundated zone; 3 = permanently inundated zone (after Cvijić 1918).

can be recognized, a lower permanently saturated zone, an intermediate zone which is intermittently saturated and an uppermost dry zone which only rarely has flowing water. When three hydrographic zones are present the karst relief has reached a mature phase in its development at which time the most advanced karst forms such as dolines, uvalas and karst poljes are present in the relief (Figure 1.4 (II)). ~~In a~~ third phase there is gradual disintegration of the limestone landforms. The impermeable beds at the base of the limestone mass begin to appear and normal stream valleys reappear (Figure 1.4 (III)). In the final fourth phase recognized by Cvijić, the limestone mass has almost completely disappeared leaving only isolated limestone residuals or hums on the impermeable beds, normal drainage is re-established. (Figure 1.4 (IV)).

Early thinking on karst landscape morphology as exemplified by Cvijić (1901; 1918), Grund (1914) and also Sawicki (1909) was to range all karst phenomena into a single evolutionary sequence or cycle. In 1936 H. Lehmann published a detailed study of karst in the Sewu Mountains of Java. In this he argued that the karst cockpit and the residual conical hills are formed at the earliest stage in karst development in the humid tropics and that they are not as Grund (1914) suggested, a later stage in the evolution of the doline. Lehmann (1936) considered conical or cockpit karst to be specific of warm and humid climates just as dolines are characteristic of areas at moderate latitudes. As Sweeting (1972) notes, H. Lehmann was something of a pioneer in suggesting that karst landform morphology is to some extent

at least, a function of the climate. With the emergence of the general concepts of climatic morphology in the 1930's and 1940's came a clearer realization that karst landscapes in contrasting climates might have independent modes of development.

Sweeting (1972) reports that at a meeting of the Karst Commission of the I.G.U. in Frankfurt in 1953 it was stated that each climate has its own 'clima-specific' karst development. She notes that the main climatic zones in which karst landforms were considered to be distinctive on the grounds of climate included the periglacial and polar zones, the high Alpine zones, the cool oceanic west European-type zones, the Mediterranean zones, the dry desert zones, and the humid tropical zones. Sweeting goes on to say that in a further meeting of the Karst Commission of the I.G.U. in Rio de Janeiro in 1956, it was noted that in view of the dependence of karst upon climatic conditions it was unfortunate that the classical karst research started in the karst regions of mid latitudes where landforms are complex because they were exposed to changing climatological conditions during their development. Sweeting (1972) comments that "Whilst it is undeniable that climate is a major determinant in the differentiation of karst landforms, it is by no means the only one, and it could be said that to a certain extent modern German and French karst morphologists have been obsessed with this one factor" (p. 254).

The climatic variable has certainly been used more often than any other to explain regional variations in the characteristics of karst landforms. In particular humid tropical and extra-tropical

landforms have been differentiated. The opinion that many of the karst landforms to be found in tropical areas can not form under anything but a humid tropical climate (Lehmann 1956) has led many workers to explain the presence of such landforms in regions outside of the tropics in terms of formerly warmer and wetter conditions during an earlier geological period (Pokorny, 1963; Šilar, 1956; Gavrilović, 1969; Marker, 1970). In other words the landforms are considered to be relict.

Climate has been widely used to differentiate karst types - that is different assemblages of landforms. Many workers have differentiated tropical karst landform assemblages from those present in colder regions. For instance Sweeting (1972) recognizes True Karst, Fluviokarst, Glacio-(Nival) Karst, Tropical Karst and Arid and Semi-arid Karst. Earlier Gvozdeckij (1965) differentiated Bare Karst; Covered Karst, Soil-covered Karst, Buried Karst, Tropical Karst and Permafrost Karst. High Mountain, Polar and Tropical Karst varieties were also recognized by Jenko (1959).

As Sweeting (1972) argues "of all types of karst it can be said that tropical karst forms are the most distinctive. It is still arguable to what extent the karst features found in tropical areas are unique to the tropics, but it is undeniable that in general the karst lands appear to show different landforms from those in extra-tropical areas; landforms that occur in temperate areas do occur in the tropics, but the reverse is so far not known" (p. 270).

Certainly the karst landform assemblages of the hot, wet regions of the world have always appeared very different from those found in cold dry regions. As Jennings (1970) has pointed out there is more morphologic variation in tropical karst landscapes than elsewhere. The many landform types such as cockpit karst, tower karst, labyrinth karst, crevice karst, polygonal karst, and arête and pinnacle karst attest to this. In addition tropical carbonate terrains are characterized by very dense karst landform assemblages often with considerable vertical development (Sweeting, 1958; Jennings & Bik, 1962; Šilar, 1965; Monroe, 1968; Williams, 1972). For instance the Gunung Sewu karst (Lehmann, 1936) is thought to be made up of 40,000 conical hills in an area of 1,300 square kilometers. Lehmann reports that the average height of hills is about 75 meters.

Karst development in the much colder and drier alpine, arctic and sub-arctic regions of the world is much less spectacular. In the alpine karst of the Mount Castleguard-Columbia icefield area of the Canadian Rocky Mountains for instance, Ford (1971(b)) reports a close juxtaposition of karst, glacial and periglacial landforms. The karst features present include all kinds of karren on limestone pavement surfaces and more than 100 sinkholes almost all of which are vertical shafts opening directly from the surface or from a confluence of grikes. Ford (1971(b)) also reports a few funnel-shaped dolines with the funneling confined to an uppermost layer of moraine. A few sinkholes he notes drain much larger closed depressions but the topographic closure he attributes to glacier erosion and deposition, not to solution directed at the modern sinkhole. Cave systems are also

common in this region. Karst forms in arctic terrains seem to be even less well developed than they are in alpine terrains. Bird (1966) notes that limestone is the most common sedimentary rock in arctic Canada south of Parry Channel where it covers about 300,000 square kilometers or more than 12% of the land surface. Despite such a wide area of soluble rock outcrop Bird notes that surface karst forms are rare, although occasionally solution effects may be observed along joints in areas of limestone pavement and surface karren are relatively common. Bird also notes that under suitable conditions subnival solution may be concentrated beneath perennial snowbanks with the formation of nivation-type limestone hollows. These features are similar to the kotlici of the Julian Alps. Bird also reports that groundwater flow is rare in the Canadian arctic with few caves and springs. Also the only sinkholes that have been discovered were found in stream beds on Alepatok Island where they are up to 5 meters wide. According to Bird (1966) "The conclusion is inescapable that under continental arctic conditions, in areas that were glaciated, and where there is continuous, deep permafrost, karst landscape due to chemical weathering has not developed" (p. 117). Bird also notes that there are few observations of karst development from northern Canada although Branden (1963) has found that in the Mackenzie lowlands region of discontinuous permafrost, there is considerable groundwater flow, some of which occurs along solution channels. Bird also points out that karst features occur in northern Alberta and may exist locally south of Great Bear Lake. No karst development is found in

the Hudson Bay lowlands, the other subarctic limestone region in Canada. As Bird (1966) says "Where karst is found in northern subarctic areas, it may be contemporary but at least in unglacierized areas, it may also be a relic feature" (p. 117). A much more thorough account of karst development in the arctic and subarctic regions of Canada is given by Ford & Quinlan (1973) but again the generally poor karst development is emphasized. Corbel (1952) has described karst development in Sweden where he reports the existence of extensive cave networks and some doline development. Both Kunaver (1965)<sup>1</sup> and Brown (1972) working in alpine areas have reported that some valleys blocked by glacial end moraines may become glaciokarstic basins when water drains underground leaving the closed basin intact.

The more varied nature and more accentuated development of karst landscapes in the humid tropics has been explained in terms of the climate and the vegetation (Lehmann 1953, Birot, 1954). Chemical reactions are thought to proceed faster because of the higher temperatures; high rainfall and rainfall intensities make for prolonged and rapid solution while rapid plant growth and decay and intense microbial activity with resulting high  $PCO_2$  makes tropical water more aggressive (Jennings, 1970).

It is clear from this short discussion on the theories of karst landform development that arctic and subarctic carbonate terrains are generally only poorly karsted with few and shallow forms. On the other hand karst development in humid tropical areas is varied and intense. In the Nahanni subarctic mountainous region

---

<sup>1</sup>See Sweeting 1972, p. 267.

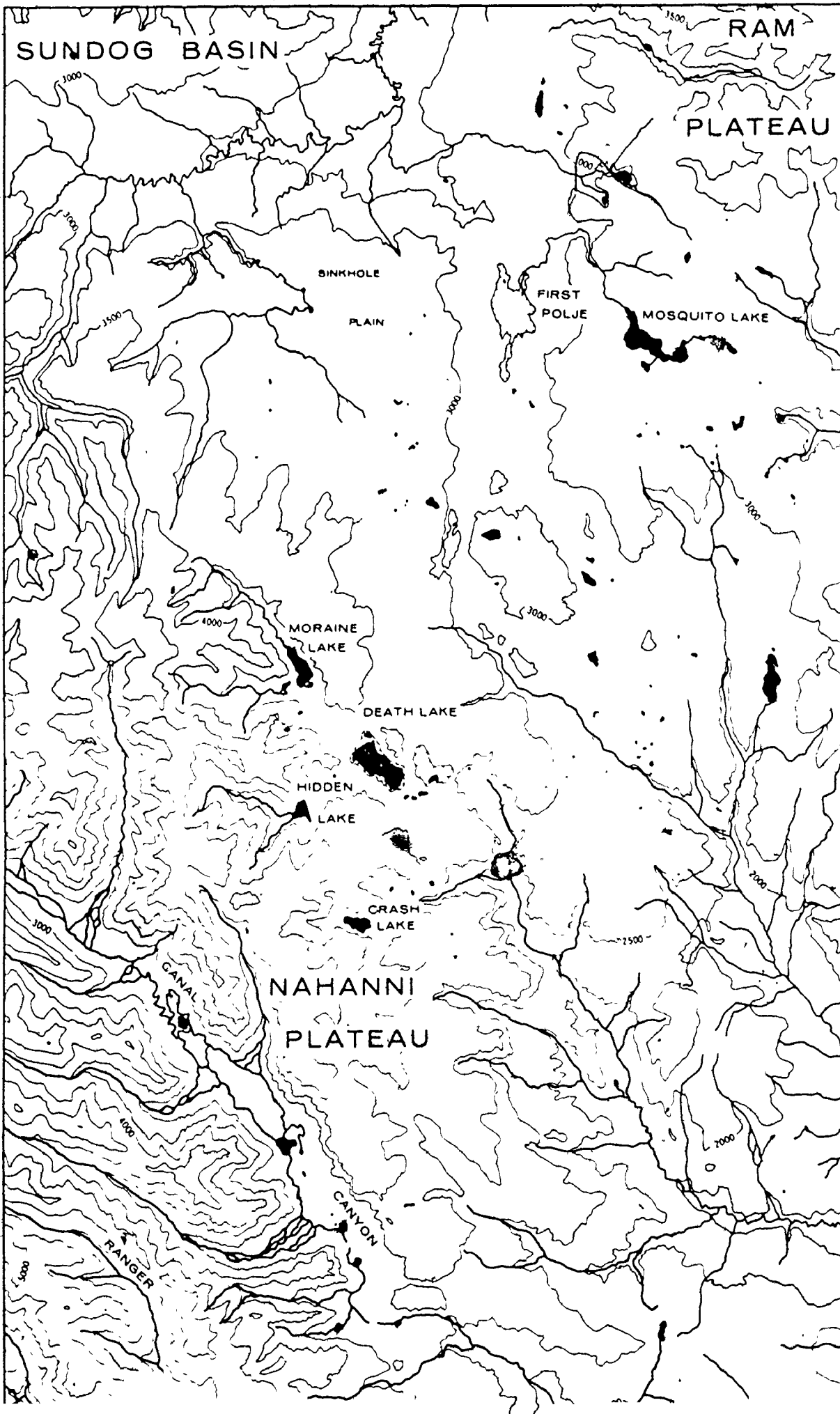
of Canada, there exists the most complex high-latitude karst yet discovered. The karst assemblage includes limestone pavements with karren forms; dense collections of dolines of solution, collapse, subjacent karst collapse, suffosion and subsidence origin with related uvala forms; highly accentuated labyrinth or crevice karst networks with residual karst towers; glacially-closed fluvial canyons of huge dimensions and the most northerly poljes known (Figures 1.5 and 1.6). This dense assemblage of karst landforms developed on a massive scale, appears exotic to a bleak subarctic landscape; it is much more characteristic of what one would expect in a humid tropical area of high relief such as is present in New Guinea or Indonesia. The problem posed by the highly developed Nahanni karst in view of the morphoclimatic concept of karst landform development supported by many workers is a simple one. Why does the Nahanni karst assemblage exist and how has it evolved?

### 3. The Structure of the Answer.

Chapters 2 through 7 are an attempt to explain the existence of the Nahanni karst landform assemblage. At the outset it was realized that a satisfactory and all-embracing explanation of the Nahanni karst might not be easy to arrive at, and that is how it turned out. Perhaps the greatest obstacle encountered was that of incomplete evidence. The Nahanni terrain has not everywhere been examined on the ground; in fact large areas still remain essentially unexplored and these may host just that small piece of geomorphic evidence that would help in piecing together the geomorphic history of this region. In the exploration of the Nahanni region restrictions on time and money had to be



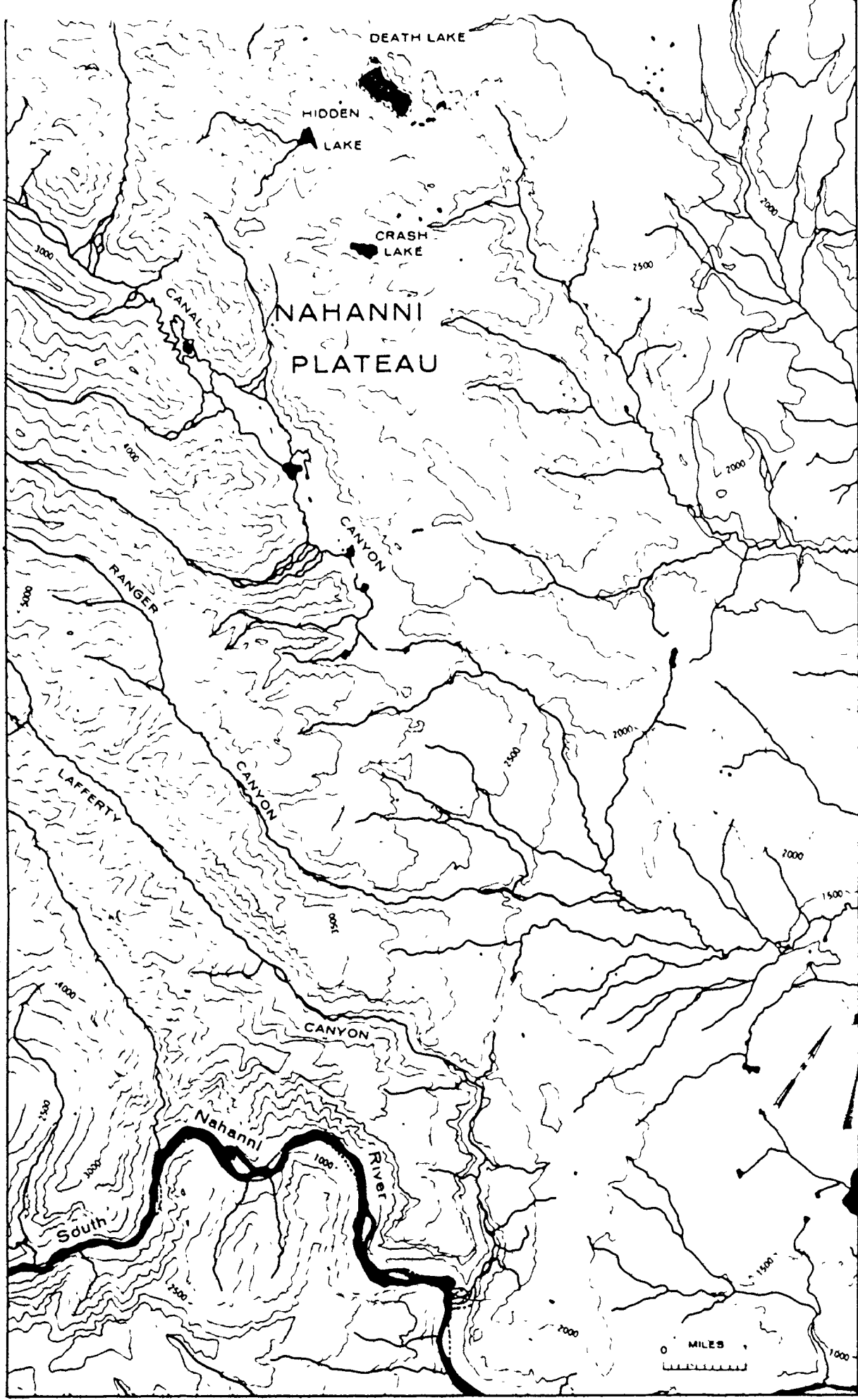
00'



30'

61° 30'

61° 30'



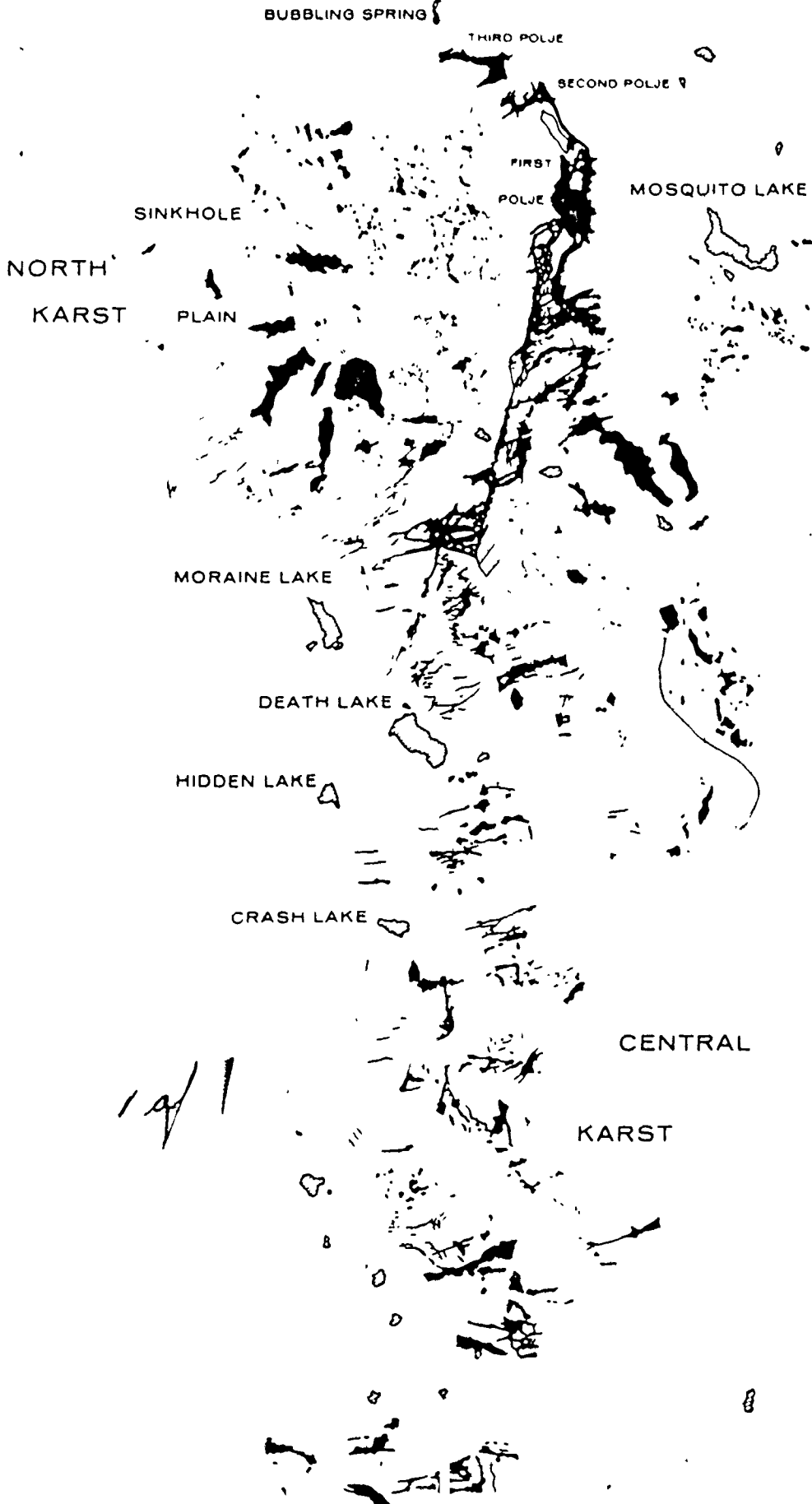
61° 20'

61° 20'

2 of 2

124° 10'

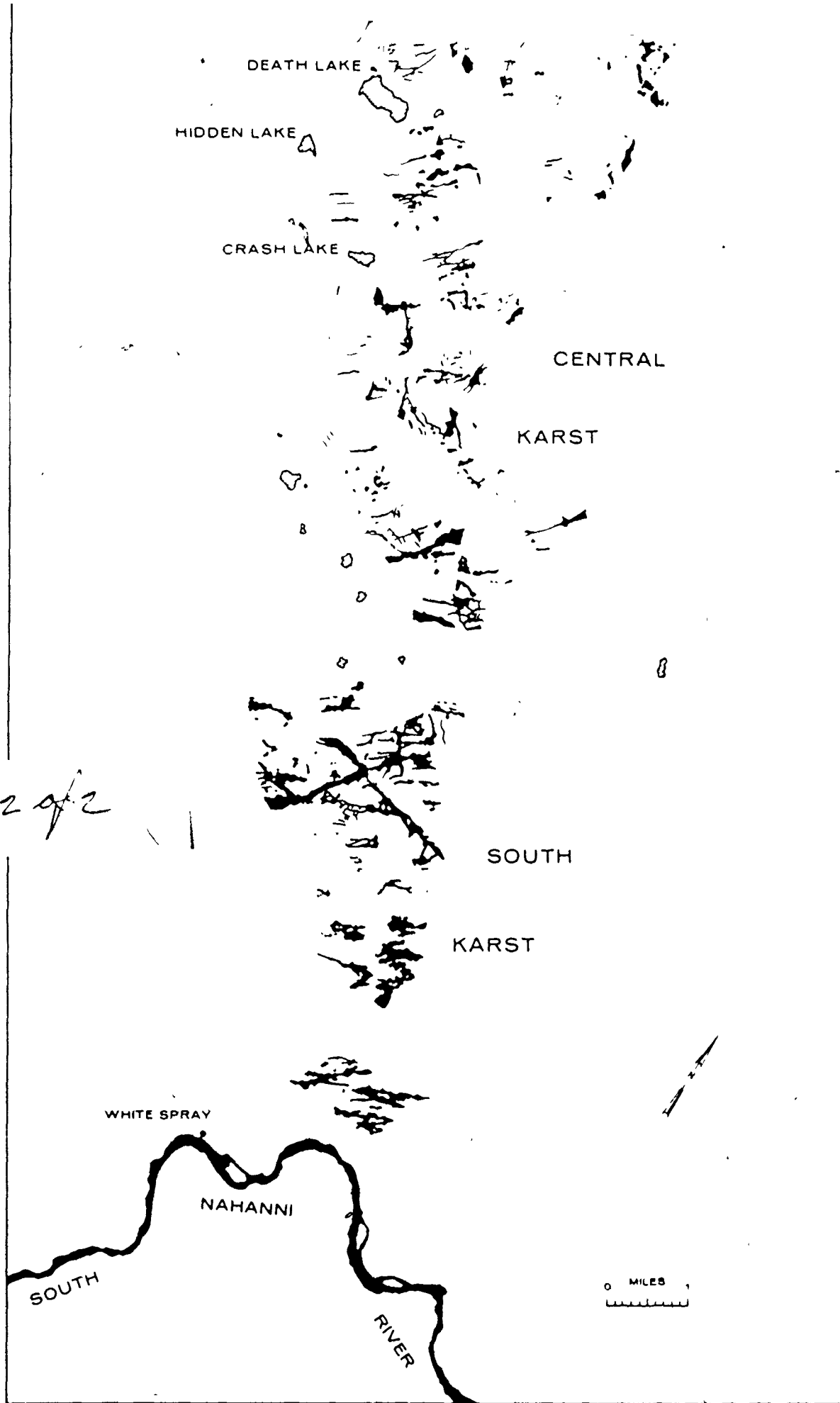
124° 00'



61° 30' -

- 61° 30'

19/1



61° 20' -

- 61° 20'

124° 10'

124° 00'

faced. The area is extensive and difficult to traverse on the ground. The only way in which the area could have been examined thoroughly, would have been by using a helicopter for weeks at a time, and these are expensive machines. The approach taken was to examine the most accentuated karst landforms in detail, view as much of the karst as possible on foot and examine the remainder from the air or by means of aerial photographs. The problem of adequately covering the area became even more severe when it was realized that a knowledge of the glacial history of the southern Mackenzie Mountains region as a whole may be necessary for a complete understanding of the genesis of the karst landscape. Patterns of glaciation have been deduced from evidence collected during fieldwork, from aerial reconnaissance observations and from a detailed analysis of the aerial photographs. There is no doubt that further work is necessary.

During the summers of 1972 and 1973 base camps were set up at Mosquito Lake and Death Lake and in 1973 a short time was spent at First Polje. These camp locations allowed relatively easy access to the northern section of the karst (Figure 1.5 and 1.6). The karst landforms north of Ranger Canyon and south of Canal Canyon have not been examined on the ground although they have been looked at from the air and one or two landings were made. For ease of discussion, the karst terrain is referred to in terms of three regions namely the North, South and Central karsts (Figure 1.6). Most of the names used in the following discussion for the various topographic features are not official but simply those adopted by the working party when in the field.

Chapter 2 examines aspects of the regional stratigraphic and structural bedrock geology of the Upper Mackenzie River area with specific reference to the South Nahanni region. Work in the field was directed at determining to what extent the structural and lithological characteristics of the bedrock sequence have affected the morphologies and modes of development of the karst landforms in this subarctic terrain.

The characteristics of the solutional landforms to be found in the Nahanni karst are documented in Chapter 3. The various landforms are described and the pattern and intensity of solution in each type is discussed. Chapter 3 is the necessary description of a newly-discovered complex karst landscape. It also serves to emphasize the great variety of forms present and provides some explanation as to their mode of development.

In Chapters 4 and 5 discussion is centered upon what is going on in the karst at present. The hydrology of the karst is discussed in Chapter 4 and its effect upon the pattern of karst landform development, both past and present is considered. Spatial variations in the intensity of solution across the karst and the factors that control it are examined in Chapter 5. Tentative estimates of present and past denudation rates in the area are proffered.

Aspects of Pleistocene glaciation in the southern Mackenzie Mountains are discussed in Chapter 6 and a tentative scheme is proposed. Not until Chapter 7, however, is the material synthesized, the various possible explanations of the Nahanni karst proposed and a conclusion

as to its origin reached. Also in this chapter a tentative structural model for the development of karst landscapes in general is introduced. Whether the explanation offered is the correct one will likely be known in time as more information on the geomorphic evolution of this remote area is collected.

In discussing the various aspects of the Nahanni karst it has proved difficult to avoid at least some duplication of argument. Solution patterns, for instance, are discussed in Chapters 3 and 5 although a detailed explanation of terms is not given until Chapter 5. To overcome this problem, brief explanations of the chemical terms used in Chapter 3 are given in Appendix I which is a glossary of terms. This glossary is included because any discussion of karst landscapes necessitates the use of a broad and often complex 'jargon.'

## Chapter 2. Geology of the Southern Mackenzie Mountains

### 1. Introduction.

The Southern Mackenzie Mountains are a part of the Cordilleran Orogen, a segment of the circum-Pacific orogenic belt. The orogen is some 500 miles wide and is a region of mountains, plateaux, trenches and valleys. The eastern part of the orogen, including the Mackenzie Mountains, embraces the parts of the Cordilleran Geosyncline that generally received miogeosynclinal and exogeosynclinal sediments and that underwent superficial deformation with little or no metamorphism, volcanism or plutonism during the orogenic phases. The central sector comprising the arcuate Mackenzie Fold Belt, made up of Liard Plateau, Mackenzie, Franklin and Wernecke Mountains and the Taiga Ranges of Porcupine Plateau, was produced during the Columbian and Laramide Orogenies. This fold belt is characterized by Paleozoic carbonate and clastic rocks thrown into broad simple folds with intervening zones of complex folds and faults (Douglas et al. 1970).

The geology of the southern Mackenzie Mountains is complicated by the fact that it is a zone of rapid facies change at several stratigraphic levels from the Ordovician to the top of the Middle Devonian. Because the sequence of Devonian sediments in the Nahanni karst area has been important in controlling the pattern of solutional landform development there, an attempt will be made to explain the characteristics of the strata.



## 2. Stratigraphy.

### (a) Regional Stratigraphy of the Upper Mackenzie River Area.

The regional Devonian geology of the upper Mackenzie River area has been thoroughly discussed by Law (1971). A brief summary of his synthesis will be presented here to explain stratigraphical and facies variations in the rocks of the southern Mackenzie Mountains. Law notes that under most of the Interior Plains, Devonian rocks rest on a thick sequence of Ordovician dolomites, shales and sandstones. In the Mackenzie and Franklin Mountains and Mackenzie Plain, on the other hand, they rest unconformably on thick Ordovician and Silurian limestones and dolomites of the Sunblood, Whittacker and lower Delorme Formations (Figure 2.1). In the upper Mackenzie River area, Devonian sediments thicken southwestwards from zero on the edge of the Precambrian Shield to more than 10,000 ft. in the southern Mackenzie Mountains, deeper into the Cordilleran miogeosyncline. The Lower and Middle Devonian consist mainly of carbonates with some shales and evaporites (Law 1971). The Upper Devonian consists of shales with some siltstones, sandstones and limestones.

#### (i) Lower Devonian.

Lower Devonian rocks outcropping in the southern Mackenzie Mountains include the Delorme, Camsell and Sombre Formations of Silurian to Early Devonian age (Douglas & D. K. Norris 1960, 1962). The Delorme, the oldest, consists of more than 3,000 ft. of thinly bedded limestones, dolomites and shales while the Camsell Formation consists of more than 1,400 ft. of unfossiliferous limestones and breccias with salt casts.

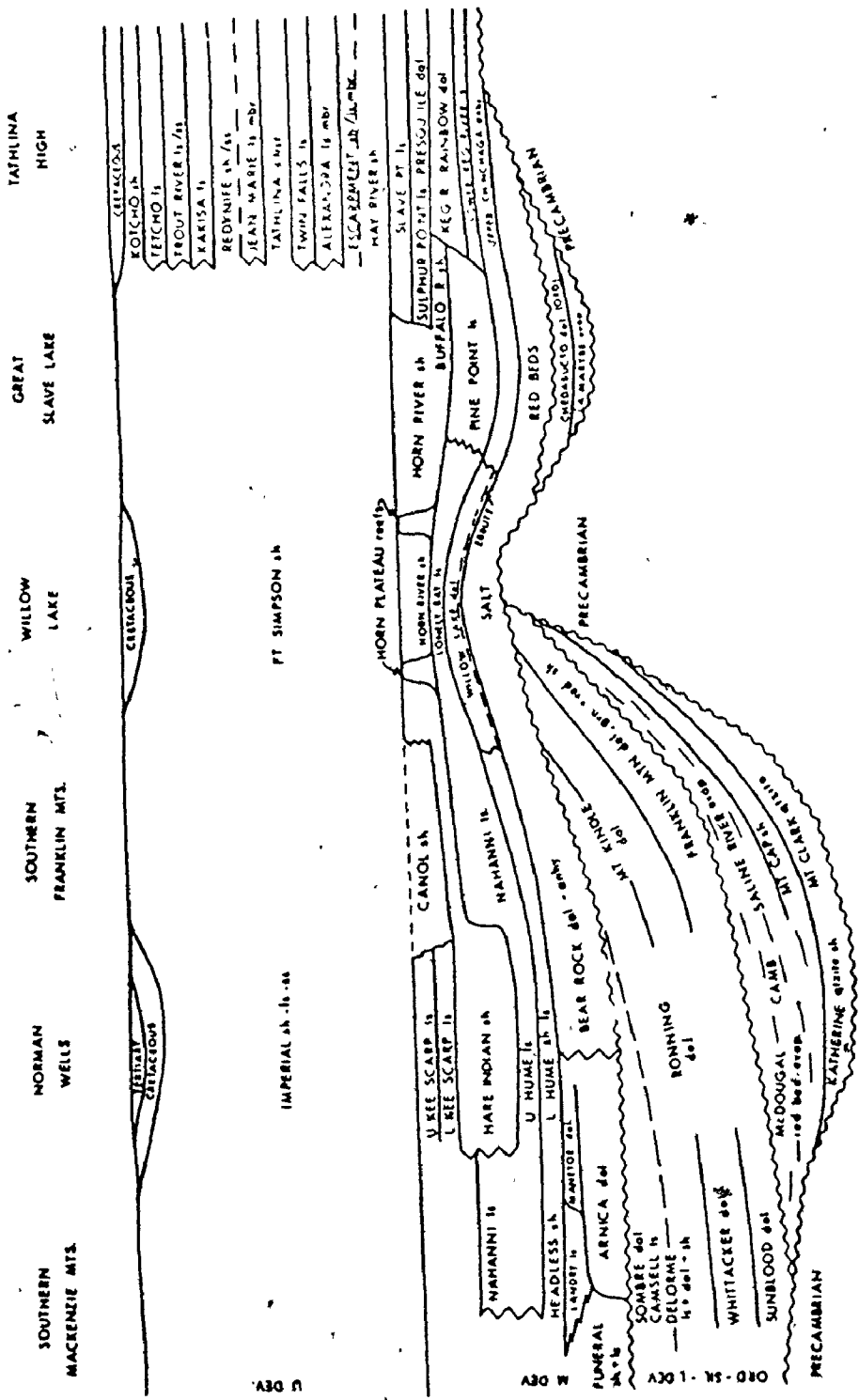


Figure 2.1. Schematic cross section through the upper Mackenzie River area, N.W.T. (after Law 1971).

Law (1971) suggests that the breccias have been formed by solution of evaporites. This sequence is overlain by several thousand feet of unfossiliferous fine-grained dolomites of the Sombre formation which is in turn overlain unconformably by Middle Devonian beds (Figure 2.1).

(ii) Middle Devonian.

Middle Devonian beds consist of limestones, dolomites and shales laid down during a series of transgressive pulses. Formational boundaries commonly occur at the beginning of each transgression and the lithofacies within a formation change from open marine in the west to restricted marine in the east (Figure 2.1).

The oldest rock unit of Middle Devonian age in the upper Mackenzie River area is the Funeral Formation which is up to 2,550 ft. thick where it outcrops in the Mackenzie Mountains. It consists of dark grey to black shales and argillaceous limestones. The Lower Funeral grades laterally into the massive fine-grained, grey-and-black banded dolomites of the Arnica Formation which may be up to 2,630 ft. thick. Law (1971) mentions that it is not yet clear whether the fine-grained dolomites of the Arnica Formation were deposited behind a reef trend fringing the Funeral embayment, or whether they are the result of algal, bacterial or inorganic agencies unrelated to reefing. Further west in the southern Franklin Mountains the Bear Rock Formation is the restricted marine environment equivalent of the Arnica and overlying Manetoe Formations (Figure 2.1). Law (1971) notes that at surface exposures in the Franklin and Mackenzie Mountains the Bear Rock Formation consists of limestone breccia which is thought to have been formed by solution and alteration of an evaporite sequence.

The Arnica is overlain by dolomites and limestones of the Manetoe and Landry Formations. The Manetoe consists of 150-500 ft. of dark grey, coarsely crystalline, massive, very porous secondary dolomite with white calcite veins. Law (1971) notes that since the Manetoe dolomites grade into the Funeral limestones and shales, they probably represent reef or bank deposits. The Landry consists of 300-700 ft. of cryptograined and pelletoid limestones. Law feels that since the Landry limestones grade southwards into the Funeral Formation, they may represent an interreef facies developed where the main Manetoe front lay further back from the Arnica front. To the east the Manetoe passes into anhydrite beds of the Upper Bear Rock Formation (Figure 2.1).

After deposition of the Landry, Manetoe and Bear Rock Formations subsidence of the geosynclinal environment caused a major transgression. This led to the deposition of normal marine carbonates and shales of the Lower Hume and Headless Formations over restricted-marine evaporites in the northern and western parts of the Upper Mackenzie area. Throughout the southern Franklin Mountains and in parts of the southern Mackenzie Mountains, the Headless Formation is about 200 ft. thick and occurs as a recessive band below the Nahanni limestones. As the marine transgression continued the amount of shale entering the shelf area declined and the entire upper Mackenzie River area became covered by normal-marine limestones and dolomites 100-200 ft. thick. These carbonates form the Upper Hume Formation of Norman Wells and the Lower Nahanni Formation of the southern Mackenzie and

Franklin Mountains. The Lower Nahanni Formation consists of dense, partly dolomitic and finely crystalline limestones while the limestones of the Hume Formation are mainly fine-grained and sometimes argillaceous with a fauna of crinoids and brachiopods with corals and stromatopoids occurring in some areas.

The Upper Nahanni was deposited at a time when the rate of subsidence in the geosyncline became rapid. Isolated reefs appeared and grew to be several hundred feet thick. According to Douglas & D.K. Norris (1962) the upper Nahanni consists of several hundred feet of limestone with alternating recessive and resistant units. The resistant units are medium to thickly bedded limestone varying from cryptocrystalline to medium grained and are coraliferous and fossiliferous with thicker fossiliferous beds more prevalent in the middle part. The recessive units, on the other hand, they report to be thinly bedded fine-grained limestones.

The isolated reef phase of deposition was eventually brought to a close by elevation of the 'Upper Mackenzie Uplift' (Law 1971). Following uplift, attrition of reef crests took place throughout most of the upper Mackenzie River area and limestone detritus was swept into the area between the reefs. The inter-reef deposition resulted in an extensive complex of carbonate sediments forming around and over the Upper Mackenzie Uplift. This complex forms the upper part of the Nahanni Formation. Following the hiatus associated with elevation of the Upper Mackenzie Uplift, there was renewed submergence and the beginning of another sedimentary cycle. The basinal shale facies

transgressed over the carbonate facies in many areas. Thus the upper part of the Hare Indian shales overlies the middle Nahanni in the southern part of the Mackenzie Plain but as Law (1971) points out, carbonate deposition was probably continuous in the southern Mackenzie Mountains at this time for here the Nahanni Formation is very thick.

(iii) Upper Devonian.

Throughout most of the upper Mackenzie River area Middle Devonian limestones and shales are overlain, apparently conformably, by shales of the Fort Simpson Formation (Douglas & D. K. Norris 1961). These consist of dark-grey to greenish-grey shales with some siltstones and fine-grained sandstones. Where not thinned by erosion, the Fort Simpson Formation may be up to 2,000 ft. thick.

(b) Stratigraphy of the Nahanni Region.

(i) The Map-units and Stratigraphic Formations.

The stratigraphy of the Nahanni region has been outlined by Douglas & D. K. Norris (1960), with correlation of formations in other areas outlined in Douglas & D. K. Norris (1961, 1962). Noble & Ferguson (1971) have conducted detailed work on facies and faunal relations in the area and have demonstrated the relationships between the various formations recognized by Douglas & D. K. Norris (1960, 1961, 1962) and faunal zones (Figure 2.2). These writers point out that in the Liard-Nahanni area an epeiric shelf to the east was bordered to the west by a marginal cratonic basin which during most of the Middle Devonian received thick clastics from some extra-cratonic source. The work of Noble & Ferguson (1971) helps explain lithological changes in the bedrock section in the Nahanni karst region.

LIARD - NAHANNI AREA		NORMAN WELLS AREA	NORTHERN ALBERTA
STRATIGRAPHIC NOMENCLATURE	ZONE		
NAHANNI	<i>Lerorhynchus castanea</i>	LOWERMOST HARE INDIAN OR TOPMOST HUME	KEG RIVER
	<i>Bilingostrea vernii</i>	HUME	
HEADLESS	<i>Schuchertella adoceta</i>		
			CHINCHAGA CLASTIC
LANDRY	<i>Warrenella</i> sp 1	BEAR ROCK	LOWER CHINCHAGA
FUNERAL	<i>Gasterocoma ? bicula</i>		
MANETOE			
ARNICA			COLD LAKE
CAMSELL			ERNESTINA LAKE

Figure 2.2. Faunal zones of the Middle Devonian in the Liard-Nahanni area and correlation with the Norman Wells and northern Alberta regions (after Noble and Ferguson 1971).

Figure 2.3 shows the geology of the Nahanni karst as mapped by Douglas & D. K. Norris (1960). Accompanying it Table 2.1 outlines the ages, lithologies and thicknesses of the various map-units while approximate stratigraphic relationships of Middle Devonian and older map-units in the Virginia Falls map-area are given in Figure 2.4. Correlations between formations and map-units in the Virginia Falls and nearby areas are presented in Figures 2.5 and 2.6. The main characteristics of the various map units important in the Nahanni karst area will now be outlined.

Map units 11-14. The Sombre Formation (Silurian-Devonian).

On the Nahanni Plateau map-units 11-14 which Douglas & D. K. Norris (1961) ascribe to the Sombre Formation (Figure 2.5) form a thick sequence of grey-weathering banded dolomites. At First Canyon these units are 650 ft. thick (Douglas & D. K. Norris 1960). The dolomites are cryptograined, dark to medium grey and in part slightly greenish-grey. They are massively and evenly bedded in beds 1-5 ft. thick.

Map-unit 16. The Arnica Formation (Middle Devonian).

At First Canyon, South Nahanni River this unit consists of 1,650 ft. of dolomite, fine-grained, dark grey to black and massive to thick bedded. This is interbedded with dolomite which is silty, very fine-grained, black to brown and massively bedded and also with light brownish-grey, thinly bedded dolomites and with vuggy and porous





Table 2.1. Table of Geologic Formations in the South Nahanni Region  
(after Douglas and D. K. Norris 1960).

Period or Epoch	Group or Formation (map-unit)	Lithology	Thickness (feet)
Pleistocene and Recent	(36)	Alluvial sands and silts of Liard and South Nahanni rivers	180+
Upper Cretaceous	Fort Nelson (35)	Sandstone, fine grained	1,000+
Lower Cretaceous	Fort St. John (34)	Shale, grey and siltstone	1,000+
Carboniferous	Upper (33a)	Sandstone, calcareous limestone shale	1,000 to 1,740
	Middle (33b)	Sandstone, massive and thick bedded	105 to 800
	Lower (33a)	Sandstone, thin bedded, shale	460 to 1,220
	(32)	Limestone, marginal and argillaceous, shales, sandstone	660 to 1,430
	(31)	Shale, fissile, black, thin bedded	50 to 815
Devonian and Carboniferous	(30)	Sandstone, thinly bedded, limestone, silty	120 to 600
	(29)	Shale, dark grey (may include equivalents of map-units 23 to 32, and possibly some older beds)	3,000±
	(28)	Shale, black, fissile, mudstone, limestone	495±
	(27)	Siltstone, calcareous, mudstone, silty (may be equivalent to map units 24 to 26)	
	(26)	Limestone, sandy	
Upper Devonian	(25)	Limestone, bioclastic, argillaceous, massive, reefy	
	(24)	Shale, dark greenish grey, sandstone, calcareous	6
	Simpson (23)	Shale, black, fissile, siltstone, thinly bedded	1,800±
	Nahanni (22)	Limestone, bioclastic, thick bedded, shale, dolomite	310 to 830
	(21)	Shale, dark grey, calcareous, limestone, argillaceous	85 to 980
Middle Devonian	(20)	Shale, dark grey, calcareous, limestone, argillaceous (undivided map units 17 and 21)	
	(19)	Limestone, massive, crypto-grained (equivalent to map unit 10)	
	(18)	Dolomite, coarsely recrystallized, massive bedded	310 to 540
	(17)	Limestone, argillaceous, thinly bedded, shale, dark grey (equivalent to map-units 16 and 18)	2,550
	(16)	Dolomite, fine-grained, black, banded dark and medium grey	495 to 2,630
	(15)	Limestone, shale, dolomite, sandstone (may include equivalents of map-units 3, 5, 8, 9, 14, 16, and possibly some younger beds)	
	(13)	Dolomite, fine-grained, black to brown, banded light and medium grey	2,370
	(12)	Dolomite, crypto-grained, black, banded dark and medium grey	570
	(11)	Dolomite, fine-grained, grey, banded light and medium grey	1,160
	(10)	Dolomite, silty, sandstone	260
Devonian (7) and older	(9)	Thinly bedded shaly beds	1,000±
	(8)	Includes sandstone, coarse-grained	1,000±
	(7)	Includes limestone, grey, orange- and pink-weathering (possibly equivalent to map-unit 1)	3,000±
	(6)	Dolomite, fine-grained, grey, limestone, grey, alternating grey and buff bands	5,020
	(5)	Shale, grey, graptolitic, limestone, thinly bedded, buff-weathering	3,800
	(4)	Dolomite, massive, porous and argillaceous, grey	1,200
	(3)	Limestone, dark grey, dolomite, massive, shale, grey-weathering	2,530
	(2)	Dolomite, crypto-grained, pink, sandstone, orange- and red-weathering	500+
	Sunblood (1)	Limestone, crypto-grained, thinly bedded, grey, orange, pink- to buff-weathering	3,490-

\*Relative position of map-units in this table does not necessarily imply relative stratigraphic position.




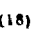

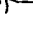
	Liard Plateau	Vicinity of Virginia Falls	Northern Funeral Range	Nahanni Plateau	Nahanni Range	
Upper Devonian	(29)	(29)	(29)	Simpson (23)	Simpson (23)	
Middle Devonian	(20)	(22) 	Nahanni (22)	Nahanni (22)	Nahanni (22)	
		(21)	(21)	(21)	(21)	
		(17) 	(18)	(17)	(18) 	(18) 
			(16)	(16)	(16) 	(16)
	(15)				(13)	
					(14)	(12)
						(11)
		(5)	(9)	(6)	(10)	
	(3)	(8)		(4)		
Ordovician	(1) or (7)	Sunblood (1)	(7)		(2)	

Figure 2.4. Approximate stratigraphic relationships of Middle Devonian and older units in the Virginia Falls map-area (after Douglas and D. K. Norris 1960).

	Virginia Falls Map-area (Douglas and Norris, 1960)		Root River Map-area		Camsell Bend Map-area	
			Southern Part	Whittaker and Delorme Ranges	Camsell and Nahanni Range	McConnell Range
Overlying beds	(16)		Arnica (11)	Arnica (11)	Arnica (11)	Bear Rock (14)
Devonian?	(14) $\frac{(13)}{(12)}$ (11)		Sombre (10) $\frac{\text{Upper}}{\text{Middle}} \frac{\text{Lower}}$	-?- Sombre (10)	-?- (9)	
Silurian	--7-- (5)	(6) --7--		(6)		
Ordovician	(3)		(2)	(3)	(8)	(7)
	Sunblood (1)		Sunblood (1)	Sunblood (1)		Franklin Mountain

Figure 2.5. Correlation of Ordovician, Silurian and Devonian formations and map-units of Camsell Bend, Root River and Virginia Falls map-areas (after Douglas and D. K. Norris 1961).

	VIRGINIA FALLS AND SIRIBSTON LAKE MAP AREAS (DOUGLAS AND D K NORRIS 1960)	CAMSELL BEND AND ROOT RIVER MAP AREAS (DOUGLAS AND D K NORRIS 1961)		DAHADDINI RIVER MAP-AREA		WRIGLEY MAP-AREA		HORN RIVER MAP-AREA (DOUGLAS AND A W NORRIS 1960)	
				WESTERN PART	EASTERN PART DAHADINI RANGE	WEST PART AND CAMSELL RANGE	EAST PART AND McCONNELL RANGE		
Overlying beds	Mississippian (30)	Mississippian 7 (26)		Cretaceous (27)	Cretaceous (27)		Cretaceous (27)	Cretaceous (27)	
DEVONIAN	UPPER	28	25	26	26	36			
		29	34						23
			27	22	24	24			34
			20	18		23			
			19						
	17								
	MIDDLE	16	15	Fort Simpson (23)	Fort Simpson (23)	Fort Simpson (23)	Fort Simpson (23)	Simpson (16)	
				Horn River (22)				Horn River (14)	
		Mahanani (23)	Mahanani (17)	Mahanani (21)	Mahanani (21)	Mahanani (21)	Mahanani (21)		
		21	Headless (16)	Headless (20)	Headless (20)	Headless (20)		12	
11		13	Landry (18)	Landry (18)	Funeral (19)	Manetoe (17)			
		Arpica (13)	Arpica (13)	Arpica (15)	Bear Rock (16)	Arpica (15)	Bear Rock (16)		
Underlying beds	14	Sombra (10)	Sombra/TTR	Camsell 7 (13)	12	Mt Kindle (9)	Ordovician (10)		

Figure 2.6. Correlation of Devonian formations of Dahadinni River, Wrigley, and adjacent map-areas (after Douglas and D. K. Norris 1962).

dolomites. In the central Nahanni Plateau the dolomites of map-unit 16 grade northward into shales and shaly limestones of map-unit 17, the same facies change occurs on the Ram Plateau.

Map-unit 17. The Funeral Formation (Middle Devonian).

On the northern part of the Nahanni Plateau map-unit 17 is 2,550 ft. thick. The lower 1,655 ft. according to Douglas & D.K. Norris (1960) comprises dark grey to black, platy, calcareous shale and calcareous mudstone, interbedded with black, silty to argillaceous, very recessive limestone. This is overlain by a locally resistant and cliff-forming unit 225 ft. thick, of black, silty and argillaceous, thinly bedded to bioclastic limestone with black shale partings. Succeeding beds 670 ft. thick are black, platy to fissile calcareous shale and black, platy mudstone alternating with thin lenticular beds of black bioclastic limestone and thick to massive-bedded, black argillaceous limestone. This unit has been equated to the Funeral Formation (Douglas & D.K. Norris 1961).

Map-unit 18. The Landry or Manetoe Facies Equivalent (Middle Devonian).

Map-unit 18 is a thin unit of coarsely crystalline dolomite which is commonly underlain by the dolomite of map-unit 16 and grades laterally into the limestones of the upper part of map-unit 17. At First Canyon this unit consists of 375 ft. of coarsely recrystallized, very massive bedded, mottled white and black dolomite, weathering light grey, and interbedded medium-grained, black dolomite with large irregular masses of white calcite and dolomite. Douglas & D.K. Norris

(1960) note that lateral gradation between the dolomites of map-unit 18 and the limestones of map-unit 17 can be observed at many localities (Figure 2.4). Douglas & D.K. Norris (1961, 1962) consider map-unit 18 to be a facies equivalent of the Landry and Manetoe Formations (Figure 2.6).

Map-unit 21. The Headless Formation (Middle Devonian).

In the Camsell Bend and Root River map-areas Douglas & D.K. Norris (1961) recognize a persistent shale and argillaceous limestone unit which separates the Nahanni from underlying formations, this is the Headless Formation. In the Virginia Falls map-area this unit was labelled map-unit 21. Douglas & D.K. Norris (1960) note that map-unit 21 and the Nahanni Formation are facies equivalents in some areas with the Nahanni limestone grading laterally into the shales and shaly limestones of map-unit 21 (Figure 2.4). These writers point out that where map-unit 21 in the Virginia Falls map-area is well developed as on Headless Range, it consists of 560 ft. of dark grey, calcareous shale, weathering pale yellowish grey; this is interbedded in the upper 150 ft. with beds of limestone, dark grey to light brownish grey, cryptograined to bioclastic, and 10-15 ft. thick. These beds are overlain by 295 ft. of massive, cliff-forming limestones of the Nahanni Formation. On southern Nahanni Plateau and Nahanni Range, map-unit 21 is thin, and is essentially only a recessive unit at the base of the cliff-forming beds of the Nahanni Formation. In Ram Plateau and northern Nahanni Plateau, shales and shaly limestones of map-unit 21 vary between 150-500 ft. in thickness.

At Nahanni Butte the Headless Formation consists of 130 ft. of argillaceous limestone which is black, fine-grained and variably dolomitized. Similar beds are 85 ft. thick at Bluefish Lake, 145 ft. thick at Little Doctor Lake and 130 ft. thick in First Canyon, South Nahanni River.

Map-unit 22. The Nahanni Formation (Middle Devonian).

At Nahanni Butte the Nahanni Formation is 350 ft. thick, and comprises dark grey limestone which is fine-grained, vaguely medium- to thick bedded and partly dolomitized to dark and light grey, fine- to medium-grained, rarely coarsely crystalline dolomite. At Bluefish Lake, Little Doctor Lake and in First Canyon the Nahanni Formation is 310, 410 and 475 ft. thick respectively. In general it thickens northwestward through Ram Plateau where it is 650 ft. thick and across northern Nahanni Plateau where it is 780 and 830 ft. thick on the east and west flanks respectively. Here it consists of massive- to thick-bedded, light to dark grey, fetid, fine-grained to bioclastic limestones weathering light grey. Douglas & D.K. Norris (1960) note that in places it is split into several small cliffs by interbedded, recessive, thinly bedded limestones but generally it is a single massive cliff.

Map-unit 23. The Fort Simpson Formation (Upper Devonian).

Douglas & D.K. Norris (1960) report that map-unit 23 may be up to 1,800 ft. thick where not eroded. The basal 220 ft. is interbedded non-calcareous, black, fissile to silty shale and sandy mudstone which is brown-weathering and partly stained with yellow sulphur.



Succeeding beds are mainly non calcareous shale which is dark grey, fissile to silty and interbedded with sandstone which is argillaceous, thinly-bedded, fine- to medium-grained, laminated and finely cross-bedded.

(ii) Facies and Faunal Relations in the Nahanni Area.

Noble & Ferguson (1971) have pointed out that the pure resistant carbonates of the Nahanni Formation pass laterally into shales, and limestones with a relatively high shale content over a distance of less than a mile. Figure 2.7 shows the details of the lithologic changes that accompany this transition and Figure 2.8 the principal faunal changes. Noble & Ferguson argue that the carbonate-shale transition is located at the margin of a shelf separated from a deeper basin by a definite slope.

The carbonate-shale transition of the Arnica-Funeral Formations according to these writers takes place even more abruptly (Figures 2.7 and 2.8). They note that at a number of localities faint relicts of stromatoporoids and corals and well-developed algal laminates may be observed in the Manetoe facies, suggesting that the shelf-basin transition was reefal with a slope angle of 30-40°. A further indication of a reefal edge to the Arnica-Manetoe shelf is the character of the sediment and fauna shelfwards of this edge. Noble & Ferguson (1971) point out that this is invariably dolomitic, barren or with a poorly developed fauna as is characteristic of restricted hypersaline lagoonal conditions. These writers suggest that in Arnica times the boundary between the shelf and the deeper basin to the east was abrupt and marked by a barrier

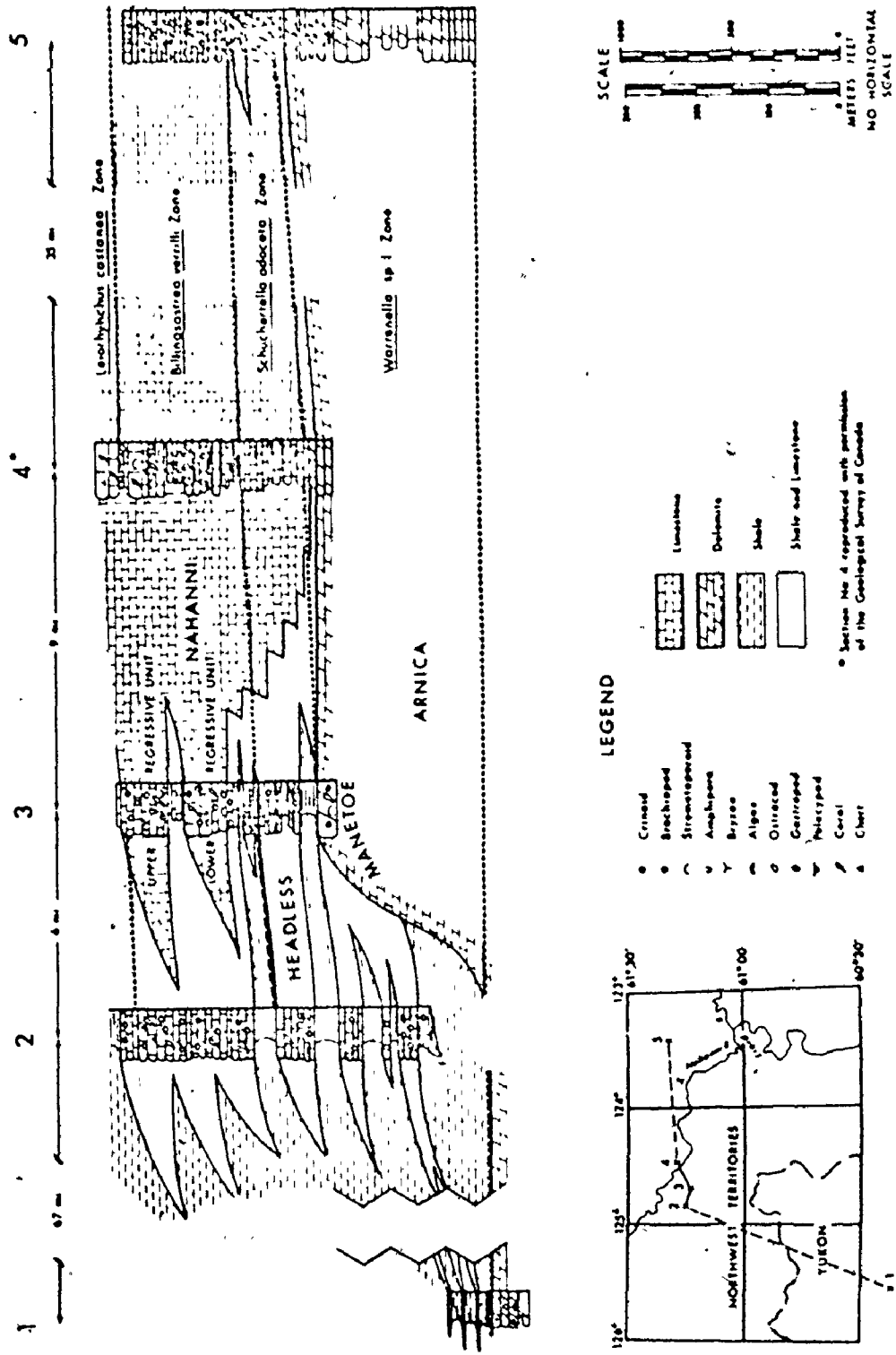
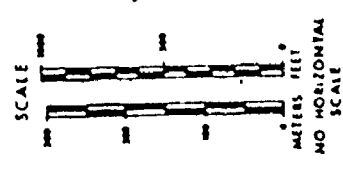
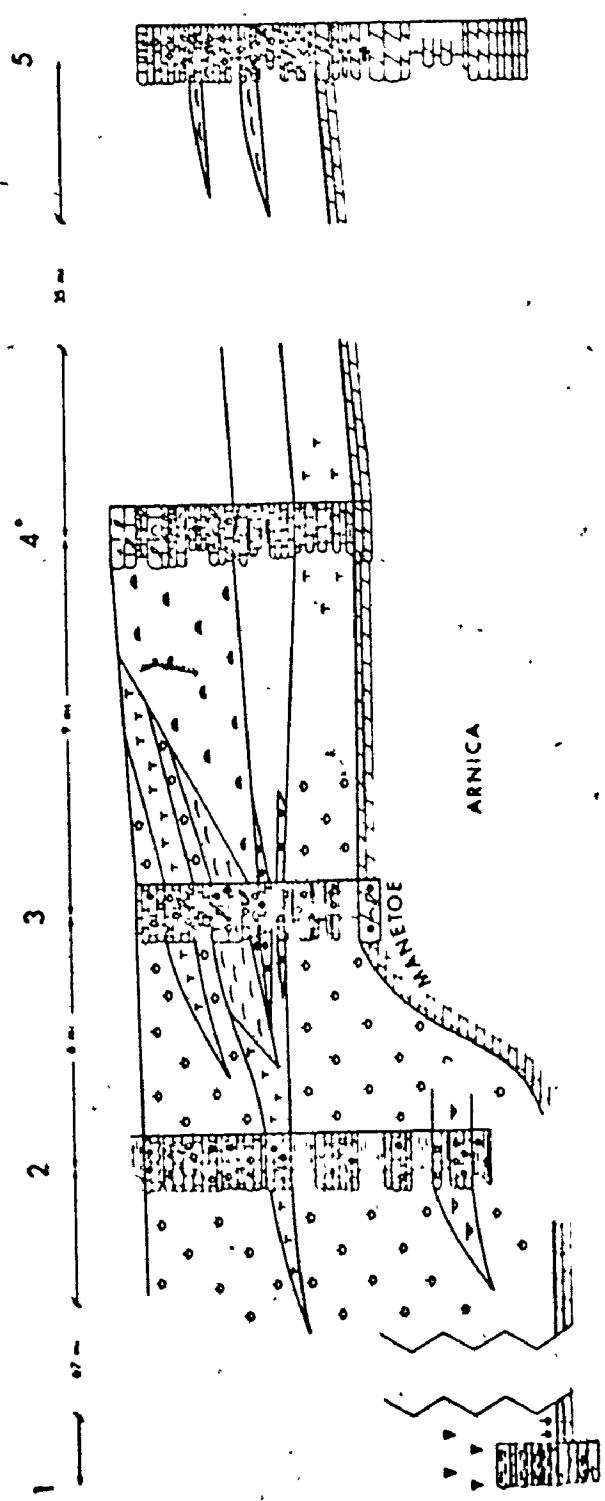


Figure 2.7. Cross section showing lithofacies changes across the shelf-basin transition, South Nahanni area, N.W.T. (after Noble and Ferguson 1971).



- LOG SYMBOLS**
- Crinoid
  - ◐ Brachiopod
  - ◑ Stromatopora
  - ◒ Amphipora
  - ◓ Bryozoa
  - ◔ Algae
  - ◕ Outcrop
  - ◖ Graptolite
  - ◗ Pelecypod
  - ◘ Coral
  - ◙ Chert
- FAUNAL COMMUNITY**
- MASSIVE STROMATOPOROID - CORAL COMMUNITY
  - LAMINAR STROMATOPOROID - CORAL COMMUNITY
  - BRANCHING TABULATE CORAL COMMUNITY
  - WABENELLA RHYNCHONELLID COMMUNITY
  - SPINULICOLA - ATRYPID COMMUNITY
  - EMANUELLA - PELECYPOD COMMUNITY
  - PELAGIC COMMUNITY
  - DOLOMITE
  - LIMESTONE
  - SHALE

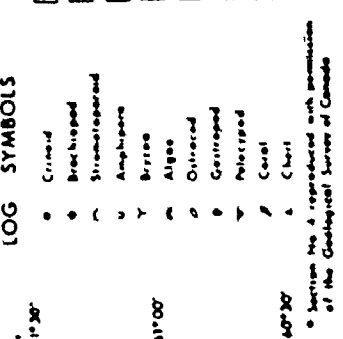


Figure 2.8. Cross section showing biofacies changes across the shelf-basin transition, South Nahanni area N.W.T. (after Noble and Ferguson 1971).

reef. They note that later as the basin filled up with terrigenous sediments, the relief between the shelf and basin decreased and true reefal development in this area diminished. With the removal of the restriction caused by the barrier reef, almost normal saline conditions were restored to this part of the shelf, and the various faunal communities present in the Nahanni and Headless Formations were able to flourish.

This work by Noble & Ferguson (1971) explains the sequence of rocks encountered in the Nahanni area. They argue that in early Middle Devonian times a broad shallow area of carbonate and evaporite deposition at least 350 miles across bordered the Canadian Shield. This carbonate shelf passed westerly into a clastic basin or marginal cratonic trough which extended hundreds of miles both north and south of the Nahanni area. They believe that it derived its sediment from a source to the west.

The dolomite shelf sediments of the *Warrenella* sp. 1 and *Gasterocoma bicaula* zones (Figure 2.2) were formed in a shallow restricted lagoonal environment probably behind a (Manetoe) barrier reef bordering the shelf and separating it from a deeper-water basin that was filling up with thick wedge of fine clastics to the west. In the succeeding *Schuchertella adoceta* zone time, the shales of the Headless Formation filled the basin, transgressed the shelf-basin slope and were deposited on much of the outer shelf. During the *Billingsastrea verrilli* zone time (Figure 2.2), the Nahanni Formation limestones were deposited not only on the outer shelf, but on the slope at the edge of the shelf. Finally a major transgression took place in *Leiorhynchus castanea* zone

time and this resulted in the widespread deposition of the Upper Devonian shales of the Fort Simpson Formation over the limestone of the Nahanni Formation and well on to the shelf.

(iii) Observed Sections in the Karst.

During the summer of 1973 a number of sections in the Nahanni North karst were examined,<sup>1</sup> in an attempt to gain further information on the characteristics of map-units outlined by Douglas & D.K. Norris (1960). This was considered desirable as a preliminary to an explanation of the karst landforms in the area as this might in some way relate to lithological characteristics (Rauch & White 1970). Samples from the various sections were analyzed for the 10 major elements by the x-ray fluorescence technique. Two carbonate standards were used giving two sets of results which were averaged to give the figures quoted in Figures 2.9 and 2.10. As neither of the two standards contained much silica and one or two of the samples did, there may be errors in some of the analyzes. Most of the beds sampled are predominantly calcite and dolomite with minor feldspar, clay mineral and silica impurities. Percentages of impurities were very small in most samples and where this was the case the rock was assumed to be made up entirely of calcite and dolomite allowing rapid calculation of weight percentages of these substances. It must be emphasized that these figures shown in Figures 2.9 and 2.10 are only broad approximations. Some rock samples contain a great deal of silica normally in the form of chert. Occasional beds in the sections were found to be rich in this substance.

---

<sup>1</sup>The writer is indebted to Ralph Ewers, McMaster University who examined a number of sections.

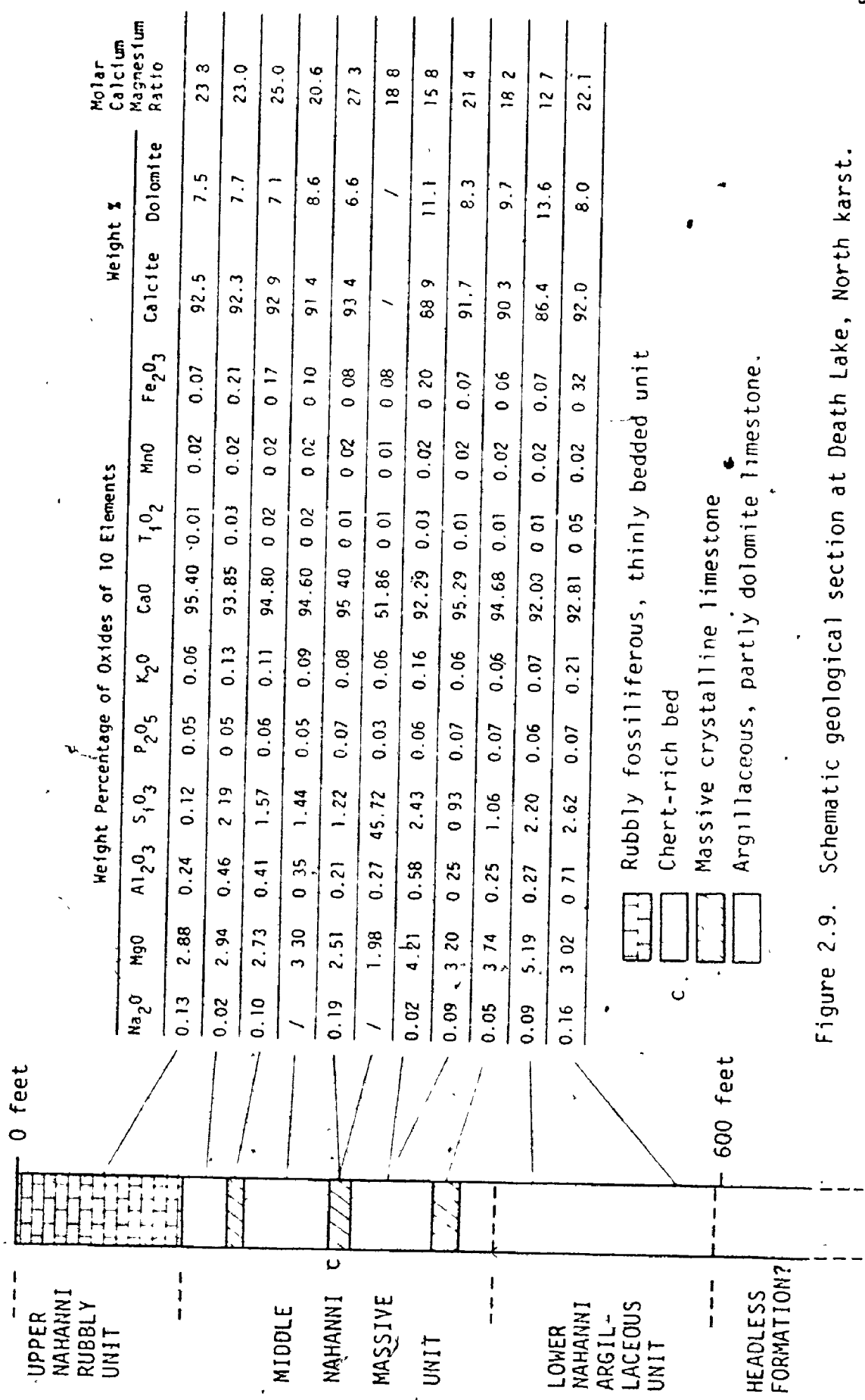


Figure 2.9. Schematic geological section at Death Lake, North karst.

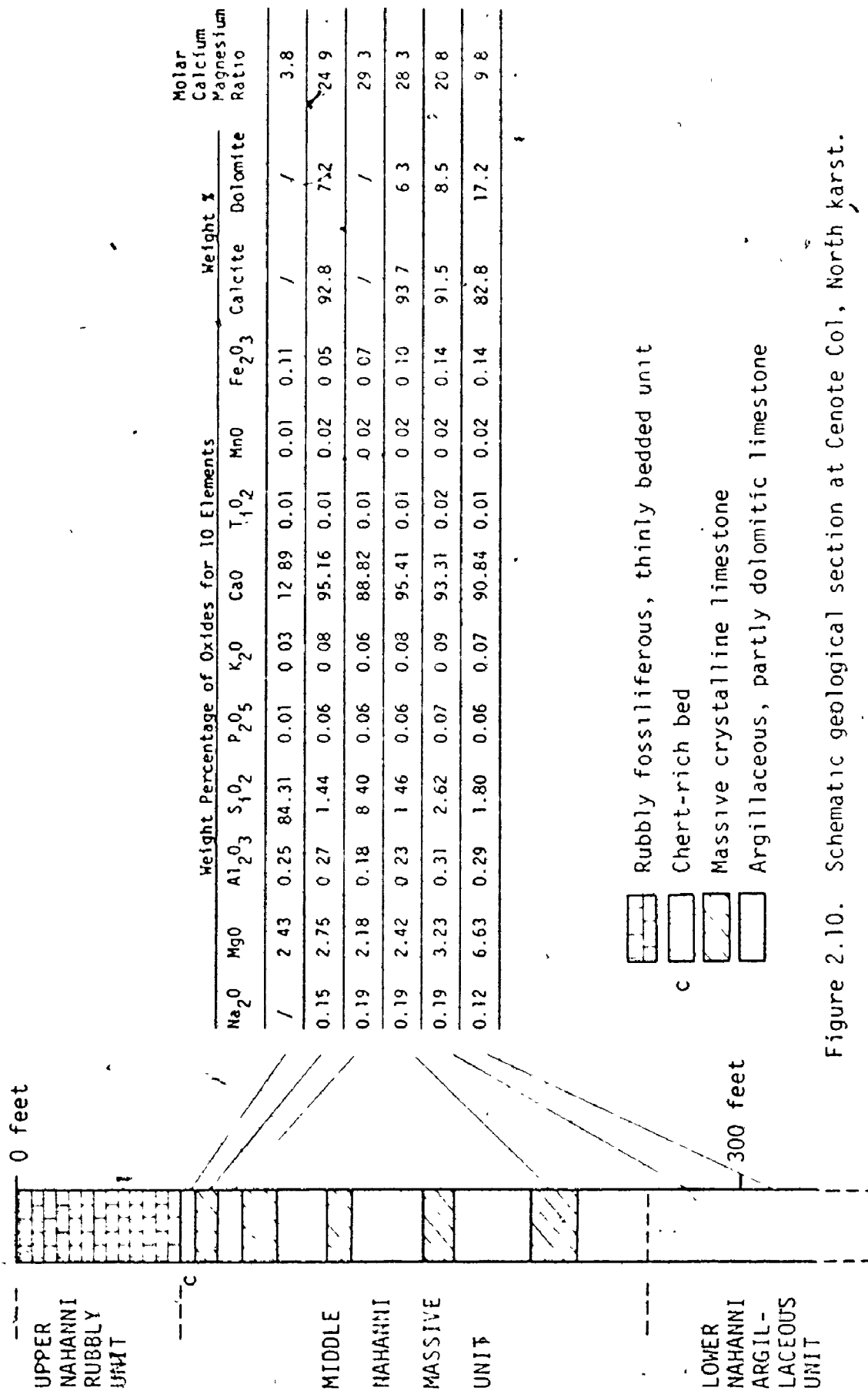


Figure 2.10. Schematic geological section at Cenote Col, North karst.

A section was examined in the wall of Death Canyon north of Death Lake (Plate 2.1). It was found to be made up of three major units in the Nahanni Formation with a basal unit that may well be a part of the Headless Formation (Figure 2.9). The total section is 680 ft. thick of which the upper rubbly unit accounts for approximately 140 ft., the middle massive unit of alternating resistant and recessive beds 260 ft., the lower argillaceous unit 200-220 ft. and the basal upper portion of the Headless Formation of argillaceous limestones with shale partings 60-80 ft. Average weight percentages of calcite and dolomite in pure beds are 91.2 and 8.8 respectively, the mean molar calcium-magnesium ratio is 20.8.

A 350 ft. section examined in the south wall of North Col Canyon below Cenote Col showed essentially similar characteristics (Figure 2.10). The upper rubbly unit here is >60 ft. thick, the middle massive unit characterized by alternating resistant and recessive beds and topped in this vicinity by a chert-rich layer is 200 ft. thick and what is visible of the lower unit >100 ft. The Headless Formation was not visible at this locality. In Second and Third Poljes and elsewhere in the karst a similar stratigraphy was recognized.

The upper rubbly unit is a slightly argillaceous limestone, often dolomitic with irregular mottling and it is in part siliceous. Textures are variable but limestones are predominantly micritic with some fossiliferous micrites and pelmicrites. Bedding varies from thin to thick or massive and is often irregular and lensoid. The biofacies includes corals, stromatoporoids and of lesser importance gastropods,





UPPER RUBBLY UNIT

MIDDLE MASSIVE UNIT

LOWER ARGILLACEOUS  
UNIT

Plate 2.1. The stratigraphical section at Death Lake.

crinoids and brachiopods. According to Noble & Ferguson (1971) such a stromatoporoid-coral community suggests deposition in a shallow-water environment with low energy conditions.

The middle massive unit is an middle alternation of light-grey-weathering, recessive and resistant units. The resistant units are medium to thickly bedded limestones varying from cryptocrystalline to medium-grained and are coraliferous and fossiliferous. The recessive units consist of thinly bedded to rubbly, dark grey, cryptocrystalline to fine-grained limestones which generally become more argillaceous towards the base of the formation. Parts of this unit may be slightly dolomitic and contain chert lenses and a slightly silicified fauna including stromatoporoids, corals, crinoids, and brachiopods. This is the case at the top of the middle massive unit below Cenote Col (Figure 2.10). Elsewhere corals appear to dominate with lesser stromatoporoids, brachiopods, gastropods and crinoids. Throughout the unit limestones are predominantly micrites with some pelmicrites, intra-micrites and biomicrites.

The lower argillaceous unit consists of medium-bedded to rubbly argillaceous limestones which are dark grey and cryptocrystalline to fine-grained. They are micrites, pelmicrites and biomicrites. The Headless Formation which underlies this lower Nahanni unit is a slightly more argillaceous limestone, thin to rubbly bedded, abundantly fossiliferous, usually micrites and biomicrites and it is occasionally interbedded with calcareous shale.

There is evidence in the Nahanni karst that the three units identified in the Nahanni Formation have had some influence on the mode

of development of the karst assemblage. Certainly the massive dolomites of the underlying Manetoe and Arnica formations appear to have been important in limiting the vertical development of many karst landforms and the overlying shales of the Fort Simpson Formation have been an important source of allogenic water to some parts of the karst.

The influence upon karst development of the various stratigraphic units discussed here will be introduced into the discussion on karst landforms in the Nahanni region.

### 3. Structure.

#### (a) Major Orogenies.

##### (i) Columbian Orogeny.

A number of orogenies affected parts of the Cordilleran Geosyncline prior to the Late Jurassic but major deformation of large areas did not occur until the start of the Columbian Orogeny. During this orogeny which lasted from the Late Jurassic to the earliest Upper Cretaceous parts of the Cordilleran Geosyncline underwent major deformation, regional metamorphism, granitic intrusion and uplift. According to Douglas et al. (1970) deformation in Selwyn and Mackenzie Mountains is difficult to assess. They believe that the arcuate Selwyn Fold Belt was created at this time for structures are cut by plutons which appear to be of Upper Cretaceous age. They also point out that in northern Mackenzie and Wernecke Mountains deformation preceded the deposition of late Cretaceous to early Tertiary sediments in Bonnet Plume Basin but it did not affect the region of Monster Syncline in southwestern Porcupine Plateau. Douglas et al. (1970) feel that much of the deformation

of Selwyn and Mackenzie Mountains was accomplished in the Columbian Orogeny. (Figure 2.11).

(11) Laramide Orogeny.

According to Douglas et al. (1970), almost all of western Canada was land in the Tertiary. The mountain belts formed during the Columbian Orogeny were rejuvenated and new mountain belts were produced by the Laramide Orogeny, the early phase of which began in the late Upper Cretaceous and the late phase probably ended early in the Oligocene. The principal effects of the orogeny were the development of most of the easternmost and northernmost structural elements of the Cordilleran region, including the arcuate Mackenzie Fold Belt and the northern Yukon Fold Complex. In the western Cordillera, in the mountainous region produced during the Columbian Orogeny, the effects of the Laramide Orogeny appear to have been limited to transverse and normal faulting and the intrusion of small granite plutons and in some areas batholiths.

During the Laramide Orogeny, the layered miogeosynclinal and exogeosynclinal sequences on the eastern and northern elements of the Cordilleran Geosyncline were deformed (Figure 2.12) and the Mackenzie Fold Belt was produced. This is composed of broad, short folds, the crests and troughs nearly flat with sharply upturned and faulted flanks. Some folds are long, narrow and tightly compressed with faults lying on either or both flanks and in the axial region. In the southern part of the Mackenzie Fold Belt, the folds are markedly segmented, the individual segments being oriented along west, northwest and northeast lines and commonly broken by faults with a small amount of thrust or

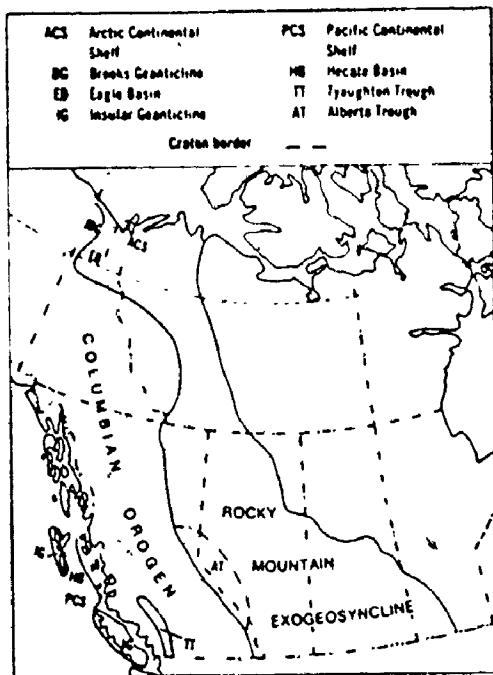


Figure 2.11. Early upper Cretaceous tectonic elements of the Cordilleran Geosyncline and Interior Platform.

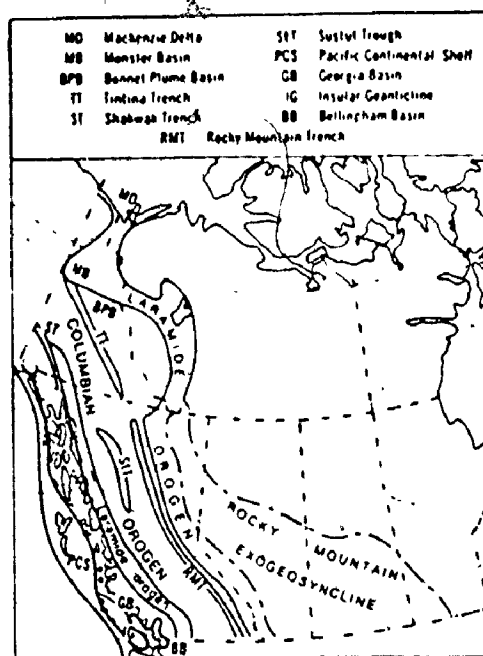


Figure 2.12. Late upper Cretaceous and early Tertiary tectonic elements of the Cordilleran Orogen and Interior Plain.

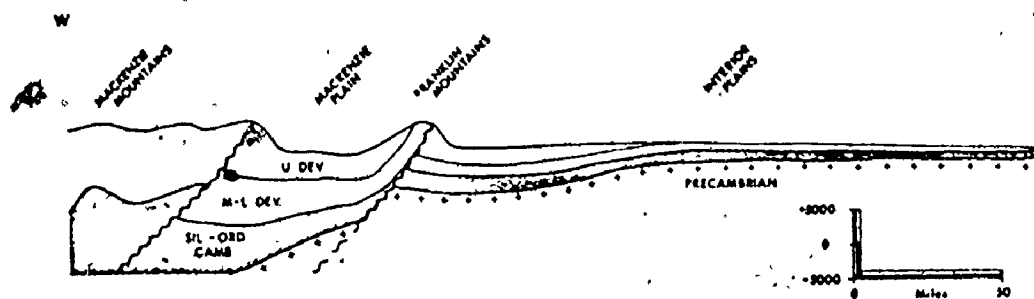


Figure 2.13. Schematic geological cross section through the upper Mackenzie River area (after Law 1971).



the Nahanni Thrust which either dips gently to the west or is flat (Douglas & D. K. Norris 1960). The structure of the range is markedly homoclinal in the northern part, with strata on the west flank dipping consistently at 20-35° west (Figure 2.14). West of the Nahanni Range, the Mackenzie Plain is also partly a structural feature paralleling the Yohin Syncline (Figure 2.14). It is a broad structure with flanks dipping at 20° and it plunges very gently southwards so that in the north Upper Devonian sandstones form the core while southwards progressively younger strata are present at the surface. In the vicinity of the South Nahanni River the structure complexes into a number of minor folds the most westerly of which is taken to be a continuation of the Yohin Syncline. In fact the structure consists of from east to west the Bluefish Syncline, the Twisted Mountain Anticline and the Yohin Syncline (Figure 2.15). Bluefish Syncline is shallow with flanks dipping at 10° while Twisted Mountain Anticline is slightly asymmetric westward with its east flank dipping at 15° and its west flank at 35°.

The Nahanni Plateau is a structural high involving Middle Devonian and older rocks. It is strongly elongate and consists of two principal structural elements. The northern two thirds of the plateau constitutes a structural terrace flanked on the west by the east-dipping homocline of Tundra Ridge (Figure 2.16). The terrace is modified into a gentle syncline and anticline in the north and into a gentle northeast-facing homocline in the south. To the southwest it is bounded by Tundra Thrust and to the south by a zone of east- and west-dipping thrust faults and associated folds which separate it from the southern one third of the Nahanni Plateau which is an area

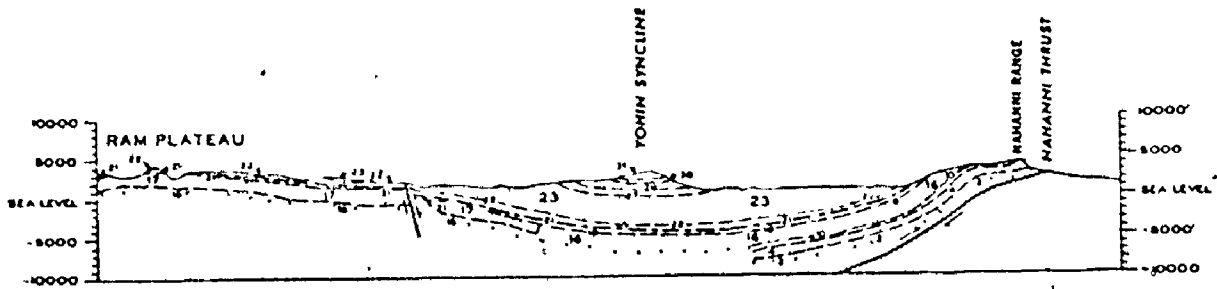


Figure 2.14. Schematic geological cross section through the Nahanni Range, Yohin Syncline and Ram Plateau (after Douglas and D. K. Norris 1960).

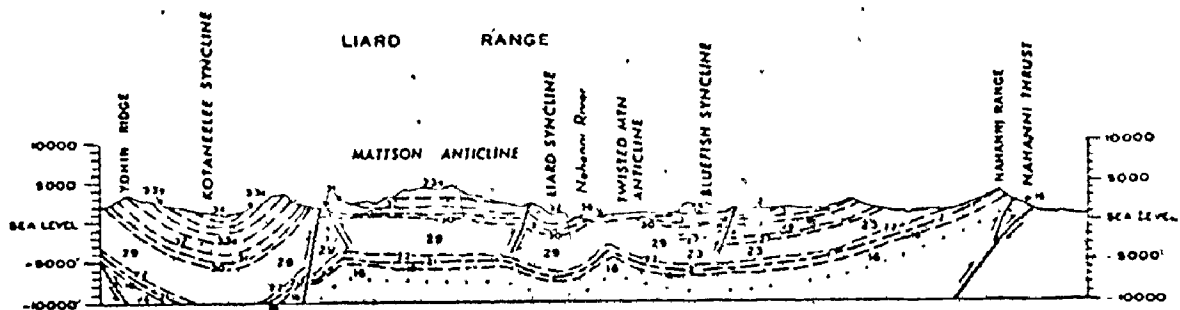


Figure 2.15. Schematic geological cross section through the Nahanni Range, Bluefish Syncline and Mattson Anticline (after Douglas and D. K. Norris 1960).



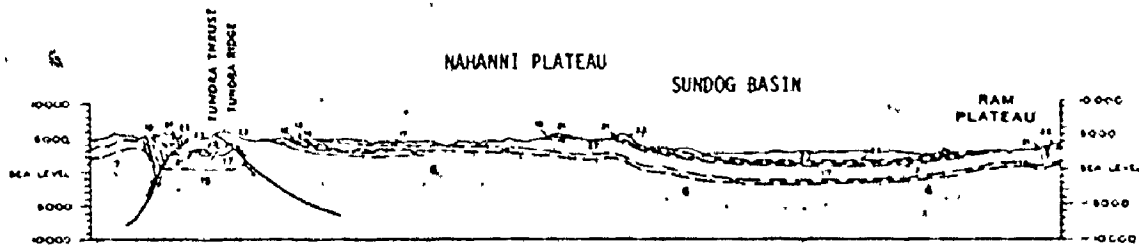


Figure 2.16. Schematic geological cross section through the Ram Plateau, Sundog Basin and Northern Nahanni Plateau (after Douglas and D. K. Norris 1960).

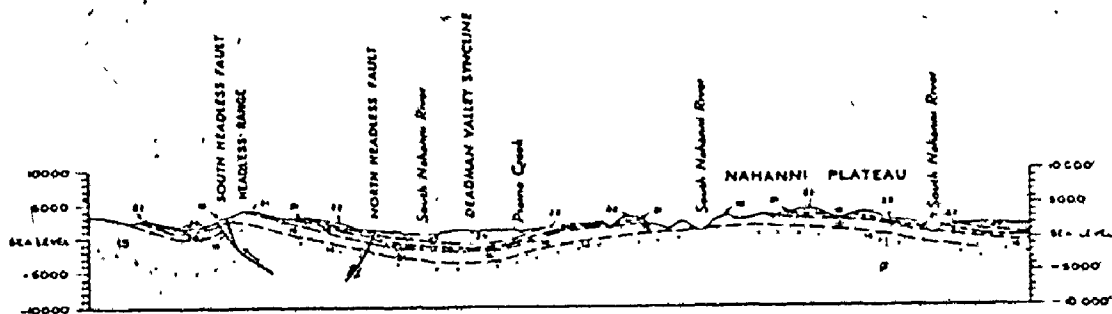


Figure 2.17. Schematic geological cross section through the Deadman Valley Syncline and the Southern Nahanni Plateau (after Douglas and D. K. Norris 1960).

of karst landform development. As Douglas & D. K. Norris (1960) point out the southern part of the plateau is open against this zone and the strata on its flanks dip gently away from the culmination (Figure 2.17).

Like the southern portion of the Nahanni Plateau the Ram Plateau is a broad dome-shaped structural high, ovate in plan with its long axis trending north (Figures 2.14 and 2.16). Between the Ram Plateau in the east and the northern Nahanni Plateau to the west is a basinal structure here referred to as the 'Sundog Basin.' Strata on its east and west flanks dip approximately 5-10° towards the center. (Figure 2.16). Both the Nahanni and Ram Plateaus have stripped bedding surfaces on Middle Devonian Nahanni limestones, these being much more resistant to erosion than the overlying shales of the Fort Simpson Formation. In the intervening synclinal valleys, however, shale is preserved. Dips on the Ram anticline are gently westward on the west flank and from 40° eastward or near vertical on the east flank where the structure appears to be broken by a west-dipping thrust fault (Douglas & D. K. Norris 1961).

(c) Patterns of Structural Deformation in the Southern Mackenzie Mountains as Suggested by Topographic Analysis.

Bostock (1970) has argued that "Probably the most notable feature of the physiography of the Cordillera is that remnants of an old erosion surface are nearly always evident" (p. 21-22). This old surface, he says, is most conspicuous in the plateau areas of the Interior System and although it has been referred to as a peneplain its relief is not sufficiently low over large areas to qualify as such. "The old surface is thought to have been formed largely in the beginning

of the Tertiary or possibly in the late Cretaceous, and to have gone through a complicated subsequent history of uplift, warping, subsidence, and renewed uplift . . . . In the early Tertiary the old surface of erosion was uplifted, the rivers entrenched, and sediments deposited in the valleys and hollows" (Bostock 1970, p. 22). The old erosion surface mentioned by Bostock is believed to have formed in the period between the Columbian and Laramide Orogenies. It was during the Laramide and Cascadian Orogenies that uplift and deformation occurred.

When deformed erosional surfaces are dissected by streams, remnants of the old surfaces may be preserved on the summits of residual hills. A number of workers have, therefore, attempted to utilize summit altitude data to assess the degree of uplift or the pattern of deformation of old erosion surfaces (King 1969; Thornes and Jones 1969; Rodda 1970; Doornkamp 1972). The technique that has been most commonly used to analyze the data has been polynomial trend surface analysis.

Summit data for a large part of the South Nahanni River region have been collected from 1:50,000 topographic maps in an attempt to determine whether they can be used to assess the pattern of deformation of the ancient erosion surface postulated by Bostock (1970), during the Laramide Orogeny. Because there is considerable doubt as to whether every hill summit in an area can be regarded as a remnant of a formerly-existing erosion surface, the data were filtered by using a variety of grids superimposed upon the 1:50,000 topographic sheets. The highest summit within each grid unit was chosen as being that most likely to

represent the level of the former erosion surface in that area (Thornes & Jones 1969). The various grids used are shown in Figure 2.18. The smallest of the grid units covers 2.5' of longitude and 1.25' of latitude or an area approximately 1.44 miles north to south and 1.38 miles east to west. Successively larger grid units have sides three, four and six times those of the smallest units so that the largest covers 15' of longitude, 7.5' of latitude and an area 8.65 miles by 8.3 miles. In all, 21-1:50,000 topographic maps of the South Nahanni region have been examined (Figure 2.19) and data sets for the various filters assembled. If every grid unit contained a closed summit contour the data sets for the finest to the coarsest grids would contain 3024, 336, 189 and 84 values respectively.

Because the elevations extracted from the topographic maps are thought to represent the high points on a pre-existing high level erosional surface, it should be possible to determine the approximate pattern of deformation of this surface in any area by simply contouring the summit data for that area. The data for the South Nahanni River region were in fact analyzed in this way. The analysis was conducted in two parts; first, the pattern of deformation in the Nahanni karst belt was looked at by considering data extracted from four map sheets using the smallest of the grids. Secondly, the broad pattern of deformation in the area covered by all 21 maps was looked into by analyzing the data sets obtained using the three coarsest grid filters. In addition the data set for the coarsest of the grid filters was subjected to polynomial trend analysis in order to compare the results

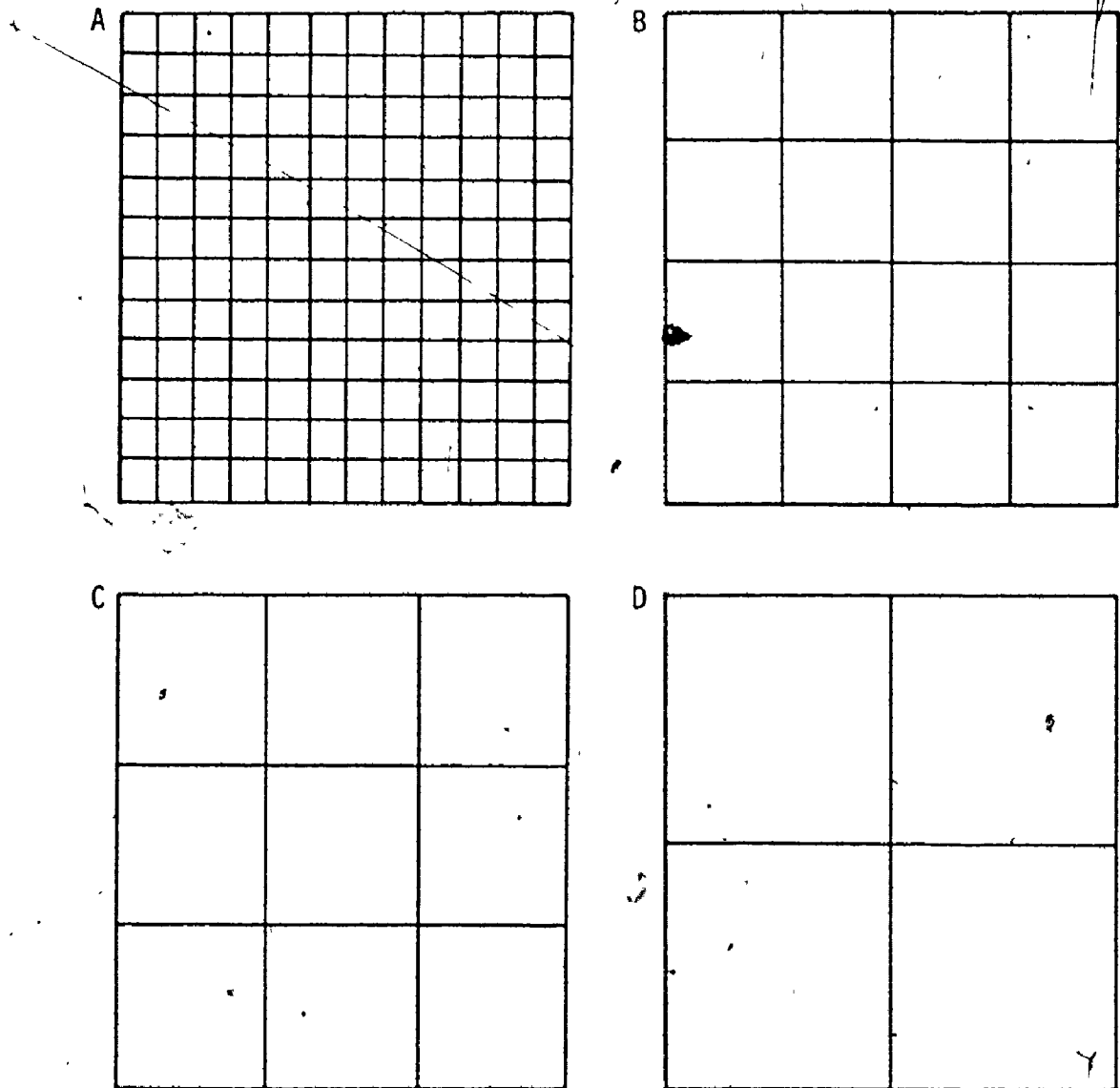
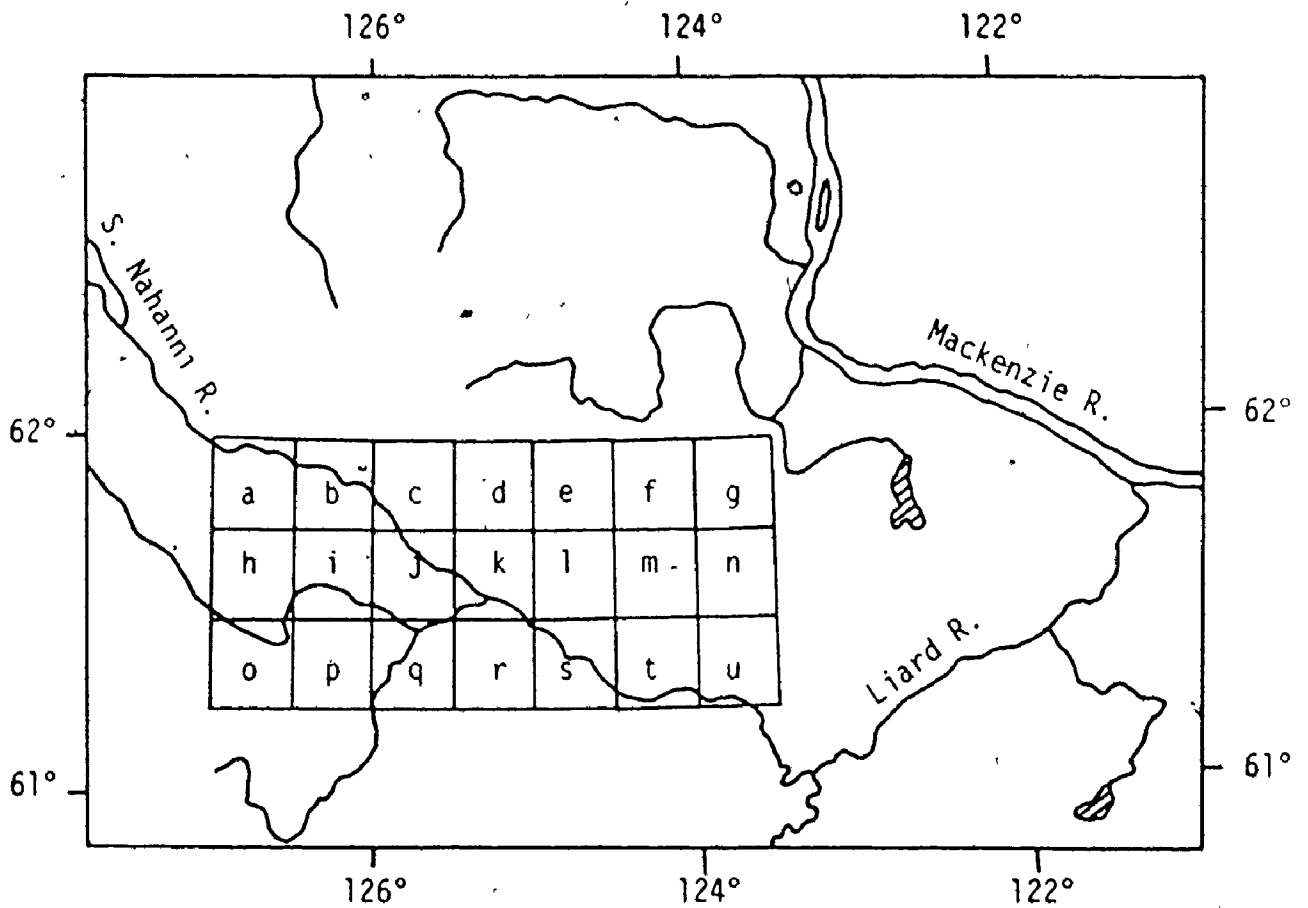


Figure 2.18. Grid filters used to extract summit altitude data from 1:50,000 topographic map sheets. The coordinates of the highest summit in each grid unit are taken to be those at the centre of the unit. For each 1:50,000 map there are potentially 144(A), 16(B), 9 (C) and 4(D) data points.



a 95 E 15	h 95 E 10	o 95 E 7
b 95 E 16	i 95 E 9	p 95 E 8
c 95 F 13	j 95 F 12	q 95 F 5
d 95 F 14	k 95 F 11	r 95 F 6
e 95 F 15	l 95 F 10	s 95 F 7
f 95 F 16	m 95 F 9	t 95 F 8
g 95 G 13	n 95 G 12	u 95 G 5

Figure 2.19. Structural deformation of the South Nahanni River region: the area of study and the 1:50,000 topographic maps analyzed.

of this elaborate technique with that of the much simpler contouring technique.

(i) Structural Deformation in the Nahanni Karst Belt.

A computer-generated contour map was prepared from summit data extracted from the eastern halves of 1:50,000 topographic sheets 95F10 and 95F7, sheets 95F9 and 95F8, and the western halves of sheets 95G12 and 95G5 (l, s, m, t, n and u respectively in Figure 2.19). Data were extracted using the finest of the four grid filters (Figure 2.18). The resulting map shown in Figure 2.20 clearly depicts the warped structures that are known to exist in this part of the South Nahanni River region. In the northern part of the area the monoclinical nature of the north Nahanni Plateau is indicated by the steep gradient on the eastern slope of this upwarped structure. A little to the east is the well-defined structural low of Sundog Basin and still further to the east the elongate structural high of the Ram Plateau. The same structures are apparent in the geological section shown in Figure 2.16. In the southwestern portion of the area the domal nature of the south Nahanni Plateau is clearly depicted with the steep east-facing limb suggesting a homoclinal structure. There is also clear evidence in the diagram of the break between the north and south portions of the Nahanni Plateau known to be the result of thrust faulting. In addition, between the south Nahanni Plateau and the Ram Plateau is depicted a marked structural col which is known from ground observations to be present. This region is also known to host the best developed surface karst landforms in the Nahanni karst belt.

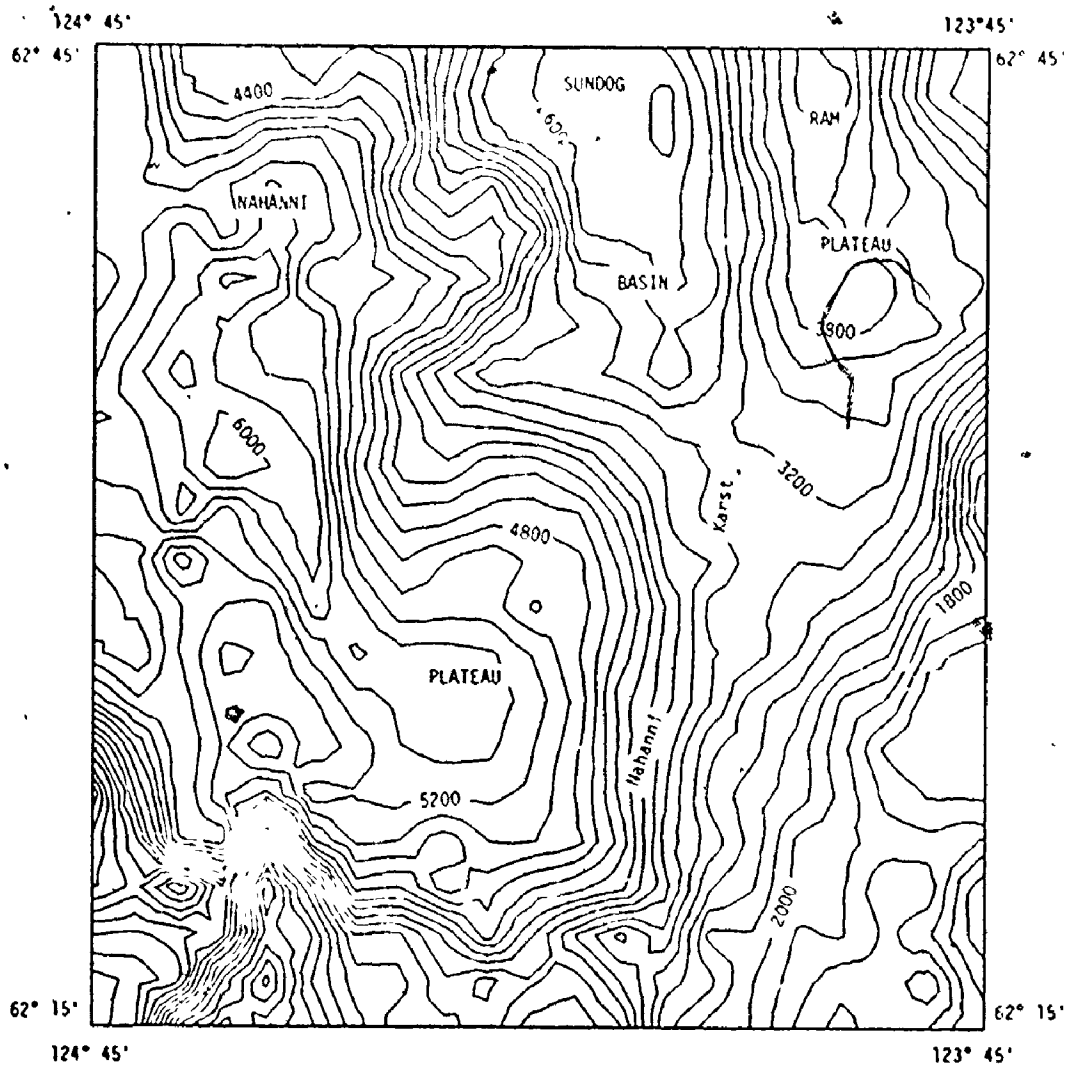


Figure 2.20. Structural deformation of the Nahanni karst belt from topographic analysis (144 grid units in each 1:50,000 topographic map).

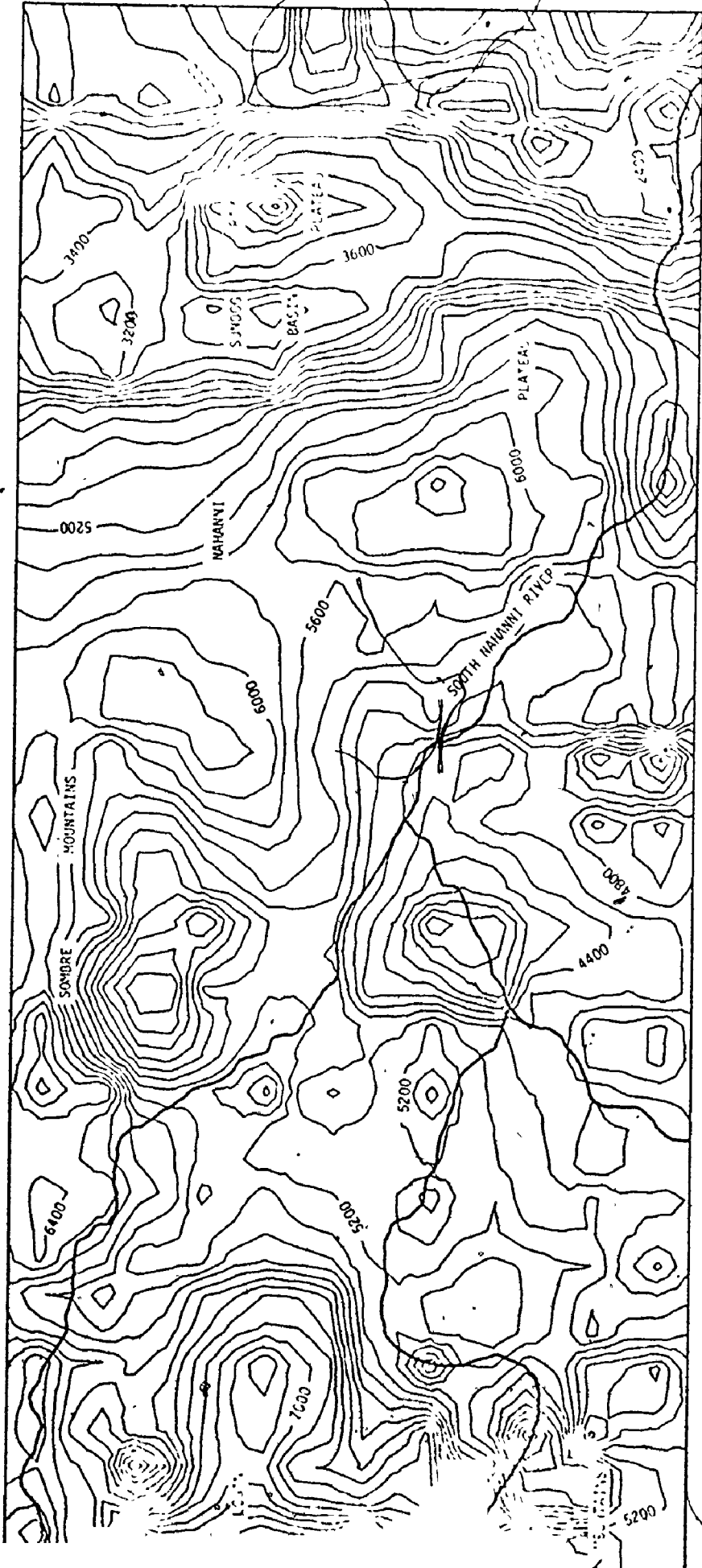


127° 00'

123° 30'

62° 00'

61° 1



127° 00'

123° 30'

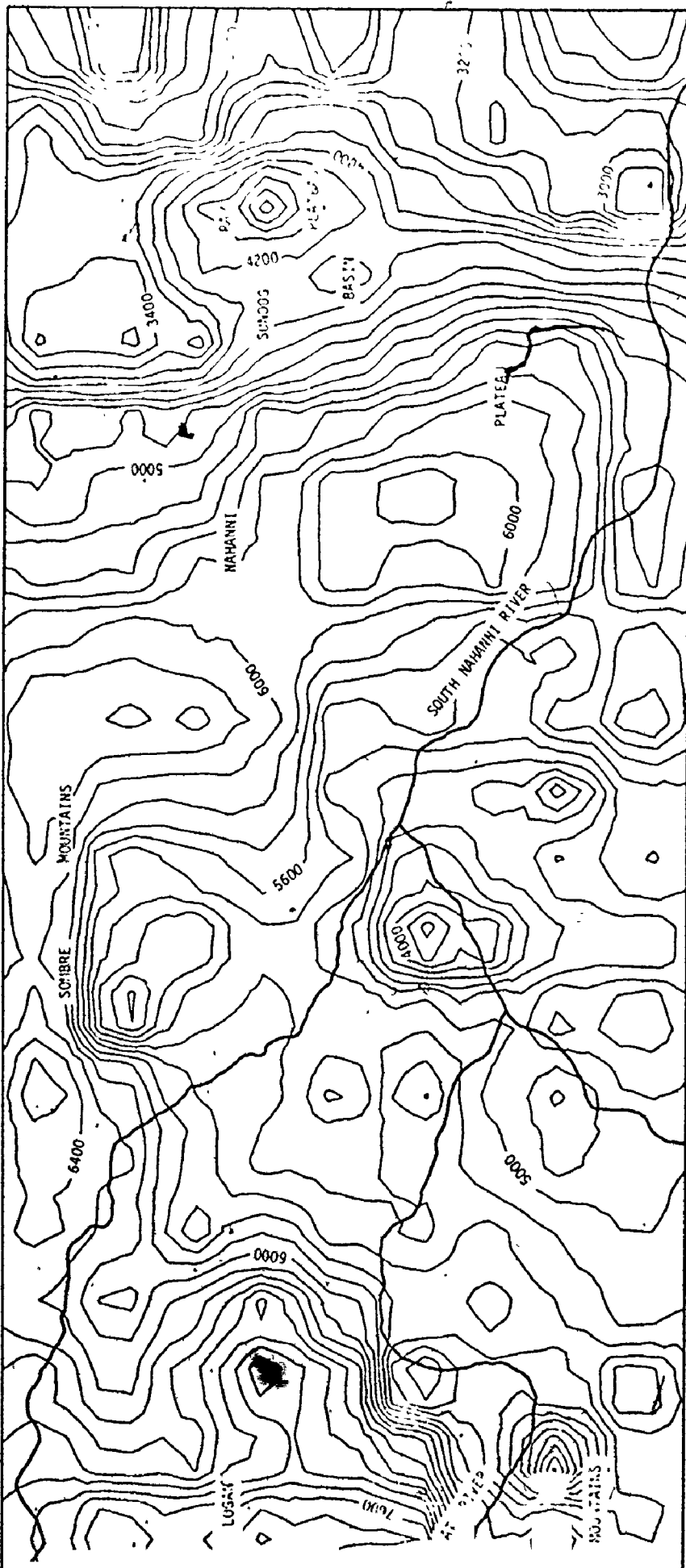
Figure 2.21. Structural deformation of the Mackenzie Mountains from topographic analysis (16 data points in each 1:50,000 topographic map).

127° 00'

123° 30'

62° 00'

61° 15'



127° 00'

123° 30'

Figure 2.22. Structural deformation of the Mackenzie Mountains from topographic analysis (9 data points in each 1:50,000 map).

a prominent structural and topographic low, named Clearwater depression. It is flanked on the east by Arnica Range, on the north by Sombre Mountains, and on the southwest by Sunblood Range. Strata of these ranges rim the depression and dip toward it at remarkably steep angles" (p. 24). Again it is clear that the contouring of filtered summit data correctly depicts a known structural depression lending further support to the view that the technique can be used to determine patterns of deformation. Much of the complexity in Figures 2.21 and 2.22, however, has clearly been introduced because irrelevant data have passed through the filters into the respective data sets. Inaccuracies are particularly evident in the western portion of the South Nahanni River area where the presence of very wide, glaciated valleys and canyons has allowed the passage of low-altitude summit values into the filtered data sets. The same appears to have happened in the vicinity of the South Nahanni River canyons in the east.

Much of the 'noise' associated with the contour maps of deformation produced using 336 and 189 data points is not evident in the map of structural deformation constructed from only 84 data values (Figure 2.23), or four values per 1:50,000 topographic map sheet. For instance there is no evidence in this diagram of the existence of the South Nahanni River Canyons and other deep canyons to the west in the Ragged Range of Logan Mountains. Not only does Figure 2.23 isolate the domal and basinal deformations that resulted in the Nahanni and Ram Plateaus and Sundog Basin, but it also demonstrates

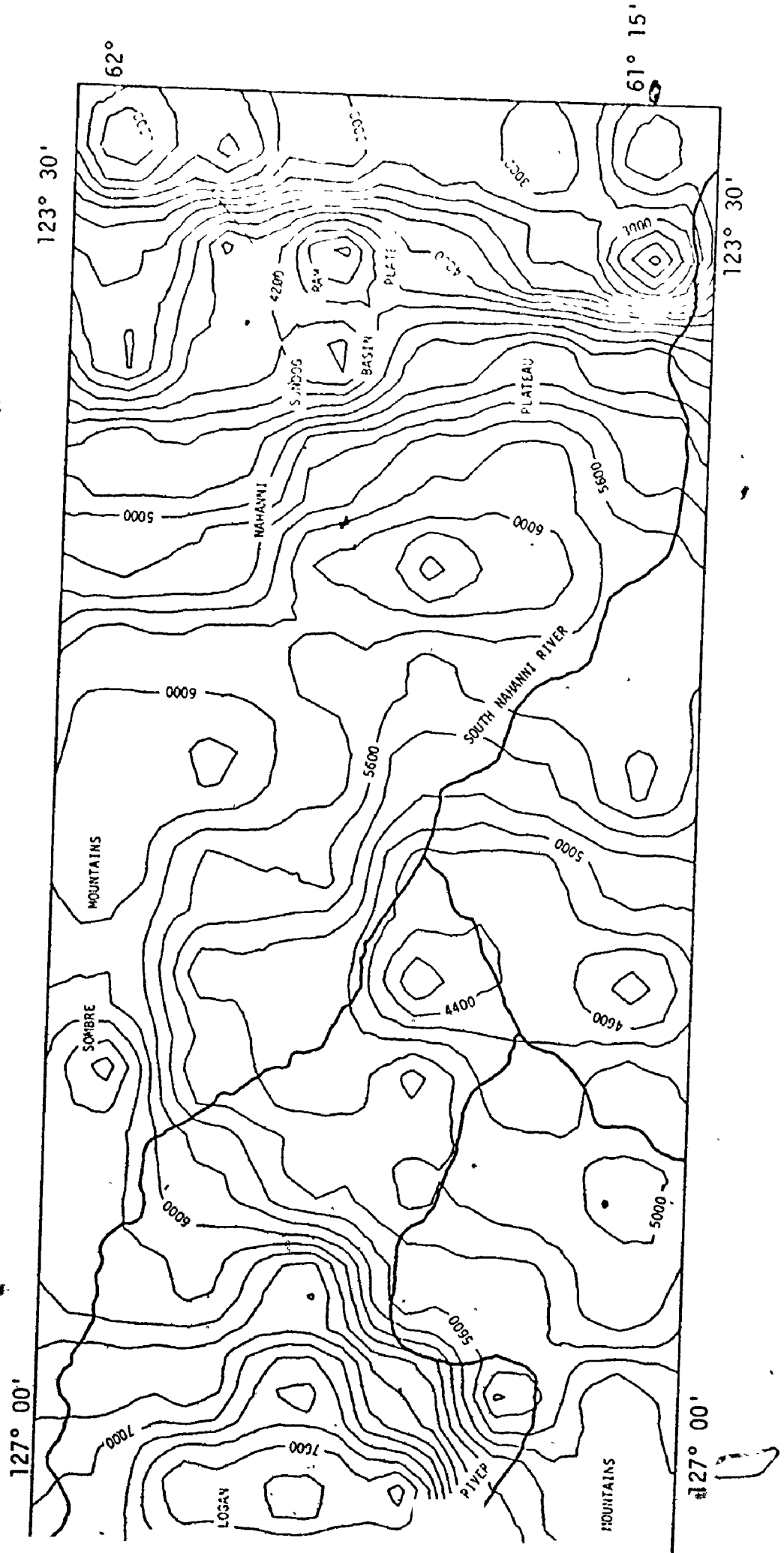


Figure 2.23. Structural deformation of the Mackenzie Mountains from topographic analysis (4 data points in each 1:50,000 map).

that there is a marked semi-circular arc of positive deformation in the South Nahanni region of the Mackenzie Mountains. Convex to the northeast, this arc runs from the Tlogotsho, Funeral and Headless Ranges in the southeast through the Nahanni Plateau, Tundra Ridge, and Manetoe and Arnica Ranges into the Sombre Mountains and eventually southwestwards into the Ragged Range of Logan Mountains. This arc of suggested positive deformation surrounds an area to the southwest in which mountain summits are at a considerably lower altitude. The broad area west of the Nahanni Plateau, and Headless and Funeral Ranges appears to be a deformational low like Clearwater Depression.

The summit altitude data set obtained by using the coarsest of the grid filters was also subjected to polynomial trend surface analysis. Linear, quadratic and cubic surfaces fitted to the 84 data points explained 49.3%, 59.2% and 80.3% of the initial variation in the data respectively. The arcuate axis of positive crustal deformation evident in Figures 2.21, 2.22 and 2.23 is also clearly apparent in the configuration of the statistically significant cubic trend surface fitted to the data (Figure 2.24). If the highest summits across the South Nahanni region were at one time part of a gently sloping erosion surface of moderate relief that has since been uplifted and deformed, then it follows that Figures 2.24 and 2.23 display the broad and more detailed patterns of Laramide-Cascadian deformation respectively.

As Figures 2.23 and 2.24 show, the course of the South Nahanni River takes it right across the upwarped crustal zone in the southern Mackenzie Mountains suggested by the results of topographic analysis.

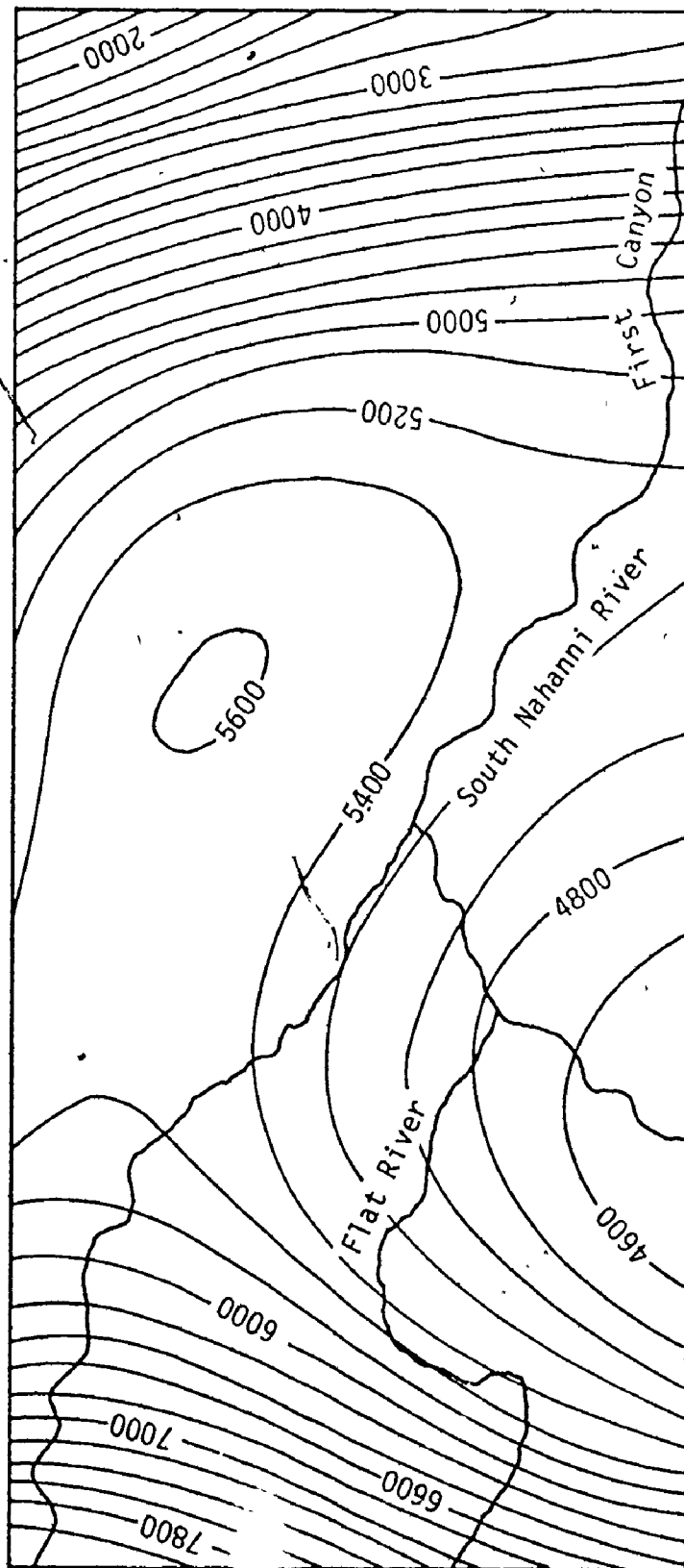


Figure 2.24. Cubic trend surface fitted to 84 data points in the South Nahanni River region. Each data point represents the highest summit elevation in one quadrant of a 1:50,000 topographic map. The linear, quadratic and cubic surfaces explained 49%, 59% and 80% of the initial variance in the data respectively.

The river has in fact cut through Funeral and Headless Ranges forming Third and Second Canyons respectively and deep into the southern limb of Nahanni Plateau with the formation of the deepest of its three canyons namely First Canyon. It is clear from Figure 2.23 that the upwarp of the Nahanni Plateau does in fact continue across First Canyon as Douglas & D.K. Norris (1960) have suggested.

As early as 1938, Cameron & Warren noted that "Certain peculiarities of the course of the South Nahanni make it appear that the valley is largely antecedent to the main structure of Mackenzie Mountains. The river cuts its way through high ranges of hard rock making immense canyons, when it could have gone round the end of the ranges by flowing a few miles farther and have traversed softer rocks all the way. It is just possible that glaciation may have had some influence in producing these drainage anomalies, but evidence of glaciation is not strongly marked in this area" (p. 17). Ford (1973) has also argued that the canyons of the South Nahanni River are of antecedent origin. Further north, the Ram River has entrenched itself into the northern limb of the Ram Plateau with the formation of canyons similar in most respects to those cut by the South Nahanni River. The Ram River canyons may also be of antecedent origin.

The drainage lines of the South Nahanni and Ram Rivers may well have been established before the region of the eastern Mackenzie Mountains was deformed during the Laramide-Cascadian Orogenies. Deformation appears to have progressed at a rate slow enough that entrenchment of at least some of the major rivers was sufficient to keep pace with it.

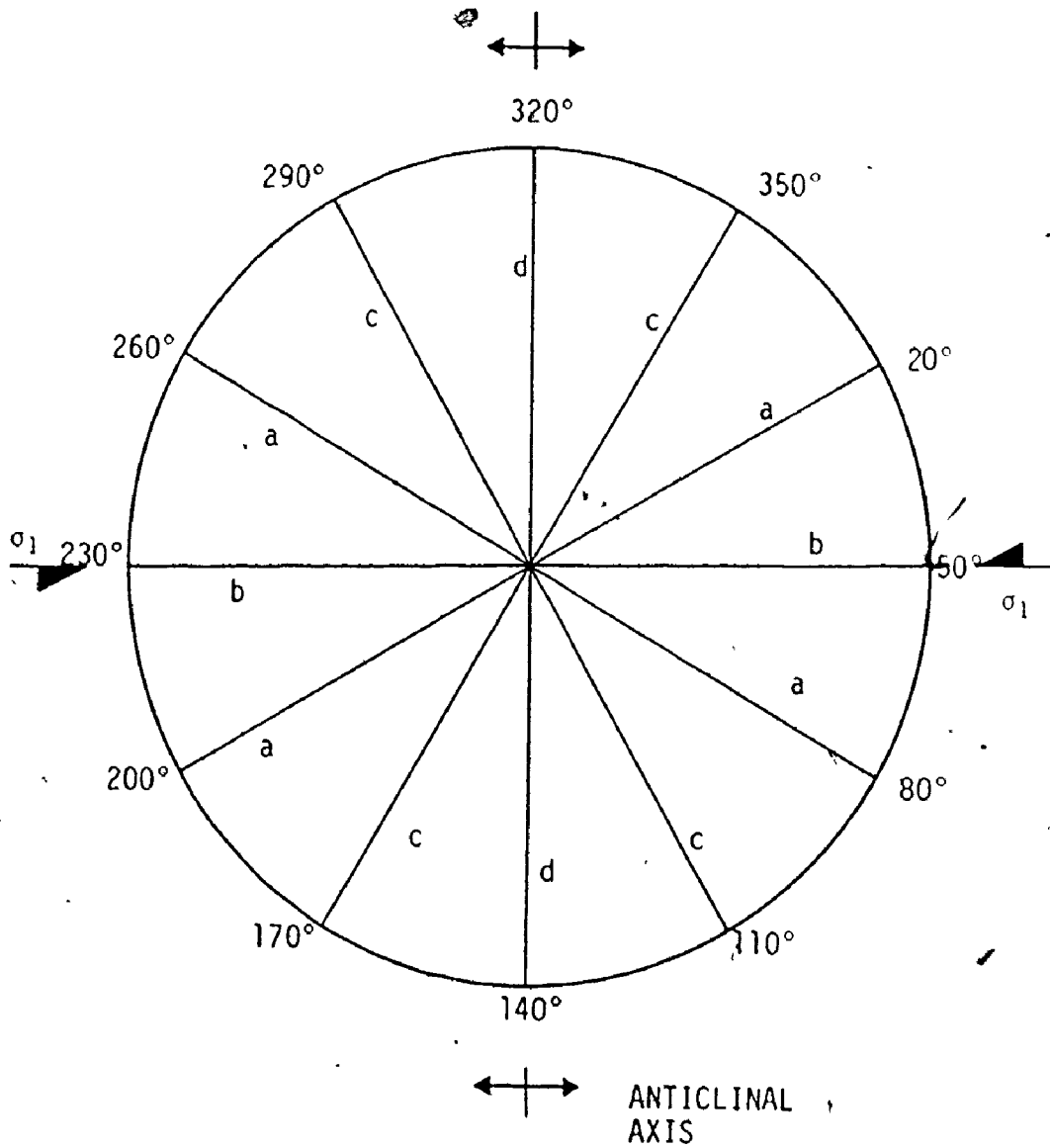
(d) Fault and Joint Patterns in the Nahanni Karst Belt.

As de Sitter (1956) has noted, almost every anticlinal structure is accompanied by a host of faults and joints particularly where the anticlinal axis plunges. All of these fractures have a common origin in the stretching that results from the three-dimensional shape produced by uplift. North of First Canyon, South Nahanni River, the limestones of the Nahanni and Ram domes are broken by dense networks of faults and joints. As these structures have certainly influenced the locations and modes of development of many of the karst landforms, it is pertinent to consider the characteristics of the fracture network and if possible to provide some tentative interpretation of its genesis.

(i) A Tentative Interpretation of Fracture Orientations.

The kinds of joints and faults that might be expected in a moderately folded limestone have been discussed by de Sitter (1956). He notes that before bending takes place primary shear fractures, including both faults and joints, which make an acute angle with the deformative stress ((a) in Figure 2.25) and tension fractures parallel to this stress (b) are to be expected. In the next stage a secondary stress condition caused by elastic bending may result in the development of a second set of shear fractures (c) with their acute angle bisected by the anticlinal axis with secondary extension fractures (d) developing parallel to the axis. de Sitter also points out that due to the elastic bending of strata and the couple induced, frictional shear fractures (d) may be developed which would be parallel to the anticlinal or synclinal axis. Also release tension fractures





- KEY:
- a Primary conjugate shear fractures
  - b Primary extension fractures, secondary release fractures.
  - c Secondary conjugate shear fractures.
  - d Secondary extension fractures, frictional shear fractures, primary release fractures, thrust faults.
  - $\sigma_1$ , Regional principal deformative stress.

Figure 2.25. The pattern of fractures that might be expected in a moderately folded limestone (after de Sitter 1964).

might form after the stress has vanished, these being either parallel or perpendicular to the axis of folding depending upon whether they release the main or the secondary stress. Finally thrust faults may develop which dip at an angle of approximately  $45^\circ$  to the bedding and with a strike parallel to the fold axis.

Fractures in the Nahanni karst were mapped from aerial photographs taken from an altitude of 30,000 ft. For the purpose of analysing these fractures the study area was divided on a north to south basis into six equally-sized regions (a-f in Figure 2.26). The lengths and orientations of all fractures in each of the regions were measured. In all, 976 fractures were identified these having a total length of 216.7 miles. No attempt was made to correct measurements for errors induced by photographic distortion although care was taken to use only the central portions of photographs for mapping purposes. In plateau areas, errors in fracture orientation are thought to be in the region of  $2-3^\circ$  but in areas of high relative relief errors may be as high as  $5-10^\circ$ . Fracture orientation-frequency histograms with  $10^\circ$  class intervals and weighted for fracture length were prepared for each region and for the whole karst area (Figures 2.27 and 2.28 (a)). These illustrate that fully 61.4% of all fractures weighted for length are oriented between  $30^\circ$  and  $70^\circ$  magnetic (Table 2.2). This fracture set will be labelled  $J_1$ . Other minor preferred orientations are apparent at approximately  $350^\circ$  ( $J_2$ ),  $315^\circ$  ( $J_3$ ) and  $280^\circ$  ( $J_4$ ) magnetic (Figure 2.28 (a)) in almost all of the regions although peaks on the histograms vary considerably in magnitude (Figure 2.27).

A

MOSQUITO LAKE

B

MORaine LAKE

DEATH  
LAKE

HIDDEN LAKE

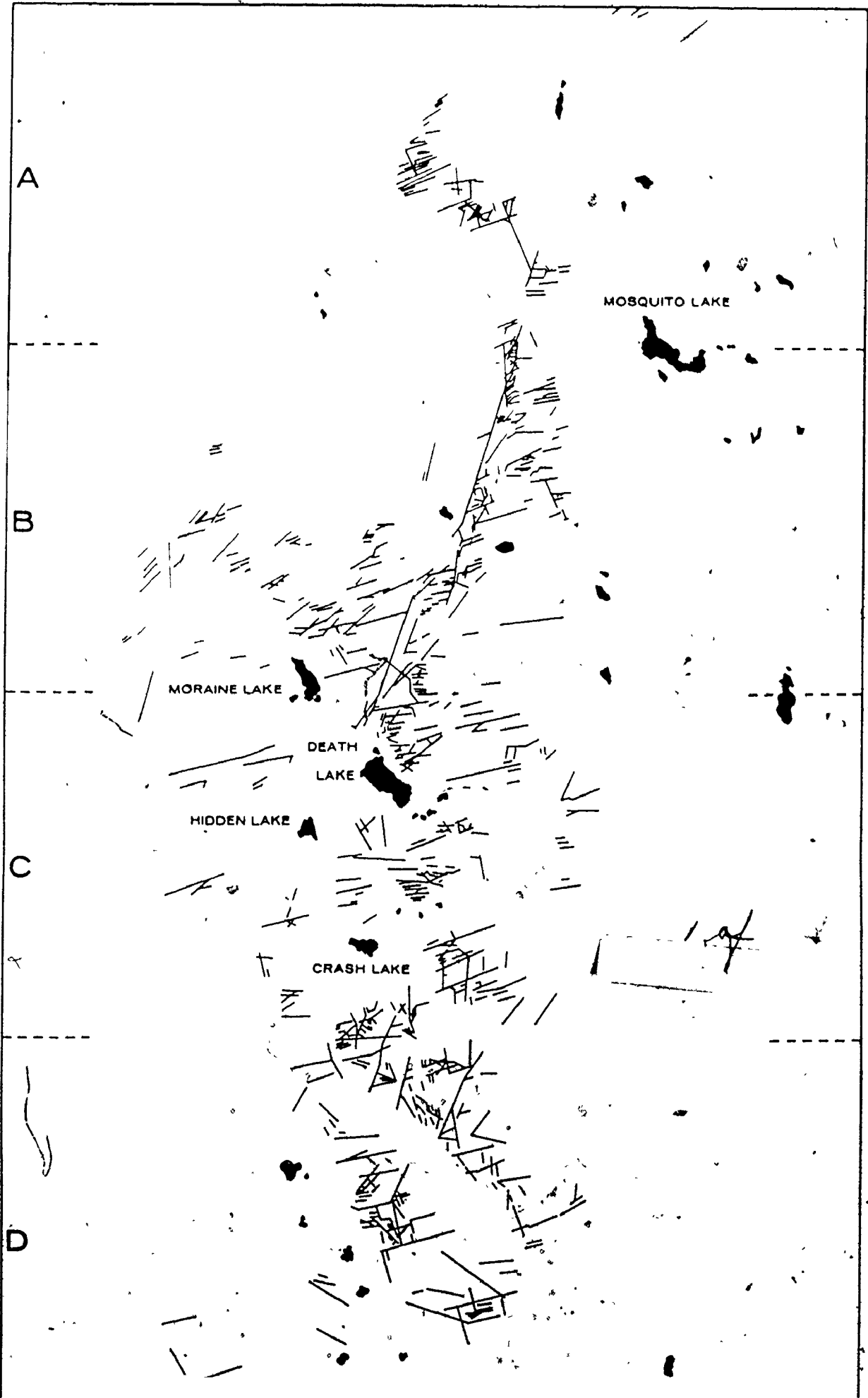
61° 30'

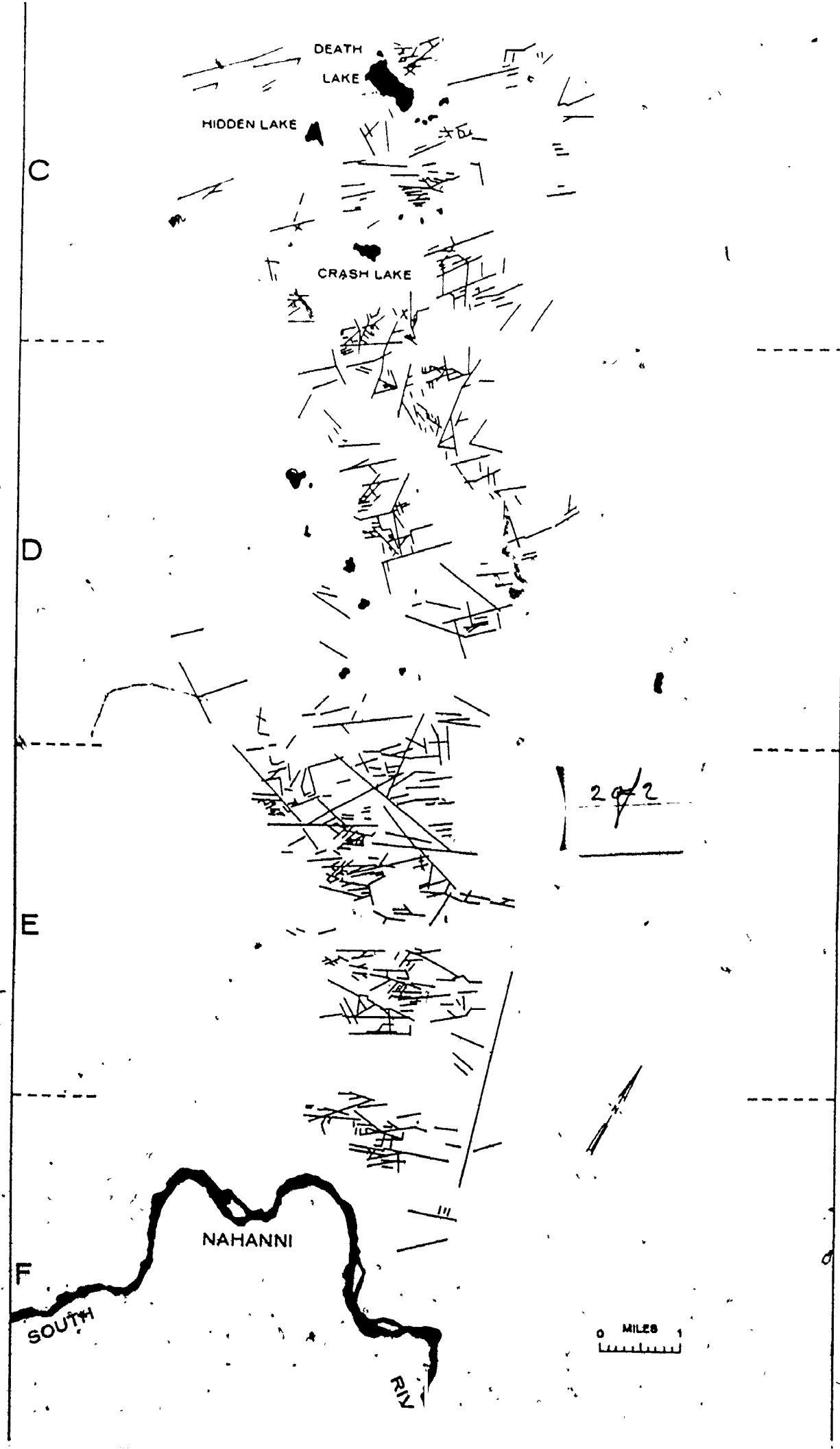
C

CRASH LAKE

D

61° 30'





DEATH  
LAKE

HIDDEN LAKE

CRASH LAKE

C

D

E

F

SOUTH

RIVER

NAHANNI

20/2

0 MILES 1  
|-----|

61° 20'

61° 20'

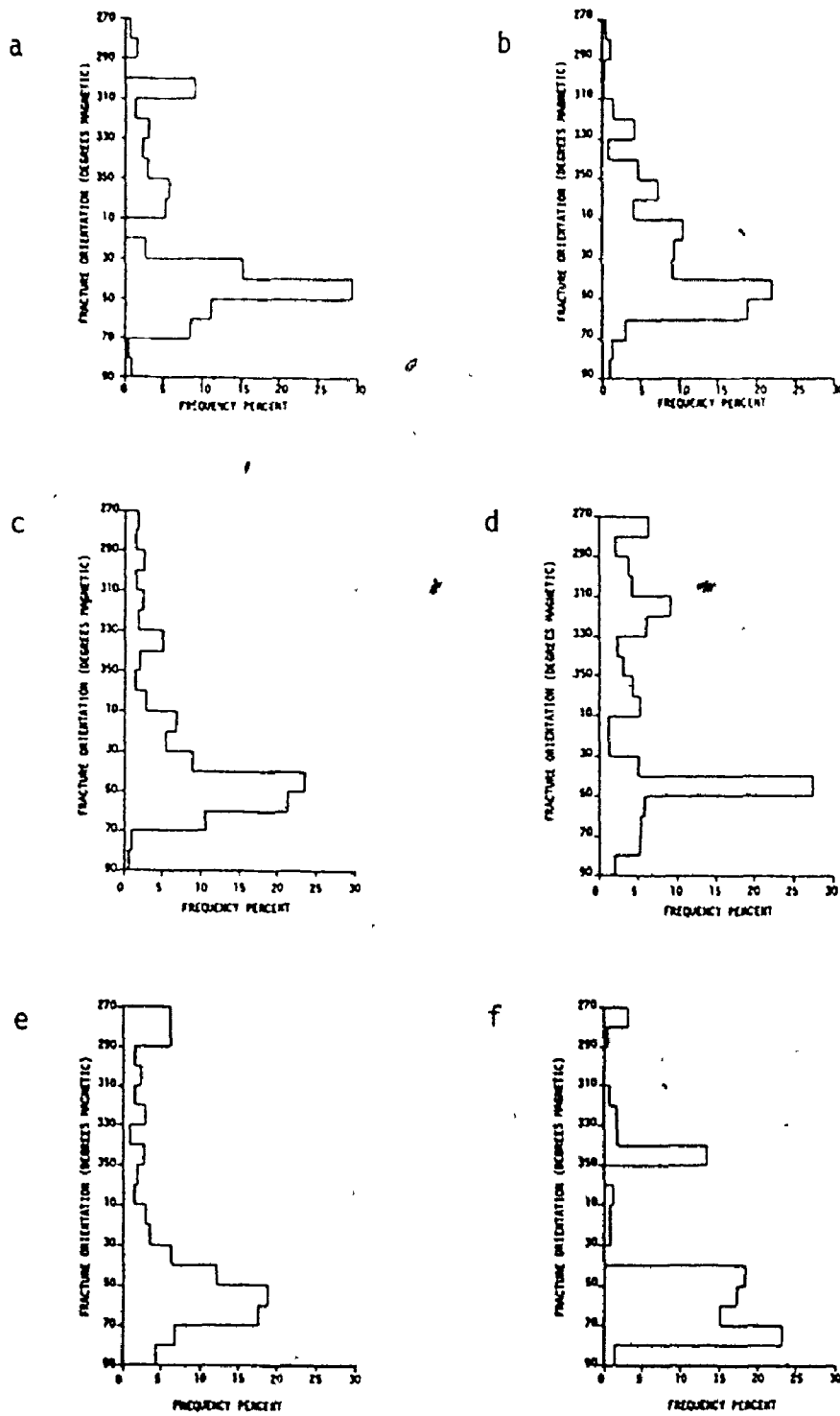


Figure 2.27. Fracture orientation histograms by region. Nahanni karst.

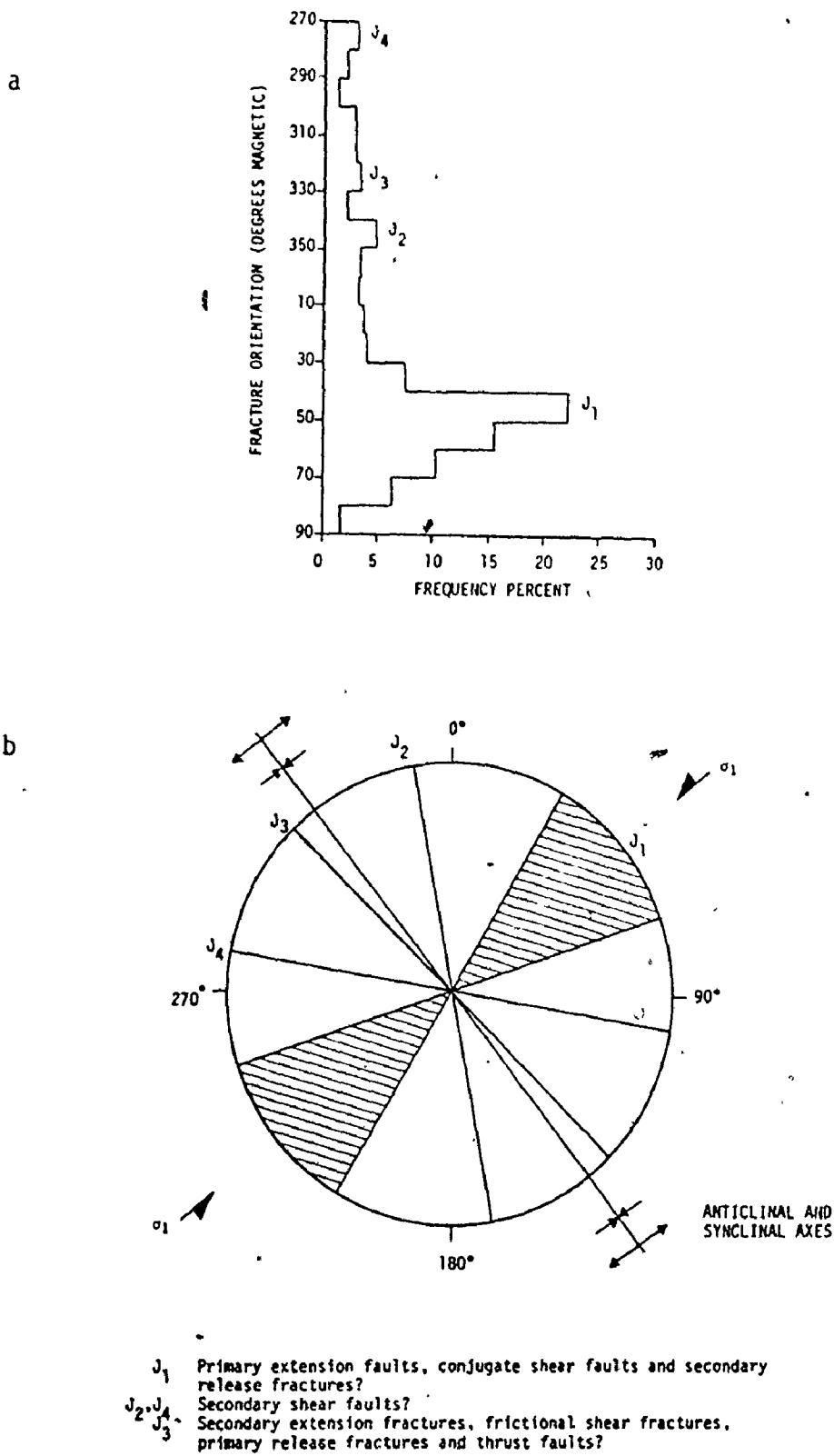


Figure 2.28. Major sets of fractures in the Nahanni karst (a) and the postulated direction of the principal stress that produced them (b).

Table 2.2. Fracture Patterns in the Nahanni Karst.

Orientation Class (° Magnetic)	Total Length of Fractures (miles)	Percentage of All Fracture Length
270-280	6.7	3.1
280-290	4.8	2.2
290-300	3.0	1.4
300-310	6.1	2.8
310-320	6.1	2.8
320-330	7.1	3.3
330-340	4.8	2.2
340-350	10.4	4.8
350-360	7.4	3.4
0-10	7.1	3.3
10-20	8.0	3.7
20-30	8.4	3.9
30-40	16.0	7.4
40-50	47.9	22.1
50-60	33.6	15.5
60-70	21.9	10.1
70-80	13.6	6.3
80-90	3.7	1.7

It is known from field observations that at least some of the fractures oriented at  $30^{\circ}$ - $70^{\circ}$ ,  $350^{\circ}$  and  $280^{\circ}$  are strike-slip faults because fracture planes are often characterized by slickenside and in many instances a layer of mylonite 1-3 inches thick which varies in color from cream to black, is present. Slickenside on many fault planes indicates that the last movements along the faults were horizontal, and together with the fact that there appears to have been little vertical displacement of beds indicates strike-slip faulting. Neither mylonite nor slickenside were discovered along the 1.6 miles extent of Main Street fault in the North karst oriented at  $352^{\circ}$  (Figure 2.26) although this too is believed to be a strike-slip fault. Any evidence of fault movements is unlikely to have been preserved for the fracture has been extensively widened by solution and a combination of freeze-thaw breakdown and gravitational collapse.

The interpretation of Main Street fault as a strike-slip form is further suggested by the presence of what appear to be secondary faults leading off from it. Both Billings (1972) and Price (1969) point out that movement along first-order shear faults may generate second-order shears which make an acute angle of close to  $30^{\circ}$  with the main form. Price (1969) has attributed the formation of these second-order faults to shock waves transmitted through the rock as movement takes place along the first-order fracture. Minor fractures leading off from Main Street fault have a preferred orientation of close to  $20^{\circ}$  magnetic and therefore make an angle of  $28^{\circ}$  with Main Street fault. As the acute angle between first- and second-order



faults points in the direction in which the block containing the second-order fault was moving, this suggests that Main Street fault is a dextral strike-slip fault.

Although interpretation of fault and joint patterns mapped from aerial photographs is anything but straightforward, a number of points can be made about the pattern observed in the Nahanni karst. The  $J_1$  fracture set for instance, which contains 61.4% of all fracture length is oriented exactly at right angles to the long axes of Ram Plateau and Sundog Basin, positive and negative elements of folding respectively (Figure 2.28 (b)). The  $J_3$  fracture set at  $315^\circ$ , on the other hand, almost parallels these axes of folding while  $J_2$  and  $J_4$  fractures subtend acute angles of  $28^\circ$  and  $42^\circ$  respectively with them.

Perhaps the simplest and most logical explanation of fracture and fold patterns in the Nahanni karst is that both were produced by a stress distribution with  $\sigma_1$  oriented at  $50^\circ$ ,  $\sigma_3$  at  $320^\circ$  and  $\sigma_2$  vertical (Figure 2.28 (b)). Following de Sitter (1956) we would expect a fracture pattern on the flanks of the Nahanni Plateau similar to that shown in Figure 2.25. In fact the observed fracture pattern in the karst area bears a close resemblance to this theoretical pattern if the  $J_1$  fracture set is considered to include primary shear faults, primary extension fractures or flank faults (de Sitter 1956, p. 193), and secondary release fractures (a & b in Figure 2.25). Additional evidence for a principal stress direction oriented at  $50^\circ$  comes from the geometries of small thrust faults in the limestones of the Nahanni Plateau (Plate 2.2). These structures dip either towards the northeast



Plate 2.2. A small thrust fault visible in the north wall of Canal Canyon. The fault appears to have been produced under conditions in which the principal stress was oriented at approximately  $50^\circ$  magnetic.

or southwest at angles of between  $30^\circ$  and  $40^\circ$  to the bedding; there is generally only minor separation along them. They form a part of the  $J_3$  fracture set. Douglas & D.K. Norris (1960) have reported numerous thrust faults in the Virginia Falls map-area. All of these dip either to the northeast or southwest. Thrust faults of this dip and orientation would require for their formation a compressive stress oriented at approximately  $45^\circ$ , a principal stress at  $50^\circ$  could certainly have produced them.

The  $J_3$  fracture set observed in the Nahanni karst is likely made up of a number of different fracture types including secondary extension fractures, frictional shear fractures, primary release fractures and thrust faults. The  $J_2$  and  $J_4$  fracture sets which subtend an acute angle of  $70^\circ$ , close to the  $60^\circ$  to be expected of conjugate shear faults are possibly secondary shear faults. A tentative interpretation of the observed fracture pattern in the Nahanni karst is, therefore, that it was produced during the Laramide and Cascadian Orogenies when the principal stress was oriented at  $50^\circ$  magnetic. Many of the faults and joints were produced before the folding of the limestone began; others were intimately related to it.

(ii) Variations in Fracture Density.

The zone of intense fracturing evident in Figure 2.26 - 'The Nahanni Fracture Belt,' follows the eastern limb of the southern Nahanni Plateau and passes between this upland region and that of the Ram Plateau. East of this zone fracture patterns could not be mapped accurately for over wide areas the limestones of the Nahanni

Formation are either overlain by shales of the Fort Simpson Formation which plastically deformed under stress rather than fractured or they lie beneath a thick cover of glacial deposits. The indication is, however, of a decrease in fracture density, in an easterly direction. To the west, despite the heavily stream-dissected nature of the Nahanni Plateau surface, there is evidence that fracture densities are much reduced.

Harris et al. (1960) have argued that the greatest concentration of compressional deformational fractures produced during folding occurs in areas of maximum curvature on the fold structure. This they say is the area of greatest rate of change in either the dip or the strike of the sedimentary beds. As comparison of Figures 1.5, 2.20 and 2.26 shows the Nahanni Fracture Belt parallels the zone of rapid change in dip associated with the steep almost monoclinial limb of the southern Nahanni Plateau. In the north it also appears to be associated with rapid variations in strike as it passes between the Nahanni and Ram Plateaus on the structural col separating these two positive structural features.

Uplift of the Nahanni and Ram Plateaus appears to have been accompanied by intensive fracturing along the eastern limb of the southern Nahanni Plateau. The dense networks of fractures provided routes by which water could enter the limestone; their presence, therefore, encouraged the development of both surface and underground karst landforms in this area. Uplift provided the relative relief necessary for the observed intense vertical development of many of the surface karst landforms.

1. Introduction.

The solutional landforms of the Nahanni region make up the most complex and intensively developed high-latitude karst landscape known (Figure 1.6). Karst forms are common on the residual surfaces of the deeply dissected Nahanni and Ram Plateaus between about 2,300 ft. and 4,300 ft. elevation. They are, however, most highly developed on the structural col which separates these two upland masses. The maximum dimensions of landforms vary from inches to miles and forms occur in bare, covered and mantled limestone regions both above and below the tree line. Six broad categories of features have been identified, namely limestone pavements, dolines, labyrinth karst, poljes, blind valleys and closed fluvial canyon systems and caves. Each will be discussed in turn.

2. Limestone Pavements.

Limestone pavements are horizontal to gently sloping rock surfaces approximately parallel to the bedding which are divided into a series of blocks by intersecting networks of widened fractures (Plates 3.1 and 3.2). The individual blocks are clints or flachkarren, the widened fissures, grikes or kluftkarren. Clint surfaces and walls are often intricately etched by a variety of micro-solutional features. Many of these, such as rillenkarren, rinnenkarren,

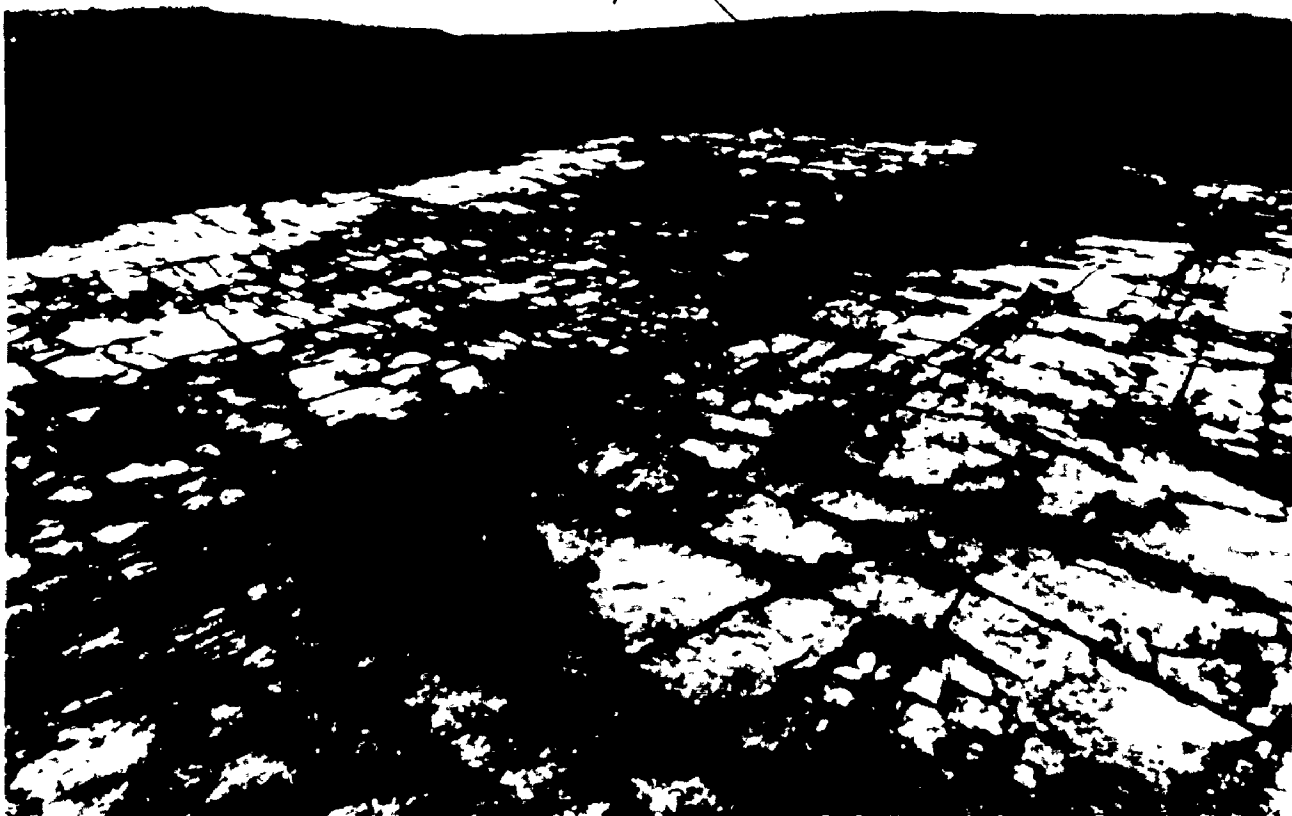


Plate 3.1. Limestone pavement on a spur in the north wall of Crash Canyon. Clint and grike systems are poorly developed because joints have as yet been little widened by solution.

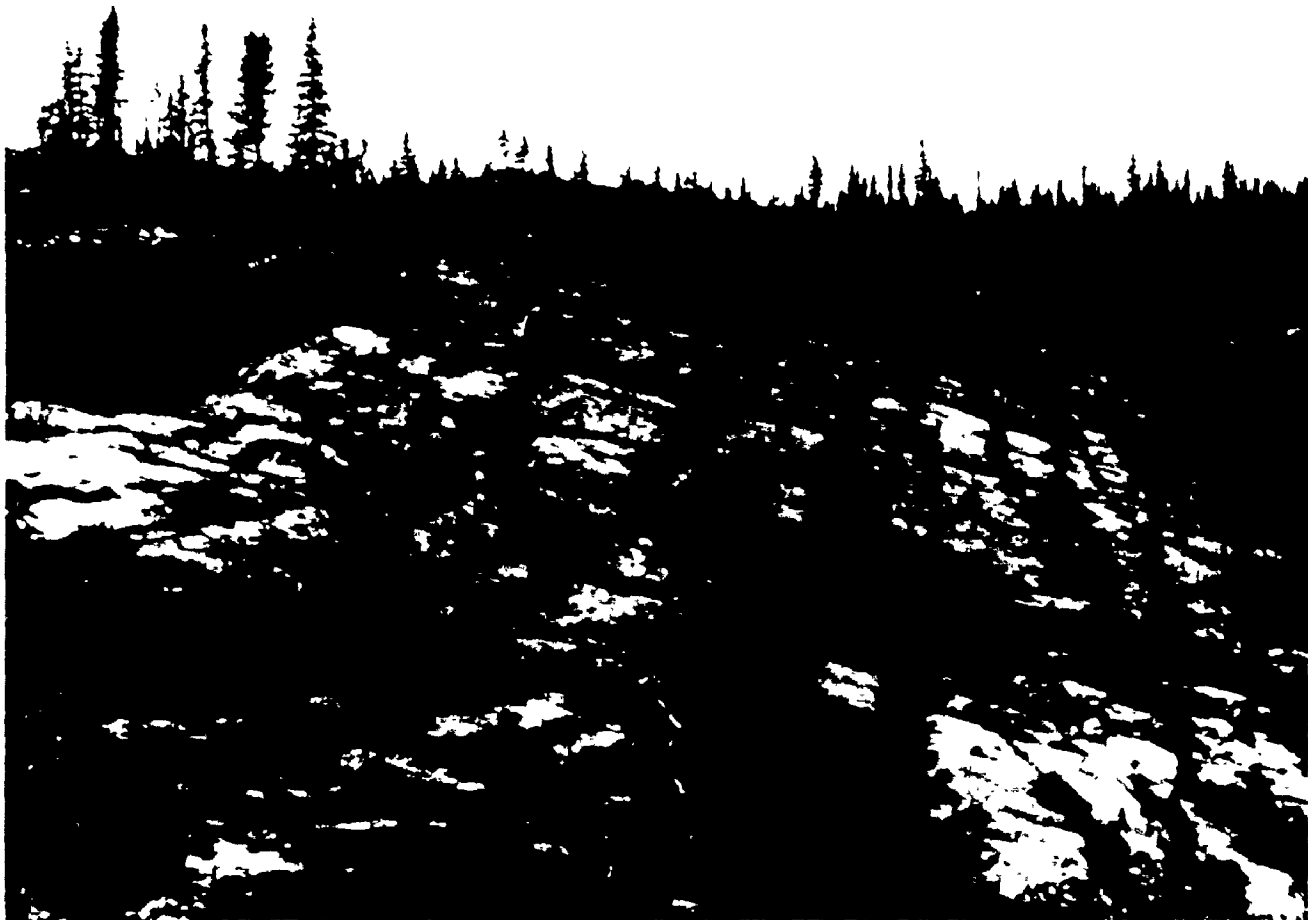


Plate 3.2: Steeply dipping pavement on the Nahanni Plateau surface south of Death Lake. The clints on this example are almost rectangular.

meanderkarren, rundkarren, trittkarren and solution basins or kamenitzas are characteristic of Nahanni pavement surfaces (Plates 3.3, 3.4 and 3.9) and have been discussed fully by Brook & Ford (1974).

On the southern portion of the Nahanni Plateau, limestone pavements are common up to an altitude of approximately 4,000 ft. Above this the plateau surface is a felsenmeer of limestone fragments patterned and sorted by periglacial processes and bare rock is only rarely visible (Plate 6.1). Many pavements occur in stepped sequences forming schicht-treppenkarst. Two basic types have been identified, the first and most ubiquitous being the sequence in which the shallow scarps or steps separating the pavement upper surfaces point down-dip, the second in which they point up-dip. Clint and grike systems are invariably best developed at or just back from these scarps, for here gravitational forces acting down-dip tend to widen fractures and often induce slight movements of clints. Fractures widened in this way provide routes by which water can percolate into the limestone encouraging karstification and bringing about the partial removal of soil from the rock surface. At relatively small distances back from these minor scarps, pavements are generally mantled by a thin soil cover supporting a tundra vegetation. In fact, broad areas of the Nahanni and Ram Plateaus are nothing more than a patchwork of irregularly shaped expanses of bare limestone pavement and areas that are thinly soil covered.

(a) Characteristics of the Bedrock.

(i) Lithology.

The pavements in the Nahanni have developed in the upper two units of the Nahanni Formation. Limestones are generally micrites,



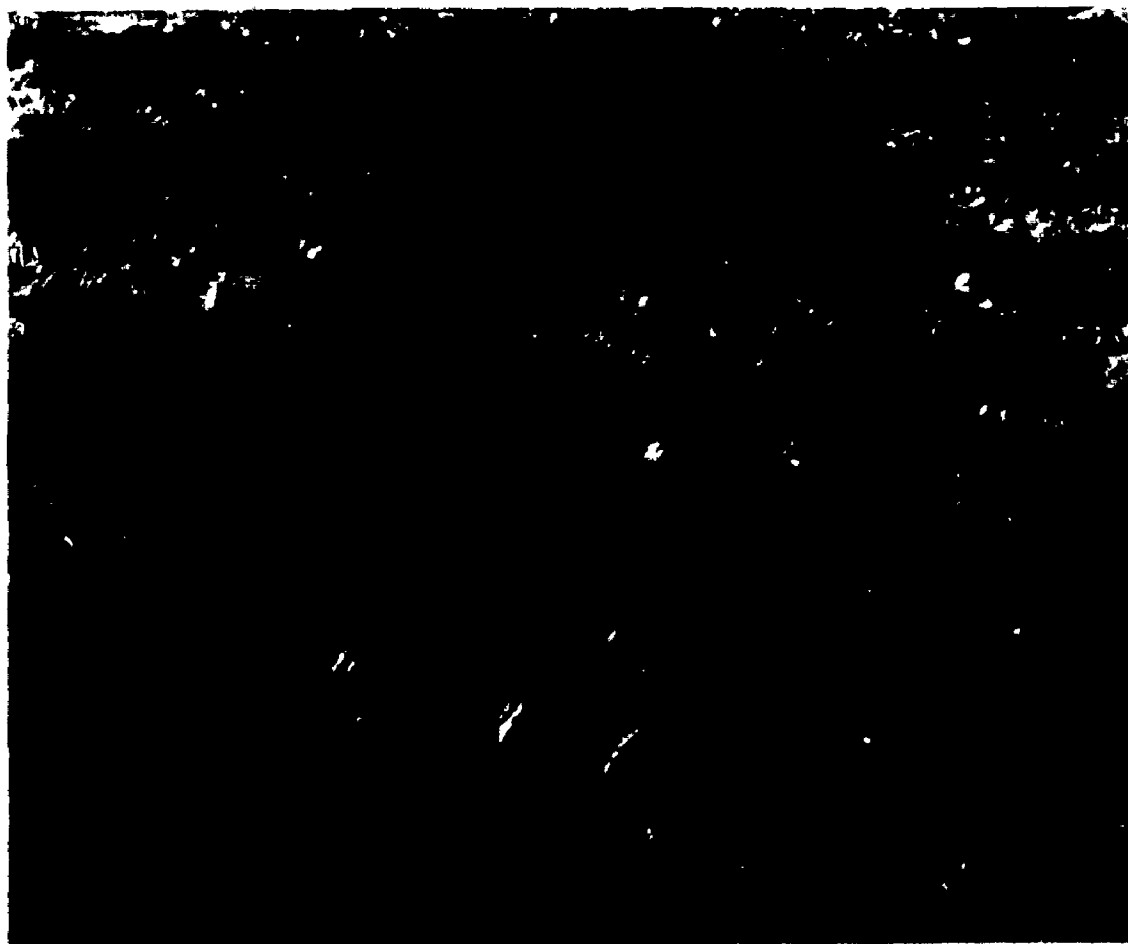


Plate 3.3. Field of rillenkarren on a little-jointed limestone pavement, Nahanni Plateau south of Crash Canyon. At left is a relict vegetation hollow that has been transformed by subaerial processes into a kamenitza.

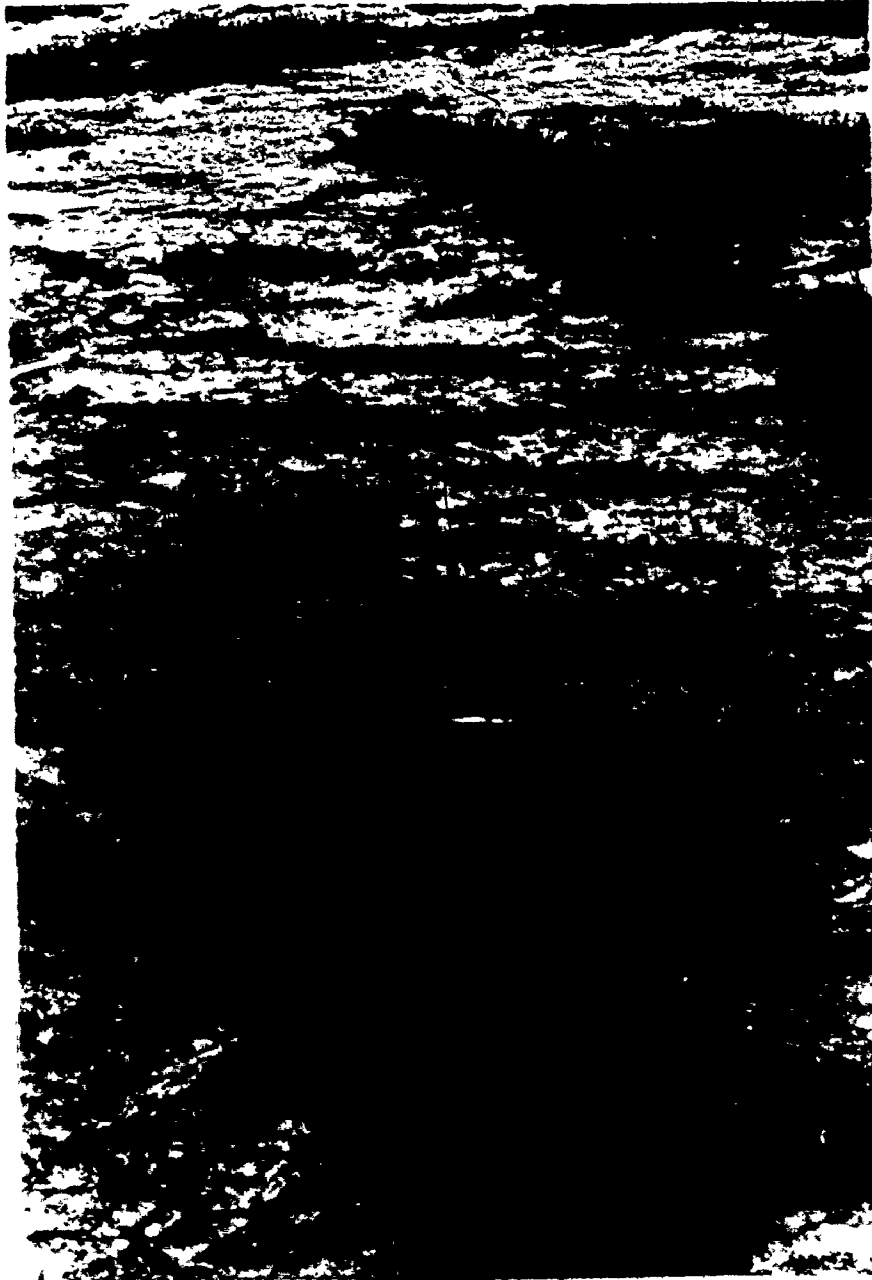


Plate 3.4. Ripple and step development on an almost unjointed limestone pavement, Nahanni Plateau. Dark grey dolomitic zones, which are more resistant to solution than the surrounding light grey limestone, give the pavement surface the mottled and rippled appearance.

pelmicrites or biomicrites with a fossil assemblage which includes stromatoporoids, corals, crinoids, brachiopods and gastropods. The corals and stromatoporoids often make up reefoid masses on a small scale and many of the fossils are partly or wholly silicified.

Massively bedded, resistant limestone beds tend to have a sparry limestone content, the thinner-bedded units are dominantly micritic. Many of the limestone beds are dolomitic giving the limestone a mottled appearance. Because the dolomite is less soluble than the dark grey limestone 'groundmass' the dolomitic zones stand out from pavement surfaces giving them an irregular rippled appearance (Plate 3.4). Silicified fossils also project out of clint surfaces so that in places these may be extremely irregular and intricately etched (Plate 3.11 (a)).

(ii) Bedding.

Limestone pavements are developed on thin and massive beds which dip at angles from  $0^{\circ}$  to  $16^{\circ}$ . Bed thickness varies between several inches (Plate 3.7) and several feet (Plate 3.6). The limestones are characterized by two kinds of bedding structure. Apart from the major planar bedding planes there are other structures which partially define the original current bedding in the limestones and which have not been entirely obliterated in the later compaction of the rock. Rarely flat or perfectly parallel to the major bedding planes for any distance, these partings may in plan show numerous minor irregularly-domed corrugations with complementary depressions (Plate 3.5). The frequency of these structures varies from bed to bed but they are present in both massive and thinly bedded limestones.



Plate 3.5. Solutionally etched current bedding structures and solution "tunnels" in a clint wall, Nahanni Plateau.

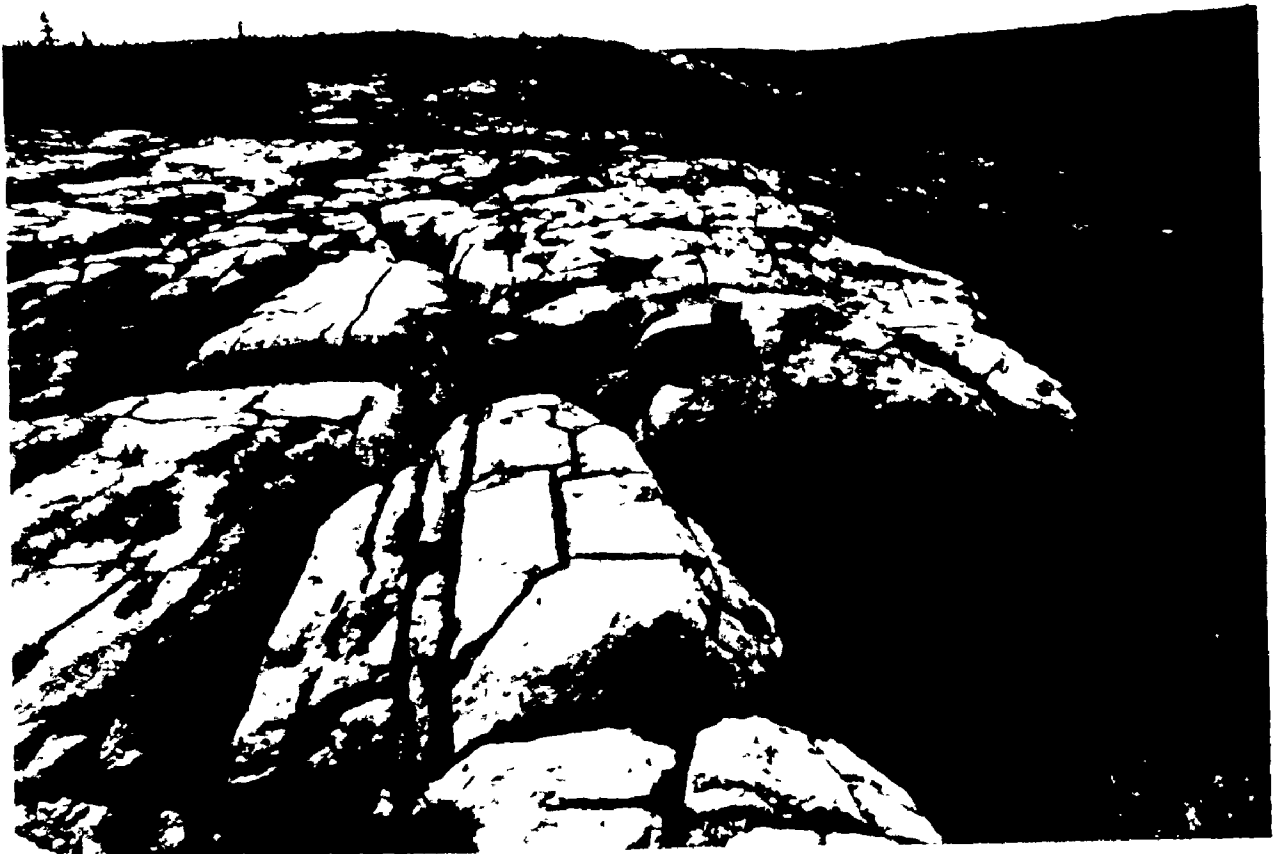


Plate 3.6. Clint and grike hierarchies, Nahanni Plateau. Solutionally rounded master clints are being destroyed as secondary clint and grike networks are opened by a combination of solutional and freeze-thaw action.



Plate 3.7. Secondary clint and grike networks making up natural crazy paving, Nahanni Plateau.

There may be as many as 10-15 or as few as 1-2 per foot. The amplitude of irregularities may be as great as 2 inches or be imperceptible (Plate 3.5). Many of these partings are filled with secondary calcite others may only become visible when they have been etched out by solution.

(iii) Fracturing.

The beds on which the Nahanni pavements have developed are characterized by both major and minor fracture systems. Major joints or small faults may extend laterally for several tens of feet and vertically for several or more feet. On the Nahanni Plateau pavements, the major fractures are oriented between  $0^{\circ}$ - $20^{\circ}$ ,  $22^{\circ}$ - $45^{\circ}$ ,  $84^{\circ}$ - $90^{\circ}$  and  $270^{\circ}$ - $307^{\circ}$ , and  $320^{\circ}$ - $358^{\circ}$ . Those at  $84^{\circ}$ - $90^{\circ}$  and  $270^{\circ}$ - $307^{\circ}$  were observed at all of the nine localities examined, those at  $22^{\circ}$ - $45^{\circ}$  at eight of the nine and the other two sets at only four out of the nine localities. Because the angles between the major fracture sets are rarely  $90^{\circ}$ , clints tend to be irregularly shaped and multi-sided.

In addition to the vertically and laterally persistent fractures which cross the limestone beds, there are networks of minor fractures which are often filled with secondary calcite and which are so fine in some cases that they are only visible once solution has widened them (Plate 3.8). These minor structures which are planar and which dip at steep angles, may pass completely through thick limestone beds and show some directional consistency (Plate 3.6). In rubbly bedded limestones, however, they rarely persist vertically for more than twelve inches before they are offset laterally at a current bedding structure. Most

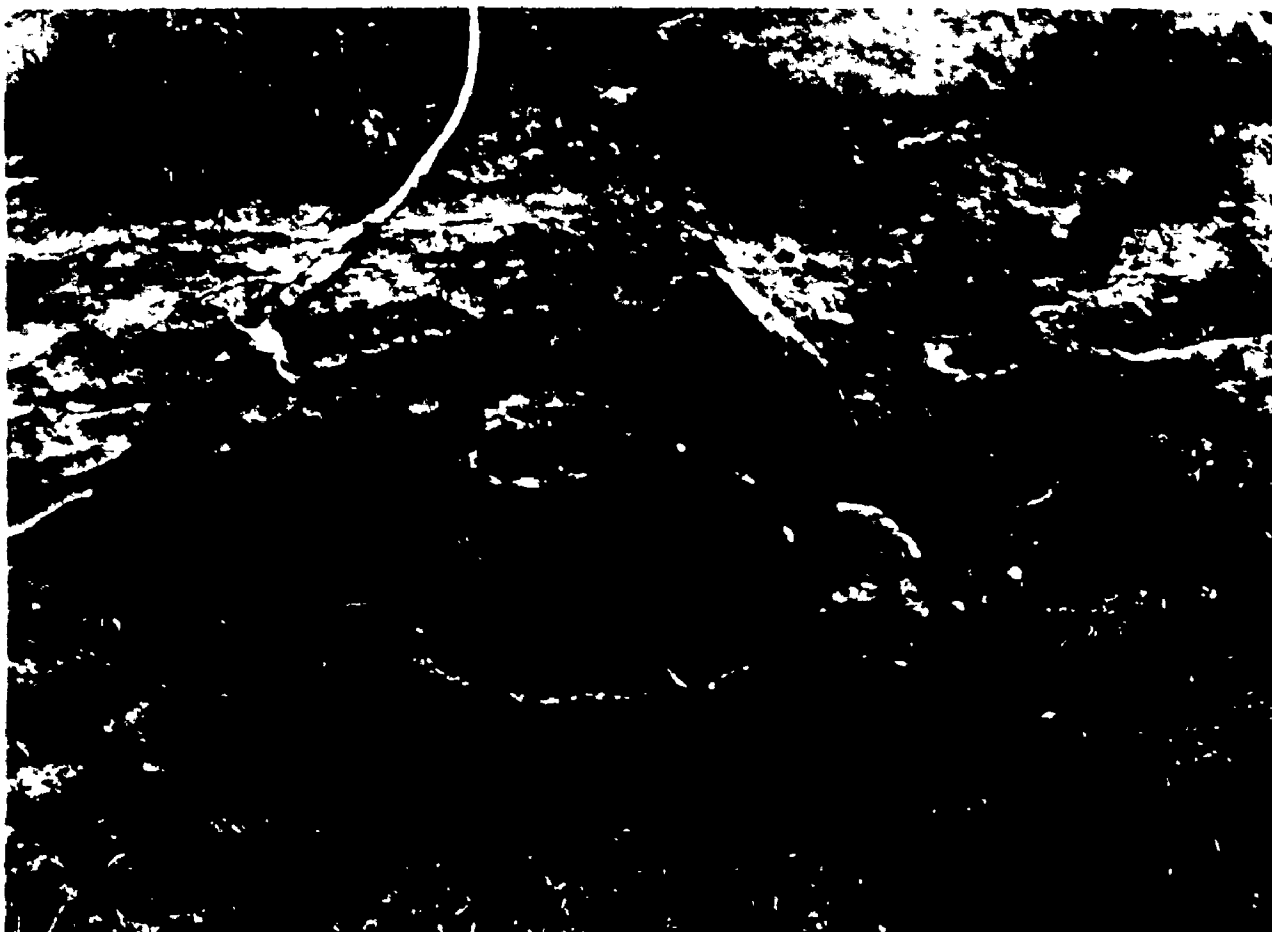


Plate 3.8. Elliptical solution pits developed in microfractures filled with secondary calcite.



commonly these fractures are offset at numerous current bedding partings and are generally less than 6 inches in vertical extent. In thinly bedded limestones five of these fractures per foot is common although as many as fifteen have been counted. In the more massive limestones one or two per foot is more usual. In thinly-bedded limestones the orientations of these minor fractures may be very variable.

(b) Some Morphological Characteristics of Nahanni Pavements.

In a morphological sense the limestone pavements of the Nahanni are similar in many respects to pavements that have already been described by Parry (1960), Sweeting (1964, 1966), Jones (1965), Clayton (1966), Williams (1966), Thomas (1969) and Pluhar & Ford (1970). Certain aspects of Nahanni pavement morphology and evolution, however, are important to an overall view of karst forms in the Nahanni region. These will now be discussed.

(i) Characteristics of Clint and Grike Systems.

Pavement morphology in the Nahanni is controlled almost entirely by the hierarchies of structural weaknesses that are present in the limestone. The networks of master joints and the master bedding planes once widened by solution, isolate the master clints. Generally these vary in size from 3 ft. by 2 ft. up to 12 ft. by 10 ft., and there is a considerable range in size across a single pavement surface (Plates 3.1, 3.2, 3.6 and 3.11 (a)). Depending upon the orientations of the master joint sets and their degree of development, clints may be rectangular or polygonal in plan (Plates 3.1 and 3.2). The master

clints may be made up of one or more beds of limestone depending upon bed thickness and the vertical persistence of the master joints. Normally master clints are from one to several feet thick. Lower joint frequencies in the more massively bedded limestone units mean that master clints in such beds are large; in thinner bedded limestone, on the other hand, master clints ~~may~~ be quite small.

Many limestone pavements in the Nahanni have only poorly developed master clint and grike systems (Plates 3.1 and 3.2) while on others these features are highly developed (Plate 3.6). On several pavements the master clints have been further broken down along secondary weaknesses with the formation of what might be regarded as secondary clint and grike systems (Plate 3.6). In massive limestone beds with few current bedding partings, where the secondary fractures have the same vertical persistence as the master grikes, the secondary clints are the same thickness as the master clints but have less extensive upper surfaces. In the pavement shown in Plate 3.6, the master clints are large with rounded edges and corners and the master grikes broad and deep with a partial soil fill. Secondary grike systems have developed in the master clints isolating secondary clints which are irregularly shaped and have sharp corners and edges. The secondary grikes are narrow and rarely contain soil. As the plate shows, many of the secondary clints are collapsing into the master grikes.

The pattern of development of secondary clint and grike systems differs in pavements where the master clints are made up of more than one bed of limestone. In this situation secondary fractures rarely

pass continuously through all of the beds, but are usually offset at the various bedding planes. Secondary clint and grike structures develop which are essentially limited to the upper bed. Where this is massive and more than six inches thick a regular rectangular or other consistent geometric pattern of secondary fractures may cross it. Where this is thin the pattern may be extremely irregular. Under such conditions the upper surfaces of many master clints are topped by thin rectangular- to polygonal-shaped secondary clints up to two feet long. Where the secondary clints are irregularly-shaped the master clint surfaces resemble crazy paving (Plate 3.7); where they are rectangular the surfaces are like that of a cobbled street.

Master clints formed in limestones characterized by numerous current bedding partings and secondary fractures develop a quite different morphology (Plate 3.10). These clints are broken down along current bedding and joint weaknesses with the formation of secondary clints and grikes. The secondary clints are irregularly shaped with straight sides but have uneven upper and lower surfaces essentially paralleling current bedding structures. In limestones where current bedding weaknesses are abundant, secondary clints may be further broken down into tertiary forms. This process goes on until what is produced is really a released rock slab rather than a clint.

Morphologic variation between Nahanni pavements is in large part related to differences in the characteristics of master and secondary clint and grike systems, themselves controlled largely by

the structural properties of the limestones. It seems likely that pavements elsewhere also show these hierarchical clint and grike characteristics.

(ii) Pit-and-Tunnel Networks.

Pluhar & Ford (1970) have differentiated between grikes of shallow depth which they have called trench karren and those which pass through a number of limestone or dolomite beds which they refer to as cleft karren. In addition, these workers have reported the existence in the dolomite pavements of the Niagara Escarpment, southern Ontario, Canada, of pit-and-tunnel systems (Figure 3.1). Both trench karren and pit-and-tunnel systems are joint-guided and almost all terminate downwards at the first readily penetrable bedding plane. The terminating bedding plane may be widely opened to either side of the trench or pit-and-tunnel line. The openings in the bedding plane are solutional anastomoses with voids ranging from 0.1 to 5.0 centimeters in height. Pluhar & Ford suggest that the anastomoses are underground runways which serve to discharge water to other trenches or to a breach to a lower bedding plane, ultimately directing it to the deep cleft karren which are the main water drains. The water to initiate anastomosing is thought in some cases to penetrate broadcast down a joint, in which case a trench is initiated directly, but more commonly it is believed to be limited to a few irregularly-spaced points along the joint with a pit developing at each point (Figure 3.1). These pits are linked by an underground tunnel which is no more than an enlarged anastomotic tube following the contact of joint and bedding plane. Pluhar & Ford

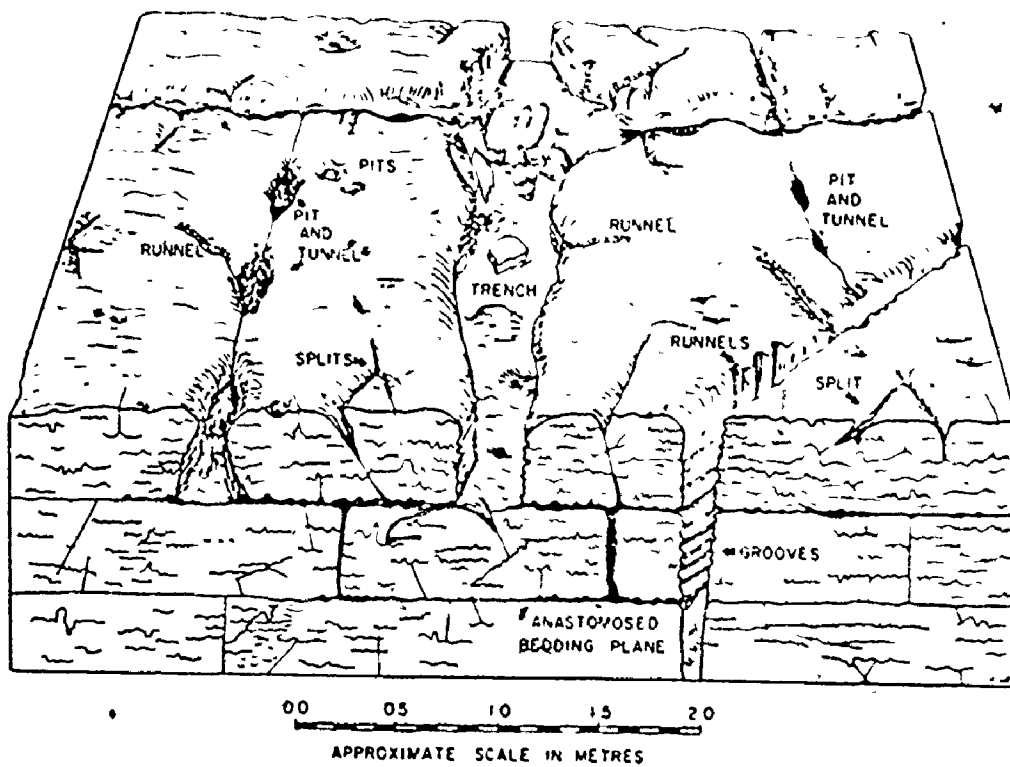



Figure 3.1. The principal karren types on the dolomite pavements of the Niagara Escarpment in the Hamilton district of Southern Ontario (after Pluhar and Ford 1970).

note that pits may amalgamate to create a trench by their elongation along the host joint.

Pit-and-tunnel systems similar to those reported by Pluhar & Ford (1970) are common on Nahanni pavements (Plate 3.8). They are characteristic of both master and secondary weaknesses. As Pluhar & Ford have argued there is clear evidence to suggest that pit-and-tunnel systems in secondary fractures enlarge to form shallow grikes or trenchkarren. In the Nahanni pavements there is also strong evidence to indicate that pit-and-tunnel systems developed in the master joints may enlarge and coalesce along the joints to form master grikes. That some master grikes on Nahanni pavements formed in this way is evidenced by the existence of paired embayments in grike walls attesting to the former presence of solution pits (Plate 3.8). In addition, on some pavements with poorly developed master grike systems, pits are evident in the major joint networks.

On many pavements pit-and-tunnel systems are highly developed in secondary structural weaknesses. In rubbly bedded limestones pits developed in secondary fractures connect with tunnels developed along current bedding partings (Plate 3.5). Often the tunnels are developed parallel to the joint hosting the pit, but many are not. There is no doubt that pit-and-tunnel networks in the master clints enlarge and coalesce to form secondary grikes. As this enlargement process proceeds numerous small natural bridges are left spanning the secondary grikes.



As Pluhar & Ford (1970) have noted, the pit-and-tunnel systems of pavements serve as discharge routes for water falling on the limestone or dolomite exposures. There is clear evidence in the Nahanni that like clints and grikes, there are hierarchies of pit-and-tunnel networks. The first pits and tunnels to develop are thought to do so in the more open master joints and bedding planes which eventually enlarge into grike systems. As the master clint and grike networks open up, secondary pit-and-tunnel systems develop in the secondary structures in the master clints. These systems funnel water to the larger pit-and-tunnel systems or master grikes.

It is evident from examination of Nahanni limestone pavements that grikes may develop by the mechanical widening of joints and they may also develop by solution as water flows broadside into an already open joint. In the majority of instances, however, grikes are believed to pass through a pit-and-tunnel stage in their development.

(iii) Natural Rock Hollows.

Four types of natural rock hollows have been identified on Nahanni pavements. These include solution basins or kamenitzas, vegetation hollows, structural hollows and what are here referred to as joint hollows. Sweeting (1972) has pointed out that where rock surfaces are more or less horizontal, water collects in pools and as a result of localized solution shallow basins maybe formed. These basins or kamenitzas, she notes, vary in size from one or more inches up to 9 feet in diameter and from a few tenths of an inch to 18 inches in depth. Kamenitzas are usually round or oval in plan, they have

steep to overhanging walls and flat floors which are often mantled by organic and inorganic debris. The flanks of these basins above the level of overflow are frequently fretted by rillenkarren forms (Plate 3.9).

Many pavements in the Nahanni show evidence that they were at one time mantled by a thin soil cover. In a number of areas there is a distinct gradation between bare limestone surfaces, surfaces irregularly soil covered and those totally soil covered. When a pavement surface reaches the stage of being a patchwork of bare rock and soil, the latter being retained in slight hollows in the pavement surface, the intensity of the solution process varies from one place to another. There can be little doubt that more limestone is removed in solution from beneath the vegetation than is removed from the bare rock surfaces. The reason for this is that any water seeping into the soil becomes more aggressive upon contact with biogenic carbon dioxide and organic acids. The enhanced solution beneath vegetation patches or hummocks leads to the development and enlargement of vegetation hollows in the limestone (Plates 3.3, 3.4 and 3.9).

When an isolated vegetation hummock was removed from the upper surface of one Nahanni pavement a smooth-sided hollow 18 inches deep, 20 inches long and 10 inches wide was revealed. Removal of the soil and vegetation mantling a bedrock surface occurs naturally in some circumstances and many hollows on Nahanni pavements are believed to be relict vegetation hollows now exposed to subaerial processes.





Plate 3.9. Relict vegetation hollow on a pavement surface. This has been partially modified into a "kamenitza." The sides of the hollow display rillenkarren solution forms.

One of the most commonly occurring bedrock depressions on Nahanni pavements is the structural hollow and there are clear relationships between structural hollows and some vegetation hollows and kamenitzas. Structural depressions essentially constitute exposed current bedding basinal irregularities. At one locality on the Nahanni Plateau, for instance, a loose slab of limestone was removed from the surface of a pavement. Beneath was a smooth, shallow structural hollow 18 inches by 10 inches containing both organic and inorganic debris. Such structural hollows vary in dimensions but are rarely more than 6 ft. in diameter and 3-4 inches in depth.

It is apparent that because many structural hollows on pavements are able to retain soil even when it is eroded from the surrounding areas that many are modified into vegetation hollows. On the other hand, under subaerial conditions there is the tendency for both structural and vegetation hollows to be modified into a kamenitza-like form. Clearly after heavy rain, water collects in these basins until it overflows. Mineral and organic debris protects the floors of hollows so that solution is concentrated at the walls which are steepened and may even be undercut. Lateral solution also tends to generate more of a circular or oval plan to the depressions. A stage may be reached where the solutionally modified structural basin or vegetation hollow differs little from a 'true kamenitza.'

It is apparent that the life spans of structural hollows and relict vegetation hollows are dependent upon the frequency of structural weaknesses in the limestone. Where weaknesses are abundant, the probability

that they intersect a structural or vegetation hollow is high and not only do they provide routes along which water in the basins can escape but they also bring about the disintegration of the surrounding limestone. Because structural basins are essentially exposed current bedding structures in the limestone, such features are more common in the rubbly bedded sequences. The density of structures in these beds, however, means that they do not generally survive for any great length of time. These hollows are less common in the more massive beds with few current bedding partings but once they are exposed, their life span is invariably long enough for them to be modified into kamenitzas.

There is a clear indication in the Nahanni that many vegetation hollows originate as structural depressions in the limestone. In addition it is apparent that many, if not all kamenitzas in this area are modified structural or vegetation hollows.

Very different from kamenitzas, structural hollows and vegetation hollows is the joint hollow, a shallow, irregularly-shaped, low-lying area on a pavement surface (Plate 3.10). Joint hollows range in size from inches across, to one or more tens of feet across, being from a few inches to a few feet deep. It is apparent that joint hollows result from the widening of dense networks of secondary grikes or trench karren, all of which terminate at the same bedding plane. As the grikes widen, the secondary clints separating them are reduced in size and ultimately removed. As all secondary clints are not of the same size the large forms often form residuals in the floors of many joint hollows (Plate 3.10).



Plate 3.10. Large joint hollow on a limestone pavement surface, Nahanni Plateau. The depression was produced by the solutional widening of a dense network of joints. It has residual secondary clints projecting from its floor.

(c) The Scale of the Solution Process.

(i) The Chemical Characteristics of Waters on Pavements.

In an attempt to learn more about the process of solution on limestone pavements in western Ireland, Williams (1966) collected and analyzed water samples from 118 rain-fed pools on bare rock surfaces. He found that on average the pool waters had a temperature of 15°C, a pH of 8.7, a magnesium content of 11 p.p.m.  $\text{CaCO}_3$  and a calcium content of 66 p.p.m.  $\text{CaCO}_3$ . Williams notes that water at 15°C in equilibrium with atmospheric carbon dioxide levels can dissolve approximately 67 p.p.m.  $\text{CaCO}_3$ . The close agreement between this theoretical figure and the measured values, Williams regards as convincing evidence that water in rock pools on limestone pavements in Ireland works towards equilibrium with atmospheric carbon dioxide levels, and derives little  $\text{CO}_2$  from other sources. He argues that these results indicate that many micro-solution features of pavements can be produced by rainwater alone, without the addition of soil  $\text{CO}_2$  and soil acids of biological origin. The chemical characteristics of pool waters on Nahanni pavements suggest somewhat different conclusions.

During the summer of 1973 12 pool waters on pavements on the Nahanni Plateau surface south of Death Lake were sampled and analyzed. Samples were collected within 2 hours of very heavy rain while light rain was still falling. Results of these analyses are given in Table 3.1 and average statistics are shown in Table 3.2. On average the pools had a temperature of 11°C, a pH of 8.19, a magnesium content of 8 p.p.m.  $\text{CaCO}_3$  and a calcium content of 64 p.p.m.  $\text{CaCO}_3$ . The striking similarity

Table 3.1. Chemical Characteristics of Waters in Pavement Areas of the Nahanni Plateau South of Death Lake.

Sample ID	Temp. °C	pH	CaCO <sub>3</sub> ppm	MgCO <sub>3</sub> ppm	SI <sub>c</sub>	SI <sub>d</sub>	LogPCO <sub>2</sub>
<u>Pools on Bare Rock Surfaces</u>							
169	12.0	8.05	52	4	-0.12	-1.32	-2.85
170	11.0	7.91	121	26	-0.15	-0.93	-2.94
176	11.0	8.30	42	7	-0.50	-1.74	-3.66
179	10.0	7.86	59	5	-0.72	-2.48	-3.12
180	10.6	7.80	59	6	-0.70	-2.36	-2.98
181	10.5	8.30	45	3	-0.44	-2.02	-3.62
185	10.0	8.30	76	10	-0.18	-1.21	-3.56
186	11.0	8.40	101	10	0.00	-0.98	-3.72
187	11.6	8.51	82	8	-0.01	-1.02	-3.88
191	10.8	8.23	44	3	-0.27	-1.68	-3.29
193	10.8	8.21	58	10	-0.45	-1.63	-3.56
194	12.0	8.40	32	2	-0.58	-2.35	-3.86

Pools on Vegetated Till

182	9.0	8.09	146	13	+0.29	-0.44	-2.89
183	3.0	7.88	139	9	-0.12	-1.37	-2.72

Seepage Water

184	8.2	8.41	116	21	+0.04	-0.62	-3.69
188	4.0	8.03	121	11	-0.05	-1.08	-2.92
125	10.0	8.35	123	2	+0.42	-0.91	-3.23

Soil Water

190	11.0	7.70	156	14	-0.04	-1.09	-2.51
-----	------	------	-----	----	-------	-------	-------

Table 3.2. Mean Chemical Characteristics of Water Types on Nahanni  
Payments.

Water Type	No. Samples	Temp. °C	pH	CaCO <sub>3</sub> ppm	MgCO <sub>3</sub> ppm	SI <sub>c</sub>	SI <sub>d</sub>	logPCO <sub>2</sub>
Pools on Bare Rock Surfaces	12	10.9	8.19	64	8	-0.34	-1.64	-3.42
Pools on Vegetated Till	2	6.0	7.98	142	11	+0.08	-0.90	-2.80
Seepage Waters	3	7.4	8.26	120	11	+0.14	-0.87	-3.28
Soil Water	1	11.0	7.70	156	14	-0.04	-1.09	-2.51

between these statistics and those quoted by Williams (1966) for pools on western Ireland pavements makes it tempting to argue that both are in equilibrium with atmospheric  $\text{CO}_2$  levels. However, a more detailed examination of the results reveals that in the Nahanni the calcium content of pool waters varied from 32 p.p.m.  $\text{CaCO}_3$  up to 121 p.p.m.  $\text{CaCO}_3$  while the pH varied between 7.8 and 8.5. The pool waters examined by Williams (1966) showed variations of similar magnitude. The calcium content of pool waters on western Ireland pavements varied from approximately 25 p.p.m.  $\text{CaCO}_3$  to more than 150 p.p.m.  $\text{CaCO}_3$  while the pH varied from approximately 7.6 up to 10.4 (Figure 3.2). Despite such variation Williams (1966) has argued that the pool waters of County Clare are in equilibrium with atmospheric  $\text{CO}_2$  levels basing his conclusion upon the use of a Trombe graph, a method that has since been shown to be inaccurate (Jacobson & Langmuir 1972).

Accurate calculation of the degree of saturation of pool waters on Nahanni pavements has shown that at the time of analysis they were undersaturated with respect to calcite, the mean  $\text{SI}_C$  being -0.47 and highly undersaturated with respect to dolomite, the mean  $\text{SI}_D$  being -1.91. In addition, it is further apparent that when analyzed these pool waters were in equilibrium with higher than atmospheric levels of  $\text{CO}_2$  for the average  $\log \text{PCO}_2$  value was -3.22 compared to the atmospheric average of -3.50 (Tables 3.1 and 3.2). Clearly these conclusions differ substantially from those arrived at by Williams, although as Figure 3.2 shows some of the pool waters examined by him appear, according to the Trombe analyses, to be undersaturated. It seems that pool waters on



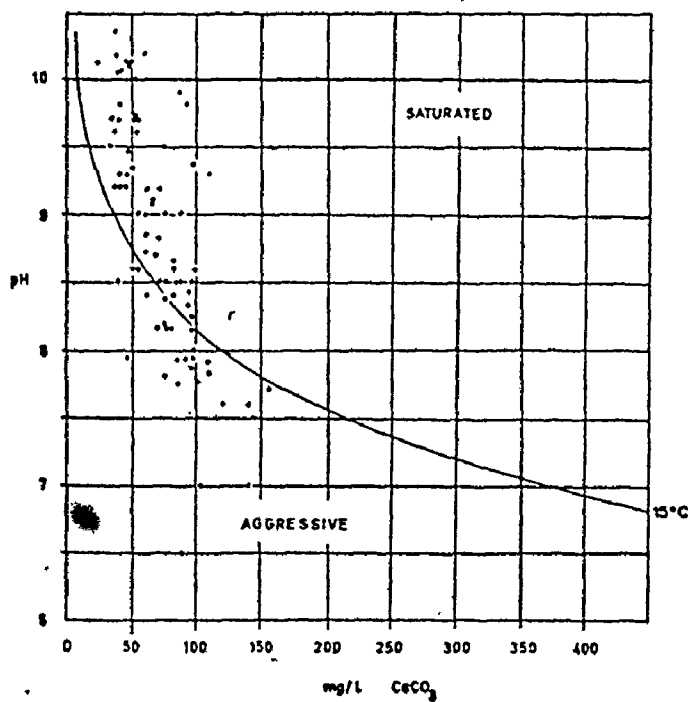


Figure 3.2. Calcium carbonate and pH of rock pools, County Clare, plotted on Trombe's graph (after Williams 1966).

Nahanni pavements have been in contact with higher than atmospheric levels of  $\text{CO}_2$  either in the soils around the pool areas or contained in the debris covering the floors of many solution basins. As to whether these pool waters do in time lose  $\text{CO}_2$  to the atmosphere as equilibration with atmospheric  $\text{PCO}_2$  levels takes place is not known but certainly it appears that at least some of the micro-solutional features on Nahanni pavements may be etched by waters containing biogenic  $\text{CO}_2$  and perhaps even organic acids.

Other water types on the limestone pavements showed very different chemical characteristics. For example, two pools on till-mantled pavements had an average temperature of  $6^\circ\text{C}$ , a pH of 7.98, a magnesium content of 11 p.p.m.  $\text{CaCO}_3$  and a calcium content of 142 p.p.m.  $\text{CaCO}_3$ . They were found to be saturated with respect to calcite (mean  $\text{SI}_C = +0.08$ ) but undersaturated with respect to dolomite (mean  $\text{SI}_D = -0.90$ ) and highly enriched in  $\text{CO}_2$  for the mean  $\log \text{PCO}_2$  is -2.80 (Tables 3.1 and 3.2). It is apparent from these statistics that these pool waters on soil-covered pavement surfaces contain approximately twice the content of dissolved calcium carbonate, are much more saturated with respect to both calcite and dolomite and are in equilibrium with higher levels of  $\text{CO}_2$  than are pool waters on bare rock surfaces. Furthermore, analysis of three seepage waters that had percolated through a soil cover and through several feet of the underlying limestone showed that these had similar chemistries to the pool waters perched on a vegetated soil surface.

One sample of soil water was also analyzed. This was extracted from soil occupying the head of a solution rannel or rinnenkarren where it left a vegetation patch. The temperature of the water was 11°C, its pH 7.7, the magnesium content 14 p.p.m.  $\text{CaCO}_3$  and the calcium content 156 p.p.m.  $\text{CaCO}_3$ . The soil water was close to saturation with respect to calcite ( $\text{SI}_C = -0.04$ ), highly undersaturated with respect to dolomite ( $\text{SI}_D = -1.09$ ) and in equilibrium with a  $\text{PCO}_2$  much above atmospheric ( $\log \text{PCO}_2 = -2.51$ ).

All of the waters on Nahanni pavements seem to contain higher than atmospheric levels of carbon dioxide even where waters reside in hollows on a bare limestone surface. There are clear differences in chemistry between waters that have had limited contact with soil and those that have infiltrated into it or rest upon it. A number of measurements of the levels of  $\text{CO}_2$  in the soils that partially or totally mantle limestone pavements in the Nahanni have been made to see if the chemical characteristics of waters can be explained in this way and to determine what influence the presence of soil on pavement surfaces has, on the evolution of these solution forms.

(ii) Soil Carbon Dioxide and Variations in Solution Intensity  
Across a Pavement Surface.

The carbon dioxide contents of soils in areas of limestone pavement development were measured at a number of localities in the Nahanni karst (Table 3.3). The apparatus used was that designed by F.-D. Miotke and fully described in Miotke (1972). The mean carbon dioxide content of nine soils examined was 0.20% by volume which is

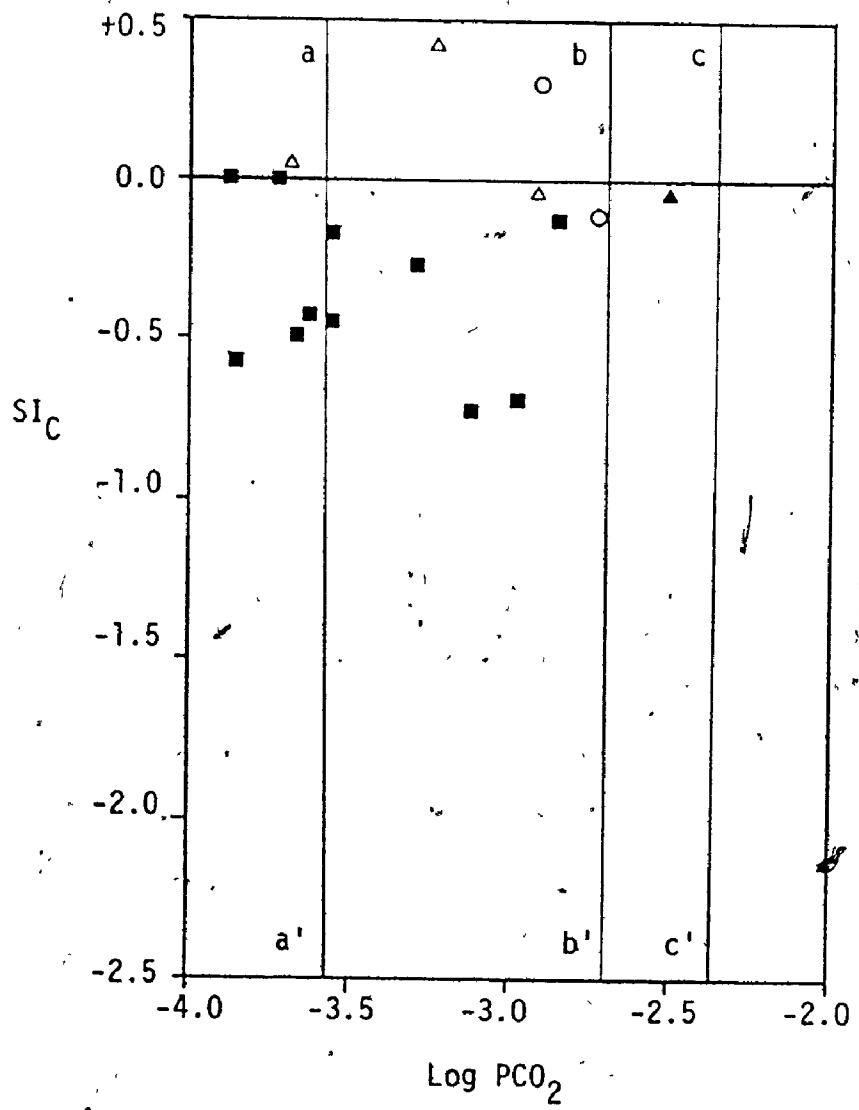
Table 3.3. Carbon Dioxide Levels in Soils on Limestone Pavements in the Nahanni.

Locality	Year	Depth cms	CO <sub>2</sub> %
On flat limestone surface close to south end of First Polje	1972	38.0	0.42
On limestone plateau surface west of Raven Lake	1972	41.5	0.07
On flat limestone surface below Corner Cave	1972	34.5	0.08
In shallow till on plateau north of Death Lake	1972	20.0	0.20
Floor of small corridor north of Death Lake	1972	45.5	0.40
Corridor floor close to Crash Valley	1972	35.5	0.03
Corridor floor on plateau south of Crash Valley	1972	37.5	0.16
Boggy hollow in plateau south of Crash Valley	1972	41.5	0.04
Grike in limestone pavement at south end of Third Polje	1973	40.5	0.43

between 6 and 7 times greater than the atmospheric level of 0.03%. Values ranged from atmospheric up to 0.43%, with the highest value, some 14-15 times atmospheric, registered for a soil filling a grike south of Third Polje. Shallow till on the Nahanni Plateau surface south of Death Lake was found to have a  $\text{CO}_2$  content of 0.2%. Overall, the results indicate that the  $\text{PCO}_2$  in the often shallow soils which mantle limestone pavements is much greater than that in the atmosphere. It is apparent that waters which come in contact with these soils should be capable of dissolving more limestone than those that do not.

Seven of the 12 pool waters on bare rock and one seepage water appear to be in equilibrium with atmospheric  $\text{PCO}_2$  while all other waters have clearly picked up additional  $\text{CO}_2$  from soils. Of the 18 samples analyzed, however, only one was found to be in equilibrium with a  $\text{PCO}_2$  level greater than the mean  $\text{PCO}_2$  measured in soils in pavement areas and none was in equilibrium with a  $\text{PCO}_2$  level greater than the maximum measured in these soils (Figure 3.3). This is strong evidence suggesting that the waters on pavements acquire their contents of  $\text{CO}_2$  from the irregularly distributed soil cover.

The fact that many pool waters on bare limestone surfaces are in equilibrium with  $\text{PCO}_2$ 's higher than atmospheric, suggests that these have been enriched by biogenic  $\text{CO}_2$ . Some water may have been enriched in this gas through contact with soils before it flowed into the rock basins. On the other hand it is also possible that at least some of it derived from the mineral and organic material which occupies the floors of many of the solution basins. Williams (1966) has essentially



- Pools on bare rock
- Pools on vegetated till
- △ Seepage waters
- ▲ Soil water
- a-a' Atmospheric  $\text{log } PCO_2$  at 3,500 ft.
- b-b' Mean  $\text{log } PCO_2$  in soils on pavements
- c-c' Maximum  $\text{log } PCO_2$  measured in pavement soils

Figure 3.3.  $SI_c$  against  $\text{log } PCO_2$  for pavement waters.

argued that carbon dioxide is not given off by this material, the Nahanni evidence, however, seems to contradict this conclusion.

Waters in constant contact with soils and equilibrated with the  $PCO_2$  in them are clearly more aggressive towards limestone. Pool waters on bare limestone surfaces, which have had little contact with soils have an average total hardness of 73 p.p.m., soil water and pools perched on soil, on the other hand, have total hardnesses of 164 and 153 p.p.m. respectively. These figures indicate that the solution of limestone on Nahanni pavements proceeds more rapidly beneath a shallow soil and vegetation cover than it does under purely subaerial conditions. As Williams (1966) has argued the magnitude of solution by waters equilibrated with atmospheric  $PCO_2$  is quite sufficient to explain many of the solution forms on Nahanni pavements. Enhanced solution beneath soils and by waters draining from soils can be invoked to explain the rest.

(d) The Development and Evolution of Nahanni Pavements.

Williams (1966) has argued that the first stage in the evolution of all limestone pavements is a period of glacial erosion when superficial material is removed and the bedrock is scoured smooth (Figure 3.4 (1)). The second stage involves the modification of the ice-scoured surface with the erasing of striations and the entrenching of grikes, runnels and small depressions. He contends that if solution proceeds beneath a permanently wet superficial cover, smooth, rounded solution forms entrenched only shallowly in the bedrock result (Figure 3.4 (2a)). On the other hand where vegetation is patchy, selective

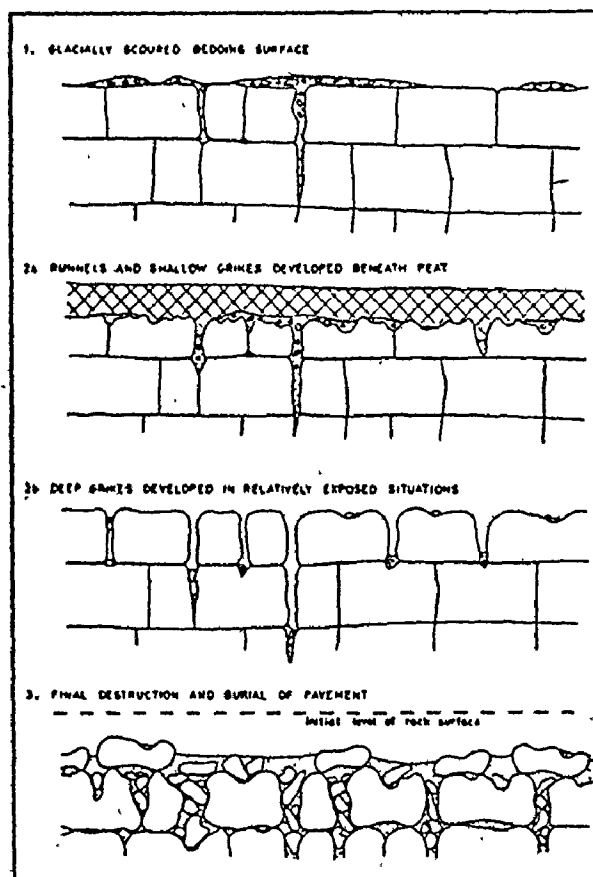


Figure 3.4. Some stages in the evolution of limestone pavements (after Williams 1966).



solution produces deep grikes and runnels and a rough, pitted surface (Figure 3.4 (2b)). Whatever the details of the solutional activity, the result is that the initial glaciated bedding plane surface is divided into clints. The third stage in pavement evolution is the destruction of the clints as grikes, runnels and rock hollows eventually consume the bed on which the pavement is developed. Broken fragments of eroded clints clog grikes and pavements are destroyed (Figure 3.4 (3)). Williams (1966) believes that pavements evolve sequentially and the sequence can only be repeated if the region is glaciated again.

As with the pavements of County Clare, Ireland, there is clear evidence that the first stage in the development of pavements in the Nahanni was one of glaciation. In fact, in regions that are thought not to have been glaciated in the recent past there are no limestone pavements. These areas are generally above 4,500 ft. and as has already been noted, they are mantled by limestone debris with little bare rock visible. That pavements appear to be restricted to areas below about 4,000 ft. - areas that show evidence of relatively recent glaciation, indicates that ice erosion is necessary to remove accumulated debris and scour the bedrock surfaces.

In the Nahanni, the glaciated rock surfaces left after the ice retreated are thought to have been almost completely mantled by a thin layer of glacial till. Even in the few predominantly bare rock areas cracks and hollows in the bedrock were probably filled with this material. This post-glacial surface was subjected to

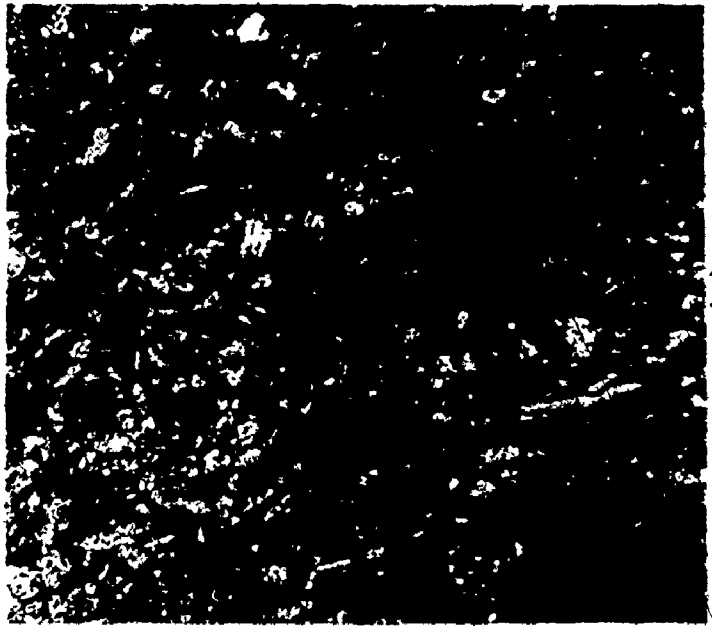
modification by a variety of processes. In areas of bare rock, fractures were enlarged and the smooth rock surfaces were etched by solution. In soil-covered areas, however, solution of the rock surface was probably insignificant until the bulk of the soluble material in the till cover had been removed. Once this had been achieved, it is likely that the intensity of solution beneath the soil cover exceeded that on nearby bare rock surfaces. This certainly appears to be the case at the present time. In any event, the glaciated rock surfaces were solutionally modified both above and beneath a soil cover as Williams (1966) has argued for western Ireland pavements.

At the same time that solutional modification of the glaciated surfaces took place, removal of the shallow till cover exposed more and more bedrock to the atmosphere. That soil erosion has been active in the Nahanni region since it was last glaciated is indicated by the widespread occurrence on pavement surfaces of now relict subsoil solution forms such as the vegetation hollow. Most of these have been substantially modified by subaerial solution processes since they were uncovered.

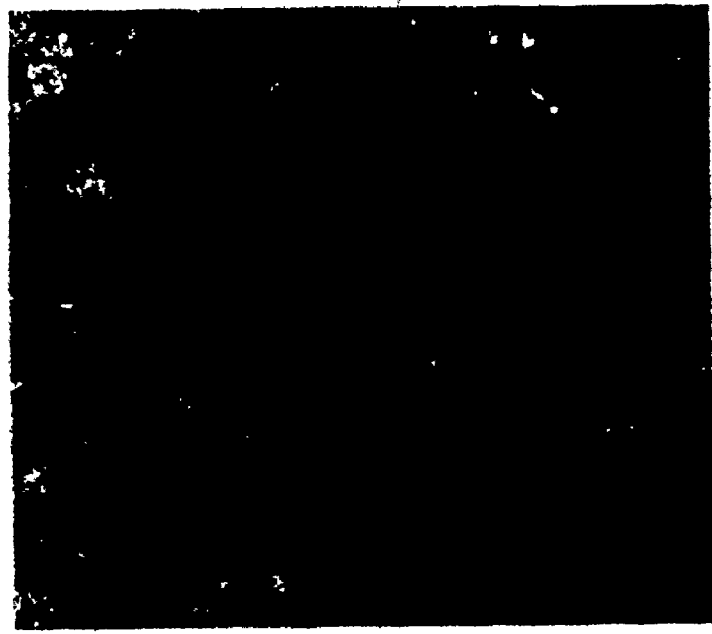
Modification of glaciated rock surfaces by solution under subaerial conditions or beneath a soil cover appears to have progressed in an extremely organized fashion. Rain falling on the pavement surfaces drained into the limestone via the most open of the joint systems - the master joints. Some of these joints had been opened by ice pressure during glaciation, others by subsequent gravitational movements of limestone blocks and in these cases the rainwater flowed

broadside down the joint widening it by solution and eventually forming a grike. Many of these open joints on bare rock surfaces were filled with soil so that solution in them was intensified by addition of biogenic  $CO_2$  to the infiltrating waters. The vast majority of master joints, however, were still tightly closed and water penetrated these at only a few irregularly-spaced weak points with the development of pit-and-tunnel drainage systems. Many solution pits on bare rock surfaces collected organic and inorganic debris and this intensified solution in them. The tunnels developed along the master, open bedding planes. Enlargement of pit-and-tunnel networks and their coalescence led to the development of master clint and grike systems (Plate 3.11 (a)). It is when the master clints and grikes have developed that a pavement has reached the peak of its formative evolution. Beyond this stage all processes seem to act to destroy it.

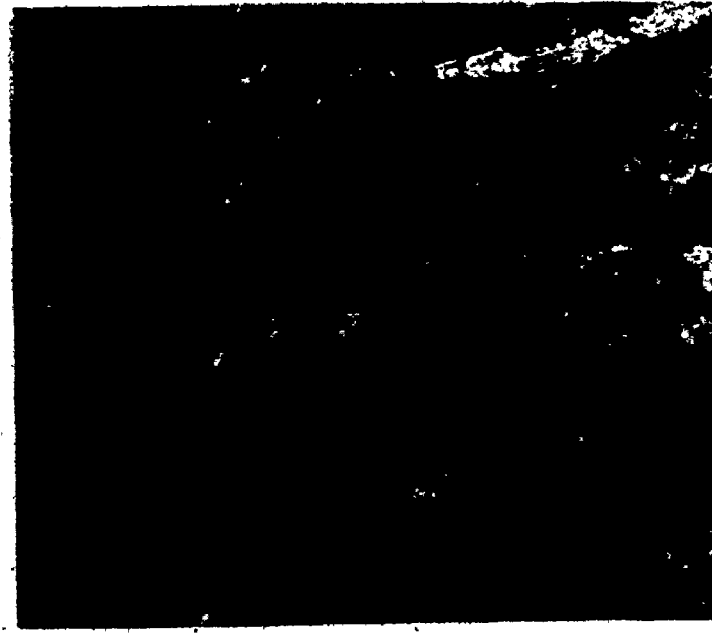
Although the breakdown of master clints can begin before they are fully isolated by the development of grike systems, in general it proceeds at some later time. Secondary fractures and minor bedding structures are often tightly closed or filled with calcite and are not as susceptible to solution as are the master joints and bedding planes. These structures, therefore, are generally opened up by solution only after the master structures have been widened. When they are eventually widened by solution, secondary clints and grikes are produced usually via a pit-and-tunnel stage. The master clints are broken down into smaller blocks which often collapse and accumulate in the master grikes. The whole breakdown process, in the Nahanni at least, is



(c)



(b)



(a)

Plate 3.11. Destruction of a limestone pavement in the Nahanni Karst. Well developed clint and grike networks (a) are gradually modified by solution and frost action. Solution etches out the minor fractures and frost breaks up the limestone into small pieces which choke the grikes (b). Eventually the pavement is reduced to a felsenneer of partially sorted, angular limestone fragments (c).

aided by freeze thaw action. Water freezing in a minor fracture widened initially by solution tends to expand the crack and speed up the breakdown of the limestone. In addition, the magnitude of contraction of the limestone at times of extremely low temperature in winter may be sufficient to induce cracking. The development of secondary clint and grike systems undoubtedly brings about the degradation of the pavement sequences (Plate 3.11 (b)), which are ultimately reduced to piles of limestone debris (Plate 3.11 (c)).

A number of important points emerge from this discussion of the evolution of limestone pavements in the Nahanni. First, it is apparent that the formative stage in pavement development is the opening up of master grike networks in the glaciated rock surfaces with the isolation of clints. Secondly, all processes that subsequently operate on the master clints serve to eventually destroy them. Thirdly, it seems certain that because the limestone pavements are presently being destroyed by both solutional and freeze-thaw processes, that they are not an equilibrium landform of sub-arctic terrains and there is considerable doubt that they are equilibrium forms of any climatic region or terrain type. Finally, as Williams (1966) has emphasized, once destroyed, pavements can only reform if the accumulated debris is removed. The only really effective mechanism for doing this seems to be glacial erosion.

### 3. Dolines.

In fluvial landscapes the diagnostic landform is the stream valley; in karst landscapes it is invariably the doline. The doline

is generally regarded as the fundamental unit of karst relief. Dolines are closed depressions of moderate size and may be dish, bowl, conical or cylindrical shaped. The diameter is usually greater than the depth with the majority of dolines being from 5-300 ft. deep and 30-3,000 ft. in diameter. Dolines may occur singly or in groups and they may be formed entirely in bedrock or entirely in unconsolidated sediment overlying bedrock. When two or more dolines increase in size and coalesce a complex closed depression known as an uvala is produced. Uvalas are generally from 1,500-3,000 ft. in diameter and are from 300-600 ft. deep; characteristically they have undulating floors. Jennings (1970) has pointed out that when a doline in bedrock approaches the form of a vertical shaft there is a transition to the pothole. When they become elongated in plan there is a transition to the karst corridor and if a stream runs into a doline there is a transition to a blind valley.

In 1893 Cvijić distinguished three main types of doline on morphological grounds. Bowl-shaped dolines he described as having a diameter to depth ratio of approximately 10 to 1, flat floors covered with soil and frequently marshy, and slope angles of  $10^{\circ}$ - $12^{\circ}$ . In funnel-shaped dolines, on the other hand, the diameter is only 2-3 times the depth and the sides, in either rock or soil, slope at angles of  $30^{\circ}$ - $40^{\circ}$ . Well-shaped dolines, the least common of the three types, have diameters usually less than their depths and have very steep to vertical sides.

Since the work of Cvijić, dolines have been variously classified. Sweeting (1972) for instance recognizes normal solution, alluvial,

solution subsidence and collapse dolines. A more comprehensive classification, and one that will be adopted here has been outlined by Jennings (1970) who recognizes solution, collapse, subjacent karst collapse, subsidence (including suffosion) and alluvial streamsink dolines (Figure 3.5).

All of the doline types recognized by Cvijić (1893), Sweeting (1972) and Jennings (1970) are to be found in the Nahanni karst. In addition a number of dolines of undoubted structural origin have been identified and these will be referred to here as 'structural dolines.' Together the various doline types and blind valleys make up an extremely dense assemblage of closed depressions (Figure 1.6) that would be more characteristic of a much warmer climatic region. It is remarkable that so many kinds of doline in such great numbers are present in this high-latitude sub-arctic region. Characteristics of the various doline types in the Nahanni will now be discussed.

(a) Structural Dolines.

A number of closed depressions in the Nahanni appear to be almost entirely structural in origin. The most impressive of these features is Palsa Basin in the North karst which is approximately 600 yards long, 400 yards wide and has a closure of 15-20 ft. (Plate 3.12; Figure 3.6). Palsa Basin appears to be little more than a structural depression in the upper surface of the Nahanni Formation limestones that has been stripped of overlying shales of the Fort Simpson Formation. The rock basin with the limestone dipping towards its center at angles from 6.5°-14° appears to be little modified by

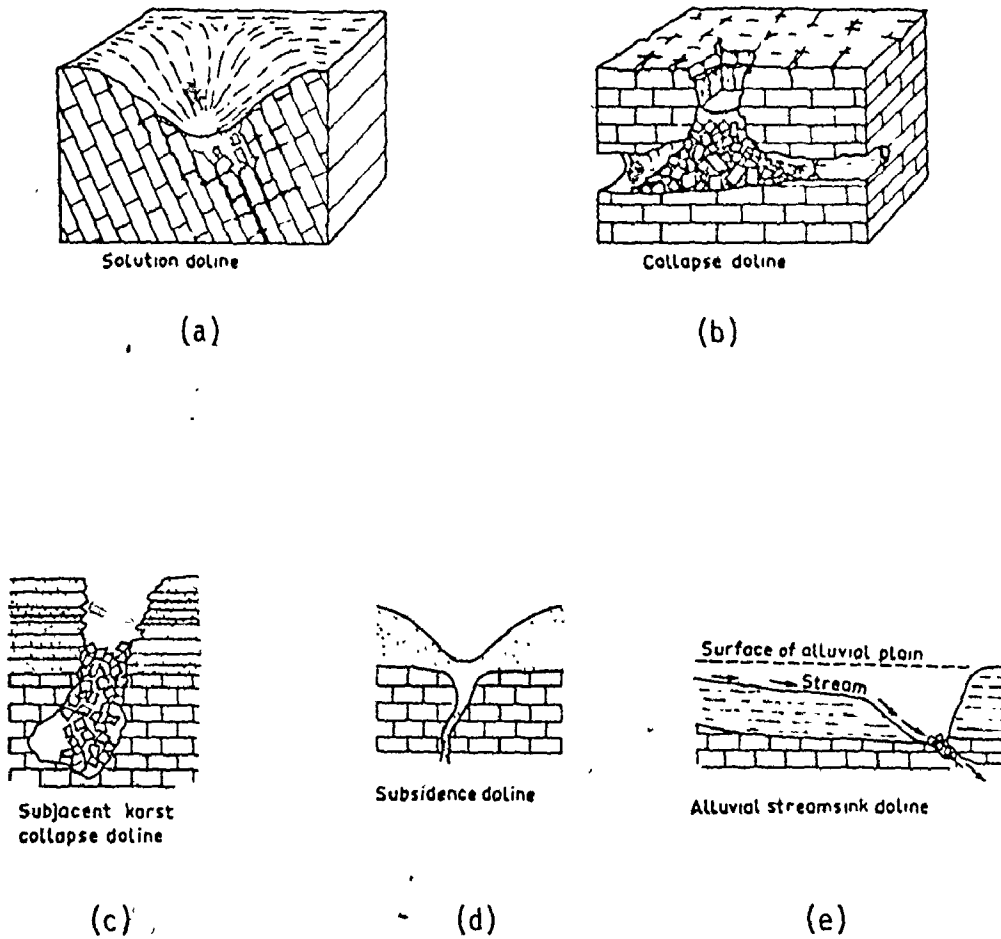


Figure 3.5. The main categories of doline (after Jennings 1970).





Plate 3.12. Palsa Basin, a structural doline. This depression is little more than a shallow basin in the upper surface of Nahanni Formation limestones. The doline is flanked on two sides by shales of the Fort Simpson Formation.

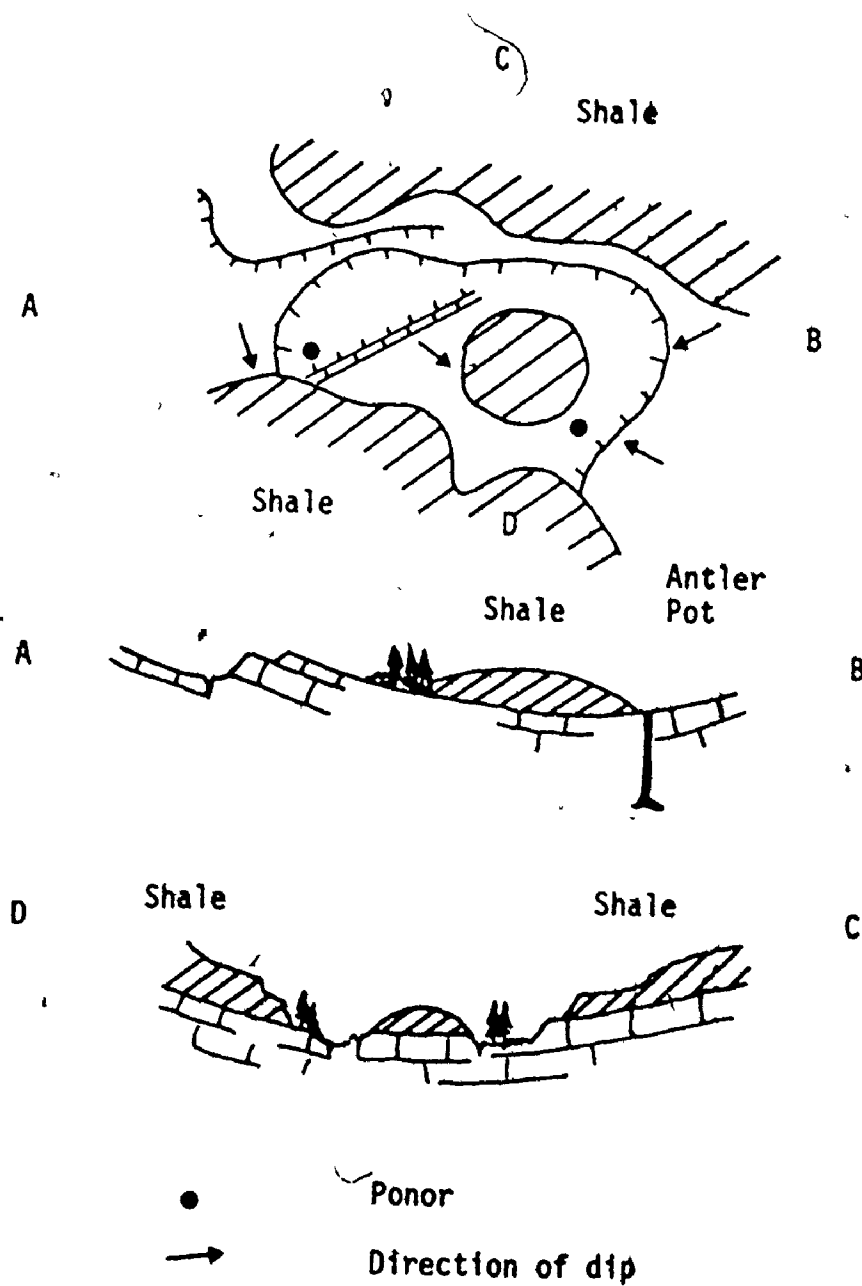


Figure 3.6. Plan and schematic geological sections of Palsa Basin, a structural doline.

solution. It is apparent from observations elsewhere in the karst that minor domal and basinal structures are common in the limestones of the Nahanni Formation (Plate 3.13). They are obviously preserved because water reaching them drains underground rather than being discharged in surface streams which would cut through the lips of such depressions.

Palsa Basin although formed entirely in limestone is flanked on two sides by shales (Figure 3.6). It likely represents a very early stage in the karstification of the Nahanni Formation limestones following removal of overlying shales. A number of small streams, their headwaters in the shales, funnel water into the doline which has a partially alluviated floor and at least three large ponor outlets. Two of the ponors are heavily alluviated; the third, Antler Pot is a vertical shaft 60-100 ft. in depth believed to be blocked by breakdown debris. In early August 1973 a small stream was plunging into it. As to just what the mechanism was that stripped the shales from the limestones in the vicinity of Palsa Basin is not known, but there is some evidence to suggest that it was stream action with the stream waters eventually draining underground. At least partial stripping by glacier erosion can not be discounted, however.

(b) Solution Dolines.

Within bare limestone regions of the Nahanni karst are ubiquitous vertical-walled dolines (Plates 3.14 & 3.15) which essentially fall into the category of well-shaped doline as differentiated by Cvijić (1893). In mantled karst areas, however, solution dolines



Plate 3.13. Synclinal structure in Nahanni Formation limestones. The upper surface of the Nahanni Formation is characterized by numerous shallow anticline, syncline, domal, and basinal structures. A shallow syncline is clearly visible in this photograph of the north wall of Death Canyon at left center.



Plate 3.14. Rappel Cenote, Cenote Col, North Karst. This vertical-walled pond doline is more than 90 feet deep. During the summers of 1972 and 1973 there was ice on the surface of the pond in its floor. Despite the narrowness of the wall between the doline and South Col Canyon (at left in photograph) water does not move laterally in this direction.



Plate 3.15. Vertical-walled solution doline in bare karst, Nahanni Plateau south of Crash Canyon.

tend to be either bowl- or saucer-shaped (Plate 3.16). Vertical-walled dolines are of two main types. First are those that have developed in a single fracture and tend to be elliptical in cross section (Plate 3.14) and second are those that have developed at locations where a number of joints or faults intersect (Figure 3.7). These are generally circular to oval in cross section. Both types have vertical walls with floors mantled in limestone debris, and commonly the bases of the walls are flanked by talus aprons. Temporary ponds which are from a few feet to 100 ft. in depth, and 60-100 yds. in diameter, are characteristic of both types (Plate 3.14).

Although vertical-walled solution dolines are present at locations throughout the Nahanni karst, the most marked concentrations of these forms is on Cenote Col a residual ridge of limestone in the natural rock labyrinths of the North karst. On this ridge, in an area a little more than 300 yds. by 100 yds., there are 23 vertical-walled solution dolines up to 100 ft. in depth. Many of them contain water (Plate 3.17, Figure 3.8). Such a marked concentration of forms is remarkable for such a high-latitude terrain.

It is apparent that many of the dolines on Cenote Col have formed by the coalescence of smaller features. For instance the shape of Surprise Doline suggests that it grew from at least three smaller dolines by the breakdown of intervening walls. Hidden Doline, on the other hand, is obviously an isolated form (Figure 3.7). Other large dolines such as Rappel Cenote (Plate 3.14) probably grew from one or more small dolines developed in the same fault or joint. A number



Plate 3.16. Solution doline on till-covered limestone. This enclosed depression and others in the area were formed as surface drainage waters were pirated underground. Limestone bedrock is visible at left.



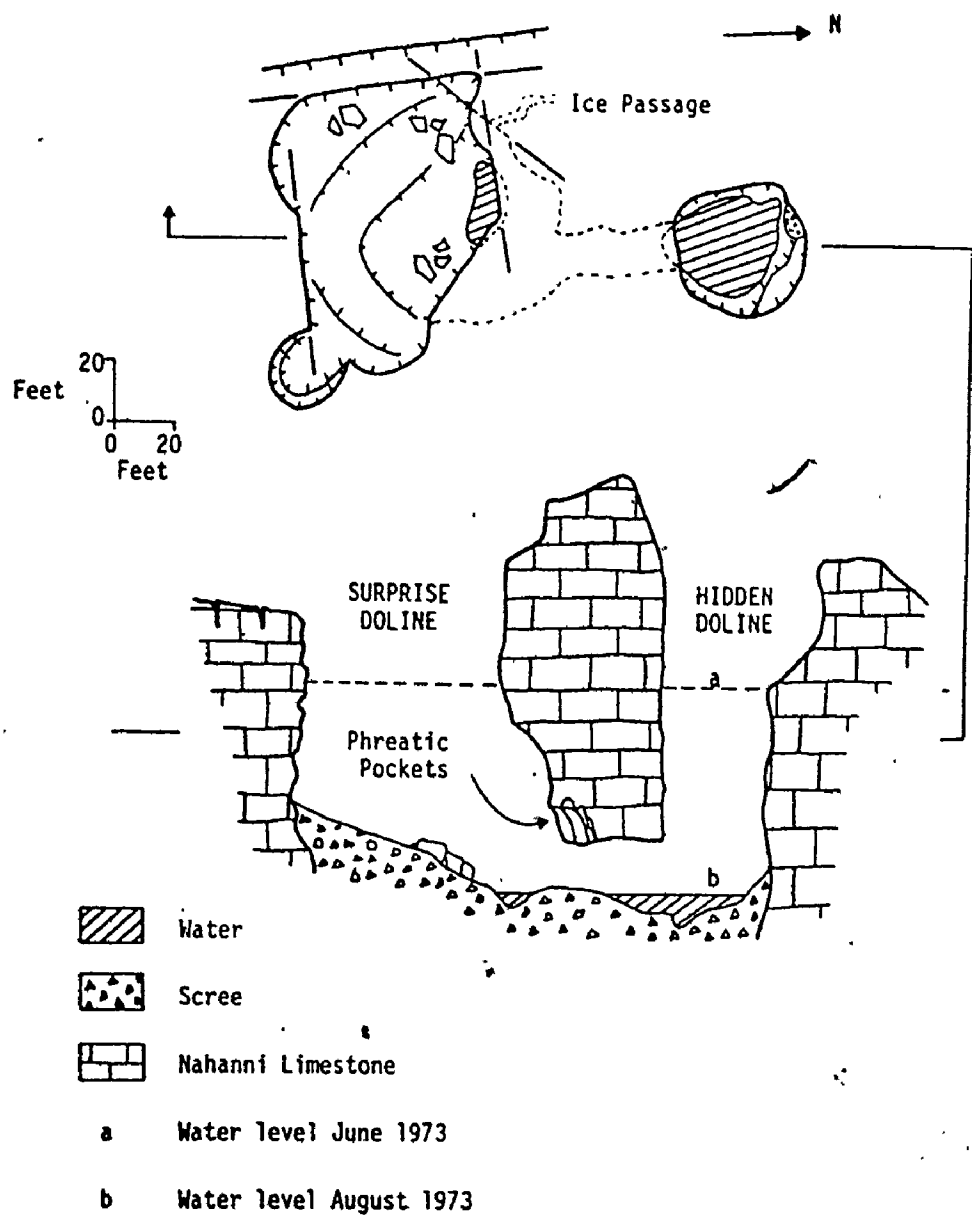


Figure 3.7. Plan and Section of Surprise and Hidden Dolines, Cenote Col, North Karst.



Plate 3.17. Aerial view of Cenote Col, North Karst labyrinths, showing the spectacular solution doline assemblage. At least 15 depressions, some with ponds are visible in the photograph. At left is North Col Canyon the largest karst pleatea in the region and at right South Col Canyon also a platea. In the background the Nahanni Formation-Simpson Formation contact is clearly visible.

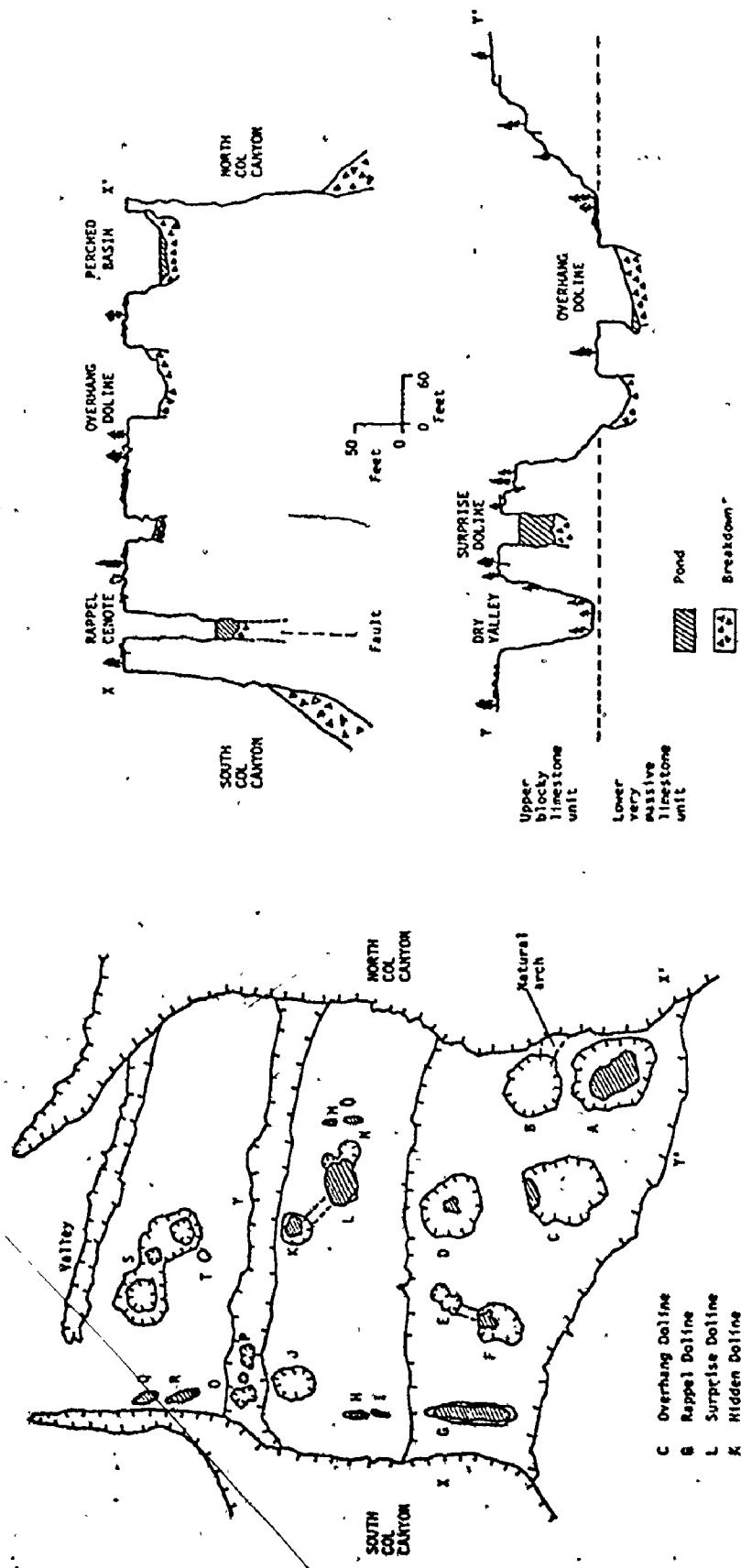


Figure 3.8. The solution dolines of Cenote Col, North karst labyrinths.

of dolines on Cenote Col look as if they will eventually coalesce to form single larger forms. For instance, in Figure 3.8(a), pond dolines H and I are close together and are developed in the same fracture; sooner or later they will coalesce. The same will probably happen to M and N, and Q and R. Other doline pairs such as Surprise and Hidden Dolines (Figure 3.7), and dolines E and F in Figure 3.8 (a), which have developed at joint intersections, are known to be connected by caves. It seems likely that these two pairs of depressions will also coalesce at some time in the future as the cave roofs collapse. Proof of doline growth and coalescence is to be found in closed depression S in Figure 3.8(a). This feature is a small uvala made up of three separate dolines.

Many of the vertical-walled dolines on Cenote Col and others elsewhere in the karst contained ponds up to 50 ft. in depth when examined during the summers of 1972 and 1973 (Plates 3.14, 3.17, 4.6). When ponds are present these dolines bear a striking resemblance to classical cenotes such as those of the Yucatan Peninsula, Mexico. Shrock (1945) has argued that these latter features are vertical-walled collapse pond dolines formed when the regional water table was at a slightly lower elevation than it is at the present time. A subsequent rise in the water table, he contends, flooded the bases of these depressions. The cenote of Chichen Itza, a very famous Mayan sacrificial well, is 210 ft. deep with the lower 140 ft. flooded. Sweeting (1972) feels that at least some of the cenotes of the Yucatan Peninsula are former springs. She believes that the water table may have been lowered

sufficiently that water can no longer flow over the lips of these structures and argues that "The conventional explanation of a simple collapse cavern origin for the cenotes does not seem entirely convincing, since their distribution and frequency are not entirely characteristic of collapse phenomena" (p. 216).

Whatever the origin of the classical cenote form, it seems certain that the vertical-walled pond dolines of the Nahanni were formed differently. Perhaps the most obvious difference between the two categories of landforms is that the ponds in the Nahanni dolines are perched so that pond levels between closely spaced water bodies on Genote Col may differ by as much as 100 ft. (Figure 3.8). Pond levels in the cenotes of the Yucatan are, on the other hand, thought to parallel the regional groundwater table which is remarkably flat. Perching of water in the Nahanni is thought to be caused by the blockage of doline drainage routes by subsurface ice. The presence of such ice is to be expected in this region of discontinuous permafrost.

The marked vertical development of dolines in the bare karst regions of the Nahanni is undoubtedly related to the structural properties of the Nahanni Formation limestones. Of particular importance have been the massiveness of the limestones and the openness and persistence of vertical faults and joints. The greater frequency of open sub-vertical fractures to open bedding planes in the limestones clearly resulted in a greater concentration of groundwater flow along fracture planes than along bedding planes. For instance, there is no evidence in the 90 foot vertical or overhanging walls of Rappel Cenote

to suggest even minor past or present water movement along bedding planes (Plate 3.14). On Cenote Col, at least, the vertical movement of groundwater still predominates at the present time for despite the narrowness of the limestone walls which separate Rappel Cenote from South Col Canyon (10-15 ft.) and Perched Basin from North Col Canyon (5-10 ft.) these dolines still contain ponds (Figure 3.8). When water has moved laterally it appears to have followed the fracture planes as evidenced by the fracture-located caves which join at least two pairs of dolines on Cenote Col (Figure 3.8 (a)). Vertical-walled solution dolines in the Nahanni have developed in both the upper rubbly and middle massive units of the Nahanni Formation (Figure 3.8 (c)). Much of the debris that mantles the floors of most dolines is derived either from the rubbly unit or from thinly bedded recessive units in the middle massive unit (Plate 3.14). The massive nature of the limestone as a whole, however, with the resulting great internal strength of the rock has allowed the development and survival of vertical-walled features. Had the rock been less resistant to breakdown by mechanical or chemical means, vertical dolines would not have developed. Nor would they have developed if the available vertical relief in the area had been of little magnitude.

The vertical-walled dolines of the Nahanni appear to have formed by the action of solution from the ground surface. There is no evidence to suggest that they are collapse features or that they were former spring outlets. Solution was concentrated in fractures with water moving down them at irregularly spaced weak or open zones. Following their initial development, solution in the dolines may have been

intensified because they accumulated snow during the winter months. Despite 9.03 inches of rainfall on the Nahanni karst in the 15 days between July 20th and August 3rd, 1972, pond levels in the dolines on Cenote Col changed little demonstrating that rainwater is not funnelled into them. Much of the water in Nahanni pond dolines is believed to be melted snow that was blown into these depressions during the winter months. Enhanced solution in them may also have occurred when drainage routes were temporarily blocked by ice and ponding of waters occurred.

It is apparent that although superficially similar to the classical cenotes of the Yucatan, the vertical-walled pond dolines of the Nahanni differ markedly in present hydrology and mode of origin from these features. They appear to be a remarkable sub-arctic variant of vertical-walled pond dolines elsewhere in the world where the perching agent is impermeable clay. In the case of the Nahanni features the perching agent appears to be ice.

In limestone areas mantled by a till cover, the morphology of solution dolines is quite different from that of features developed in bare limestone regions (Plate 3.16). Dolines are generally basin-shaped with flat alluviated floors and many contain ponds perched on this impermeable material. Individuals may be up to 100 ft. in depth and 300 yards in diameter with side walls sloping at 30°-40°. The smooth rounded forms of the dolines are in marked contrast to the sharp outlines of solution dolines developed in bare limestone regions. This roundness is undoubtedly related to the presence of the till

cover which not only mantles vertical limestone walls in some places but also tends to encourage solution at the doline walls as well as in their floors. Water is held by the till and subsoil solution proceeds everywhere beneath it. In the Nahanni karst, at least, smoothness of doline form appears to be related to the presence or absence of a cover on the limestone.

The majority of solution dolines in the mantled karst areas of the Nahanni appear to represent karstified stream drainage networks. These networks are thought to have developed on the impermeable till cover shortly after glacier retreat and waters were pirated underground once the stream cut into the underlying limestone. These features appear, therefore, to be the end product of blind valley development from an initial surface stream network. Surface runoff into these features after heavy rain is characteristic and this has probably been far more significant in their evolution than has solution by melting snowdrifts accumulated during the winter. Because of the surface runoff on the impermeable till after rain, small stream valleys cut into the walls of these dolines are characteristic.

(c) Collapse and Subjacent Karst Collapse Dolines.

The least common of the various doline types that have been recognized in the Nahanni karst is the collapse doline. Only one definite example has been discovered although it is suspected that more do exist and also that some vertical-walled solution dolines in bare limestone regions may be at least partly of collapse origin. This doline, in the limestone surface to the north of Stal Gorge in



the North karst, is 80-100 ft. in diameter and 40-50 ft. deep with vertical to overhanging ragged walls. The depression which can be entered via a large cave in the north wall of Stal Gorge was clearly formed by the partial collapse of the roof of this cave. The floors of both doline and cave are covered by uneven accumulations of breakdown blocks. It is evident that large portions of the roof of the cave collapsed at some time in the past but in only one small area was collapse total.

By comparison with simple collapse dolines, subjacent karst collapse dolines are relatively common and show their most marked development in the region to the south of Mosquito Lake where both dolines and uvalas are present (Figure 3.9). In this region the depressions may be up to 250 yards long, 60 yards wide and 150 feet deep. Most are bowl-shaped with steep sides sloping at  $30^{\circ}$ - $50^{\circ}$  and have flat floors because of a fill of shale-derived alluvium. Because this material is at least partially impermeable, depression floors are often marshy and many contain ponds. All forms have a rounded appearance because of a cover of glacial till 1-10 ft. thick. Streams flow into these depressions after rain so that shallow stream valleys are common in their walls.

Nowhere in any of the depressions south of Mosquito Lake was an outcrop of limestone discovered but exposures of shale were observed in the walls of two dolines. It is apparent that these features are at least partly developed in shale and the absence of limestone suggests that they may be of subjacent karst collapse origin. The

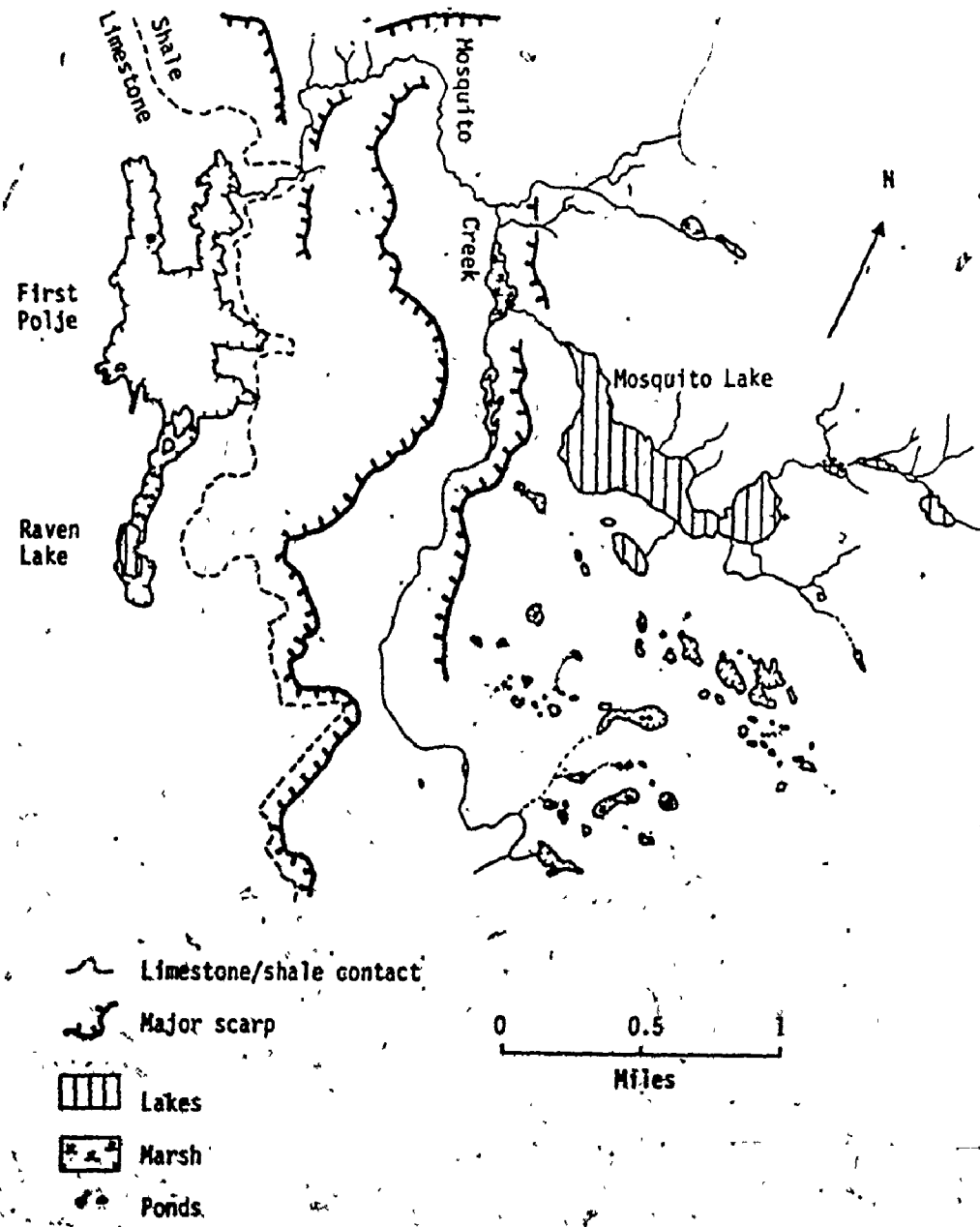


Figure 3.9. Distribution of subjacent karst collapse dolines, south of

most likely explanation is that they were formed by the collapse of parts of a shale cover into solution cavities in the underlying limestones (Figure 3.10). The sizes of some of the closed depressions suggest that the solution cavities must be of considerable dimensions. The discovery of a very recent, small collapse doline 40 ft. in diameter and 10-15 ft. deep during an aerial reconnaissance in 1974 indicates that collapses are still occurring. This depression is circular in shape, has vertical walls cut in either shale-derived alluvium or weathered shale and contains a perched water body. Although bedrock is not visible in its walls, it likely connects with a solution cavity in limestone at shallow depth.

Water entering these subjacent karst collapse dolines in shale is believed to percolate underground through collapse breccia zones in the shale and then enter caves in the underlying limestone. Once the water reaches the limestone it moves approximately down the dip, its actual path being controlled by single fractures or zones of fractures in the limestone. It is ultimately thought to emerge at spring points in the east wall of First Polje, the main one being Tufa Spring (Figure 3.10). The water which emerges at Tufa Spring contains on average 55 p.p.m. sulphate ion which is thought to be picked up from the shale - a rock which commonly contains minor percentages of impurities including sulphur.

The initial cavities in the limestone, into which the shale collapsed, were probably produced by movement of groundwater through the limestone aquifer from a recharge area to the east of Mosquito

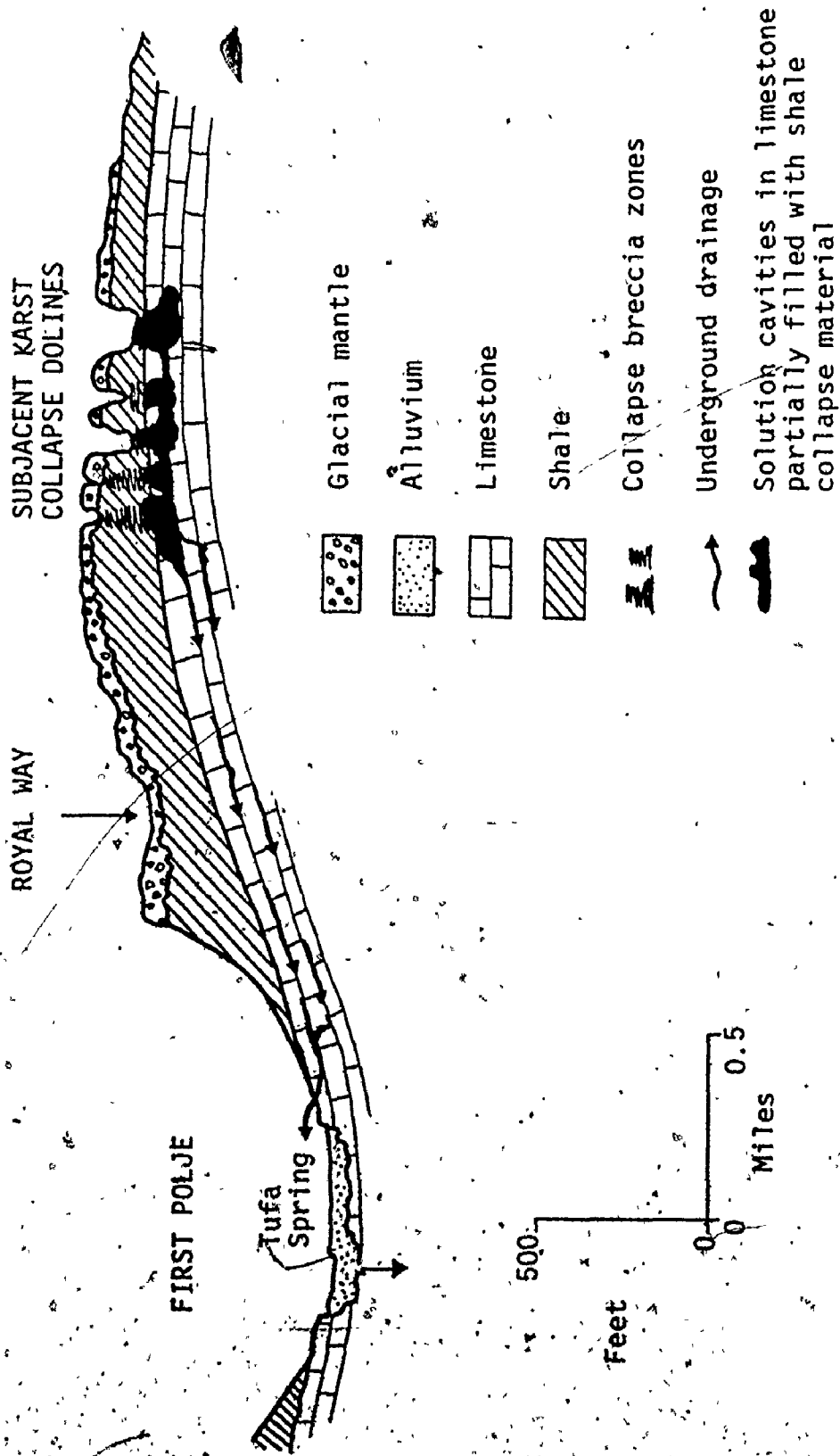


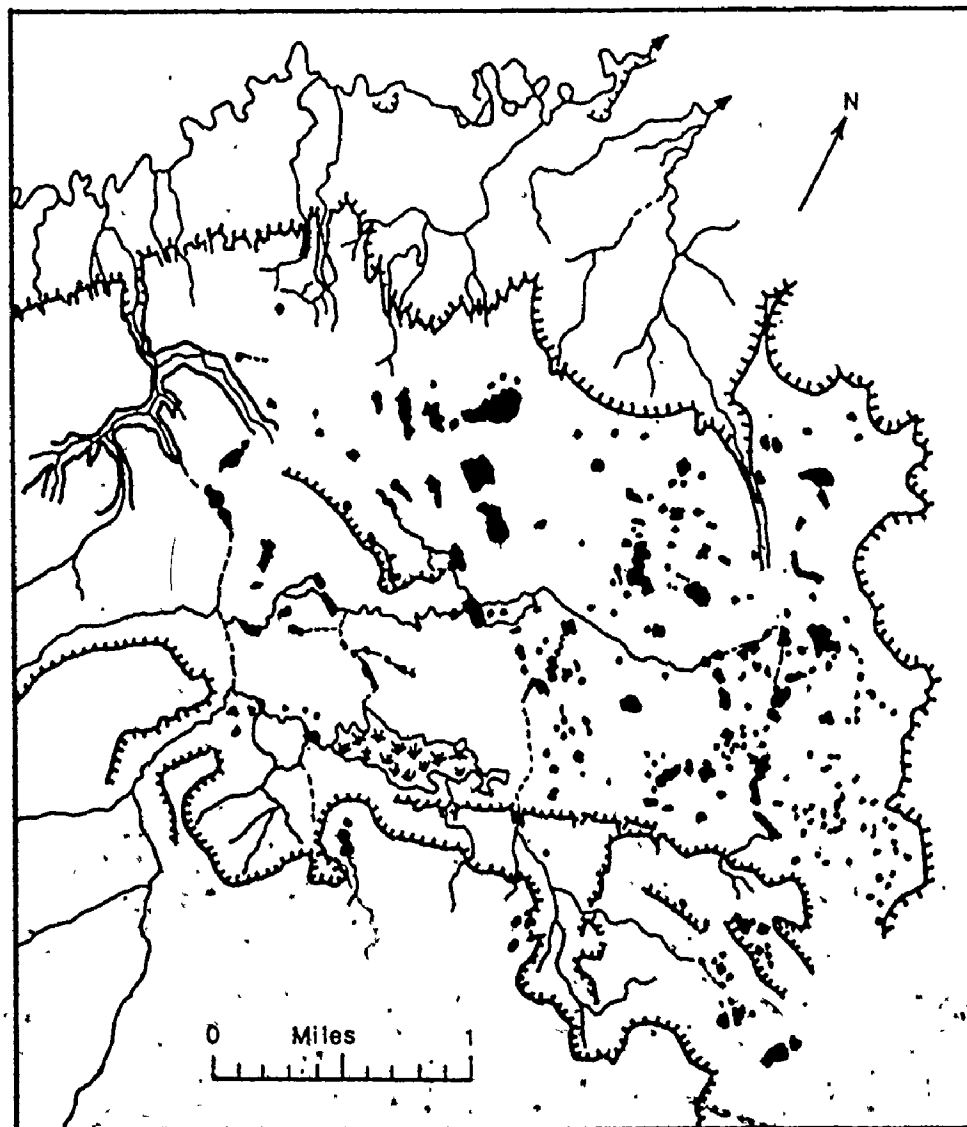
Figure 3.10. Schematic geologic and topographic section through the subjacent karst collapse dolines south of Mosquito Lake. The diagram shows the likely hydrological relationship between water sinking in these depressions and that emerging in springs in First Polje.

Lake where limestone again outcrops at the surface although it is mantled by glacial till. In addition, there may have been minor movement of water through fault breccia zones in the shale.

(d) Subsidence, Suffosion and Alluvial Streamsink Dolines.

Subsidence, suffosion and alluvial streamsink dolines are all formed partly in limestone and partly in overlying unconsolidated sediments and it is often difficult to differentiate between them in the field. All are common in mantled karst regions of the Nahanni. Alluvial streamsink dolines or ponors are well developed in the floors of the three Nahanni poljes. Streams entering the poljes sink at these ponors after flowing across the alluvial floor of the depressions. The ponors are largely developed in the alluvium mantling the limestone although bedrock is visible in some features.

Subsidence and suffosion dolines develop through spasmodic subsidence and more continuous piping or suffosion of unconsolidated materials overlying soluble rocks, into widened joints and solution pipes in the bedrock beneath. Dolines of both kinds may be of variable shape and size. Rapid subsidence may temporarily produce a cylindrical hole which rapidly weathers into a gentler conical- or bowl-shaped depression. Gradual suffosion of material underground also initiates and maintains with enlargement conical- and bowl-shaped dolines so that differentiation of the two forms in the field is difficult. Both types of doline are common in two mantled karst areas of the Nahanni, the first an area east of Insel Tower and the second the area of the 'Sink-hole Plain' (Figure 3.11). Both areas are in the North karst region.







-  Major scarps
-  Marshy terrain
-  Closed surface depressions
-  Indeterminate drainage lines

Figure 3.11. Map of Suspected Subsidence and Suffosion Dolines on the Sinkhole Plain, Nahanni North Karst.

East of Insel Tower a number of subsidence or suffosion dolines pock-mark the flat upper surface of a layer of alluvium that rests on limestone. The dolines are up to 150 ft. in diameter and 100 ft. deep and have a marked funnel shape (Plate 3.18). They occur in strings that obviously parallel solutionally widened fractures in the underlying limestone. Parent-daughter patterns are often evident. Bedrock is not visible in any of the forms, which appear to be entirely developed in the surficial cover. An excavation at 30 ft. depth in the side of one doline showed the cover to be a poorly sorted, poorly bedded fluvial deposit made up of shale fragments and erratic igneous and metamorphic pebbles in a sandy matrix. Both subsidence and suffosion likely played some part in the development of these forms.

West of First Polje on the Sinkhole Plain is a dense assemblage of saucer-, basin- and funnel-shaped dolines that appear to be entirely developed in a thick, poorly-sorted glacio-fluvial deposit resting on limestone. The deposit consists of rounded pebbles of sedimentary, igneous and metamorphic material up to 4 inches long in a sandy-silt matrix. Numerous saucer-shaped depressions up to 300 yds. in length and 50 ft. in depth appear to be suffosion dolines formed by the transport of material into cavities in the underlying limestone via networks or small joints. The floors of these depressions are nearly always marshy and some contain ponds.

More spectacular are the well developed bowl- and funnel-shaped dolines of this region (Plate 3.19), which are up to 250 ft. in diameter and 100 ft. in depth and often contain water. Unlike the saucer-shaped

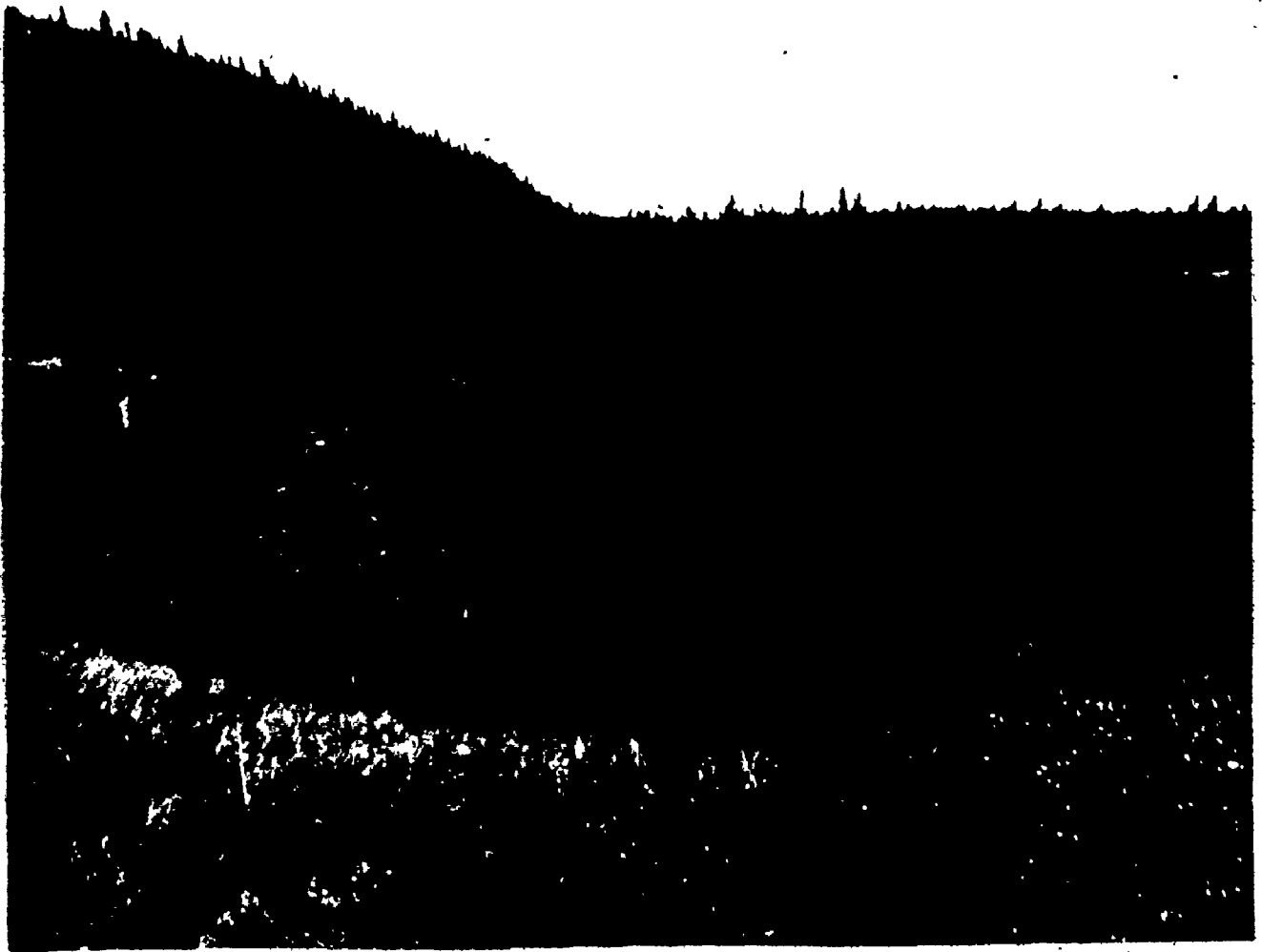


Plate 3.18. Suffosion doline in fluviably-reworked glacial debris resting on limestone, Insel Tower region, North Karst.



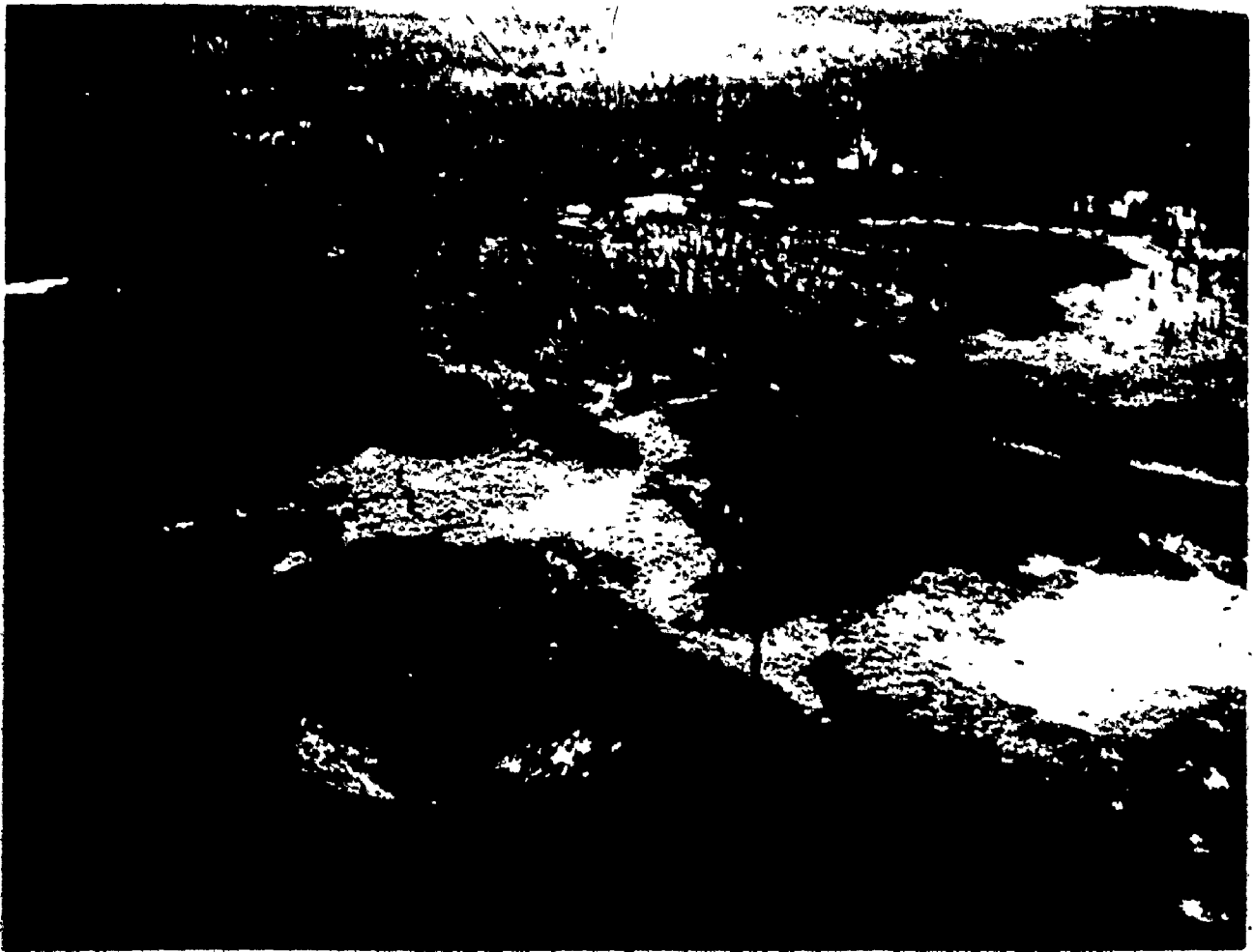


Plate 3.19. Funnel-shaped suffosion dolines developed in superficial glacial debris resting on limestone, Sinkhole Plain, North Karst.

dolines on the Sinkhole Plain, basin- and funnel-shaped depressions appear to have been produced by movement of material into single cavities in the underlying limestone. Once formed, many of these depressions grow laterally as their sides slump - particularly after heavy rain. At the same time, because much of this material is washed towards the centers of these depressions they become shallower. Further subsidence leads to a 'doline within a doline' depression, a number of which have been identified on the Sinkhole Plain.

Much of the water sinking in this region is thought to drain either to Bubbling Springs or to a number of small springs that have been discovered in the west wall of First Polje. The high density of sinkholes on the Sinkhole Plain indicates the existence of numerous large and small solution cavities in the underlying limestone.

(e) Characteristics of Solution in Nahanni Dolines.

During the summer of 1972, samples of pool, pond and seepage waters were taken from solution dolines in bare and mantled karst areas and also from subjacent karst collapse dolines in shale. All samples were collected within the North karst region, their chemical characteristics are shown in Tables 3.4 and 3.5. Summary statistics are given in Table 3.6 and the data is graphed in Figure 3.12.

Solution doline pond waters in areas of bare limestone have an average pH of 7.97, a total hardness of 83 p.p.m., an  $SI_C$  of -0.37 and a  $\log PCO_2$  of -3.06. They are clearly in equilibrium with partial pressures of  $CO_2$  higher than that of the atmosphere and are slightly undersaturated with respect to calcite. This suggests that waters

Table 3.4. Chemical Characteristics of Some Waters Associated with Solution Dolines in Bare Limestone Regions of the North Karst.

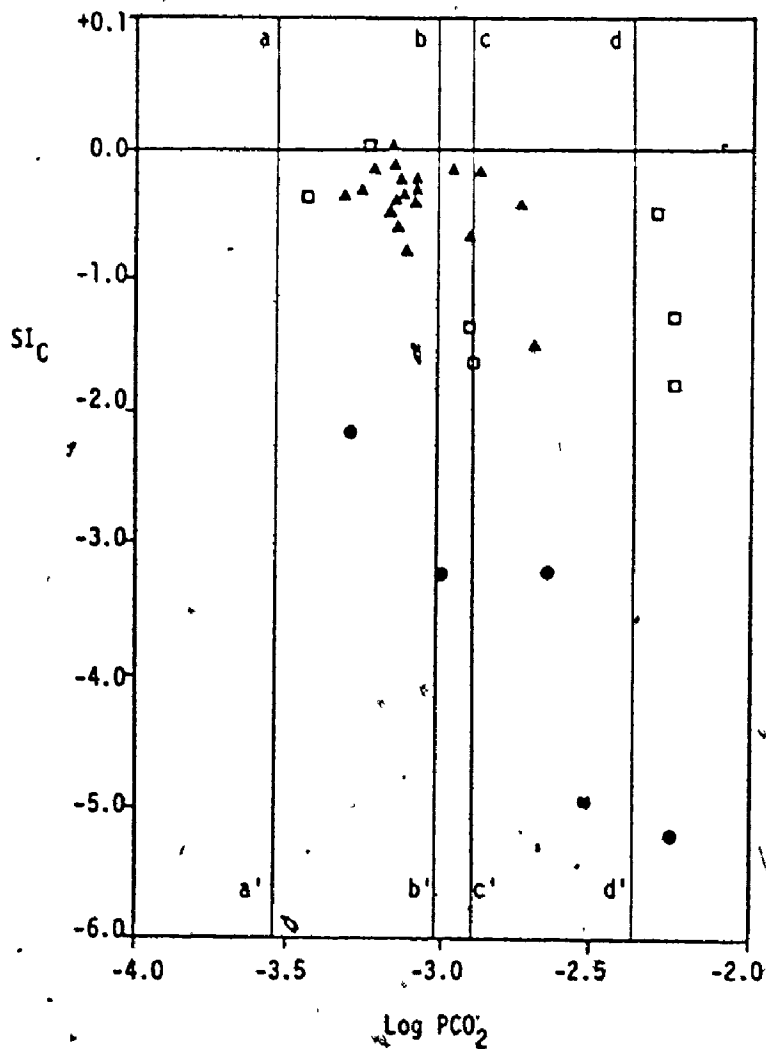
Date	Water Type	Sample ID	Temp °C	pH	CaCO <sub>3</sub> ppm	MgCO <sub>3</sub> ppm	SI <sub>C</sub>	SI <sub>D</sub>	Log PCO <sub>2</sub>
9/7/72	Pond	34	15.0	8.00	61	5	-0.36	-1.79	-3.15
"	Pool	32	4.5	7.80	75	9	-0.66	-2.22	-2.91
	Pond	35	16.0	7.94	62	7	-0.38	-1.69	-3.09
"	Pond	36	17.0	8.05	64	12	-0.21	-1.13	-3.14
10/7/72	Pond	37	4.5	8.15	76	5	-0.31	-1.75	-3.26
9/7/72	Pond	38	5.0	8.20	102	15	+0.01	-0.77	-3.16
10/7/72	Pond	39	5.5	7.80	96	20	-0.39	-1.41	-2.75
"	Pond	40	6.0	7.40	41	9	-1.46	-3.53	-2.70
16/7/72	Pond	56	15.0	7.90	89	21	-0.15	-0.91	-2.88
"	Pond	58	14.0	8.10	74	10	-0.12	-1.10	-3.16
"	Pool	57	11.5	8.00	65	31	-0.43	-1.15	-3.17
9/7/72	Seepage	33	9.5	8.00	96	13	-0.12	-1.07	-2.97
28/7/72	Pond	82	12.5	8.00	74	11	-0.27	-1.34	-3.08
14/7/72	Pond	51	15.0	8.15	65	21	-0.12	-0.71	-3.22
16/7/72	Pond	59	15.5	8.00	66	13	-0.26	-1.21	-3.08
9/7/72	Pond	31	13.0	8.00	62	9	-0.39	-1.60	-3.14
"	Seepage	30	7.0	8.15	68	5	-0.35	-1.79	-3.32
"	Stream Sink	29	9.5	7.95	63	7	-0.56	-2.04	-3.15
"	Stream	28	7.5	7.85	54	12	-0.82	-2.26	-3.11

Table 3.5. Chemical Characteristics of Some Standing Waters in Subjacent Karst Collapse Dolines on Shales South of Mosquito Lake and in Solution Dolines in Mantled Karst Areas North of Death Lake.

Date	Water Type	Sample ID	Temp °C	pH	CaCO <sub>3</sub> ppm	MgCO <sub>3</sub> ppm	SP <sub>C</sub>	SI <sub>D</sub>	Log PCO <sub>2</sub>
<u>Subjacent Karst Collapse Dolines</u>									
6/7/72	Pond	6	17.0	6.70	10	4	-3.18	-6.75	-2.67
"	"	7	19.0	6.60	5	2.5	-3.19	-8.27	-3.02
"	"	8	19.5	5.50	2	0.5	-5.18	-12.22	-2.26
"	Lake	9	19.0	7.50	11	5	-2.14	-4.62	-3.30
<u>Solution Dolines on Till-covered Limestone</u>									
25/8/72	Marsh	139	14.0	7.40	113	23	-0.48	-1.62	-2.28
"	Pond	140	13.5	7.55	28	14	-1.36	-3.01	-2.91
"	Pond	141	17.0	7.40	26	8	-1.62	-3.75	-2.90
"	"	142	16.0	8.20	72	20	+0.02	-0.50	-3.24
"	Marsh	143	7.0	7.15	72	13	-1.26	-3.22	-2.25
"	Pond	144	14.0	6.95	38	11	-1.78	-4.08	-2.26
"	"	145	17.0	8.20	45	17	-0.34	-1.10	-3.44

Table 3.6. Mean Chemical Characteristics of Some Waters in Dolines in the Nahanni North Karst Region.

Water Type	Temp °C	pH	CaCO <sub>3</sub> ppm	MgCO <sub>3</sub> ppm	SI <sub>C</sub>	SI <sub>D</sub>	Log PCO <sub>2</sub>
Pond waters in dolines formed in till covered limestone	14.1	7.55	56	15	-0.97	-2.47	-2.75
Pond waters in sub-jacent karst dolines on shale	18.6	6.57	7	3	-3.42	-7.96	-2.81
Pond and pool waters in solution dolines on bare limestone	11.3	7.97	71	12	-0.37	-1.49	-3.06



- Ponds in subjacent karst collapse dolines
- Ponds in dolines on till-mantled limestones
- ▲ Ponds and seepage waters in dolines and blind valleys in bare karst

a-a' Atmospheric log  $PCO_2$  at 3,500 ft.

b-b' Mean log  $PCO_2$  level in soils on limestones covered by thick till

c-c' Mean log  $PCO_2$  level in soils on limestones

d-d' Mean log  $PCO_2$  level in soils on shales

contact with soils. As Figure 3.12 demonstrates, all but three ponds were in equilibrium at the time of measurement, with partial pressures of  $\text{CO}_2$  less than the average  $\text{PCO}_2$  measured in soils in bare limestone regions, suggesting that at least part of the  $\text{CO}_2$  in them is acquired from this source. The chemistry of water found trickling into Perched Doline on Cenote Col (Figure 3.8) supports such a view. This water had a higher hardness than most doline pond waters (109 p.p.m. as opposed to an average of 83 p.p.m.) and was in equilibrium with a higher  $\log \text{PCO}_2$  (-2.97 as opposed to an average of -3.06). The equilibrium  $\text{PCO}_2$  of -2.97 calculated for this water is virtually the same as the average statistic of -2.90 for  $\text{CO}_2$  in soils on limestone. Clearly its increased aggressiveness relates to contact with soils.

Pond waters in subjacent karst collapse dolines in shale south of Mosquito Lake have very different chemistries to those occupying depressions in bare limestone (Table 3.5). They have an average pH of 6.57, a total hardness of 10 p.p.m., an  $\text{SI}_C$  of -3.42 and a  $\log \text{PCO}_2$  of -2.81.<sup>1</sup> These waters are highly undersaturated with respect to calcite and have very low hardnesses because of limited contact with soluble carbonate material. The very high  $\text{PCO}_2$  with which they are in equilibrium probably relates to contact with soils on shales where average

---

<sup>1</sup>Errors in calcium and total hardness titration results are, on a percentage basis quite sizeable when waters of very low hardness are analyzed. Errors in measurement are carried through to the derived variables  $\text{SI}_C$ ,  $\text{SI}_D$  and  $\log \text{PCO}_2$ . Values such as -12.22 for the  $\text{SI}_D$  of sample 8 in Table 3.5 are of dubious accuracy as are the mean statistics for these variables quoted in Table 3.6.

Once they drain underground they must enlarge drainage conduits suggesting that these depressions are actively deepening today.

Waters entering solution dolines in bare limestone tend to approach saturation before they reach their floors so that solution by rainwater is concentrated at the upper lips of the depressions. Such an uneven distribution of corrosion would tend to produce dolines with steep but not vertical walls. Because most of the water that enters solution dolines in the bare karst areas of the Nahanni enters in the form of snow and not as running water, these forms are deepening at a far quicker rate than they are growing laterally. Solution by snowmelt water is concentrated in doline floors and at the bases of side-walls so that as depressions are deepened their walls are undercut so that they become vertical or overhanging. Although processes are operating to widen Nahanni dolines in bare karst terrains, other processes are operating to deepen them. It is apparent that during the period of their growth these latter gained the upper hand.

#### 4. Labyrinth Karst.

The most ubiquitous solutional landforms in the Nahanni are networks of widened fractures or karst streets<sup>1</sup> and irregularly-shaped closed depressions or karst platea<sup>2</sup> (Plates 3.20, 3.21 and 3.22, and

---

<sup>1</sup>The analogy is made between the complicated networks of negative linear forms constituting labyrinth karst and the streets in an urban area.

<sup>2</sup>The analogy is made between the market place or square of an urban center which constitutes a large open space within a street network and the closed depressions characteristic of karst labyrinths. The term platea (pl. platea) is derived from the Latin noun platea and the



Figure 1.6) which together make up a karst type best described as 'labyrinth karst'<sup>1</sup> (Plate 3.23). Landforms that resemble the karst streets of the Nahanni have been described by Cvijić (1893), Milojević (1936, 1938), Pannekoek (1948), Blanc (1958), Sunartadirdja & Lehmann (1960), Tricart & da Silva (1960), Jennings & Bik (1962), Jennings & Sweeting (1963), Verstappen (1964, 1969), Monroe (1964, 1968), Croce (1964), Wilford & Wall (1965), Jennings (1969), Waltham (1970), Bauer & Zötl (1972) and Cooke (1973). Jennings & Sweeting (1963) and Jennings (1969) have also reported features which appear at least outwardly to resemble karst platea.

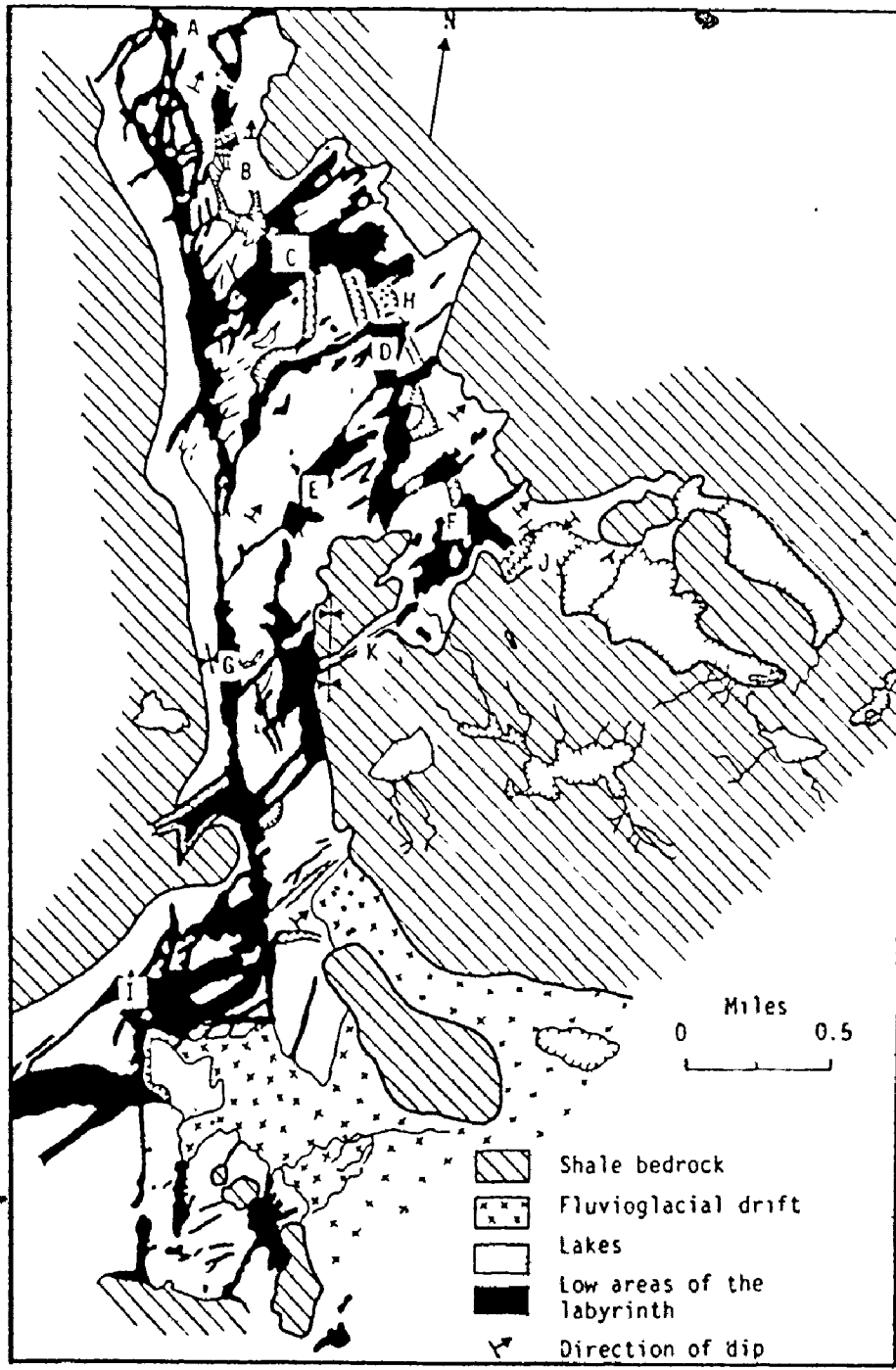
Prior to the discovery of the Nahanni karst in 1971, the most highly developed limestone labyrinths known were those of the Limestone Ranges in the Fitzroy Basin, Australia. These have been thoroughly described by Jennings & Sweeting (1963) who report the existence there of karst streets up to 100 ft. deep, 20 ft. wide at the base and hundreds of yards long. The natural rock labyrinths of the Nahanni North karst region are as much as 600 ft. deep and 3.5 miles long. The largest karst platea, North Col Canyon, is approximately 900 yds. long, 450 yds. wide and 300 ft. deep (Plate 3.22). The Nahanni forms clearly dwarf those of Australia and now represent the most spectacular examples of labyrinth karst known.

(a) Karst Streets.

Solutionally widened fractures 10 or more feet in depth have been variously referred to as bogaz or strugas (Cvijić (1893), Milojević

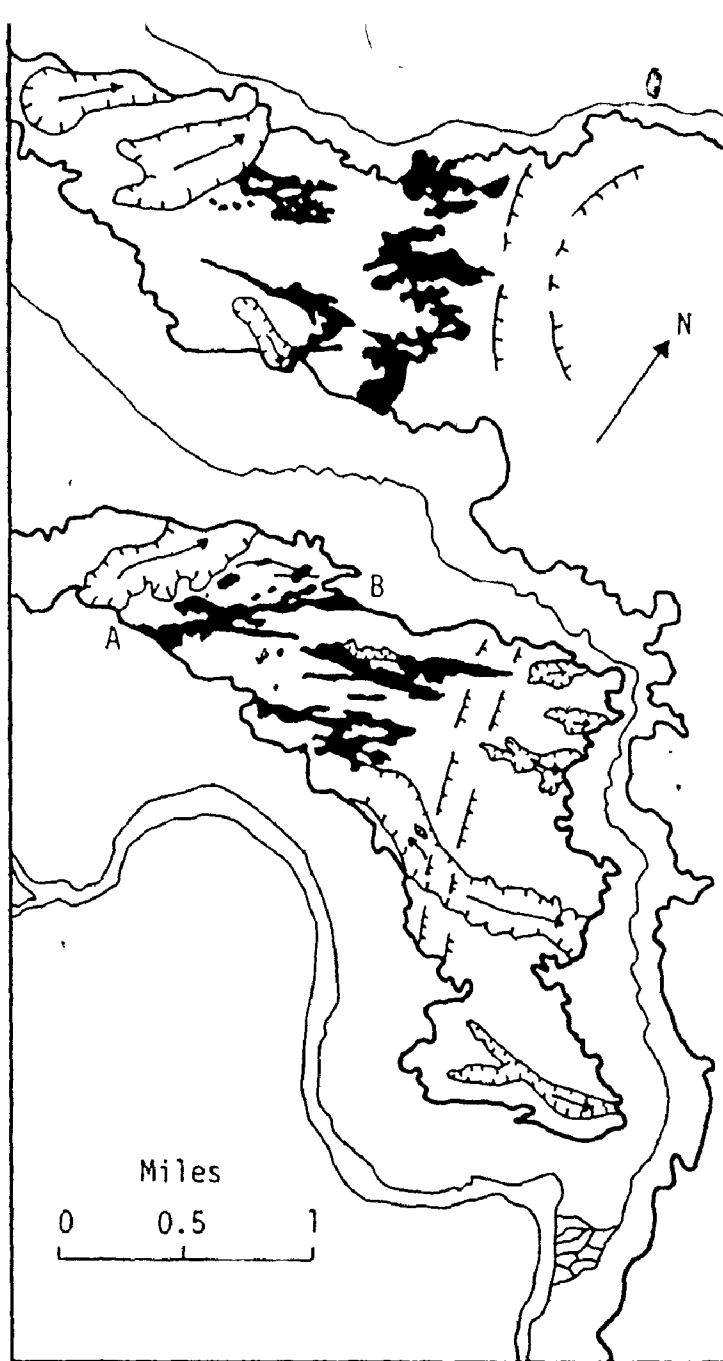
---

<sup>1</sup>Verstappen (1969) has used the same term for a very different karst type that is perhaps better called 'honeycomb karst.'



- |   |                  |   |             |
|---|------------------|---|-------------|
| A | First Polje      | G | Main Street |
| B | Raven Lake       | H | Cenote Col  |
| C | North Col Canyon | I | Insel Tower |
| D | South Col Canyon | J | Palsa Basin |
| E | Simpson Platea   | K | Lost Valley |
| F | Polaski Platea   |   |             |

Figure 3.13. The North Karst Labyrinths.







-  Labyrinth karst
-  Pond
-  Line of hills of glacial debris
-  Shallow valleys on plateau surface

Figure 3.14. Networks of karst streets on residuals of the Nahanni Plateau, South Karst.

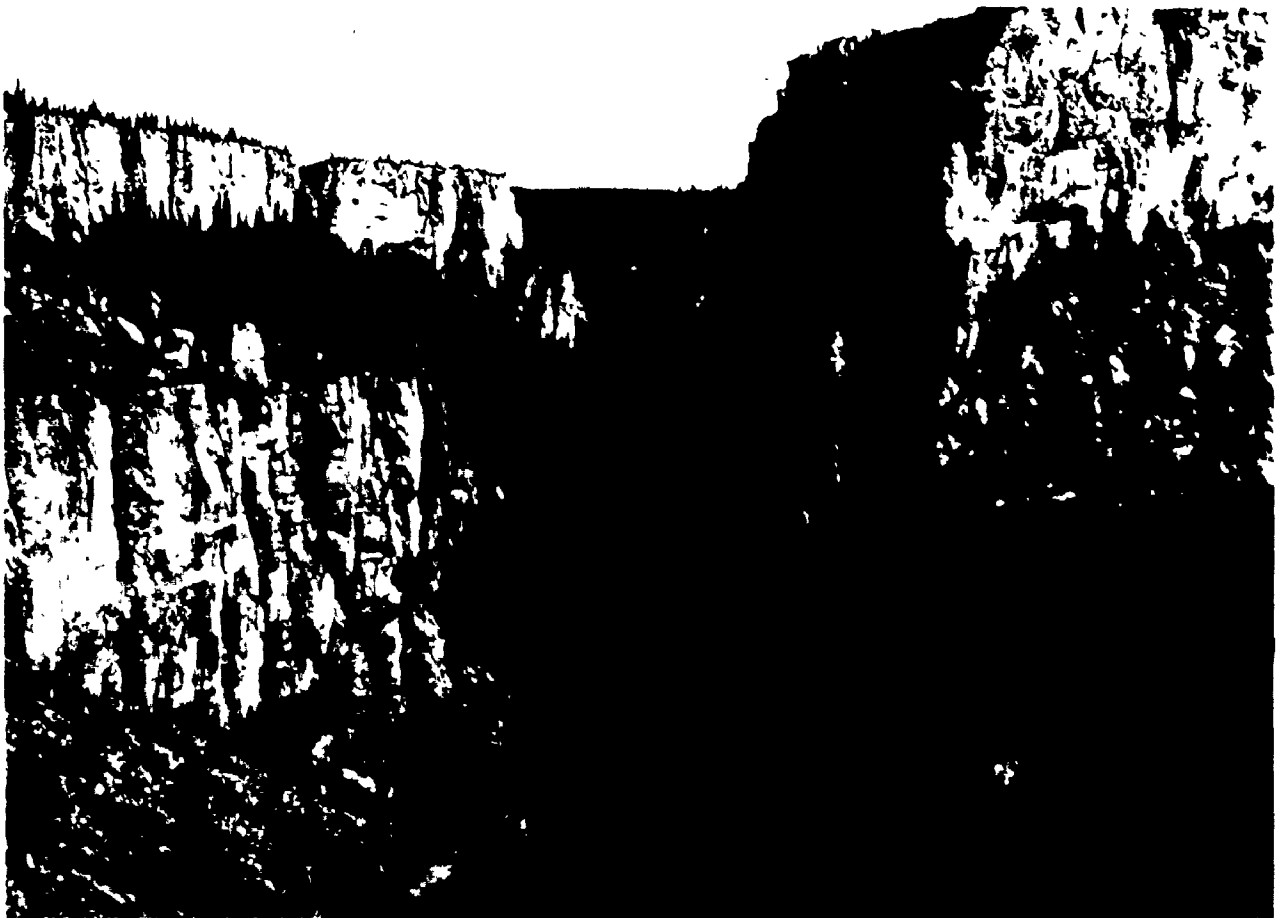


Plate 3.20. Stal Gorge, a moderately sized karst street 150-250 feet deep. The floor has been divided into a series of closed depressions by the irregular accumulation of breakdown debris. The walls contain fragments of phreatic caves.

of individual streets are believed to be related to the vertical and horizontal persistences of the host fractures and to the stage of development. Streets formed in single fractures tend to be deep and narrow, those formed in narrow fracture zones wider and generally shallower. Perhaps the best example of a large karst street developed in a single fracture is one that cuts right across the Nahanni Plateau residual between First Canyon, South Nahanni River and Lafferty Creek (A-B in Figure 3.14). This feature which is about 0.75 miles long, 50-200 ft. deep and only 40-60 ft. wide is a slightly widened strike-slip fault and is little more than a slot in the plateau surface. At its southwest end it is cut deeply into the almost vertical north wall of First Canyon, its floor some 1,900 ft. above river level.

Street floors are heavily mantled with limestone debris and in forms close to shale outcrops this may be mixed with shale-derived alluvium. In the larger streets talus cones and aprons with slope angles of  $25^{\circ}$ - $30^{\circ}$  are characteristic (Plate 3.20). Long profiles are always irregular (Figure 3.17) for floors consist of a series of shallow closed basins either in bedrock or in surficial material where talus cones on opposite walls coalesce (Figures 3.15, 3.16 and 3.18). Rarely visible in the larger features, bedrock basins are common in the smaller streets and function as ponor systems. The streets shown in Figures 3.15 and 3.18, for instance, are made up of numerous, often nested shallow depressions in bedrock with a superficial cover of limestone breakdown material. Two of the depressions shown in Figure 3.15 are connected by a short fissure cave which has formed a small natural rock br' .

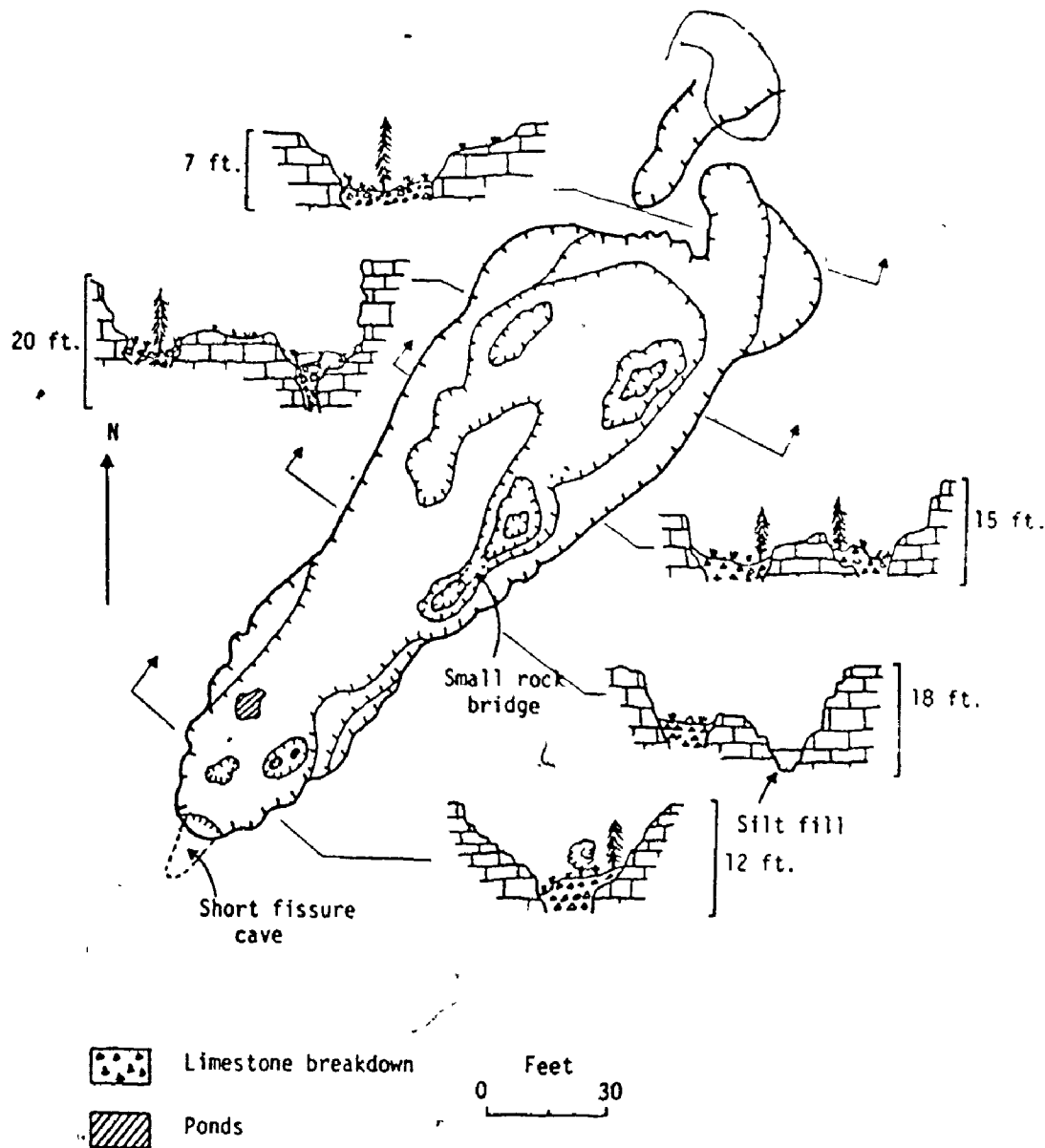


Figure 3.15. Plan and Sections of a small karst street on the Nahanni Plateau, south of Death Lake.

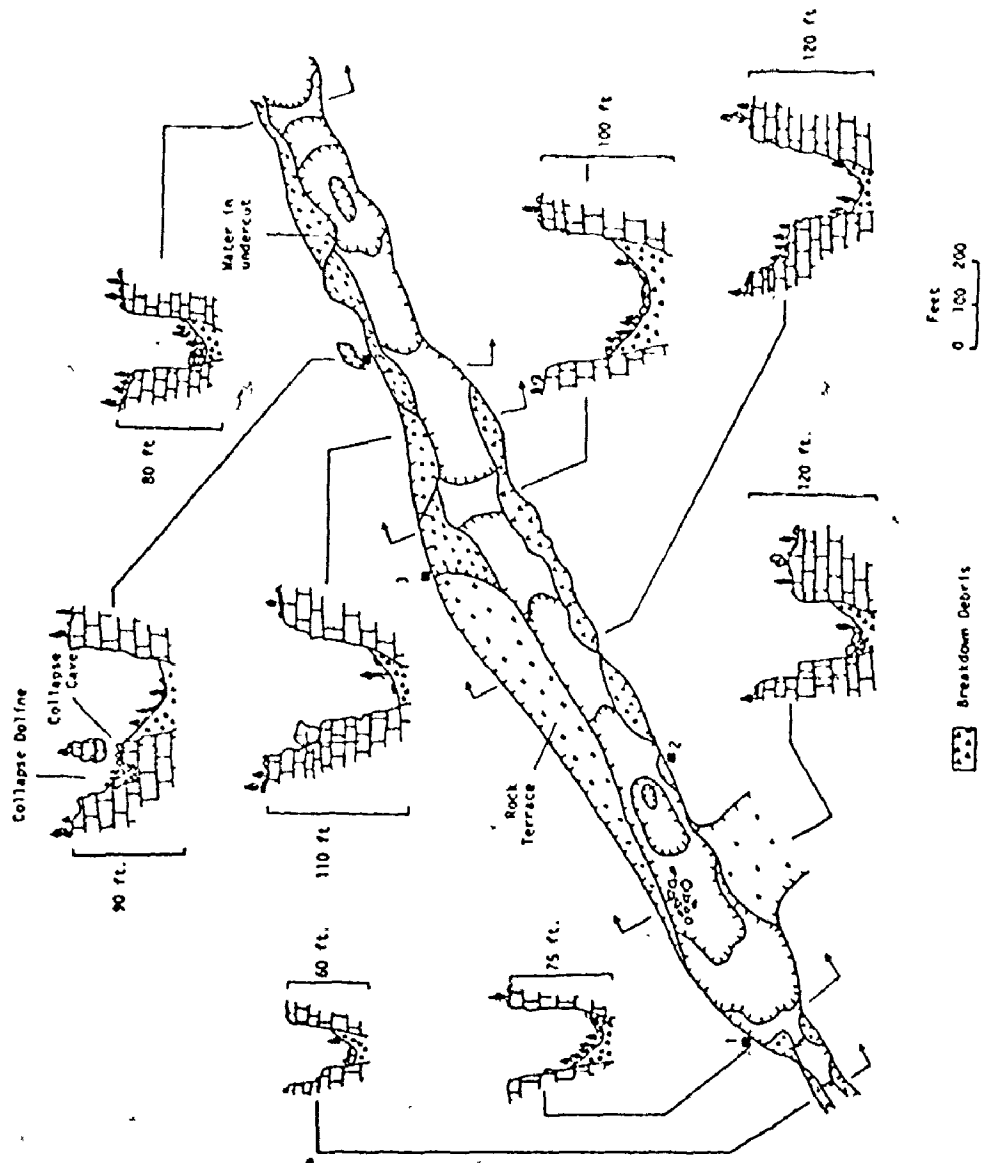


Figure 3.16. Plan and sections of Stal Gorge, a large karst street.

NE

SW

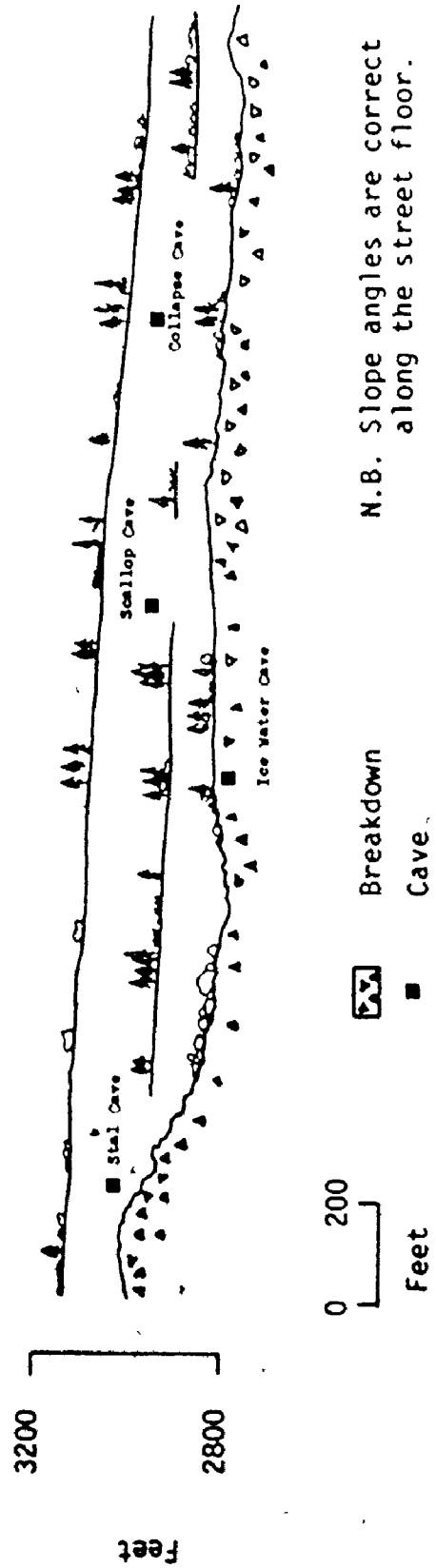


Figure 3.17. Longitudinal profile of Stal Gorge, North Karst.



The majority of karst streets are largely bare of vegetation (Plate 3.20) and have no surface flow of water in them or into them although ponds may be present where drainage-routes have been blocked by ice (Figures 3.15 and 3.18). Like vertical-walled solution dolines, they are thought to derive much of their water supply from snow trapped in them during winter. Streets near outcrops of shale (Figure 3.13), on the other hand, have allogenic streams flowing into them after heavy rain so that one or more of the walls of these depressions may be dissected by shallow stream valleys. Because of the input of shale-derived sediment these karst streets are almost invariably at least partially alluviated with streams flowing across their floors and eventually sinking in alluvial streamsink dolines usually at the bases of the vertical side walls but sometimes in the center of the street floor. The partial soil cover generally supports a dense vegetation cover including conifers up to 30 ft. high (Plate 3.30).

Some karst streets continue for short distances as fissure caves (Figure 3.15) and fragments of phreatic caves are common in most side walls. Four large and numerous small caves have been discovered in the walls of Stal Gorge, for instance (Figures 3.16 and 3.17, and Plate 3.20); one of these has an entrance 40-50 ft. high and 60-70 ft. wide and connects a short distance back into the plateau with a collapse doline. Caves do in fact often connect karst streets formed in the same fracture or fracture zone and link closely-spaced parallel forms via rock windows and rock bridges. For instance, Raven Canyon a 600 ft. deep karst street in the North karst (Figure 3.13)

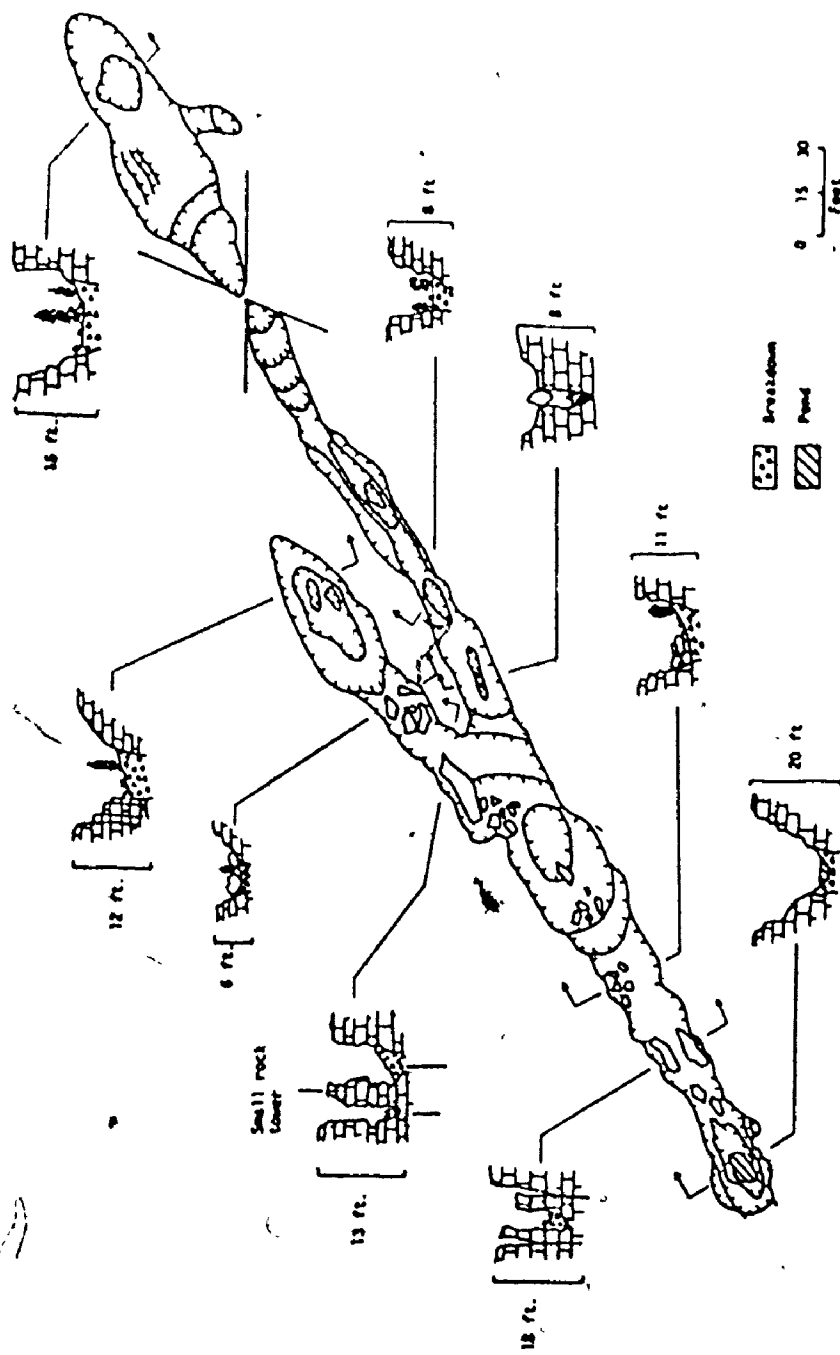


Figure 3.18. Shallow karst street on the Nahanni Plateau south of Death Lake.

is connected to shallow labyrinth karst forms to the west by a steeply sloping fissure spanned by three large and two small natural rock bridges. The whole system clearly represents a former cave connection in which only portions of the original roof remain intact.

(b) Karst Platea.

Karst platea are irregularly-shaped closed depressions which vary from a few tens of feet to several hundred yards in diameter and from several feet to a few hundred feet in depth (Plates 3.21 and 3.22). Shapes may be relatively simple (Figure 3.19) or extremely complex (Figure 3.20) but common to all features are extensive linear walls controlled by major fractures. Walls are generally vertical to overhanging with considerable scree development in the larger forms (Plate 3.22). Floors are irregular and mantled by limestone debris which may be of huge size and are often characterized by residual limestone towers and pinnacles with vertical sides (Plate 3.31, and Figures 3.19 and 3.20). Exceptionally these towers and pinnacles may be up to 200 ft. in height. Karst towers and platea frequently contain fragments of phreatic fissure and bedding plane caves which may be high up in their walls (Figure 3.19).

Water enters karst platea as surface streams with headwaters in shale or via resurgences in the side walls which are generally hidden by talus accumulations. All of the larger karst platea have developed close to shale outcrops suggesting that allogenic flow from the shales after rain may have been partly instrumental in producing them. Streams generally enter platea via shallow fissure-located valleys but occasionally they plunge over the vertical side

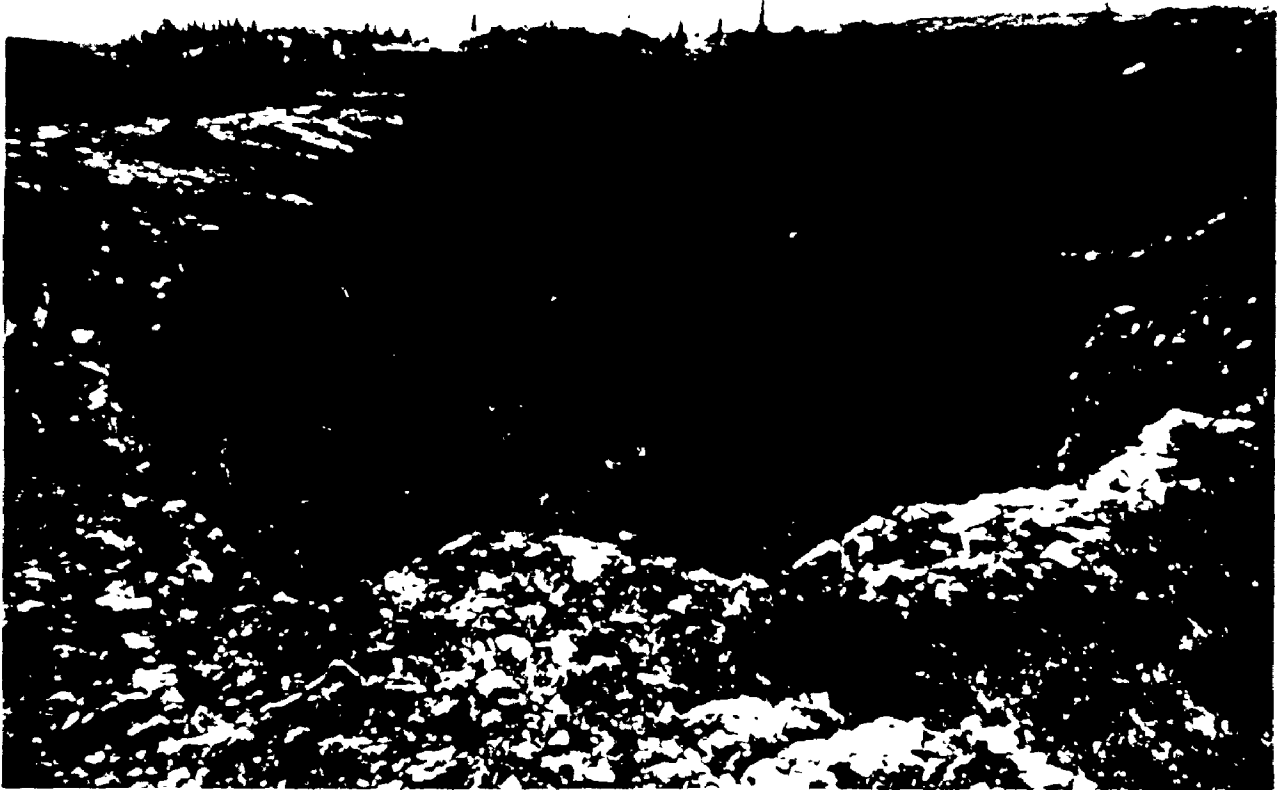


Plate 3.21. Shallow karst platea in the surface of the Nahanni Plateau between Death and Crash Canyons.



Plate 3.22. North Col Canyon, the largest karst platea in the Nahanni Karst is approximately 900 yards long, 450 yards wide and more than 300 feet deep.

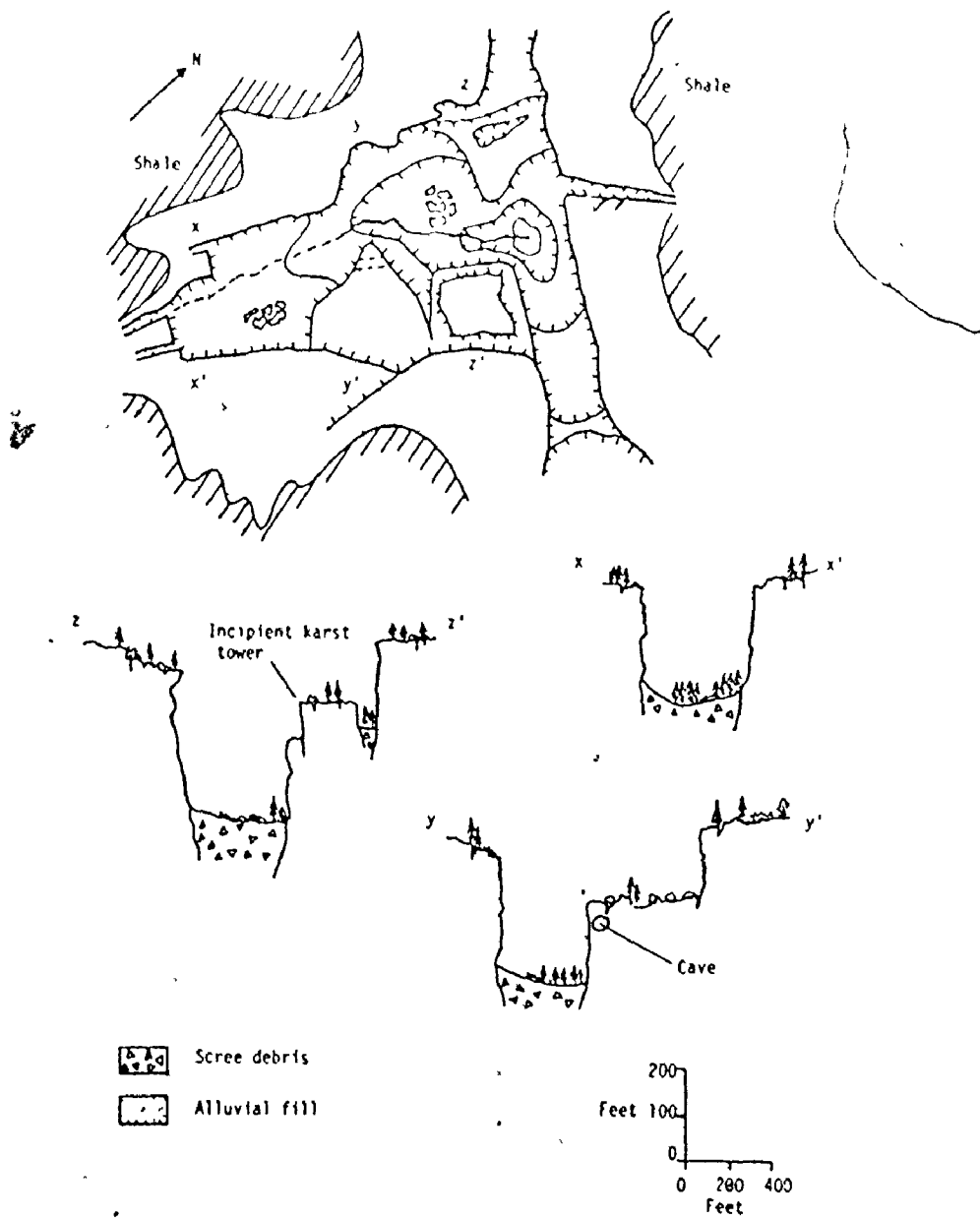


Figure 3.19. Polaski Plateau, North Karst.

walls in small waterfalls (Figure 3.20). Shale-derived sediment brought in by allogenic streams often mantles the low-lying ponor areas of platea floors (Plate 3.22).

The majority of the smaller karst platea and some of the larger forms are single depressions with water sinking at the lowest point (Plate 3.21). Of the larger forms Polaski Platea is of this type (Figure 3.19). In this feature the floor gradient is everywhere towards the base of the southwest-facing wall where the major ponor systems are located in an area that is heavily alluviated. Although the platea is entirely developed in limestone it is surrounded by outcrops of shale so that allogenic stream flow into it is common especially after heavy rain. The largest and most persistent stream flow into the platea is via fissures in the southwest extremity of the depression. Once inside the platea stream waters disappear into talus material but eventually emerge on to alluvium, winding their way across this and eventually sinking in alluvial streamsink dolines at the base of the northeast wall.

The floors of the majority of karst platea, however, consist of more than one depression with alluvial streamsink dolines in each. The floor of North Col Canyon, for instance, is made up of two large basins and one small one all developed in bedrock and all alluviated at the ponor systems (Figure 3.20). Four streams funnel water to the ponor systems in each of the two larger depressions which are liable to flood after very heavy rain. The much smaller Simpson Platea is also made up of three separate basins. The main one is 600 yards long and 150 yards wide and slopes towards the south end which is

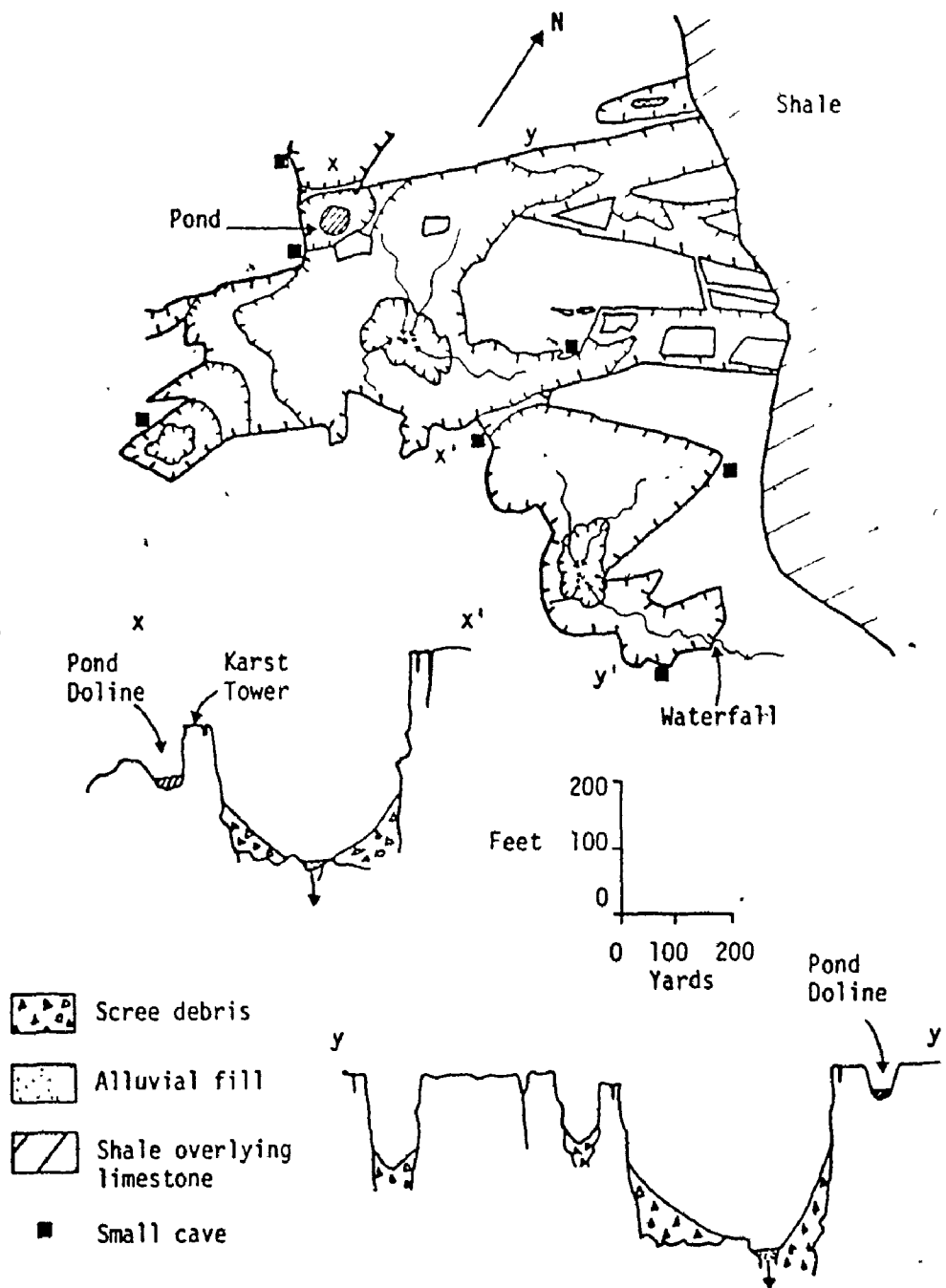


Figure 3.20. North Col Canyon, the largest karst platea in the Nahanni karst region.



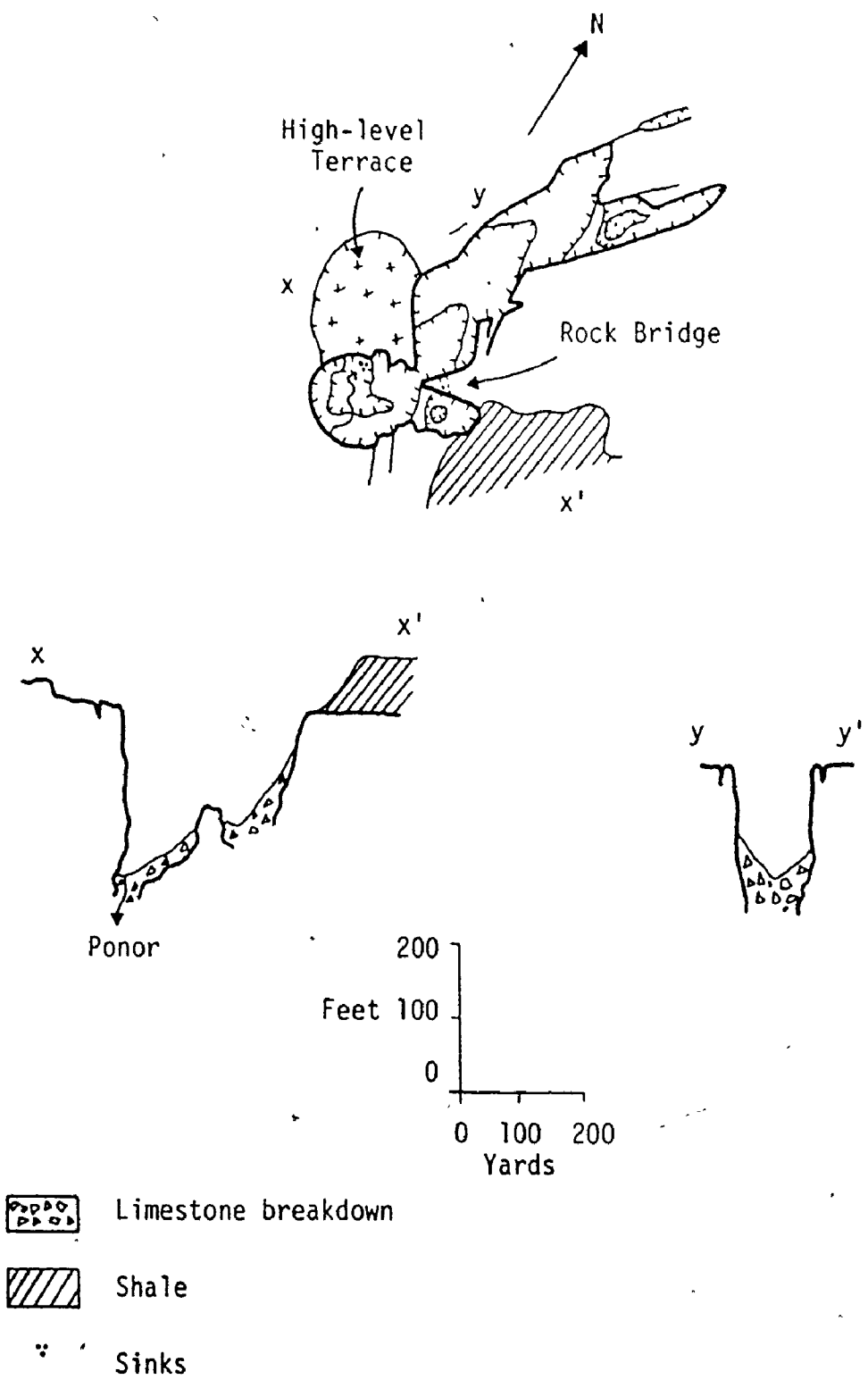


Figure 3.21. Simpson Platea, North Karst Labyrinths, Nahanni:



Plate 3.23. The natural rock labyrinths of the Nahanni North Karst looking south towards the Nahanni Plateau. In the foreground are North Col Canyon and Cenote Col, in the background Main Street, the longest karst street in this region and the Nahanni Plateau.

alluviated. The ponor systems are at the base of the southeast-facing wall (Figure 3.21). Two smaller basins have developed in 'arms' of the platea; these are 100 yards and 200 yards long respectively and both are approximately 50 yards wide. Water sinks at the centers of these depressions. Because of the accumulation of sediment in karst platea - on the Nahanni Plateau derived from the till cover and in the North karst from weathered shale - most are quite densely vegetated. A reindeer moss and sphagnum ground cover with conifers up to 40 ft. high is typical (Plates 3.21 and 3.22).

(c) Characteristics of Solution in Karst Streets and Platea.

Solution is not the only process that has operated to produce or is presently modifying the natural rock labyrinths of the Nahanni karst. There can be no doubt that both freeze-thaw action and gravitational collapse have played and are still playing a part. Solution is, however, necessary for the formation and continued development of karst streets and platea, making an examination of the present distribution of solutional activity in these forms a relevant one. During the summers of 1972 and 1973 stream, pond, lake and seepage waters in these depressions were analyzed. The chemical characteristics of waters in the Central karst, at an average elevation of 3,500 ft. are shown in Table 3.7, those in the North karst, generally below 3,000 ft. in Table 3.8. Summary statistics are given in Table 3.9.

Streams in the North karst depressions have a mean temperature of 3.7°C, a pH of 7.75 and a total hardness of 117 p.p.m. On average they are undersaturated with respect to both calcite and dolomite

Table 3.7. Chemical Characteristics of Some Pond and Seepage Waters in the Karst Streets of the Central Karst Region, Nahanni.

Date	Sample ID	Temp °C	pH	CaCO <sub>3</sub> ppm	MgCO <sub>3</sub> ppm	SI <sub>C</sub>	SI <sub>D</sub>	Log PCO <sub>2</sub>
<u>Pond Waters</u>								
16/8/72	110	2.0	8.40	69	25	-0.15	-0.69	-3.49
17/7/73	199	1.0	8.22	66	20	-0.40	-1.25	-3.34
"	198	2.5	8.12	81	9	-0.33	-1.56	-3.20
20/8/72	111	9.0	8.25	72	10	-0.12	-1.07	-3.35
"	112	10.0	8.20	88	8	+0.01	-1.00	-3.22
12/8/72	104	17.0	7.90	85	19	-0.11	-0.86	-2.86
14/7/73	171	1.2	8.20	81	7	-0.25	-1.51	-3.24
"	172	9.0	8.00	91	7	-0.18	-1.43	-3.00
"	173	2.8	8.19	69	6	-0.36	-1.72	-3.31
"	174	11.2	8.20	94	5	+0.10	-1.05	-3.18
"	175	15.0	8.41	80	7	+0.28	-0.49	-3.43
15/7/73	189	1.0	8.36	70	8	-0.23	-1.34	-3.48
24/8/72	135	9.5	8.15	62	9	-0.31	-1.43	-3.29
"	136	5.5	8.05	80	15	-0.33	-1.34	-3.12
"	137	10.5	8.55	66	7	+0.13	-0.68	-3.69
"	138	11.0	8.40	103	18	+0.35	-0.04	-3.36
<u>Seepage Waters</u>								
15/7/73	188	4.0	8.03	121	11	-0.05	-1.08	-2.92

(mean  $SI_C = -0.55$ ; mean  $SI_D = -1.69$ ) and are in equilibrium with a  $\log PCO_2$  of  $-2.72$  which is substantially above the atmospheric average (Figure 3.22). Many of the streams have their headwaters in outcrops of shale and flow across shale-derived alluvium in floors of streets and platea before sinking. There is some evidence to suggest that when these streams reach limestone they are in equilibrium with carbon dioxide levels typical of shale soils and then proceed to lose  $CO_2$  to the atmosphere as they re-equilibriate with levels of  $CO_2$  in soils on limestone. For instance one stream which flows into the southeast end of North Col Canyon via a waterfall (Figure 3.20 and Sample 41 in Table 3.8), is in equilibrium with a  $\log PCO_2$  of  $-2.33$  as it enters the platea. This value corresponds well with the mean  $\log PCO_2$  of  $-2.39$  measured in soils on shale (Figure 3.22). After percolating through limestone talus and soil in the floor of the platea and surfacing at an alluviated ponor system, however, the stream water is in equilibrium with a much lower  $\log PCO_2$  of  $-2.81$  which is close to the average  $\log PCO_2$  of  $-2.90$  measured in soils on limestone. Because most streams that enter karst streets and platea are thought to lose  $CO_2$  in this fashion and because most of the waters analyzed were taken from streams in the floors of these depressions, most are in equilibrium with a level of  $CO_2$  typical of that in limestone soils (Figure 3.22).

Pond and lake waters in the North karst labyrinths have a mean temperature of  $14.4^\circ C$ , a pH of  $8.13$ , a total hardness of  $101$  p.p.m., an  $SI_C$  of  $-0.04$ , an  $SI_D$  of  $-0.78$  and a  $\log PCO_2$  of  $-3.17$ . Pond waters

Table 3.8. Chemical Characteristics of Some Stream, Pond, Lake and Seepage Waters in the North Karst Labyrinths, Nahanni.

Date	Sample ID	Temp °C	pH	CaCO <sub>3</sub> ppm	MgCO <sub>3</sub> ppm	SI <sub>C</sub>	SI <sub>D</sub>	Log PCO <sub>2</sub>
<u>Stream Waters</u>								
16/7/72	60	3.0	7.90	75	15	-0.55	-1.75	-2.96
"	64	9.0	7.95	84	10	-0.29	-1.47	-2.98
10/7/72	41	1.0	7.45	135	29	-0.65	-1.89	-2.33
"	45	2.0	7.35	95	22	-0.96	-2.49	-2.33
"	44	1.0	7.75	80	17	-0.73	-2.07	-2.81
"	42	1.0	7.65	89	9	-0.78	-2.49	-2.71
"	43	8.0	7.80	83	14	-0.47	-1.68	-2.82
"	49	3.0	8.00	91	65	-0.17	-0.43	-2.83
"	50	5.0	7.90	89	54	-0.37	-0.92	-2.88
<u>Pond and Lake Waters</u>								
14/7/72	54	12.5	8.30	93	24	+0.23	-0.10	-3.26
"	53	10.0	8.30	86	35	+0.13	-0.10	-3.28
3/8/73	273	12.5	8.30	95	40	+0.15	-0.06	-3.36
16/7/72	61	15.5	7.30	99	15	-0.67	-2.14	-2.25
14/7/72	55	18.5	8.35	76	16	+0.27	-0.12	-3.35
3/8/73	270	15.0	8.45	80	16	+0.22	-0.24	-3.57
16/7/72	62	17.0	7.85	65	8	-0.41	-1.72	-2.96
"	63	17.0	8.10	71	8	-0.11	-1.15	-3.19
18/7/72	65	12.0	8.20	67	15	-0.14	-1.38	-3.30
<u>Seepage Waters</u>								
14/7/72	52	5.50	8.20	77	21	-0.17	-0.85	-3.24

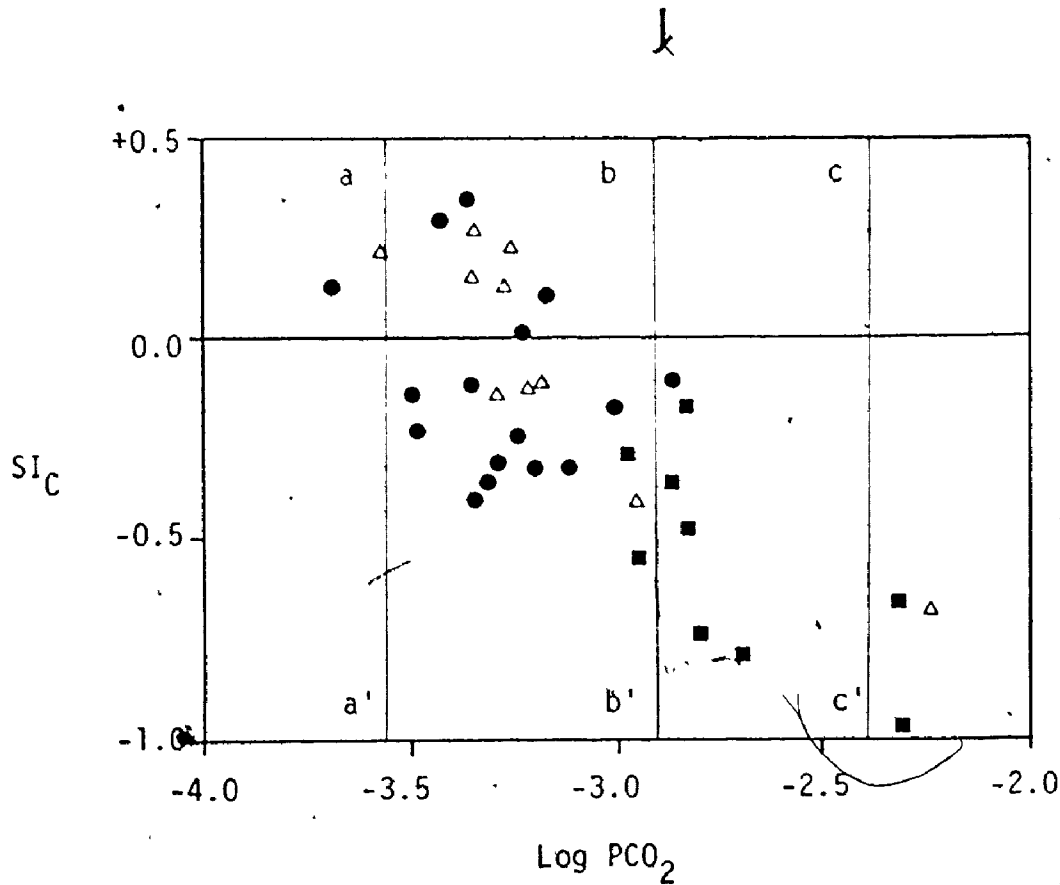
Table 3.9. Chemical Means of Some Waters in Karst Streets and Platea of the Central and North Karst Regions, Nahanni.

Location	Temp °C	pH	CaCO <sub>3</sub> ppm	MgCO <sub>3</sub> ppm	SI <sub>C</sub>	SI <sub>D</sub>	Log PCO <sub>2</sub>
<u>Stream Waters</u>							
North karst	3.7	7.75	91	21	-0.55	-1.69	-2.74
<u>Pond and Lake Waters</u>							
North karst	14.4	8.13	81	20	-0.04	-0.78	-3.17
Central karst	7.4	8.22	79	10	-0.12	-1.09	-3.28
<u>Seepage Waters</u>							
North karst	5.5	8.20	77	21	-0.17	-0.85	-3.24
Central karst	4.0	8.03	121	11	-0.05	-1.88	-2.92

at a higher elevation in the Central karst, on the other hand, have an average temperature of  $7.4^{\circ}\text{C}$ , a pH of 8.13, a total hardness of 89 p.p.m., an  $\text{SI}_\text{C}$  of -0.12, an  $\text{SI}_\text{D}$  of -1.09 and a  $\log \text{PCO}_2$  of -3.28. It is evident from these statistics that the level of  $\text{CO}_2$  in pond and lake waters in both regions is partly the result of contact with soils on limestone and partly due to equilibration with atmospheric  $\text{PCO}_2$  (Figure 3.22). Both sets of standing waters are close to saturation with respect to calcite and undersaturated with respect to dolomite and as would be expected, there is a slightly higher average level of  $\text{CO}_2$  in North karst waters than there is in Central karst waters because of the greater soil thicknesses and denser vegetation cover in this former area. Compared to stream waters, ponds in the North karst are closer to equilibrium with atmospheric  $\text{CO}_2$  levels and are more highly saturated. Both differences are to be expected, for as water loses  $\text{CO}_2$  to the atmosphere it moves towards saturation with respect to both calcite and dolomite.

The chemical characteristics of waters in the karst streets and plateaus of the North and Central regions of the Nahanni, indicate that the intensity of solution in North karst depressions is greater than it is in Central karst forms. Stream and pond waters in the North karst have average total hardnesses of 112 p.p.m. respectively while ponds in Central karst depressions have a hardness of only 89 p.p.m. It is clear from this evidence that at the present time the North karst labyrinths are evolving at a more rapid rate than are similar forms further south. Further, it is clear that more water





- Streams in the North Karst
- △ Ponds and lakes in the North Karst
- Ponds in the Death Lake region
- a-a' Atmospheric  $\text{log PCO}_2$ , 3,500 ft.
- b-b' Mean  $\text{log PCO}_2$  in limestone soils
- c-c' Mean  $\text{log PCO}_2$  in shale soils

Figure 3.22.  $SI_c$  and  $\text{Log PCO}_2$  graph of stream, pond and lake waters in streets and plateaus in the North and Central karst regions.

sinks in the North karst features than in those further south because these collect allogenic stream water rich in  $\text{CO}_2$  from nearby shale outcrops. The greater intensity of solution in the North karst streets and plateaus and their increased water supply, in comparison with similar features in the Central karst may at least in part explain the more accentuated development of labyrinth karst forms in this region than elsewhere.

#### 5. Poljes.

Sweeting (1972) describes poljes in the Classical and Dinaric karst regions of Yugoslavia as large closed depressions with conspicuously flat floors. They vary in size from 2 km. to 60 km. long and most are elongate and aligned in the direction of the major tectonic lines. Floors are either planed in bare rock or are mantled by alluvium; the sides usually rise steeply from the floors at angles close to  $30^\circ$  so that the transverse profile is a wide open U-shape. Isolated residuals of limestone rising above the floor are common; these are known as hums. Poljes may be drained by one river and be little more than a single large depression; more commonly however, polje floors consist of several separate hydrological basins. Drainage is underground through ponors which may be either alluvial stream-sink dolines or fissures in bare rock. The largest polje in Yugoslavia, for instance, is the Livno Polje which is 70 km. long and 10 km. wide; its floor is made up of three hydrologically distinct basins.

Lehmann (1959) differentiated three types of polje in the Apennines. First, are poljes formed in high level erosion surfaces, second are poljes formed within a former valley system and third are

semi-poljes with one wall in impermeable rocks not liable to karstification. Sweeting (1972) suggests that the most significant classification of poljes is into those features that are completely surrounded by limestones and those developed at the contact of limestones with impermeable rocks and formed by differential corrosion. The first type she notes are frequently though not always closed poljes - that is all water entering them leaves by ponor systems; the second are quite often open poljes - that is they are fully comparable with closed poljes except that they have external drainage along a narrow defile.

Many workers have argued that poljes are primarily tectonic features that have been only slightly modified by solution, while others contend that they may form entirely by solution. Poljes occupying fault troughs, fault angle depressions and synform structures in bedrock support the first contention, while poljes in the crests of anticlinal structures support the second (Jennings, 1970). Sweeting (1972) has argued that perhaps 99% of poljes in the Classical and Dinaric karsts are guided by tectonic lines in these areas - either folds or faults. She also notes that they are always associated with the appearance of impermeable strata.

Three poljes have been discovered in the Nahanni karst. They represent the only poljes known in the sub-arctic and the only features of this kind in Canada<sup>1</sup> (Figure 1.6). Gams (1969) has suggested

---

<sup>1</sup>Brown (1972) has claimed the existence of poljes in the Maligne Basin area of the southern Canadian Rocky Mountains. These features, however, which are known to the writer are closed fluvial canyon systems rather than poljes.

that before a closed depression should qualify as a polje it should have a floor area of several square kilometers and although the largest of the Nahanni depressions is only 1.4 km. long and 0.8 km. wide, all three display virtually all of the characteristics that are normally associated with poljes and will therefore be regarded as such.

(a) Morphological Characteristics of Nahanni Poljes.

The three Nahanni poljes have formed in the limestone floor of a narrow 300-400 ft. deep 'corridor' cut in the shales of the Fort Simpson Formation. The corridor walls are steep in shale and although the corridor is between 0.75 and 1.5 miles wide only a strip of limestone little more than 0.5 miles wide is exposed in its floor. The poljes have developed in the portion of this strip that lies between the highly accentuated North karst labyrinths in the south and Bubbling Spring in the north (Figures 1.6 and 3.23).

(i) First Polje.

First Polje is approximately 1,600 yards long and 900 yards wide. Its floor is at an elevation of about 2,450 ft. a.s.l. and although the depression has a closure of only a little more than 100 ft. in directions parallel to the line of the shale corridor which it occupies, the walls to east and west; at first in limestone and then in shale, rise 550 ft. (Figure 3.24 and Plate 3.24). The floor of the depression consists of two separate basins separated by a 5-10 ft. high rock threshold. The larger of these is Camp Basin in the south which is an oval, saucer-shaped depression approximately 1,000 yards by 900

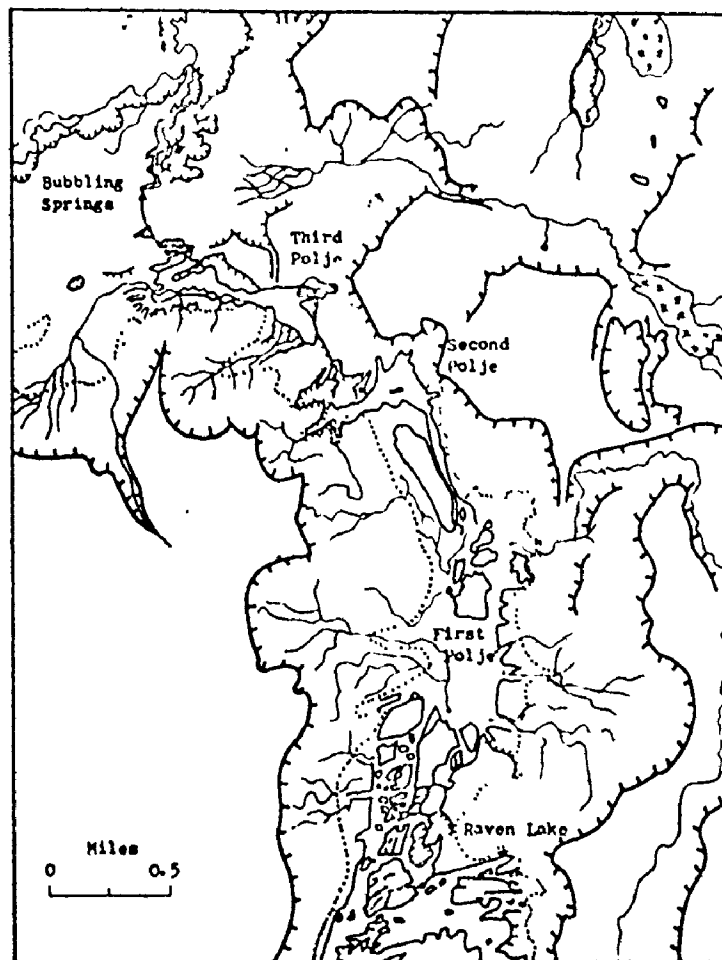
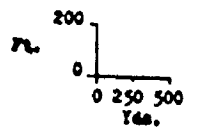
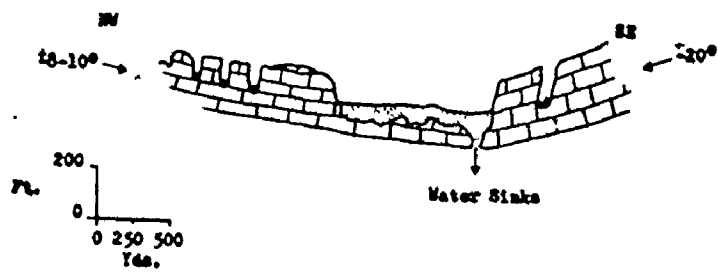
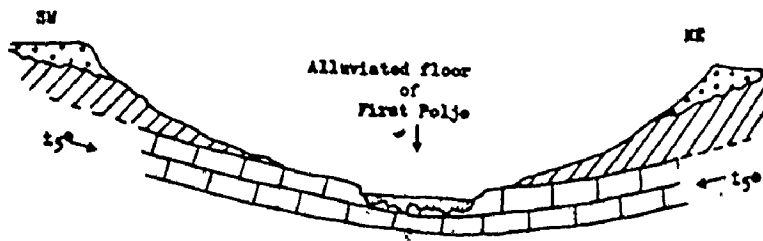
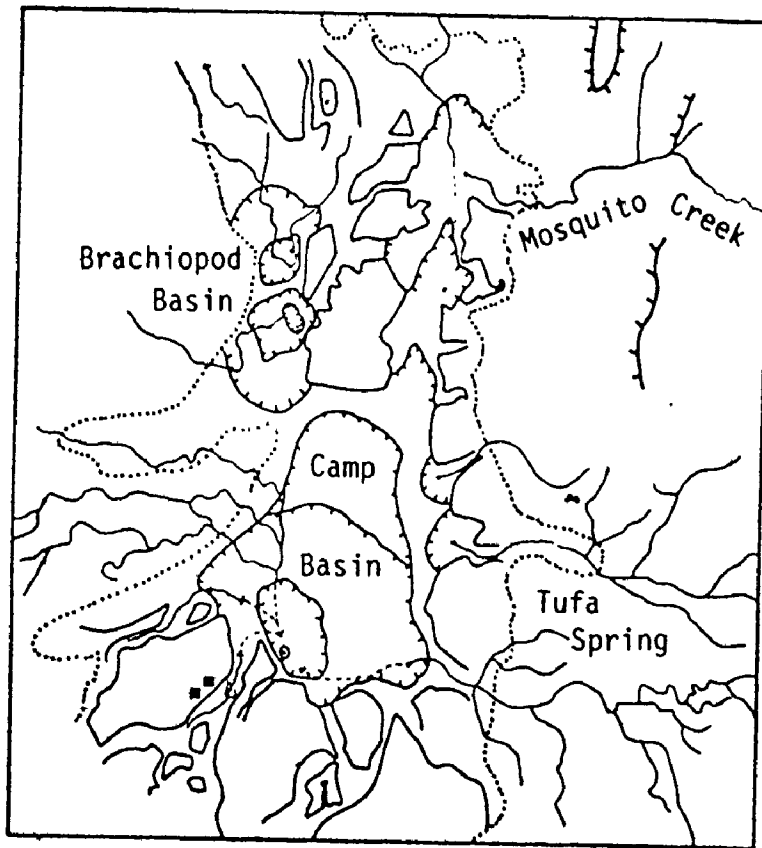


Figure 3.23. Geomorphic map of the northern section of the labyrinths showing the Nahanni poljes.

yards. The smaller is Brachiopod Basin in the northwest which is close to 500 yards long and 250 yards wide. Both are at least partially alluviated and both have their own ponor systems (Plate 3.24).

The two basins differ considerably in morphology. Brachiopod Basin is bounded by steep limestone walls 30-40 ft. high and is only partially alluviated. Camp Basin, on the other hand, is highly alluviated and is bordered by steep to vertical limestone walls 10-15 ft. high. From the tops of these walls the sides of the basin follow the exposed bedding surfaces of the limestone which slope gently away from the center of the basin. Only when shale is encountered at some distance from the alluviated floor do the sides steepen once more (Figure 3.24). This marked difference in morphology is due to different origins for the two basins. Camp Basin is little more than a solutionally-modified, simple shallow downfold in the Nahanni Formation limestones that has been alluviated. Brachiopod Basin, on the other hand, appears to have been produced entirely by solution acting along intersecting networks of faults and joints. Around the periphery of Camp Basin, the bedrock dip varies up to 20° but is everywhere towards the basin (Figure 3.24 and Plate 3.24).

Water drains into First Polje via surface streams and springs. Most of the streams flow only after heavy rain but one or two such as Mosquito Creek flow throughout the summer season. Springs are located in the steep side walls of the polje, waters emerging at the shale-limestone junction. The largest example is Tufa Creek in the east wall. The springs flow all through the summer months but are believed to freeze over in winter. If dry all of the



- |  |                   |  |                         |
|--|-------------------|--|-------------------------|
|  | Nabanni Limestone |  | Shale-limestone contact |
|  | Simpson Shales    |  | Stream sink             |
|  | Glacial Deposits  |  | Cave                    |
|  | Alluvial Fill     |  | Surface water           |

Figure 3.24. First Polje.



Plate 3.24. Aerial view of First Polje, Nahanni North Karst. Unlike Second and Third Poljes which are alluviated karst plateaus, this depression is a solutionally modified downfold in the upper surface of Nahanni Formation limestones. The absence of trees on the floor suggests frequent inundation. Camp Basin is at center, Brachiopod Basin at left. Raven Lake is in the right foreground.



streams both spring derived and surface runoff derived, sink at the margins of the alluviated floor in shallow alluvial streamsink dolines. Under wet conditions, however, with an increase in surface runoff some peripheral ponors are not always capable of absorbing the volume of runoff into them and streams continue across the polje floor eventually sinking in deep ponors in the southwest portion of the basin. These ponors are mostly alluvial streamsink dolines although bedrock is visible in the largest of them. These depressions are up to 10 ft. deep and absorb water from a number of small streams even during dry conditions.

Input of water to Brachiopod Basin is largely through surface stream flow which increases substantially after heavy rain. Unlike those in Camp Basin, the ponor systems in Brachiopod Basin are vertical shafts in bedrock that are choked with limestone breakdown at shallow depth. Some stream waters simply disappear into limestone rubble. The vertical shafts are widened fissures about 6 ft. long and 2-3 ft. wide, the deepest being 20-25 ft.

The floors of Camp and Brachiopod Basins are flat and alluviated (Plates 3.24 and 4.1 (a)). A shallow excavation into the floor of Camp Basin in 1972 showed the fill to be horizontally bedded, black, and made up of a fine shale gravel in a matrix of sand and shale-derived silt. The sand is believed to have originated from glacial sands and gravels such as are exposed in the valley of Mosquito Creek between Mosquito Lake and First Polje. The present bedload of Mosquito Creek was found to be identical to the alluvial material in First Polje

suggesting that such material was and still is being carried into this basin by allogenic streams.

The structural basin that initially located Camp Basin, First Polje, has since been modified by solution. The magnitude of this modification is not known. If the basin was alluviated soon after shales were stripped from the top surface of the Nahanni Formation, it may be essentially intact beneath this 'protective' cover. If the basin was exposed to subaerial solution and freeze-thaw processes for a long period before alluviation occurred, however, the likelihood is that the alluvial fill in the floor of Camp Basin is a deep one and that it hides an uneven bedrock surface much etched by solution. Whatever the bedrock surface beneath the present alluvial floor of Camp Basin looks like, it was likely acted upon by the same processes that produced the labyrinth karst region to the south - processes that seem to have generated markedly vertical karst landforms. Alluviation of the basin certainly altered the distribution of solution across it.

The abrupt break in slope between the alluviated floor of Camp Basin and the shallow limestone walls at its margins are clearly the products of lateral solution. Within poljes, vertical solution is concentrated only at the ponors for elsewhere the bedrock is protected by an almost impermeable cover of alluvium. The lateral growth of Camp Basin appears to have resulted from two processes. Most important has been the frequent flooding which is indicated by the complete lack of tree growth in the floors of either Camp or Brachiopod Basins (Plate

3.24). During periods of flood, the bedrock floors of alluviated depressions like First Polje are protected by the impermeable cover so that solution is concentrated in those regions where bare rock is exposed - that is at the margins of the polje. Solution occurs at or below the surface of standing water in the basin so that walls are undercut and collapse. The overall result is lateral corrosion at or slightly above the level of the alluviated floor. Walls are steepened and collapse as a solution niche is cut and the flat floor is gradually extended.

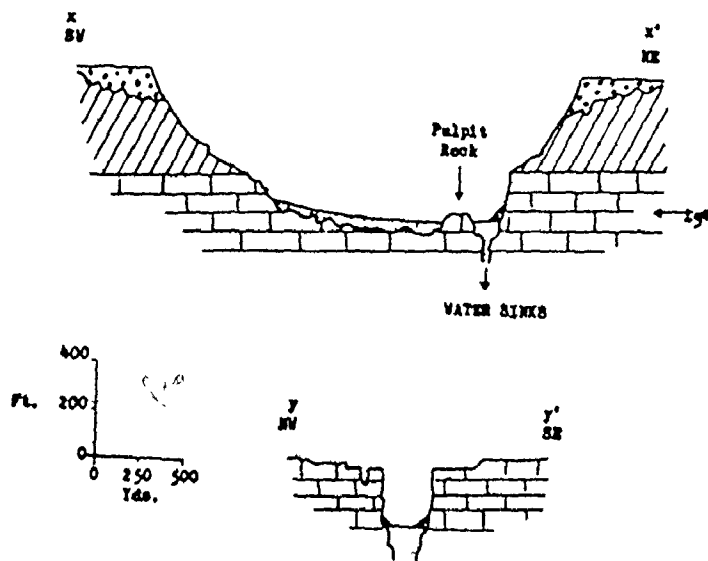
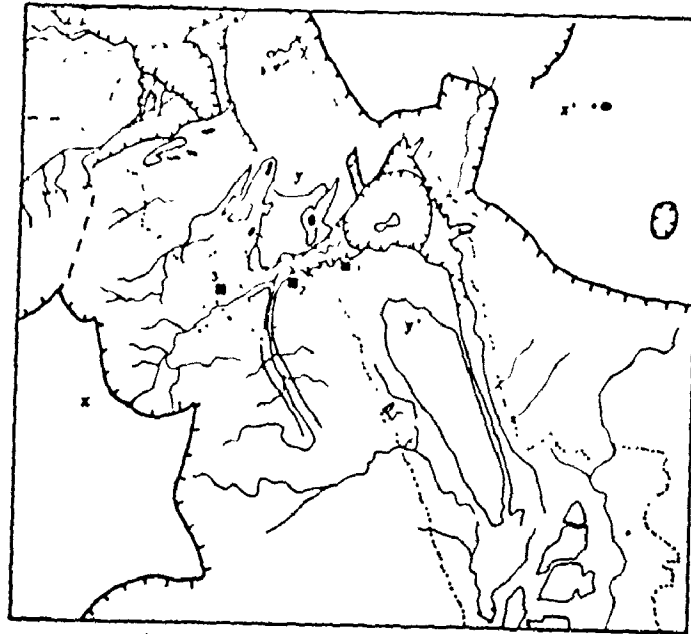
The floor of Camp Basin is also being extended by a second process that appears to be of considerable importance. In moderate flow conditions, streams entering the polje sink in shallow alluvial stream-sink dolines as soon as they encounter the alluviated floor which constitutes the base level of erosion for them. As these streams develop sinks nearer and nearer to their headwaters, the abandoned stretches close to the polje floor are used only at times of high flow and tend to become alluviated. The polje floor, therefore, extends into them. Fluvial incision graded to the level of the polje floor and lateral solution of the polje walls during periods of flood have together resulted in the extension of the alluviated floor of Camp Basin in the past. There can be no doubt that these processes continue today.

It is apparent that First Polje is a structurally located depression. Its existence lends support to the hypothesis that many poljes may well be solutionally modified structural depressions and

(ii) Second and Third Poljes.

Whereas First Polje appears to be at least partially structural in origin, Second and Third Poljes show all of the characteristics of having been formed almost entirely by the action of solution in networks of faults and joints. Variations in the bedrock dip across both depressions are of minor magnitude while both features are bounded by vertical walls that parallel major fractures in the limestone. Caves in the walls of both poljes suggest a former period of groundwater flow in the limestone before these surface basins developed - again supporting a solutional rather than a structural origin for these two features.

Second Polje is a triangular-shaped depression 700 yards long and 500 yards wide which has a closure of close to 100 ft. (Plate 4.4, Figure 3.25). It is bounded by vertical limestone walls up to 200 ft. high generally above massive screes from 50-100 ft. high. The west-facing wall has been deeply etched by solution into 50 ft. limestone pinnacles and cutters (Howard, 1963) which appear to have been eroded by acid allogenic waters originating on shales just back from the wall. Such highly developed features appear to be absent where shale outcrops are not present (Plate 3.25). Third Polje is an irregularly-shaped depression 1,300 yards long and from 100-500 yards wide. It has a closure of only 25-30 ft. (Plate 4.2 (a), Figure 3.26). Like Second Polje, Third Polje is bounded by vertical to overhanging walls which vary from 130 ft. above massive screes 100 ft. high in the southeast, to 20 ft. where screes are not present in the northwest. Only the higher walls are characterized by talus cones and aprons suggesting that the shallower walls can not support these.



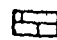
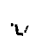



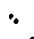



- |   |                   |   |                         |
|---|-------------------|---|-------------------------|
|  | Mahanni Limestone |  | Shale-limestone contact |
|  | Stepsen Shale     |  | Caves                   |
|  | Glacial Deposits  |  | Stream sinks            |
|  | Alluvial Fill     |  | Not for scarps          |
|  | Scree Debris      |   |                         |

Figure 3.25. Second Polje.



Plate 3.25. Second Polje partially inundated. This depression, the smallest of the three Nahanni poljes, floods regularly up to the lower limit of tree growth. The residual rock mass projecting above water level is Pulpit Rock - a small hum. Cutters and pinnacles are visible in the far wall.

The alluviated floors of both Second and Third Poljes slope gradually in an approximate west to east direction so that the lowest portions of their floors are in the east. No bedrock is visible in the floor of Third Polje but a bedrock residual in Second Polje - Pulpit Rock - resembles a small hum. Both floors are crossed by meandering, often dry stream channels and both are characterized by a complete grass cover indicating that they are frequently flooded (Plates 4.2 (a) and 3.25). In both basins the upper level of flooding is clearly marked by the lower limit of tree growth on screes (Plate 3.25). In Third Polje, the lower limit of tree growth on screes parallels solution notches and small caves in limestone walls with no scree development (Figure 3.26 (a)). Three small caves in the southwest-facing wall of Third Polje just at the upper limit of flooding were examined in early July 1972 when the polje was dry. They were found to be small, horizontal bedding-plane tubes 3 ft. in diameter and 10-12 ft. long, that connect with extremely narrow fissure passages too small to be penetrated. Caves of this type are common in poljes and serve to funnel floodwaters underground. They tend to develop at the upper limit of flooding for it is at the air-water-limestone interface that solution is most active. The upper limit of flooding in Third Polje is controlled by the elevation of the lowest point in the depression's rim; lakes formed during flood periods overflow towards Bubbling Spring once they reach this level. This fact may explain why solutional undercutting is particularly marked in the walls of Third Polje and entirely absent in those of Second Polje which does not

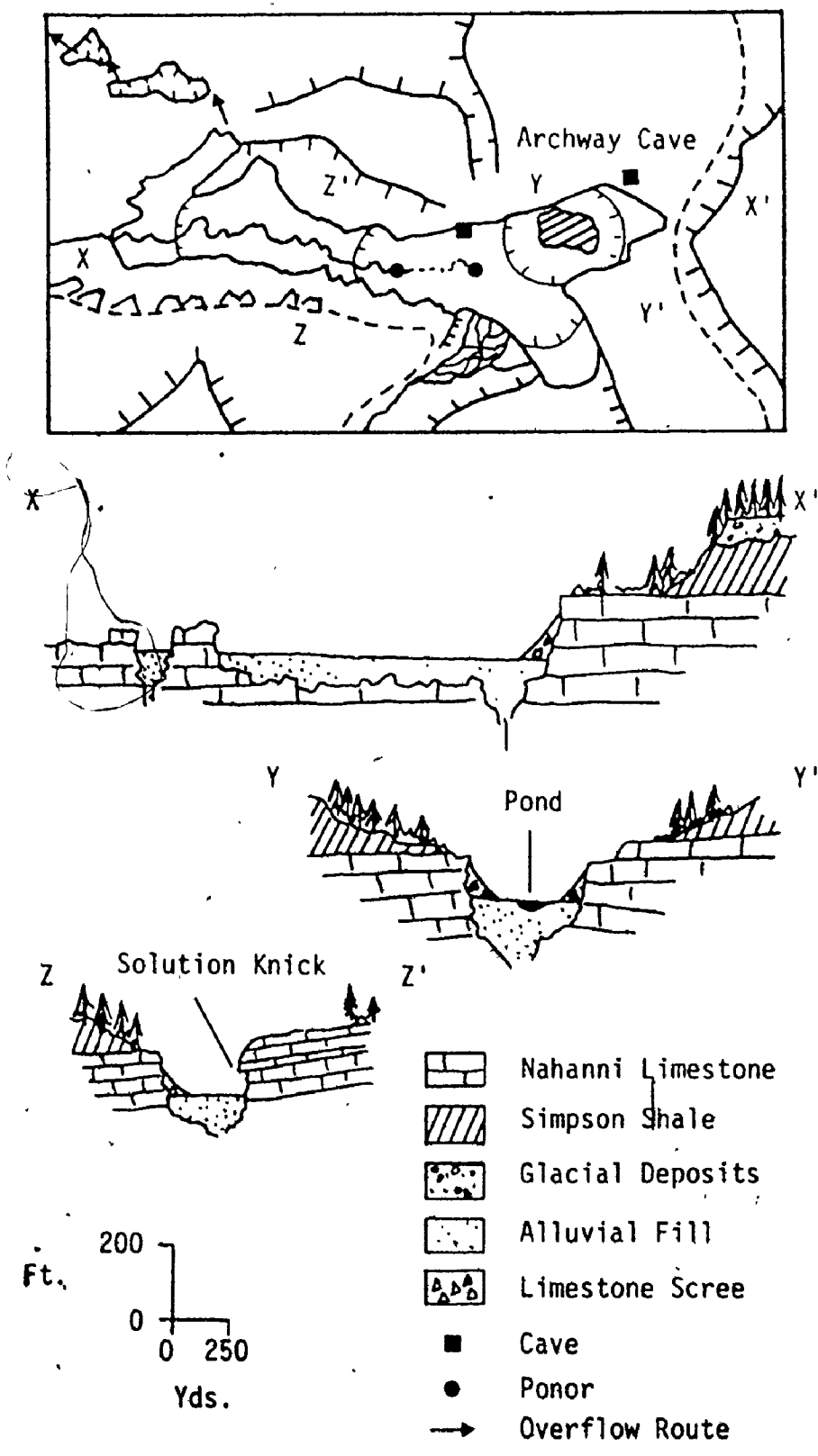


Figure 3.26. Third Polje.



overflow. The upper limit of flooding in Second Polje must relate to the balance between input to the depression and underground drainage from it. Whereas Second Polje may dry out completely after flooding, there is some evidence to suggest that a pond, a few feet in depth at the eastern end of Third Polje, may be a semi-permanent feature retained by perching of water on impermeable alluvium.

Although a number of springs discharge water into First Polje none have been discovered in the walls of either Second or Third Poljes. All of the water that enters these depressions does so via surface streams which generally flow for only short periods after rain, or during snowmelt. The main inputs are from the southwest; stream catchments are on shale mantled by a thick cover of glacial debris (Figures 3.25 and 3.26). Although a number of large streams discharge water into Third Polje after rain, only one stream funnels significant quantities of water into Second Polje. This stream enters the southwestern narrow end of the depression in a restricted, steep-sided valley (Plate 4.4) and meanders its way across the floor of the polje. Water appears to be gradually absorbed into the relatively coarse alluvium for there are no definite alluvial stream sink dolines in the floor of this depression. Streams entering the southeastern portion of Third Polje disappear in small ponors once they encounter the polje floor. The large stream which drains into the western extremity of Third Polje after rain, however, flows in a meandering path eastwards across the polje floor. Water appears to be lost underground at a variety of alluvial stream sink dolines along the

route. Any one ponor does not appear capable of absorbing the whole flow of the stream and so flow normally continues for some distance. When the polje is flooding, all streams may flow across the floor adding their water to the slowly growing lake in the depression.

The alluvial fill in the floors of both Second and Third Poljes appears slightly different to that in First Polje. The material is a poorly sorted fluvial deposit with cobbles up to 18 inches in diameter in a silt, sand and gravel matrix. Much of the material is derived from outcrops of weathered shale; the rest appears to be reworked glacial material with igneous and metamorphic constituents up to cobble size present. The difference between the material covering the bedrock floor of First Polje and that in Second and Third Poljes is clearly related to the source of the material. The streams discharging sediment into Second and Third Poljes derive that sediment from the glacial deposits that mantle the Sinkhole Plain to the west at an elevation of 3,000 ft. Most of the streams that have funnelled sediments into First Polje did not have their headwaters in such material. There can be no doubt that this glacial material is being funnelled into both depressions today.

Second and Third Poljes are believed to have formed entirely by the action of solution in networks of faults and joints. The Nahanni poljes, therefore, provide evidence that some poljes occupy structural depressions in the bedrock and that other poljes are entirely solutional in origin. The indication is that poljes in general do not all occupy structural basins nor are they all entirely of solutional origin.

(b) Characteristics of Solution in Nahanni Poljes.

Stream, spring, lake and overflow waters in the three Nahanni poljes were sampled and analyzed during the summers of 1972 and 1973. The chemical characteristics of stream and spring waters are illustrated in Table 3.10, those of lake and overflow waters in Table 3.11. Summary statistics are given in Table 3.12. Streams flowing into First Polje which derive their water from surface runoff have an average temperature of 7.5°C, a pH of 8.03, a total hardness of 138 p.p.m., an  $SI_C$  of -0.03, an  $SI_D$  of -0.69 and a  $\log PCO_2$  of -2.92. Streams deriving their water from springs in the polje walls, on the other hand, have an average temperature of 8.6°C, a pH of 8.02, a total hardness of 302 p.p.m., an  $SI_C$  of 0.66, an  $SI_D$  of 0.87 and a  $\log PCO_2$  of -2.80 where these sink in the polje's floor (Table 3.12). It is clear from these statistics that the stream waters sinking in First Polje tend to be saturated with respect to calcite but are still undersaturated with respect to dolomite.

Streams flowing into Second and Third Poljes differ in chemistry from those entering First Polje. The large stream that enters the western end of Second Polje, for instance, has an average temperature of 3.7°C, a pH of 7.97, a total hardness of 83 p.p.m., an  $SI_C$  of -0.68, and  $SI_D$  of -1.77 and a  $\log PCO_2$  of -3.18. In addition one of the streams entering the southwest end of Third Polje had a temperature of 4.0, a pH of 7.20, a total hardness of 167 p.p.m., an  $SI_C$  of -0.86, an  $SI_D$  of -2.04 and a  $\log PCO_2$  of -2.05. Clearly when sampled, the streams entering Second and Third Poljes were much less saturated with respect to both calcite and dolomite than the streams that discharge water into First Polje. This difference in chemistry probably relates to the fact that

Table 3.10. Chemical Characteristics of Some Stream and Spring Waters in Nahanni Poljes.

Date	Water Type	Sample ID	Temp °C	pH	CaCO <sub>3</sub> ppm	MgCO <sub>3</sub> ppm	SI <sub>C</sub>	SI <sub>D</sub>	Log PCO <sub>2</sub>
<u>First Polje</u>									
7/7/72	Stream	27	10.0	8.30	73	32	-0.004	-0.40	-3.38
4/8/73	"	286	10.0	8.50	108	32	+0.41	+0.31	-3.49
12/7/72	"	46	19.5	7.85	78	22	-0.16	-0.86	-2.81
"	"	47	20.5	7.75	99	23	+0.02	-0.57	-2.52
"	"	48	25.5	8.00	100	26	+0.29	0.00	-2.83
18/7/73	"	66	3.0	8.10	104	17	-0.11	-0.96	-3.04
"	"	67	1.5	7.80	106	12	-0.47	-1.81	-2.77
"	"	68	2.0	7.85	92	15	-0.49	-1.70	-2.85
"	"	70 <sup>1</sup>	9.0	8.05	146	50	+0.26	+0.09	-2.83
5/8/73	"	288	2.2	7.85	125	25	-0.14	-0.91	-2.61
"	"	292	5.0	8.10	162	33	+0.35	+0.06	-2.78
18/7/72	Spring	71 <sup>2</sup>	13.0	8.45	229	72	+1.02	+1.56	-3.08
4/8/73	"	274	7.2	7.85	240	84	+0.30	+0.19	-2.52
18/7/72	"	69 <sup>3</sup>	5.0	8.00	237	47			
5/8/73	"	287	12.2	7.55	224	70			
"	"	289	5.2	7.50	275	40			
"	"	290	6.5	8.50	185	90			
<u>Second Polje</u>									
28/7/72	Stream	79	3.5	7.85	63	23	-0.88	-2.15	-3.14
"	"	80	4.0	8.10	62	20	-0.48	-1.39	-3.23
<u>Third Polje</u>									
28/7/72	Stream	83	4.0	7.20	118	49	-0.86	-2.04	-2.05

<sup>1</sup>Samples 70 and 288 are of the same stream.

<sup>2</sup>Samples 71 and 274 are of Tufa Spring waters where these sink in First Polje. These waters contain on average 55 p.p.m. sulphate ion.

<sup>3</sup>The high hardnesses of samples 69, 287, 289, and 290 suggest spring sources. As no sulphate determinations were made SI<sub>C</sub>, SI<sub>D</sub> and log PCO<sub>2</sub> are not quoted.

streams flowing into First Polje cross a broad expanse of limestone before reaching the alluviated floor. Streams entering Second and Third Poljes, however, flow almost directly from shale on to the alluviated floors and, therefore, do not pick up as much  $\text{CaCO}_3$  so they remain aggressive.

During the summers of 1972 all three poljes flooded - Third Polje to the extent that it overflowed. The lake waters were first examined on July 28th 1972; at this time the lake water in First Polje had a total hardness of 74 p.p.m., that in Second Polje 115 p.p.m. and that in Third Polje 87 p.p.m. The lake in Third Polje was also sampled and analyzed on August 27th 1972 and in the following year on August 2nd 1973. The lake water had a total hardness of 152 and 145 p.p.m. respectively on these occasions. The low hardness of lake water in Third Polje on July 28th 1972 and the fact that it was highly undersaturated with respect to both calcite and dolomite at this time (Table 3.11) suggests that surface runoff into the depression had been rapid and of considerable magnitude so that waters had only limited contact with limestone. By August 27th 1972 the water in Third Polje was saturated with respect to calcite and had picked up an additional 65 p.p.m. total hardness. As the only contact that the lake water had with limestone, was at the depression walls, solution must have taken place there. Under flood conditions, therefore, lateral solution at the walls of Third Polje must be of substantial importance. Solution niches in the walls support such a conclusion.

The overflow stream out of Third Polje was also sampled at two localities on July 27th 1972. The chemical characteristics of

Table 3.11. Chemical Characteristics of Lake and Overflow Waters in Nahanni Poljes During Flood.

Location	Date	Water Type	Sample ID	Temp °C	pH	CaCO <sub>3</sub> ppm	MgCO <sub>3</sub> ppm	SI <sub>C</sub>	SI <sub>D</sub>	Log PCO <sub>2</sub>
First Polje	28/7/72	Lake	87	14.0	7.90	57	17	-0.53	-1.56	-3.06
Second Polje	"	"	81	8.0	7.90	96	19	-0.28	-1.22	-2.89
Third Polje	"	"	84	11.5	7.55	64	23	-0.80	-2.02	-2.63
"	27/8/73	"	152	10.0	8.00	105	47	+0.01	-0.29	-2.87
"	2/8/73	"	264	13.3	7.45	100	45	-0.58	-1.48	-2.42
At Third Polje	27/8/72	Over-flow	146	6.0	8.10	102	36	-0.04	-0.49	-3.03
At Bubbling Spring	"	"	147	6.0	8.20	104	13	+0.06	-0.87	-3.14

Table 3.12. Mean Chemical Characteristics of Waters in Nahanni Poljes.

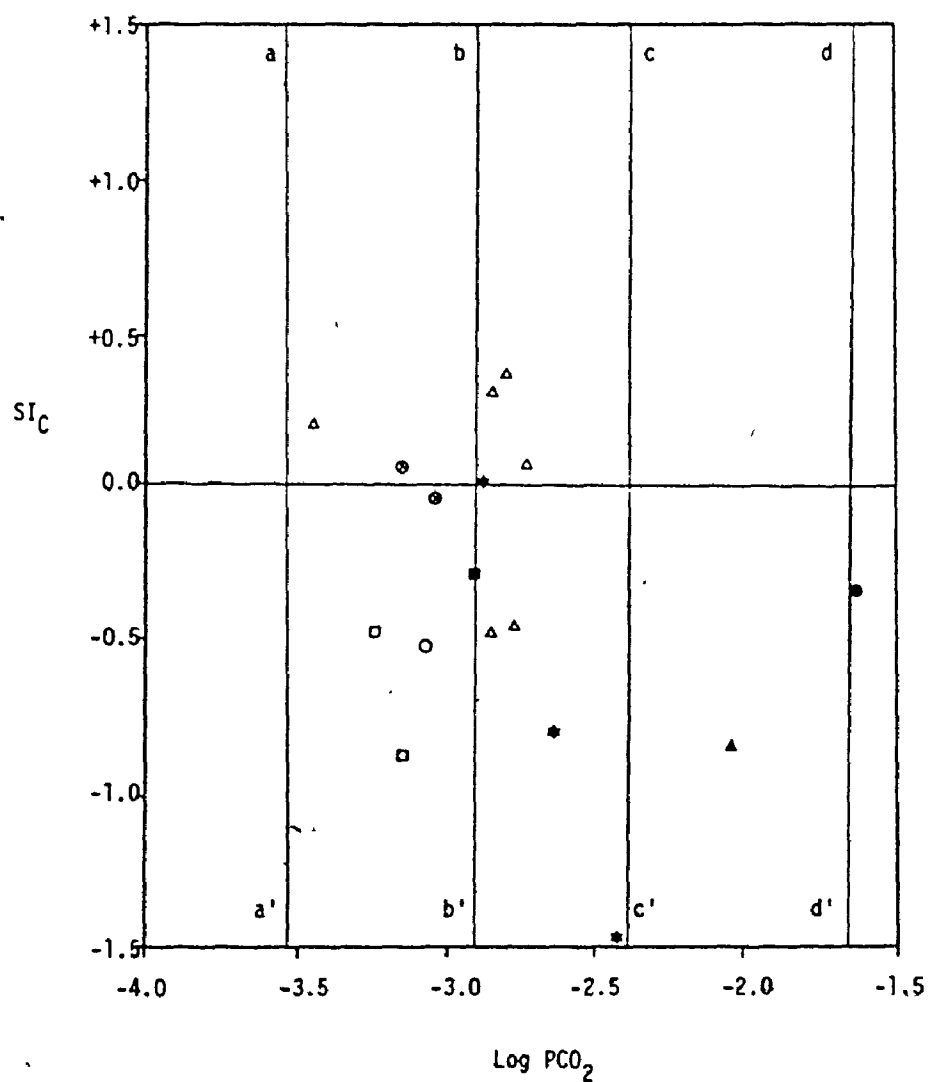
Description	No. of Samples	Temp °C	pH	CaCO <sub>3</sub> ppm	MgCO <sub>3</sub> ppm	SI <sub>C</sub>	SI <sub>D</sub>	Log PCO <sub>2</sub>
First Polje Streams	7	7.5	8.03	113	25	-0.03	-0.69	-2.92
Second Polje Streams	2	3.7	7.97	62	21	-0.68	-1.77	-3.18
Third Polje Streams	1	4.0	7.20	118	49	-0.86	-2.04	-2.05
<u>Average Stream Chemistry</u>		6.4	7.93	103	27	-0.24	-1.04	-2.88
First Polje Springs		8.6	8.02	232	70	+0.66	+0.87	-2.80
First Polje Lake		14.0	7.90	57	17	-0.53	-1.56	-3.06
Second Polje Lake		8.0	7.90	96	19	-0.28	-1.22	-2.89
Third Polje Lake		11.6	7.67	90	38	-0.46	-1.26	-2.64
<u>Average Lake Chemistry</u>		11.2	7.82	81	25	-0.42	-1.35	-2.86
Third Polje Overflow		6.0	8.15	103	27	+0.01	-0.53	-3.08

these two samples - one taken where the overflow left Third Polje, the other where it tumbled over a small waterfall to join the outflow from Bubbling Spring - indicate that once water leaves the polje its flow is turbulent and it loses  $\text{CO}_2$ . On July 27th, for instance, the pH rose from 8.00 in the lake to 8.20 at the waterfall, the hardness remained more or less the same but the calculated  $\log \text{PCO}_2$  dropped from -2.87 to -3.14 reflecting the loss of  $\text{CO}_2$  due to turbulence.

Figure 3.27 demonstrates that all stream and spring waters that enter the three Nahanni poljes are enriched in  $\text{CO}_2$ . Most are in equilibrium with a  $\log \text{PCO}_2$  similar to that present in soils on limestone. Some waters, however, especially those emerging at Tufa Spring, appear to have picked up  $\text{CO}_2$  from soils on shale. Many stream waters were probably in equilibrium with  $\text{CO}_2$  levels in shale soils but lost  $\text{CO}_2$  once they encountered limestone areas. Because lakes in poljes derive their water from streams flowing into these depressions they are generally in equilibrium with similar  $\text{CO}_2$  levels. The mean calculated  $\log \text{PCO}_2$  in streams flowing into poljes is -2.88, that for the lake waters is -2.86.

The chemical characteristics of waters in the Nahanni poljes support the view that lateral corrosion is far more important in these depressions than is vertical corrosion. The mean total hardness of streams when they reach the alluvial floors of the poljes is 130 p.p.m. and the mean  $\text{SI}_c$  is -0.24. Clearly solution by these waters is concentrated on the limestone surfaces that surround the poljes, not in their floors, although after very heavy rain aggressive waters may reach





- |      |  |   |                      |
|------|--|---|----------------------|
| △    | Streams entering First Polje                         | ○ | Lake in First Polje  |
| □    | Streams entering Second Polje                        | ■ | Lake in Second Polje |
| ▲    | Streams entering Third Polje                         | * | Lake in Third Polje  |
| ●    | Tufa Creek Spring First Polje                        | ⊙ | Third Polje overflow |
| a-a' | Atmospheric log PCO <sub>2</sub> , 3,000 ft.         |   |                      |
| b-b' | Mean log PCO <sub>2</sub> in limestone soils         |   |                      |
| c-c' | Mean log PCO <sub>2</sub> in shale soils             |   |                      |
| d-d' | Maximum log PCO <sub>2</sub> measured in shale soils |   |                      |

Figure 3.27.  $SI_C$  -  $\log PCO_2$  relationships for waters in the three Nahanni Poljes.

alluvial streamsink dolines, particularly those in Second and Third Poljes (Table 3.10). In addition, the flooding of poljes with aggressive stream water results in considerable lateral solution at the polje walls as well as some widening of the ponor systems. Not only does the alluvial fill in the polje floors protect the underlying bedrock surface from corrosion, concentrating this at the polje walls, but this material is also a rich source of  $\text{CO}_2$  for waters in the poljes. Log  $\text{PCO}_2$  levels of -2.80 and -3.10 were measured in dry parts of the alluvial floor of Second Polje and levels of -2.85 and -3.22 were measured in First Polje. Clearly waters crossing polje floors pick up  $\text{CO}_2$  and become more aggressive before reaching ponors; also flood waters must be enriched as  $\text{CO}_2$  is expelled from the saturated alluvial material. Even in dry conditions, corrosion must take place below soil level at the polje walls because soil water, rich in  $\text{CO}_2$ , must be highly aggressive. This will lead to the undercutting of the bounding walls and their subsequent collapse.

#### 6. Blind Valleys and Closed Fluvial Canyon Systems.

Many closed depressions in karst terrains are produced when surface streams or rivers are pirated underground. When a large proportion of the water in a stream sinks at one location, there is a substantial reduction in the erosional capability of the stream down valley of this point. As a result, a threshold develops in the valley long profile. As the underground drainage route is enlarged, a point may be reached when it absorbs all of the streamflow at normal stages but surface runoff continues down valley at periods of high flow.

At this point in time a semi-blind valley is said to have formed upstream of the sink. When the sink can absorb the entire streamflow even during periods of flood, so that the stream never overflows the threshold in its valley, the depression upstream of the sink is termed a blind valley and the valley downstream of it a dry valley. Blind, semi-blind and dry valleys are particularly common where allogenic stream waters encounter limestone and almost immediately sink underground. Karst processes do not completely break down the drainage system, however, because surface flow from the impervious rock cover on to the limestone continues. Instead, there is a continuous deepening of the blind valley upstream of the sink.

The disorganization of stream systems on limestone does not stop with the formation of blind valleys. Cvijić (1960) for instance, has noted that in time a swallow hole situated higher up in a blind valley may become enlarged and entirely absorb the stream so that the lower sink will become 'dead.' This process can be repeated several times with the development of a series of sinks each one nearer to the headwaters of the stream. Sweeting (1972) has also pointed out that dry valleys downstream of the blind valley swallow holes, are favored locations for the development of dolines. Water collects in irregularities in the valley floor and drains underground where fissures are most highly developed. Ultimately the dry valley floor may become a series of shallow solution dolines. Normal stream valleys in carbonate rock areas are, therefore, completely integrated by karst processes. Valleys in karst areas may be at all stages of disorganization from those that are still occupied by a large stream with little loss of water underground

to those in which the former stream valley is now little more than a string of dolines.

In areas that have recently been glaciated many closed depressions may have originated by glacial scour or have been produced by the blockage of valleys and canyons by glacial morainic material. In areas of soluble rock, these depressions may undergo karstification and therefore not be destroyed by post-glacial fluvial erosion. Barrère (1964), for instance, has reported that glacial cirques in the Pyrenees that have developed subterranean drainage systems have been transformed by solution into glacio-karstic depressions that are essentially cirque-dolines. Likewise, Ford (1971(b)) has interpreted many of the shallow closed depressions in the Mount Castleguard area of the southern Canadian Rockies as being of glacio-karstic origin. In the Triglav area of the Julian Alps, the seven lakes of Triglav which occupy a glaciated limestone valley have been dammed by valley and lateral moraines (Kunaver, 1965).<sup>1</sup> Similar closed canyon systems, blocked by glacial moraines, have been identified in the Maligne Lake area of the southern Canadian Rockies (Brown, 1972).

All stages of stream valley disorganization are to be found in the Nahanni karst. Blind valleys have been formed by allogenic streams; they have also been formed by streams with their headwaters entirely in limestone. Dwarfing these entirely karstic depressions, however, are a number of huge closed fluvial canyon systems that have been formed by a combination of fluvial, glacial and karstic processes.

---

<sup>1</sup>See Sweeting 1972, p. 267.

(a) Stream Networks Disorganized Entirely by Karstic Processes.

Many stream networks in the Nahanni, some with their headwaters in impermeable rocks have become disorganized as karstic processes have taken over. In the North karst region, disorganized networks appear to be of three main types (i) those with their headwaters in shale (ii) those developed entirely in limestone and (iii) those developed on till-covered limestone. Examples of each will be discussed.

(i) Networks with Headwaters in Shale.

A number of streams in the Nahanni North karst region have their headwaters in shale and sink almost as soon as they encounter limestone so that shallow blind valleys produced by allogenic streams are relatively common. An interesting example of such a closed depression is Lost Valley (B in Figure 3.28) which collects water from an area of shale and channels it south westwards into the labyrinth karst region of the North karst where it disappears underground. Lost Creek, which flows parallel to the bedrock dip, has cut a V-shaped valley in shale exposing limestone in the floor (Figure 3.29). At the downstream end of the valley, the creek crosses a shallow closed depression isolated on two sides by the shale walls of the valley and on the other two by a synclinal structure in the upper surface of the limestones. This depression has been filled by an alluvium clearly derived from weathered shale. Some of the water in Lost Creek sinks in this section of the valley which is characterized by several small cylindrical-shaped subsidence dolines up to 30 ft. in diameter and 20 ft. deep; some of these contain water and Lost Creek discharges into the largest of them (Figure 3.29). The presence of these subsidence dolines clearly indicates that

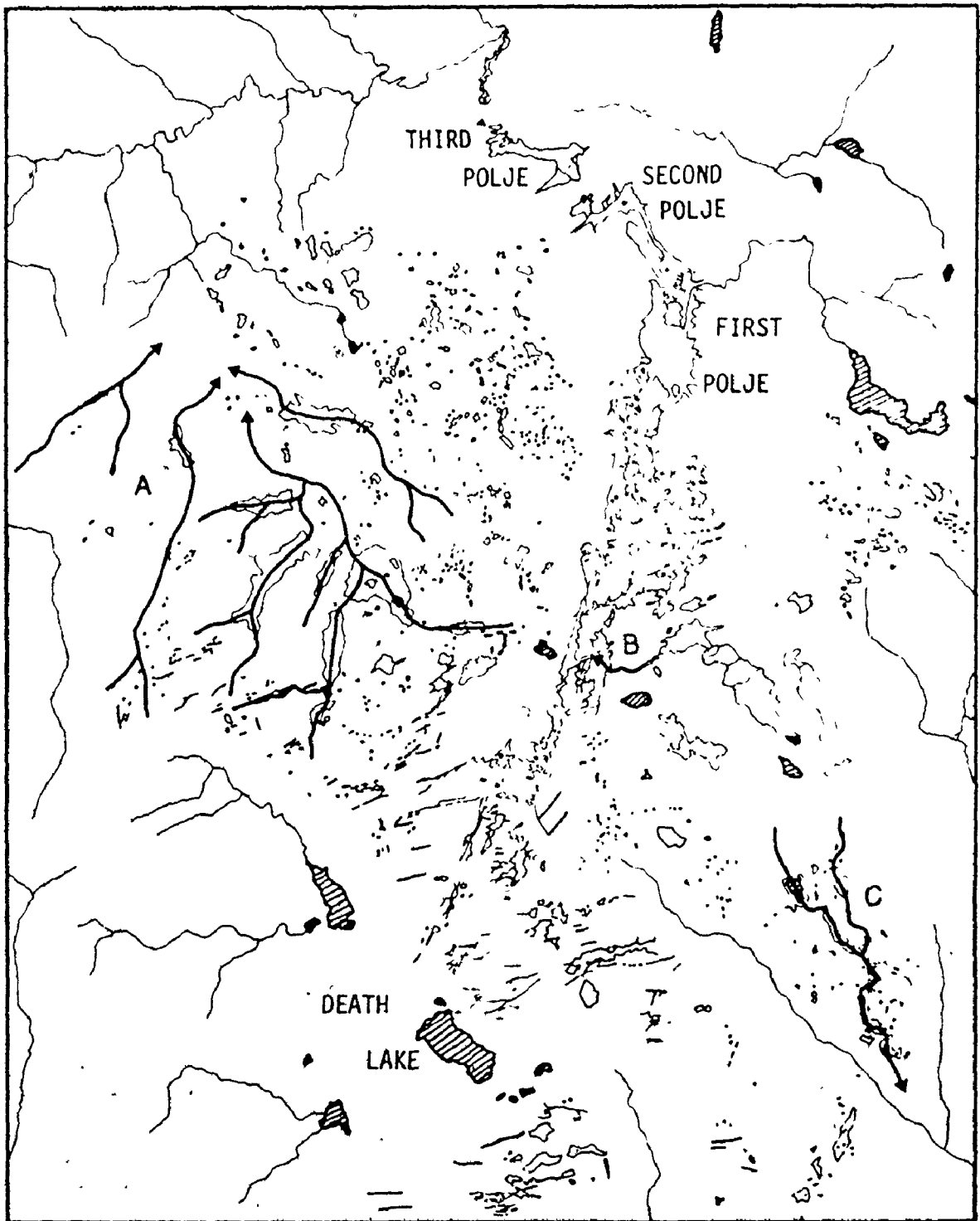


Figure 3.28. Disorganized valley systems in the North Karst, Mahanni.

solution cavities are present in the underlying limestone and that these are transmitting some water deep underground. Lost Creek leaves this alluviated stretch much reduced in volume and finally sinks underground in the floor of a karst plateau a few tens of yards further on.

Lost Creek valley is an unusual blind valley for it contains in its floor an alluviated partly structural depression. There is in fact a distinct similarity of form between this alluviated stretch of Lost Valley and Palsa Basin. It may well be that a period of stream incision through shales with blind valley development, preceded the development of Palsa Basin - a structural doline developed entirely in limestone but flanked on two sides by walls of shale.

(ii) Networks Entirely in Limestone.

Between Moraine Lake, Death Canyon and the Sinkhole Plain to the north are a number of large closed depressions which appear to have formed because of the disorganization of a surface stream valley network (A in Figure 3.28). Depressions vary up to 1500 yds. long and 900 yds. wide. They generally occupy a stretch of a stream valley which may continue up-valley of the depression for as much as two miles. All of the depressions have alluviated floors and bedrock or alluvial streamsink dolines are always present. It is apparent that water entering these depressions sinks underground. These basins are essentially blind valleys developed in a stream network entirely in limestone bedrock.

Many of the depressions have very rounded walls that appear to have been smoothed by glacial abrasion. There is some evidence, therefore, to suggest that a period of stream development on the

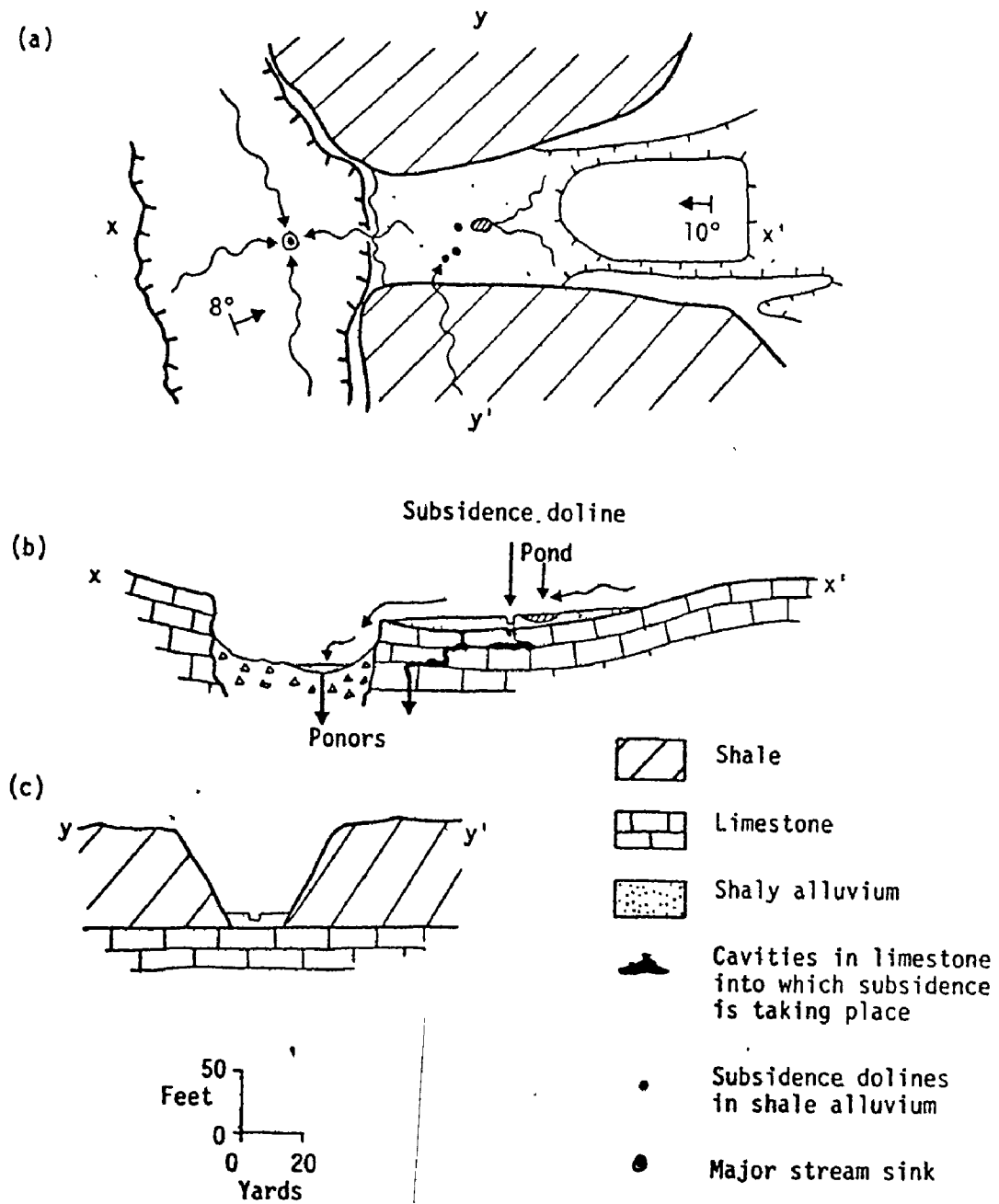


Figure 3.29. Schematic plan and profiles of Lost Valley, a blind valley formed by an allogenic stream, North Karst, Nahanni.



limestone was followed by a period of glaciation during which time the valleys were smoothed. In the post-glacial period surface flow was re-established and blind valleys formed as streams were pirated underground. A tentative reconstruction of the original drainage network is presented in Figure 3.28. It can be seen from this that the drainage was to the north or northwest. Because much of the original stream valley system is preserved in this area, it is clear that the disorganization by karstification has not yet reached an advanced stage.

(iii) Networks Developed on Till-Covered Limestone.

Over large areas of the Nahanni karst, surface stream networks are developed on impermeable glacial till which overlies large areas of limestone. Many of these streams have cut through the till into the underlying limestone and karst processes operating in the valley floors have transformed them into blind and dry valley systems. One former stream network 3 miles northeast of Death Lake (C in Figure 3.28) has been totally disorganized by karst processes. This network has been transformed into a string of linear dolines and uvalas up to 800 yds. long that are all located in very narrow corridors usually no more than 200 yds. wide. These corridors are obviously all that remain of the original stream valleys. Like the disorganized drainage system northwest of Moraine Lake this area northeast of Death Lake suggests that a fluvial system was developed on a till surface after a period of glaciation and that

this system was subsequently disorganized as karst processes operated upon it.

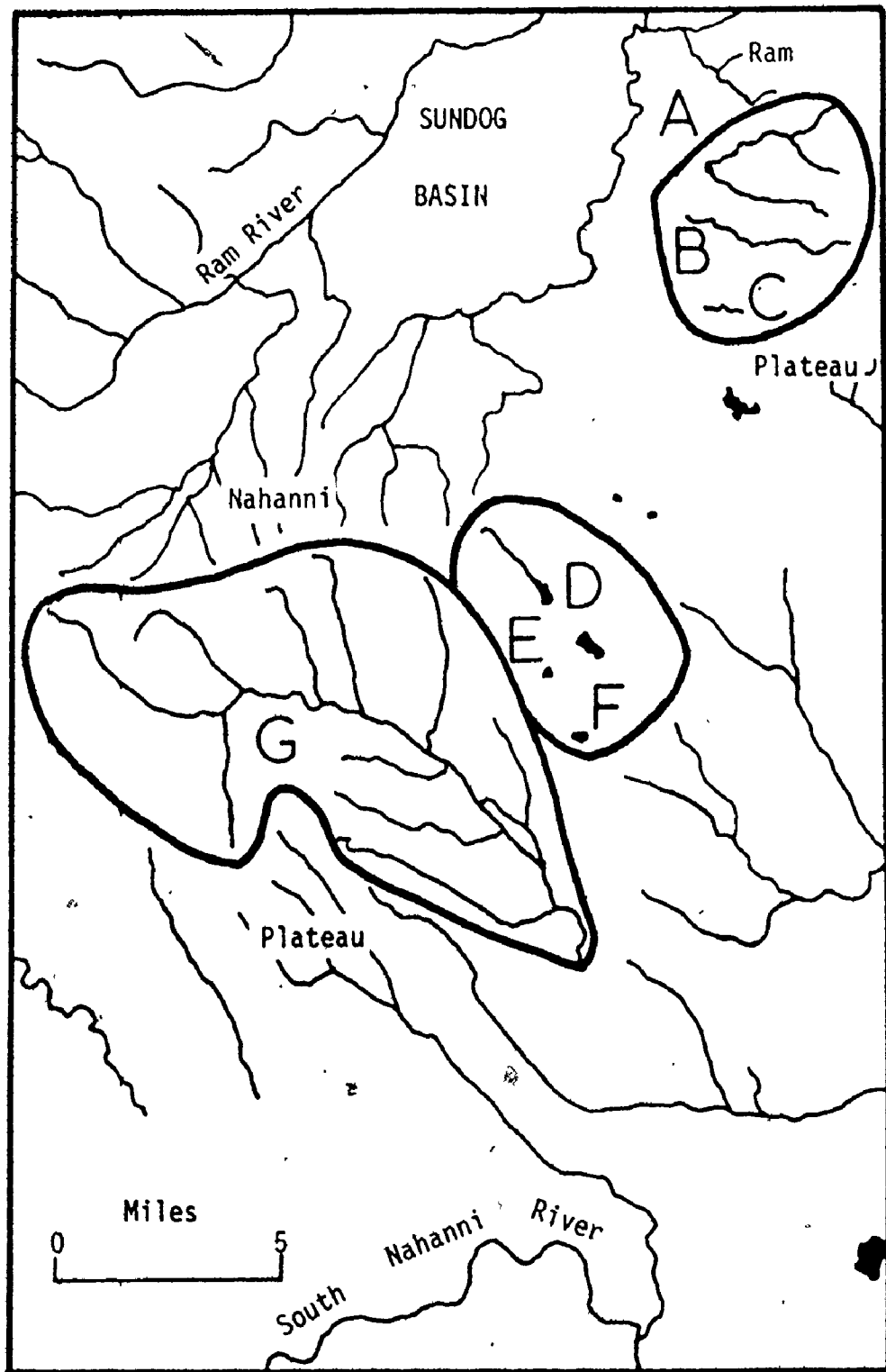
(b) Closed Fluvial Canyon Systems of Glaciokarstic Origin.

(i) Morphological Characteristics.

Six large closed fluvial canyon networks have been identified in the Nahanni karst and the likelihood is that more exist. Three of these are located on the southwest flank of the Ram Plateau and prior to closure, streams in them used to drain westwards into Sundog Basin to join the Ram River. The other canyons are located on the eastern limb of the Nahanni Plateau south of Sundog Basin and prior to closure, streams in these canyons used to discharge water eastwards to the Tetcela River. The smallest of the closed canyons is Wigchruss Canyon about three miles east of Bubbling Spring; this is about 1,000 yds. long, 200-300 yds. wide and 200-300 ft. deep. The largest is Canal Canyon on the eastern limb of the Nahanni Plateau which is approximately 18 miles long, 1.0-1.5 miles wide and from 1,000-2,500 ft. deep (Figure 3.30). Small lakes are present in the floors of all of the closed canyons.

The Closed Canyons of the Ram Plateau.

The closed canyon networks of the Ram Plateau were examined on August 2nd and 3rd 1972 after very heavy rain in July. Ground observations were made in Hiller Canyon; Texas and Wigchruss Canyons were looked at only from the air. The canyons are dendritic, up to 4 miles long and are cut into shales and limestones on the west flank of the Ram Plateau which dip at 12° to the southwest. Plateau remnants



- |   |                  |   |               |
|---|------------------|---|---------------|
| A | HILLER CANYON    | E | HIDDEN CANYON |
| B | TEXAS CANYON     | F | CRASH CANYON  |
| C | WIGCHRUSS CANYON | G | CANAL CANYON  |
| D | DEATH CANYON     |   |               |

Figure 3.30 The closed fluvial canyons of the Nahanni karst.

between the canyons are generally capped by a layer of shale from 50-150 ft. thick (Figure 3.31). All of the canyons have vertical walls in limestone which are from 100 ft. to 700 ft. high and talus cones and aprons are characteristic. The canyons are blocked at their downstream ends by accumulations of glacial debris (Plate 3.26). The magnitude of closure varies from canyon to canyon; in Hiller Canyon it is of the order of 50-75 ft., in Texas and Wigchruss Canyons it appears to be less than 30 ft. (Figure 3.32). The floors of the canyons are alluviated back from their points of closure so that the canyons are distinctly U-shaped in these stretches (Figure 3.32). Nearer the headwaters, however, the canyon floors are cut in bedrock and cross profiles are much more V-shaped. The canyon floors have been alluviated to approximately the same level. The floor of Wigchruss Canyon is at an elevation of about 3,000 ft. a.s.l., that in Texas Canyon at a little less than 2,900 ft. and the floor of Hiller Canyon varies between 2,700-2,800 ft. in altitude.

Lakes are present in all three of the Ram Plateau closed canyons, they appear to be semi-permanent features perched on insoluble material and are fed by surface runoff waters. After heavy rain and probably at snowmelt there is rapid surface runoff into the canyons from surrounding areas of shale and at these times streamflow in the canyon floors is vigorous. In early August 1972, for example, after 10.5 inches of rainfall in July some streams were entering the canyons via short valleys; others were simply plunging over the canyon walls. All of the tributaries of the Hiller Canyon network had sizeable streams flowing across

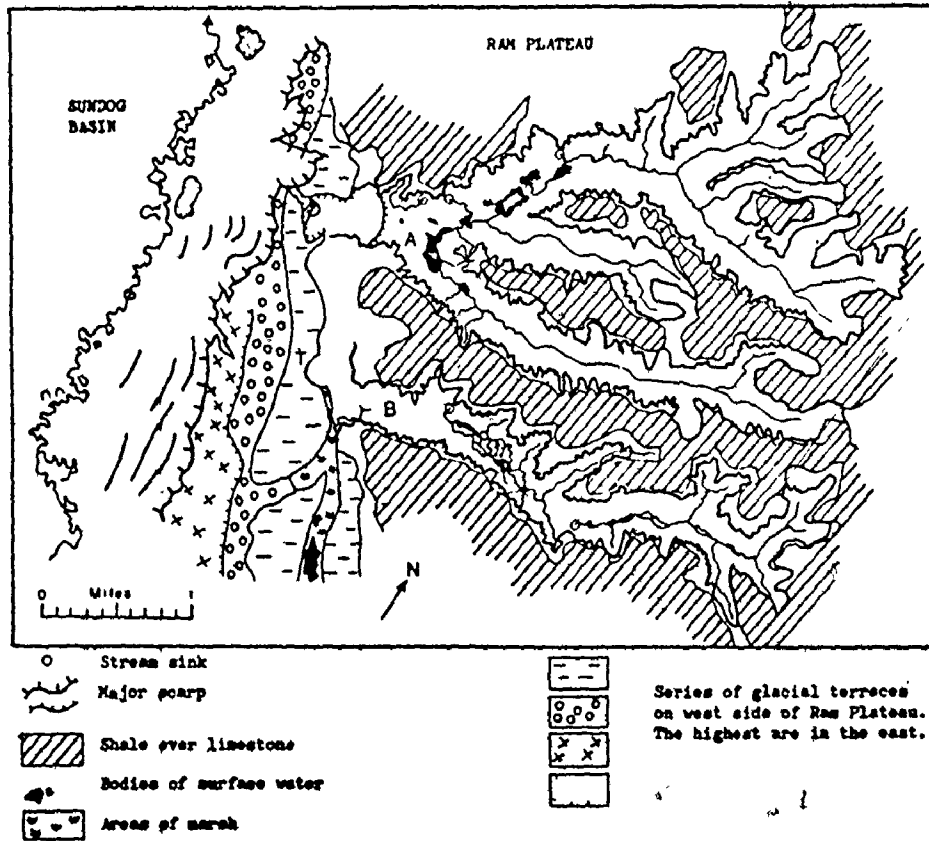


Figure 3.91. Geomorphic map of Hiller and Texas closed canyons, Ram Plateau.



Plate 3.26. Hiller Canyon, a closed fluvial canyon dissecting the western edge of the Ram Plateau.

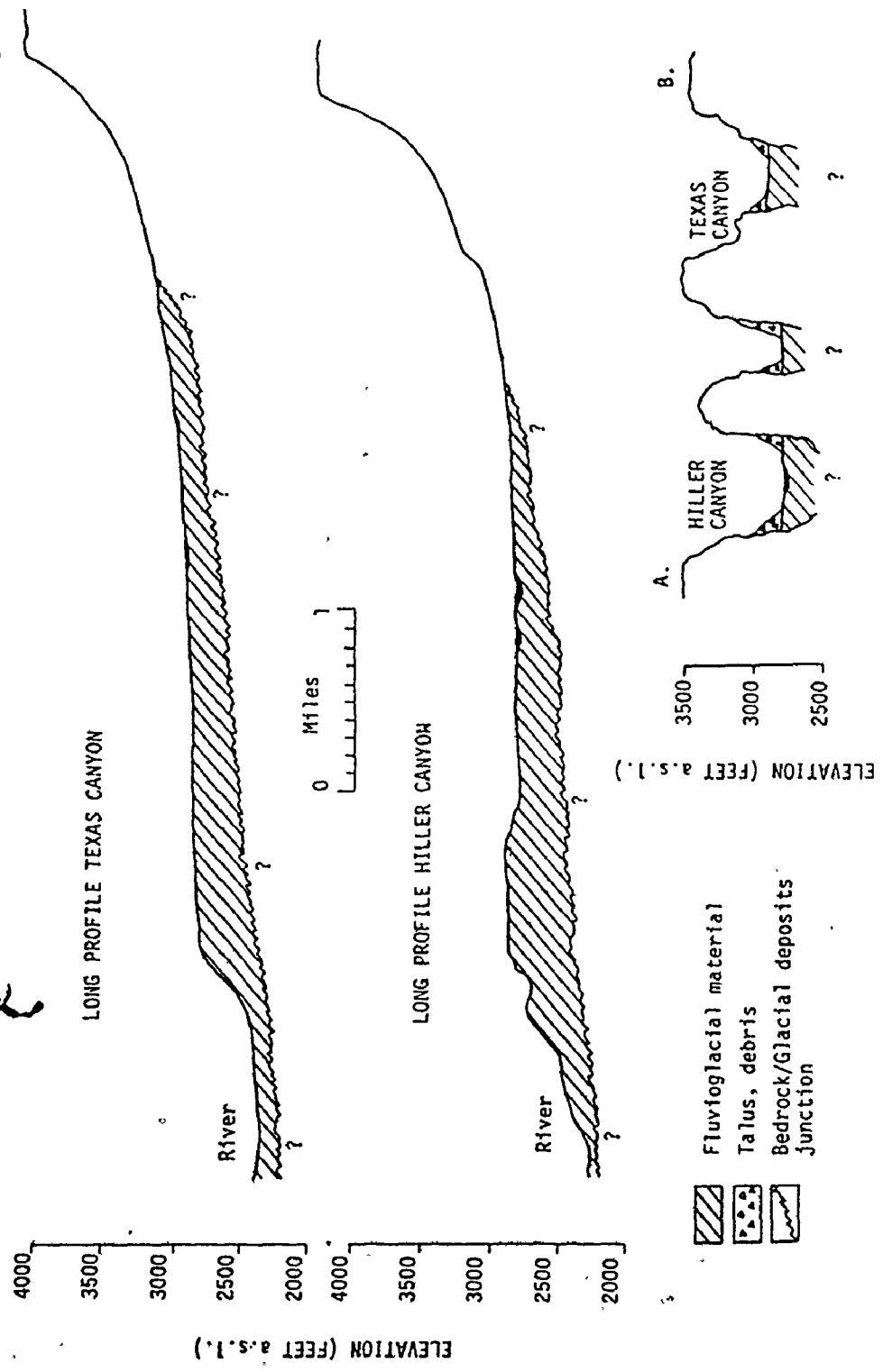


Figure 3.32. Long profiles of Hiller and Texas Canyons; Ram Plateau.

their floors. These were channeling water into the lakes in the alluviated stretch of the canyon system. Water that enters Hiller Canyon finally drains underground via alluvial streamsink dolines that appear to be concentrated at the base of the north wall in the alluviated area (Figure 3.31). Although ground observations were not made in Texas Canyon, it appears from the aerial photographs of the area that waters sink at the base of the south wall in this system. In early July 1972, three members of the McMaster party stumbled into Wigchruss Canyon after losing their way en route from Third Polje to Mosquito Lake. They described the canyon as having a lake at its mouth, vertical walls in limestone, a flat alluviated floor and noted that there was no surface drainage out of it. It is clear that waters in this canyon also sink underground.

#### The Closed Canyons of the Nahanni Plateau.

The closed canyons of the Nahanni Plateau are much larger features than those of the Ram Plateau and differ slightly in morphology. The simplest and the largest of them is Canal Canyon, a dendritic network 18 miles long and in places more than 2,500 ft. deep (Figure 3.33). The upper 600 ft. of the canyon is cut in limestones of the Nahanni Formation dipping at  $10^\circ$  to the southeast, the rest into underlying dolomites (Plate 3.27). Walls are steep to vertical in the limestones and steeply sloping in the dolomites above extensive talus accumulations. The mouth of the canyon is blocked by a glacial end moraine, its crest at 2,800 ft. a.s.l. For a distance of 5 miles upstream of this barrier the alluviated floor slopes imperceptibly around a mean elevation of close to 2,700 ft. giving the canyon a closure of approximately



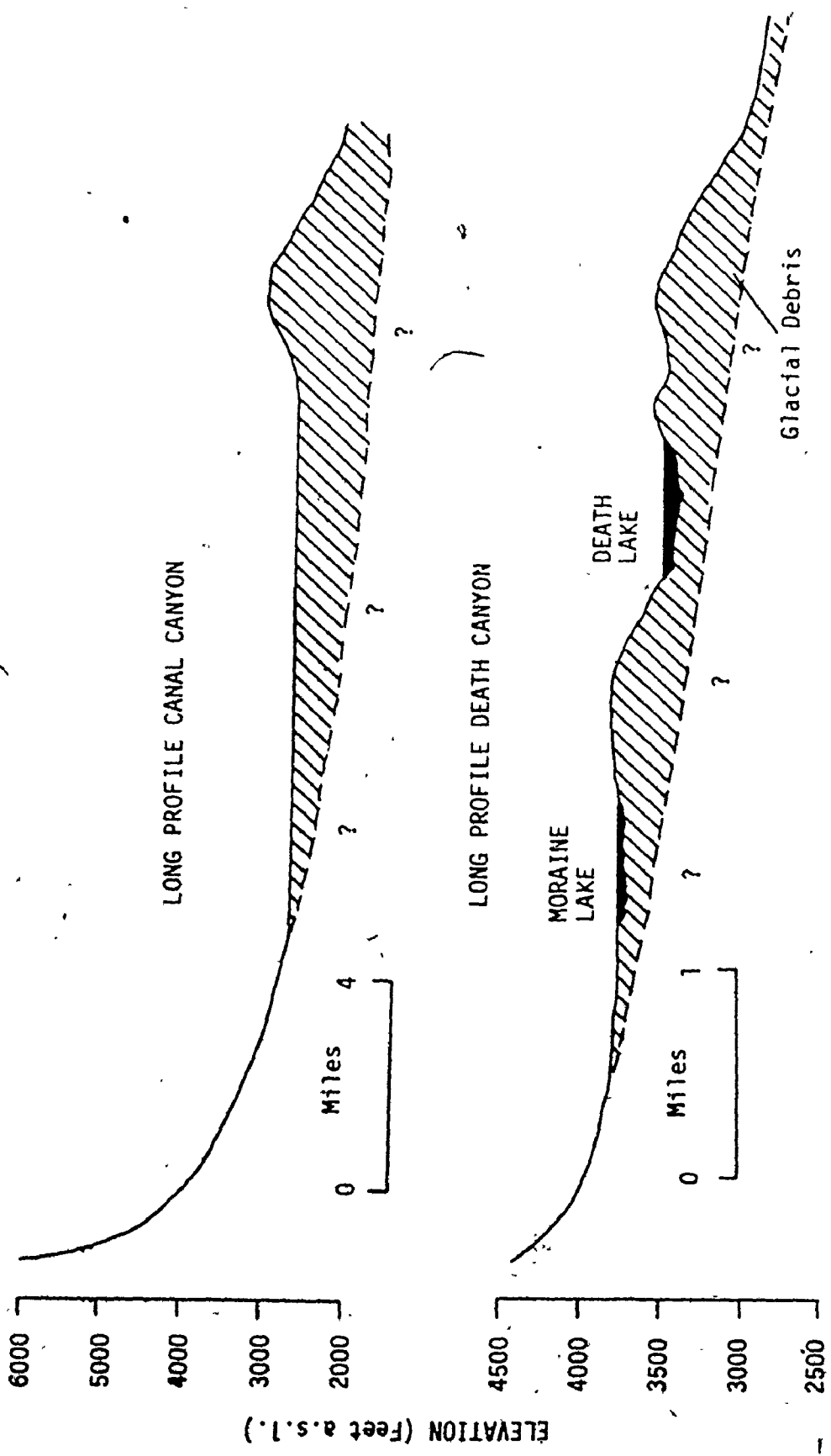


Figure 3.33. Long profiles of Canal and Death Canyons.

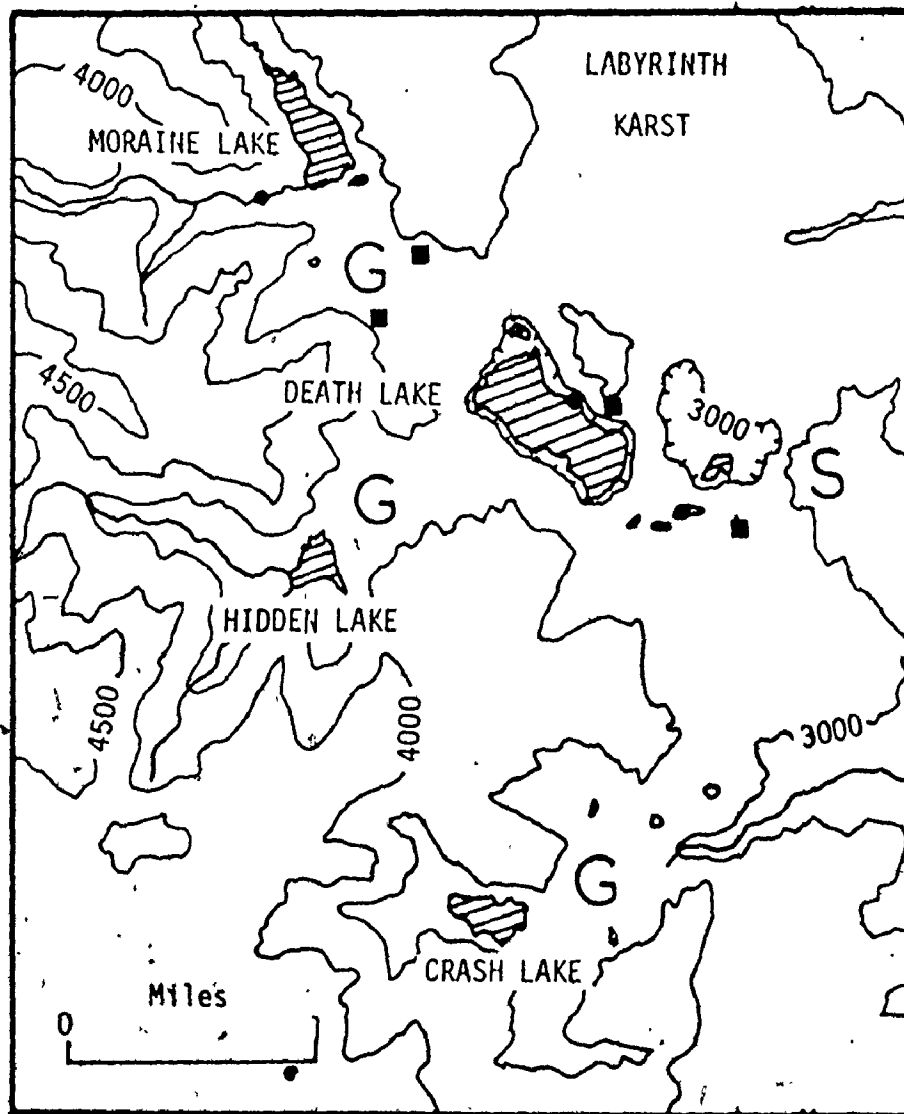


Plate 3.27. Canal Canyon, a glacio-karstic depression. In places this canyon which is cut in limestones and underlying dolomites is more than 3,000 feet deep. Its mouth is blocked by glacial debris laid down by ice moving in the up-valley direction. There is no surface drainage out of the canyon at present. All water is thought to drain underground through dolomites to White Spray in the north wall of First Canyon, South Nahanni River.

100 ft. (Plate 3.27). The alluvial fill consists of a fine sand that appears to be a weathering product of the dolomites.

The catchment of the Canal Canyon network is substantial so that the amount of water that flows into the system during snowmelt or after heavy rainfall must be considerable. Huge alluvial fans which are made up of limestone and dolomite boulders sometimes more than 3 ft. in diameter, have been built out into the main canyon by tributary streams. These attest to the intensity of fluvial activity in this canyon complex today (Figure 3.33 and Plate 3.27). Despite evidence of vigorous fluvial activity there is no surface flow of water out of the canyon at the present time. A series of lakes connected by sluggish, meandering streams that resemble canals, dot the alluviated section of the canyon which becomes extremely marshy after heavy rain. Water reaching this portion of the canyon floor is believed to sink into ponors at the base of the south wall of the canyon and flow underground to White Spray - a spring in the north wall of First Canyon, South Nahanni River.

The most complex of the closed fluvial canyon networks in the Nahanni karst is the Death Canyon assemblage which includes Death Canyon and two of its tributaries Hidden and Crash Canyons (Figure 3.34). Unlike the other closed canyon networks, the Death Canyon system consists of not one but four major closed basins each closed by glacial end moraine deposits and each occupied by a sizeable lake (Figure 3.35). Death Canyon itself hosts two of these basins, the one nearest the headwaters occupied by Moraine Lake and a second occupied by Death Lake. The closed canyons, which have vertical walls above huge screes and a relative relief of



- G Glacial moraine barrier
- S Bedded sands and gravels
- Caves
- Sinks

Figure 3.34. Geomorphic map of Death Canyon.

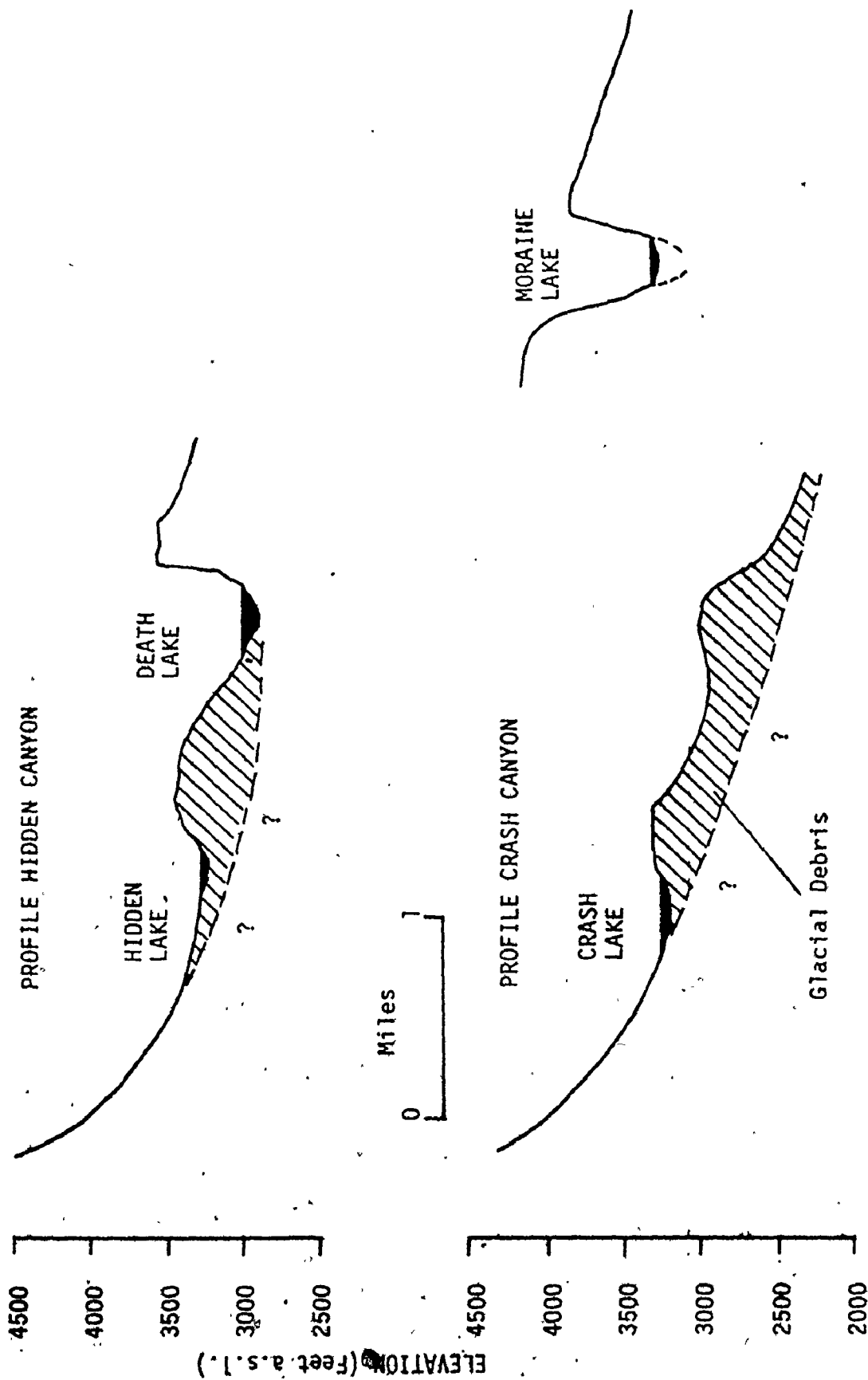


Figure 3.35. Sections across Death Canyon.

300-500 ft., are almost entirely developed in limestones of the Nahanni Formation; neither dolomites nor shales are exposed in their walls. The largest of the glaciokarstic depressions is more than a mile long, has a closure of about 150 ft. and is occupied by Moraine Lake. The smallest is less than 1,000 yds. long, has a closure of less than 100 ft. and is occupied by Crash Lake (Figure 3.35). Down-valley of the end moraine complex that has blocked the upper portion of the Death Canyon drainage system, the canyons are choked with glacial debris that has been dissected by stream action and which is characterized by numerous small depressions, many containing ponds (Figure 3.34).

All four lakes in the Death Canyon area have surface streams flowing into them after rain, and in addition, some water is supplied to Death Lake by a spring in the south wall of the canyon. All of the lakes are believed to drain underground although definite proof of this has only been obtained for Death Lake. This lake, 1,200 yds. long, 300-400 yds. wide and more than 100 ft. deep, drains into a sink in the north wall of Death Canyon (Figure 3.34); the water is known to resurge at Bubbling Spring in the north. The aerial photographs of Hidden Lake, which is generally less than 20 ft. deep, show that a stream channel continues right across the floor of the lake to the base of the western wall. The existence of this channel suggests that a sink exists in the western wall and that during dry periods Hidden Lake may dry up completely. The floor of Crash Lake, which in 1972 appeared to be less than 10 ft. deep, is covered by limestone boulders up to 3 ft. in diameter. Although no sinks have been identified it is possible that the

water in this lake percolates through this coarse debris into fissures in the underlying bedrock. No evidence that Moraine Lake drains underground could be found.

(ii) Characteristics of Solution.

The pattern of solution in the closed canyons of the Ram Plateau is very different to that in the closed canyons of the Nahanni Plateau because of basic differences in bedrock and surficial geology. Variations in the intensity of solution in Hiller Canyon and in the Death Canyon assemblage will now be discussed to illustrate this point.

The Pattern of Solution in Hiller Canyon, Ram Plateau.

Lake, stream and marsh waters in Hiller Canyon were sampled and analysed on August 2nd and 3rd 1972. The chemical characteristics of the samples taken are shown in Table 3.13, mean statistics are given in Table 3.14. The mean chemical characteristics of streams flowing into Hiller Canyon from surrounding areas of shale were found to be temperature 4.1°C, pH 7.75, total hardness 78 p.p.m.,  $SI_C$  -0.84,  $SI_D$  -2.56 and  $\log PCO_2$  -2.92 (Table 3.14 and Figure 3.36). These waters are clearly in equilibrium with a  $PCO_2$  higher than the atmospheric figure and are highly undersaturated with respect to both calcite and dolomite. Stream waters in the alluviated floor of the canyon, on the other hand, were found to have a mean temperature of 3.7°C, a pH of 7.8, a total hardness of 109 p.p.m., an  $SI_C$  of -0.48, and  $SI_D$  of -1.71 and a  $\log PCO_2$  of -2.80. Stream waters in the alluviated floor of Hiller Canyon, therefore, clearly have a higher pH, a higher hardness, are closer to saturation and are in equilibrium with a higher level of  $CO_2$  than streams flowing into the canyon from shale areas (Figure 3.36).

Table 3.13. Chemical Characteristics of Some Waters in Hiller Canyon,  
Ram Plateau.

Date	Sample ID	Temp. °C	pH	CaCO <sub>3</sub> ppm	MgCO <sub>3</sub> ppm	SI <sub>C</sub>	SI <sub>D</sub>	Log PCO <sub>2</sub>
<u>Streams in the Canyon Floor</u>								
3/8/72	103	2.0	7.90	93	16	-0.43	-1.57	-2.90
"	101	4.0	7.70	93	16	-0.53	-1.88	-2.70
"	97	5.0	7.80	97	14	-0.44	-1.67	-2.90
<u>Streams Entering the Canyon From Shale Areas</u>								
3/8/72	99	1.0	7.85	76	7	-0.69	-2.36	-2.96
"	98	1.0	8.05	79	7	-0.46	-1.90	-3.14
2/8/72	95	1.0	7.80	121	19	-0.35	-1.44	-2.69
"	94	6.0	7.90	63	8	-0.66	-2.18	-3.08
"	93	7.0	8.05	72	3	-0.41	-2.15	-3.20
"	89	6.5	7.30	43	8	-1.55	-3.79	-2.63
"	90	6.5	7.30	34	7	-1.74	-4.13	-2.72
<u>Lakes</u>								
3/8/72	102	5.0	7.80	93	15	-0.46	-1.66	-2.80
2/8/72	96	4.0	7.55	98	13	-0.72	-2.26	-2.56
"	91	7.5	7.50	79	16	-0.82	-2.28	-2.55
3/8/72	100	9.0	7.60	95	17	-0.53	-1.78	-2.57
<u>Marsh Waters</u>								
2/8/72	92	6.0	4.10	2	4	-8.23	-16.41	-1.62



It would be expected that the shallow lakes in Hiller Canyon would have similar chemical characteristics to the streams which feed them. The mean characteristics of these waters, however, with the mean temperature  $6.4^{\circ}\text{C}$ , pH 7.61, total hardness 106 p.p.m.,  $\text{SI}_C$  -0.63,  $\text{SI}_D$  -1.99 and  $\log \text{PCO}_2$  -2.62 indicate that they have a higher temperature, a lower pH, are less saturated and are in equilibrium with higher levels of  $\text{CO}_2$  than are these stream waters (Table 3.14 and Figure 3.36). One additional water sample was collected from a marshy area in the canyon floor (sample 92 in Table 3.13). This water was found to have a temperature of  $4.1^{\circ}\text{C}$  a pH of 4.1 and a total hardness of approximately 6 p.p.m.  $\text{SI}_C$  and  $\text{SI}_D$  values of -8.23 and -16.41 are of dubious accuracy because of the very low hardness of the water but there can be no doubt that it is highly undersaturated. A calculated  $\log \text{PCO}_2$  of -1.62 indicates that it is highly enriched in  $\text{CO}_2$ .

Chemical differences between the various water types in Hiller Canyon, appear to be related to the degree of contact with biogenic  $\text{CO}_2$  and limestone. Streams that discharge water into the canyon and which have their headwaters in shale, have had only limited contact with limestone and therefore have a relatively low mean total hardness of 70 p.p.m. These waters have picked up  $\text{CO}_2$  from the soils on the shales but much of this gas is lost to the atmosphere as streams tumble into the canyon in small waterfalls or enter it via steep, narrow valleys. As Table 3.13 shows, the calculated values of  $\log \text{PCO}_2$  for these waters range from -2.62, which is close to the mean  $\log \text{PCO}_2$  of -2.39 measured in soils on shale (Figure 3.36), down to -3.20;  $\text{SI}_C$  values vary from -1.74 to -0.35.

Table 3.14. Mean Chemical Characteristics of Some Waters in Hiller and Death Canyons, Nahanni Karst.

Location	Temp. °C	pH	CaCO <sub>3</sub> ppm	MgCO <sub>3</sub> ppm	SI <sub>C</sub>	SI <sub>D</sub>	log PCO <sub>2</sub>
<u>Streams</u>							
Hiller Canyon	4.0	7.76	77	10	-0.73	-2.30	-2.88
Death Canyon	6.0	8.04	103	11	-0.13	-1.25	-3.00
<u>Lakes</u>							
Hiller Canyon	6.4	7.61	91	15	-0.63	-1.99	-2.62
Death Canyon	17.0	8.21	76	16	+0.10	-0.50	-3.22

The most saturated stream waters and those containing the least  $\text{CO}_2$ , are invariably those that have entered the canyon in small waterfalls, lost  $\text{CO}_2$  quickly as they were rapidly aerated and thus became more saturated.

Figure 3.36 demonstrates that lake and stream waters on the alluviated floor of Hiller Canyon are generally in equilibrium with higher  $\log \text{PCO}_2$ 's than are the streams entering the canyon from shales. This difference is undoubtedly due to the fact that waters in the canyon floor came in contact with extremely acid marsh waters rich in biogenic  $\text{CO}_2$  and acquire some of their properties.

The Pattern of Solution in the Death Canyon Assemblage, Nahanni Plateau.

Data on the pattern of solution in the Death Canyon assemblage of closed canyons was collected during the summer of 1972 and 1973. The chemical characteristics of the stream and lake waters that were sampled and analyzed are given in Table 3.15, mean statistics are listed in Table 3.14. Lake waters in the Death Canyon area have a mean temperature of  $17.0^\circ\text{C}$ , a pH of 8.21, a total hardness of 92 p.p.m., an  $\text{SI}_\text{C}$  of +0.1, an  $\text{SI}_\text{D}$  of -0.5 and a  $\log \text{PCO}_2$  of -3.22. The average chemical characteristics of some of the stream waters that feed them are temperature  $6.0^\circ\text{C}$ , pH 8.04, total hardness 114 p.p.m.,  $\text{SI}_\text{C}$  -0.13,  $\text{SI}_\text{D}$  -1.25 and  $\log \text{PCO}_2$  -3.00. On average, therefore, lake waters in the Death Canyon region have a higher temperature and pH and a lower hardness than stream waters on limestone. In addition they are more saturated with respect to both calcite and dolomite and are in equilibrium with lower  $\log \text{PCO}_2$  levels. Although some of the chemical difference, particularly in

Table 3.15. Chemical Characteristics of Some Waters in the Death Canyon Area.

Date	Sample ID	Temp. °C	pH	CaCO <sub>3</sub> ppm	MgCO <sub>3</sub> ppm	SI <sub>C</sub>	SI <sub>D</sub>	log PCO <sub>2</sub>
<u>Streams</u>								
21/8/72	123	8.0	8.00	107	4	-0.11	-1.60	-2.97
"	124	4.0	8.10	91	17	-0.21	-1.09	-3.11
"	121	7.0	7.50	95	15	-0.69	-2.14	-2.48
"	117	4.5	8.15	109	12	-0.04	-0.99	-3.13
"	116	3.0	8.15	96	18	-0.14	-0.95	-3.14
22/8/72	126	7.0	8.00	134	4	+0.09	-1.30	-2.83
"	128	7.0	8.40	94	4	+0.20	-0.94	-3.39
"	131	7.5	8.00	99	17	-0.14	-0.99	-2.95
<u>Lakes</u>								
14/8/72	108	18.0	8.05	64	13	-0.16	-1.01	-3.11
"	105	15.0	8.40	81	24	+0.31	+0.11	-3.37
16/7/73	204	14.9	8.38	85	28	+0.38	+0.29	-3.27
21/8/72	122	18.0	8.20	81	9	+0.12	-0.70	-3.22

hardness, may be due to dilution of lake waters by rainfall and the input of low-hardness surface runoff waters from glacial material after rain, most is probably due to the partial equilibration of lake waters with atmospheric  $PCO_2$  levels. Such a loss in  $CO_2$  would result in a slight increase in pH, a move towards saturation with respect to both calcite and dolomite and a slight lowering of the calculated log  $PCO_2$ . Figure 3.36 illustrates that the stream and lake waters in the Death Canyon area are all in equilibrium with log  $PCO_2$  levels that lie somewhere between atmospheric and the maximum that has been measured in soils on limestone in this region.

As Table 3.14 shows, lake and stream waters in Hiller Canyon are highly undersaturated with respect to both calcite and dolomite and have average total hardnesses of 106 and 87 p.p.m. respectively. Similar waters in the Death Canyon complex have average hardnesses of 92 and 114 p.p.m. respectively and are generally saturated with respect to calcite but undersaturated with respect to dolomite. Slightly more solution is therefore accomplished by surface waters in the Death Canyon area and because stream waters in this area are close to saturation before they discharge water into lakes in the canyon floors, this solution appears to be concentrated in the sides of the canyons rather than in their floors. In the Hiller Canyon area, especially in the alluviated, marshy stretch of the canyon floor, solution is concentrated at the bases of the canyon walls in contact with the acid shale-derived alluvium. Lateral solution in Hiller Canyon and in the other closed and alluviated canyons of the Ram Plateau is concentrated (at the canyon walls) at or just below the upper level of the impermeable alluvium.

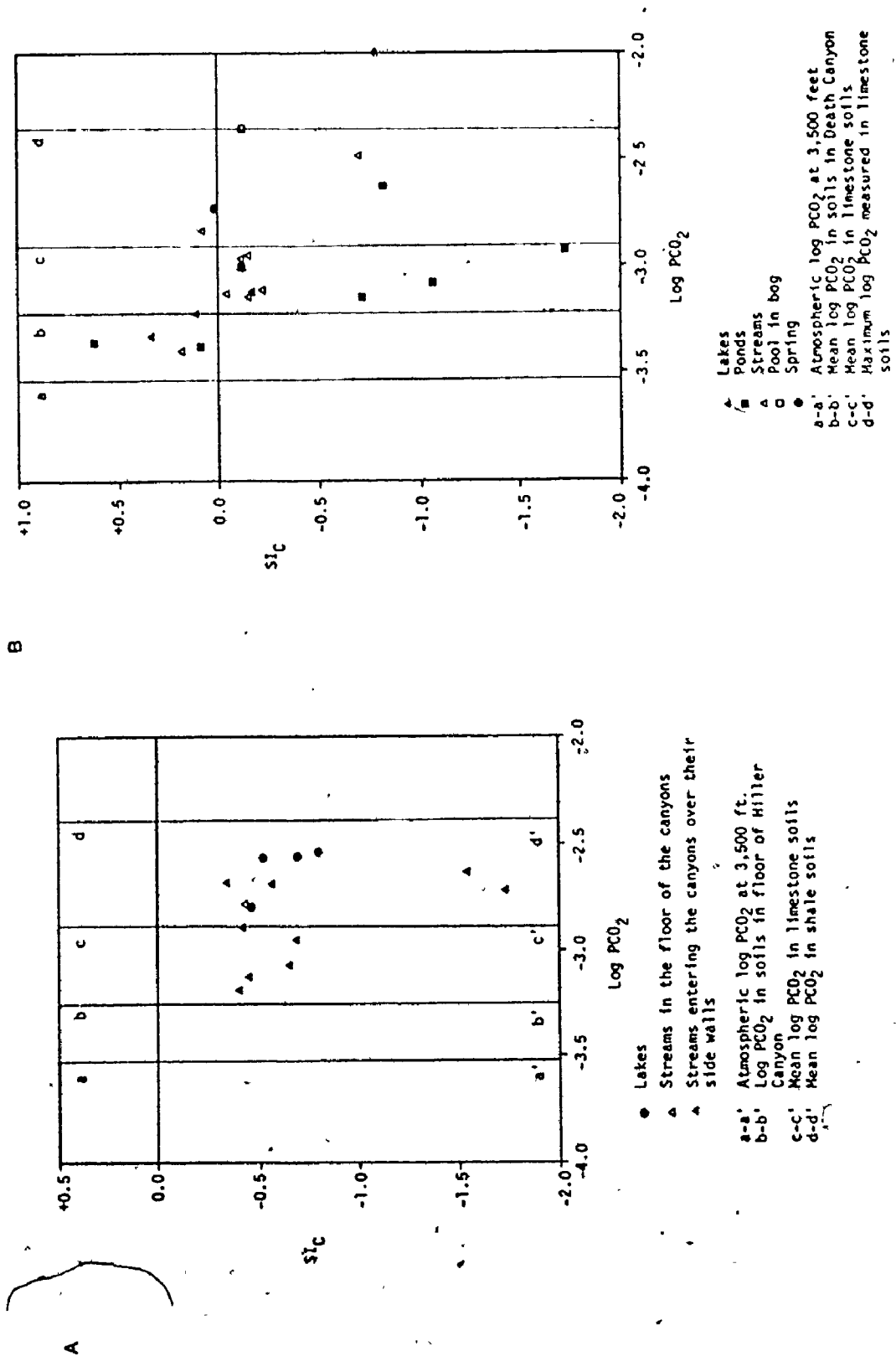


Figure 3.36.  $SI_c - \log PCO_2$  graphs for waters in the Hiller Canyon network (a) and in the Death Canyon network (b).

In this respect the pattern of solution in the closed canyon systems of the Ram Plateau is similar to that operating in the poljes of the Nahanni. Concentrated lateral corrosion of this kind could well transform these closed canyons into poljes at some time in the future. It should be noted that similar processes seem to be operating in Canal Canyon in the Nahanni Plateau where solution in the alluviated, marshy section of the basin is also concentrated at the bases of the side walls.

Water sinking underground in the closed basins of the Death Canyon complex is generally saturated or very close to saturation with respect to calcite. This is not the case in Hiller Canyon, however, where sinking waters are highly aggressive (Table 3.14 and Figure 3.36). It is clear that the underground drainage routes leading out of Hiller Canyon are being rapidly widened by the waters passing through them, those draining water from the Death Canyon area on the other hand are being only slowly widened. That waters in Hiller Canyon are highly undersaturated when they sink underground while those of Death Canyon are virtually saturated is clearly due to differences in the surficial cover in the floors of these two canyon systems. In Hiller Canyon, surface waters are in contact with a marshy environment before they sink and they pick up additional  $\text{CO}_2$ . In the Death Canyon area, waters are saturated by the time they reach the depression floors and because there is no additional source of  $\text{CO}_2$  they remain saturated when they sink.

Solution in the closed fluvial canyon networks of the Ram Plateau and in Canal Canyon of the Nahanni Plateau, appears to be concentrated at the bases of the bounding limestone or dolomite walls in the alluviated sections and in the alluvial streamsink dolines. The pattern of solution

is, therefore, similar to that observed in the poljes of the Nahanni - a pattern typical of poljes elsewhere in the world. There is, therefore, the possibility that these basins will develop into poljes as they continue to evolve. In the Death Canyon area, however, solution is not concentrated at the bases of the bounding limestone walls, it is instead more equally distributed over the vertical extent of these walls. Nevertheless, the intensity of solution in the closed basins of this complex suggests that in time, poljes might evolve here too.

(iii) Origin of the Closed Fluvial Canyon Networks.

There have clearly been three major phases in the development of the closed fluvial canyon networks of the Nahanni area. The first stage was a period of intense fluvial activity during which time the Nahanni and Ram Plateau were dissected by river canyons up to 3,000 ft. deep (Figure 3.30). In the second stage, the mouths of many of these canyons were blocked by glacial material laid down by a Laurentide ice sheet that invaded the area from the east. Some of the canyons were completely covered by ice at this time while ice occupied only the mouths of others. Many of the canyons, not entirely covered by ice, may have been occupied by lakes during this period; others may have developed underground drainage routes.

Ice retreat almost certainly left a large number of canyons blocked by accumulations of glacial debris. Those canyons that had already developed underground drainage routes or that subsequently developed them, remained closed. Surface drainage was re-established in many of the canyons and the morainic barriers were gradually eroded.



Surface drainage out of canyons that developed efficient alternative subsurface routes was never re-established.

The third and present stage in the development of the closed canyons is one of karstification. Underground conduits are being enlarged and vertical and lateral corrosion is taking place. The original glacially-produced basins are becoming true karstic depressions and as has already been pointed out, could eventually evolve into true poljes. The closed canyon systems of the Nahanni are, therefore, complex fluvio-glacio-karstic landforms that are rapidly evolving today.

## 7. Caves.

### (a) Cavern Morphology.

The vast majority of caves that have been discovered in the Nahanni karst appear to be of the phreatic type. They consist of one or more of three passage elements - vertical shafts, fissure passages and bedding plane tubes. The vertical shafts generally intersect the plateau surfaces, the horizontal passages the vertical walls of fluvial canyons, karst streets, karst plateaus and poljes. Although most of the caves that have been discovered are choked at shallow depth by limestone breakdown, ice or silt, it is clear that at one time they functioned to collect and discharge groundwater from many sink points on the plateaus into a few big springs in the evolving canyons. Today, none of these caves contain streams so all are fossil. Vertical shafts that transmit water at the present time have been discovered on the Nahanni Plateau surface south of Death Lake and in the floors of Brachiod Basin, First Polje and Palsa Basin. These can be entered to shallow

depth but all are blocked by limestone breakdown through which the streamwaters infiltrate.

From the limestone plateau surfaces in the Nahanni, caves are entered via vertical shafts of elliptical cross section that have developed in faults or joints. The deepest cave of this type is Raven Lake Pit in the plateau surface west of Raven Lake in the north karst. This cave consists of a vertical shaft 240 ft. deep and 40 ft. in diameter which connects with a bedding plane tube 20 ft. in diameter (Figure 3.37). The north end of this tube intersects the south wall of Raven Canyon at a point approximately 200 ft. above the level of Raven Lake. The tube ends 600 ft. to the south in a boulder choke and at this point the passage is floored by ice. Several small joints cross the bedding plane tube and one of these has been widened by solution with the formation of a 60 ft. high phreatic dome. The presence of this feature indicates that the bulk of the cave is solutional in origin and that enlargement took place under conditions of phreatic groundwater flow in the limestone.

Although Raven Lake Pit is a fossil cave, conduit systems of similar morphology have been discovered that are still active. One of these was discovered in the upper surface of the Nahanni Plateau south of Death Lake in 1973. The cave is a vertical shaft of elliptical cross section 60 ft. deep and 6-10 ft. in diameter which at the time it was examined had a small stream plunging into it. At depth, the shaft is blocked by frost and collapse breakdown (Figure 3.43).

More common than vertical shaft caves, however, are more or less horizontal bedding plane tubes and f are

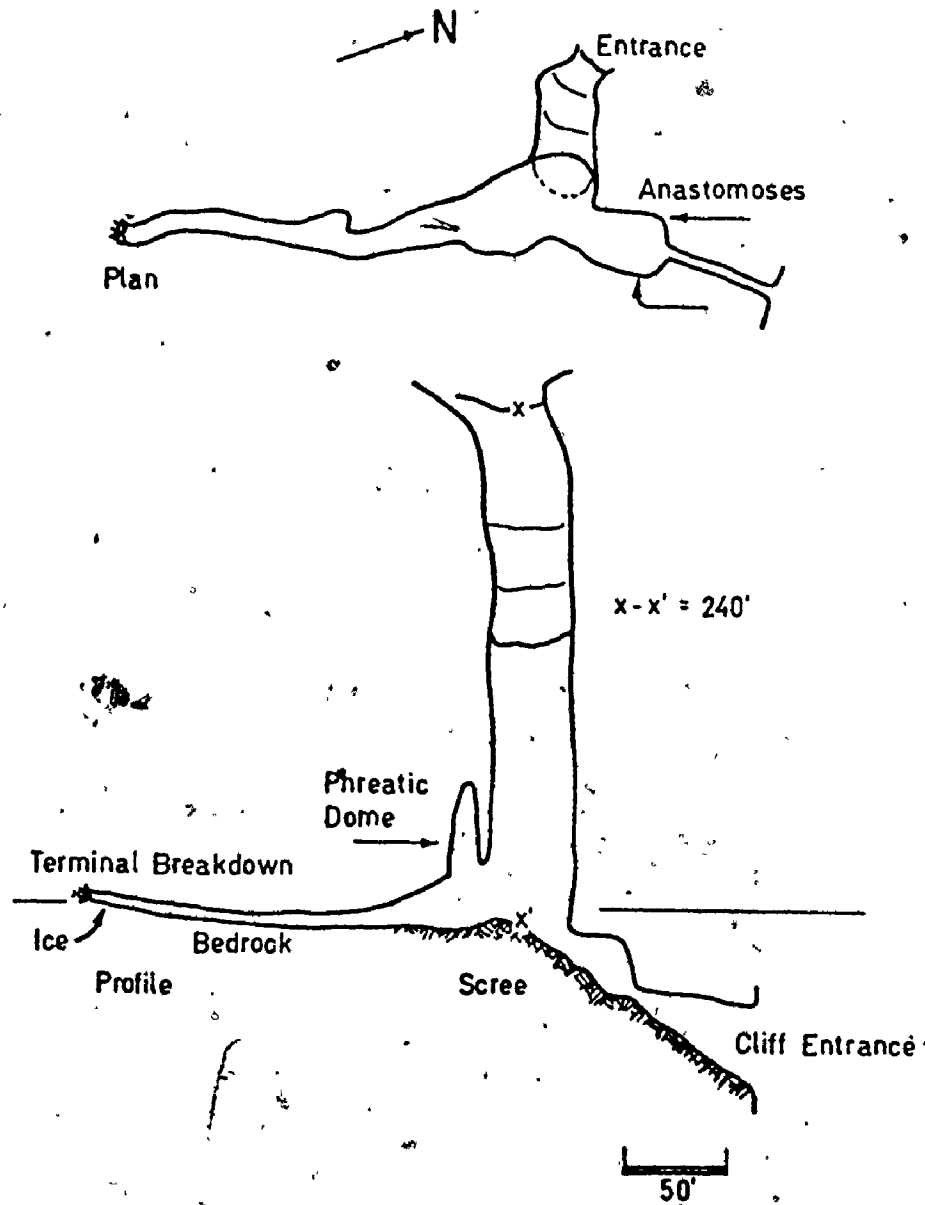


Figure 3.37. Raven Lake Pit, Nahanni North Karst (surveyed by R. Ewers and L. Simpson).

present throughout the karst in the vertical walls of fluvial canyons and karst depressions. Igloo Cave, for instance, intersects the south wall of Death Canyon between Death and Moraine Lakes. It is entered via a short bedding plane tube which leads into a partially collapsed chamber which in turn connects with narrow but high fissure passages which run parallel to the wall of the canyon (Figure 3.38). The intensively scalloped walls of the fissure passage indicate that there must have been a considerable flow of water through this cave at one time; today it is fossil. Ice Curtain Cave, in the north wall of Death Canyon is also a bedding plane tube with an entrance 50 ft. high and 20 ft. wide. Like virtually all of the horizontal caves in the area, it shows evidence of an entirely solutional origin under conditions of phreatic groundwater flow (Figure 3.39).

The active and fossil caves that have been discovered in the Nahanni, the largest of them Grotte Valerie in the north wall of First Canyon, South Nahanni River (Ford 1971, 1973) all indicate that a period of channelled groundwater flow in the limestone preceded the development of many of the surface karst landforms and fluvial canyons in whose walls they now hang (Figure 3.41 and Plate 3.28). Cavern geometry suggests that water entered the limestone via small vertical shafts that developed in fissures and that at depth this water collected and flowed laterally along bedding plane or fissure conduits to resurgences located in the walls of shallow fluvial canyons.

(b) The Past and Present Microclimates of Nahanni Caves.

In summer, many of the larger fossil caves in the Nahanni karst

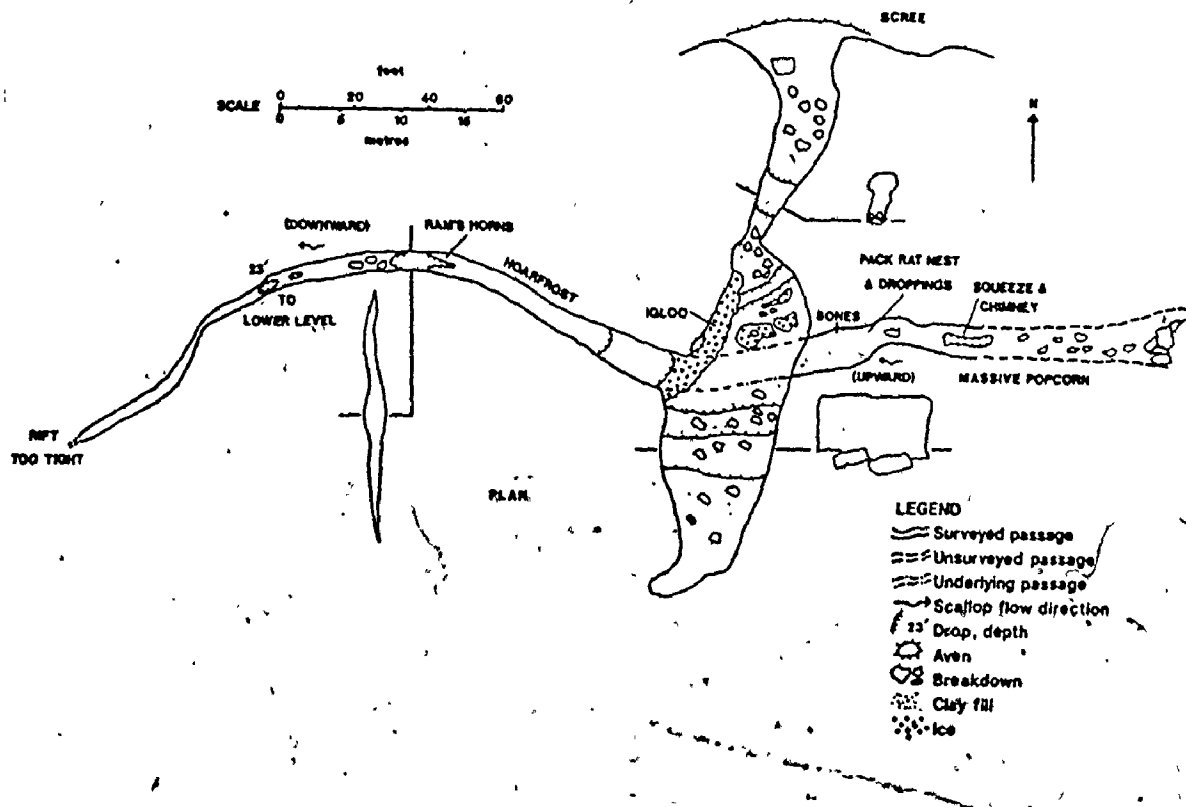


Figure 3.38. Igloo Cave, Death Canyon, Nahanni North Karst (surveyed by L. Simpson, R. Ewers and N. Prout).

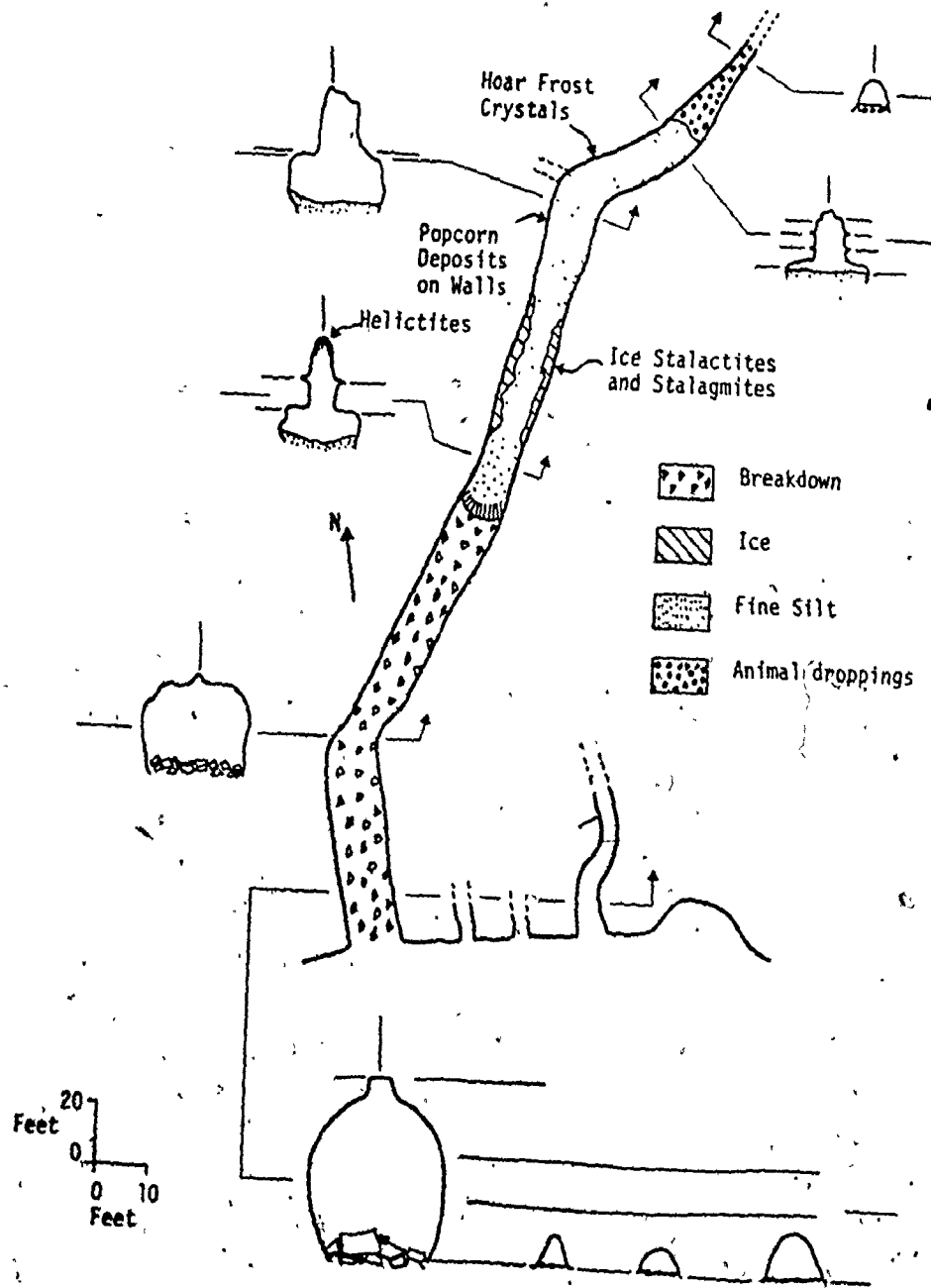


Figure 3.39. Plan and sections of Ice Curtain Cave, Death Canyon.

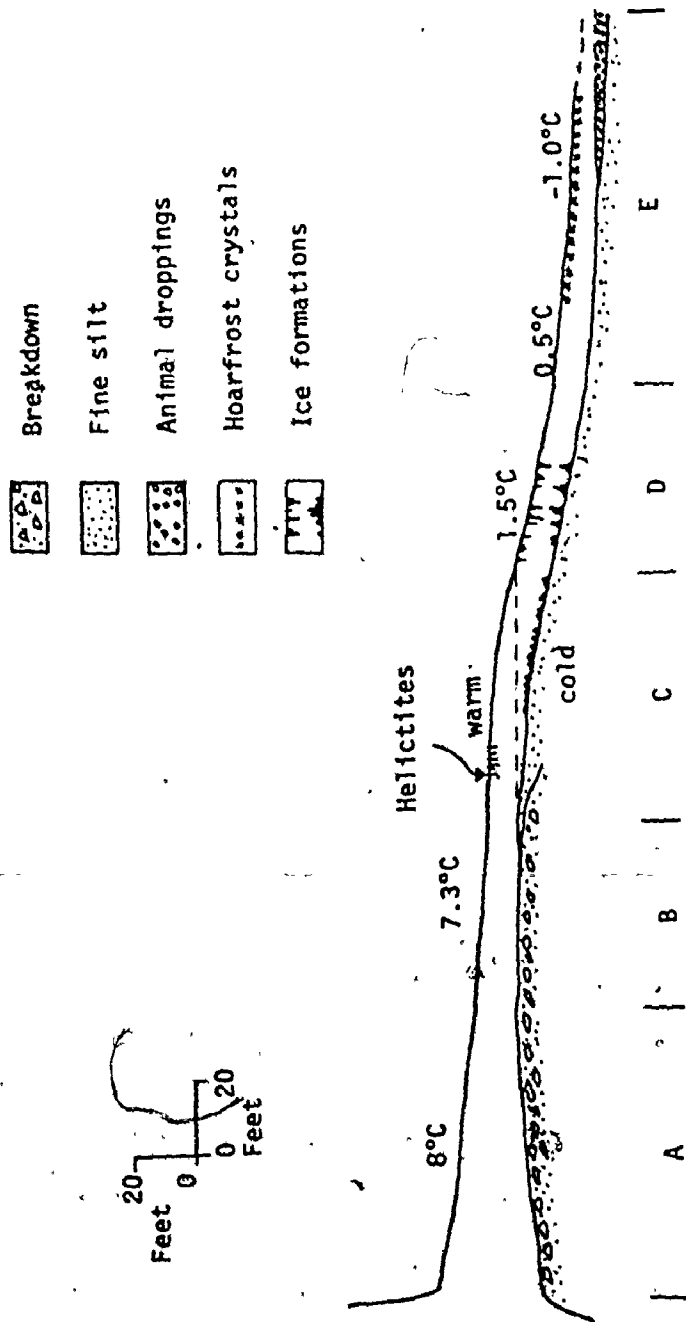


Plate 3.28. Tunnel Cave. The cave passes completely through a spur in the south wall of Death Canyon. Although it is now fossil, it must at one time have been part of an extensive underground drainage system that was dissected by the deepening of fluvial canyon networks.

for instance, high up in the north wall of First Canyon, South Nahanni River, is warmed by the inflow of air during the summer months. Temperatures in this zone range from  $1^{\circ}$ - $3^{\circ}\text{C}$ ; water has, therefore, been able to seep through the roof and deposit small stalactites and stalagmites. Further from the entrance is a second climatic zone in which temperatures are at or very close to freezing. During summer a small amount of seepage water is still able to penetrate the shallow overhead rock cover and more trickles in from the entrance zone. In addition, water vapour diffuses into this zone from the cave entrance. This water and water vapour freezes when it encounters the cold air so that ice sheets, ice stalactites and stalagmites, and hoarfrost crystals are characteristic. In deeper parts of the cave where passages descend below the levels of the cave entrances, very cold, dense winter air remains throughout the summer months. Temperatures are always below freezing ( $-3^{\circ}\text{C}$  in the summer of 1972) and water is unable to penetrate the frozen rock cover. Passages are dry and dusty and there are no deposits of either calcium carbonate or ice.

Igloo and Ice Curtain Caves in the south and north walls of Death Canyon respectively display a similar climatic zonation to that in Grotte Valerie. Air in the entrance zone of Ice Curtain Cave on July 23rd 1973 was between  $7^{\circ}$ - $8^{\circ}\text{C}$ ; water was dripping from the roof which has several small calcium carbonate helictites hanging from it (Figures 3.39 and 3.40). In the cave passages that are below the level of the entrance, two zones can be differentiated. Back from the entrance area is a zone in which temperatures are close to  $1.5^{\circ}\text{C}$  and ice formations are abundant. The die ing for





- A Zone of sunlight penetration; water abundant.
- B No sunlight; air mixes.
- C Upper air warm, underlain by cold air. Ice stalagmites form in colder air.
- D Cold air; ice stalagmites and ice stalactites form.
- E Zone of hoar frost crystals in very cold dry atmosphere.

Figure 3.40. The summer microclimate of Ice Curtain Cave, Death Canyon, July 23rd, 1973. Floor-slopes are exaggerated 2x for clarity.

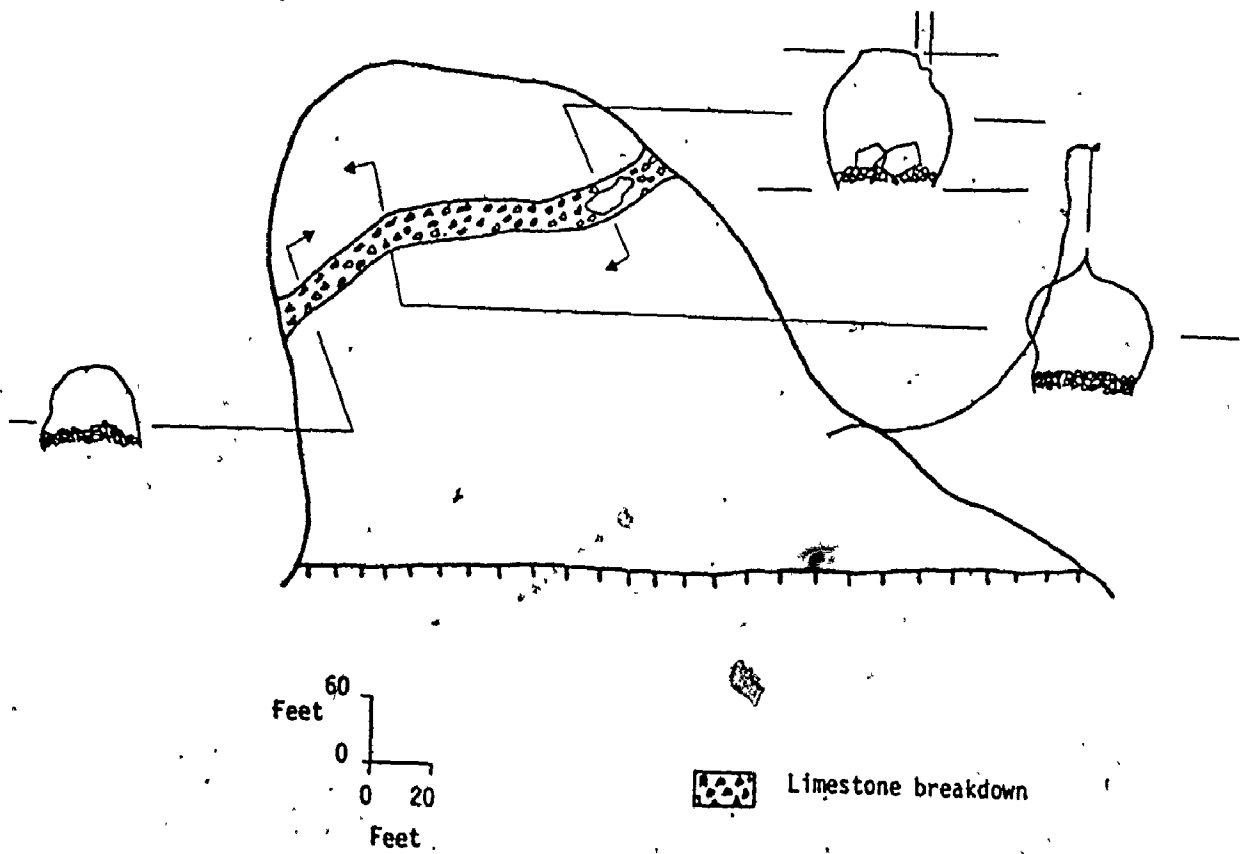


Figure 3.41. Tunnel Cave, Nahanni karst. This cave passes completely through a bedrock spur projecting from the south wall of

layer of warmer air near the ceiling which overlies a colder air layer at the floor (Figure 3.40). The boundary between the warm and cold air clearly advances into the cave as the outside temperatures rise during the summer months. As winter approaches, this boundary retreats towards the cave entrance. It is the warm air at the ceiling of the cave that allows water to percolate into it. When the water reaches the cold air below, it freezes into ice stalagmites and ice sheets. Advance and retreat of the warm air also causes the formation of ice stalactites. These are not present in the warm air zone itself but just into the cave from it. Deeper into the cave temperatures drop to as low as  $-1^{\circ}\text{C}$ . In this zone there are no ice formations as the ceiling of the passages are never warmed to the extent that water can percolate through them. Diffusion of water vapor does occur, however, so that walls and ceiling are covered by hoarfrost crystals.

Most of the chambers and passages making up Igloo Cave are below the level of the entrance and in July, 1973, the temperature in these was  $-4^{\circ}\text{C}$ . Above this cold air in the main chamber (Figure 3.38), was a zone of slightly warmer air near the roof with hoarfrost crystals developed on walls and ceiling (Plate 3.29). This air warms substantially in the direction of the entrance zone. It is apparent that in some years (although not in 1973), this upper layer of air becomes warm enough to allow percolation of water into the cave from above for ice stalactites, stalagmites and curtains are highly developed in the main chamber (Plate 3.29). Many of the ice deposits in the cave at present appear to be old, suggesting that the upper layer of air in the cave



Plate 3.29. Spectacular ice formations in Igloo Cave, Death Canyon. Samples of stalagmite from the cave have been dated at > 350,000 years B.P. Under present conditions calcium carbonate is not being deposited because water entering the cave freezes in the 25°F air. The presence of stalagmite, therefore, suggests that temperatures in the cave have been much warmer on one or more occasions in the past. Hoarfrost crystals cover the upper sections of the cave walls.

or even tens of years. Unlike the ice formations in Ice Curtain Cave, those in Igloo Cave are clearly not deposited and melted in an annual cycle.

Ice and not calcium carbonate is presently being deposited in many Nahanni caves because of the cold winter air that is trapped in them during the summer months. Large calcium carbonate formations have been laid down in many of these caves in the past, however, and this can only indicate that at these times temperatures inside the caves were higher than they are at present. Because the microclimates of Nahanni caves are largely a function of outside sub-arctic temperature fluctuations, this also suggests that during periods of calcium carbonate deposition the climate of the Nahanni area was warmer than it is at present. In a warmer period, speleothem deposition in caves would also be encouraged by a more complete vegetation cover on the plateau surfaces overhead. Percolating waters would be enriched in  $\text{CO}_2$ , would contain more calcium carbonate in solution and would deposit this material in subsurface voids filled with relatively warm air.

Massive speleothem deposits have been collected from a number of caves in the Nahanni karst including Grotte Valerie and Igloo Cave. Formations from these two caves were collected from passages that are at present too cold in summer for calcium carbonate deposition to occur. A number of these formations have been uranium-series dated (Thompson *et al.* 1974; Harmon *et al.* 1975) and these dates indicate that the climate of the Nahanni area has been much warmer than it is at present during more than one period of the last 350,000 years.

(c) Evolutionary History of Fossil Caves in the Nahanni Karst.

The fossil caves of the Nahanni have provided a great deal of information on aspects of the geomorphic evolution of the southern Mackenzie Mountains region. Ford (1973), for instance, has isolated six phases in the history of Grotte Valerie in the north wall of First Canyon, South Nahanni River (Table 3.16). Ford argues that in Phase 1 the Grotte Valerie system with 6,300 ft. of explorable passages, was created by solution under conditions of phreatic groundwater flow. He notes that the cave may then have been drained and lain fossil for a long period before the commencement of Phase 2 during which time more than half of the volume of the cavern was infilled by a poorly sorted fluvial deposit containing erratic pebbles that was washed in from the plateau overhead. The emplacement of this coarse material implies a considerable streamflow through the cave.

The third phase in the history of Grotte Valerie appears to have been a period of speleothem deposition when stalagmites and columns of calcite were built upon the First Clastic Fill. The phase was of long duration for some calcite columns in the cave are 30 ft. high and have basal diameters as great as 3 ft. Because very little of the First Clastic Fill is preserved in the cave today, Ford (1973) has suggested that a period of fluvial re-excavation followed the period of speleothem deposition: During this phase, streams were active in Grotte Valerie and swept away most of the First Clastic Fill and removed much of the stalagmite of the Major Stalagmite Phase (Table 3.16).

Table 3.16. Phases in the History of Grotte Valerie in the North Wall of First Canyon, South Nahanni River. (after Ford 1973).

Phase	Event	Notes
6	Modern Phase	-newly initiated, local, light stalactite deposition, ice elsewhere
5	Second Clastic Fill	-homogeneous silt-clay mix of loessic character
4	Fluvial Re-excavation	-most deposits of Phases 2 and 3 removed but little new erosional cave development
3	Major Stalagmite Phase	-large and extensive stalactite and stalagmite deposits
2	First Clastic Fill	-cave largely infilled with clay-pebble fluvial deposit, containing erratics
1	Origin and Development of Solutional Cavern	-under shallow phreatic groundwater conditions

Ford notes that locally this deposit is more than 20 ft. thick but that it does not appear to have filled the cavern to the extent that the First Clastic Fill did. Ford (1973) interpreted this as a water-laid, reworked loess deposit but in a later work (Ford 1976) re-interpreted it as a lacustrine deposit laid down in an ice-dammed lake. The most recent phase in the complex history of Grotte Valerie identified by Ford (1973) is one of local light stalactite deposition, samples of which have been dated at 2,000 yrs. B.P.

Many of the smaller caves in the Náhanni north karst region show evidence of a history similar to that outlined by Ford (1973) for Grotte Valerie. In most caves the evidence is incomplete but in Stal Cave, in the north wall of Stal Gorge (Figures 3.16 and 3.17, and Plate 3.20) there is evidence for a history that includes all of the six phases listed in Table 3.16. The presence of solutional pockets in the walls and ceiling of Stal Cave which is less than 100 ft. long, indicates that it was created by solution under conditions of phreatic groundwater flow. An ancient phase of infilling is indicated by remnants of a poorly sorted clastic deposit cemented to the passage walls 2-3 ft. above the present floor level. This fill, which contains shale fragments of gravel size in a matrix of reddish-brown silt, was probably emplaced by streams flowing into the cave from the plateau above and it is clear that at this time the cave passages were filled to a higher level than they are today. Following this, the cave dried out and massive stalagmite and flowstone formations were laid down upon the coarse fill. This long period of deposition in the cave was followed by a phase of intense stream activity when much of the fill was eroded and the overlying stalagmite and flowstone deposits



disturbed. Broken speleothems are common amongst breakdown in the cave entrance; many of these remnants are cemented to a coarse clastic fill. Today the bedrock floor of the cave is covered by a yellow-brown, clay-silt deposit which appears equivalent to the Second Clastic Fill identified by Ford (1973) in Grotte Valerie. Ford (1976) has interpreted this fill as having been deposited in an ice-dammed lake with its upper surface at about 1,950 ft. despite the fact that passages in Grotte Valerie range from about 2,040-2,100 ft. a.s.l. - that is they are higher than the lake surface. Caves in the North karst up to elevations of greater than 3,500 ft. contain the same fill suggesting that Ford's original interpretation of it as a reworked loess deposit (Ford 1973) may well be the correct one.

That the major events in the histories of both Stal Cave and Grotte Valerie correlate exactly, suggests that the Major Stalagmite Phase and the First and Second Clastic Fill events (Table 3.16) were the result of broad changes in outside conditions and were not due to local changes in the cave environments. Because the oldest stalagmite deposits laid down during the Major Stalagmite Phase are older than 350,000 yrs. B.P., the First Clastic Fill must have occurred prior to this. As massive speleothem deposits could not have been laid down until the caves were emptied of water, it is clear that the streams in the area began downcutting at some time prior to 350,000 yrs. B.P. There can be no doubt that the now fossil caves of the Nahanni are extremely old. It is unlikely that they began to form later than 500,000 yrs. B.P. and there is every likelihood that they began to form many tens of        nds of

## 8. Relationships Between the Karst Landforms of the Nahanni Region.

The karst landform assemblage that has developed in the Nahanni region is a remarkable one for a sub-arctic terrain. The various component landforms include dolines, karst streets, karst platea, poljes, limestone pavements and caves. In some respects what is even more remarkable are clear interrelationships between many of these forms.

### (a) The Size Hierarchy of Karst Landforms.

Many of the karst landforms in the Nahanni have remarkably similar morphological characteristics but differ considerably in size. Solution pits in limestone pavement surfaces, for instance, only a few inches deep bear a striking resemblance to many vertical-walled solution dolines and vertical caves several tens of feet deep (Plates 3.8 and 3.14). The solution pits connect at depth with tunnels formed in bedding planes or current bedding partings, the dolines and vertical shafts connect with horizontal caves developed in major open bedding planes. Just as pit-and-tunnel systems function to drain water from limestone pavement surfaces, doline-cave systems drain it from more extensive areas of bare limestone.

Other solutional landforms that bear a striking resemblance to one another include grikes and karst streets (Plates 3.11 (a) and 3.23), joint hollows and karst platea (Plates 3.10, 3.21 and 3.22), and structural hollows on limestone pavements, structural dolines and poljes developed in natural bedrock depressions (Plates 3.9, 3.12 and 3.24). Grikes and karst streets are little more than solution slots produced by the etching out of fractures in the limestone by a combination of solutional and

mechanical processes. Joint hollows and karst platea are both irregularly-shaped depressions that may have residual limestone blocks or towers projecting from their floors. Both sets of features are produced by solution acting in dense intersecting networks of fractures in the limestone. The Nahanni karst also hosts a series of closed depressions that are little more than solutionally modified structural basins in limestone. On pavement surfaces these depressions are simply irregularities in current structures; elsewhere they occupy basinal structures in the upper surface of the Nahanni Formation limestones. Relatively small basins of this kind may become structural dolines like Palsa Basin; larger structures may become poljes like First Polje. All may be alluviated and all ultimately develop subsurface drainage routes. They are eventually modified by solutional and mechanical processes.

Morphologically similar karst landforms in the Nahanni, therefore, range in size from inches up to several tens or even several hundreds of feet. All of these landforms are developed in structures in the limestone - either in faults, joints, bedding planes or structural basins. Their sizes are undoubtedly controlled by the horizontal and vertical extents of the host structure or structures. Solution pits, grikes and joint hollows on pavement surfaces, have developed in joints that are rarely more than a few tens of feet long and a few feet deep. Vertical-walled solution dolines, karst streets and karst platea such as those in the North Karst labyrinths, have developed in networks of faults that are several hundreds to several thousands of feet in length and several tens to a few hundred feet in depth. In the same way rock hollows on

limestone pavements have developed in structural basins several inches to a few feet in diameter while structural dolines and structural poljes have developed in natural rock basins that range from several hundred feet to several thousand feet in diameter. Although there can be no doubt that many very small solution forms such as solution pits can develop in very large structures, it is clear that the size of a structure imposes an upper limit upon the size of the karst landform that can develop in it.

To produce a karst assemblage like that in the Nahanni with such a great size range between morphologically similar landforms, requires a limestone sequence that has similar hydrogeological properties no matter what the size of the rock mass being considered. Grikes and karst streets, and solution pits, dolines and vertical shafts, form because water can drain far more easily through the vertical structures in the Nahanni limestones than it can through the horizontal structures and also because the limestone is massive enough to support vertical walls. If vertical fractures in a cube of limestone with 20 ft. sides are better developed than bedding plane partings and the limestone is massive, the likelihood is that solution pits and small grikes will develop in it. If the size of the limestone cube is increased and the ratio between its ability to transmit water vertically and its ability to transmit it horizontally, remains more or less constant, it is clear that large karst streets, vertical-walled solution dolines and vertical shafts should develop in it. If, however, as the volume of the limestone cube is increased it becomes far easier for water to move horizontally

than to move vertically through it, then the larger solutional forms may bear little resemblance to the smaller ones and very large karst streets would likely not form. It is possible that they would be replaced by true dolines. It is clear that in the Nahanni the hydrological properties of the Nahanni Formation limestones remain remarkably constant no matter what size the 'cube' considered. It is for this reason that there is such a wide range in size between similar landforms.

Not only are there definite relationships between morphologically similar karst landforms in the Nahanni that differ considerably in size but there are also relationships between landforms of similar size that differ in morphology.

(b) The Sequential Development of Karst Landforms in the Nahanni.

Sweeting (1972) has pointed out that in 1918, Cvijić "supposed a cyclic evolution of karst landforms, from the doline through the uvala to the polje." This she argues "both perpetuated an incorrect idea of the origin of the polje and also added to the confusion of the terminology" (p. 192). Cvijić was also well aware that poljes can be present at a very early stage of karst development for he knew that many poljes are located in structural hollows. Since Cvijić outlined his ideas on karst landform development, there has been much controversy about the origin of poljes. Majority opinion seems to be that most of these landforms are of structural rather than solutional origin. The opinion that poljes can form by the gradual coalescence of smaller depressions is no longer a widely held one. In the Nahanni, many of the karst landforms appear to be part of a developmental cycle that links the smaller karst

forms to the larger. It is apparent that in this area at least, there is some support for Cvijić's contention that poljes can form by the coalescence of dolines.

Three stages in the transformation of a highly fractured limestone surface into a natural rock labyrinth are depicted in Figure 3.42. In the first stage, water moving vertically down fractures in the limestone forms strings of vertical-walled solution dolines and vertical caves (Figures 3.42 (a), 3.43 and 3.44, and Plates 3.14 and 3.17). These connect at depth with sub-horizontal cave passages which funnel the groundwaters laterally towards springpoints. At a later stage, the growth of dolines and vertical shafts along the host fractures brings about their coalescence so that the landscape is now characterized by strings of shallow elongate depressions, irregularly interspersed with steep-walled dolines (Figures 3.42 (b), 3.15 and 3.18). In the final stage, further coalescence of depressions along the host fractures produces networks of karst streets (Figures 3.42 (c), 3.13, 3.14 and 3.16, and Plates 3.20 and 3.23).

The denudation of the limestone terrain does not stop here, however, for the karst streets continue to enlarge. As they do so, the limestone ridges which separate them (Figures 3.42 (c) and 3.45 (a)) are gradually consumed until eventually all that remains of them are vertical-walled rock towers (Plate 3.30). When the residual limestone masses within dense networks of karst streets are consumed, karst plateaus with limestone towers in them, are produced (Figures 3.45 (b), and

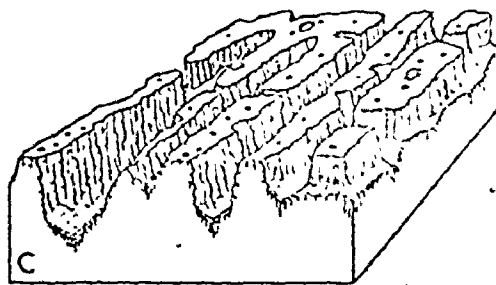
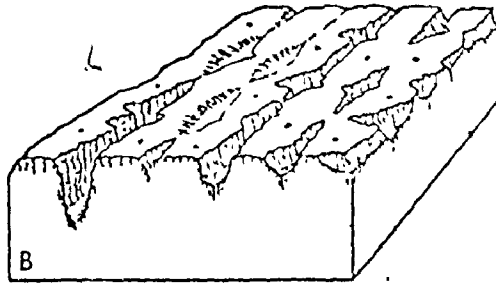
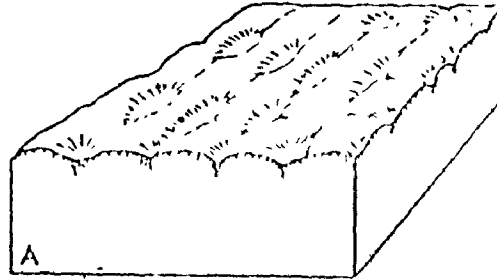


Figure 3.42. Three stages in the development of a natural rock labyrinth in a highly fractured limestone surface. Strings of elliptical dolines (A) coalesce along the host fractures (B) until eventually they become elongate vertical-walled karst streets (C).

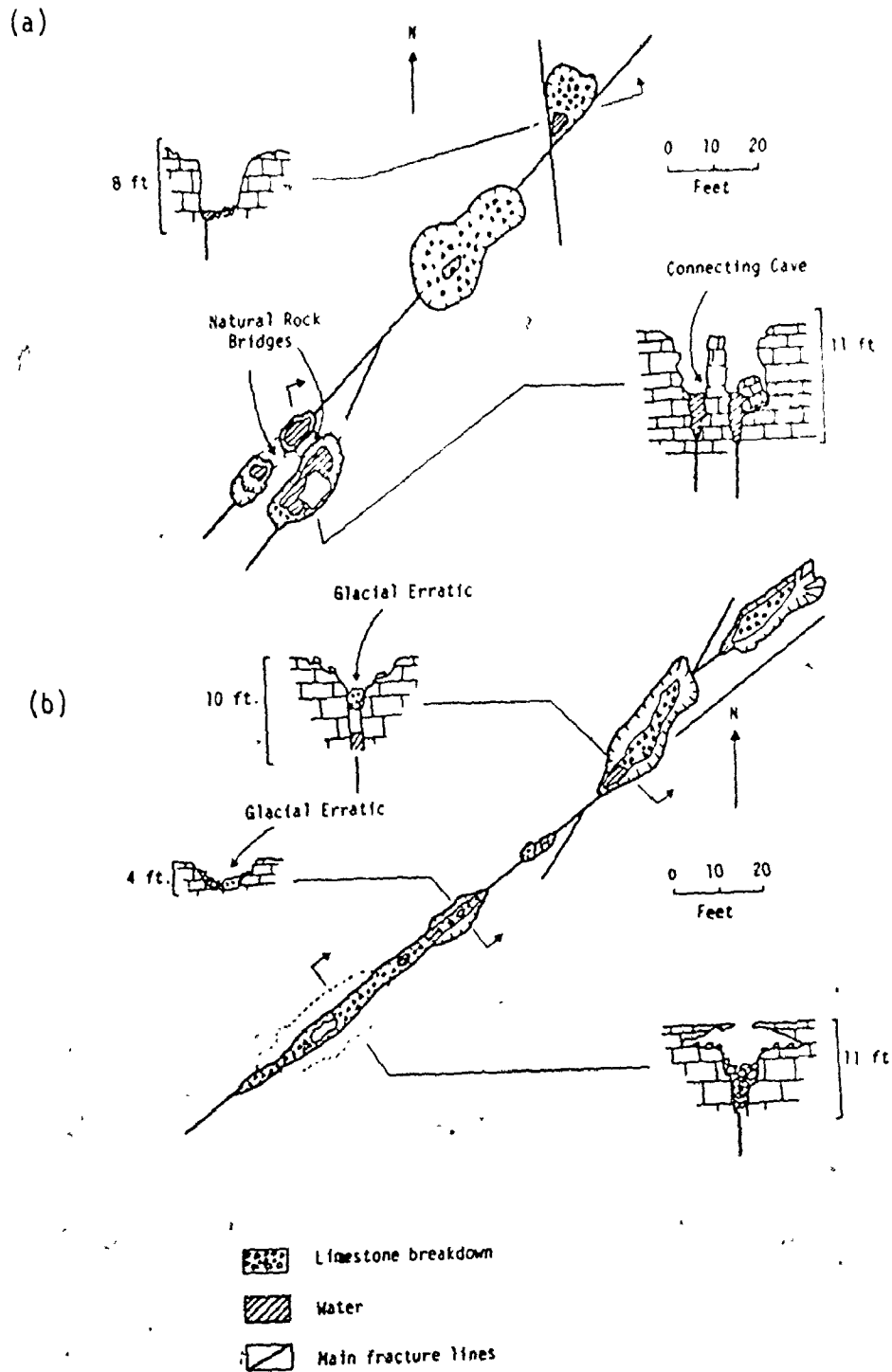


Figure 3.43. Strings of ellipsoidal, vertical-walled dolines, Nahanni Plateau. This is the first stage in the widening of a fracture network into a series of small karst streets.



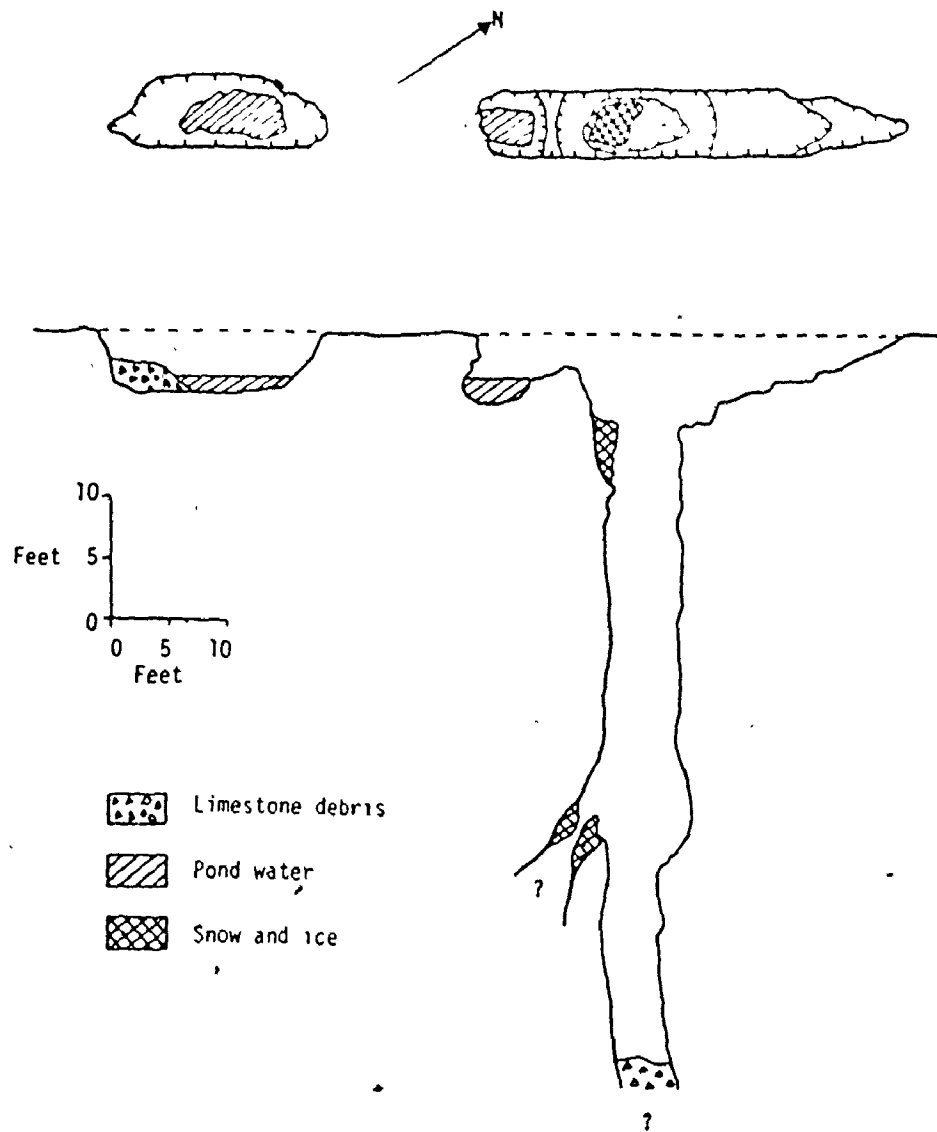


Figure 3.44. Diane Cave, an early stage in the modification of a fracture into a karst street via the development of a vertical shaft.

3.20, and Plates 3.21, 3.22 and 3.31). All stages in the evolution of a highly fractured limestone surface to one displaying karst platea have been observed in the Nahanni. What is more, this evolutionary process has been observed in karst features of all dimensions. Joint hollows on limestone pavements, for instance, have clearly been produced by destruction of secondary clints within dense networks of grikes. It has already been argued that grikes on limestone pavements which are equivalent to small karst streets are produced by the coalescence of strings of solution pits along the host joint. On limestone pavements, therefore, solution pits develop into grikes and grikes develop into joint hollows. On a larger scale solution dolines develop into karst streets and streets develop into karst platea. At all scales the limestone surface passes through the stages shown in Figures 3.42 and 3.45 (a & b).

It is unlikely that a landscape of karst streets and platea such as that of the Nahanni region, is the final stage in the evolution of the labyrinth karst type. There can be no doubt that streets and platea increase in size and coalesce to form larger and larger depressions with more and more isolated limestone towers (Plate 3.31). A situation can be envisaged in which the landscape is no longer dominated by the closed depressions - be they dolines or karst platea, but is instead characterized by irregularly spaced vertical-walled karst towers up to 500 ft. high which are separated by broad, shallow closed depressions. This final stage in the evolution of a labyrinth karst landscape would be similar to the

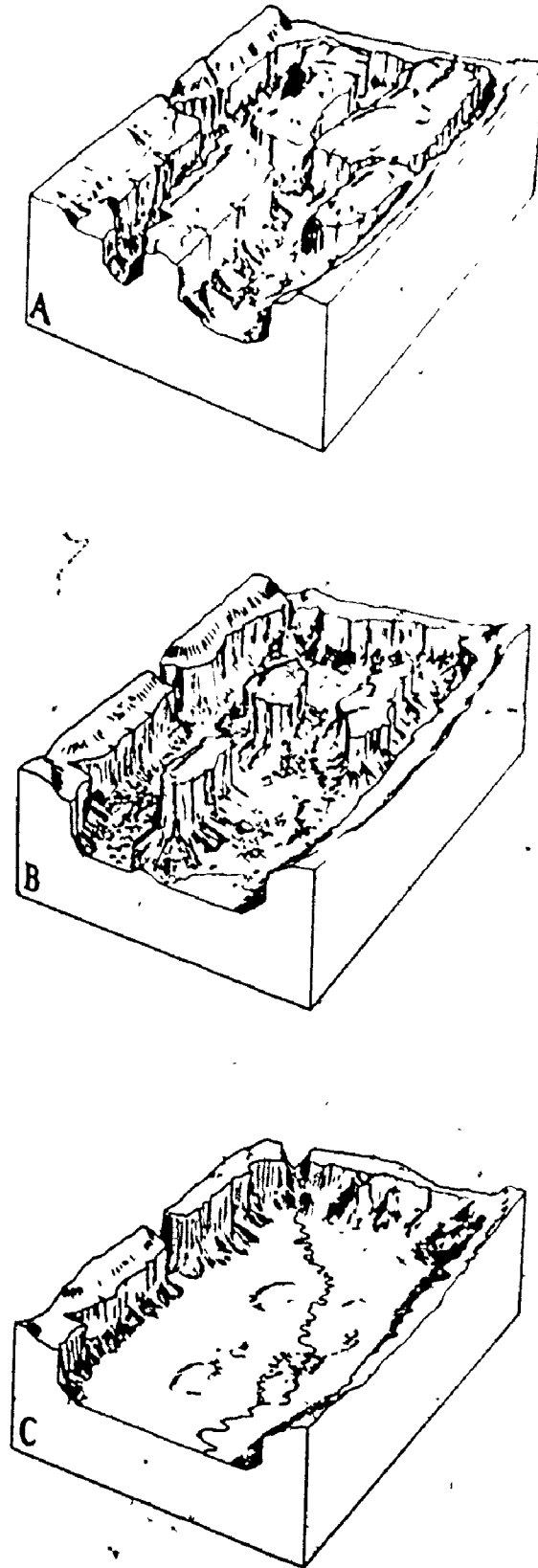


Figure 3.45. The development of karst plateaus, towers and poljes from networks of karst streets. Karst plateaus with residual towers (B) form as karst streets (A) widen and coalesce. Eventually the residual rock towers are denuded and where





Plate 3.30. Moderate-scale labyrinth karst to the west of Raven Canyon. The widening of a dense network of karst streets 100-150 feet deep has resulted in the formation of a karst platea which has numerous residual karst towers and pinnacles projecting from its floor.

'old' karst stage of Grund (1914) that is depicted in Figure 1.3. Given a sufficient depth of limestone, the cycle could be repeated if a lower base level of erosion was established in the area.

The labyrinth karst cycle as described above may be slightly modified if there is a source of insoluble sediment available to the developing karst depressions. Where sediment is supplied to karst platea these features may be alluviated (Plate 3.32) with the eventual formation of poljes which flood at irregular intervals (Figure 3.45 (c) and Plates 3.25, 4.4 and 4.2). The similarity in size and form between Polaski Platea (Figure 3.19) and Second Polje (Figure 3.25), leaves no doubt that Second and Third Poljes in the Nahanni karst are little more than totally alluviated karst platea. First Polje, on the other hand, is an alluviated bedrock depression in the limestone.

It is apparent that two factors have been important in bringing about the alluviation of only three out of the many large closed depressions in the Nahanni North Karst (Figure 3.13). First, and probably the most important factor is that all three poljes have large surface streams flowing into them. These streams which have their headwaters in the surrounding shales and unconsolidated glacial deposits, have clearly transported and are still transporting a considerably volume of insoluble sediment into these basins, bringing about their alluviation. Depressions of similar size such as North Col Canyon and Polaski Platea do not have large surface streams flowing into them and they are not, therefore, alluviated.

Although the steady input of insoluble sediment to large closed basins in the Nahanni would almost certainly bring about their eventual



Plate 3.31. Insel Tower. Some workers have suggested that karst towers form only under humid tropical conditions. In the Nahanni there are numerous examples of such landforms, the most impressive being Insel Tower in the southern portion of the North Karst labyrinths. The residual mass is 150-200 feet high.



Plate 3.32. Karst platea south of Insel Tower, North Karst. Water drains across the floor of the depression to the alluviated stretch in the foreground where it sinks underground. Solutionally-moulded pinnacles project from the depression floor at right.



alluviation, a second factor may have played a part in the filling of the Nahanni poljes. It is almost certain that prior to alluviation the bedrock floors of what are now the three Nahanni poljes, extended to elevations much below that of the present hydrological base level in the area - Bubbling Spring. There is a considerable body of evidence to suggest that the original base level was much lower, and that at some period this was raised by the infilling of Sundog Basin with sediment. Lakes may have existed in Sundog Basin and in the Nahanni poljes at this time and all four basins may have been alluviated at the same time. It may well be, therefore, that the sediments carried by streams into First, Second and Third Poljes were deposited into shallow lakes which would have encouraged an even distribution of fine sediment across the polje floors. The final stage in the evolution of a labyrinth karst network in an area close to a supply of insoluble sediment - and perhaps the Nahanni North Karst falls into this category - would be an irregular alluviated plain with shallow ponor systems characterized by irregularly distributed rock towers of various dimensions. The landscape characteristics of this final stage are strikingly similar to many present-day tower karst landscapes in humid tropical areas.

The Nahanni karst, therefore, contains conclusive evidence that poljes do form by the alluviation of structural depressions in bedrock, and that they can form by the alluviation of karstic depressions formed by the gradual coalescence of solution dolines - just as Johann Cvijić suggested as long ago as 1918.

## Chapter 4. Surface and Groundwater Hydrology.

### 1. Climatology.

#### (a) Mean Temperature and Precipitation.

Only a very sparse network of climatological stations serves the Upper Mackenzie Valley area (Figure 4.1) and because of this very little is known of conditions in the Mackenzie Mountains. Average temperature and precipitation figures for the karst have been estimated from climatic data at nearby stations and also in the case of precipitation, from stream runoff records.

#### (i) Estimates from Climatological Data.

The nearest station to the Nahanni karst with a long and reliable climatic record is Fort Simpson at the confluence of the Liard and Mackenzie Rivers (Figure 4.1). Data for this location are available from 1927. Mean annual temperature is 25.1°F and mean precipitation is 13.6 inches of which 38.7% falls as snow (Table 4.1). Unfortunately, conditions at Fort Simpson are likely to differ considerably from those in the karst because this station is situated in the Interior Plains region of northern Canada, well to the east of the western cordillera but still within their rain shadow zone. Within the southern Mackenzie Mountains, data have been collected at two mining settlements, Tungsten on Flat River and Cadillac Mine on Prairie Creek (Figure 4.1). Observations were made at Tungsten during the seven years from 1967-1973 but the record is far from

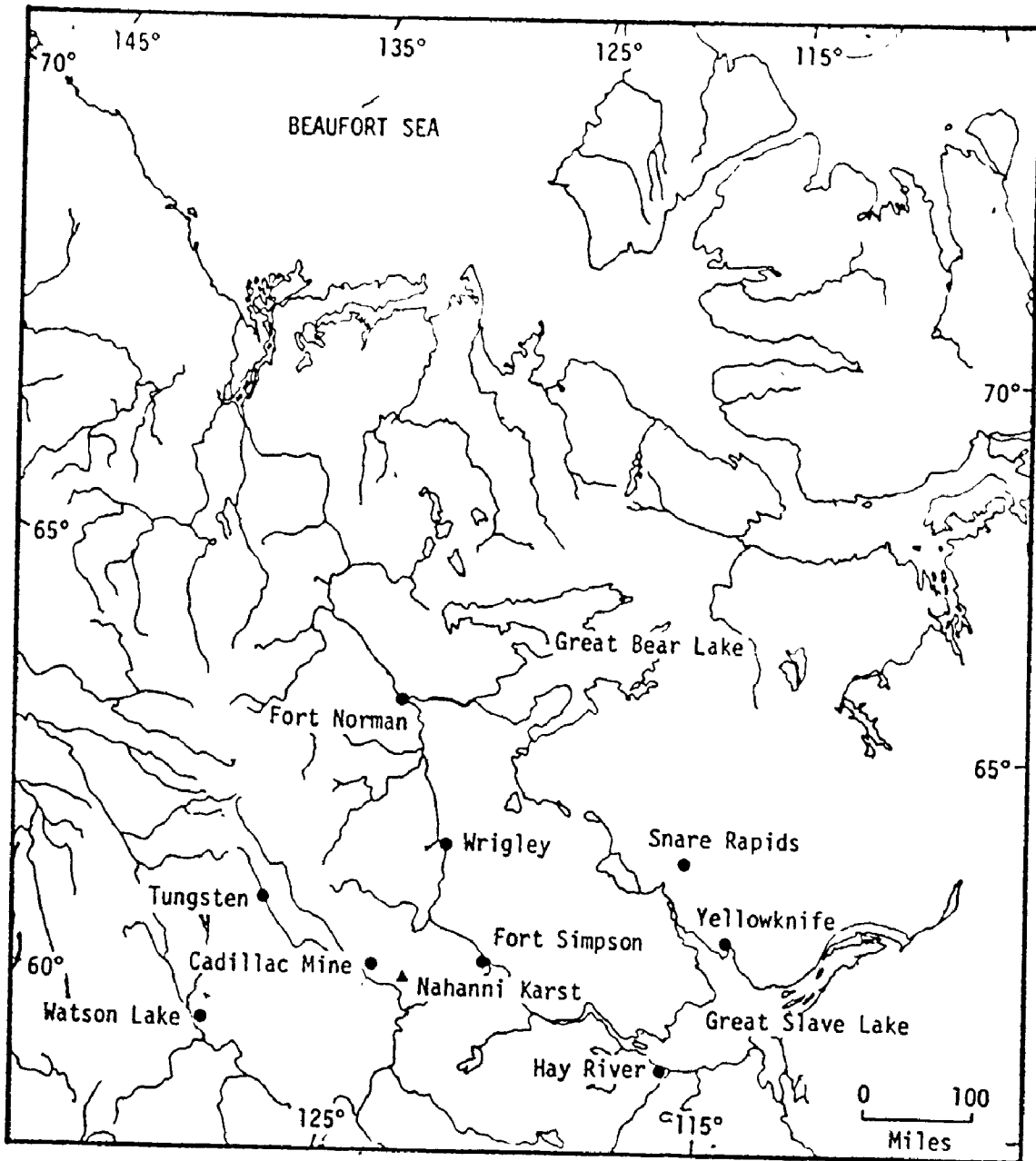


Figure 4.1. Location of Nahanni karst and climatic stations in its vicinity.

Table 4.1. Mean Temperature and Precipitation Data, Fort Simpson, N.W.T.

	TEMPERATURE (°F)			PRECIPITATION (inches)	
	Mean Daily Maximum	Mean Daily Minimum	Mean Daily	Mean Total	Mean Snowfall
JAN	-6.8	-22.7	-14.8	0.82	8.2
FEB	-1.3	-18.5	-9.9	0.57	5.7
MAR	15.8	-5.9	5.0	0.73	7.3
APR	36.0	14.3	25.2	0.85	6.1
MAY	57.1	34.9	46.0	0.82	1.7
JUN	69.0	46.6	57.8	1.72	0
JUL	73.6	51.1	62.3	1.96	0
AUG	68.9	47.5	58.2	1.84	0
SEP	54.7	37.2	45.9	1.59	1.0
OCT	36.4	23.6	29.9	1.03	5.9
NOV	12.3	0.6	6.5	0.92	9.2
DEC	-3.8	-17.8	-10.8	0.75	7.5
YEAR	34.3	15.9	25.1	13.60	52.6

complete. Data were collected at Cadillac Mine only in 1970 but again there are many gaps in the record.

Although mean temperature statistics for Tungsten can be calculated from the published data, this is not possible with the precipitation statistics for there are no published figures for precipitation in May. It is clear from Figure 4.2, however, that there is a reasonable linear relationship between mean monthly precipitation at Tungsten and that at Fort Simpson. This relationship is given by the regression equation

$$Y = 0.33 + 1.45 (X),$$

where Y is the mean monthly precipitation at Tungsten and X the corresponding precipitation at Fort Simpson. The correlation coefficient between these two variables is 0.83 for the eleven data pairs, while the standard error of the estimate is 0.48. The mean precipitation in May at Tungsten calculated by means of this equation is 1.52 inches. As Table 4.2 shows, the mean temperature at Tungsten, where conditions are likely to be reasonably similar to those in the Nahanni, is 21.8°F and the mean annual precipitation is 23.7 inches with some 51.5% falling as snow.

Figure 4.2 also demonstrates that there is a general linear relationship between monthly precipitation at Cadillac Mine in 1970 and precipitation at Fort Simpson in the same year. This relationship is

$$Y = -0.25 + 2.22 (X),$$

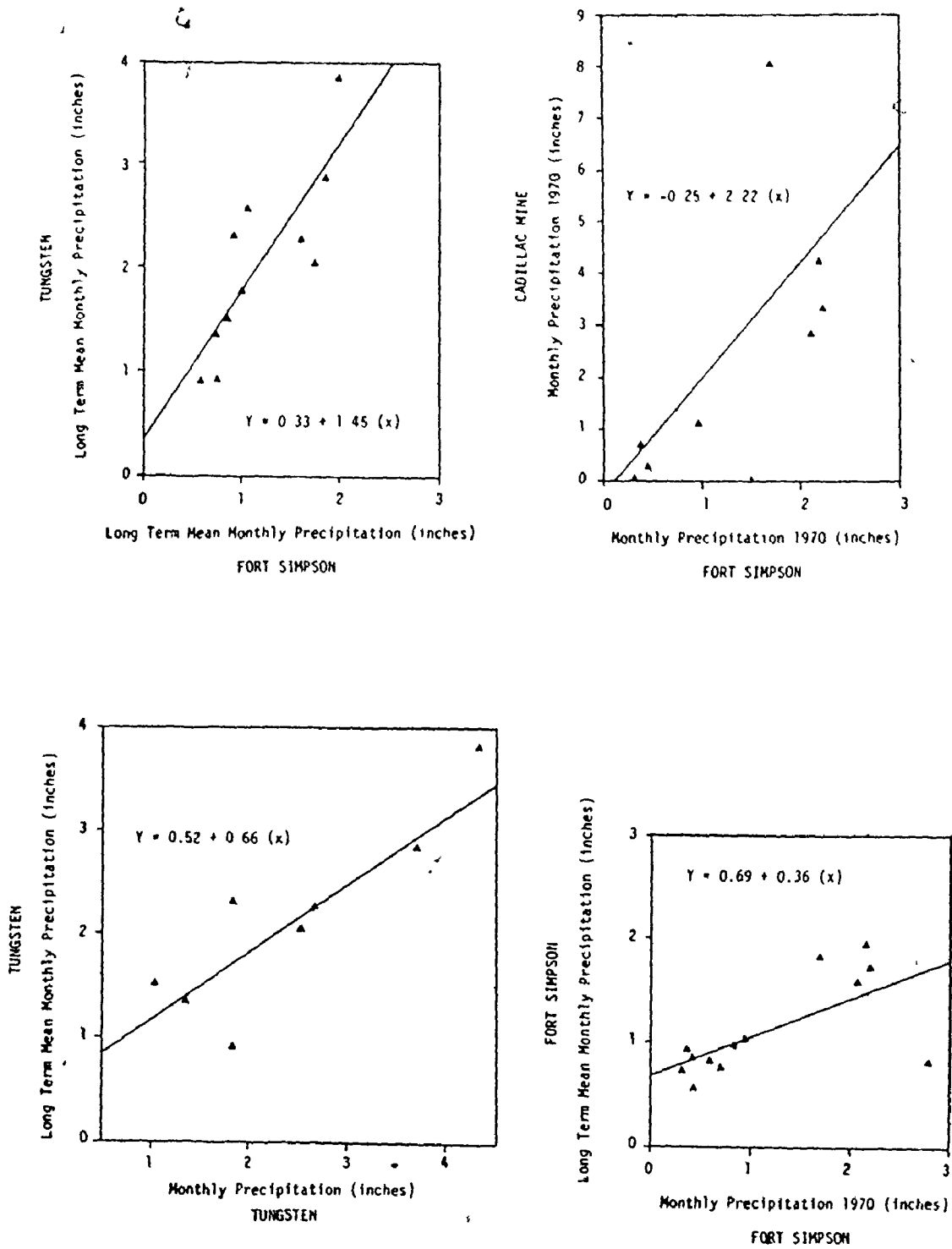


Figure 4.2. Monthly precipitation relationships between Cadillac Mine, Fort Simpson and Tungsten

Table 4.2. Mean Temperature and Precipitation Data, Tungsten, N.W.T.

	TEMPERATURE (°F)		Mean Daily	PRECIPITATION (inches)	
	Mean Daily Maximum	Mean Daily Minimum		Mean Total	Mean Snowfall
JAN	-7.0	-25.0	-16.0	1.53	15.3
FEB	12.3	-10.6	1.8	0.90	9.0
MAR	20.5	-1.7	9.4	1.37	13.7
APR	32.9	11.1	22.0	1.50	15.0
MAY	46.6	26.2	36.5	1.52 E	9.8 E
JUN	60.8	37.5	49.2	2.06	0
JUL	61.5	40.7	51.1	3.85	0
AUG	59.1	37.1	48.5	2.88	0
SEP	43.9	29.1	36.5	2.28	4.9
OCT	30.5	15.0	22.8	2.57	24.2
NOV	14.2	-3.9	5.1	2.32	20.0
DEC	2.9	-15.2	-5.7	0.92	10.3 <sup>1</sup>
YEAR	31.5	11.7	21.8	23.7	122.2

E Estimated values.

<sup>1</sup> Snowfall and total precipitation means were calculated from the available data. In some months only total precipitation data are available, in others only snowfall data. This can lead to a snowfall mean being larger than a total precipitation mean as in this case.

where Y is the monthly precipitation at Cadillac Mine and X the corresponding value at Fort Simpson. The correlation coefficient for the eight data pairs is 0.70 and the standard error of the estimate 1.80. This and other regression relationships for mean daily maximum, mean daily minimum and mean daily temperature, have been used to estimate missing data in the 1970 Cadillac Mine climatic record. Missing snowfall values were calculated by averaging the mean percentages of monthly precipitation falling as snow at Fort Simpson and Tungsten. A complete climatological record for Cadillac Mine in 1970 is presented in Table 4.3

Table 4.4 and Figure 4.2 clearly demonstrate that 1970 monthly climatological data at Tungsten and Fort Simpson, are related to long term mean values at these stations in a linear manner. For instance, in the case of precipitation where Y is the long term mean and X the 1970 value, the relationship at Fort Simpson is

$$Y = 0.69 + 0.36 (X),$$

the correlation coefficient is 0.66 and the standard error of the estimate 0.35. At Tungsten, on the other hand the relationship is

$$Y = 0.52 + 0.66 (X),$$

in this case the correlation coefficient is 0.86 and the standard error of the estimate 0.42. As Table 4.4 shows, mean temperature statistics are highly correlated with 1970 figures, all correlation coefficients being 0.99 and all standard errors less than 4°F.



Table 4.3. Temperature and Precipitation at Cadillac Mine N.W.T., 1970.

	TEMPERATURE (°F)			PRECIPITATION (inches)	
	Mean Daily Maximum	Mean Daily Minimum	Mean Daily	Total	Snowfall
JAN	0.5 E	-17.7 E	-8.6 E	1.05 E	10.5 E
FEB	18.4	-8.2	5.1	0.28	2.8
MAR	27.7	-1.6	13.1	0.03	0.3
APR	39.6	12.7	26.2	0.65 E	5.6 E
MAY	52.2	30.2	41.2	5.93 E	24.9 E
JUN	63.9	38.7	51.3	3.36	0
JUL	66.1	41.3	53.7	4.24	0
AUG	62.5	39.0	50.8	8.06	0
SEP	48.1	30.3	39.2	2.81	8.1
OCT	33.6	12.8	23.2	1.10	10.1
NOV	8.0	-6.5	0.8	0.68	6.8
DEC	1.7 E	-17.4 E	-7.8 E	1.30 E	13.0 E
YEAR	35.2	12.8	24.0	29.49	82.1

E Estimated values. Where Y is the Cadillac Mine figure and X the Fort Simpson figure both for 1970. The relationships used to estimate missing values were:

Mean Daily Maximum Temperature (°F)	$Y=7.47 + 0.80(X)$	( $r=0.98$ ; Std. Err. =4.00)
Mean Daily Minimum Temperature (°F)	$Y=0.13 + 0.81(X)$	( $r=0.99$ ; Std. Err. =2.41)
Mean Daily Temperature (°F)	$Y=3.79 + 0.80(X)$	( $r=0.99$ ; Std. Err. =3.10)
Monthly Precipitation (inches)	$Y=2.22(X) - 0.25$	( $r=0.70$ ; Std. Err. =1.80)

Table 4.4. Linear Regression Relationships between 1970 Temperature and Precipitation Values and Long Term Means for Fort Simpson and Tungsten.

CLIMATIC PARAMETER	Regression Equation Y = Long Term Mean X = 1970 Value	Number of Data Pairs	Correlation Coefficient	Standard Error of the Estimate
<u>Fort Simpson</u>				
Mean Daily Maximum Temp (°F)	$Y = 1.01 (X) - 0.68$	12	0.99	3.67
Mean Daily Minimum Temp (°F)	$Y = 0.29 + (X)$	12	0.99	2.77
Mean Daily Temp (°F)	$Y = (X) - 0.20$	12	0.99	3.06
Monthly Precipitation (inches)	$Y = 0.69 + 0.36 (X)$	12	0.66	0.35
<u>Tungsten</u>				
Mean Daily Maximum Temp (°F)	$Y = 1.08 (X) - 2.30$	8	0.99	3.62
Mean Daily Minimum Temp (°F)	$Y = 1.06 (X) - 1.91$	7	0.99	3.57
Mean Daily Temp (°F)	$Y = 1.07 (X) - 1.60$	7	0.99	3.49
Monthly Precipitation (inches)	$Y = 0.52 + 0.66 (X)$	8	0.86	0.42

That long term temperature and precipitation means at a given station are approximately related to 1970 statistics, suggests a way in which long term figures for Cadillac Mine can be calculated. As this mining camp is within 20 miles of the Nahanni karst, these long term means could well reflect conditions in this region also. Two sets of figures have been calculated. In the first case, relationships between mean values and 1970 statistics at Fort Simpson were used and in the second, the relationships estimated for Tungsten were employed (Table 4.4). The resulting data are shown in Tables 4.5 & 4.6, averages of these figures in Table 4.7 and a climagraph of these average statistics in Figure 4.3. The estimates indicate that the mean annual temperature at Cadillac Mine and in the Nahanni karst lies between 23.8°F and 24.1°F with a likely average figure being 23.9°F. There is less certainty about precipitation but there is a high degree of probability that it is between 19.0 inches and 25.7 inches with a likely mean annual total close to 22.3 inches.

(ii) Precipitation Estimates from Stream Discharge and Evapotranspiration Data.

Mean annual precipitation can be calculated from mean annual stream discharge and evapotranspiration data if it is assumed that there is no change in water storage. The water balance equation then becomes:

$$\text{Total Precipitation} = \text{Effective Precipitation} + \text{Evapotranspiration},$$

Table 4.5. Long Term Mean Temperature and Precipitation Estimates at Cadillac Mine Using Fort Simpson Relationships.

	TEMPERATURE (°F)			PRECIPITATION (inches)	
	Mean Daily Maximum	Mean Daily Minimum	Mean Daily	Mean Total	Mean Snowfall
JAN	-0.2	-17.4	-8.8	1.07	10.7
FEB	17.7	-7.9	4.9	0.79	7.9
MAR	27.0	-1.3	12.9	0.70	7.0
APR	38.9	13.0	26.0	0.92	6.6
MAY	51.5	30.5	41.0	2.85	5.9
JUN	63.2	39.0	51.1	1.91	0
JUL	65.4	41.6	53.5	2.23	0
AUG	61.8	39.3	50.6	3.63	0
SEP	47.4	30.6	34.0	1.71	1.1
OCT	32.9	13.1	23.0	1.09	6.2
NOV	7.3	-6.2	0.6	0.93	9.3
DEC	1.0	-17.1	-8.0	1.16	11.6
YEAR	34.5	13.0	23.8	19.0	66.3

1 Mean snowfall was estimated by assuming that the same percentage of mean total precipitation falls as snow at Cadillac Mine as it does at Fort Simpson.

Table 4.6. Long Term Mean Temperature and Precipitation Estimates at Cadillac Mine Using Tungsten Relationships.

	TEMPERATURE (°F)			PRECIPITATION (inches)	
	Mean Daily Maximum	Mean Daily Minimum	Mean Daily	Mean Total	Mean <sup>1</sup> Snowfall
JAN	-1.8	-20.7	-10.8	1.21	12.1
FEB	17.6	-10.6	3.9	0.70	7.0
MAR	27.6	-3.6	12.4	0.54	5.4
APR	40.5	11.5	26.4	0.95	9.5
MAY	54.1	30.1	42.5	4.43	28.6
JUN	66.7	39.1	53.3	2.74	0
JUL	69.1	41.9	55.9	3.32	0
AUG	65.2	39.4	52.8	5.84	0
SEP	49.6	30.2	40.3	2.37	5.1
OCT	34.0	11.7	23.2	1.25	11.8
NOV	6.3	-8.8	-0.7	0.97	8.4
DEC	-0.5	-20.3	-9.9	1.38	13.8
YEAR	35.7	11.7	24.1	25.7	101.7

1 Mean snowfall was estimated by assuming that the same percentage of mean total precipitation falls as snow at Cadillac Mine as it does at Tungsten.

where effective precipitation is that proportion of the rainfall and snowfall that becomes surface runoff. In the South Nahanni River drainage basin, stream discharge figures are available from 1960 for three stations although in many years observations were only made in the summer months. Two of the stations are located on the South Nahanni itself, one above Virginia Falls and the other above Clausen Creek at the downstream end of First Canyon; the third station is located on the Flat River near its confluence with the South Nahanni.

The drainage area of the South Nahanni River basin above Clausen Creek is 12,900 square miles and the average annual volume of runoff is 5,234,976 million cubic feet. This means that the average effective precipitation on the basin as a whole is 18.4 inches. In fact effective precipitation varies considerably from place to place. The portion of the South Nahanni basin above Virginia Falls, for instance, has an average effective precipitation of 21.0 inches annually, while in the Flat River basin it is only 17.4 inches. Surface runoff from the 3,970 square miles below Virginia Falls, excluding the Flat River basin is 3,670 cubic feet per second on average, giving an effective precipitation in the eastern portion of the basin, where the main tributaries are Mary River, Meilleur River and Prairie Creek, of 12.6 inches. The precipitation that eventually becomes surface runoff in the South Nahanni basin appears to increase from 12.6 inches in the east, through 17.4 inches in the Flat River area, up to 21.0 inches nearer the headwaters in the Selwyn Mountains.

Table 4.7. Tentative Estimates of Mean Temperature and Precipitation at Cadillac Mine Obtained by Averaging the Estimates from Fort Simpson and Tungsten Relationships.

	TEMPERATURE (°F)			PRECIPITATION (inches)	
	Mean Daily Maximum	Mean Daily Minimum	Mean Daily	Mean Total	Mean Snowfall
JAN	-1.0	-19.0	-9.8	1.14	11.4
FEB	17.6	-9.2	4.4	0.74	7.4
MAR	27.3	-2.4	12.6	0.62	6.2
APR	39.7	12.2	26.2	0.93	8.0
MAY	52.8	30.3	41.7	3.64	17.2
JUN	64.9	39.0	52.2	2.32	0
JUL	67.2	41.7	54.7	2.77	0
AUG	63.5	39.3	51.7	4.73	0
SEP	48.5	30.4	39.6	2.04	3.1
OCT	28.4	12.4	23.1	1.17	9.0
NOV	6.8	-7.5	-0.0	0.95	8.8
DEC	0.2	-18.7	-8.9	1.27	12.7
YEAR	35.1	12.3	23.9	22.3	84.0

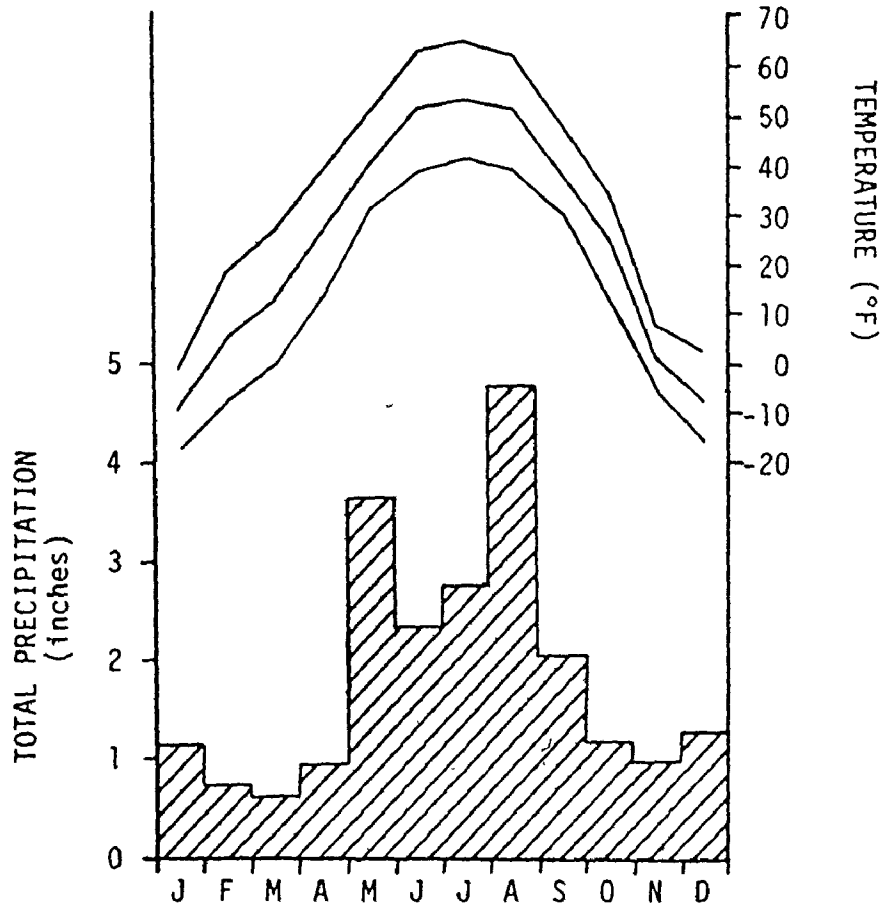


Figure 4.3. Climograph for Cadillac Mine, N.W.T. The figure was prepared from data contained in Table 4.7.



Possible explanations for this are that there is a general increase in precipitation westwards and with altitude and also that perhaps the magnitude of evapotranspiration decreases in this direction.

Mean total precipitation at Tungsten on the Flat River is 23.7 inches or some 6.3 inches more than the average effective precipitation calculated for the Flat River basin from stream discharge data. This suggests that 6.3 inches of moisture, or 26.6% of the actual precipitation falling on the Flat River area, is returned to the atmosphere by evapotranspiration. Annual evapotranspiration can be calculated by a variety of methods only the simplest of which can be employed here because of the general lack of data. Turc (1954), for instance, has developed a formula based on a statistical study of data collected from 254 watersheds located in all parts of the world, that relates evapotranspiration, precipitation and temperature over watersheds. He suggests that annual evapotranspiration may be estimated from the empirical equation:

$$E = \frac{P}{\left[0.90 + \left(\frac{P}{I_T}\right)^2\right]^{1/2}},$$

in which E is the annual evapotranspiration (mm) and P is the annual precipitation (mm). The quantity  $I_T$ , the "evaporation capacity" of the air, is defined as:

$$I_T = 300 + 25T + 0.05T^3,$$

where T is the mean annual air temperature ( $^{\circ}\text{C}$ ). The main advantage of the Turc equation is that no net radiation data are required for the estimation of evapotranspiration.

Anderson (1973) has applied a different method for computing the annual evapotranspiration. This is based upon the existence of a strong linear relationship between annual evapotranspiration (E) and annual precipitation (P) within a drainage basin. The general equation in this case is:

$$E = a(P) + b,$$

where a and b are numerical coefficients which differ from one drainage basin to another. Anderson has estimated these coefficients for the Hay, Athabasca and Liard River drainage basins. For the Hay basin in the Interior Plains of northern Canada, the relationship reduced to

$$E = 0.95(P) - 36,$$

while for the Liard it became

$$E = (P) - 249,$$

where both evapotranspiration and precipitation are expressed in millimeters.

Evapotranspiration at Tungsten, Cadillac Mine and Fort Simpson has been estimated by using the Turc equation and by using the empirical relations outlined by Anderson (1973). The Hay River basin relationship between precipitation and evapotranspiration was used on the Fort Simpson data while that for the Liard was used on the Tungsten and Cadillac Mine figures. Evapotranspiration figures derived

by these means have been used to estimate effective runoff at the three stations; these statistics are shown in Table 4.8. The Turc model suggests that average evapotranspiration ~~at~~ Tungsten on the Flat River should be 5.72 inches per year, which agrees very well with the 6.3 inches estimated here from stream discharge and precipitation data. The Anderson model for the Liard basin, of which the South Nahanni basin is a part, suggests 13.90 inches of evapotranspiration for the Tungsten area - between 2 and 3 times that suggested by the Turc equation. It is clear from this and the other statistics in Table 4.8 that the Anderson model for the Liard can not be applied to smaller basins in the Mackenzie Mountain area. As the figures show, the empirical equation for the Liard can not realistically be applied to other stream basins, for it suggests a constant effective precipitation from basin to basin because the coefficient (a) in the equation is equal to unity. Hence effective precipitation in millimeters (E-P) is given by

$$E - p = 249.$$

It is difficult, therefore, to accept the rationale of this equation which overestimates evapotranspiration in the drainage basins of the Upper Mackenzie Valley to a marked degree. The much more realistic estimates using the Turc equation suggest an effective precipitation in the Nahanni karst somewhere between 12.28 and 18.63 inches, with the likelihood that the figure is close to 15.51 inches. This result agrees well with the effective precipitation estimate for the eastern portion of the South Nahanni basin of 12.6 inches.

Table 4.8. Evapotranspiration and Effective Precipitation Estimates for Fort Simpson, Tungsten and Cadillac Mine.

STATION	EVAPOTRANSPIRATION (inches)		EFFECTIVE PRECIPITATION <sup>4</sup> (inches)	
	Turc Model	Anderson Model	Turc Model	Anderson Model
Fort Simpson	6.94	11.50 (H)	6.66	2.1
Tungsten	5.72	13.90 (L)	17.98	9.80
Cadillac Mine <sup>1</sup>	6.72	9.20 (L)	12.28	9.80
Cadillac Mine <sup>2</sup>	7.07	15.90 (L)	18.63	9.80
Cadillac Mine <sup>3</sup>	6.79	12.50 (L)	15.51	9.80

H Hay River basin model.

L Liard River basin model.

1 Data contained in Table 4.5.

2 Data contained in Table 4.6.

3 Data contained in table 4.7.

4 Cogley (1975) contends that, on average, actual precipitation in the Canadian high arctic may be 400% greater than measured precipitation (p. 257). If gross precipitation is also underestimated in the sub-arctic, say by as little as 50%, then this would imply that precipitation in the Cadillac Mine region lies not between 19.0 and 25.7 inches but rather between 28.5 and 38.5 inches. In this case evapotranspiration estimated by the Turc model would vary between 6.95 and 7.21 inches and effective precipitation between 21.5 and 31.3 inches.

The estimates of temperature, precipitation, and evapotranspiration presented here are considered to be the best available for the southern Mackenzie Mountains region at the present time. Other workers have attempted to estimate conditions in this remote area. Burns (1974), for instance, has estimated precipitation from runoff and evapotranspiration data and his work suggests that the Nahanni karst receives between 23-24 inches of precipitation annually, a figure very similar to the 22.3 inches estimated here (Table 4.7). Hare & Hay (1971), on the other hand, suggest 12-16 inches with some 4-8 inches of this being lost to the atmosphere as evapotranspiration.

Temperature, precipitation and evapotranspiration estimates for the Nahanni karst have been derived by using methods that give reasonably accurate results in fluvial terrains. The bulk of water in the Nahanni karst does not, however, flow into surface streams; most of it passes quickly underground where it is no longer susceptible to evapotranspiration losses. There is a strong possibility that evapotranspiration in the Nahanni karst is less than the Turc model would suggest and that effective precipitation is greater than the figures calculated. Although no published figures are available for a karst region such as this, intuition would suggest that effective precipitation is 1-2 inches greater here than it is in nearby fluvial landscapes. If this is the case, then effective precipitation in the Nahanni likely falls between 14 inches and 21 inches with an average figure probably being close to 17.5 inches per annum.

(b) Effective Snowfall in the Karst and the Geomorphic Significance of its Distribution.

Mean annual snowfall at Tungsten is 122 inches and that at Fort Simpson 52.6 inches amounting to 51.5% and 38.7% of the total annual precipitation at these two locations respectively. Estimates of snowfall in the Nahanni, range from 66 to 101 inches with a likely figure being close to 84 inches (Tables 4.5-4.7). Unlike statistics for rainfall, however, those for snowfall, even if accurate, say little of the actual distribution of snow over a given region. As such workers as Harrison (1963), Barnett (1963(a)), Gardner (1964), Meinman (1970), and McKay (1970) have noted, there are substantial variations in snow depth and density even in very small areas.

Some of the variation in the structure and depth of snow across a snowpack results from spatial variations in the intensity and duration of snowfall during the parent snowstorms. Most, however, is the result of subsequent wind transport and energy exchanges with the atmosphere which together can often bring about a redistribution of snow in patterns that bear little resemblance to those of the original snowfalls (McKay 1970). It is apparent that the action of the wind modifies primary storm snowfall patterns more than any other parameter. Loose or friable snow is susceptible to transport at wind speeds as low as 3m/sec (6 mph) although the formation of a glaze by condensation or melting with subsequent refreezing may inhibit transport (Harrison 1963). Nevertheless as McKay notes, under very strong wind conditions even large sheets of glazed snow

may be moved about. The amount of snow in transport over a friable snow surface is a function of windspeed. Above wind speeds of 8-9 m/sec (18-20 mph) at the one meter level, there is a rapid increase in the amount of snow that can be transported (Komorov 1954).<sup>1</sup>

The mean annual hourly wind speed at Fort Simpson is 6.3 mph, the high recorded 38 mph with gusts estimated at 54.8 mph (Burns 1973). In all months maximum hourly wind velocities above 23 mph have been recorded with the highest values of 32, 25 and 38 mph recorded in the winter months of December, January and February respectively (Table 4.9). Average and maximum hourly wind velocities in the Nahanni are likely to be higher than those measured at Fort Simpson, particularly on bare upland surfaces. Nevertheless, even the Fort Simpson statistics indicate that wind transport of snow in winter must result in a marked redistribution of storm snowfall in the Nahanni karst terrain.

As McKay (1970) has pointed out, wind transport of snow can result in a decrease or an increase in snow cover. Whenever wind speeds increase where air flow lines converge, as between hills or on the tops of ridges, erosion occurs. Where flow lines diverge and wind speeds drop, as in the lees of obstructions, snow is deposited from an airstream fully laden with drifting snow. The rate of transport is greatest over flat open areas while favored deposition sites are the lee sides of ridges, in depressions and along the windward edges of forests.

---

<sup>1</sup>As quoted in Kuzmin 1960.

Table 4.9. Hourly Wind Speeds (m.p.h.) at Fort Simpson, N.W.T. (after Burns 1973).

	MONTH												YEAR
	J	F	M	A	M	J	J	A	S	O	N	D	
Mean	5.5	6.1	6.8	7.2	7.1	6.3	6.0	6.0	6.4	6.4	6.2	5.2	6.3
High	35	38	24	28	27	27	27	26	28	28	26	32	28

Table 4.10. Snow Retention Coefficients for Various Surfaces Relative to Virgin Soil (after Kuzmin 1960).

Virgin soil	1.0
Open ice	0.4 to 0.5
Arable land	0.9
Hilly land	1.2
Large forest tracts	1.3 to 1.4
River beds	3.0
Rushes	3.0
Forest cuttings 100 to 200 m radius and edges of forests	3.2 to 3.4



As a result of snow drifting, actual reserves of snow may vary considerably across an area. McKay (1970) has argued that almost every object in arctic and alpine regions has a profound effect on the accumulation of snow. In an area 0.25 miles square in the eastern Canadian Rockies, he found variations in snowpack thickness from zero up to 30 ft. over very small distances. In late winter 1961-1962 Barnett (1963(a)) found differences in snow depth on Ferriman Ridge, Schefferville, Quebec, of more than 60 inches in an area of a little less than one square mile. In the Denault Lake region nearby, differences of 24 inches were noted in an area 170 yds. long and 130 yds. wide. The greater depths of snow on the Ferriman Ridge, Barnett ascribed to its more diversified relief giving favorable conditions for heavy drifting.

Kuzmin (1960) has compared a variety of surfaces in terms of their ability to catch and retain snow. His findings indicate that hilly land, forest tracts, forest clearings and topographic depressions such as river beds all retain more snow than do flat unvegetated regions. In fact topographic depressions and their vegetative equivalents forest clearings, seem to have the ability to collect and retain three times more snow than flat unvegetated areas (Table 4.10). Kuzmin also found that the smaller clearings in woodland areas have a greater catch efficiency than the larger clearings (Table 4.11), which may suggest a similar relationship between the catch in large and small closed topographic depressions. Both Harrison (1963) and Gardner (1964) have found that exposed locations in the Schefferville district of Quebec-Labrador have the shallowest cover of snow in winter. Snow depths in

woodland regions are much greater while the deepest cover is encountered on the windward edges of forests. Gardner (1964) did in fact conduct a probe survey of snow depths in a plot 1300 ft. square at a time when snow depths were thought to have reached a maximum. The survey revealed considerable variations in snow depth depending upon the vegetation cover, with minimum depths of less than 25 inches in cleared or muskeg areas and maximum depths of greater than 60 inches on the windward edges of forested terrain. This evidence from northeastern Canada generally supports Kuzmin's observations.

In assessing spatial variations in water equivalent across a snowpack, both depth and density changes are important. Seligman (1962) has estimated average snowpack densities for snow in different states of consolidation (Table 4.12). His measurements clearly demonstrate that snow increases in density as it is wind toughened. This fact suggests that in winter, areas of heavy snow accumulation particularly on the windward sides of obstructions, are also likely to be areas of highest snow density. Irregular accumulation and compaction of snow across a region clearly means that some areas receive more moisture per year than others.

It is apparent from this brief discussion of the variations in depth and density across a snowpack that may be induced by wind transport, that an extremely irregular snowpack is to be expected in the Nahanni karst in winter. Broad patterns of snow accumulation in this region, in all likelihood parallel the major topographic

Table 4.11. Snow Accumulation in Clearings of Various Sizes for the Observation Period 1945-59 (after Kuzmin 1960).

Variable	Size of Clearing (m)						
	100x100	60x500	250x500	500x500	500 x 1000	700 x 1000	700 x 2000
Snow depth (cms)	53	52	51	44	43	41	40
Water equivalent (cms)	14.8	14.7	14.1	12.8	12.5	12.0	11.0

Table 4.12. Average Snowpack Densities (after Seligman 1962).

Snow Type	Density
Wild snow	0.01 to 0.03
Ordinary new snow immediately after falling in still air	0.05 to 0.065
Settling snow	0.07 to 0.19
Settled snow	0.2 to 0.3
Very slightly toughened by wind immediately after falling	0.063 to 0.08
Average wind-toughened snow	0.28
Hard wind slab	0.35
New firn* snow	0.4 to 0.55
Advanced firn snow	0.55 to 0.65
Thawing firn snow	0.6 to 0.7

\*snow consolidated partly into ice

structures and vegetation types. Snow depths are probably greater in densely forested topographic basins like Sundog Basin than they are on the tundra-vegetated upland surfaces of the Nahanni Plateau. In addition, on a micro scale, surface karst landforms must greatly influence snowpack characteristics. Canadian Department of Forestry workers centered in Fort Simpson, who have flown over the eastern ranges of the Mackenzie Mountains in winter, report that the upland tundra-vegetated surfaces of the Nahanni and Ram Plateaus are windswept at this time and retain very little snow.<sup>1</sup> Snowdrifts are of sufficient thickness in valley and canyon floors, however, that movement across them even in snow shoes might be dangerous. Such qualitative observations clearly indicate that in winter low-lying sheltered areas collect and retain the snow that is swept from the upland surfaces.

Transport of snow from higher more exposed upland surfaces to more sheltered areas at lower elevations probably generates thick snowdrifts along the windward edges of the forest cover at the tundra-forest junction. As McKay (1970) points out, the forest edge acts somewhat like a wall of variable permeability with snow banks generally extending into and out of it for a distance approximately equal to five times the height of the trees. McKay notes that in the Prairies region of Canada, 30-40% of snowfall is removed from grassland areas by wind transport in winter. Because of this,

---

<sup>1</sup>Alan Jackson personal communication.

spring thaws often leave grassland regions clear of snow while farmyards, with attendant shelter belts, may be ringed by snow drifts 5-10 ft. in depth.

Accumulation of snow at the forest edge in winter, as well as retention of storm snowfall by forest, may help explain why karst landforms are better developed in some parts of the Nahanni than in others. On the eastern slopes of the Nahanni Plateau north of First Canyon, South Nahanni River, for example, well developed surface karst forms are restricted to the lower slopes where there is a thicker soil cover and forest as opposed to tundra vegetation. The more accentuated karst development in these regions is obviously partly a function of higher  $PCO_2$  in soils and resultant more acid groundwaters. It may also be related in some degree to the fact that compared to tundra areas at only a slightly greater elevation, these areas accumulate considerably more snow in winter and are therefore subject to a higher annual precipitation. It seems highly likely that in arctic and alpine regions, the higher effective precipitation in forest regions together with the greater acidity of percolating waters are sufficient to explain the often better development of surface karst landforms in these regions as opposed to tundra areas. The occurrence of quite well developed karst forms above the tundra-forest junction on the eastern slopes of the Nahanni Plateau may indicate a somewhat higher tree line at some time or times in the past, possibly during one or more warmer interglacial periods. Certainly over much of the Nahanni Plateau surface, there is strong evidence that soil erosion is presently active.

The pattern of winter snowcover in the highly developed karst region of the Nahanni is probably complex. The vertical-walled dolines, karst streets and karst platea must represent some of the most efficient natural traps for drifting snow imaginable. There can be no doubt that these closed depressions collect a greater volume of snow in winter, per unit area, than do surrounding flat limestone surfaces. Quantification, however, is difficult for the only work on the influence of solutional depressions on snow distribution in a karst area, has been undertaken by Dubljanskij (1963) in the Ai-Petra Massif of the Crimean Mountains, U.S.S.R. Dubljanskij has estimated average reserves of moisture in the different elements of karst relief. These results show that wooded areas retain 1.5 times as much snow as bare, non-wooded areas, while sinkholes retain 1.65 times and regions under structural promontories 2.6 times this value (Table 4.13).

From the data presented by Kuzmin (1960) and Dubljanskij (1963), there can be little doubt that the vertical-walled depressions in the Nahanni, which must be able to collect and retain snow at least as well as river beds, forest cuttings (Table 4.10) and structural promontories (Table 4.13), trap 3-4 times the depth of snow that accumulates on surrounding little-vegetated limestone surfaces in winter. Evidence presented in Table 4.11 may also indicate that the smaller depressions accumulate slightly more snow than the larger features. If we assume for the sake of argument that the North Karst labyrinth area is made up of 50% essentially flat, little vegetated

Table 4.13. Average Reserves of Moisture in the Different Elements of Karst Relief in the Ai-Petra Massif, Crimean Mountains, USSR (after Dubljanskij 1963).

Surface Element	Percentage <sup>1</sup>
Bare non-wooded areas	100
Slopes of western and eastern exposure	75
Slopes of northern exposure	115
Slopes of southern exposure	147
Wooded areas	150
Sinkholes and thalwegs of temporary streams	165
Areas under structural promontories	260
Areas neighboring structural promontories	55

<sup>1</sup> The percentages are quoted in relation to reserves of moisture in bare non-wooded areas which are set at 100%.

limestone surfaces and 50% steep-walled closed depressions, then it is to be expected that at least three times more snow will be retained in the depressions than on the surrounding exposed surfaces. If this is the case and the average snowfall in the Nahanni is taken to be 84 inches (Table 4.7), then ignoring ablation, bare limestone surfaces in the North Karst labyrinths should retain a total of 42 inches of snow in winter while nearby depressions retain 126 inches. These figures could well be significantly higher if there is, as suspected, a considerable movement of snow into the labyrinth area from surrounding upland regions.<sup>1</sup>

These statistics imply that the actual precipitation reaching closed depressions in the Nahanni could be as high as 26.5 inches while that affecting the surrounding limestone surfaces may only be 18.1 inches. Whatever the truth, there can be no doubt that snow transport by wind during winter with its enhanced accumulation in already existing topographical depressions, is one factor that is leading to an accentuation of present karst features rather than the development of new ones. Precipitation in the form of snow is clearly affecting the direction karst development is taking at the present time in the Nahanni region, it may also have been of considerable importance in moulding this sub-arctic landscape in the past.

---

<sup>1</sup> If the arguments presented in footnote (4) of Table 4.8 are considered valid this figure could be substantially higher.



(c) Temperature and Precipitation Measurements During the Summers of 1972 and 1973.

(i) Precipitation.

Daily precipitation summaries for the summer months of 1972 and 1973, as determined by use of standard raingauges, are presented in Table 4.14 and the data is illustrated in Figure 4.4. In 1973 a Meteorological Service of Canada (MSC) tipping-bucket raingauge<sup>1</sup> was also installed to determine both the hourly distribution of rainfall and its intensity. As recommended, daily rainfall amounts recorded by this gauge were corrected to standard raingauge values before rainfall intensities were calculated. A summary of rainfall intensities for those days in the summer of 1973 with rain is presented in Table. 4.15.

During the 57 days of observation in 1972 a total of 12.17 inches of rain fell on the karst or an average of 0.21 inches per day. Between July 5th and July 31st rainfall totalled 10.5 inches while in August it amounted to 1.67 inches. During the 8 day period from July 19th to 26th alone 7.99 inches fell while in the 16 days between July 19th and August 3rd., 9.54 inches was recorded. The summer of 1973 was considerably drier than that of 1972 for in the 51 days of observation only 5.13 inches of rain was recorded, 2.43 inches in June, 2.00 inches in July and 0.7 inches in the first five day of August.

---

<sup>1</sup>The gauge is described in Instrument Manual 41 issued by the Canadian Department of Transport, Meteorological Branch, Downsview, Ontario.

Table 4.14. Daily Precipitation Summary, Nahanni Karst. Summers of 1972 and 1973.<sup>1</sup>

DATE	RAINFALL (inches)		DATE	RAINFALL (inches)		DATE	RAINFALL (inches)		DATE	RAINFALL (inches)	
	1972	1973		1972	1973		1972	1973		1972	1973
June			July			July			Aug		
16		0.38	5	0.32	0.06	25	0.74	0.20	13		
17		0.38	6		0.14	26	0.74	0.02	14		
18		0.38	7	0.46		27			15		
19			8	0.46		28	0.04		16		
20			9		0.20	29	0.66		17		
21			10		0.07	30	0.12	0.04	18	0.62	
22		0.01	11	0.08		31		0.07	19	0.04	
23			12		0.02	Aug			20		
24			13			1			21		
25			14		0.02	2	0.30	0.01	22		
26		1.17	15	0.18	0.24	3	0.43	0.09	23		
27		0.10	16	0.19	0.07	4		0.20	24		
28		0.01	17		0.11	5		0.40	25		
29			18			6			26		
30			19	0.51		7			27		
July			20	0.25		8	0.04		28	0.04	
1		0.01	21	1.36		9	0.07		29	0.13	
2			22	2.72		10			30		
3			23	0.97		11					
4		0.32	24	0.70	0.23	12					

<sup>1</sup> In 1972 measurements were taken at Mosquito Lake, July 5th to August 10th and at Death Lake, August 11th to August 30th. In 1973 measurements were taken at Mosquito Lake, June 16th to June 30th and July 29th to July 31st at Death Lake July 1st to July 28th and at First Polje August 1st to August 5th. All dates are inclusive.

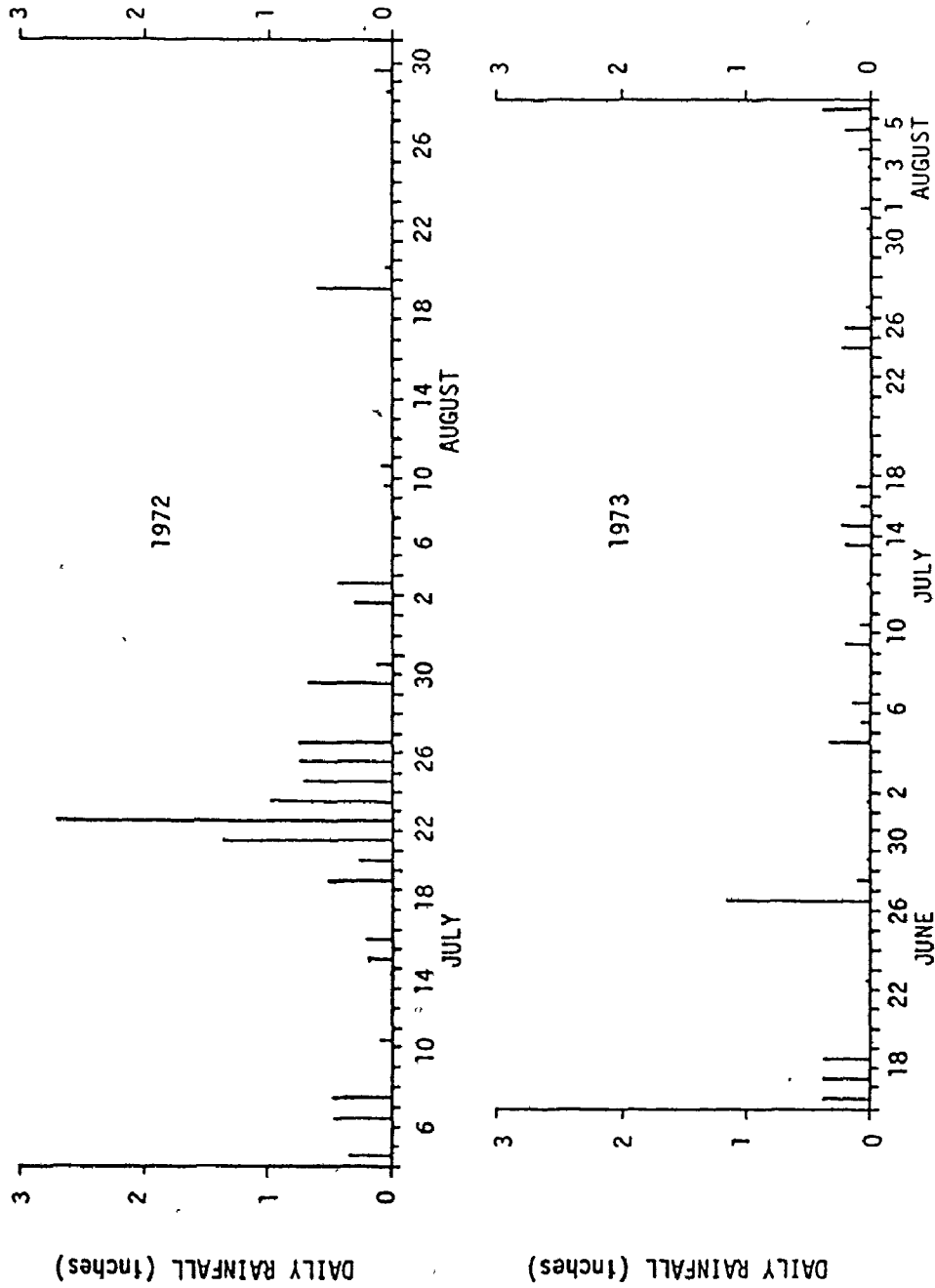


Figure 4.4. Daily rainfall histograms, Nahanni karst belt 1972 and 1973.

Maximum rainfall intensities in 1973 for periods of 5, 10, 15 and 30 minutes, and 1, 2, 6 and 12 hours are given in Table 4.15 below daily values. The maximum 12 hour intensity measured in 1973 was 0.81 inches. In 1972 the maximum rainfall in a 24 hour period, as recorded by a standard rain gauge, was 2.72 inches giving an absolute minimum 12 hour intensity of 1.36 inches, a value far greater than the intensity of any storm in 1973. Diagrams contained in Gray (1970) on the return periods of rainfalls of particular duration and intensity, suggest that 2.72 inches in 24 hours has a return period of considerably more than 25 years (p. 2.82). Storms that affected the Nahanni in 1973 appear to have relatively short return periods. For instance the maximum 24 hour intensity of 1.17 inches has a return period of close to 2 years, the maximum 60 minute intensity of 0.3 inches a return period of 5-10 years and the maximum 30 minute intensity of 0.23 inches a return period of 2-5 years.

Published records of daily rainfall at Cadillac Mine in August 1970 when 8.06 inches of rain was recorded, show that 3.52 inches and 1.67 inches of rain fell on two separate days. A storm of 1.67 inches in 24 hours has a return period of approximately 5 years while one of 3.52 inches occurs only once in from 25-50 years. The available evidence suggests that in the three years from 1970 to 1972 a number of storms with apparent return periods of more than 25 years affected the karst and other nearby areas. It appears that either these years were abnormally wet or this general area of the mountains experiences far more intense rainfall and in greater amounts

Table 4.15. Rainfall Intensities in the Nahanni Karst, Summer 1973.

Day*	Month	Greatest fall of rainfall (inches) in							
		5 min.	10 min.	15 min.	30 min.	1 hr.	2 hr.	6 hr.	12 hr.
<u>Station</u>		<u>Mosquito Lake N.W.T.</u>							
22	June	.010	.010	.010	.010	.010	.010	.010	.010
26	June	.032	.043	.054	.076	.119	.195	.455	.812
27	June	.010	.020	.030	.050	.050	.050	.070	.080
28	June	.010	.010	.010	.010	.010	.010	.010	.010
<u>Station</u>		<u>Death Lake N.W.T.</u>							
4	July	.085	.139	.172	.235	.299	.299	.320	.320
5	July	.024	.036	.036	.036	.036	.036	.060	.060
6	July	.021	.032	.043	.054	.065	.075	.140	.140
9	July	.044	.089	.111	.167	.189	.200	.200	.200
10	July	.030	.040	.050	.070	.070	.070	.070	.070
12	July	.010	.010	.010	.010	.010	.010	.010	.020
14	July	.021	.042	.053	.084	.137	.189	.200	.200
15	July	.010	.021	.031	.031	.052	.094	.146	.188
16	July	.040	.060	.060	.070	.070	.070	.070	.070
17	July	.061	.085	.110	.110	.110	.110	.110	.110
24	July	.140	.220	.230	.230	.230	.230	.230	.230
25	July	.087	.125	.137	.162	.200	.200	.200	.200
26	July	.020	.020	.020	.020	.020	.020	.020	.020
<u>Station</u>		<u>First Polje N.W.T.</u>							
2	August	.010	.010	.010	.010	.010	.010	.010	.010
3	August	.013	.026	.039	.051	.090	.090	.090	.090
4	August	.022	.033	.033	.033	.067	.111	.167	.167
5	August	.021	.021	.032	.063	.116	.189	.305	.337
<u>Maximum Rainfall Intensities</u>		.140	.220	.230	.235	.299	.299	.455	.812

\* Readings were taken from 11 P.M. to 11P.M. The day indicated is the one contributing 23 hours to the readings.

than published statistics and those estimated here for Cadillac Mine and the Nahanni karst would suggest.

(ii) Temperature.

In 1973 outside air temperature fluctuations were monitored with two Simpson Thermoscript Model 413 temperature recorders. Maximum, minimum and mean daily temperatures extracted from the continuous temperature trace obtained are listed in Table 4.16 and illustrated in Figure 4.5. The overall mean daily maximum temperature for the field season was 60°F and the mean daily minimum 38.5°F. The 10 days of June had an average daily maximum temperature of 57.7°F and an average daily minimum of 35.7°F. Temperatures in July were 60.1°F and 40.4°F respectively while the 5 days of August had maximum and minimum daily temperatures of 64.7°F and 30.3°F. Clearly there was a general rise in daily temperatures from June to August although as Figure 4.5 shows the trend is masked by sizeable day to day fluctuations. The highest temperature recorded during the 1973 season was 76°F on June 23rd, the lowest 23°F on August 3rd. This very low temperature was recorded when a temporary base camp was set up in the floor of First Polje, a closed basin which appears to collect and retain cold air during the night. In a highly developed karst area such as the Nahanni with a multitude of small and large closed basins, it is to be expected that maximum and minimum temperatures, as was demonstrated for overhang Doline on Cenote Col, will vary considerably from one location to another. It is interesting to note that on 6 out of 41 days of record in 1973, minimum temperatures fell below freezing even in the summer months of June, July and August.

Table 4.16. Mean Daily and Daily Maximum and Minimum Temperatures in the Nahanni Karst, Summer 1973.

DATE	MAXIMUM	TEMPERATURE (°F) MINIMUM	MEAN DAILY
June 21	67	34	50.5
22	62	40	51
23	76	36	56
24	59	36	47.5
25	60	38	49
26	48	40	44
27	45	39	42
28	50	37	43.5
29	53	29	41
30	57	28	42.5
July 1	Moved to Death Lake	31	-
2	59	35	47
3	61	41	51
4	59	41	50
5	52	40	46
6	53	40	46.5
7	56	35	45.5
8	58	33	45.5
9	59	32	45.5
10	56	34	45
11	62	38	50
12	64	49	56.5
13	60	39	49.5
14	53	45	49
15	49	44	46.5
16	55	48	51.5
17	60	37	48.5
18	66	34	50
19	69	53	61
20	67	52	59.5
21	59	40	49.5
22	63	35	49
23	68	36	52
24	68	41	54.5
25	60	43	51.5
26	59	47	53
27	64	46	55
28	65	43	54
	Moved to First Polje		
Aug. 2	69	-	
3	70	23	46.5
4	68	27	47.5
5	52	41	46.5

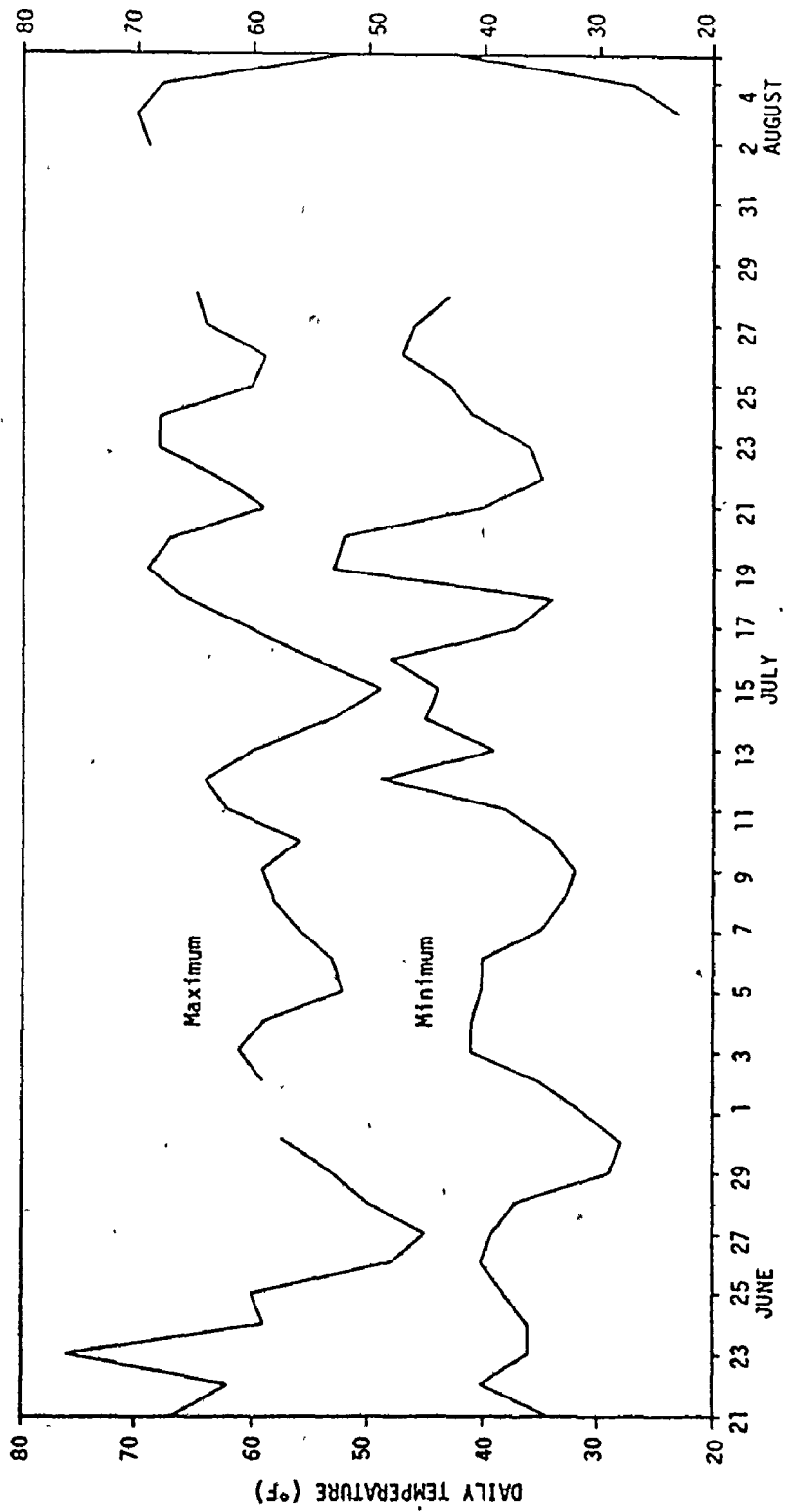


Figure 4.5. Maximum and minimum daily temperatures, Nahanni karst 1973. Measurements were made at Mosquito Lake (Jun. 16-30, Jul. 29-31), Death Lake (Jul. 1-28) and First Polje (Aug. 1-5).



(d) Seasonal Distribution of Precipitation.

It is clear from Figure 4.3 and Table 4.17 that precipitation in the Upper Mackenzie Valley is distinctly seasonal in its distribution. At Fort Simpson an average of 40.5% of the annual precipitation falls in June, July and August; at Tungsten and Cadillac Mine,<sup>1</sup> corresponding figures are 37.0% and 43.5% respectively. Furthermore, at Tungsten 67.2% of the annual precipitation falls in the 6 months from June to November while at Cadillac Mine 68.7% falls in the 5 months from May to September and at Fort Simpson 52.2% in the 4 months from June to September. Much of this summer rainfall is deposited by cyclonic storms which at least in the eastern ranges of the Mackenzie Mountains seem to produce particularly intense rains with some degree of regularity (Hench 1960).

Mackay et al. (1973) have documented an extreme summer storm that affected approximately 30,000 square miles of the eastern Mackenzie Mountains immediately west of Norman Wells on the 19th-21st July 1970. This caused severe flooding of the Redstone, Keele, Mountain and Arctic Red Rivers. The same storm has been discussed by Bowkett (1974) who has also outlined the events that led up to the intense storm in the Mackenzie Mountains of July 16-31, 1972, which had such a pronounced effect on conditions in the Nahanni North Karst. Since 1970 at least two storms which produced intense rains are known to have affected the area. These will be discussed briefly.

---

<sup>1</sup>Calculated for data in Table 4.7.

Table 4.17. The Seasonal Distribution of Precipitation at Fort Simpson, Tungsten and Cadillac Mine.

MONTH	PERCENTAGE OF ANNUAL PRECIPITATION OCCURRING BY MONTH				
	FORT SIMPSON	TUNGSTEN	CADILLAC MINE <sup>1</sup>	CADILLAC MINE <sup>2</sup>	CADILLAC MINE <sup>3</sup>
JAN	6.0	6.5	5.6	4.7	5.1
FEB	4.2	3.8	4.2	2.7	3.5
MAR	5.4	5.8	3.7	2.1	2.9
APR	6.2	6.3	4.8	3.7	4.2
MAY	6.0	6.4	15.0	17.2	16.1
JUN	12.6	8.7	10.0	10.7	10.3
JUL	<del>14.4</del>	16.2	11.7	12.9	12.3
AUG	13.5	12.1	19.1	22.7	20.9
SEP	11.7	9.6	9.0	9.2	9.1
OCT	7.6	10.8	5.7	4.9	5.3
NOV	6.8	9.8	4.9	3.8	4.3
DEC	5.5	3.9	6.1	5.4	4.7

1 From data in Table 4.5.

2 From data in Table 4.6.

3 From data in Table 4.7.

(i) The Storm of August 15th-17th 1970.

Although there were three storms that moved across the South Nahanni River area in August 1970, the most severe was the intense low pressure system of August 16th and 17th. The center of the storm formed near Fort Simpson by the evening of the 15th and developed rapidly on the 16th to a low of 988 mb (Figure 4.6). It is clear that in the eastern-portion of the South Nahanni River basin very strong winds varying in direction from northeast to northwest resulted from this pressure development. The heaviest rains were recorded at Muncho Lake (1.52 inches), Tungsten (1.47 inches) and Cadillac Mine (4.20 inches) as shown in Figure 4.7. It is an interesting fact that the rainfall at Cadillac Mine was more than twice that recorded elsewhere. The storm persisted near Fort Simpson until it moved towards Hudson Bay on the 18th.

(ii) The Storm of July 16th-31st 1972.

The formation of a low pressure system in north-central British Columbia, and the development of a strong high centered over the south coast of the Beaufort Sea (Figure 4.8), resulted in a strong northeasterly persisting surface wind over the eastern ranges of the southern Mackenzie Mountains from July 16th-31st 1972. An isohyetal chart for the period July 16-27, 1972 is presented in Figure 4.9 while mass curves of rainfall are presented in Figure 4.10. The Nahanni karst received 9.00 inches of rainfall in the 16 days between July 16th-31st and at the height of the storm between July 20th-23rd some 4.33 inches was recorded. The easterly gradient was less evident between July 27th-31st although instability showers and thunderstorms persisted

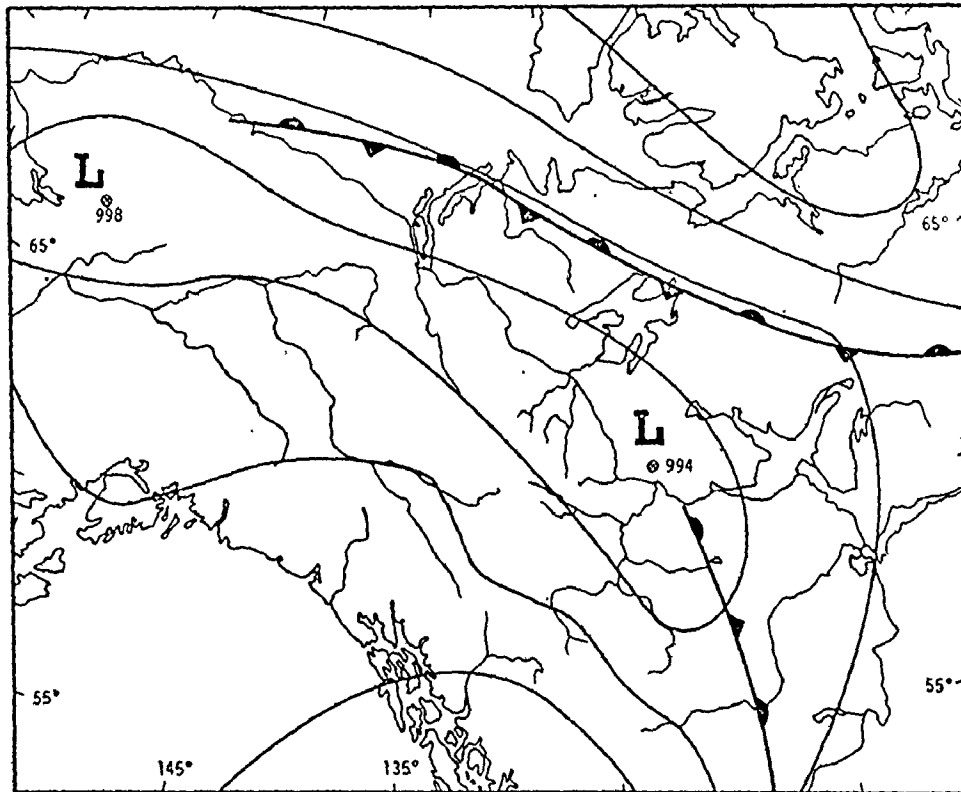


Figure 4.6. Surface pressure characteristics, district of Mackenzie, August 15, 1970.

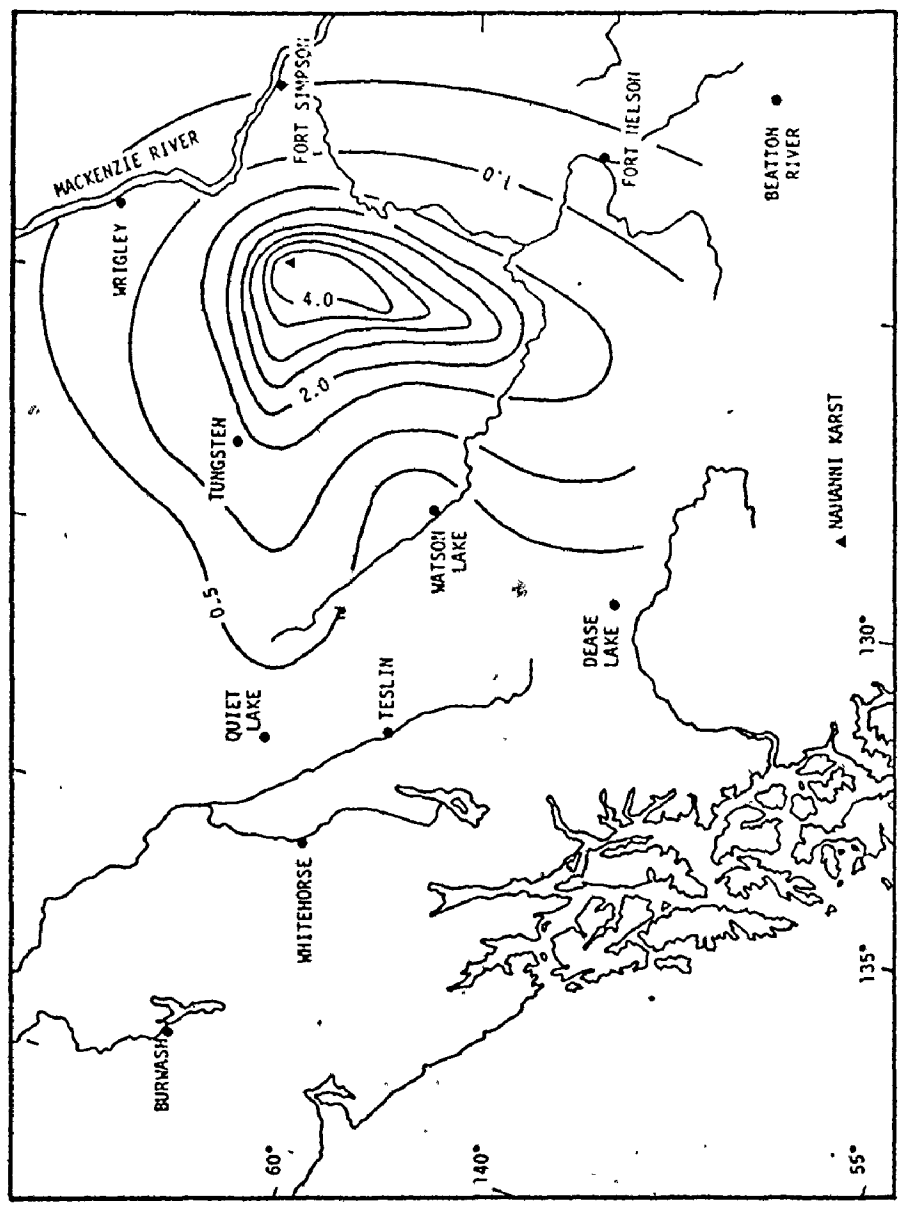


Figure 4.7. Rainfall in the southern Yukon, southwest district of Mackenzie and northern British Columbia, August 14-19, 1970 (rainfall is given in inches).

and an additional 0.82 inches of rainfall was deposited on the Nahanni area (Figure 4.4). The rainfall recorded at Mosquito Lake in the Nahanni karst appears to have been just short of twice that recorded elsewhere within the boundaries of the storm, which is estimated to have affected approximately 80,000 square miles. Between July 19th-26th when the storm was most active, 7.99 inches of rainfall was recorded in the Nahanni karst, Quiet Lake in the Yukon received 4.38 inches, Fort Nelson and Dease Lake in northern British Columbia 3.75 and 2.13 inches respectively and Wrigley, N.W.T. 2.33 inches. The mass curves (Figure 4.10) demonstrate that the movement of air was in a westerly direction for the most intense rains occurred in the Nahanni karst and at Fort Nelson and Wrigley on July 22nd. The effects of the north easterly air flow were not properly felt at Dease Lake and Quiet Lake until July 24th.

Both storms appear to have deposited the heaviest rains in the eastern ranges of the southern Mackenzie Mountains. Although some of the precipitation from both storms may have been induced by the dynamics of the low pressure systems, most of it likely resulted from the orographic lift involved in a north-easterly air flow enhanced markedly by a moist and unstable atmosphere. In both cases warm, moist air appears to have been funnelled into the South Nahanni basin where orographic uplift resulted in very intense rains. It seems possible from the evidence, that the Nahanni karst may experience a greater magnitude of and more intense rainfall than areas around it. Similar synoptic conditions are common elsewhere in the eastern ranges of the western cordillera as reported by Warner & Thompson (1974).

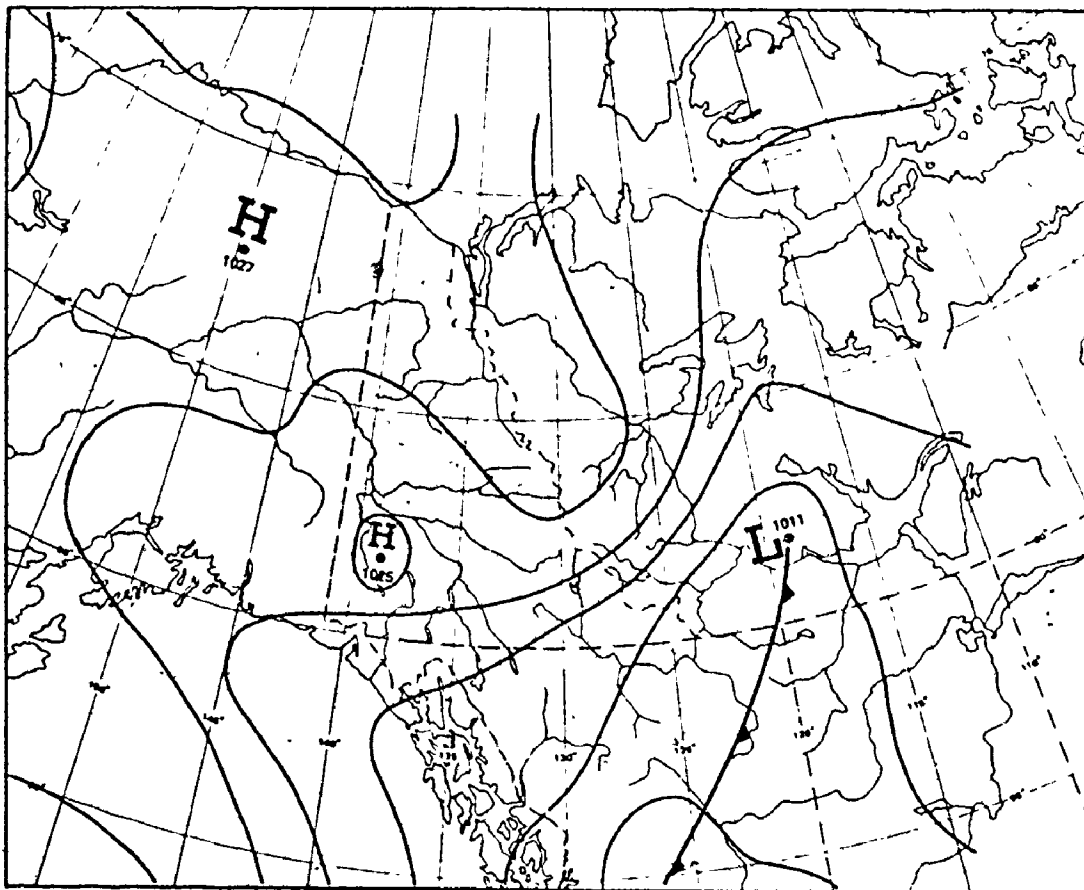


Figure 4.8. Surface pressure characteristics, district of Mackenzie, 0000Z July 22, 1972 (after Bowkett 1974).

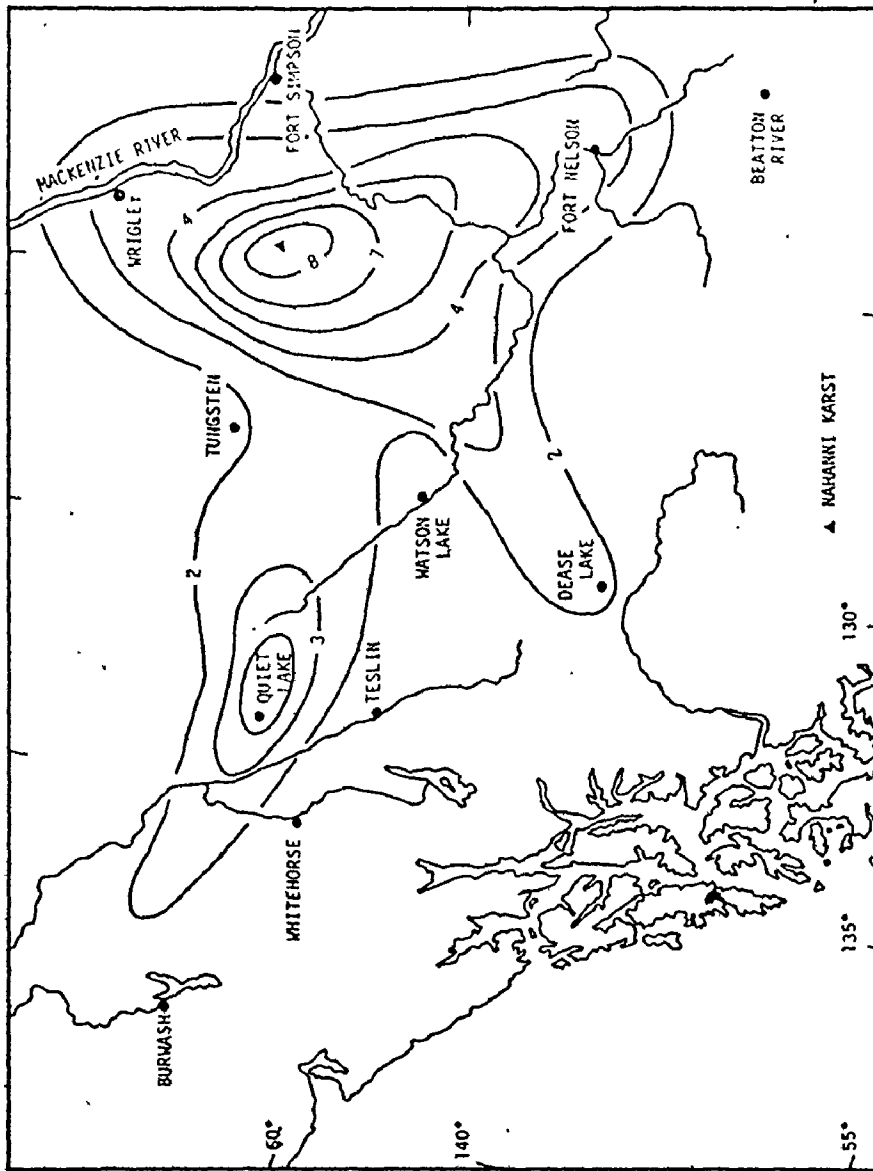


Figure 4.9. Rainfall in the southern Yukon, southwest district of Mackenzie and northern British Columbia, July 16-27, 1972 (rainfall is given in inches).



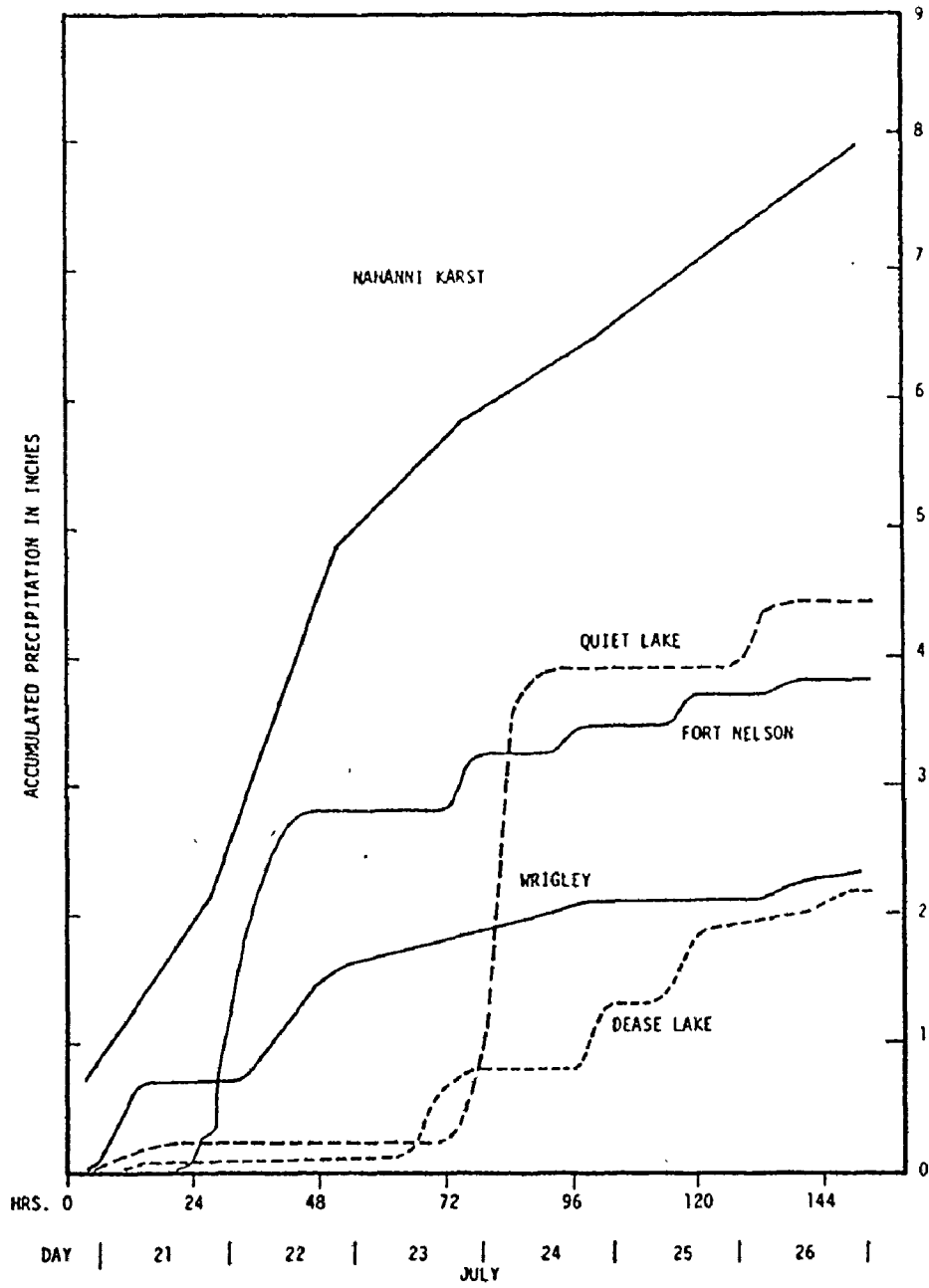


Figure 4.10. Mass curves of rainfall, July 20-27, 1972.

As Burns (1974) has noted, the seasonality of precipitation in the Mackenzie Valley is related to the movements of the various air masses that affect the area. In winter the cold dome of arctic air forms a block to migrating frontal lows which normally travel along the periphery of the air mass. In winter they seldom penetrate the Upper Mackenzie region but with the shift of the mean high pressure area northward in summer, the reverse is the case. In the spring, the increase in sensible heat limits the build-up of arctic air so that there is a steady northward retreat of its southern boundary. As this occurs, storms follow more northerly paths. In summer, upper level short-wave troughs from around a major vortex in the Russian sector develop frontal lows in Siberia and the Bering Sea. These move east or southeast and together with cyclones of Pacific origin are the primary sources of summer precipitation in the Upper Mackenzie region. The dominant circulation in winter is therefore anticyclonic but cyclonic activity increases in other seasons and reaches a maximum in July and August. This latter fact explains why such a high percentage of precipitation falls in the eastern ranges of the cordillera in the summer months.

If the Nahanni karst does receive an abnormally large amount of precipitation for its location, two aspects of the synoptic picture in the Upper Mackenzie region may explain why. First of all, corridors of primary and secondary lows (Figure 4.11) demonstrate that this area is affected not only by cyclones which move south eastwards down the Mackenzie Valley but also by those that move in an easterly direction from the southern Yukon and then down the South Nahanni Valley. It

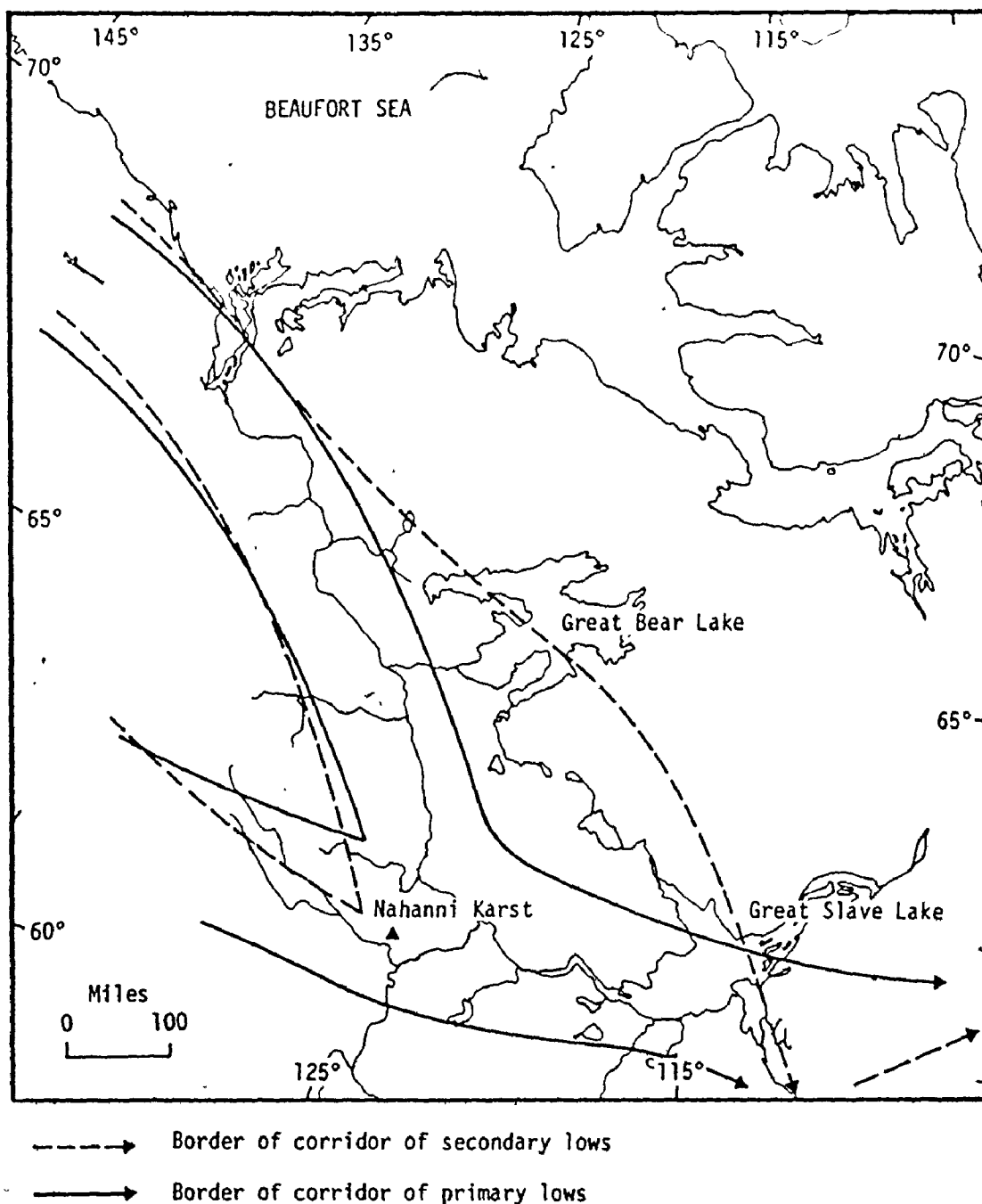


Figure 4.11. Corridors of 'primary' and 'secondary' lows in the Mackenzie River basin (after Burns 1973). Primary lows move down the corridor parallel to the Mackenzie River most frequently in July, secondary lows in May, June and July. Primary lows in the South Nahanni corridor are more frequent in August, secondary lows in April, June, July, September and October.

is clear that not only do these pressure systems generate cyclonic precipitation in this area but once centered close to Fort Simpson they induce a northeasterly airflow towards the eastern ranges of the Mackenzie Mountains which brings intense orographic storms. In addition to this, Burns (1973) points out that studies by Klein (1957) and Chung & Reinelt (1972) on the occurrence of cyclogenesis in the lee of the western cordillera have indicated two favored locations in the Mackenzie Valley, one near Norman Wells, N.W.T. and one near Fort Nelson, British Columbia. It has been shown already in relation to the July 1972 storm in the southern Mackenzie Mountains, that storms centered over north-central British Columbia can profoundly affect weather conditions in the Upper Mackenzie Valley, for in many instances these induce a northeasterly pattern of airflow into the mountains and this can produce substantial orographic precipitation when associated with a warm unstable airmass.

## 2. General Patterns of Surface and Groundwater Flow in the Nahanni Karst.

### (a) Groundwater Recharge.

Within the bounds of the Nahanni karst virtually all of the precipitation that is not lost to the atmosphere through evapotranspiration, drains underground. Over much of the karst area, where bare or thinly till-mantled limestone surfaces are characteristic, rain or snowmelt water infiltrates rapidly into the bedrock, encouraged by networks of open joints and a sparse forest cover at lower elevations, or a tundra cover at higher altitudes. This infiltrating water

represents the diffuse or percolation component of groundwater recharge to the karst aquifer.

In areas where limestone is covered by impermeable materials the volume of percolation to the limestone aquifer is significantly reduced. Where limestone is overlain by shale, or where it is mantled by thick glacial deposits, rainfall and snowmelt becomes surface runoff as soon as the soil moisture deficit is satisfied. Surface streams with catchments in these areas sink almost immediately when they encounter limestone bedrock. Water added to the limestone and dolomite aquifer in this way makes up the conduit or swallet groundwater recharge component.

Although diffuse recharge varies little in magnitude over wide areas of the karst, the same can not be said of conduit recharge for this is concentrated within the narrow zone of highly faulted and jointed limestone and dolomite making up the 'Nahanni Fracture Belt.' It is noticeable, for instance, that Hiller, Texas and Canal Creeks show no tendency whatever to sink underground until they encounter this zone, at which point they sink almost immediately, - Canal Creek into dolomite and Hiller and Texas Creeks into limestone. In addition, streams flowing from shale and glacial drift areas in the North karst, among them Mosquito Creek, also sink in this zone as does Death Lake a little to the south. There is no doubt, therefore, that overall, recharge to the limestone and dolomite aquifer is concentrated within the relatively narrow 'Nahanni Fracture Belt.' This may in part explain why the most accentuated

surface karst landforms are also located in this region. It may also point to the fact that the aquifer is anisotropic in terms of its ability to transmit groundwater with zones of concentrated groundwater flow characteristic.

(b) Groundwater Discharge.

Although several springs discharging groundwater have been identified in the Nahanni karst, only two have been discovered that actually discharge water out of the karst area. In the south White Spray adds to the flow of the South Nahanni River and in the north Bubbling Spring supplies water to a tributary of the Ram River (Figure 4.12).

White Spray in the north wall of First Canyon, emerges from scree some 40-50 ft. above the level of the South Nahanni River. Water emerges from dolomites almost 1,700 ft. below the limestone-dolomite contact clearly visible far above in the shear walls of First Canyon, South Nahanni River. On July 4th 1973 the main resurgence was discharging an estimated 180 cubic feet per second (c.f.s.) while several smaller flows of 0.5-1.5 c.f.s. meant that the total discharge was 183-189 c.f.s. at this time (believed to have been a period of relatively high flow). Because at least two more resurgences were discharging from beneath the water level in the South Nahanni River, it is clear that this flow estimate is conservative.

When White Spray was examined in 1973 it seemed possible that the spring derived its water from surface runoff into Lafferty Canyon

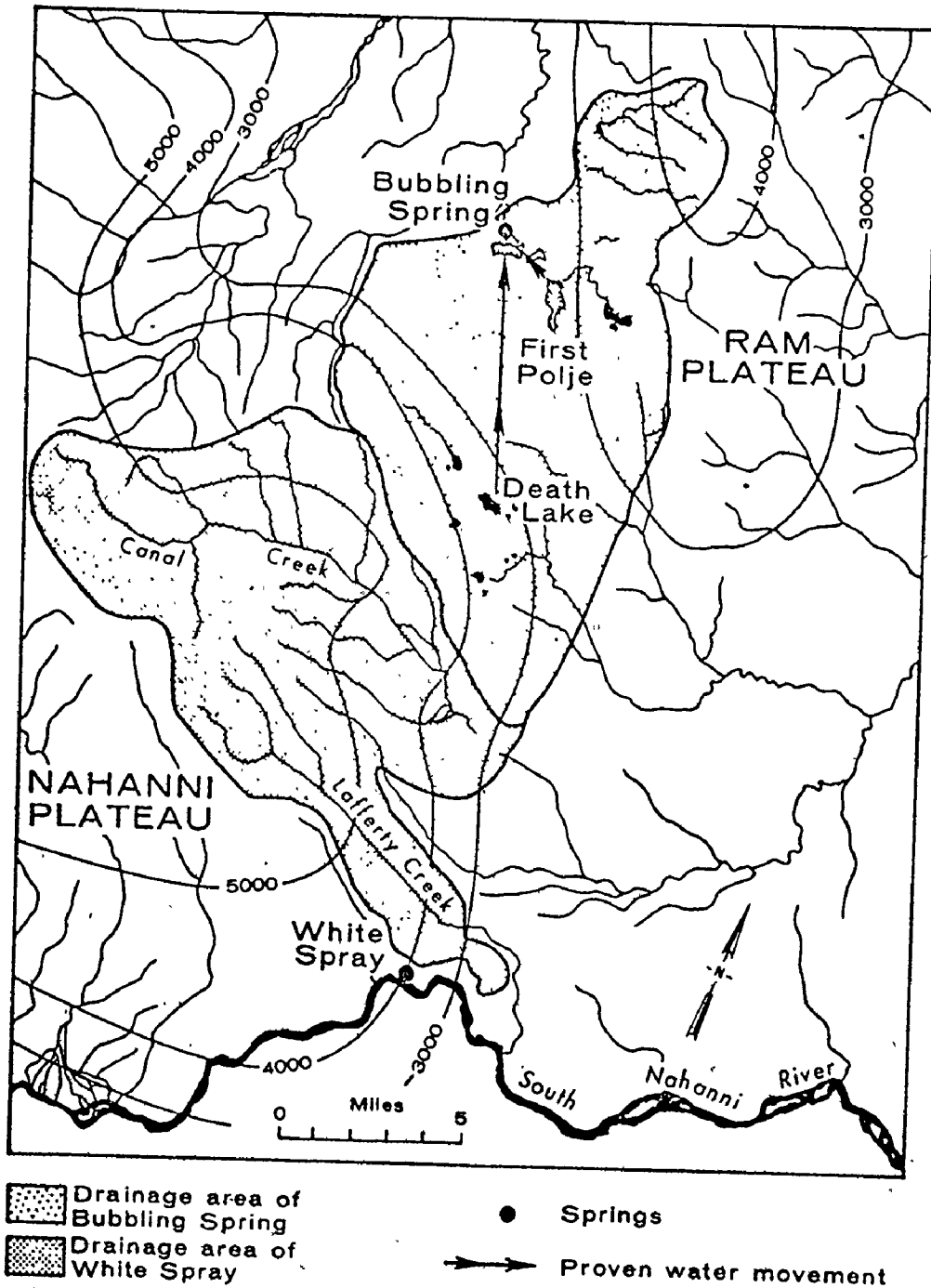


Figure 4.12. The Nahanni karst: surface and groundwater hydrology.

which during the three summers it has been examined, has never had a sizeable surface stream in its floor, despite a maximum depth of more than 2,500 ft. and an extremely large catchment area. In addition, the fact that the floor of Lafferty Canyon immediately to the north of White Spray is 1000 ft. above the spring, means that there is a more than adequate hydraulic head available to encourage such a groundwater movement. To test this hypothesis in the most rapid way possible the temperature of the spring was accurately monitored for several days using a thermocouple attached to a Rustrak continuous recording device. It was expected that if the water emerging at White Spray had originated in the floor of Lafferty Canyon, there would be a small diurnal variation in the temperature of the spring. As the temperature of the spring water remained constant at 4.5°C during the period of measurement, it is clear that White Spray discharges water that has had a relatively long residence time in the limestone and dolomite aquifer and also that a great deal of the water probably comes from much farther afield than Lafferty Canyon.

In the northern part of the karst belt Bubbling Spring issues not from dolomite but from the upper units of the 'Nahanni Limestone Formation.' Eight major resurgences have been identified along the base of a shallow vertical limestone wall located about 0.5 miles north of Third Polje (Plate 4.5). The water forces its way up through unconsolidated sands which choke the outlets. Because there is no



diurnal variation in the temperature of the spring water, the spring clearly has a relatively large catchment area. In June 1973 a stage recorder was installed at a suitable location along the out-flow channel of the spring, a cross section of the channel was surveyed and water velocities were measured. On August 2nd the spring was discharging close to 260 c.f.s. a slightly larger flow than that estimated by much less accurate methods for White Spray.

The temperatures of White Spray and Bubbling Spring waters are remarkably similar. In the summer of 1973 for instance, the only summer when measurements were made at both locations, the average temperature of White Spray water was  $4.8^{\circ}\text{C}$  while that of Bubbling Spring water was  $4.6^{\circ}\text{C}$ . In 1972 the average temperature of water at the Bubbling Spring outlet was  $5.2^{\circ}\text{C}$ . This unusually high value was due to mixing of spring water with relatively warm surface overflow water from Third Polje. The similarity in temperature and the coldness of White Spray and Bubbling Spring waters suggests that they are derived from groundwater that has spent some time in the karst aquifer. Because the average temperature of all surface waters examined in the Nahanni karst during the summers of 1972 and 1973 was  $9.5^{\circ}\text{C}$ , it is clear that the temperature of groundwater in this region results from a mixing of spring snowmelt water at or very close to  $0^{\circ}\text{C}$  with water derived from summer rainfall. This mixing, which must take place in the aquifer, is probably followed by a general cooling of the mix for the temperature of rock at depth even in the summer months is likely to be close to or possibly even below  $0^{\circ}\text{C}$ .

The fact that only two springs have been discovered that transmit water out of the karst despite an extremely large number of water input points in the limestone, suggests that there is a considerably degree of linkage between conduits.

(c) Groundwater Flow Directions and Velocities as Determined by Dye Tracing Experiments.

In an attempt to gather factual information about the area drained by Bubbling Spring and if possible to determine approximate groundwater flow velocities in the North karst area, two dye tracing experiments were conducted in the summer of 1973. A Dupont 20% rhodamine WT solution was used. This particular dye has been used by Brown & Ford (1971) in the Maligne Basin area of the southern Canadian Rockies and these workers regard it as the most economical, efficient tracer available.

The first of two experiments was conducted on a small stream that sinks in Brachiopod Basin in the northwest extremity of First Polje. Water disappears down a small, narrow vertical fissure that is blocked at shallow depth by breakdown material. On 23rd June at 11:00 A.M. approximately three gallons of 20% rhodamine WT solution was added to the stream a short distance from the sinking point. On the same day bags of activated charcoal were inserted into the water of Bubbling Spring to pick up any dye reaching this rising. The first batch of detectors was removed and replaced by a fresh batch on June 30th. This second batch was replaced on July 28th and the third batch on August 6th. The charcoal detectors were

replaced as frequently as possible so that some idea of flow velocities between First Polje and Bubbling Spring could be gained in the event that a connection was proved. Upon removal, the charcoal detectors were stored in airtight plastic bags.

Any dye that may have been adsorbed by the activated charcoal was extracted in the laboratory using an elutant of 1-proponol alcohol plus 20% aqueous solution of ammonium hydroxide in a 51:43 proportion. Fluorescence of the elutant plus any dye present was measured with a Turner Model III fluorometer using either a Corning 1-60 or a Wratten 58 primary filter and a Wratten 23A secondary filter. This fluorometer has four ranges giving the scale a length of 3,000 divisions in units of fluorescence. One division corresponds to a rhodamine concentration of about one part in  $10^{10}$ , which is 1/1000 of visibility. The instrument was set to zero at the fluorescence of an elutant mix from charcoal that had been in the spring water before any dye was inserted into sinking waters. Such a procedure eliminates the possibility of mistaking the natural fluorescence of elutant and spring water for rhodamine dye.

Only a few of the charcoal detectors in the first batch contained dye and then in trace amounts. Batch 2 detectors, however, inserted on June 30th had clearly picked up considerably quantities of dye while batch 3 detectors inserted in July 28th and removed on August 6th contained no dye whatsoever. The first tracing experiment carried out between First Polje and Bubbling Spring proves conclusively that at least some of the water sinking in Brachiopod Basin, First Polje, travels underground to Bubbling Spring (A in Figure 4.12).

It is apparent from analysis of batch 1 charcoal that some of the dye travelled the straight-line distance between sink and spring, a distance of 2.1 miles, in under 6 days. Most of the dye was, however, picked up not in batch 1 collectors but in batch 2 collectors. The bulk of the dye, therefore, took more than 6 days but less than 28 days to reach the spring from First Polje. This suggests that water sinking in Brachiopod Basin, First Polje, travels via different routes to Bubbling Spring with some routes transporting water more rapidly than others. The evidence indicates the existence of different-sized, partially integrated cavities in the limestone. As some dye reached the spring in under 6 days, a maximum flow velocity of 77 ft./hour or 1.28 ft./minute is indicated if the distance travelled is assumed to be equivalent to the shortest distance between sink and spring. As the actual distance travelled by the water was likely much more than the 2.1 miles straight-line path, velocities may be somewhat greater than those calculated. It should be noted that at the time the experiment was carried out, Third Polje, Second Polje and Raven Lake were all flooded so that underground conduits must have been overloaded. In view of this, the calculated flow velocities are probably slightly higher than average groundwater flow rates.

The second tracing experiment was timed so as not to interfere with that conducted on First Polje. Approximately 7 gallons of 20% rhodamine WT solution was added to the sinking point of Death Lake in the central portion of the karst. The dye was inserted at 3:00 P.M.

on July 20th to test the possibility of at least some flow to Bubbling Spring in the north. At the time of insertion, charcoal detectors were already in the waters of Bubbling Spring, for the First Polje trace. Detectors were changed at 8:00 P.M. on July 28th and again on August 6th, the last set of charcoal detectors inserted were not removed until late June of the following year 1974. It was hoped that because Death Lake is some 7.4 miles almost directly south of Bubbling Springs, all of the dye inserted at First Polje would have emerged at the spring long before the slug of dye inserted at Death Lake reached it. This is in fact what appears to have happened.

It has already been pointed out that batch 2 charcoal detectors inserted on June 30th, 1973 contained dye which has been ascribed to the First Polje experiment. Charcoal inserted on July 28th and removed on August 6th was found to contain no dye whatsoever, suggesting that the dye from First Polje had all reached Bubbling Springs by this date. The absence of dye in these detectors also indicates that dye from Death Lake had not reached the spring by this time, some 17 days after its insertion. Activated charcoal detectors placed in the spring on August 6th 1973 and finally removed in late June 1974, were found to contain substantial quantities of dye suggesting an underground connection between Death Lake in the south and Bubbling Spring in the north (B in Figure 4.12). Because no dye was picked up by batch 3 detectors, the maximum flow velocity of underground waters between Death Lake and Bubbling Spring, calculated on the basis of

the most direct route, must be less than 95.8 ft./hour or 3.99 ft./minute. This figure does not contradict the estimated maximum flow velocities calculated from the results of the First Polje - Bubbling Spring trace. There seems every reason to believe that maximum groundwater flow velocities in the Death Lake - Bubbling Spring region are between 77 and 110 ft./hour assuming that the actual distance travelled by waters lies somewhere between 1.0 and 1.5 times the shortest distance between sinks and spring.

Results of dye tracing experiments support the contention that at least some of the water sinking in the northern section of the karst belt drains northwards to Bubbling Spring. It is important to realize, however, that ideally when water tracing experiments were being carried out, charcoal detectors should also have been inserted into the waters of White Spray to test the possibility that some of the water sinking at Death Lake and First Polje Passes also to this spring. Unfortunately in the summer of 1973 it was not economic to do this.

(d) Spring Catchment Areas and Possible Concentrated Groundwater Flow in the Nahanni Karst.

The catchment areas of Bubbling Spring and White Spray, as shown in Figure 4.12, were delimited on the basis of known drainage connections as well as a great deal of what might be regarded as 'circumstantial evidence.' Canal Canyon for instance, which cuts deeply into the upwarped dome of the Nahanni Plateau, appears to be a major catchment divide primarily because to north and south the

structural dip is always away from the canyon (Figure 4.13). Water percolating into limestone north of Canal Canyon appears to make its way to Bubbling Spring by draining more or less in the direction of the structural dip. If this water was draining south small springs might be expected at the base of Canal Canyon's north wall. Examination of this area in 1972, however, did not reveal even one resurgence.

Surface runoff into Canal Canyon, on the other hand, is thought to sink at one or more locations at the base of the south wall close to the glacial moraine barrier that blocks its exit and make its way along the structural dip to White Spray some miles to the south. At its point of closure Canal Canyon is more than 1,500 ft. deep and is cut more than 1,000 ft. in dolomites which underly the limestones of the 'Nahanni Formation.' It is evident that if drainage out of Canal Canyon is via underground routes (and a lengthy helicopter reconnaissance in 1973 revealed no evidence of water movement through the extremely massive glacial barrier) these routes are in dolomite not in limestone. One strong reason for believing that surface runoff into Canal Canyon, which sinks into dolomites at an altitude of 2,700 ft. a.s.l., drains to White Spray, is that there is a more than adequate hydraulic gradient in this direction, for White Spray waters emerge at an elevation of 900 ft. a.s.l. (Figure 4.14). Another is that White Spray waters emerge from dolomites so that flow from sinks to spring would be through this rock type. If flow was towards Bubbling Spring the drop in elevation would be only 400 ft., flow would be against the dip and water would need to rise up through the stratigraphic section from dolomites into limestones before emerging at

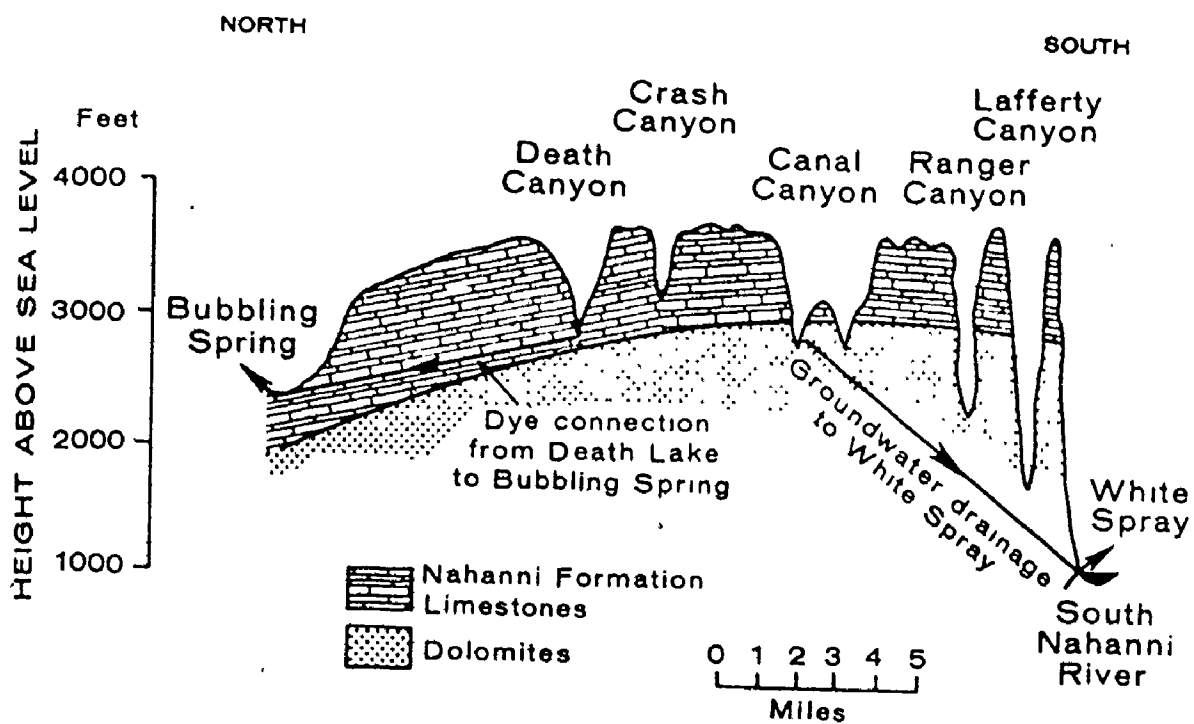


Figure 4.13. Topographic and geologic section through the Nahanni karst from Bubbling Spring to White Spray.



the spring. The likelihood is that water follows the direction of the greater hydraulic gradient and the structural dip and remains in dolomites, that is it flows to White Spray. If water in Canal Canyon drains south it is almost certain that water sinking into the plateau remnants south of it does so also.

As shown in Figure 4.12, the catchment areas of Bubbling Spring and White Spray cover 103 and 100 square miles respectively. If the average annual precipitation in the Nahanni is taken to be 22.3 inches (Table 4.7) and the effective precipitation calculated by using the Turc equation 15.5 inches (Table 4.8), then average discharges for the two springs can be calculated if it is assumed that there is no long-term change in groundwater storage. If each catchment area is taken for simplicity to be 100 square miles, then the volume of water draining to each spring in an average year must be  $3601 \times 10^6$  cubic ft. giving a constant discharge at each of 114 c.f.s. As both springs were discharging close to 200 c.f.s. during the summer of 1973, it is clear that discharge volume varies with season. If a mean discharge of 200 c.f.s. is assumed during 4 months of the year, mean discharge during the other 8 months would be of the order of 72 c.f.s. There is little doubt that spring discharges during the winter, when there is no recharge to the aquifer, are considerably less than in spring and summer when recharge reaches a peak.

Horizontal groundwater movements in the Nahanni are clearly controlled to a marked degree by the structural dip with waters tending to drain from domal to basinal structures. Zones of fracturing in the bedrock often associated with axes of flexure are

also thought to exert an influence upon the patterns of groundwater movement in the area. Although the structural dip is thought to control the direction of groundwater movement in a general way, fracture zones are considered to influence the actual paths taken by groundwaters to reach points of discharge.

Many workers have attested to the fact that groundwater flow in limestones and dolomites is often concentrated along zones of intense fracturing. Kiersch & Hughes (1952), for instance, noted such localization in the limestones of the 'Big Bend District,' Texas-Mexico. In this area groundwater flow in many areas is along conduit systems confined to fracture zones which often parallel the strike of flexures in the limestone. Lattman & Parizek (1964) obtained caliper logs from wells drilled in fracture zones in dolomite and sandy dolomite and from those drilled in areas between such zones. The logs showed that numerous cavernous openings were encountered down to a depth of 350 ft. in wells drilled in fracture zones while only a few were encountered by wells in inter-fracture areas. Lattman & Parizek argue that zones of fracture concentration appear to markedly affect both the occurrence and movement of groundwater in carbonate and other rock types. Moore et al. (1969) arrived at similar conclusions from their work in the Upper Stones River basin, Tennessee, where they found that in a few areas where high-yielding wells were close together a line connecting the wells was oriented either northeast or northwest, the average directions of the regional joint system. This fact, they feel, indicates that the

trend of subsurface solution cavities and lines of concentrated groundwater flow are joint controlled. Similar controls upon groundwater flow have been documented in the Edwards Plateau region of Texas (Abbott 1975). Here groundwater flow in the Edwards limestone parallels the Balcones Fault Zone and does not move in the direction of the structural dip. Further evidence of structural localization of groundwater flow comes from northwestern Lawrence County, Indiana, where Palmer (1969) has found that the yield of wells in the lower karst aquifers is determined to a large degree by whether or not the wells penetrate joints and fracture zones. Palmer notes that the distribution of successful wells in these formations may show alignments similar in trend to fracture systems and groundwater flow patterns. Such trends, he emphasizes, are not because wells encounter single joints but because they penetrate linear fracture zones.

Present groundwater flow in the Nahanni karst is thought to be highly localized within the 'Nahanni Fracture Belt,' already recognized as a region of concentrated conduit-flow recharge. Diffuse and conduit input to the aquifer likely gravitates towards this heavily fractured zone via numerous conduits of small size. The structural dip and minor faults and joints are thought to control the actual paths of movement. At the fracture belt the numerous small conduits connect with fewer but much larger features developed along open faults and joints and the groundwater is channelled either north or south along the fracture zone to either Bubbling Spring or White S / res

That groundwater does move in this manner in the Nahanni karst, is supported by evidence of a former flow pattern in the limestone as indicated by the characteristics and distribution of relict caves. Large, now inactive caves which must at one time have channelled considerable volumes of groundwater, have been discovered mainly within the boundaries of the 'Nahanni Fracture Belt.' Cave remnants within this region are quite numerous and generally of fairly sizeable dimensions. The largest discovered to date is Grotte Valerie with entrances in the north wall of First Canyon, South Nahanni River. This cave has in excess of one mile of passageways which form a branching pattern. Many of them are more than 20 ft. in diameter. Away from the fracture belt, however, caves are less frequently encountered and those that have been discovered are generally of very small diameter. The distribution of relict caves and their sizes indicate that at some time in the past groundwater movement in the Nahanni was concentrated, as it is thought to be today, within the 'Nahanni Fracture Belt.' Within this narrow zone, water clearly moved in conduits of considerable diameter with these larger conduits collecting water funnelled to them from nearby areas via smaller underground 'pipe' networks.

Palmer (1969) has argued that in northwestern Lawrence County, Indiana, "The dip of the strata and the configuration of joint systems exert the strongest control over the horizontal pattern of groundwater movement" (p. 103). It is apparent that the same statement could be used to describe horizontal groundwater flow patterns in the Nahanni karst.

3. The Flooding and Draining of Depressions in the North Karst Region: An Account and an Explanation.

Sweeting (1972) has noted that according to the type of or absence of inundation, poljes are classified as dry poljes if they are never inundated, periodically inundated or overflow poljes if they are flooded during part of the year or intermittently, and as waterlogged poljes if they are permanently inundated. In early July 1972 all three Nahanni poljes were dry and there was no way of knowing to which of these hydrological classes each belonged. By August 1972 it became all too apparent that First and Second Poljes are periodically inundated while Third Polje is an overflow form. What is known about the flooding and draining of poljes and other closed depressions in the North Karst from aerial photographs and ground and aerial reconnaissance observations, will now be outlined and an attempt will then be made to explain how and why flooding occurs.

(a) Flooding and Draining: The Evidence.

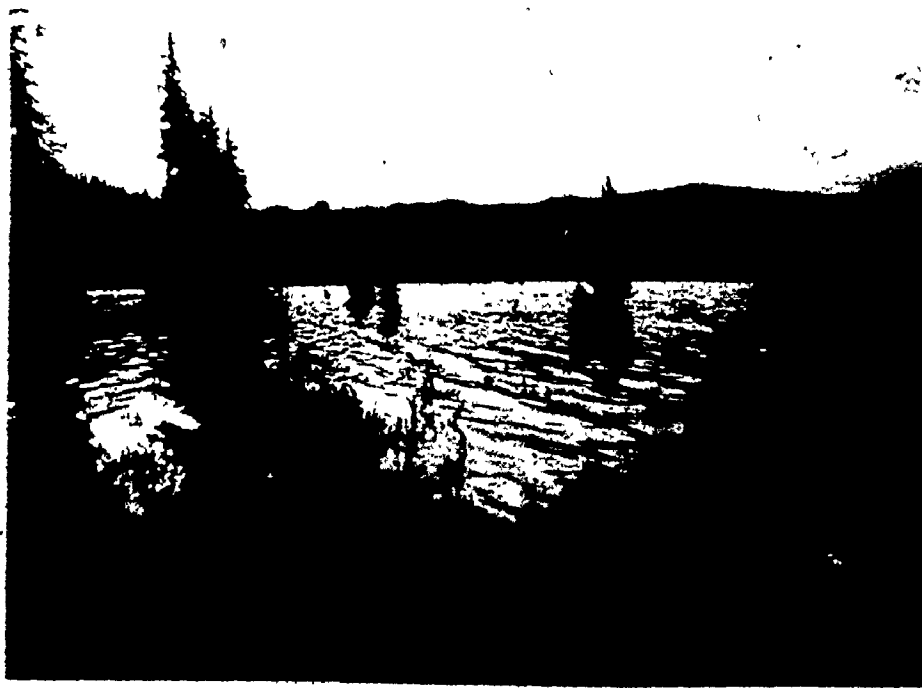
(i) A Chronological Account of Flooding and Draining for the Period 1971-1975 Based Upon Ground and Aerial Reconnaissance Observations.

On July 3rd and 4th 1972 the three Nahanni poljes were dry except for a small pond at the eastern extremity of Third Polje at its lowest point (Plates 4.1(a) and 4.2(a)). The poljes were in essentially the same condition when examined in late August of the previous year during a brief aerial reconnaissance of the area.

There was no surface flow into Second and Third Poljes in early July 1972.



(a)



(b)

Plate 4.1. First Polje dry and in flood. After approximately eight inches of rainfall in ten days, the flat alluviated floor of First Polje was submerged beneath 10-15 feet of water.



(a)



(b)

Plate 4.2.- Third Polje dry and in flood. After heavy rain in early July 1972 the polje was transformed into a lake. The level of the lake rose until eventually water spilled out of the enclosed basin at its northern end.

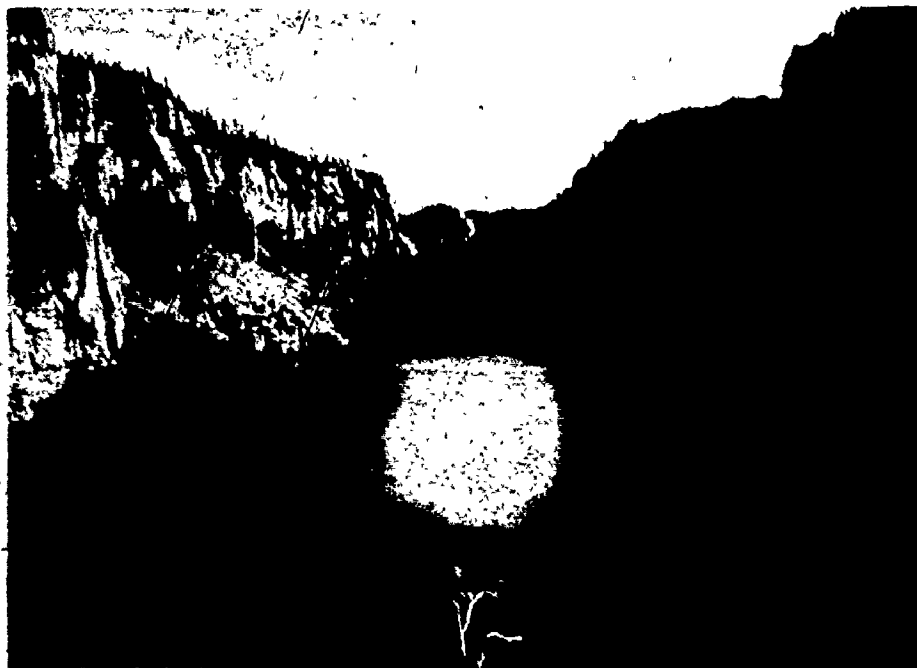
but a number of small springs were discharging water into First Polje, the water sinking as soon as it encountered the polje's flat alluviated floor. Raven Lake was first examined on the ground on July 16th 1972 and at this time it was flanked on all but its eastern shore by huge talus aprons which made it possible to walk around the western edge of the lake (Plate 4.3 (a)).

In the 8 days between July 19th and July 26th 1972, 7.99 inches of rain was deposited on the Nahanni North Karst terrain including 2.72 inches in one day (Table 4.14 and Figure 4.4). When the poljes were next visited after one day without rain, on July 27th, it became apparent that a remarkable transformation had taken place. By July 28th the floors of the three poljes, which had been all but dry earlier in the month, were either partly or wholly submerged beneath a considerable depth of sediment-laden water. Lakes occupied both Camp and Brachiopod Basins in the floor of First Polje, with the lake in the smaller basin overflowing into that occupying the larger basin (Plate 4.1 (b)). Numerous streams were funnelling water into the polje as a result of the rapid surface runoff that followed the heavy rains. Many of these streams were not flowing on July 18th while those that were had increased in volume. Mosquito Creek, for example, was sinking as soon as it encountered the polje floor on July 18th; 10 days later its discharge had increased to the extent that it was flowing all the way across the polje floor into Camp Basin. All surface streams were clearly transporting substantial volumes of sediment similar in character to that presently mantling the bedrock floor of the polje.





(a)



(b)

Plate 4.3. Raven Lake at low and high levels. Raven Canyon which is more than 600 feet deep is the largest karst street in the Nahanni region. After heavy rain in July 1972, the level of the lake occupying its floor rose by an astounding 160 feet.

A lake 20-30 ft. deep occupied Second Polje on July 28th (Plate 4.4). Pulpit Rock, a residual bedrock hill projecting out of the alluviated floor of the depression, was totally submerged. A number of streams were funnelling water into the polje, the largest entering the polje at its western extremity. Several small surface flows were plunging over the vertical walls of the depression to talus aprons 150 ft. or more below. The most remarkable transformation of all, however, had undoubtedly taken place in Third Polje which on July 28th was simply one large lake (Plate 4.2 (b)). The lake level was still some feet below a number of solution notches in the walls of the polje which suggested that the level was likely to rise still further. Several small but fast-flowing, sediment-laden streams were discovered flowing into the southwest side of the depression. These streams were certainly not active on July 5th. The flooding of the three poljes was accomplished in a matter of 9 or 10 days following the onset of heavy rainfall on July 19th.

By August 5th, after a further 1.55 inches of rain on the karst, the lake in Camp Başın, First Polje, was visibly more extensive. Since July 28th the ponors in the polje floor had evidently been unable to cope with the volume of spring and stream input to the basin. Raven Lake, which had not been visited since July 16th - three days before the onset of the heavy rain, was also examined on August 5th. The level of the lake was found to have risen an astounding 160 ft. in only 17 days indicating a rise of close to 10 ft. per day. The level of the lake had risen so much, that it was no longer possible to walk around the western shore of the lake on the talus material as this



Plate 4.4. Second Polje in flood. The maximum depth of water in the depression is 46 feet sufficient to completely submerge Pulpit Rock, a small hum.

had been entirely submerged (Plate 4.3 (b)). The rise in the level of Raven Lake helped explain the presence of logs jammed in a small solution pocket 60-70 ft. above the lake level on July 16th, for these logs were some feet below the lake level on August 5th. Ravirst Uvala, between Raven Canyon and First Polje, had also flooded since July 16th and small ponds had formed at the two lowest ponor discharge points in North Col Canyon south of Raven Canyon.

Final observations on the state of North karst depressions in 1972 were made on August 28th when a working party was transported by helicopter from Death Lake to Bubbling Spring. On this date, it was discovered that Third Polje had filled to the extent that it was overflowing, the overflow of approximately 50 c.f.s. joining the discharge from Bubbling Spring via a 10-15 ft. waterfall (Plate 4.5). A short helicopter reconnaissance also revealed a more extensive lake in Second Polje than had existed on July 28th. The lakes in Raven Canyon and First Polje however, seemed to have changed little since that date.

In 1973 an advance party arrived at Mosquito Lake on June 16th in poor weather conditions. Clouds were so low that the rest of the party with the bulk of the equipment had to wait two days in Fort Simpson for the weather to clear. Between June 16th and 18th an improvised raingauge recorded 1.14 inches of rain before the container beneath the Tunnel overflowed. The ground was extremely wet when First Polje was examined on June 21st. Overall, the polje had drained substantially since August 28th 1972 for only small ponds were present at the low points in Camp and Brachiopod Basins. Evidence of the more

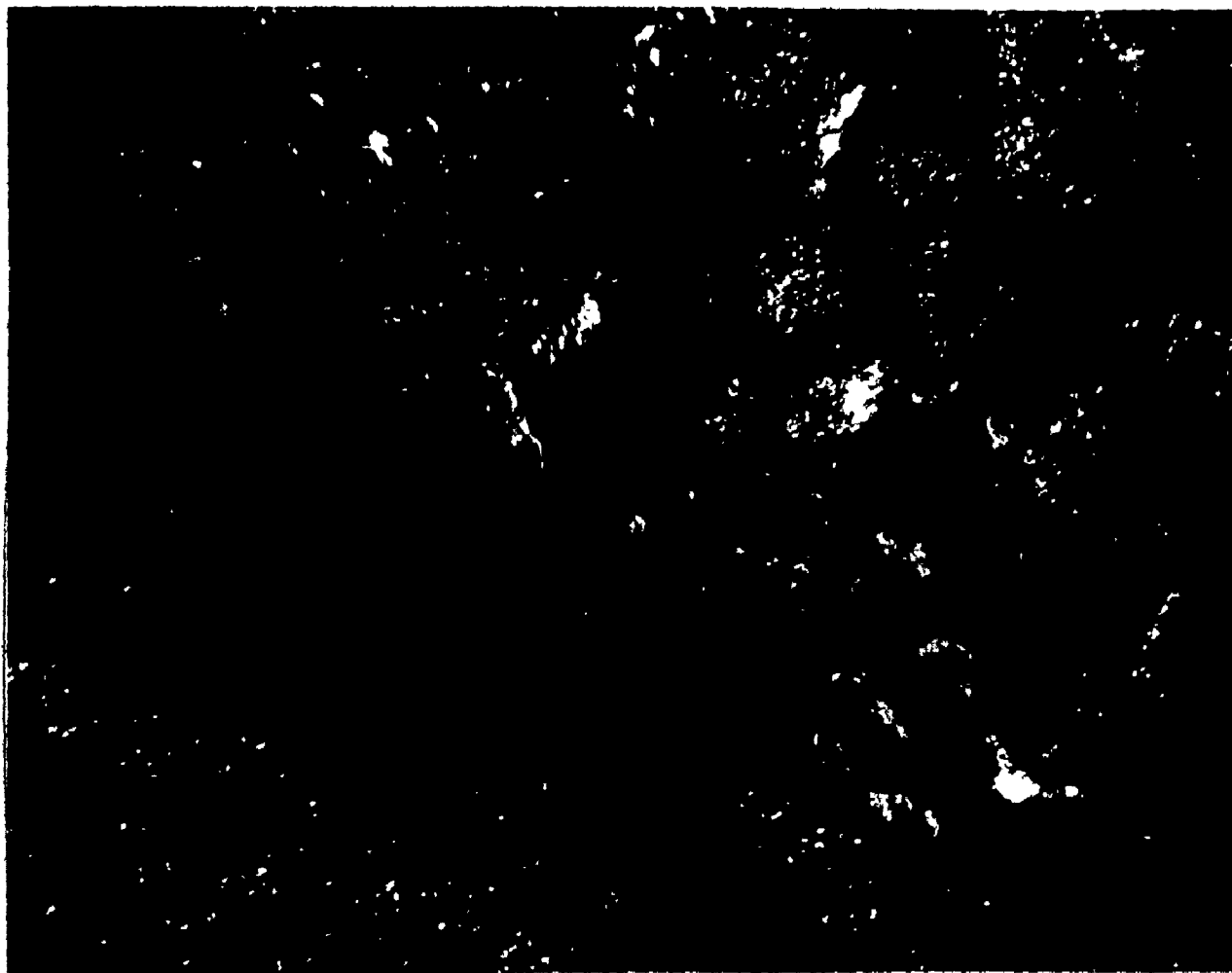


Plate 4.5. Aerial view of Bubbling Spring, North Karst. At right foreground is a small waterfall where overflow water from Third Polje is joining the spring outflow.

widespread flooding of 1972 was, however, everywhere plain to see. Around the periphery of the polje, for instance, 8-10 ft. above the level of the alluvial floor was a horizontal line marking the upper limit of brown dead vegetation. In addition, isolated or groups of conifers growing on the floor of the polje all had dead branches up to what must have been the maximum level of flooding in 1972; above this level branches and pine needles still retained a fresh appearance. The lake in Second Polje was also found to be lower in relation to its level of late August 1972 for the crest of Pulpit Rock was much above water level. The lake in Third Polje, on the other hand, appeared to have changed little from the previous year for it was still overflowing.

On June 23rd it became apparent that the poljes were again flooding for the level of the lake in Second Polje had clearly risen some 2-3 ft. since June 21st. The flooding was probably induced by the heavy rain of 16th-18th June. When next visited on June 28th after a further 1.17 inches of rain on the 26th and 0.1 inches on the 27th, the lakes in First and Second Poljes were visibly more extensive. The level of the lake in Second Polje had risen at least 15 ft. for Pulpit Rock was submerged beneath several feet of water. In addition the overflow from Third Polje seemed to have increased since June 21st. By June 30th the level of the lake in Second Polje had risen a further 3-6 ft. and it was no longer possible to walk around the talus mantling the base of the southern wall of the depression, for in at least one  
this had

below its highest position of 1972. The lake occupying Ravirst Uvala between Raven Canyon and First Polje was also considerably shallower than it had been in late August of the previous year.

Two helicopter reconnaissance trips with geological exploration parties allowed aerial examination of the North karst on July 20th and July 27th while the field party was based at Death Lake. First Polje was seen to be dry on both of these dates despite 0.45 inches of rainfall in the three days from July 24th to July 26th. The lakes in Second and Third Poljes did not appear to have drained a great deal, if at all, since June 30th. Pulpit Rock was still submerged on July 27th and the lake in Third Polje was still overflowing. In the 7 days between July 20th and 27th the level of Raven Lake appeared to have dropped by an estimated 20-30 ft. or some 3-4 ft. per day. Moving base camp from Death Lake to Mosquito Lake on July 28th provided a further opportunity to examine the North karst from the air and in addition, a party was dropped at Bubbling Spring to check the stage recorder installation and to change charcoal dye detectors suspended in the spring waters. At 8:00 P.M. on June 28th the overflow stream from Third Polje was no longer joining the discharge from Bubbling Spring as it had been on the afternoon of July 27th. Instead, a much reduced overflow, losing water at a number of locations along its channel bed, was finally draining underground some 100-200 yds. from the site of Bubbling Springs. The temperature of the sinking water at this time was 12°C, that of the spring water 5°C.

After a short period at Mosquito Lake in late July - early August 1973, a camp was set up in First Polje - a location which

allowed frequent examination of North karst depressions. Short lines were painted on the talus material at the north end of Raven Lake at the water level. Similar lines had been painted on talus in Second Polje much earlier in the season. At 8:00 P.M. on August 5th it was discovered that a paint line made at the level of the lake in Second Polje on June 23rd was 10 ft. under water, indicating a net rise in the lake level of 10 ft. during this period. Raven Lake was observed closely for six days during which time the lake level fell a total of 24.45 ft. at an average rate of 0.19 ft./hr. or 4.67 ft./day. This figure is close to the 3-4 ft./day estimated from aerial observations for the period July 20th to July 27th.

Observations of the North karst from aircraft were all that was possible during the summers of 1974 and 1975. In June 1974 the floor of First Polje was completely dry, the lake in Second Polje was shallow enough that Pulpit Rock was clearly visible and only the eastern half of Third Polje remained flooded. Clearly visible from the air was a stream channel meandering across the exposed floor of Third Polje. Between mid-June and early August 1974 a number of storms are known to have crossed the Nahanni area and although accurate figures are not available, rainfall is known to have been considerable. One storm induced a 9 ft. rise in the stage of the Ram River in Ram Canyon for instance. The heavy rain caused many depressions in the North karst to fill with water. By August 1974 ven



Lake had risen to a level equal to the highest it reached in 1972. Sizeable lakes had been ponded in Camp and Brachiopod Basins, First Polje, and Second Polje appeared to be exceptionally full from the air for Pulpit Rock was completely submerged. Third Polje had filled to overflowing.

By early July 1975 when the North karst was next viewed from the air, the depressions appeared to have drained. First and Second Poljes were completely dry, only the extreme eastern end of Third Polje was under water and Raven Lake appeared to have returned to its early July 1972 level for talus aprons were clearly visible.

A number of conclusions can be drawn from these ground and aerial reconnaissance observations on the North karst during the period 1971-1975. First, there can be no doubt that much of the observed flooding was induced by heavy summer rainfall and second it is clear that hydrological activity in this sub-arctic karst landscape is comparable to anything that is known to occur in the highly developed karst landscapes of warm temperate and humid tropical areas such as Yugoslavia, Jamaica and Puerto Rico. In a hydrologic sense, the Nahanni karst can in no way be regarded as a relict landscape. Additional information on the flooding of North karst depressions has been obtained from aerial photographs, this will now be discussed.

(ii) Data on the Flooding of North Karst Depressions Obtained from Aerial Photographs.

On July 5th 1949 aerial photographs of the Nahanni karst were taken from an altitude of 20,000 ft. but because of an incomplete  
of the the region was again on

These two flights did, in fact, capture an interesting hydrologic event. On July 5th, 1949, Raven Lake was clearly at a low level, Brachiopod Basin, First Polje, contained only a small pond and approximately half of the floor of Third Polje was under water (Figure 4.14(a)). By August 31st, the floor of Third Polje was totally inundated with water overflowing at the northwestern extremity of the depression and sinking a short distance away (Figure 4.14(b)). In addition, a lake had formed in Second Polje, deep enough that it had submerged Pulpit Rock, while Raven Lake was visibly more extensive and presumably somewhat deeper than it had been on July 5th. The floor of First Polje, on the other hand, apart from a small pond in Brachiopod Basin was still dry. The flooding recorded by the 1949 aerial photographs does not appear to have been anywhere near as extensive as that which occurred in July 1972 (Figure 4.14(d)), suggesting that the events which induced such widespread flooding in that year may occur only infrequently.

Aerial photographs of the North karst taken on June 26th 1952 from 20,000 ft. and on August 3rd 1961 from 30,000 ft., show that on each of these dates, depressions were dry except for small ponds in Third Polje and Brachiopod Basin, First Polje. It is apparent that these may well be semi-permanent features (Figure 4.14(c)). Conditions in the karst on these dates were similar to those observed during an aerial reconnaissance of the area in late August 1971. The small size of Raven Lake is particularly noticeable in the photographs.

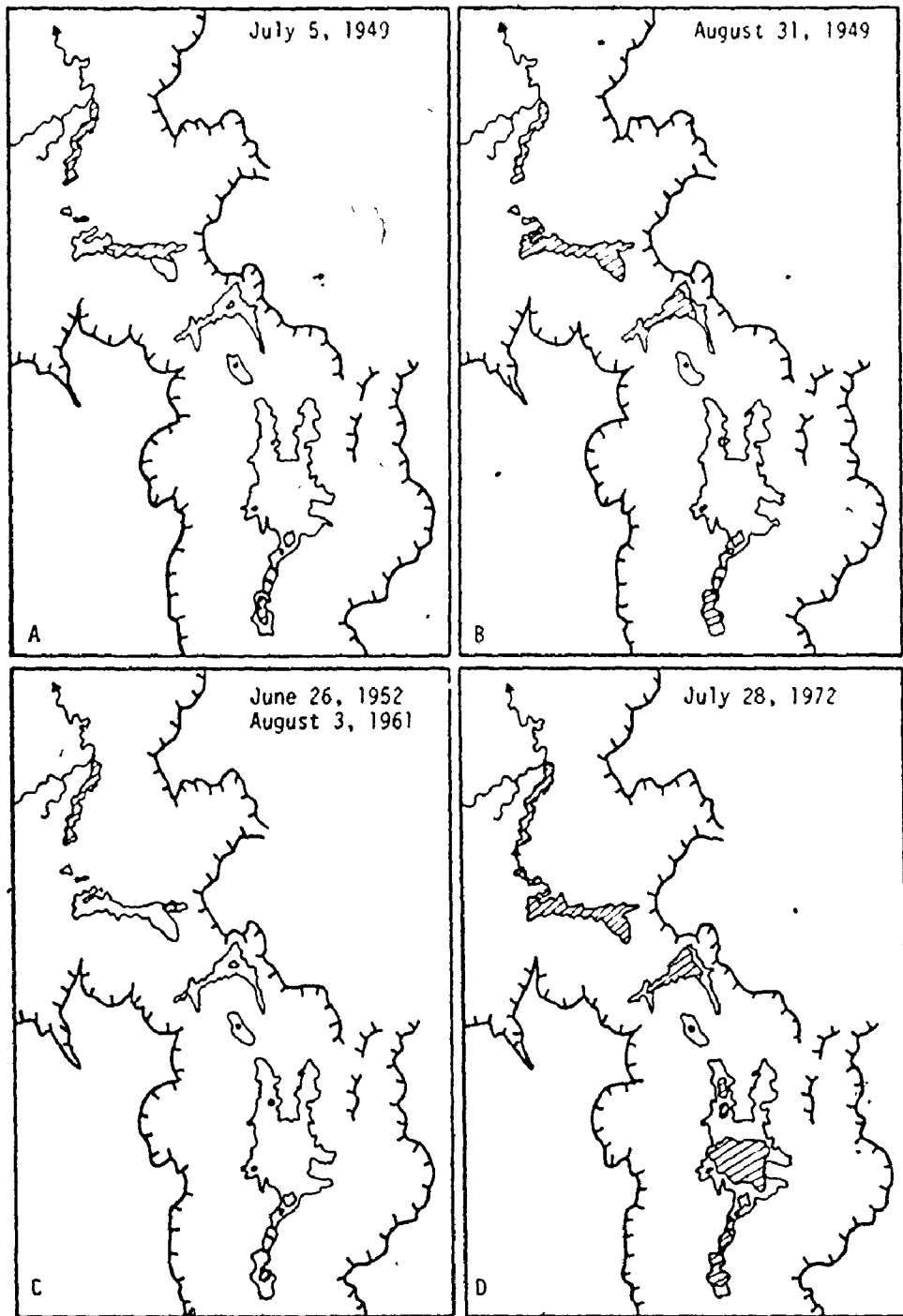


Figure 4.14. Flooding characteristics of Nahanni North karst depressions as determined from aerial photographs and ground observations.

(iii) Order, Frequency and Seasonality.

From observations that have been made in the Nahanni North karst, it is apparent that depressions flood in a set order and drain in the reverse order. During the summer of 1973, for instance, the first depression to drain was First Polje (North Col Canyon was dry at this time), followed shortly afterwards by Ravirst Uvala. Second and Third Poljes were still flooded in early August. In June 1974, First Polje was dry and Second and Third Poljes flooded, indicating that these depressions were either the last to drain, or alternatively the first to flood.

Aerial photographs taken on July 5th 1949 show all depressions to be dry except Third Polje, indicating that this is the first depression to flood or the last to drain. By August 31st 1949, both Second and Third Poljes were completely inundated confirming that these two depressions do indeed flood before others (Figure 4.14(a) and (b)). The available evidence indicates that North karst depressions are inundated in the order Third Polje, Second Polje, Ravirst Uvala and First Polje and that they drain in the reverse order.

It is also apparent that some depressions in the North karst flood more frequently than others, although observations have not been made for a sufficiently long period for precise figures to be quoted. First Polje was dry on July 5th and August 31st 1949, for instance, suggesting that it remained dry throughout this year. It was also dry on June 26th 1952, August 3rd 1961, July 28th 1971 and in late July 1975. The polje was inundated, on the other hand, in

July and August 1972, was flooded in June 1973 but drained by mid-July and was dry in June 1974 but was flooded again by early August. Out of a somewhat irregularly distributed series of observations, it is evident that First Polje was inundated at some time during the summers of 3 out of 8 years although in all of these years the polje was dry for part of the summer. These data suggest that First Polje floods approximately once every 3 years.

Second and Third Poljes appear to flood more frequently than this. On July 5th 1949, Third Polje was partially flooded and Second Polje was dry but by August 31st both basins were totally inundated. The two depressions were dry on June 26th 1952, August 3rd 1961, July 28th 1971 and in late July 1975 but were inundated from early July 1972 until at least the end of August and were flooded throughout 1973. In 1974, partial drainage occurred but by August 15th both features were again full of water. Second and Third Poljes are known to have been inundated, therefore, during the summer months of 4 out of 8 years of observations. In only one of these 4 years was Third Polje dry at some time during the summer, while Second Polje was dry in 2 of the 4 years. The evidence suggests that Second and Third Poljes flood perhaps once every 2 years, and that Third Polje tends to remain flooded for longer periods than either First or Second Poljes.

That Second and Third Poljes flood more often than First Polje and remain flooded for longer, is also suggested by the vegetation covering the floors of these depressions. The trees and bushes in First Polje are in marked contrast to the short grass cover in the

other two depressions. As grass can survive frequent and lengthy submergence and trees can not, this implies that Second and Third Poljes are flooded so often and for such long periods that trees can not survive in them.

Depressions in the Nahanni North karst are known to have flooded between July 5th and August 31st 1949, in July 1972, during the summer of 1973 and at some time between mid-June and early August 1974. In all of these years, the observed flooding was induced by heavy summer rains, suggesting that flooding may be distinctly seasonal in nature - occurring most frequently in the summer months.

It has been pointed out that depressions in the Nahanni North karst flood and drain in a particular order, that flooding appears to be distinctly seasonal and that some depressions flood more often and for longer periods than others. Any explanation of flooding and draining should, therefore, be able to account for such characteristics. Possible explanations will now be reviewed.

(b) Flooding and Draining: An Explanation.

It is not unusual for closed depressions in karst areas, particularly poljes, to flood either annually or at irregular intervals. As Sweeting (1972) notes, many poljes in the Classical and Dinaric karst areas of Yugoslavia, flood during the autumn and winter and are dry in summer. Others may remain flooded for a number of years. Cerknica Polje in Slovenia, for example, often remains flooded for 2-3 years and in 1714 it remained flooded for 7 years. In many cases flooding is extremely rapid. Popova Polje in Yugoslavia, which is more

than 40 km. long and 1.5 km. wide, is liable to flooding at the northwest end by the Trebinjica River which rises in large springs. The springs are so large that the polje may be flooded to a depth of more than 40 m. in winter and contain a lake with a volume of more than 900 million cubic meters. Flooding may occur in 1-2 days and drainage may be just as rapid. Sweeting (1972) reports that in June 1951 a lake of several square kilometers in this polje drained through the large alluvial ponors in only a few hours. As both Jennings (1970) and Sweeting (1972) point out, many karst depressions are believed to flood during the period of snowmelt or after heavy rain because the volume of surface flow into them exceeds the drainage capacity of ponors. This possible explanation of the periodic flooding of depressions in the Nahanni North karst terrain will now be examined.

(i) Flooding as a Result of Rapid Surface Runoff and the Ponding of Water in Depressions.

In an attempt to determine the effect of heavy rain on the magnitude of surface runoff into North karst depressions, a stage recorder was installed in the Mosquito Creek valley downstream of Mosquito Lake. A second recorder was installed at Bubbling Spring to monitor variations in groundwater discharge and a tipping-bucket rain gauge was set up to record the duration and intensity of rainfall. As it turned out, it was not possible to measure flow velocities in Mosquito Creek or in the Bubbling Spring outflow stream often enough for the plotting of rating curves. In fact, only two weeks were spent within walking distance of the two stage recorders during the entire

1973 field season. Variations in stage, together with isolated discharge measurements did, however, prove to be of considerable value in assessing relationships between rainfall and surface and groundwater flows. One further problem experienced was that at the time the stage recorder was installed at Bubbling Spring, the stream-flow measured was made up of the discharge from the spring and the overflow from Third Polje; there was no way of separating these two components or of monitoring each separately. Unfortunately the overflow from Third Polje continued until July 28th. It was only in early August that the discharge of Bubbling Spring could finally be calculated.

At least 1.14 inches of rainfall fell on the Mosquito Lake area in the three days of June 16th-18th. Apart from 0.01 inches of rain on June 22nd, no further rainfall was recorded until June 26th when 1.17 inches was deposited (Table 4.14). It is apparent that the precipitation of June 16th-18th produced a rise in the stage of Mosquito Creek, for after June 20th the stage was falling steadily (Figure 4.15 (b)). Heavy rainfall on June 26th, however, produced an almost immediate rise in the levels of both Mosquito Creek and the combined spring and polje overflow stream at Bubbling Spring. Rainfall began at sometime between 2 and 3 A.M. on the morning of the 26th. An increase in rainfall intensity between 4 and 5 A.M. produced a small but sharp rise in the stages of both streams (V in Figure 4.15) but stages levelled off as the intensity of rainfall dropped. A second increase in the intensity of precipitation produced a further sharp rise in stage at both localities, but again stage levelled off as intensities dropped once again



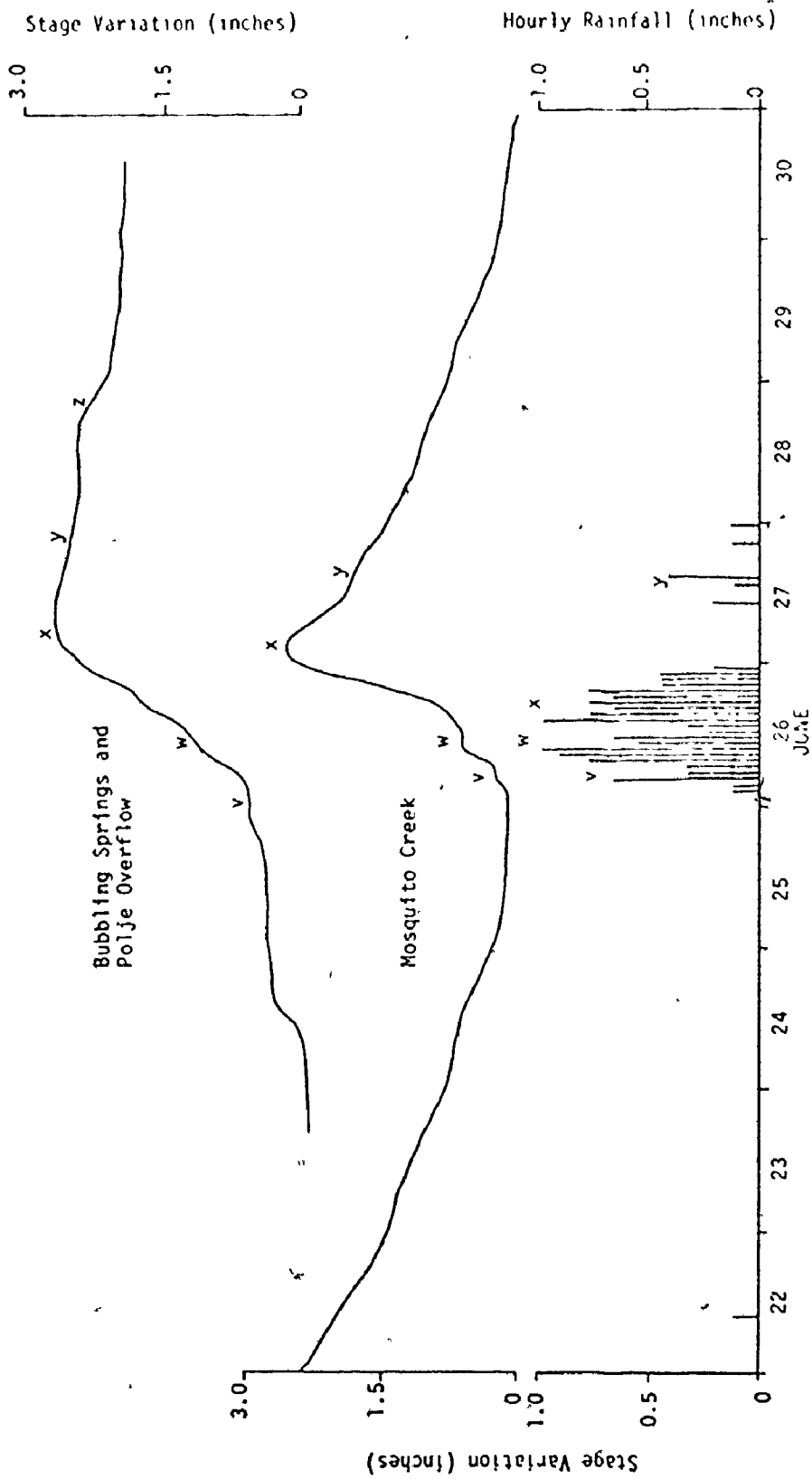


Figure 4.15. Relationships between rainfall and groundwater and surface runoff, Nahanni karst, June 1973.

(W in Figure 4.15). A further period of heavy rainfall during the afternoon and evening of June 26th lasted for several hours and caused stages at Mosquito Creek and Bubbling Spring to rise steadily until they peaked 25 and 28 hours after the onset of rainfall, rising 2.4 and 2.25 inches respectively (X in Figure 4.15).

After peak discharges were reached on the morning of the 27th both stream levels began to fall, although a further 0.11 inches of rainfall during the afternoon of the 27th slowed the drop for a while (Y in Figure 4.15). The level of Mosquito Creek fell steadily from the 28th to the 30th of June at which time its level was lower than it had been on June 25th. The 1.27 inches of rain on June 26th and 27th swelled the discharge of this stream for only 5 days, during which time all of the effective precipitation falling on the Mosquito Creek drainage basin was funnelled into First Polje.

The drop in discharge of the combined spring and surface flow at Bubbling Spring was quite different to the pattern observed at Mosquito Creek. First of all discharges dropped much more slowly at Bubbling Spring and secondly, late in the evening of June 28th there was in fact a very slight increase in flow (Z in Figure 4.15(a)). This increase can only be put down to the fact that the peak discharge from Bubbling Spring, resulting from the heavy rains of June 26th and 27th, did not occur until 36 hours after the peak discharges of the polje overflow and Mosquito Creek had been reached. Peak groundwater discharge clearly occurred some 60 hours after the onset of rain, with the peak level of recharge to the aquifer taking 36 hours to affect

the discharge at Bubbling Spring. As dye tracing has demonstrated that maximum ground water flow velocities in the North karst aquifer at times of flood are between 77 ft./hr. and 110 ft./hr., this implies the movement of a kinematic wave through the groundwater body to affect the spring discharge only a short time after maximum recharge occurred. As conduit recharge to the aquifer takes place at a number of points, this also indicates a fair amount of groundwater integration between input and discharge points. The much lower gradient of the recessional limb of the Bubbling Spring - Third Polje overflow hydrograph (Figure 4.15(a)), is clearly related to an overall increase in the groundwater 'base flow' component.

After June 28th when the peak discharge from Bubbling Spring is thought to have occurred, there was a steady recession in the Bubbling Spring - Third Polje overflow hydrograph despite the fact that between June 28th-30th the level of the lake in Second Polje rose by 3-6 ft. Because the flood pulse was passed at the spring as the polje continued to fill, this implies less than perfect integration between Second Polje and Bubbling Spring, and suggests that at least some of the flood water in the three Nahanni poljes is perched water.

Prior to June 26th 1973, the Mosquito Lake area was extremely wet because of 1.14 inches of rain earlier in the month. In drier conditions, surface runoff does not increase quite so rapidly for the soil moisture deficit must first be satisfied. The period from July 18th to 29th inclusive was a relatively dry one in the karst with only 0.45 inches of rain falling (Table 4.14). The level of Mosquito Creek

was falling steadily by July 30th and continued to do so for the next few days despite 0.07 inches of rain on July 31st, 0.01 inches on August 2nd and 0.09 inches on August 3rd (Figure 4.16). On August 5th the level of the creek did rise but only after 0.20 and 0.20 inches of rainfall on August 4th and 5th respectively. It is evident from the stream hydrograph that the rains prior to noon of August 5th were merely satisfying the soil moisture deficit acquired during the previous dry spell. The indication is that this deficit amounted to more than 0.80 inches. Once it had been satisfied, however, surface runoff increased rapidly during the afternoon of August 5th 1973 but discharges were already beginning to fall by early morning August 6th - only some 15-16 hours after the peak discharge was recorded. Surface runoff peaked 46 hours after the beginning of rainfall on August 3rd with the maximum increase in stage being 1.0 inches. Under the wet conditions already discussed and with slightly heavier rains, the peak flow in Mosquito Creek was reached after only 25 hours and the maximum rise in stage was 2.40 inches.

The two examples discussed leave no doubt that surface runoff into the depressions of the Nahanni North karst, particularly from nearby shale areas, is rapid after heavy rainfall especially when soil moisture requirements have already been satisfied. Runoff may be so rapid, in fact, that increased streamflows may last for only a few days after the onset of rain. A number of observations made during the course of the 1973 field season lend support to such a conclusion. On the way to Bubbling Spring on June 23rd, one stream entering the eastern margin of First Polje was observed to be sinking

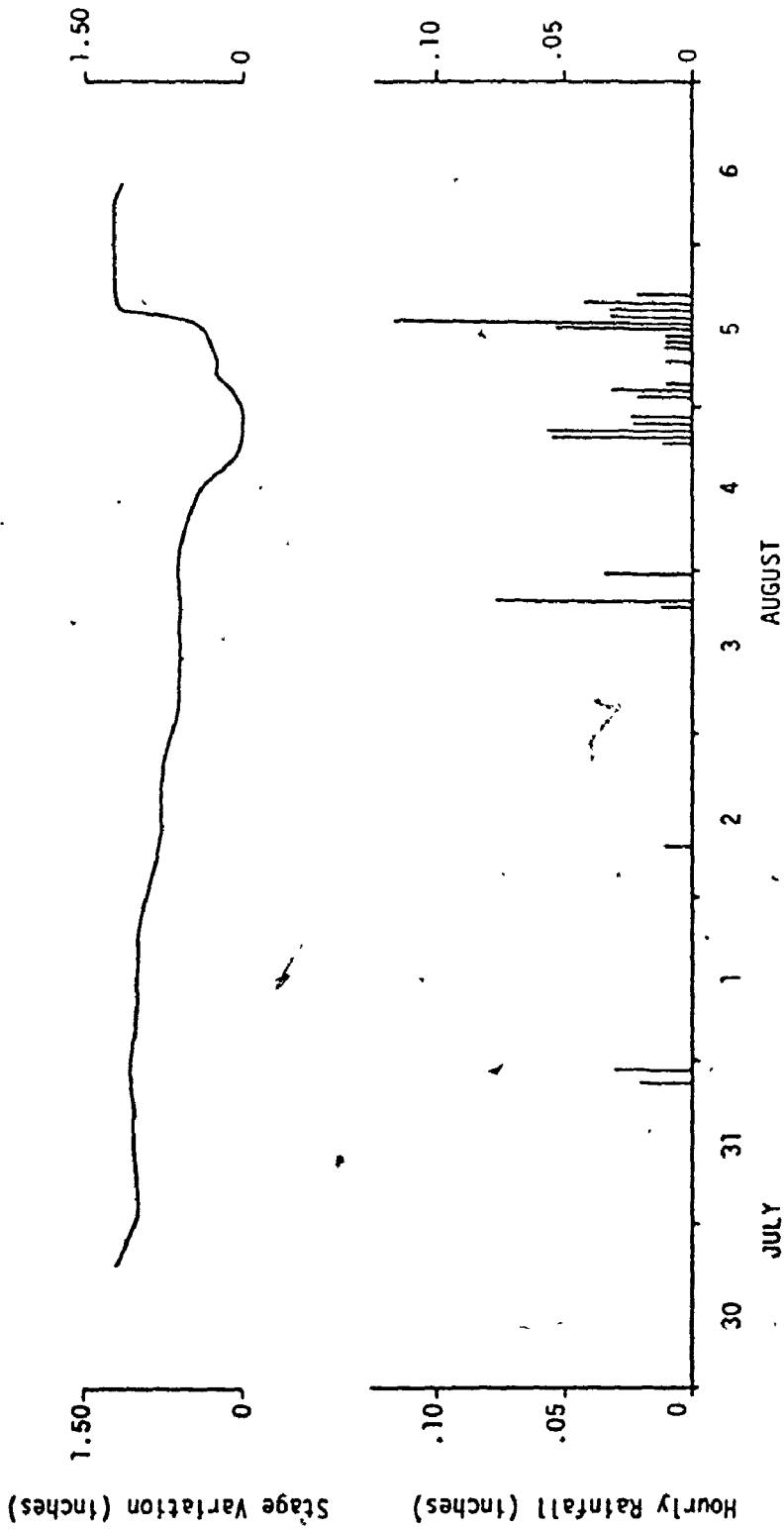


Figure 4.16. Rainfall-stage relationships, Mosquito Creek, July and August 1973.

some distance across the polje floor at 10:00 A.M. By 11:30 P.M. on the same day, the volume of this stream was substantially reduced and it was sinking almost as soon as it encountered the alluviated floor of the polje. At 12:00 noon a large stream flowing into the western end of Second Polje was used to fill water bottles. When the party returned to the same location at 11:00 P.M., however, after installing a stage recorder at Bubbling Spring, there was no longer surface flow into the depression. It is thought that both streams had begun to flow after 1.14 inches of rainfall had been deposited on the area between June 16th-18th. Obviously for one stream at least, the surface runoff generated by this rainfall lasted only 5 days.

It is clear that after extremely heavy rains such as occurred in July of 1972, tremendous volumes of surface runoff water are rapidly funnelled into many of the depressions in the Nahanni North karst. The question is, can the volume of input to these depressions ever exceed the drainage capacities of their ponor systems. Certainly, as Sweeting (1972) has pointed out, alluvial ponors such as those that characterize the three Nahanni poljes, are much less capable of absorbing water rapidly than are ponors in bare rock. Furthermore, perching of water is not uncommon in the Nahanni karst. Evidence from aerial photographs and from aerial and ground observations, made during the summers of 1971-1975 inclusive, indicate that ponds are commonly present in the southeast portion of Third Polje and in Brachiopod Basin; First Polje, throughout the summer months. These are believed to be perched on

impermeable alluvium because other depressions such as Second Polje, with floors at lower elevations, may at the same time be dry.

Ponding due to the blockage of underground drainage routes by subsurface ice is also common in many solution dolines in the Nahanni karst (Plates 3.14 and 4.6). In late June 1973, for instance, Surprise and Hidden Dolines on Cenote Col contained ponds 50-60 ft. deep (Figure 3.7). In early August, however, after a forest fire had gutted the northern section of the labyrinth karst belt, these dolines emptied-presumably because the ice blockage had melted. Perched Basin, also on Cenote Col, drained in mid-July 1972 after 8 inches of rain, indicating that a variety of factors control the drainage of perched water from dolines in this area.

It is obvious that rapid surface runoff into the Nahanni poljes and the perching of water on the alluvium in their floors is likely one reason why these depressions flood. At least one piece of evidence, however, suggests that the situation is not as simple as it may first appear. There are no surface streams flowing into Raven Canyon, yet in 1972 the level of Raven Lake rose by 160 ft. in only a few days. The possibility must be considered that depressions in the North karst flood because the upper level of phreatic groundwater in the limestone aquifer - the 'karst water table,' rises as the ratio of recharge to discharge increases.

(11) Flooding and Draining of North Karst Depressions Due to Fluctuations in a 'Karst Water Table.'

During 12 consecutive days of July 1972, 8.81 inches of rain was deposited on the Nahanni karst. If the of ibbling Spring



Plate 4.6. Eyehole Doline, Nahanni Plateau north of Death Lake.  
In 1973 this vertical-walled depression contained a pond more than  
40 feet deep.



during this period is assumed to have been 200 c.f.s. (the value of outflow measured in early August 1973 under flooded conditions) then, the total discharge during the 12 days was  $20,736 \times 10^4$  cubic feet. If 75% of the rainfall drained underground, the rest being lost to evapotranspiration, the catchment area necessary to supply the amount of water that flowed out of Bubbling Spring would be close to 13.5 square miles or an area 2 by 6.75 miles. The catchment of Bubbling Spring, however, is thought to be close to 103 square miles (Figure 4.12), so that during this particular 12 days of July more water was added to the aquifer than was discharged from it. Cavities in the limestones and dolomites may have filled with water and, using the term in a loose sense, there may have been a rise in the groundwater table.

If a groundwater table of sorts does exist in the limestone and dolomite aquifer of the North karst terrain, fluctuations in its level may bring about the flooding or draining of North karst depressions. If a water table is present, there should be a gradual increase in its elevation (as represented by lake levels in karst depressions during flood) away from the groundwater outlet for this acts as a base level. That is, lake levels should increase away from Bubbling Spring. During the summer of 1973 an attempt was made to test whether this is in fact the case.

In early August 1973 many depressions in the North karst were flooded and the high water marks of 1972 were still visible. Ideal conditions existed, therefore, for a survey of high and medium 'water table' levels in the

a series of altimeter surveys from a base camp at the southern end of First Polje. In each depression three elevations were determined, namely the present lake level if any, the high lake level of 1972 and the lowest point of the depression floor. In many cases this final elevation could only be calculated following depth sounding from a portable two-man rubber dinghy carried for this purpose. Elevations of many other points within the karst were also determined (Table 4.18). Two altimeters were used in the survey; one was left in base camp to record changes in atmospheric pressure and was read at 15-minute intervals, the other was carried by the survey party. Elevations recorded by the 'roving altimeter' were corrected on the basis of changes in atmospheric pressure during the survey as recorded by the 'base altimeter.' All elevations were ultimately adjusted to correspond with an estimated altitude for Bubbling Spring (as determined from a 1:50,000 topographic map) of 2,365 ft. a.s.l. The elevations obtained can only be considered approximate because the altimeter method of survey is not exactly renowned for its fineness of accuracy.

It is apparent from Figure 4.17, that during periods of flood lake levels in the North karst do in fact increase in elevation away from Bubbling Spring. This implies the existence of a water table in at least this part of the Nahanni karst. A water table with a gradient of 36 ft./mile would adequately explain conditions in late July 1972 (Figure 4.17(a)) and one with a slope of 14 ft./mile conditions in early August 1973 (Figure 4.17(b)).

If the flooding and draining of depressions in the labyrinth karst and polje belt are related to fluctuations in the level of a

Table 4.18. Altitudes of Important Levels in the North Karst as Determined by Altimeter Survey in 1973.

Locality	1973		1972		Elevation of the Lowest Point in Depression Floor
	Lake Level (ft. a.s.l.)	Lake Depth (ft.)	Highest Water Level (ft.)	Max. Lake Depth (ft.)	
Camp Basin First Polje			2,477	28	2,449
Brachiopod Basin First Polje	2,439			8/2	
Second Polje	2,403	43	2,441	8/2	2,360
Third Polje	2,405	26	2,405	8/2	2,379
Raven Lake	2,337 2,325	60 48	2,496	8/3 8/5	2,277
Ravirst Uvala (north ponor)			2,461	43	2,418
Ravirst Uvala (south ponor)			2,461	46	2,415

1 Altitudes relate to an assumed elevation a.s.l. at Bubbling Spring of 2,365 ft.

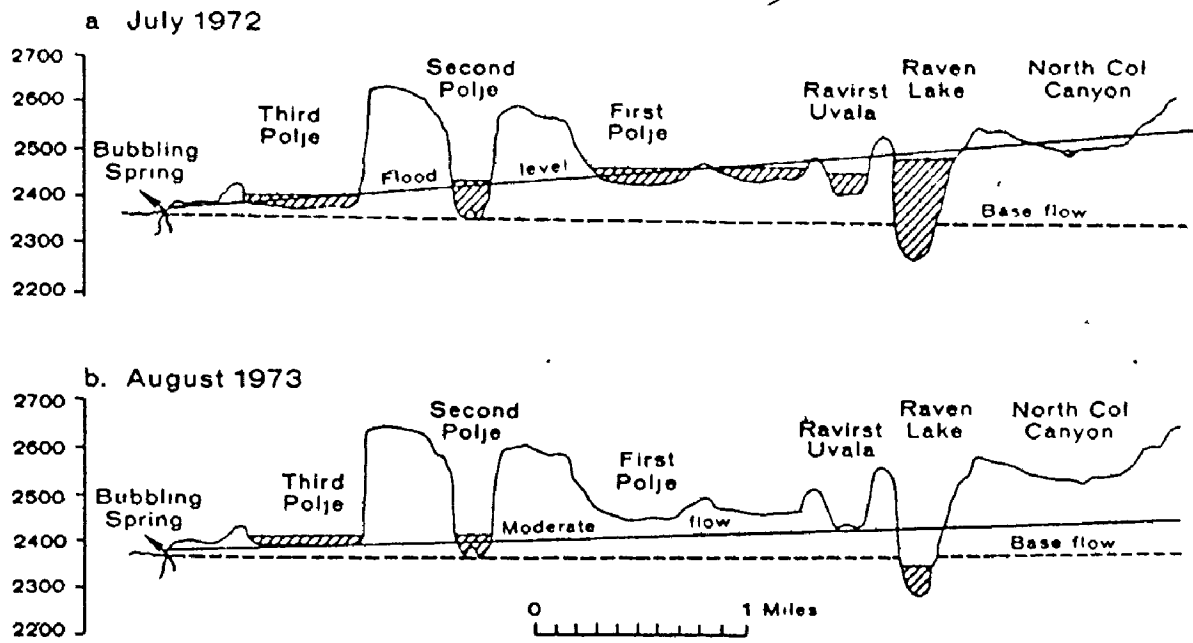


Figure 4.17. Water levels in Nahanni North karst depressions, July 1972 and August 1973.

water table, then flooding should occur in the order Second Polje, Third Polje, Ravirst Uvala, First Polje and North Col Canyon, and should be accompanied by a steady rise in the level of Raven Lake. After severe flooding depressions should drain in the reverse order and be accompanied by a steady drop in the level of Raven Lake. The order of flooding predicted by a simple 'water table model' is, therefore, very similar to the actual order of flooding with the exception of Third Polje which floods before Second Polje and not the reverse. In addition, the water table model would predict that because First Polje is the first to drain and the last to flood, it should be inundated less frequently and for shorter periods than either of the other two poljes. As we have already seen this appears to be the case.

Although many aspects of North karst hydrology can be adequately explained in terms of a simple water table model, it cannot explain all. The surface of Raven Lake, for instance, appears on occasions to fall below the level of Bubbling Spring - the supposed base level in the area (Figure 4.17(b)). This suggests that at least some water in Raven Canyon drains to a lower-level outlet - perhaps even to White Spray some 17.5 miles distant at an elevation of 900 ft. a.s.l. as compared to the floor of Raven Canyon at approximately 2,277 ft. a.s.l. (Figure 4.13). The existence of small ponds in some depressions when the floors of nearby depressions at lower elevations are totally dry and the fact that Third Polje floods before Second Polje, are both difficult to explain in terms of a 'water table model.'

A simple 'water table model' can not explain all aspects of Nahanni North karst hydrology and although flooding may occur in some depressions due to the perching of water on alluvium it is difficult to explain flooding in Raven Canyon and Ravirst Uvala in this way. A 'compromise' model will now be outlined that it is believed explains many of the seemingly contradictory characteristics of North karst hydrology.

(iii) A Compromise Hydrologic Model for the North Karst.

Many workers have experienced difficulties in attempting to explain the hydrological characteristics of limestone terrains. The idea that there is a water table in limestones with associated vadose, intermediate and phreatic zones, (e.g. Grund 1903, Davis 1930, Davies 1960, Wolfe 1964 and Bedinger 1966), is not universally accepted. Many karst hydrogeologists feel that water in limestones moves in independent, largely unintegrated conduits or multiple aquifers - systems that operate like rivers but in three-dimensional space (e.g. Katzer 1909, Martel 1910, 1921, Palmer 1969, Drew 1969). Under multiple aquifer conditions water levels are controlled not by an approximate equalisation of hydrostatic pressure through the system, but more by input-discharge relationships in the conduit networks and variations from conduit to conduit in the resistance to flow.

As neither the water table nor the multiple aquifer hypothesis seem to be able to explain all of the characteristics of groundwater flow in limestone regions, many compromise hypotheses have been proposed (e.g. Cvijić 1918, Lehmann 1932, Gèze 1965). Lehmann (1932), for example, has suggested that when a dense limestone is first

exposed to the atmosphere, it is not permeable and so a normal surface drainage develops on it. Seepage water eventually opens up the structural planes of weakness in the rock which develops a considerable secondary permeability. Ultimately a mature karst hydrology develops, with numerous independent conduit systems which are not integrated and there is no water table. As solutional enlargement progresses, passages are widened and intervening obstacles removed. Eventually the limestone mass is riddled with passages and it is at this old stage of degenerate karst hydrology that something approximating to a karst water table is established. On the basis of work conducted in the Austrian Calcareous Alps, an area that can not be regarded as being in an old stage of geomorphic development, Zötl (1957, 1965) has argued that underground drainage routes in karst areas establish interconnections much earlier in their evolution than Lehmann has suggested. Despite such criticism, Lehmann's ideas are interesting.

In the Nahanni North karst the hydrologic evidences are contradictory. Some suggest that there is a reasonably well integrated conduit network in the aquifer and that depressions at the surface flood because of a rise in the level of a karst water table. Other evidence seems to point to a poorly integrated underground system in which there is great variation in the resistance to flow, and to perching as an explanation of flooding. What is the truth?

It is questionable whether water table conditions do, in fact, exist in the North karst region. A water table with a slope of 35 ft./mile (to explain the flooding of 1972) is much in excess of typical gradients. In addition it is difficult to envisage a water table in

Raven Canyon when water levels there can drop below the supposed regional base level. Perching of water, on the other hand, is known to occur. In 1972, for instance, the two water bodies in First Polje were at different elevations and eventually water in Brachiopod Basin, which is nearer to Bubbling Spring, flowed into Camp Basin. This is difficult to explain other than in terms of perching which is also indicated for water in Third Polje and in many smaller depressions within the karst. For these reasons it is considered that there is no highly integrated underground conduit system in the labyrinth karst and polje region of the North karst and that depressions do not flood because of a rise in the level of a karst water table.

Flooding is, instead, believed to be due to the perching of water both above and below ground at times of particularly rapid input to the aquifer. There seem to be two possibilities, first that essentially multiple aquifer conditions exist and secondly that a reasonably well integrated conduit system has been highly alluviated introducing great variability to the resistance offered to groundwater flow. As it is clear that the altitude of Bubbling Spring has been raised by alluviation, the second of these two possibilities seems the most likely.

Flooding at the surface is thought to be induced in two main ways. First it can occur when conduits in the aquifer fill with water, there is no regional water table because filling is irregular due to variable flow resistance in the network. In localized areas such as the Raven Canyon-Ravirst Uvala region, however, where there appears to be greater groundwater integration, local water levels may be



Flooding can also occur when the volume of inflow into a depression exceeds the drainage capacity of ponor systems. This is more common where ponors are in alluvium for there is more resistance to drainage in this case, than when they are in bare rock. In 1972, the level of Death Lake which drains at least in part underground to Bubbling Spring, rose approximately 12 inches for this very reason. Some of the difficulties experienced in interpreting the hydrologic evidence from the North karst region, may be due to the fact that the floors of the three Nahanni poljes increase in elevation away from Bubbling Spring. This means that even if all three flood because of perching, the impression is of a rise in the level of a karst water table.

South of Raven Canyon are numerous huge karst plateaus none of which are liable to severe flooding. Many have alluviated ponors, however, where water may be ponded after heavy rain. It is apparent that beneath these depressions there is a deep vadose zone otherwise they would flood as cavities in the limestone filled with water. If these depressions had large surface streams flowing into them after heavy rain and they were highly alluviated, would they still drain almost immediately? The answer is probably no, because the conduit system would be partially clogged with sediment and alluviated ponors would provide a substantial resistance to rapid drainage. In all likelihood they would flood, just as the poljes to the north flood at the present time. So although there is clearly some integration in the conduit system in the North karst region, flooding of surface depressions is believed to result because of the overall lack of it. A partial water

table' situation exists because of irregular ponding of water both above and below ground.

Such complexities in karst hydrogeology are not restricted to the Nahanni region, for similar conditions have been reported from Dalmatia in Yugoslavia by Roglić (1965) and Petrik (1967). One of a number of karst lakes in the Imotski region, Crveno Jezero (the Red Lake) with a diameter of 400 meters, occupies an immense collapse abyss its rim at more than 520 meters a.s.l. and its base 4.1 meters a.s.l. The lower part of Crveno Jezero is filled with water which periodically changes level. Roglić (1965) has demonstrated that the varying levels of this water bear no relationship to water levels in the floor of Imotski Polje which is only a few meters away. Petrik (1967) has compared the elevations of lake surfaces in the Imotski region at various times during 1955-1957. He notes that individual lake levels varied greatly during this period but in an irregular fashion so that changes were not always in the same direction. The observed levels of Crveno Jezero fluctuated by 20 meters, those of Modro Jezero by more than 100 meters. Petrik contends that all observations were in harmony with the argument that water enters the depressions through their floors. In fact he says that "on the bottom of Modro Jezero are clearly visible holes which perform the double function of feeding and draining the lake." (p. 579).

In the winter period there is no recharge to the Nahanni karst aquifer because all surface water is in the form of snow or ice. Water continues to be discharged from the aquifer, however, because groundwater

temperatures remain above freezing.<sup>1</sup> In winter therefore, groundwater levels must drop and in spring, summer and fall they must rise. The available evidence does, in fact, suggest that flooding occurs more frequently after intense summer and fall rainstorms, than it does during the period of spring snowmelt. There may be two reasons for this. First, flooding due to perching above ground requires a greater volume of input to depressions than they can cope with. If snowmelt is not particularly rapid in this sub-arctic region, these conditions may only be satisfied after extremely intense summer or fall frontal/orographic rainstorms such as affected the area in 1972. There can be no doubt that surface runoff is rapid enough in cases like this. Secondly, flooding due to perching of groundwater below ground takes place only when sufficient water is added to the aquifer to fill up the underground channels. It may well be that in most years the volume of spring snowmelt is not sufficient to cause flooding and may simply add to a body of groundwater depleted by continuous, if reduced springflow during the winter months. After the groundwater body has been swollen by the addition of snowmelt water, however, intense summer rainfall may be sufficient to fill up the remainder of the air-filled conduits in the aquifer and cause flooding at the surface.

Sweeting 1972 has noted that in karst areas where precipitation and groundwater recharge are more or less evenly distributed throughout the year, surface runoff cuts depressions only rarely exceeds the drainage

---

<sup>1</sup>Gus Krause who used to live at the entrance to First Canyon, South Nahanni River near the hot springs reports that White Spray flows all winter.

capacities of ponor systems. However, in regions where there is great seasonality to groundwater recharge this may occur fairly frequently. Recharge to the Nahanni karst aquifer is extremely seasonal with maximum inputs during the spring snowmelt period and immediately after heavy summer and fall rainstorms. It is clear that conduits in the limestone and dolomite aquifer are not efficient enough, perhaps because of alluviation, to cope with the maximum rates of input to them at these times. The marked seasonality of recharge in the North karst is clearly a further reason why depressions there are susceptible to flooding and why flooding is so common in the summer months.

The magnitude of hydrologic activity in the Nahanni karst, although not everywhere the same, emphasizes that this is not a relict landscape. Because it is the locus for allogenic streams from surrounding areas, the labyrinth karst and polje belt shows a degree of activity not evident elsewhere in the region. This enhanced activity could well be one reason why karst landforms are so highly developed within this extremely narrow corridor floored by limestone.

## Chapter 5.

## Characteristics of Solution.

### 1. Introduction.

#### (a) Karst Solution.

Chemical reactions may be described by the Law of Mass Action, so that in the dissociation of a weak acid for instance



at equilibrium, the activity of un-ionised acid [HB], the activity of the hydrogen ion [H<sup>+</sup>] and the activity of the conjugate base ion [B<sup>-</sup>] all in moles per liter are interrelated by the expression

$$\frac{[\text{H}^+][\text{B}^-]}{[\text{HB}]} = K_a \quad 5.2$$

where  $K_a$  is known as the equilibrium constant for the weak acid HB at a temperature stated. However, the equilibrium constant for a salt only slightly soluble, for instance  $A_a B_b$  which dissolves according to



at equilibrium the activities of ions in solution for a given temperature is given by

$$K_{sp} = [A]^a [B]^b \quad 5.4$$

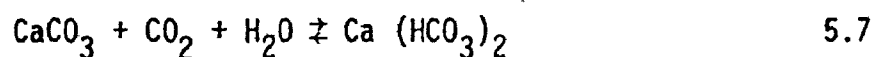
the solubility product. There is no denominator as the solid has no molecular existence in the solution.

The most commonly occurring rocks which are highly susceptible to solution and in which solution is likely to be the dominant geomorphic process are limestone, dolomite, gypsum, anhydrite and halite. The carbonate rocks are by far the most widespread and it is in limestone and dolomites that the Nahanni karst has developed. As Drake (1974) has pointed out, the solution of gypsum or anhydrite and halite in water is a two-phase ionic dissociation:



Although the solution of limestone and dolomite can be represented in a similar simple form, the process is complicated by the instability of the  $\text{CO}_3^{2-}$  ion in the range of pH encountered in most natural waters in karst terrains. Because the  $\text{Cl}^-$  and  $\text{SO}_4^{2-}$  ions are stable in the natural situation, the solution of gypsum or anhydrite and of halite is completely described by equations 5.5 and 5.6. The stable form of the carbonate species in water with a pH of 7 - 9 is in fact the bicarbonate ion,  $\text{HCO}_3^-$  which accounts for more than 80% of the total dissolved carbonate species.

The solution of limestone is generally explained in terms of the following equation



The calcium carbonate is broken down by water enriched in carbon dioxide to give calcium bicarbonate which is soluble in water. The

equation merely indicates the reactants and products of the reaction but says little of just how the reaction takes place.

An important stage in the solution process is the slight dissociation of calcium carbonate in water



This is a reversible reaction and the position of equilibrium can be defined for a given temperature in terms of the solubility product  $K_c$  where

$$[\text{Ca}^{2+}][\text{CO}_3^{2-}] = K_c \quad 5.9$$

The square brackets denote the activities of the ions concerned. Clearly if carbonate ions are removed from solution to decrease  $[\text{CO}_3^{2-}]$ , then more calcium ions are produced by solution of calcium carbonate until the product  $[\text{Ca}^{2+}][\text{CO}_3^{2-}]$  returns to  $K_c$ .

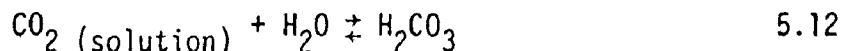
A mechanism by which the activity of carbonate ions can be reduced is by their reaction with hydrogen ions  $\text{H}^+$  to produce bicarbonate ions  $\text{HCO}_3^-$ . In pure water small concentrations of hydrogen ions are produced by dissociation of the water molecule



but the main source of hydrogen ions in natural waters comes from the dissociation of weak acids; the carbonate solution process is obviously pH dependent.



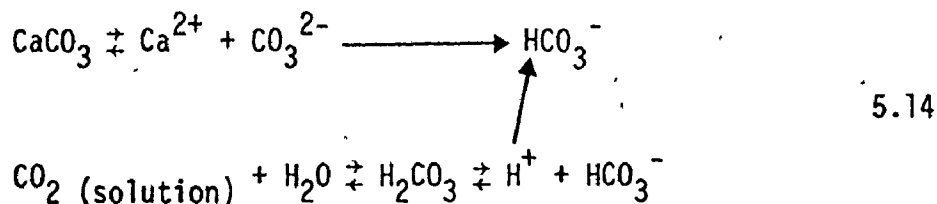
In effect, the most commonly occurring acid present in karst waters is carbonic acid which is produced by carbon dioxide gas dissolving in water.



The amount of carbon dioxide which can dissolve in water depends upon the partial pressure of the gas in the atmosphere above the water and upon the water temperature. According to Henry's Law, as the partial pressure of the gas increases, so does the amount that can dissolve. Furthermore, carbon dioxide is more soluble in colder waters. As with all weak acids, carbonic acid ionises to give hydrogen ions and anions; in this case bicarbonate ions:



Hydrogen ions produced in this way react with the carbonate ions produced in reaction 5.8 as described in 5.11 to increase the solubility of calcium carbonate. The overall scheme of the solution process much simplified is represented by the following reactions:



As can be seen, bicarbonate ions are derived from two distinct sources, namely calcium carbonate and carbon dioxide. In fact, the main parameters which control the solubility of calcium carbonate are the partial



pressure of carbon dioxide and to a lesser degree the water temperature. The importance of these parameters in the Nahanni will be examined shortly.

Not only is the process of solution of limestone and dolomite fairly well understood, but recently many workers have detailed the essential steps in deriving an estimate of the saturation state of solutions so that these too can be accurately calculated from the measured chemical characteristics of natural waters. In this it is necessary to take into account all significant ion pairing in the system and consider activities of relevant species rather than their concentrations alone. The pertinent chemical reactions and their equilibrium constants necessary for calculating saturation states are given in Table 5.1. Use of activities corrects for an increase in the magnitude of all equilibrium constants with increasing ionic concentrations. Such increases are greater for salts whose ions bear a greater charge.

From field measurements of temperature, concentrations of  $\text{Ca}^{2+}$ ,  $\text{Mg}^{2+}$  and  $\text{HCO}_3^-$ , and pH, the first stage in assembling the saturation states of natural waters is to compute the activities of ions in solution. The activity of a given ion is given by:

$$a_i = \delta_i m_i \quad 5.15$$

where  $a_i$  is the activity,  $\delta_i$  is an activity coefficient and  $m_i$  is the molar concentration of the ion (i) in solution. To convert the concentrations of the various ions to activities, the activity coefficient ( $\delta$ ) is calculated using the Debye-Hückel equation:

Table 5.1. Chemical equations and equilibrium constant relationships pertinent to the calculation of saturation indices (after Garrels & Christ 1965)\*

$\text{CaCO}_3 \rightleftharpoons \text{Ca}^{2+} + \text{CO}_3^{2-}$	1
$\text{Ca Mg} (\text{CO}_3)_2 \rightleftharpoons \text{Ca}^{2+} + \text{Mg}^{2+} + 2\text{CO}_3^{2-}$	2
$\text{CO}_2 + \text{H}_2\text{O} \rightleftharpoons \text{H}_2\text{CO}_3$	3
$\text{H}_2\text{CO}_3 \rightleftharpoons \text{H}^+ + \text{HCO}_3^-$	4
$\text{HCO}_3^- \rightleftharpoons \text{H}^+ + \text{CO}_3^{2-}$	5
$\text{H}_2\text{O} \rightleftharpoons \text{H}^+ + \text{OH}^{2-}$	6
$K_C = [\text{Ca}^{2+}] [\text{CO}_3^{2-}]$	1(a)
$K_D = [\text{Ca}^{2+}]^{1/2} [\text{Mg}^{2+}]^{1/2} [\text{CO}_3^{2-}]$	2(a)
$K_{\text{CO}_2} = [\text{H}_2\text{CO}_3] / p\text{CO}_2$	3(a)
$K_1 = [\text{H}^+] [\text{HCO}_3^-] / [\text{H}_2\text{CO}_3]$	4(a)
$K_2 = [\text{H}^+] [\text{CO}_3^{2-}] / [\text{HCO}_3^-]$	5(a)
$K_W = [\text{H}^+] [\text{OH}^-]$	6(a)

\* Chemical equations for reactions are given in 1 - 6 inclusive while the corresponding equilibrium constant relationships are numbered 1(a) - 6(a).

$$-\log \delta_i = \frac{Az_i^2 \sqrt{I}}{1 + \frac{a_i}{B} \sqrt{I}} \quad 5.16$$

A and B are constants characteristic of the water for given temperatures and pressures. The constant  $a_i$  relates to the effective diameter of the specified ion in solution. The charge of the ion enters the equation as  $z_i$  while  $I$  is the ionic strength of the total solution. Values used for these constants are those given by Garrels & Christ (1965). The value of the ionic strength is given by the equation

$$I = \frac{1}{2} \sum m_i z_i^2 \quad 5.17$$

where  $m_i$  is the molar concentration and  $z_i$  is the valence of ionic species (i).

Essentially, if the activities of substances involved in a particular reaction are known, an ion activity product ( $K_{iap}$ ) can be calculated. For instance the ion activity products for calcite and dolomite are given by:

$$K_{iap_C} = [Ca^{2+}] [CO_3^{2-}] \quad 5.18$$

$$K_{iap_D} = [Ca^{2+}]^{1/2} [Mg^{2+}]^{1/2} [CO_3^{2-}] \quad 5.19$$

where the square parentheses denote activities of the enclosed species as calculated from field measurements. In general such calculated ion activity products will not be the same as the equilibrium constants (1(a) and 2(a)) for reactions 1 and 2 in Table 5.1. Only when these reactions are in thermodynamic equilibrium will  $K_{iap_C} = K_C$  and  $K_{iap_D} = K_D$ .

If  $K_{iaP_C} < K_C$  the reactions in equation 1(a) will proceed in sum to the right, if on the other hand  $K_{iaP_C} > K_C$  they will proceed to the left.

Ion activity products for calcite and dolomite can be calculated from pH and the individual ion activities by assuming equilibrium among the dissolved carbonate species  $H_2CO_3$ ,  $HCO_3^-$  and  $CO_3^{2-}$  and correcting for the complexes  $CaHCO_3^+$ ,  $CaSO_4^0$  and  $MgSO_4^0$ . The saturation indices ~~for~~ for calcite and dolomite ( $SI_C$  and  $SI_D$ ) can then be calculated using the following relationships defined by Langmuir (1971)

$$SI_C = \log K_{iaP_C} / K_C \quad 5.20$$

$$SI_D = \log K_{iaP_D} / K_D \quad 5.21$$

Essentially when  $SI_C$  or  $SI_D$  equals zero, the karst water is considered to be saturated with respect to the carbonate in question. Negative saturation indices denote undersaturation and positive indices supersaturation. Langmuir (1971) notes that ion pairs which are sometimes present in local carbonate groundwaters in significant amounts are  $CaSO_4^0$ ,  $MgSO_4^0$  and  $MgHCO_3^+$ . The  $CaHCO_3^+$  ion pair he considers unimportant and feels that it can be ignored. He notes that the maximum effect of ion pairs on  $SI_C$  and  $SI_D$  values for some well waters in Pennsylvania is about some -0.02 units and for spring waters -0.01 units.


Substitution of hydrogen ion concentrations and  $HCO_3^-$  activities in equation 4(a) of Table 5.1 allows the determination of  $[H_2CO_3]$  which can then be substituted in equation 3(a) to allow computation of a theoretical  $PCO_2$  level. This derived partial pressure of carbon dioxide is hypothetical. It essentially refers to the gas phase that would be

in equilibrium with the solution if the solution were in equilibrium with a gas phase. The  $PCO_2$  level so calculated is normally expressed as a logarithm, that is it is referred to as  $\log PCO_2$ . In terms of a  $\log PCO_2$  level, atmospheric carbon dioxide constituting 0.03% by volume converts to a value of approximately -3.52. Lower percentages of carbon dioxide convert to lower  $\log PCO_2$  values for instance 0.01% is -4.0 while higher percentages convert to higher  $\log PCO_2$  values, 1.0% carbon dioxide is -2.0 when expressed as a logarithm of partial pressure. Throughout this and other chapters reference will constantly be made to  $SI_C$  and  $SI_D$  and  $\log PCO_2$  values for natural waters.

(b) Analytical Methods.

During the summers of 1972 and 1973 some 214 water samples were collected from various localities within the Nahanni karst belt. Temperatures and where possible hydrogen ion and bicarbonate ion concentrations were determined at site. Samples for calcium and total hardness were collected in polyethylene bottles and returned to base camp where the analyses were carried out.

The most important uncertainty amongst chemical variables measured from natural waters is the pH. Langmuir (1971) has pointed out that an error of  $\pm 0.05$  pH units leads to an uncertainty of  $\pm 0.05$  units in  $SI_C$  and  $SI_D$ . Because of uncertainties in  $Ca^{2+}$ ,  $Mg^{2+}$  and  $HCO_3^-$  concentrations used in calculation of ion activity products, and in values of  $K_C$  and  $K_D$ , Langmuir believes that the total uncertainty is probably about  $\pm 0.1$  units of  $SI_C$  and may be larger for  $SI_D$ . He suggests therefore that any water with a saturation index of between -0.1 and



+0.1 be considered saturated with respect to the mineral concerned. pH of waters in the Nahanni was determined by means of a portable pH meter. As the pH measurement is very sensitive to temperature differences between sample, buffer and electrode differences resulting in a considerable instrument drift (Shuster & White 1971), care was taken with this measurement. The buffer was immersed in the water being sampled until it acquired the same temperature. At the same time the electrode was chilled in a plastic beaker of the water. These precautions reduced instrument drift and allowed accurate determination of water pH.

Bicarbonate ion concentrations were determined by field titration, in 1972 with 0.003 N HCl and in 1973 with 0.01 N HCl. The end point was determined potentiometrically using the pH meter. Although this method strictly speaking measures total alkalinity, other carbonate species were assumed negligible and the total analysis was assigned to  $\text{HCO}_3^-$ . The titrations were probably precise to  $\pm 2$  ppm.

Calcium and magnesium ion concentrations were determined in base camp using a commercially available Schwarzenbach titration kit containing indicators, buffer solutions and a standard EDTA titrating solution for calcium and total hardness titrations. Titrations are believed accurate to 1 - 2 ppm. Calcium and total hardness is expressed in ppm.  $\text{CaCO}_3$  and magnesium in the same units is determined by subtraction. Titrations were run only once generally within 24 hours of collection but never more than 72 hours after it.

Free carbon dioxide was also measured at site using a commercially available titration kit. The accuracy of the titration itself is 2 ppm.

$\text{CO}_2$  and in reality the accuracy is far less than this perhaps as much as 5 - 10 ppm.

Calcium, total hardness and alkalinity titrations in the field were conducted using a 'microtitration kit.' Only 10 ml. of the sample is required for titrating instead of the more normal 50 ml. This necessitated corresponding reductions in the amounts of buffer and indicator added. EDTA was titrated via a 1 ml. hypodermic syringe. The technique was tested in the laboratory prior to the 1972 season and was found to give results as accurate as could be obtained using a 50 ml. sample, titrating with a buret. Despite the smaller sample size, accuracy is retained because, whereas the buret is calibrated to only 0.1 ml., the syringe is calibrated to 0.01 ml. The great advantages of using a microtitration technique in a remote area like the Nahanni are that bulky, breakable burets need not be transported to and within the area and, secondly, the volumes of chemicals used in water analysis are greatly reduced both in a spatial and a weight sense.

All sample data were processed using a computer program written by Wigley (1972). Using the measured chemical data, the activities of the various ions are calculated, ion activity products are generated. The most important outputs of the program are values for  $\text{SI}_C$ ,  $\text{SI}_D$ ,  $\text{SI}_G$  (gypsum) and  $\log \text{PCO}_2$ . Details of the steps taken in this program have been listed by Drake (1974) and are given in Appendix II.

## 2. Aspects of the Total Data Set.

The 214 water samples collected in the Nahanni karst belt were taken from a wide variety of hydrogeologic settings. Stream, lake, pond, pool, soil, seepage and spring waters were all analysed for their chemical contents. Samples were collected from bare limestone terrains, others from areas of shale bedrock and still others from regions mantled by glacial drift.

Table 5.2 outlines the means of chemical variables both measured and derived for all 214 samples. Mean temperature of all waters is 9.5°C although values ranged from 0.7 to 25.5°C. The mean pH is 7.8 suggesting that most waters are slightly alkaline which in a carbonate terrain is not surprising. The range in pH, however, from 4.1 to 8.8 emphasizes the great diversity in water types in the Nahanni region. Clearly, extremely acid and extremely alkaline waters exist very close to one another both in a two- and a three-dimensional sense.

Although the mean total hardness of Nahanni waters in ppm.  $\text{CaCO}_3$  is 110 ppm., with the mean calcium content 87 ppm. and the mean magnesium content 22 ppm., there is again a very considerable range from a total hardness of 2.5 ppm. to one of 375 ppm. As with pH, this reflects the very different environments present in the area. The molar calcium to magnesium ratio is often useful in determining the extent to which natural waters have been in contact with limestone and dolomite beds. Where this ratio exceeds 1.5 the waters have not been in contact with substantial amounts of dolomite. The mean molar Ca/Mg ratio of 5.9 suggests that most Nahanni waters have had little contact with dolomite. This is not unexpected for the Nahanni limestone formation



Table 5.2. Mean Chemical Characteristics of All Water Samples Taken in the Nahanni Karst in 1972 and 1973.

VARIABLE	MEAN	STANDARD DEVIATION	STANDARD ERROR OF THE MEAN	SAMPLE SIZE	MAXIMUM VALUE	MINIMUM VALUE	RANGE
Temperature (°C)	9.5	5.8	0.39	214	25.5	0.7	24.8
pH	7.81	0.58	0.04	214	8.80	4.10	4.70
Calcium (ppm CaCO <sub>3</sub> )	86.6	53.8	3.7	214	302.0	2.0	300.0
Magnes. (ppm CaCO <sub>3</sub> )	22.4	20.5	1.4	214	104.0	0.5 <sup>e</sup>	103.5
Total Hardness	109.9	71.1	4.9	214	375.9	2.4	372.5
Molar Ca/Mg	5.9	6.0	0.4	214	61.4	0.9	60.6
Alkalinity mM/l	1.98	1.19	0.08	214	6.78	0.01	6.77
log PCO <sub>2</sub>	-2.92	0.44	0.03	214	-1.21	-3.88	2.67
SI <sub>C</sub>	-0.58	1.09	0.07	214	1.02	-8.23	9.25
SI <sub>D</sub>	-1.78	2.10	0.14	214	1.56	-16.41	17.97
Ionic Strength M/l	0.0031	0.0020	0.0001	214	0.0107	0.0001	0.0106
Error Percent	5.2	12.5	0.9	214	86.0	-46.4	134.4

in which the karst has predominantly developed contains only moderate amounts of dolomite. Molar Ca/Mg ratios, however, from 0.87 up to 61.43 suggest that some waters have had considerable contact with dolomite beds. The high value of 61.43 is the result of large errors induced from titration results when natural waters contain only minor amounts of dissolved material.

The graph of calcium hardness in ppm.  $\text{CaCO}_3$  against magnesium hardness in the same units (Figure 5.1) stresses two points. First that the bulk of natural waters in the Nahanni karst have calcium hardnesses less than 110 ppm. and magnesium hardnesses less than 40 ppm., and second that there is a fairly strong relationship between calcium and magnesium concentrations in Nahanni waters. Regression of magnesium against calcium gives a correlation coefficient of 0.71, the standard error of the estimate of magnesium hardness at the mean is 14.5 ppm. The linear regression equation relating these two measured variables is

$$\text{Mg (ppm. CaCO}_3) = 0.272 (\text{Ca (ppm. CaCO}_3)) - 1.13$$

Figure 5.2, a graph of pH against log total hardness, also emphasizes that most waters have a pH in the range 7.5 to 8.5 and a very narrow range in total hardness. The correlation coefficient between these two variables is 0.57 and the standard error of the estimate of pH at the mean 0.48. The regression equation relating the two parameters is

$$\text{pH} = 1.06 (\log \text{ total hardness}) + 5.74$$

The relationship between pH and total hardness is an expectable one for an increase in the dissolved content of the waters should cause an

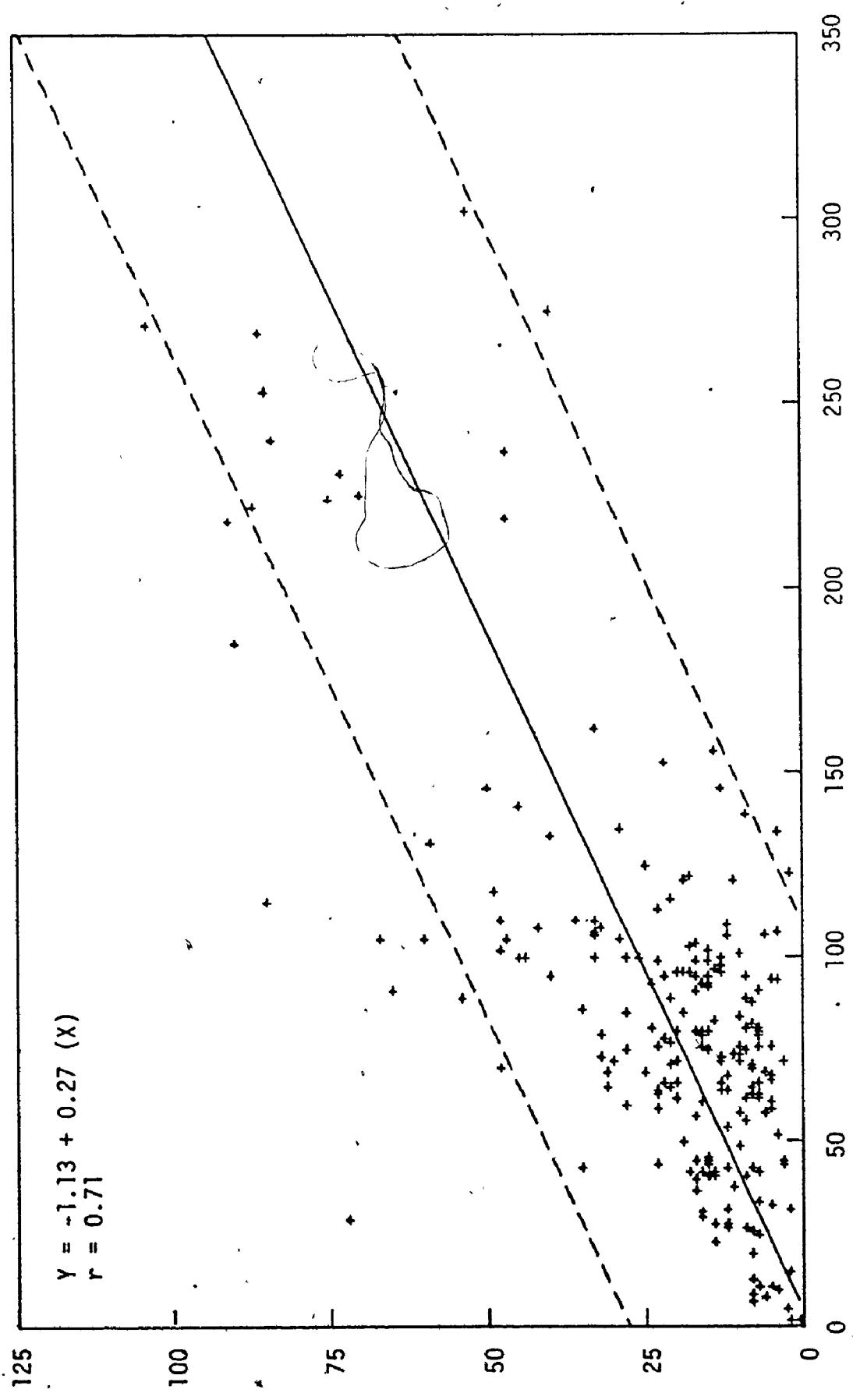


Figure 5.1. The Chemistry of Nahanni Waters: Calcium - Magnesium.

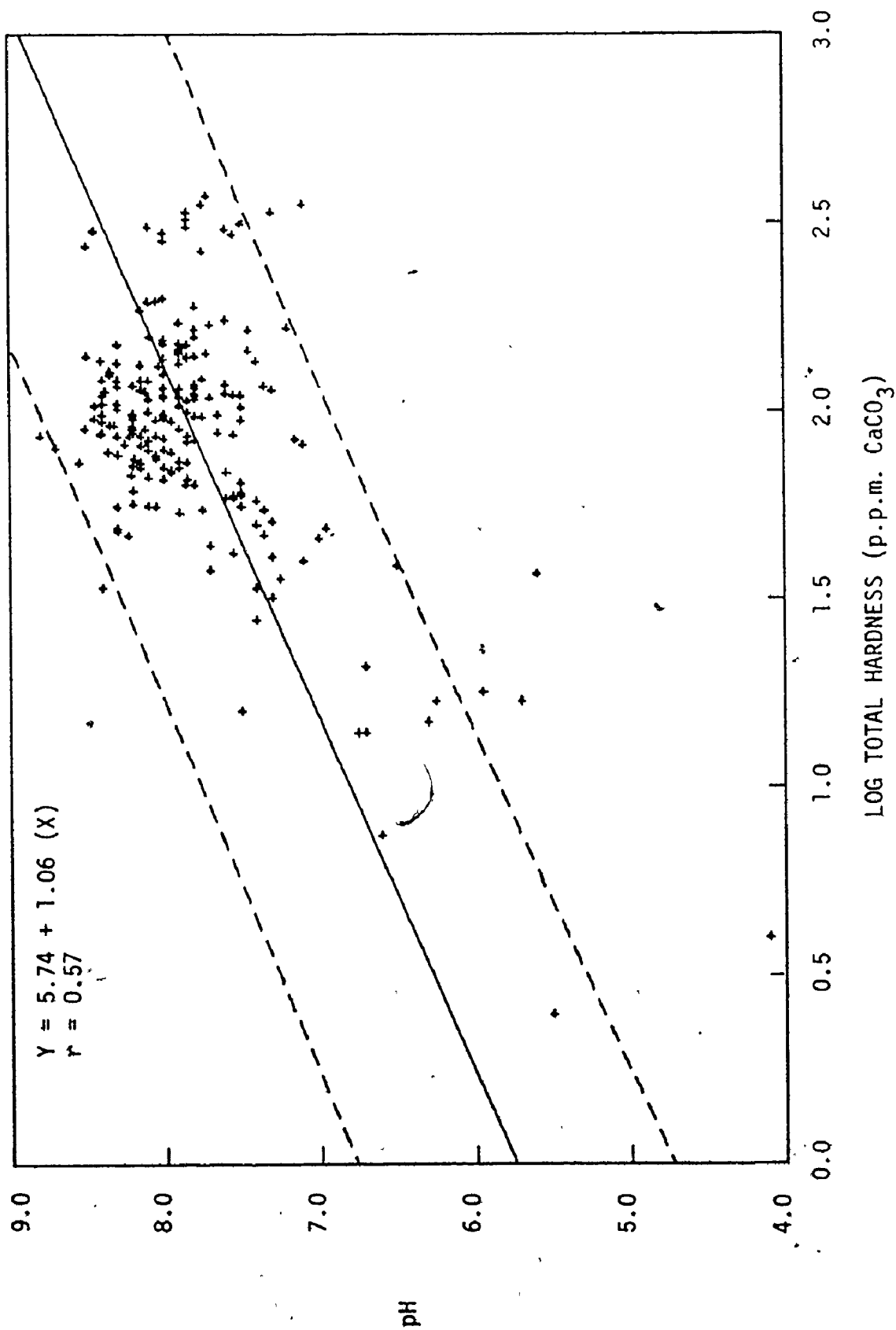


Figure 5.2. The Chemistry of Nahanni Waters: Log Total Hardness - pH.

increase in the pH as the water becomes more alkaline. However, an extremely low pH and a low total hardness is a function more of a lack of limestones and dolomites to dissolve, for acid waters are not characteristic of limestone terrains. There is no doubt that pH and total hardness are in some respects directly related; but in many situations the pH is also a function of available carbon dioxide which, dissolved in water, forms carbonic acid which dissociates increasing the hydrogen ion concentration of natural waters; controls such as this probably account for the relatively low correlation coefficient between these two variables.

The mean alkalinity of all waters is 1.98 mM/liter or in terms of a bicarbonate ion concentration  $\text{HCO}_3^-$ , 121 ppm. If the waters contain only carbonate derived species, there should be a strong correlation between total hardness and alkalinity. Where waters contain considerable amounts of sulphate and chloride, the relationship would be expected to weaken. The correlation coefficient calculated for these two variables is 0.94 and the standard error of the estimate of the alkalinity at the mean is 0.42. The regression equation relating the two parameters is

$$\text{alkalinity (mM/liter)} = 0.02 (\text{total hardness (ppm. CaCO}_3)) + 0.26$$

The small size of the intercept on the y axis and the very good correlation coefficient (Figure 5.3) indicate that most waters in the Nahanni are free of other than carbonate derived anions in solution.

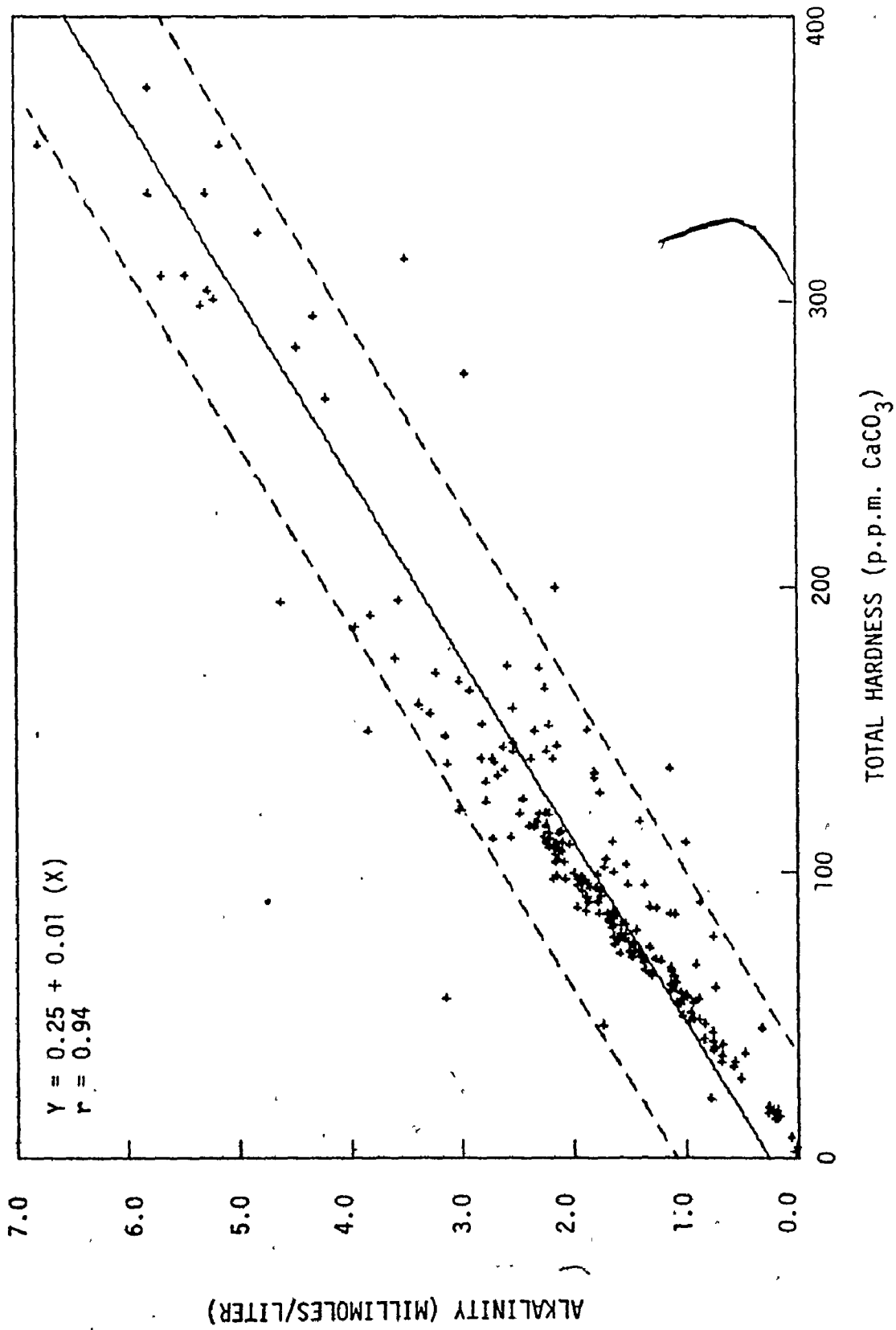


Figure 5.3. The Chemistry of Nahanni Waters: Alkalinity - Total Hardness.

Interesting relationships are also evident in the derived variables  $SI_C$ ,  $SI_D$  and  $\log PCO_2$ . Mean saturation indices for calcite and dolomite are -0.58 and -1.78 respectively indicating that the bulk of waters are undersaturated with respect to both of these minerals. Figure 5.4 demonstrates that there is a strong relationship between  $SI_C$  and  $SI_D$ . Regression of  $SI_C$  on  $SI_D$  shows that these two derived variables are related by the following linear equation

$$SI_C = 0.52 (SI_D) + 0.34$$

The correlation coefficient is 0.99 and the standard error of the estimate of  $SI_C$  at the mean is 0.15. It is also clear from this graph that waters in the Nahanni range from being highly undersaturated with respect to both calcite and dolomite, to being highly supersaturated. The regression relationship indicates that when waters are saturated with respect to calcite (that is  $SI_C > 0.0$ ) they are still undersaturated with respect to dolomite for an average  $SI_D$  is equal to -0.65. When waters are saturated with respect to dolomite they are supersaturated with respect to calcite for an average  $SI_C$  is equal to -0.34. The very strong correlation between  $SI_C$  and  $SI_D$  suggests that the magnesium and calcium sources are linked in the same rock type in approximately equal amounts. Clearly this hydrogeologic evidence suggests that the limestones of the Nahanni Formation have a small but persistent dolomite content.

The final variable of interest is the calculated  $\log PCO_2$ . This value gives some idea of the partial pressure of carbon dioxide with

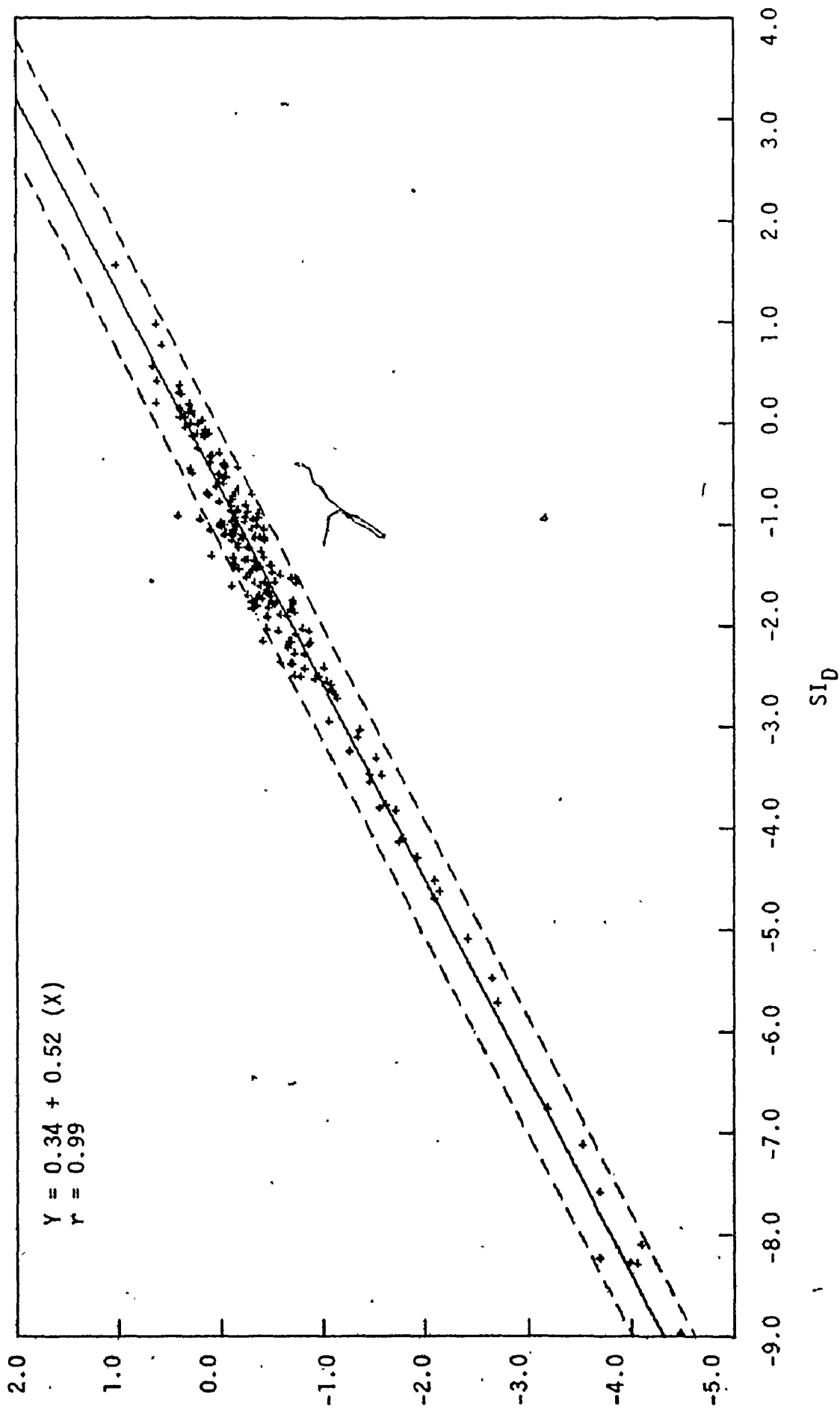


Figure 5.4. The Chemistry of Nahanni Waters: SI<sub>C</sub> - SI<sub>D</sub>.



which waters are in equilibrium. The mean  $\log PCO_2$  of waters in the Nahanni is -2.92. This indicates that most of the ~~karst~~ waters are in equilibrium with a very much higher partial pressure of carbon dioxide than is present in the atmosphere, for the atmospheric  $\log PCO_2$  is approximately -3.52. The range in  $\log PCO_2$  values for Nahanni waters, which is between -3.88 and -1.21, indicates that some waters are in equilibrium with atmospheric conditions while others are immensely enriched in carbon dioxide, presumably through contact with soil atmospheres which are generally thought to be enriched in carbon dioxide produced by biogenic processes. Figure 5.5 shows the calculated regression relationship between  $\log PCO_2$  and  $SI_C$ , this is:

$$SI_C = -0.97 (\log PCO_2) - 3.36$$

The correlation coefficient between the two variables is -0.47 and the standard error of the estimate of  $SI_C$  at the mean is 0.79. There is a tendency therefore for  $SI_C$  to be closer to saturation as  $\log PCO_2$  tends towards atmospheric. On the other hand waters in equilibrium with a considerable partial pressure of carbon dioxide tend to be undersaturated with respect to calcite. This may be a function of hydrogeologic environment rather than due to a tendency for rapid saturation of waters in equilibrium with low levels of carbon dioxide. In general waters with high calculated  $\log PCO_2$  values are those on shales and glacial drift. Because these waters have limited contact with limestone and are in contact with high levels of biogenic carbon dioxide, they will tend to be undersaturated with respect to both calcite and dolomite.

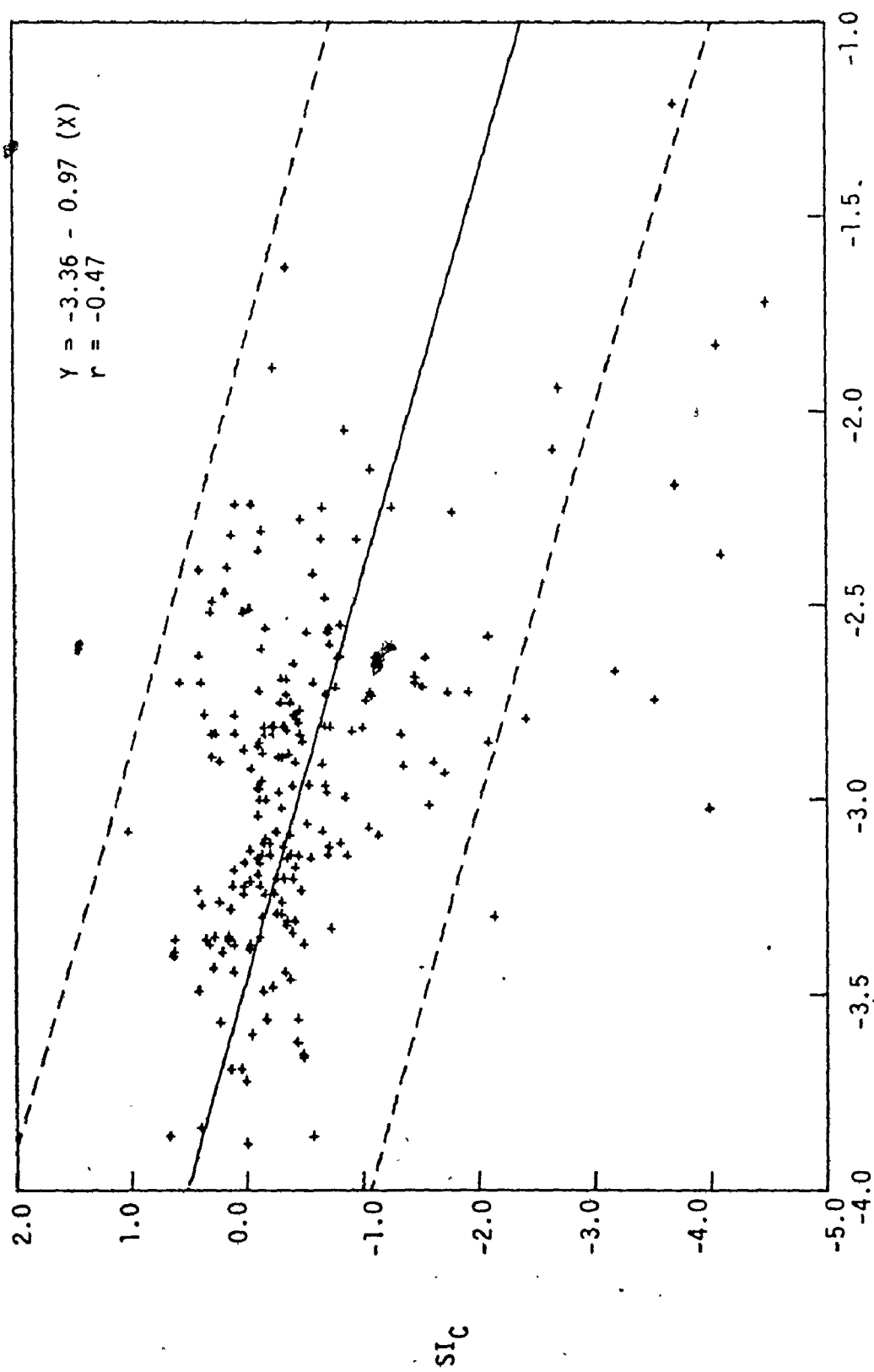


Figure 5.5. The Chemistry of Nahanni Waters:  $SI_c - \log PCO_2$ .

Figure 5.5 does emphasize two points very clearly, however; first that most waters in the Nahanni are very close to saturation with respect to calcite and second that virtually all waters contain levels of carbon dioxide higher than those characteristic of the atmosphere at the various altitudes encountered in the Nahanni.

### 3. Hydrochemical Classification of Waters in the Nahanni Karst.

Within any karst terrain there are marked spatial variations in the intensity of solution. In order to understand such patterns it is first necessary to determine what kinds of water are present within a given area, what the mean chemical characteristics of such waters are and what interrelationships exist between them. Following this it is possible to better explain the geomorphology of the solutionally moulded terrain. Outside of remote areas, the identification of natural water categories with particular hydrochemical characteristics is a great aid in pollution control and water resource planning.

Wigley et al. (1973) and Drake & Harmon (1973) have demonstrated that within karst terrains it is possible to differentiate water varieties on hydrochemical grounds. In both cases linear discriminant function analysis was applied to chemistry data to determine the statistical significance of a priori hydrogeological groupings of waters in karst terrains. When performed in a stepwise manner, this technique (King 1969; Davis 1973) can be used to determine the most powerful discriminating variables between groups.

Wigley et al. (1973) grouped waters in a gypsum karst into five categories, namely gypsiferous springs, surface rivers downstream of

springs, surface rivers upstream, Lussier Valley sinkhole waters, and Coyote Valley sinkhole waters. The chemical variables used in the discriminant analysis were: temperature; pH; calcium, magnesium and sulphate concentrations; alkalinity,  $SI_C$ ,  $SI_D$ ,  $SI_G$ ,  $\log PCO_2$ , calcium/sulphate ion ratio and calcium/magnesium ion ratio. The analysis showed that the three most important discriminating variables were calcium concentration, temperature and  $SI_G$ . Over 99.9% of the variance between the groups was explained by these variables alone.

Waters in two carbonate regions of Pennsylvania were divided into six groups by Drake & Harmon (1973). The groups were allogenic surface recharge from non-carbonate rocks, soil zone recharge, conduit springs, diffuse springs, well waters, and basin surface recharge. As these writers point out, linear discriminant function analysis normally requires a set of orthogonal variables that are usually constructed from the interrelated set of measured or observed variables by a principal components analysis. Such derived components are however very difficult to interpret in a physical or chemical sense. Drake & Harmon argue that the geochemical variables  $SI_C$ ,  $SI_D$  and  $\log PCO_2$ , because they reflect the geochemical constraints on the chemical system  $CO_2 - CaCO_3 - CaMg(CO_3) - H_2O$  can be considered as 'factors' in the sense that they are orthogonal and are derived from various, though non-linear loadings of the measured variables. Any separation of water groups in terms of these variables is much easier to interpret geochemically.

The discriminant analysis on the chemical characteristics of Pennsylvanian waters by Drake & Harmon (1973) was therefore conducted

in two parts. First, an attempt was made to differentiate the six groups using six measured chemical variables, namely temperature, pH,  $\text{Ca}^{2+}$ ,  $\text{Mg}^{2+}$ ,  $\text{HCO}_3^-$  and specific conductance. Secondly, the analysis was carried out using the three derived variables,  $\text{SI}_C$ ,  $\text{SI}_D$ , and  $\log \text{PCO}_2$ . Using the measured variables the groups were found to be separate at the 0.005 confidence level after two steps; pH was entered first and then  $\text{HCO}_3^-$  concentration. At this stage some 41 out of 166 waters were misclassified by the discriminating function or 25% of the total. Using the derived variables, the groups were also found to be separate at the 0.005 confidence level after two steps.  $\text{SI}_C$  was entered in to the analysis first and then  $\log \text{PCO}_2$ . At this stage some 39 out of the 166 waters were misclassified or 23% of the total. Drake & Harmon argue from these results that not only can the water classes common to a typical carbonate terrain be distinguished according to the geochemical variables,  $\text{SI}_C$  and  $\log \text{PCO}_2$ , but that these parameters vary between groups in a manner that can be used to define the chemical evolution of a water as it moves through a carbonate drainage basin. They note that  $\text{SI}_C$  is a direct measure of the residence time of a water within the drainage basin and the  $\log \text{PCO}_2$  an indication of the conditions under which recharge waters entered the carbonate aquifers. These workers conclude that geochemical measures provide a sound basis for distinguishing the various water types within a carbonate drainage basin.

The Nahanni karst is a somewhat more complicated environment in a surficial and bedrock geology sense than either of the areas considered by Wigley et al. (1973) or Drake & Harmon (1973). It contains a large

number of hydrogeological water classes. From hydrological considerations alone, six groups can be differentiated, namely springs, streams, pools and ponds, lakes, soil and marsh waters, and limestone seepage waters (Table 5.3). In turn each major hydrologic group contains waters from a variety of surficial and bedrock geological environments so that sub-groups can be defined. For example waters on shale clearly differ in their chemical characteristics from waters on bare limestone. The full list of hydrogeological water groups that can be identified in the Nahanni is given in Table 5.3.

In order to determine whether water groups in the Nahanni karst region can be differentiated on chemical grounds and to find out the degree of chemical interaction between groups, chemical data was subjected to stepwise linear discriminant function analysis. It was hoped that this would also isolate the important group distinguishing variables. The linear discriminant function program used in this study was BMD 07M from Dixon (1970). The analysis was conducted in a manner similar to that outlined by Drake & Harmon (1973) where measured and derived chemical variables were considered separately. Similarly, because it is very difficult to interpret orthogonalized variables constructed by a principal components analysis, no such technique was employed. In order to eliminate highly correlated measured and derived chemical variables from the analysis therefore, a correlation matrix for the 214 water samples was prepared (Table 5.4). The measured variables chosen for entry into the analysis were temperature, pH, calcium concentration, magnesium concentration and alkalinity.

Table 5.3. Hydrogeological Water Types in the Nahanni Karst.

HYDROLOGICAL GROUPS	SYMBOL	HYDROGEOLOGICAL SUB-GROUPS	SYMBOL
Springs	U	Springs with recharge areas on limestone	A
		Springs with recharge areas on shale	B
Ponds	V	Ponds on shale	C
		Ponds on sandy glacial drift	D
		Ponds on till-mantled limestone	E
		Pools and ponds on limestone	F
Lakes	W	Lakes on shale	G
		Lakes on shale-derived alluvium	H
		Lakes on sandy glacial material	I
		Lakes on limestone	J
Streams	X	Streams on shale	K
		Streams on limestone	L
Soil Waters	Y	Soil waters on shale	M
		Soil waters on limestone	N
Seepage Waters	Z	Seepage waters on limestone	O

Table 5.4. Correlation Matrix of 12 Chemical Variables from Analysis of 214 Water Samples, Nahanni Karst, 1972-1973.

	1	2	3	4	5	6	7	8	9	10	11	12
1	1.00											
2	0.07	1.00										
3	-0.34	0.24	1.00									
4	-0.25	0.10	0.71	1.00								
5	-0.06	0.25	0.06	-0.37	1.00							
6	-0.33	0.27	0.91	0.73	0.05	1.00						
7	-0.16	-0.66	0.09	0.10	-0.14	0.08	1.00					
8	0.22	0.80	-0.23	-0.25	0.22	-0.26	-0.68	1.00				
9	0.02	0.91	0.53	0.33	0.22	0.56	-0.49	0.50	1.00			
10	0.02	0.89	0.54	0.42	0.11	0.57	-0.47	0.47	0.99	1.00		
11	-0.32	0.23	0.94	0.84	-0.04	0.97	0.10	-0.26	0.52	0.55	1.00	
12	-0.32	0.23	0.95	0.86	-0.06	0.94	0.09	-0.24	0.52	0.55	0.99	1.00

List of Variables

- 1 Temperature ( $^{\circ}\text{C}$ )
- 2 pH
- 3 Calcium Hardness (ppm  $\text{CaCO}_3$ )
- 4 Magnesium Hardness (ppm  $\text{CaCO}_3$ )
- 5 Molar Ca/Mg Ratio
- 6 Alkalinity mM/liter
- 7 Carbon Dioxide (ppm)
- 8  $\log \text{PCO}_2$
- 9  $\text{SiC}$
- 10  $\text{SiD}$
- 11 Ionic Strength M/liter
- 12 Total Hardness (ppm  $\text{CaCO}_3$ )



Essentially, temperature is not highly correlated with any of the other measured or derived variables while pH is only strongly correlated with derived variables which does not present a problem. Initially it was decided to include the Ca/Mg molar ratio and alkalinity as the other two variables which would leave four measured variables with poor correlation between them. However the Ca/Mg molar ratio is essentially a function of calcium and magnesium concentrations which it was decided to include instead to add an extra discriminating variable. The correlations between calcium, magnesium and bicarbonate concentrations are not thought to have significantly affected the importance of the analysis. Because of the extremely high correlation between  $SI_C$  and  $SI_D$  (0.99),  $SI_D$  was not entered into the discriminant analysis involving derived variables; only  $SI_C$  and  $\log PCO_2$  were utilized.

The stepwise linear discriminant function analysis of Nahanni waters was conducted for a variety of groups in an attempt to determine what realistic hydrochemical groups do exist in this area. In such an analysis at each step the chemical variable entered in the discrimination is that which gives the greatest improvement in the F-ratio of between-group variation to within-group variation. Initially only the six main hydrological groups were considered. The analysis was conducted first for the five measured chemical variables and then for the two calculated variables  $SI_C$  and  $\log PCO_2$ . Results of the analysis are shown in Table 5.5. For the measured variables, 100 of 214 samples were misclassified by this technique after five steps or some 46.7% of the total. Using the derived variables, 136 of 214 samples were

Table 5.5. Stepwise Linear Discriminant Function Analysis of the Chemistries of Major Water Types in the Nahanni Karst.<sup>1</sup>

Step at Which Groups are Separate at the 0.005 Confidence Level<sup>2</sup>

	U	V	W	X	Y	Z
Measured Variables <sup>3</sup>						
U	-					
V	1	-				
W	1	1	-			
X	1	1	3	-		
Y	1	2	2	2	-	
Z	1	1	3	(<0.05)	2	-
Derived Variables <sup>4</sup>						
U	-					
V	1	-				
W	1	2	-			
X	1	1	(<0.5)	-		
Y	1	1	1	1	-	
Z	1	(<0.25)	(<0.05)	(<0.025)	1	-

Classification Matrices from the LDF Analysis

	U	V	W	X	Y	Z	Originally Classified	Mis-Classified
Measured Variables <sup>5</sup>								
U	21	0	0	1	0	8	30	9
V	0	41	12	4	4	9	70	29
W	0	5	16	6	0	0	27	11
X	4	9	12	25	5	13	68	43
Y	0	0	0	2	4	1	7	3
Z	2	3	0	0	0	7	12	5
Derived Variables <sup>6</sup>								
U	21	0	8	0	0	1	30	9
V	3	31	7	6	4	19	70	39
W	5	6	3	7	0	6	27	24
X	11	13	12	17	5	10	68	51
Y	2	0	0	0	5	0	7	2
Z	2	5	4	0	0	1	12	11

1 A list of groups and symbols is given in Table 5.3.

2 Where the groups are not separate at the 0.005 level the level at which they are separate is given in parentheses.

3 Variables were entered in the order Magnesium, pH, temperature, alkalinity, Calcium.

4 Variables were entered in the order log PCO<sub>2</sub>, SI<sub>c</sub>.

5 Out of 214 water samples 100 were misclassified after 5 steps.

6 Out of 214 water samples 136 were misclassified after 2 steps.

misclassified after two steps or 63.5%. Many groups were found to be separate at the 0.005 confidence level after one or more steps, but clearly the results demonstrate that Nahanni waters cannot be classified into hydrological groups purely on the basis of their water chemistry. Obviously there is a great deal of chemical overlap between such groups.

Because the first part of the discriminant analysis convincingly demonstrates that waters in the Nahanni do not differ in water chemistry for purely hydrological reasons, an attempt was made to determine whether there are significant differences in water chemistry between the hydrogeological sub-groups within each of five of the hydrologic classes. Each of the hydrologic groups was therefore considered in turn and the geologic sub-groups were subjected to a discriminant analysis. The results of this analysis which was conducted for both measured and calculated variables are shown in Tables 5.6 - 5.10 inclusive.

As Table 5.6 shows, the limestone springs of the Nahanni with recharge areas on limestone and sulphate springs with recharge areas on drift-mantled shale can be differentiated according to either alkalinity or saturation index with respect to calcite, at the 0.005 confidence level. A discriminant function utilizing all five of the measured chemical variables classified all spring water samples correctly while one using the two calculated variables misclassified only one water. Obviously the different chemistries of these two springs are related to the different geological environments in their recharge areas.

Four kinds of pond can be differentiated in the Nahanni karst according to the geological terrain they occupy. The four categories

Table 5.6. Stepwise Linear Discriminant Function Analysis of the Chemistries of Spring Water Types in the Nahanni Karst.<sup>1</sup>

Step at Which Groups are Separate at the 0.05 Confidence Level

	A	B	
			Measured Variables <sup>2</sup>
A	-		
B	1	-	
			Derived Variables <sup>3</sup>
A	-		
B	1	-	

Classification Matrices from the LDF Analysis

	A	B	Originally Classified	Mis-Classified
			Measured Variables <sup>4</sup>	
A	13	0	13	0
B	0	17	17	0
			Derived Variables <sup>5</sup>	
A	12	1	13	1
B	0	17	17	0

1 A list of groups and symbols is given in Table 5.3.

2 Variables were entered in the order alkalinity, temperature, calcium, pH, magnesium.

3 Variables were entered in the order  $SI_C$ ,  $\log PCO_2$ .

4 All 30 water samples were correctly classified after 5 steps.

5 Out of 30 water samples 1 was misclassified after two steps.

are to be found on limestone, shale, till-mantled limestone and sandy glacial drift. As the results of discriminant analysis show (Table 5.7) only ponds on limestone and those on sandy glacial drift cannot be differentiated according to pH at the 0.005 confidence level. Differentiation of these two groups is effected by consideration of water temperature which is much higher in ponds on sandy glacial drift. Using  $SI_C$  and  $\log PCO_2$ , only four group separations are achieved and the results emphasize in particular, the fact that ponds on limestone and ponds on sandy glacial drift have very similar  $SI_C$  and  $\log PCO_2$  characteristics, as using both variables these two groups are only separate at the 0.95 confidence level. The discriminant function derived from the measured variables misclassified only 17 of the 70 samples or some 23.4%. Using the calculated variables 35 of 70 samples were misclassified or 50%. Clearly the measured chemical variables differentiate pond waters more efficiently than do the calculated variables.

As with ponds, there are four principal categories of lake in the Nahanni. These include lakes on drift-mantled shale, those purely on limestone, those held up by shale-derived alluvium filling closed depressions in limestone areas, and those surrounded by sandy glacial drift choking limestone canyons (Table 5.3). As Table 5.8 shows, virtually all of these water types can be separated at the 0.005 significance level using the measured chemical variables employed in the discriminant analysis. Only lakes on limestone and lakes on shale-derived alluvium in limestone depressions are not significantly different after five steps at this confidence level. These groups are different at the 0.025 level however.

Table 5.7. Stepwise Linear Discriminant Function Analysis of the Chemistries of Pond Water Types in the Nahanni Karst.

Step at Which Groups are Separate at the 0.005 Confidence Level<sup>2</sup>

	C	D	E	F
	Measured Variables <sup>3</sup>			
C	-			
D	1	-		
E	1	1	-	
F	1	2	1	-

	C	D	E	F
	Derived Variables <sup>4</sup>			
C	-			
D	1	-		
E	1	( 0.025)	-	
F	1	( 0.95)	1	-

Classification Matrices from the LDF Analysis

	C	D	E	F	Originally Classified	Mis-Classified
	Measured Variables <sup>5</sup>					
C	4	0	0	0	4	0
D	0	6	3	0	9	3
E	0	2	5	0	7	2
F	0	8	4	38	50	12

	C	D	E	F	Originally Classified	Mis-Classified
	Derived Variables <sup>6</sup>					
C	4	0	0	0	4	0
D	0	1	3	5	9	8
E	0	1	5	1	7	2
F	0	20	5	25	50	25

1 A list of groups and symbols is given in Table 5.3.

2 Where the groups are not separate at the 0.005 level the level at which they are separate is given in parentheses.

3 Variables were entered in the order pH, temperature, calcium, magnesium, alkalinity.

4 Variables were entered in the order  $SI_C$ ,  $\log PCO_2$ .

5 Out of 70 water samples 17 were misclassified after 5 steps.

6 Out of 70 water samples 35 were misclassified after 2 steps.

Table 5.8. Stepwise Linear Discriminant Function Analysis of the Chemistries of Lake Water Types in the Nahanni Karst.

Step at Which Groups are Separate at the 0.005 Confidence Level<sup>2</sup>

	G	H	I	J
Measured Variables <sup>3</sup>				
G	-	-	-	-
H	1	-	-	-
I	3	1	-	-
J	2	(<0.025)	4	-

	G	H	I	J
Derived Variables <sup>4</sup>				
G	-	-	-	-
H	(<0.01)	-	-	-
I	1	1	-	-
J	1	(<0.025)	(<0.95)	-

Classification Matrices from the LDF Analysis

	G	H	I	J	Originally Classified	Mis-Classified
Measured Variables <sup>5</sup>						
G	10	0	0	0	10	0
H	1	10	0	0	11	1
I	0	0	4	0	4	0
J	0	0	0	2	2	0
Derived Variables <sup>6</sup>						
G	6	4	0	0	10	4
H	2	8	1	0	11	3
I	0	0	3	1	4	1
J	0	0	0	2	2	0

1 A list of groups and symbols is given in Table 5.3.

2 Where the groups are not separate at the 0.005 level the level at which they are separate is given in parentheses.

3 Variables were entered in the order temperature, pH, alkalinity, magnesium, calcium.

4 Variables were entered in the order  $SI_C$ ,  $\log PCO_2$ .

5 Out of 27 water samples only 1 was misclassified after 5 steps.

6 Out of 27 water samples 8 were misclassified after 2 steps.

Using the calculated variables only three group separations are possible at the 0.005 level, and particularly lakes on limestone and lakes on sandy glacial drift are difficult to separate using these two variables; they are different only at a 0.95 confidence level. As with ponds and streams, water class differentiation according to chemical parameters is more efficient using measured as opposed to calculated variables. The discriminant function derived from the five measured variables misclassified only one of 27 cases while that for two derived variables misclassified 8 of 27 cases or 29.6%. Lake waters in different surficial and bedrock geological environments clearly differ in their overall water chemistries and can be classified on this basis. Although similar hydrologically, such waters differ because of the environment in which they are found.

Only two major categories of stream water exist in the Nahanni karst although there is a great deal of interaction between the two types. Identified are streams which in the majority of cases have headwaters in areas of drift-covered shale and streams which flow in limestone regions. These latter are often extensions of streams on shale but some streams have headwaters on limestone. Although a group of 'mixed' stream waters could have been differentiated waters would have been very difficult to isolate. The group of streams on limestone refers both to streams that have headwaters in this rock type and to those that do not. Streams on limestone and streams on shale can be differentiated at the 0.005 confidence level using either calcium concentration in ppm.  $\text{CaCO}_3$  or saturation index with respect to calcite



(Table 5.9). The discriminant function derived from calcium concentration, temperature, pH and magnesium concentration misclassified only 5 samples out of 68 or 7.4%; alkalinity was not entered at the 0.005 level. Eleven samples were misclassified using the discriminant function utilizing the calculated variables, this is 16.3% of the total. Thus despite a known interaction between stream waters on shale and those flowing on limestones, these water groups can be differentiated according to their chemistries.

Water contained in soils resting on both limestone or shale bedrock were sampled and analyzed in 1972 and 1973. These water groups as Table 5.10 shows can be separated at the 0.005 confidence limit on the basis of their alkalinity alone. They are not different at the 0.005 level on the basis of  $SI_C$  and  $\log PCO_2$ , however, but are different at the 0.25 confidence level. All seven waters were correctly classified using both the measured and derived variables.

There is no doubt that the second stage in the discriminant analysis of water classes in the Nahanni has demonstrated that hydrologically similar waters owe their characteristic chemistries in large part to the surficial and bedrock geological characteristics of the environments which they occupy. Once waters have been classified into hydrological categories, the environment to which they relate can be determined according to their water chemistry. Of some 202 water samples initially divided into five hydrological groups, some 179 were correctly classified according to environment on the basis of measured chemical variables and 147 on the basis of calculated chemical variables. This is 88.6% and 72.8% correctly classified respectively.

Table 5.9. Stepwise Linear Discriminant Function Analysis of the Chemistries of Stream Water Types in the Nahanni Karst.<sup>1</sup>

Step at Which Groups are Separate at the 0.005 Confidence Level.

	K	L		
			Measured Variables <sup>2</sup>	
K	-			
L	1	-		
			Derived Variables <sup>3</sup>	
K	-			
L	1	-		
Classification Matrices from the LDF Analysis				
	K	L	Originally Classified	Mis-Classified
			Measured Variables <sup>4</sup>	
K	23	1	24	1
L	4	40	44	4
			Derived Variables <sup>5</sup>	
K	17	7	24	7
L	4	40	44	4

1 A list of groups and symbols is given in Table 5.3.

2 Variables were entered in the order calcium, temperature, pH, magnesium, alkalinity was not included at the 0.005 level.

3 Variables were entered in the order  $SI_C$ ,  $\log PCO_2$ .

4 Out of 68 water samples 5 were misclassified after 4 steps.

5 Out of 68 water samples 11 were misclassified after 2 steps.

Table 5.10. Stepwise Linear Discriminant Function Analysis of the Chemistries of Soil Water Types in the Nahanni Karst.

Step at Which Groups are Separate at the 0.005 Confidence Level<sup>2</sup>

	M	N		
			Measured Variables <sup>3</sup>	
M	-			
N	1	-		
			Derived Variables <sup>4</sup>	
M	-			
N	(<0.25)	-		
Classification Matrices from the LDF Analysis				
	M	N	Originally Classified	Mis-Classified
			Measured Variables <sup>5</sup>	
M	5	0	5	0
N	0	2	2	0
			Derived Variables <sup>6</sup>	
M	5	0	5	0
N	0	2	2	0

1 A list of groups and symbols is given in Table 5.3.

2 Where the groups are not separate at the 0.005 level the level at which they are separate is given in parentheses.

3 Variables were entered in the order alkalinity, magnesium, calcium, temperature, pH.

4 Variables were entered in the order  $SI_C$ ,  $\log PCO_2$ .

5 All 7 water samples were correctly classified after 5 steps.

6 All 7 water samples were correctly classified after 2 steps.

The third and final stage in the discriminant analysis of Nahanni water classes is an attempt to determine the extent to which hydrologically different waters in the same environment differ in water chemistry. Two environments have been chosen for this study. The first is the drift-covered shale area of the region, the second the irregularly mantled limestone terrain. Certain spring, pond, lake, stream and soil waters in the Nahanni are either found on drift-mantled shale or are thought to derive their chemical characteristics from this type of environment. Out of 60 samples, 48 were correctly classified by a discriminant function using measured chemical parameters and 42 using derived chemical parameters (Table 5.11). Only two groups separations were not significant at the 0.005 level using the measured variables and the same two could not be separated at this level using the derived variables. Two of the groups that could not be separated are lakes and streams on shale. Clearly there is mixing between these two waters as streams flow into and out of lakes and therefore there is an expected overlap in chemical characteristics. The other two groups, soil waters and ponds, also mix to a great degree in nature and therefore again overlap in properties is to be expected. Despite minor difficulties in separating some groups, overall the results indicate that in a given 'homogeneous' environment natural waters do differ according to their hydrological category. Some 80% and 70% of water samples on shale can be correctly classified into their hydrological group by measured chemical variables and derived chemical variables respectively.

In limestone terrains 127 samples have been taken of spring, pond, lake, stream, soil and seepage waters. Only two pairs of groups

Table 5.11. Stepwise Linear Discriminant Function Analysis of the Chemistries of Some Water Types on Shales in the Nahanni Karst.<sup>1</sup>

Step at Which Groups are Separate at the 0.005 Confidence Level<sup>2</sup>

Measured Variables<sup>3</sup>

	B	C	G	K	M
B	-				
C	1	-			
G	1	2	-		
K	1	3	(<0.05)	-	
M	1	(<0.025)	2	2	-

Derived Variables<sup>4</sup>

	B	C	G	K	M
B	-				
C	1	-			
G	2	1	-		
K	1	1	(<0.25)	-	
M	1	(<0.025)	1	1	-

Classification Matrices from the LDF Analysis

	B	C	G	K	M	Originally Classified	Mis-Classified
Measured Variables <sup>5</sup>							
B	17	0	0	0	0	17	0
C	0	4	0	0	0	4	0
G	0	0	9	1	0	10	1
K	0	0	7	14	3	24	10
M	0	0	0	1	4	5	1
Derived Variables <sup>6</sup>							
B	16	0	1	0	0	17	1
C	0	4	0	0	0	4	0
G	0	0	7	3	0	10	3
K	2	1	8	11	2	24	13
M	0	0	0	1	4	5	1

1 A list of groups and symbols is given in Table 5.3.

2 Where the groups are not separate at the 0.005 level the level at which they are separate is given in parentheses.

3 Variables were entered in the order alkalinity, pH, temperature, magnesium, calcium.

4 Variables were entered in the order  $SI_C$ ,  $\log PCO_2$ .

5 Out of 60 water samples, 12 were misclassified after 5 steps.

6 Out of 60 water samples, 18 were misclassified after 2 steps.

were not separate at the 0.005 confidence level when measured chemical variables were fed into discriminant analysis. The discriminant function derived, misclassified 53 samples or some 41.7% of the total (Table 5.12). The two pairs of groups that were not separate at the 0.005 level after five steps were ponds and lakes, and streams and seepage waters. It is to be expected that there would be some similarity between what are in some cases large ponds and fairly small lakes. These groups were separate at the 0.025 level, however, after five steps. Similarly seepage waters often derived from sinking stream waters should bear some chemical similarities to the latter group. Again these two groups were separate at the 0.025 level after five steps. Discriminant analysis employing derived variables misclassified 66 of the 127 total or 52% and only nine of fifteen group separations were significant at the 0.005 level after two steps. In particular lakes and seepage waters are only separate at the 0.5 confidence level after two steps. Clearly these two groups have very similar average  $SI_c$  and  $\log PCO_2$  values. The reason for this is that the only lake in the region that can truly be classified as a 'limestone' lake is Raven Lake occupying Raven Canyon. This lake derives its water from underground sources thought to represent accumulated seepage waters. These results demonstrate that some 58.3% and some 48% of water samples in limestone areas can be correctly classified into their hydrological group by measured chemical and calculated variables respectively. This result is clearly not as convincing as that obtained from analysis of waters in the shale environment but is to be expected considering the great diversity of

Table 5.12: Stepwise Linear Discriminant Function Analysis of the Chemistries of Some Water Types on Limestone in the Nahanni Karst.<sup>1</sup>

Step at Which Groups are Separate at the 0.005 Confidence Level<sup>2</sup>

	A	F	J	L	N	O
	Measured Variables <sup>3</sup>					
A	-					
F	1	-				
J	1	(<0.025)	-			
L	1	1	2	-		
N	1	1	1		-	
O	4	1	2	(<0.025)	1	-
	Derived Variables <sup>4</sup>					
A	-					
F	1	-				
J	1	(<0.05)	-			
L	(<0.025)	1	2	-		
N	(<0.01)	1	1	2	-	
O	1	(<0.01)	(<0.5)	(<0.01)	1	-

Classification Matrices from the LDF Analysis

	A	F	J	L	N	O	Originally Classified	Mis-Classified
	Measures Variables <sup>5</sup>							
A	12	0	0	1	0	0	13	1
F	0	29	9	7	1	4	50	21
J	0	0	6	0	0	0	6	0
L	6	7	3	21	1	6	44	23
N	0	0	0	0	2	0	2	0
O	2	3	0	1	2	4	12	8
	Derived Variables <sup>6</sup>							
A	11	0	0	1	1	0	13	2
F	4	27	7	6	1	5	50	23
J	0	0	5	0	0	1	6	1
L	7	8	3	15	4	7	44	29
N	0	0	0	0	2	0	2	0
O	3	4	2	2	0	1	12	11

1 A list of groups and symbols is given in Table 5.3.

2 Where the groups are not separate at the 0.005 level, the level at which they are separate is given in parentheses.

3 Variables were entered in the order calcium, temperature, magnesium, pH, alkalinity.

4 Variables were entered in the order log PCO<sub>2</sub>, SI.

5 Out of 127 water samples 53 were misclassified after 5 steps.

6 Out of 127 water samples 66 were misclassified after 2 steps.

surficial if not bedrock geological conditions within the limestone exposure. By comparison the shale environment is far more homogeneous.

Discriminant analysis of Nahanni waters has been of value in that it has provided statistical proof that surface and sub-surface waters in the region derive their chemical content not only from their position in the hydrological cycle but also from the environment in which they are to be found. Marked differences have been found between hydrologically similar waters in different geological environments and also between a variety of water types in the same environment. Clearly waters in the Nahanni acquire their chemical characteristics according to these two controls.

#### 4. Spatial Variations in the Biogenic Carbon Dioxide Content of Nahanni Soils.

##### (a) Importance of Biogenic Carbon Dioxide.

Under ordinary atmospheric conditions the carbon dioxide in the atmosphere exerts a partial pressure of 0.0003 atmospheres or it has a log  $P_{CO_2}$  of -3.52. Water at 16°C in equilibrium with atmospheric conditions can dissolve close to 63 ppm.  $CaCO_3$ . As concentrations of  $CaCO_3$  in Nahanni waters are far in excess of this value (average total hardness is 110 ppm.  $CaCO_3$ ) they have clearly been enriched in carbon dioxide. As early as 1937 Adams & Swinnerton pointed out that soil atmospheres are often characterized by  $PCO_2$  levels as much as several hundred times as great as that of the atmosphere. They pointed out that waters passing through soils should be capable of dissolving large quantities of calcium carbonate. Swinnerton (1942) mentions that



although the carbon dioxide enrichment of ground water through contact with soil may not be the complete answer to extremely high solute concentrations in natural waters, it is in many cases an adequate one. Foster (1942) also feels that "It is probable that the greater part of the carbon dioxide content of meteoric waters is derived from the soils through which they pass" (p. 649).

In 1959 Corbel argued that temperature and not soil carbon dioxide is the most important control on the rate of limestone solution in different environments. He suggested that because carbon dioxide is three times more soluble in water at 0°C than it is in water at 30°C, colder natural waters are richer in carbon dioxide than are warmer waters and are therefore capable of dissolving more limestone. As early as 1942, however, Swinnerton noted that "The temperature factor is not highly significant in the ordinary ranges, but it is complicated. In general it may be said . . . that whereas the solubility of calcium carbonate in water free from carbon dioxide increases with increase in temperature, the reverse is true in the presence of carbon dioxide" (p. 659).

Drake (1974) divides the environmental controls upon limestone solution into two groups. First are those which influence the chemical reactions, such as temperature and the availability of carbon dioxide, and secondly are those which influence the intermixing of the solute and solvent such as the type of fluid flow, the geometry of the interface and whether the system is open or closed. As Drake notes, temperature influences not only the rate of the dissociation process but also

the final equilibrium state. For a solid-liquid system, the dependence, as Swinnerton (1942) noted, is positive so that more of the solute may be dissolved with an increase in temperature. For a gas-liquid system, however, the reverse is true. Using values for dissociation constants given by Wigley (1972), Drake (1974) has calculated the theoretical temperature dependence of the equilibrium  $\text{Ca}^{2+}$  concentrations of the calcite-water system (Figure 5.6). It is apparent that the solubility of calcite decreases with increasing temperature. As Drake notes this is because for calcite (and dolomite) solution, the magnitude of the temperature dependence of the carbon dioxide-water sub-system is greater than that of the  $\text{H}_2\text{CO}_3$  - calcite sub-system, resulting in an overall negative  $\text{Ca}^{2+}$  temperature relationship - a result noted by Ek (1969).

In general, most workers recognize that although there are many controls upon the solution of limestone, the dominant control is that exerted by the carbon dioxide content of the water. It is also realized that this is primarily a function of carbon dioxide levels in soil atmospheres. Despite this realization, little work has been conducted to determine relationships between soil carbon dioxide levels and the chemical characteristics of nearby natural waters. In the summers of 1972 and 1973 an attempt was made to do this in the Nahanni karst.

(b) Soil Carbon Dioxide Levels in the Nahanni.

During the summers of 1972 and 1973 some 32 spot measurements of soil carbon dioxide were made. Sites varied in setting, vegetation and surficial and bedrock geology, and were chosen to provide some insight

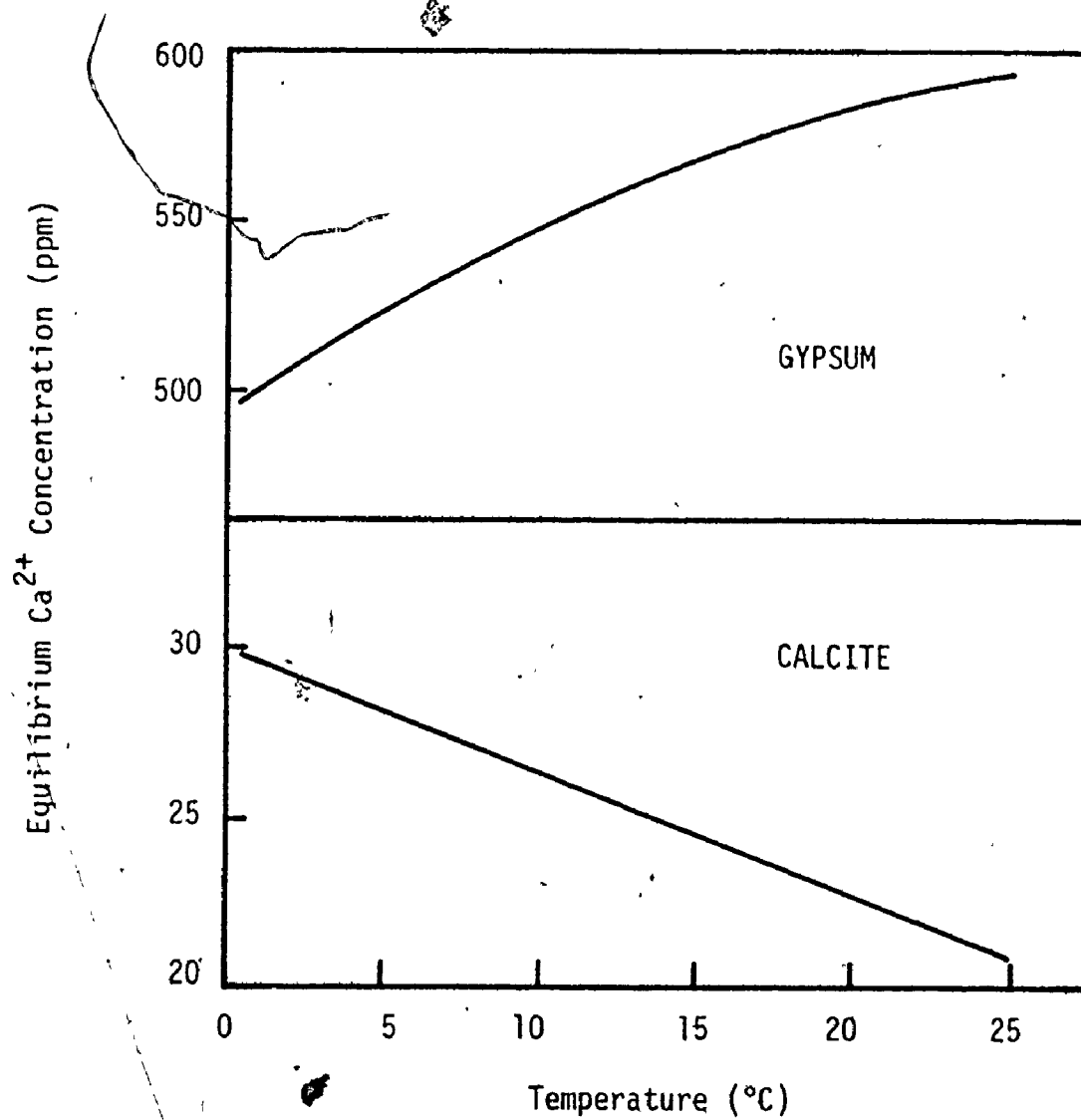


FIGURE 5.6. Temperature Dependence of the Solubilities of Calcite and Gypsum (after Drake 1974).

into the differences in water chemistry between the various hydrological water groups in this region. Soil carbon dioxide was measured with apparatus designed and manufactured by Franz-Dieter Miotke. The apparatus, technique of utilization and accuracy is thoroughly described in Miotke (1972). At each of the 32 sites the sampling depth was recorded and a brief and probably inadequate description of the vegetation was made.

As Table 5.13 shows, the average carbon dioxide content of the 32 soils examined was 0.3% or ten times the atmospheric level. Soil carbon dioxide content varied considerably, however, with values ranging from atmospheric up to 2.25%. To determine whether soil carbon dioxide levels vary systematically with geological environment measurements were divided into four groups reflecting predominantly limestone, shale, till-mantled limestone and sandy glacial drift environments. The mean carbon dioxide contents of soils in these environments were found to be 0.17%, 0.70%, 0.11% and 0.06% respectively, demonstrating the likelihood that soil carbon dioxide levels are related to environment.

Carbon dioxide evolution in soils is related to the metabolic activity of the soil biota. This gas is produced by soil fauna, microbes and flora including root respiration. Shilova (1967) argues that most of the  $\text{CO}_2$  in the atmosphere of cropped soils comes from respiration of roots during plant growth. Kosonen (1968) tested this argument by examining  $\text{CO}_2$  production at a number of sites in a grazing meadow in Finland. He found that at measuring points covered with vegetation  $\text{CO}_2$  production was 125% higher on average than at sites where the vegetation had been cut. Vadyunina & Korchagina (1965) on the other hand contend

Table 5.13. Mean Carbon Dioxide Levels in Nahanni Soils.

VARIABLE	MEAN	STANDARD DEVIATION	STANDARD ERROR OF THE MEAN	SAMPLE SIZE	MAXIMUM VALUE	MINIMUM VALUE	RANGE
ALL SOIL TYPES							
Depth (cms)	35.6	9.7	1.7	32	59.0	17.5	41.5
CO <sub>2</sub> %	0.30	0.45	0.08	32	2.25	0.03	2.22
log PCO <sub>2</sub>	-2.80	0.46	0.08	32	-1.65	-3.52	1.87
SOILS ON LIMESTONE							
Depth (cms)	34.9	9.1	2.3	16	48.0	17.5	30.5
CO <sub>2</sub> %	0.17	0.13	0.03	16	0.43	0.03	0.40
log PCO <sub>2</sub>	-2.90	0.33	0.08	16	-2.37	-3.52	1.16
SOILS ON SHALES							
Depth (cms)	35.9	10.1	3.3	9	57.0	25.5	31.5
CO <sub>2</sub> %	0.70	0.70	0.23	9	2.25	0.07	2.18
log PCO <sub>2</sub>	-2.39	0.52	0.17	9	-1.65	-3.15	1.51
SOILS ON TILL-COVERED LIMESTONE							
Depth (cms)	43.5	10.7	5.3	4	59.0	35.0	24.0
CO <sub>2</sub> %	0.11	0.05	0.02	4	0.15	0.04	0.11
log PCO <sub>2</sub>	-3.01	0.25	0.13	4	-2.82	-3.40	0.57
SOILS ON SANDY GLACIAL DRIFT							
Depth (cms)	28.0	7.2	4.2	3	36.0	22.0	14.0
CO <sub>2</sub> %	0.06	0.02	0.01	3	0.08	0.05	0.03
log PCO <sub>2</sub>	-3.23	0.12	0.07	3	-3.10	-3.33	0.23

that in semi-desert soils  $\text{CO}_2$  content varies with the number of microorganisms in the soil and is also dependent on the soil moisture content. When moisture levels fall,  $\text{CO}_2$  production is reduced.

A number of workers have reported differences in  $\text{CO}_2$  content between soils supporting different vegetation communities. Zonn & Li (1960) for instance note that in evergreen geroniera forest in the Yunan province of China the  $\text{CO}_2$  content of the soil air varied throughout the year from 0 - 5.1% at 10 cms. depth and from 3.4 - 6.3% at 200 cms. The corresponding figures in bamboo forest were from 0.2 - 3.5% and from 4.1 - 10.8%. Not only do Zonn & Li suggest vegetal controls upon soil  $\text{CO}_2$  production but they also note that in both vegetal types  $\text{CO}_2$  content was highest in the wet season from May to October inferring temperature and moisture controls. Matskevich (1957) also notes soil  $\text{CO}_2$  differences according to supporting vegetation. Carbon dioxide content of soils supporting tree coenoses was found to be 2.5 - 3.4% while that of soils supporting herbaceous coenoses 1.2 - 2.0%. Both workers therefore report a greater soil  $\text{CO}_2$  level in soils supporting the denser vegetation cover.

Yamaguchi et al. (1967) suggest that the primary factors that govern the concentrations of  $\text{CO}_2$ ,  $\text{O}_2$  and  $\text{N}_2$  in the soil atmosphere are microbiological activity, solubility of gases in the soil solution, and gaseous diffusion. As microbiological activity relates to soil temperature and moisture conditions many workers have reported relationships between  $\text{CO}_2$  levels and these essentially climatic variables. Matskevich (1957) noted an increase in the  $\text{CO}_2$  content of soil air

in spring and a decrease at the end of summer. In fact when easily available moisture was present in the root zone, changes in the  $\text{CO}_2$  content of the soil air practically paralleled changes in soil temperature. The  $\text{CO}_2$  content of the soil in summer was also found to depend upon the moistness of the soil in spring and the amount of summer precipitation. Morozova & Bogdanova (1965) found that increasing soil temperatures at optimum soil moisture conditions contribute to  $\text{CO}_2$  release as does the accumulation of vegetal residues which are readily oxydized by microorganisms. Witkamp (1969) found a daily cycle in  $\text{CO}_2$  evolution from a variety of biotopes with a predawn minimum and an afternoon maximum that paralleled the daily temperature cycle. From a statistical analysis of the results of a multi-factorial laboratory experiment with soil temperatures of 5 - 30°C and moisture levels 20 - 80% Tamm & Krzysch (1963) were able to quantitatively estimate the effects of temperature and moisture on  $\text{CO}_2$  production. They found that some 50% of the variation in  $\text{CO}_2$  content in the soil is due to temperature and only 20% to moisture.

The solubility of  $\text{CO}_2$  in the soil solution and its gaseous diffusion from the soil to the outside atmosphere largely explain the general increase in  $\text{CO}_2$  with depth in the soil profile. Kurl'ykova (1962) for instance reports that in the humus horizon of soddy peats  $\text{CO}_2$  concentrations in summer reached 3.3% at 10 cms., 5.6% at 25 cms., 8.2% at 50 cms. and 14% at one meter. Also in peaty bog soils Starikova (1965) notes an increase in soil  $\text{CO}_2$  with depth from 0.6 - 4.0%. One of the reasons why there is  $\text{CO}_2$  enrichment of the soil profile with

depth is because as Hoffmann & Hoffmann (1962) have noted from lysimeter tests on sandy, calcareous and loam soils much of the  $\text{CO}_2$  produced by biochemical processes does not escape to the soil surface but because it is very soluble in water (at least in relation to oxygen) it moves with the seepage water to deeper layers. Furthermore when soil water moves upwards to an evaporating soil surface it comes into contact with air containing less  $\text{CO}_2$  and more  $\text{O}_2$ . Consequently  $\text{CO}_2$  is released from solution into the air pores again enriching the lower layers of the soil profile in  $\text{CO}_2$  first (Enoch & Dasberg 1971).

A further important factor that controls the level of  $\text{CO}_2$  in a soil is its degree of aeration. Zakke (1961) notes low  $\text{CO}_2$  contents of 0.25 - 1.1% in sandy podzolic soils with good aeration and higher  $\text{CO}_2$  levels of 1.26 - 2.4% in calcareous loams and gleyed loams in which moisture accumulation in depressions in the ground surface has obstructed aeration and promoted anaerobic processes. Clearly good aeration promotes more rapid diffusion of  $\text{CO}_2$  from soils than does poor aeration and diffusion also results in a decrease in  $\text{CO}_2$  in the soil profile closer to the soil-atmosphere interface.

This brief discussion of some of the characteristics of soil  $\text{CO}_2$  helps in the interpretation of the Nahanni data. It is apparent from the literature that soil  $\text{CO}_2$  levels up to 14% or 467 times the atmospheric average are not uncommon. The range in soil  $\text{CO}_2$  percentages given in Table 5.13 fits in well with what other workers report for a wide variety of areas. It is noticeable that the sub-arctic Nahanni soils do, in summer at least, contain quite significant quantities of



carbon dioxide and are not as might be expected deficient in this gas compared to warmer areas. A second important point that emerges from discussion of the literature is that  $\text{CO}_2$  content generally increases with depth. As many of the measurements of  $\text{CO}_2$  in the Nahanni were made at relatively shallow depth, maximum  $\text{CO}_2$  levels in soils must clearly be substantially higher than the maximums listed in Table 5.13. This may be important when the effects of soil  $\text{CO}_2$  on water chemistry are considered.

Two major environmental controls may explain differences in soil  $\text{CO}_2$  from one geological situation to another. One of the most important is clearly the density of vegetation which appears to control  $\text{CO}_2$  production in two ways. First,  $\text{CO}_2$  is emitted through roots as the plant grows and secondly microbial oxidation of litter generates  $\text{CO}_2$ . The densest vegetation in the Nahanni occurs where soils are relatively thick, on drift-covered shale areas. Here is found extremely dense boreal forest of white spruce and jackpine with an underlayer of sphagnum, reindeer moss and matt grass. In other geological environments especially in limestone and sandy glacial terrains trees are sparse and the region relatively open. In the dense forests on shale it is impossible to see more than 10 yards ahead. Vegetation density is clearly one explanation of the high  $\text{CO}_2$  contents of shale soils.

The second factor which may be of importance in controlling soil  $\text{CO}_2$  levels in the Nahanni may well be spatial differences in the degree of soil aeration. Soils on sandy glacial material have by far the lowest soil  $\text{CO}_2$  content presumably because they are extremely well

aerated. Diffusion of biogenic  $\text{CO}_2$  out of these soils is rapid so that levels are only slightly higher than atmospheric. On the other hand, many soils on shale and till-covered limestone are very poorly aerated so higher  $\text{CO}_2$  percentages are to be expected. In many locations within these geological environments in fact where marshy conditions prevail, anaerobic processes operate. In these situations  $\text{CO}_2$  production must be considerable. Unfortunately the apparatus designed by Miotke (1972) cannot be used in soils with a high moisture content. Clearly again the conclusion must be that the averages and maximum soil  $\text{CO}_2$  values listed in Table 5.13 are low for the shale and till-covered limestone environments. In fact this is definitely the case for the till-covered limestone area examined, for the majority of the area was too wet for soil  $\text{CO}_2$  determinations to be made. The values quoted for this landscape are then likely to be very low and do not truly reflect soil  $\text{CO}_2$  production in such an environment.

Soil carbon dioxide levels in the Nahanni therefore vary considerably with geological environment. Levels are high on drift-mantled shales because of poor soil aeration in these clay-rich soils and also because of a very dense vegetation canopy.  $\text{CO}_2$  levels are low on sandy glacial deposits because of rapid diffusion of  $\text{CO}_2$  from the soil because of its good aeration and also because of low vegetation densities. Soils on limestone are moderately well aerated on account of marked jointing in the rock but many soils are clay rich. As they support a sparse vegetation, their  $\text{CO}_2$  content falls somewhere between that of shales and that of sandy glacial drift. Because of measurement difficulties, the figures quoted for soils on till-covered

limestone are undoubtedly low for such a terrain and should probably fall somewhere between the figures quoted for shale and limestone.

##### 5. Carbon Dioxide and the Chemistries of Natural Waters in the Nahanni.

Discriminant analysis of water types in the Nahanni has demonstrated that the chemical characteristics of waters vary according to hydrogeological type, while examination of soil carbon dioxide levels has shown that they too vary spatially according to surficial and bed-rock geological environment. Clearly variations in soil  $\text{CO}_2$  as well as other factors may explain differences in water chemistry in this sub-arctic area.

The mean calculated  $\log \text{PCO}_2$  for all samples of Nahanni water is -2.92 while the mean  $\log \text{PCO}_2$  determined from measurements of soil atmosphere characteristics is -2.80. The carbon dioxide levels in soils are therefore slightly higher on average than they are in natural waters. Figure 5.7 shows that most Nahanni waters have a  $\log \text{PCO}_2$  which lies somewhere between -3.5 and -2.5, while soil carbon dioxide levels are generally between -3.5 and -2.0. It is apparent therefore that the  $\text{CO}_2$  levels in soils are on average higher than they are in waters. This relationship is to be expected for natural waters after they have picked up  $\text{CO}_2$  from soils, tend to lose some of it to the atmosphere for the  $\text{PCO}_2$  in the water is greater than it is in the air. That all waters do not have  $\text{CO}_2$  contents closer to the atmospheric level can probably be attributed to the slow rate at which  $\text{CO}_2$  dissolved in water equilibrates with atmospheric conditions. The evidence therefore suggests that the  $\text{CO}_2$  content of waters in the Nahanni is largely a function of previous equilibration with  $\text{CO}_2$  levels in soils.

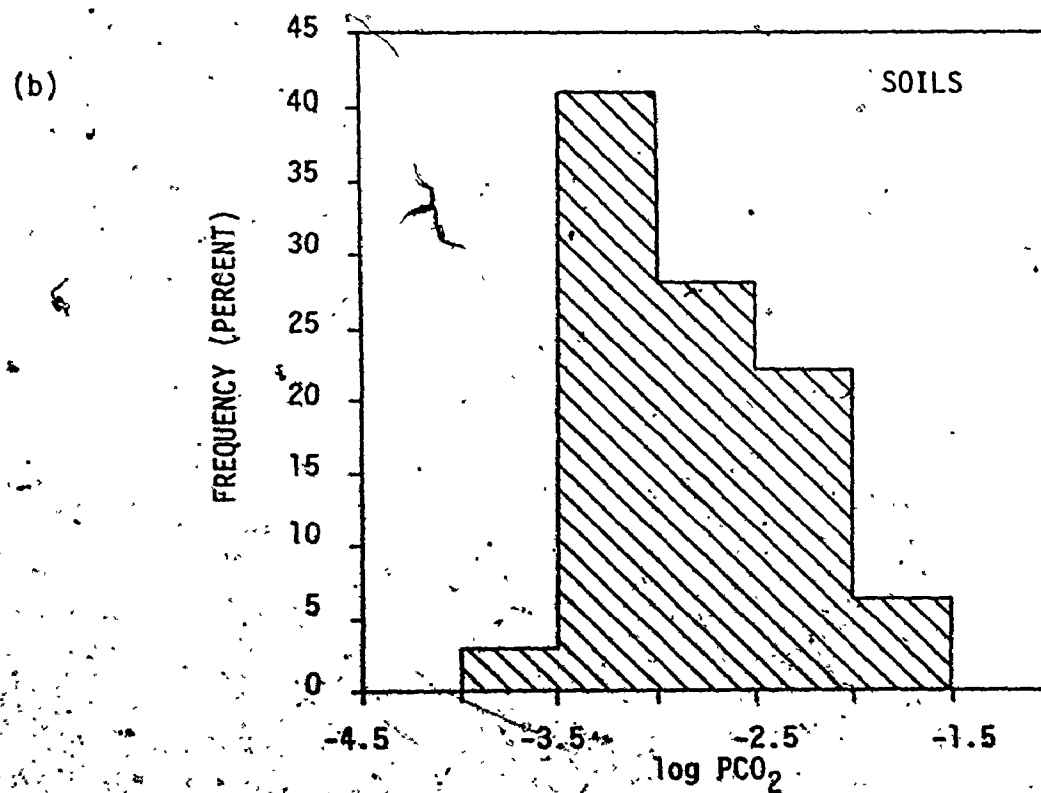
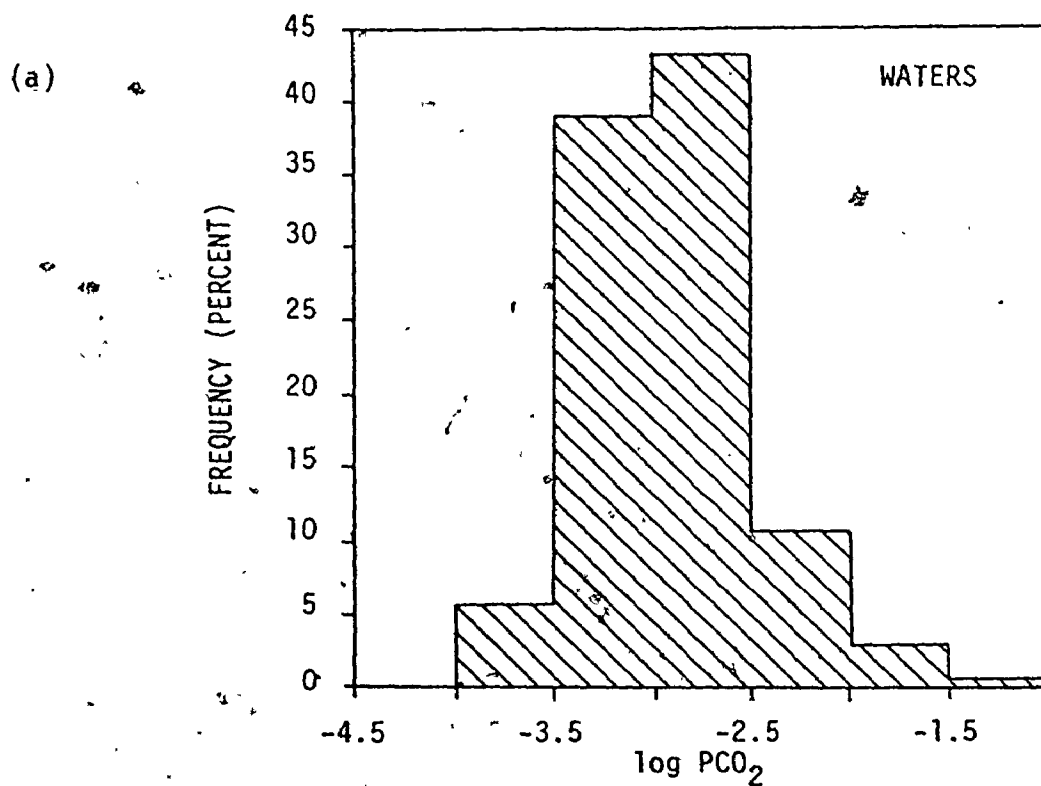


FIGURE 5.7. Frequency Histograms of Calculated log PCO<sub>2</sub> in Nahanni Waters (a) and Measured log PCO<sub>2</sub> in Nahanni Soils. (b)

Averages of hydrogeologic log  $PCO_2$  group means on shale, limestone, sandy glacial drift and till-mantled limestone are remarkably similar to the average  $CO_2$  contents of soils in these areas. On shales the average log  $PCO_2$  of waters is -2.59 while that of soils is -2.39. On limestone the averages are respectively -2.97 and -2.90, on sandy drift -3.24 and -3.23 and on till-mantled limestone -2.75 and -3.01. A strong relationship is apparent in every case except the till covered limestone results, and as has already been explained, the measured soil  $CO_2$  levels in this terrain are thought to be much lower than those that influence water characteristics. In the other three environments soil  $CO_2$  levels are all slightly higher than the levels of  $CO_2$  to be found in natural waters. This has already been explained in terms of a slow loss of  $CO_2$  to the atmosphere following equilibration with higher soil  $PCO_2$  levels. Very strong relationships are suggested between soil  $PCO_2$  and  $PCO_2$  in natural waters in this region. An attempt will now be made to determine the effect of soil  $PCO_2$  levels on the chemistries of the hydrogeologic groups of waters in the Nahanni and then to describe particular instances where  $PCO_2$  variations in natural waters bring about changes in their water chemistry.

(a) The Chemistry of Hydrogeological Water Groups and Soil Carbon Dioxide Levels.

Table 5.14 is an attempt to demonstrate the broad relationships that exist between  $PCO_2$  in natural waters and  $PCO_2$  in the soils of the local environments. In general there is a reasonable agreement between mean log  $PCO_2$  in natural waters and mean soil log  $PCO_2$  in the environment from which the water was derived. Furthermore in the

Table 5.14. Relationships Between Soil log PCO<sub>2</sub> in the Source Area and log PCO<sub>2</sub> in Natural Waters, Nahanni Karst, N.W.T.

WATER TYPE	SURFICIAL AND/OR BEDROCK GEOLOGY	CALCULATED log PCO <sub>2</sub> IN WATER			MEASURED log PCO <sub>2</sub> IN SOILS AT SOURCE AREA		
		Mean	Max.	Min.	Mean	Max.	Min.
Tufa Spring		-1.63	*	*			
Ponds		-2.81	-2.26	-3.30			
Lakes	Shale	-3.00	-2.57	-3.46	-2.39	-1.65	-3.15
Streams		-2.72	-1.72	-3.65			
Soil Waters		-1.96	-1.21	-2.79			
Bubbling Spring		-2.78	-2.65	-2.89			
Moraine Spring		-2.73	-2.56	-3.35			
Ponds		-3.24	-2.25	-3.88			
Lakes	Limestone	-3.32	-3.28	-3.36	-2.90	-2.37	-3.52
Streams		-2.93	-2.04	-3.49			
Soil Waters		-2.43	-2.36	-2.51			
Seepage Waters		-3.14	-2.72	-3.69			
Ponds	Till-Mantled Limestone	-2.75	-2.25	-3.44	-3.01	-2.82	-3.40
Ponds	Sandy Glacial	-3.24	-2.63	-3.86	-3.23	-3.10	-3.33
Lakes	Drift in Canyons	-3.24	-3.11	-3.37			
Lakes	Shale-Derived Alluvium on Limestone	-2.71	-2.42	-3.06	-2.90	-2.37	-3.52 <sup>1</sup>
					-2.39	-1.65	-3.15 <sup>2</sup>

\* Only one measurement was made right at the point of issue.

1 Values for measurements made in the alluvial material.

2 Values for measurements in shale soils.

majority of cases the range in  $\log PCO_2$  in waters lies within the range in  $\log PCO_2$  in soils. Admittedly differences do occur and these can generally be explained in terms of loss of  $CO_2$  to the atmosphere following equilibration with soil  $CO_2$  levels or by low mean and maximum soil  $CO_2$  values that are brought about by inadequate sampling and difficulties in measuring soil  $CO_2$  in saturated waters where the greatest concentrations are to be expected.

(i) Spring Waters.

Altogether four large springs have been identified in the Nahanni and more probably remain to be discovered. Three of these four springs, Bubbling, Moraine and Tufa, have been examined in detail and their respective chemistries suggest two main kinds of spring in the area, depending upon the geology of the recharge area (Table 5.14). One type, of which Tufa Spring is an example, collects water that sinks through the floors of subjacent karst collapse dolines in a drift-covered shale environment. Tufa Spring has an average total hardness close to 355 ppm.  $CaCO_3$ . A second type, which includes Bubbling Spring and Moraine Spring, collects and discharges water that sinks in essentially bare limestone terrain. Springs of this type have total hardnesses in the region of 144-188 ppm.  $CaCO_3$ .

Differences in water chemistry between these two spring types can largely be explained by soil  $PCO_2$  levels in the recharge zone and the relative importance of diffuse and conduit flows to the overall spring discharge (Shuster & White 1971). Brook, Cowell & Ford (1975) have already noted a marked agreement between  $PCO_2$  in spring water

and  $\text{PCO}_2$  in soils in their respective recharge areas. As Table 5.15 shows, the range of  $\log \text{PCO}_2$  in Bubbling Spring and Moraine Spring waters falls well within the range of  $\log \text{PCO}_2$  in the soils of their recharge areas. Mean  $\log \text{PCO}_2$  in soils is -2.90 while that in the springs is -2.78 and -2.73 respectively - a relatively close agreement. The  $\log \text{PCO}_2$  in Tufa Spring waters of -1.63 falls just beyond the maximum  $\log \text{PCO}_2$  measured in shale and drift soils in its recharge area, which on average have a soil atmosphere  $\log \text{PCO}_2$  of -2.39. It is noticeable in fact that all three spring waters have a higher mean  $\text{PCO}_2$  than the mean  $\text{PCO}_2$  in soils in their respective recharge areas. In all likelihood this is probably related to the fact that only a relatively small number of soil  $\text{CO}_2$  measurements were made and that the means and maximums of those that were made are low for reasons that have already been outlined. Despite problems of this type it is clear that there are definite relationships between soil  $\text{PCO}_2$  in the recharge area and  $\text{PCO}_2$  in groundwaters in the Nahanni. Groundwaters obviously derive the bulk of their  $\text{CO}_2$  content from the soil atmospheres through which they pass as they percolate into the limestone aquifer.

The  $\text{PCO}_2$  differences in the two types of groundwater in the Nahanni largely explain their respective water chemistries. The very high  $\text{CO}_2$  contents of waters that have percolated through collapse breccia zones in shale means that these waters when they encounter limestone underground dissolve large amounts of this rock. Despite high mineral concentrations, however, pH is kept relatively low by the



Table 5.15. Mean Chemical Characteristics of Spring Water Types in the Nahanni Karst.

VARIABLE NUMBER*	MEAN	STANDARD DEVIATION	STANDARD ERROR OF MEAN	SAMPLE SIZE	MAXIMUM VALUE	MINIMUM VALUE	RANGE
<u>Springs with Recharge Areas on Limestone</u>							
1	4.3	0.9	0.3	13	5.5	2.2	3.3
2	7.86	0.10	0.03	13	8.15	7.72	0.43
3	110.6	11.8	3.3	13	141.0	100.0	41.0
4	40.1	14.2	3.9	13	60.0	6.0	54.0
5	-3.8	4.1	1.1	13	17.4	1.7	15.7
6	2.72	0.55	0.15	13	3.96	2.22	1.74
8	-2.77	0.09	0.03	13	-2.56	-2.90	0.34
9	-0.27	0.16	0.04	13	0.22	-0.42	0.64
10	-0.97	0.40	0.11	13	0.00	-1.81	1.81
<u>Springs with Recharge Areas on Shales</u>							
1	6.0	4.5	1.1	17	18.0	1.0	17.0
2	7.82	0.36	0.09	17	8.50	7.10	1.40
3	224.4	60.5	14.7	17	302.0	29.0	273.0
4	71.9	20.6	5.0	17	104.0	33.0	71.0
5	3.5	1.3	0.3	17	6.7	2.1	4.7
6	4.98	0.91	0.22	17	6.78	2.96	3.82
8	-2.48	0.41	0.10	17	-1.63	-3.40	1.77
9	0.24	0.34	0.08	17	1.02	-0.36	1.38
10	0.00	0.73	0.18	17	1.56	-1.39	2.95

\* See Table 5.4 for a list of variables.

high  $\text{CO}_2$  content; the pH of Tufa Spring is 7.10. Much lower  $\text{PCO}_2$ 's in Bubbling Springs and Moraine Spring waters mean that these are capable of considerably less solution and so have lower hardnesses. In addition a reduced concentration of hydrogen ions, because of a lower  $\text{PCO}_2$ , give higher pH's of 7.8 and 8.0 respectively. The fact that Moraine Spring is saturated with respect to calcite while Bubbling Springs is not can probably be explained by differences in their inputs. All of the water emerging at Moraine Spring is believed to be derived from infiltration water, none from sinking stream water. Moraine Spring is therefore a diffuse flow spring (Shuster & White 1971) and its water has likely had a relatively long residence time in the limestone aquifer. Like Tufa Spring which also appears to be of diffuse flow type, the water temperature is clearly related to mean annual conditions in the Nahanni region. Moraine Spring with a temperature of  $2.3^\circ\text{C}$  and Tufa Spring with a temperature of  $2.0^\circ\text{C}$  are much colder than Bubbling Springs which has a temperature of  $4.7^\circ\text{C}$ . Water emerging at Bubbling Springs is believed to have had a shorter residence time in the limestone aquifer than that emerging at the other two spring points. Bubbling Springs discharges water from the aquifer that has been added via both diffuse and conduit inputs; in fact the bulk of the discharge from Bubbling Springs which is thought to be predominantly of conduit flow type may be derived from stream inputs. This fact would also explain the slightly low  $\log \text{PCO}_2$  in Bubbling Springs as opposed to Moraine Spring waters. That Tufa Spring waters are not saturated with respect to calcite despite the fact that the spring is of diffuse

(ii) Pool and Pond Waters.

Four main categories of pool and pond waters have been identified in the Nahanni on the basis of surficial and bedrock geological environment (Table 5.3). The mean chemical characteristics of these water categories are shown in Table 5.16. Pools and ponds derive their water from the local environment. In general the water that flows into ponds has been in contact with soils and their content of carbon dioxide so that a relationship between soil  $PCO_2$  and water  $PCO_2$  is to be expected. Examination of Table 5.14 shows that there is in fact a broad relationship. Ponds on shale have an average  $\log PCO_2$  of -2.81, soils nearby an average of -2.39; ponds on limestone a  $\log PCO_2$  of -3.24, soils -2.90; ponds on till-mantled limestone -2.75, soils -3.01; and ponds on sandy glacial drift -3.24 and soils -3.23. However it is noticeable that in three out of the four pond categories  $\log PCO_2$  in waters is less than  $\log PCO_2$  in soils, while for till-covered limestone the soil  $CO_2$  mean is considered to be low for reasons that have already been given. In fact this is to be expected for a second process clearly operates in determining  $PCO_2$  in pond and pool waters and that is the tendency to equilibrate with atmospheric  $PCO_2$ . It is evident that the  $PCO_2$  of pond waters results from first equilibration with soil  $PCO_2$  and second from loss of  $CO_2$  to the atmosphere.

The chemistries of the four pond types relate to the  $CO_2$  content and to the geology of the environment in which they are found. Ponds on limestone, because they have contact with carbonate bedrock,

Table 5.16. Mean Chemical Characteristics of Pond Water Types in the Nahanni Karst.

VARIABLE NUMBER*	MEAN	STANDARD DEVIATION	STANDARD ERROR OF MEAN	SAMPLE SIZE	MAXIMUM VALUE	MINIMUM VALUE	RANGE
<u>Ponds on Limestone</u>							
1	10.6	4.7	0.7	50	18.5	1.0	17.5
2	8.13	0.25	0.04	50	8.55	7.30	1.25
3	73.0	17.9	2.5	50	122.0	32.0	90.0
4	11.1	6.5	0.9	50	31.0	2.0	29.0
5	8.3	3.9	0.5	50	18.7	2.1	16.6
6	1.66	0.49	0.07	50	3.15	0.68	2.46
8	-3.24	0.30	0.04	50	-2.25	-3.88	1.63
9	-0.23	0.33	0.05	50	0.62	-1.46	2.08
10	-1.30	0.69	0.10	50	0.42	-3.53	3.95
<u>Ponds on Till-Covered Limestone</u>							
1	14.1	3.4	1.3	7	17.0	7.0	10.0
2	7.55	0.48	0.18	7	8.20	6.95	1.25
3	56.3	31.3	11.8	7	113.0	26.0	87.0
4	15.1	5.2	2.0	7	23.0	8.0	15.0
5	3.6	1.2	0.5	7	5.5	2.0	3.5
6	1.35	0.71	0.27	7	2.62	0.57	2.05
8	-2.75	0.50	0.19	7	-2.25	-3.55	1.19
9	-0.97	0.70	0.26	7	0.02	-1.78	1.80
10	-2.47	1.39	0.52	7	-0.50	-4.08	3.58
<u>Ponds on Shale</u>							
1	18.6	1.1	0.5	4	19.5	17.0	2.5
2	6.57	0.82	0.41	4	7.50	5.50	2.00
3	7.0	4.2	2.1	4	11.0	2.0	9.0
4	3.0	2.0	1.0	4	5.0	0.5	4.5
5	2.7	0.9	0.4	4	4.0	2.0	2.0
6	0.14	0.11	0.06	4	0.27	0.03	0.24
8	-2.81	0.45	0.22	4	-2.26	-3.30	1.04
9	-3.78	1.55	0.77	4	-2.14	-5.81	3.67
10	-7.96	3.21	1.60	4	-4.62	-12.22	7.60
<u>Ponds on Sandy Glacial Drift</u>							
1	19.2	2.2	0.7	9	23.5	16.0	7.5
2	8.08	0.51	0.17	9	8.80	7.40	1.40
3	57.7	23.8	7.9	9	95.0	20.0	75.0
4	12.4	5.5	1.8	9	23.0	5.0	18.0
5	5.2	2.6	0.9	9	10.6	2.2	8.5
6	1.38	0.54	0.18	9	2.16	0.51	1.65
8	-3.24	0.41	0.14	9	-2.63	-3.86	1.23
9	-0.29	0.83	0.27	9	0.66	-1.71	2.37
10	-1.24	1.55	0.52	9	0.57	-3.81	4.38

\* See Table 5.4 for a list of variables.

contain the most material in solution and have the highest pH of the four groups, total hardness is 84 ppm.  $\text{CaCO}_3$  and pH is 8.1. They are very nearly saturated with respect to calcite  $SI_C = -0.23$  and undersaturated with respect to dolomite  $SI_D = -1.30$ . Ponds on sandy glacial material in limestone canyons also have a relatively high dissolved content for the sandy drift has a content of soluble material. Also, many ponds are recharged by waters that flow from limestone screens. These ponds have a total hardness of 70 ppm.  $\text{CaCO}_3$ , less than that of ponds on limestone because of the lower  $\text{CO}_2$  content and they have a similar pH of 8.1. Ponds on glacial material are also similarly close to saturation with respect to calcite  $SI_C = -0.29$  and undersaturated with respect to dolomite  $SI_D = -1.24$ .

Ponds on till contain more  $\text{CO}_2$  than either ponds on limestone or ponds on glacial drift but because of restricted contact with limestone they only have a hardness of 71 ppm.  $\text{CaCO}_3$ . The excess carbon dioxide means that these waters are still aggressive ( $SI_C = -0.97$ ,  $SI_D = -2.47$ ) and they have a low pH of 7.5. Ponds on shale have virtually no contact with soluble material as indicated by their very low hardness of 10 ppm.  $\text{CaCO}_3$ . These waters contain large amounts of  $\text{CO}_2$  as they are highly undersaturated, ( $SI_C = -3.78$ ;  $SI_D = -7.96$ ) and are acid, pH = 6.6.

The chemical characteristics of pond waters can then be explained in terms of soil  $\text{PCO}_2$ , partial equilibration with atmospheric  $\text{PCO}_2$  levels and availability of soluble material.

(iii) Lake Waters.

The chemistries of lake waters (Table 5.17) are essentially the products of the same controls that have just been outlined for pool and pond waters. The  $\text{CO}_2$  contents of lake waters are essentially similar to those of pond waters in the same environment. For instance, ponds on shale and lakes on shale have average  $\log \text{PCO}_2$ 's of -2.81 and -3.00 respectively, ponds and lakes on limestone -3.24 and -3.32, ponds and lakes on sandy glacial drift -3.24 and -3.24. Differences in water chemistry are apparent however between ponds and lakes and perhaps these differences should be outlined here.

Lakes on shale, at least the ones sampled in 1972 and 1973, have much higher hardnesses than do ponds. This is because the large lakes on shale in the Nahanni have headwater inputs which come from regions of carbonate rock. Ponds on the other hand derive their water entirely from shale regions. This explains the higher average pH of lakes and their lower degree of undersaturation with respect to both calcite and dolomite. Differences between ponds on limestone and the only semi-permanent lake on limestone, Raven Lake, result from differences in their water supply. Raven Lake is supplied by groundwater which quickly loses  $\text{CO}_2$  to the atmosphere under subaerial conditions and tends towards saturation with respect to both calcite and dolomite, ( $\text{SI}_C = +0.14$ ;  $\text{SI}_D = -0.08$ ). The low undersaturation with respect to dolomite suggests that the groundwaters have contact with this rock. A lens of dolomite has been discovered in the north wall of Raven Canyon, a karst street occupied by the lake. The higher hardness of Raven Lake when

Table 5.17. Mean Chemical Characteristics of Lake Water Types in the Nahanni Karst.

VARIABLE NUMBER*	MEAN	STANDARD DEVIATION	STANDARD ERROR OF MEAN	SAMPLE SIZE	MAXIMUM VALUE	MINIMUM VALUE	RANGE
<u>Lakes Entirely in Contact with Limestone</u>							
1	11.2	1.8	1.2	2	12.5	10.0	2.5
2	8.30	0.00	0.00	2	8.30	8.30	0.00
3	90.5	6.4	4.5	2	95.0	86.0	9.0
4	37.5	3.5	2.5	2	40.0	35.0	5.0
5	2.4	0.1	0.0	2	2.4	2.4	0.1
6	2.02	0.29	0.21	2	2.22	1.81	0.41
8	-3.32	0.06	0.04	2	-3.28	-3.36	0.08
9	0.14	0.01	0.01	2	0.15	0.13	0.02
10	-0.08	0.03	0.02	2	-0.06	-0.10	0.04
<u>Lakes on Sandy Glacial Material in Contact with Limestone</u>							
1	16.5	1.8	0.9	4	18.0	14.9	3.1
2	8.26	0.16	0.08	4	8.40	8.05	0.35
3	77.7	9.4	4.7	4	85.0	64.0	21.0
4	18.5	9.0	4.5	4	28.0	9.0	19.0
5	5.1	2.7	1.4	4	9.0	3.0	5.9
6	2.02	0.43	0.21	4	2.56	1.59	0.97
8	-3.24	0.11	0.05	4	-3.11	-3.37	0.26
9	0.16	0.24	0.12	4	0.38	-0.16	0.54
10	-0.33	0.63	0.31	4	0.29	-1.01	1.30
<u>Lakes on Shales</u>							
1	16.2	1.7	0.5	10	19.0	14.0	5.0
2	7.76	0.30	0.09	10	8.20	7.35	0.85
3	52.2	18.3	5.8	10	79.0	31.0	48.0
4	24.7	11.2	3.5	10	48.0	12.0	36.0
5	2.3	0.6	0.2	10	3.0	1.2	1.8
6	1.14	0.33	0.10	10	1.66	0.75	0.90
8	-3.00	0.35	0.11	10	-2.57	-3.46	0.89
9	-0.75	0.34	0.11	10	-0.38	-1.52	1.14
10	-1.83	0.68	0.22	10	-1.12	-3.30	2.18
<u>Lakes on Shale-Derived Alluvium in Contact with Limestone</u>							
1	9.6	3.6	1.1	11	15.0	4.0	11.0
2	7.68	0.22	0.07	11	8.00	7.35	0.65
3	87.5	25.2	7.6	11	133.0	43.0	90.0
4	24.0	13.3	4.0	11	47.0	12.0	35.0
5	4.2	1.7	0.5	11	7.4	2.2	5.2
6	1.99	0.53	0.16	11	2.82	0.94	1.88
8	-2.71	0.19	0.06	11	-2.42	-3.06	0.64
9	-0.55	0.42	0.13	11	0.09	-1.46	1.55
10	-1.66	0.90	0.27	11	-0.29	-3.45	3.16

\* See Table 5.4 for a list of variables.

compared to ponds (128 ppm. to 84 ppm.  $\text{CaCO}_3$ ) probably relates to a reasonable residence time for the groundwaters that supply the lake.

Ponds on sandy glacial material generally have a lower hardness than lakes on the same material. This is easily explained for in fact most of the lakes in such environments directly abut limestone walls or screes and are also supplied by some water from limestone areas. Apart from this difference these two water types have very similar characteristics.

(iv) Stream Waters.

Stream waters on shale do in general have a higher  $\text{PCO}_2$  than those on limestone and each appears to be related to soil  $\text{PCO}_2$  in the two environments. Mean log  $\text{PCO}_2$  in streams on limestone is -2.93, that in soils on limestone -2.90 - a very close agreement. Mean log  $\text{PCO}_2$  in streams on shale is -2.72, that in soils -2.39. Differences in chemistry also relate to the availability of soluble material in the local environment (Table 5.18). Average total hardness of streams on limestone is 110 ppm., that of streams on shale 60 ppm.  $\text{CaCO}_3$ . In fact the relatively high hardnesses of streams on shale is related to the fact that many streams have headwaters in limestone areas that are heavily drift covered. The higher  $\text{PCO}_2$  and lower hardness of streams on shale means that these have a lower pH than those on limestone (7.4 to 7.9) and are less saturated ( $\text{SI}_C$  -1.45 to -1.39;  $\text{SI}_D$  -3.34 to -1.50). The fact that streams from shale often flow directly on to limestone has been important in landform development in the Nahanni region for clearly these waters highly aggressive to  $\text{CaCO}_3$  and are



Table 5.18. Mean Chemical Characteristics of Stream Water Types in the Nahanni Karst.

VARIABLE NUMBER*	MEAN	STANDARD DEVIATION	STANDARD ERROR OF MEAN	SAMPLE SIZE	MAXIMUM VALUE	MINIMUM VALUE	RANGE
<u>Streams on Limestone</u>							
1	5.6	4.4	0.7	44	25.5	1.0	24.5
2	7.91	0.29	0.04	44	8.60	7.20	1.30
3	90.7	23.4	3.5	44	146.0	34.0	112.0
4	19.4	14.2	2.1	44	65.0	3.0	62.0
5	7.4	6.7	1.0	44	33.1	1.4	31.7
6	2.11	0.65	0.10	44	3.84	0.76	3.08
8	-2.93	0.30	0.04	44	-2.05	-3.49	1.44
9	-0.39	0.44	0.07	44	0.41	-1.74	2.15
10	-1.50	0.91	0.14	44	0.31	-4.13	4.44
<u>Streams on Shales</u>							
1	10.9	6.3	1.3	24	21.5	1.0	20.5
2	7.38	0.65	0.13	24	8.40	5.70	2.70
3	44.1	24.7	5.0	24	100.0	8.0	92.0
4	15.6	7.9	1.6	24	33.0	2.0	31.0
5	2.9	7.3	0.3	24	7.5	1.1	6.4
6	1.08	0.62	0.13	24	3.03	0.19	2.84
8	-2.72	0.47	0.09	24	-1.72	-3.65	1.93
9	-1.47	1.22	0.25	24	0.02	-4.48	4.50
10	-3.34	2.28	0.48	24	-0.42	-8.97	8.55

\* See Table 5.4 for a list of variables.

capable of dissolving considerable quantities of limestone very quickly and in highly localized belts near the shale/limestone contact.

(v) Soil Waters.

As Table 5.14 shows and as would be expected, soil waters on both limestone and shale are equilibrated with log  $PCO_2$  levels close to the maximums that have been measured. Soil waters on limestone have a mean log  $PCO_2$  in them of -2.43; the maximum measured in limestone soils is -2.37 and the mean -2.90. Soil waters on shale have a mean log  $PCO_2$  of -1.96 while soils have a maximum log  $PCO_2$  of -1.65 and a mean of -2.39. Because of the very high  $CO_2$  contents of these waters those on limestone have a very high dissolved solid content namely 172 ppm.  $CaCO_3$  while those on shale, where soluble rock is scarce, have very low pH's which average 5.8 and low total hardnesses of 24 ppm. Soil waters on limestone are close to saturation, ( $SI_C = -0.08$ ,  $SI_D = -1.06$ ) while those on shale are highly undersaturated, ( $SI_C = -4.50$ ,  $SI_D = -9.08$ ). Mean chemical characteristics of both water types are given in Table 5.19.

(vi) Seepage Waters on Limestone.

Seepage waters on limestone with a mean log  $PCO_2$  of -3.14 clearly derive their  $CO_2$  content from soils on limestone but lose  $CO_2$  as they percolate from the soils through fissures in the limestone or down exposed limestone surfaces. Contact with limestone and soil  $CO_2$  means they have relatively high hardnesses of 131 ppm., high pH on average 8.1 and are close to saturation with respect to calcite,

Table 5.19. Mean Chemical Characteristics of Soil Water Types in the Nahanni Karst.

VARIABLE NUMBER*	MEAN	STANDARD DEVIATION	STANDARD ERROR OF MEAN	SAMPLE SIZE	MAXIMUM VALUE	MINIMUM VALUE	RANGE
<u>Soil Water in Limestone Areas</u>							
1	10.7	0.3	0.2	2	11.0	10.5	0.5
2	7.65	0.07	0.05	2	7.70	7.60	0.10
3	154.5	2.1	1.5	2	156.0	153.0	3.0
4	18.0	5.7	4.0	2	22.0	14.0	8.0
5	8.9	2.9	2.1	2	11.0	6.8	4.1
6	3.41	0.25	0.18	2	3.59	3.23	0.36
8	-2.43	0.11	0.07	2	-2.36	-2.51	0.15
9	-0.08	0.06	0.04	2	-0.04	-0.12	0.08
10	-1.06	0.03	0.02	2	-1.04	-1.09	0.05
<u>Soil Water in Shale Areas</u>							
1	6.9	2.8	1.2	5	11.0	4.5	6.5
2	5.79	1.08	0.48	5	7.00	4.10	2.90
3	14.6	11.6	5.2	5	30.0	2.0	28.0
4	9.4	5.6	2.5	5	16.0	2.0	14.0
5	1.4	0.4	0.2	5	1.9	0.9	1.0
6	0.25	0.18	0.08	5	0.48	0.01	0.47
8	-1.96	0.62	0.28	5	-1.21	-2.79	1.58
9	-4.50	2.19	0.98	5	-2.42	-8.23	5.81
10	-9.08	4.29	1.92	5	-5.07	-16.41	11.34

\* See Table 5.4 for a list of variables.

Table 5.20. Mean Chemical Characteristics of Seepage Water of Limestone in the Nahanni Karst.

VARIABLE NUMBER*	MEAN	STANDARD DEVIATION	STANDARD ERROR OF MEAN	SAMPLE SIZE	MAXIMUM VALUE	MINIMUM VALUE	RANGE
1	6.2	3.1	0.9	12	10.0	0.7	9.3
2	8.14	0.18	0.05	12	8.41	7.88	0.53
3	106.4	25.3	7.3	12	146.0	68.0	78.0
4	24.7	25.4	7.3	12	85.0	2.0	83.0
5	11.5	16.4	4.7	12	61.4	1.3	60.1
6	2.25	0.68	0.20	12	3.39	1.14	2.25
8	-3.14	0.28	0.08	12	-2.72	-3.69	0.97
9	-0.06	0.24	0.07	12	0.42	-0.37	0.79
10	-0.88	0.41	0.12	12	-0.32	-1.79	1.47

\* See Table 5.4 for a list of variables.

$SI_C = -0.05$ , and undersaturated with respect to dolomite,  $SI_D = -0.88$ . Chemical characteristics of seepage waters in the Nahanni are given in Table 5.20.

The evidence presented clearly demonstrates that the chemistry of water in the Nahanni is related to soil  $PCO_2$  levels in the local environment, to the availability of soluble material and to whether  $CO_2$  is lost to the atmosphere as the water equilibrates with new conditions once it leaves the soil. The previous discussion has emphasized that the  $PCO_2$  which a natural water is subjected to is not static but extremely dynamic and examples have been given of changes in water chemistry that take place when a water loses  $CO_2$  to the atmosphere. Two examples of dynamic  $CO_2$  - water relationships will now be discussed. The first example is one of tremendous and rapid  $CO_2$  loss to the atmosphere and the chemical changes that result, the second one of gains and losses of  $CO_2$  throughout a surface water system and again the resulting changes in chemistry.

(b) Changes in the Chemistry of Tufa Spring Waters Under Atmospheric Conditions and Reasons for Tufa Deposition in this Cold Sub-arctic Spring.

♦ As might be expected from the fact that many springs with recharge areas on shale supersaturate with respect to calcite and dolomite once they encounter atmospheric as opposed to subsurface conditions, tufa deposition is common. It is known that spring water close to the orifice can differ considerably in chemistry from surface water some distance from it and waters very often supersaturate but precipitation

of calcite does not always follow. A short study of Tufa Spring water was made in order to determine how its chemical characteristics change after it emerges from bedrock. It was hoped that such a study might isolate the reasons for tufa deposition. Spring water was therefore sampled and analyzed where it issued from bedrock and at intervals along its surface course until it finally disappeared underground in the floor of First Polje.

Variations in the water chemistry of Tufa Spring waters as they adjust to subaerial conditions are shown in Figure 5.8. It is clear from these diagrams that considerable changes do occur. Temperature at the spring outlet was 2.0°C and this rose to 13.0°C where the water sank in First Polje, a distance of approximately 600 meters. Over the same distance the total hardness of the water dropped from 355 to 301 ppm.  $\text{CaCO}_3$  emphasizing the fact that the spring water deposits tufa in its bed. This overall drop in total hardness however hides what is really happening to the water chemistry for as Figure 5.8 shows, the calcium concentration in the stream drops while its magnesium concentration actually rises in fact from 302 - 229 ppm. and 53 - 72 ppm.  $\text{CaCO}_3$  respectively. At the same time the pH of the water rises from 7.1 up to 8.4.

Just exactly what brought about these changes is partially evident from an examination of changes in the carbon dioxide content of the spring water. On its emergence from bedrock the water is in equilibrium with a  $\log \text{PCO}_2$  level of -1.63 considerably higher than atmospheric conditions. At the same time the water has an  $\text{SI}_C$  value

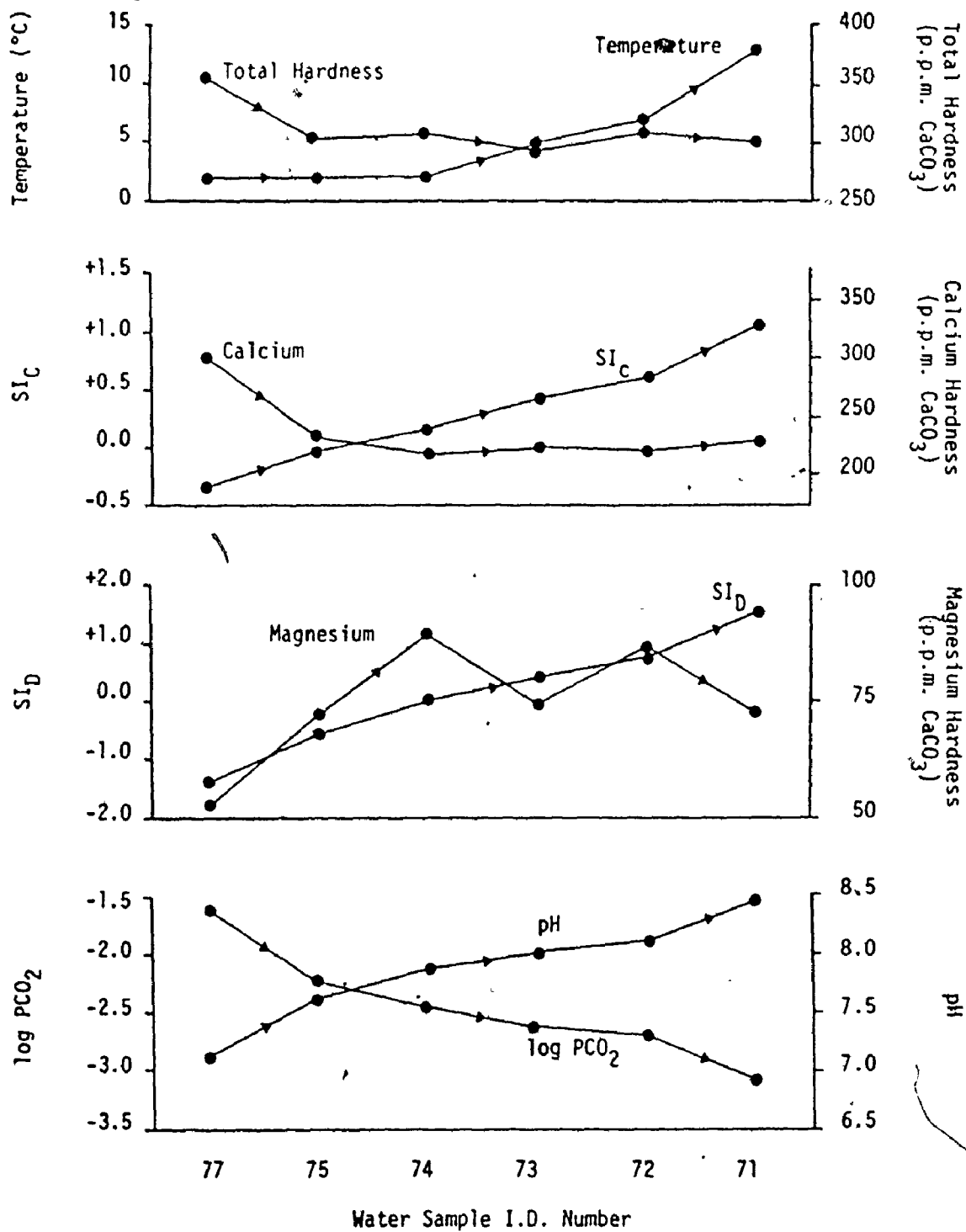



Figure 5.8. Changes in the chemistry of Tufa Spring waters under atmospheric conditions.

of -0.34 and a  $SI_D$  value of -1.35, it is therefore undersaturated with respect to both calcite and dolomite. Because the  $PCO_2$  of the water is substantially higher than that of the atmosphere,  $CO_2$  gas diffuses into the atmosphere and as Figure 5.8 shows, this is a very rapid process. Before it sinks Tufa Spring waters lose  $CO_2$  to the extent of a drop in  $\log PCO_2$  to -3.08, much closer to the atmospheric level. It is this tremendous loss of  $CO_2$  that explains the gradual rise in pH for the  $CO_2$  in the water forms carbonic acid which dissociates to give hydrogen ions. Loss in  $CO_2$  lowers the hydrogen ion concentration in the water, that is, it raises the pH. A loss in  $CO_2$  and an accompanying increase in pH means that the water loses some of its aggressivity towards carbonate minerals and therefore it becomes more saturated with respect to both calcite and dolomite. As Figure 5.8 clearly shows,  $SI_C$  and  $SI_D$  increase up to +1.04 and +1.60 respectively at the sink in First Polje, that is the waters are highly supersaturated with respect to both minerals. It should be noted that supersaturated conditions are neither uncommon nor contradictory in carbonate areas. They are attributable to the fact that  $CO_2$  loss from the water proceeds at a more rapid rate than the precipitation of calcite, and the inability of dolomite to precipitate under such conditions. In fact the tremendous supersaturation with respect to calcite has clearly induced precipitation in the form of tufa, but has not induced deposition of dolomite. As the figures show, as calcite is deposited, dolomite is picked up. This can partly be explained by the fact that the solution was still undersaturated with respect to this mineral for a period after

emergence from bedrock, however the solution proceeded to supersaturate with respect to dolomite.

Langmuir (1971) has pointed out that groundwaters from dolomite rocks frequently contain an excess of magnesium over calcium. He notes that this can come about only if the solution of dolomite is accompanied by concurrent precipitation of calcite and would necessarily lead to a calcium-deficient incongruent solution of dolomite. Wigley (1973) has considered this problem with reference to calcium-rich dolomite. His findings show that addition of dolomite to a solution saturated with respect to calcite will cause calcite to be precipitated if temperature and carbon dioxide conditions remain constant. Wigley notes that when this happens more calcite is precipitated than dolomite is dissolved. Wigley also notes that because of the highly ordered structure of ideal dolomite precipitation even for supersaturated conditions is unlikely. It is apparent therefore that Tufa Spring loses  $\text{CO}_2$  and saturates with respect to calcite; at the same time it picks up dolomite. Eventually calcite is deposited and dolomite continues to dissolve until the water is highly supersaturated with respect to this mineral. From the spring point to the sink some 73 ppm.  $\text{CaCO}_3$  calcium is lost and is the same distance 19 ppm.  $\text{CaCO}_3$  magnesium is picked up. As Wigley noted, the incongruent solution of dolomite results in more calcite being deposited than dolomite dissolved. On the whole therefore the changes in the chemistry of Tufa Spring, as it changes from a sub-surface to a surface flow, can be accounted for by first, a rise in





temperature which encourages loss in  $\text{CO}_2$  due to the instability of  $\text{CO}_2$  in the water at partial pressures considerably higher than atmospheric and thirdly the incongruent solution of dolomite present in the Nahanni limestones.

In most cases spring waters lose  $\text{CO}_2$  to the atmosphere. Shuster & White (1971) attempted to determine how long it takes a spring water to equilibrate with atmospheric  $\text{CO}_2$  and to determine the effect of this change on the equilibrium of the water with respect to calcium carbonate. Elk Creek, which at the time of sampling derived all of its flow from Elk Creek Rising, was sampled at 200 m. intervals on November 3rd, 1968. They found that the  $\text{Ca}^{2+}$  ion concentration changed by less than 2 ppm. over the 2000 m. of sampling while the  $\text{HCO}_3^-$  ion concentration showed no change over the first 1200 m. and increased by only 6 ppm. over the last 800 m. The pH however increased steadily until it stabilized after 800 m. At the same time the  $\log \text{PCO}_2$  in the water dropped from -2.46 to -3.22 at 800 m. Furthermore as the water lost  $\text{CO}_2$  it approached saturation with respect to calcite until eventually it was supersaturated. The  $\text{SI}_c$  level remained constant, however from 800 - 2000 m. indicating that the water by this point was more or less in equilibrium with atmospheric carbon dioxide levels. Shuster & White report that the supersaturation of Elk Creek was never sufficient to nucleate  $\text{CaCO}_3$  since no travertine deposits were observed in the creek bed. From diagrams presented by these writers it is apparent that Tufa Creek supersaturates to a greater degree than does Elk Creek, maximum  $\text{SI}_c$  values are +1.04 and approximately +0.25 respectively. Also,  $\text{CO}_2$  in Tufa Spring waters is

considerably more out of equilibrium with atmospheric conditions than is Elk Creek Rising. The  $\log PCO_2$  in Elk Creek Rising water is on average -2.54 while that in Tufa Spring is -1.63. The probable more rapid loss of  $CO_2$  from Tufa Spring waters and their higher degree of supersaturation in relation to waters of Elk Creek Rising may explain tufa deposition in the former case and not in the latter.

Barnes (1965) examined the mechanisms that operate in the deposition of tufa by Birch Creek, a spring-fed creek under an arid climate in California. Barnes notes that the relatively sluggish mineral-water reactions controlling the groundwater state are no longer effective when the water reaches the surface as a spring, for there is an increase in transport rate and rapidly changing ambient conditions. Groundwater contributions to Birch Creek come from four sources: a clear seep, an iron depositing seep and two headwater springs. Barnes calculated  $PCO_2$  and  $IAP_C/K_C$  for each of these waters. Expressed as  $\log PCO_2$  and  $SI_C$ , but without recalculating the data using revised equilibrium constants and taking other complicating factors into account, these values are  $\log PCO_2$  -2.92, -2.28, -2.15 and -2.19;  $SI_C$  +0.62, +0.17; -0.02 and -0.10 respectively. Barnes examined changes in the  $IAP_C/K_C$  of Birch Creek waters downstream from the springs and seeps. Extracting approximate data from Barnes' diagrams, the max.  $SI_C$  of creek water changed downstream of the springs from +0.06 through +1.00, +1.15 to +1.23. In 1962 the changes were from +0.54 through +0.84, +1.00 to +0.95. In other words Birch Creek waters were becoming more and more supersaturated with respect to calcite downstream of the

springs. As Barnes notes, this is the result of  $\text{CO}_2$  loss from the waters. The question is why do some springs deposit tufa and others not. The answer may be contained within an observation made by Barnes (1965) who found that for water samples where  $\text{IAP}_C / K_C \leq 4$  (ie  $\text{SI}_C \leq +0.60$ ) there was no significant difference in the results of calcium analysis of acidified or non-acidified duplicate samples. In some samples however with  $\text{SI}_C > 0.60$  calcium was found to be metastable and some came out of solution in samples not acidified. This admittedly qualitative evidence suggests that before calcite is precipitated by natural waters it must be supersaturated to a certain level - from Barnes' evidence  $\text{SI}_C = +0.60$ . Clearly from the evidence already presented, Tufa Creek waters have  $\text{SI}_C$  values as high as +1.04 while Birch Creek has an approximate maximum  $\text{SI}_C$  of +1.23. Both of these streams deposit tufa. On the other hand the highest  $\text{SI}_C$  value given for Elk Creek waters by Shuster & White (1971) is +0.25 and this creek does not deposit tufa.

Although it is tempting to argue that tufa deposition requires only a sufficiently high level of supersaturation with respect to calcite, it is true as Barnes (1965) has pointed out that although thermodynamic potentials exist for the loss of  $\text{CO}_2$  to the air and for the precipitation of calcite, it would be dangerous to conclude either reaction to be entirely free of organic agencies. Tufa in both Birch and Tufa Creeks is deposited around vegetation leaves and stems or scattered through algal colonies. Barnes has noted that the profuse vegetation growth along the bed of Birch Creek may be related to the sizeable supply of carbon dioxide, needed for photosynthesis, that is

contained in the creek waters. He notes vegetal effects in the hourly change of  $PCO_2$  in the water. Because vegetation aids in the rapid removal of  $CO_2$  from these waters it may encourage calcite deposition; however it still seems likely that the principal reason for tufa deposition in Tufa Creek is the rapid loss of  $CO_2$  to the atmosphere and the great supersaturation of the waters.

The Tufa Springs of First Polje, Nahanni, are extremely interesting because of their considerable contents of carbonate minerals in solution and also because they represent one of the few known cold, tufa depositing springs in a sub-arctic terrain. That tufa can be deposited by spring waters in a variety of climates suggests that such deposition is not related to climate but universally to excessive supersaturation as a result of rapid loss of  $CO_2$  when atmospheric conditions are encountered.

(c) Spatial Variations in the Chemistry of the Mosquito Creek Drainage System.

The Mosquito Creek drainage system shown in Figure 5.9 is directly east of First Polje. Along the creek are a number of lakes the longest of which, Mosquito Lake is more than one mile in length. The headwaters of the stream system traverse a drift-mantled limestone terrain before flowing into Mosquito Lake on drift-mantled shale. The flow out of Mosquito Lake which is at an altitude of approximately 3,050 ft., has cut a steep, narrow gorge in shales of the Simpson Formation and closer to First Polje in the upper beds of the underlying Nahanni Limestone Formation. Mosquito Creek eventually sinks into a number of ponors in the limestone in the floor of First Polje at an

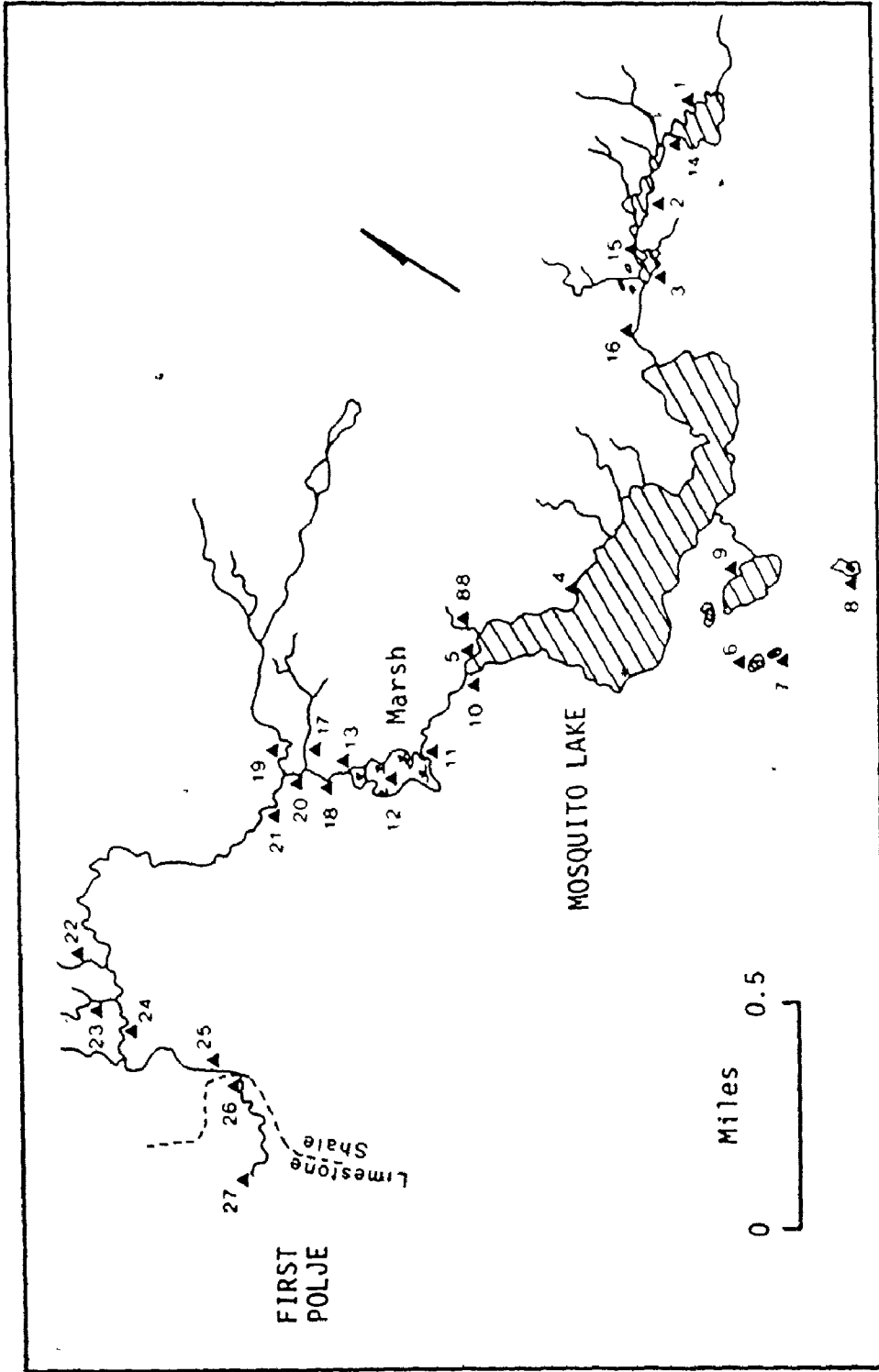


FIGURE 5.9. Spatial Variations in Water Chemistry within the Mosquito Creek Drainage Basin: Sample Locations.

x

altitude of close to 2,600 ft. and therefore from headwaters to sink it drops approximately 500 ft. Shortly after passing from shale to limestone the stream passes over a series of waterfalls, the highest being 40 - 50 ft. high. On limestone the stream flows in a very steep sided gorge with almost vertical side walls.

During the summer of 1972 samples were taken of the various water types evident in the Mosquito Creek drainage basin: stream, marsh, pond and lake waters were all analyzed for their chemical contents. Sites were chosen so as to monitor spatial variations in the chemical characteristics of the main streams and tributaries. Pond and marsh waters were examined in order to assess their contribution, if any, to stream chemical characteristics. Most samples were collected and analyzed in a single day so that hydrological conditions were constant during sampling and variations in discharge would not have to be considered in the interpretation of the chemical data. Sample sites and sample numbers are shown in Figure 5.9 while relevant chemical data for each site is given in Table 5.21.

The headwaters of Mosquito Creek are interrupted by a series of small lakes and drainage is in general indeterminate on a drift mantled limestone. As would be expected in this generally marshy terrain, log  $PCO_2$  in waters is high ranging from -3.09 to -2.57 (samples 1, 14, 2, 15, 3, 16). Contact with limestone in the drift means that total hardnesses may be high (44 - 118 ppm.  $CaCO_3$ ) while the range in pH is from 7.3 to 7.7. All waters are undersaturated with respect to calcite  $SI_C$  varying from -1.52 up to -0.68.

Table 5.21. Mosquito Creek Sample Sites and Water Chemistry Data.\*

SAMPLE ID.	SAMPLE DESCRIPTION	TOTAL HARDNESS ppm (CaCO <sub>3</sub> )	pH	SI <sub>c</sub>	log PCO <sub>2</sub> <sup>a</sup>
1	Lake	47	7.35	-1.52	-2.71
14	Stream	44	7.70	-1.14	-3.09
2	Lake	111	7.50	-0.71	-2.57
15	Stream	103	7.50	-0.72	-2.60
3	Lake	118	7.60	-0.69	-2.73
16	Stream	88	7.65	-0.68	-2.81
4	Lake	67	8.10	-0.42	-3.31
5	Lake	56	8.10	-0.50	-3.37
6	Pond	14	6.70	-3.18	-2.67
7	Pond	7.5	6.60	-3.99	-3.02
8	Pond	2.5	5.50	-5.81	-2.26
9	Lake	16	7.50	-2.14	-3.30
88	Stream	17	5.70	-4.48	-1.72
10	Stream	57	8.20	-0.38	-3.46
12	Stream in marsh	56	7.50	-1.04	-2.74
13	Stream	58	7.40	-1.12	-2.63
18	Stream	59	7.60	-0.92	-2.82
17	Stream	17	6.25	-3.70	-2.19
19	Stream	32	7.30	-2.09	-2.85
22	Stream	59	7.55	-1.34	-2.83
23	Stream	40	7.10	-2.09	-2.58
20	Stream	61	7.50	-1.07	-2.72
21	Stream	60	7.50	-1.09	-2.73
24	Stream	69	7.60	-1.01	-2.81
25	Stream after waterfall	100	8.10	-0.27	-3.20
26	Stream	102	8.30	-0.04	-3.38
27	Stream at sink	105	8.30	-0.04	-3.38

Once the headwaters enter Mosquito Lake, however, there is a marked change in their chemical characteristics. The water of Mosquito Lake (samples 4 and 5) has a lower total hardness of 61 ppm., a higher pH of 8.1 and is more saturated with respect to calcite -  $SI_C = -0.46$ . Such a radical change in chemistry is relatively simple to explain for two main processes are operating. First when the headwaters leave their marshy environment they have a  $PCO_2$  in them in excess of that in the atmosphere. In equilibrating with atmospheric conditions  $CO_2$  is lost. The  $\log PCO_2$  drops to -3.34 in the lake water which is very close to the atmospheric value of -3.52. Loss of  $CO_2$  reduces the acidity of the water and its potential to dissolve limestone and so there is a rise in pH and a move towards saturation with respect to calcite. Secondly, Mosquito Lake also collects water from the surrounding shale area. Ponds south of the lake (samples 6, 7, 8 and 9) all have very low hardnesses, low pH, are very much undersaturated with respect to calcite and are in equilibrium with high  $PCO_2$ . At least one of these pond waters is known to overflow into Mosquito Lake. After heavy rain there is rapid runoff of water into the lake via a number of small streams with characteristics similar to those listed for sample 88. Like the ponds these streams have low hardness, low pH, low saturation and are very aggressive. They work to dilute the waters of Mosquito Lake lowering hardness, pH and saturation but even these stream waters when added to the lake lose  $CO_2$  to the atmosphere. The effect of Mosquito Lake within the Mosquito Creek drainage basin is to permit loss of  $CO_2$ . It effectively lowers the solutional potential of waters entering it.



Mosquito Lake is drained only at its north west extremity where Mosquito Creek passes through a broad expanse of marshy terrain before passing through a gorge in shale and limestone to First Polje. The stream waters do not flow quickly through this marshy area but instead tend to mix with marsh waters. This process has been encouraged by the construction of a beaver dam where the creek leaves this marshy belt. The chemistry of the creek water changes dramatically as it passes through this marshy terrain. Upon entering the marsh the creek has a total hardness of 57 ppm., pH 8.2,  $SI_C$  -0.38 and  $\log PCO_2$  -3.46 (sample 10). By the time it leaves the marsh the creek has a hardness of 59 ppm., pH 7.6,  $SI_C$  -0.92 and  $\log PCO_2$  -2.82 (samples 12, 13 and 18). The creek waters have obviously picked up substantial amounts of  $CO_2$  in passing through the marsh where  $PCO_2$  in marsh waters is believed to be extremely high in such anaerobic conditions. This caused a lowering of pH as carbonic acid dissociated to give a higher hydrogen ion concentration and the water became effectively less saturated with respect to calcite.

After leaving the marsh, Mosquito Creek is joined by a number of small tributary streams which generally flow for only a short time after rain. These streams have low hardnesses (17 - 59 ppm.), their pH's range from 6.2 - 7.5, they are undersaturated with respect to calcite ( $SI_C$  is from -3.70 to -1.34) and they are in equilibrium with partial pressures of  $CO_2$  much above atmospheric ( $\log PCO_2$  is from -2.85 to -2.19). Their effect on the chemistry of the main stream as can be seen by comparing the characteristics of samples 18 and 21 in Table

5.21 is to lower the pH slightly, increase the  $\log PCO_2$  and reduce saturation without significantly changing hardness values. In fact as the main stream picks up soluble material from drift deposits along its banks it is diluted by addition of small amounts of lower hardness tributary water.

Just before it leaves shale to pass on to limestone bedrock, Mosquito Creek has a hardness of 69 ppm.  $CaCO_3$ , pH 7.6,  $SI_C$  -1.01 and  $\log PCO_2$  -2.81. As soon as the water encounters limestone its chemistry alters radically. As samples 25, 26 and 27 show, there is an increase in total hardness up to 105 ppm., an increase in pH to 8.3,  $\log PCO_2$  in the water decreases to -3.38 and the water approaches saturation with respect to calcite -  $SI_C = -0.04$ . Clearly as soon as soluble material was made available the stream picked up calcium carbonate and by so doing increased its hardness, its pH and brought the water closer to saturation. However because the  $PCO_2$  of the water was reduced it is apparent that a second process was operating. Loss of  $CO_2$  can largely be explained by the fact that almost as soon as Mosquito Creek passes on to limestone it passes over a 40 - 50 ft. waterfall and then a series of smaller ones. As the water tumbles over these obstructions it is aerated and loses  $CO_2$  to the atmosphere. As this happens pH rises and the water becomes more saturated. Clearly the changes in the chemistry of Mosquito Creek as it flows from shale to limestone can be explained by loss of  $CO_2$  and availability of soluble rock.

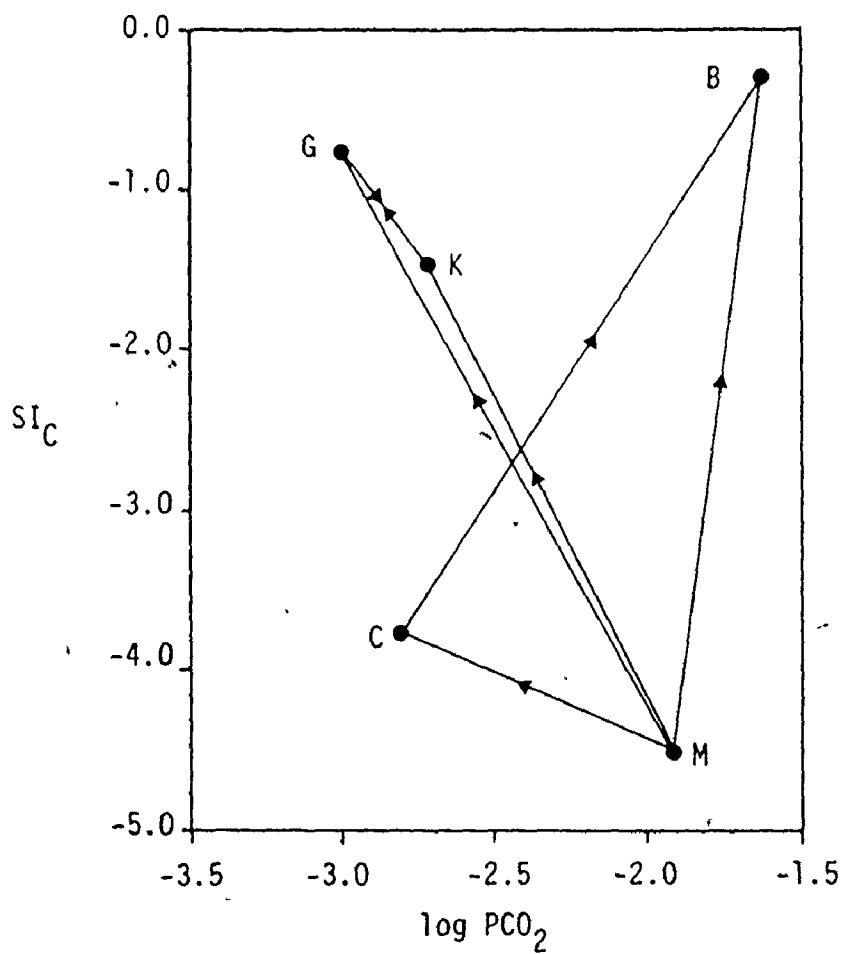
Detailed chemical analysis of waters in the Mosquito Creek drainage system has shown that waters vary not only on a temporal basis but also in a spatial sense. The chemical characteristics of waters seem to be controlled by the character of the environment, particularly the availability of soluble material, and also to changes in carbon dioxide, within any drainage system. It is clear that lakes and waterfalls act to remove  $\text{CO}_2$  from the water and make it less aggressive towards limestone while marshy terrains along the course act to enrich waters in  $\text{CO}_2$  and make them more aggressive. Mosquito Creek is a spatially dynamic chemical system.

Examination of carbon dioxide levels in soils and waters of the Nahanni has shown these to be related. In addition, examples have been given to illustrate that the  $\text{CO}_2$ -water relationship is a dynamic not a static one and that  $\text{CO}_2$  may be added or lost by a water as it moves vertically or laterally through a terrain. The question is, can we model the chemical changes that take place in any one environment, showing that if a water takes a particular path in its evolution its chemistry will change in a predictable way. Consideration will be given to this matter now.

## 6. Models of Chemical Interaction Between Waters in Similar Geological Environments.

### (a) The Drift-mantled Shale Environment.

Chemical interaction between water types in a given environment essentially involves changes in the  $\text{PCO}_2$  in the water and changes in saturation state or  $\text{SI}_c$ . Figure 5.10 is an attempt to model interactions



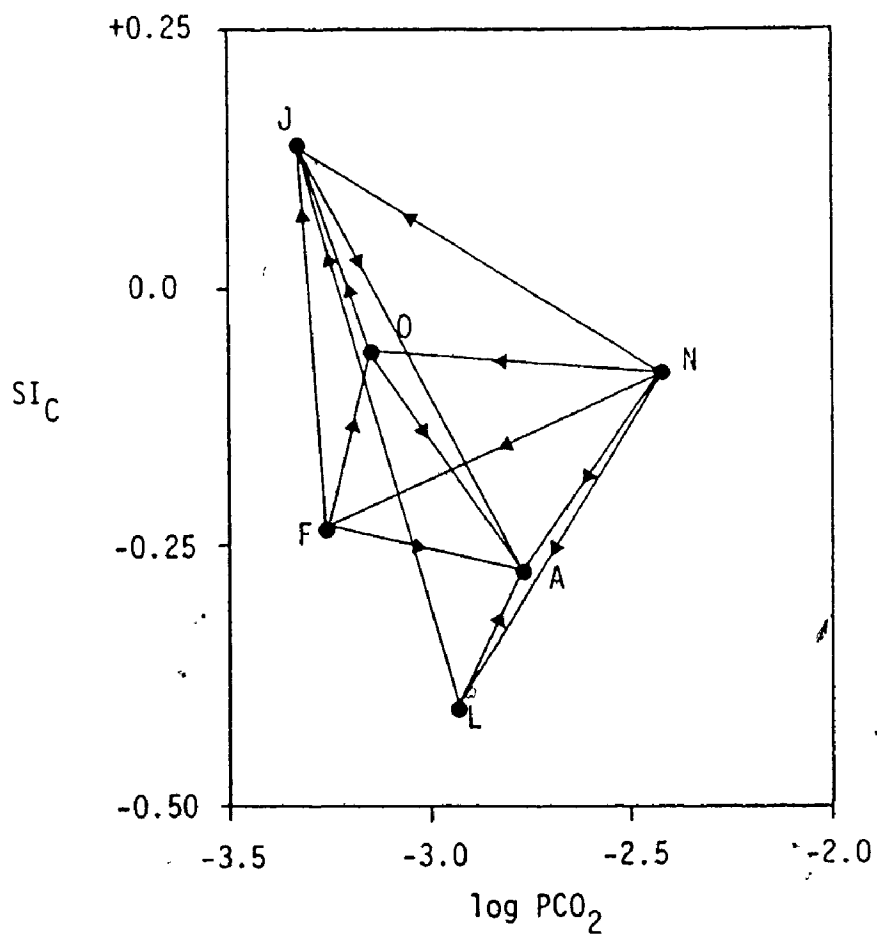
KEY: B Spring  
 C Ponds  
 G Lakes  
 K Streams  
 M Soil Waters

FIGURE 5.10. Chemical Interaction Between Waters in the Drift-mantled Shale Environment.

for a shale terrain. It shows very simply the fact that spring, pond, lake and stream waters are all supplied by water that has had contact with the soil. As the water moves from the soil into ponds, streams, and lakes it loses carbon dioxide and because of slightly more contact at least in the Nahanni environment with soluble minerals it becomes more saturated with respect to calcite. In fact the magnitude of this change for the moves from soil to both lakes and streams is clearly far less in reality than is depicted in Figure 5.10, for streams and lakes on shale used in calculating the means shown have some input from drift-covered limestone terrains. Streams flowing into lakes lose carbon dioxide and become more saturated while lake water outflow has the tendency to pick up  $\text{CO}_2$  and become less saturated with respect to calcite. In the shale environment soil water close to the surface also percolates through collapse breccia zones and in doing so has contact with high  $\text{PCO}_2$  deeper in the soil profile. Following contact with limestone, the water quickly moves towards saturation with respect to calcite. Pond waters also drain underground in the same manner and they have a similar subsurface history. Figure 5.10 therefore depicts the simple relationships that exist between waters in a shale environment and shows the changes that take place as waters move and fall into a new hydrological category.

(b) The Limestone Environment.

Figure 5.11 is an attempt to depict water chemistry interactions in a limestone terrain like the Nahanni. Clearly relationships are far more complex than those just outlined for the shale terrain. Soil



KEY: A Spring  
 F Ponds  
 J Lakes  
 L Streams  
 N Soil Water  
 O Seepage Water

FIGURE 5.11. Chemical Interaction Between Waters in the Limestone Environment.

water in a limestone area can move in any one of a number of directions either towards ponds, lakes, streams or springs or it may become seepage water. As Figure 5.11 clearly shows, whatever move is made the soil water tends to effectively have a lower  $PCO_2$  in it. In some case this is due to a real loss of  $CO_2$  to the atmosphere; in others such as the move from soil to spring it may be due to closed system evolution of waters (Drake & Wigley 1975). Normally a loss in  $CO_2$  should be accompanied by a move towards saturation as it was in the case of the shale environment, but with the Nahanni situation certain complications are introduced. First, many stream waters on limestone have headwaters in shale so that their chemistries are not entirely related to the limestone environment; streams on limestone therefore tend to be less saturated with respect to calcite than are soil waters. Because springs on limestone derive some of their water from sinking streams they too are less saturated than are soil waters. Pond waters too do not fit the pattern to be expected for in many situations these are not supplied purely by soil waters even via small streams. Many ponds in the Nahanni are supplied by melted drifted winter snow while others especially in the North Karst labyrinths rest on a shale-derived alluvium. Obviously the average  $SI_C$  of such ponds will be a little below the saturation level.

Apart from soil water interactions, other interactions are apparent in the limestone environment. For instance pond, lake, stream and seepage waters also pass underground at conduit and diffuse input points to become part of the groundwater. In relation to ponds, lakes and seepage waters the resulting groundwater mix is less saturated with

respect to calcite and is enriched in carbon dioxide while for streams only small differences are apparent, indicating the substantial contribution made to groundwater in this terrain by stream waters that sink when they encounter the limestone.

The other important set of interactions that may not be entirely obvious from Figure 5.11 is that relating to point J which is Raven Lake. It is thought to collect water from the soil, small amounts of seepage water, and pond and lake waters that have entered the aquifer and then emerged again into Raven Lake. Raven Lake is not supplied by any major direct surface inputs. In all cases as waters move towards Raven Lake they lose  $\text{CO}_2$  and become saturated with respect to calcite; at least this relationship seems to be uncomplicated.

Discussion of the chemical interactions of waters in two environments of the Nahanni that strictly speaking cannot be entirely divorced from each other's influence, has shown how dynamic regional water chemical characteristics are, and how virtually all changes involve gain or loss of only one substance - carbon dioxide gas. Evidence presented indicates that soil water is without doubt the most aggressive of the waters that can be identified in either terrain. As soil water becomes surface water it loses carbon dioxide, if it becomes diffuse-flow spring water it gains it, if it joins with predominantly conduit-flow spring water it loses it. Carbon dioxide in karst water without any doubt controls the extent of solution of limestone; any other variables are of extremely minor importance by comparison.



## 7. Nahanni Solution Rates Placed in a Regional Context.

Marked morphological differences between the karst landforms characteristic of humid tropical terrains and those of temperate, arctic and alpine climates have led to an examination of the magnitude of the solution process as a possible explanation. It is evident that enormous quantities of limestone have been removed to create the complex karst landscapes of tropical areas while substantially smaller amounts have been removed in the formation of poorly developed arctic and alpine karst terrains. In hot wet climates chemical reactions are thought to proceed quickly and the magnitude of the annual rainfall means that a considerable volume of rock is removed annually in solution. Because plant growth and decay is rapid and microbial activity intense in hot areas, soil carbon dioxide levels are thought to be higher than in colder climates. For this reason many workers feel that tropical karst waters are more aggressive, contain greater concentrations of solute and remove more material in solution per year than arctic waters. As to whether this is in fact the case will now be examined.

### (a) Solution Potential and the Actual Intensity of Solution in Different Climatic Environments.

In many karst terrains all of the water reaching the surface percolates underground and is finally discharged from the region via a number of springs. This is the case in the Nahanni for instance, where water is funnelled underground and ultimately reaches one of two springs which discharge it into major rivers. In cases like this all of the material removed in solution is present in spring waters. These

waters then, provide a useful measure of potential and actual solution in a karst area.\* Knowledge of spring discharges and solute relationships also allows calculation of the amount of rock removed in solution from an area in a year - that is, the denudation rate.

Harmon et al. (1972, 1973, 1975) have used spring water chemistry data in an attempt to determine whether the maximum rate of solution takes place under arctic climates where carbon dioxide is more soluble in water or whether it takes place in tropical environments where greater biogenic activity should in theory mean higher  $PCO_2$  in soil atmospheres. These workers have attempted to show how the chemistry of spring waters varies with water temperature, which they have argued is highly correlated in most instances with mean annual air temperature.

Harmon et al. (1973, 1975) analyzed data from 305 springs in Canada, the United States and Mexico. The data were grouped into coherent sets with analyses for climatically similar, geographically restricted areas forming a set. Mean  $Ca^{2+}$ ,  $HCO_3^-$ ,  $SI_C$  and  $\log PCO_2$  were determined for spring waters in each region. Regional means were employed as this is considered to rid the data of variability due to hydrogeological setting and seasonal fluctuations in spring temperature and chemistry. Regression analysis showed significant positive linear relationships between water temperature and the chemical parameters  $Ca^{2+}$ ,  $HCO_3^-$ ,  $SI_C$  and  $\log PCO_2$ . These relationships imply the warmer groundwaters of tropical and sub-tropical regions contain greater concentrations of  $Ca^{2+}$  and  $HCO_3^-$  ions in solution, are closer to saturation with respect to calcite because of higher partial pressures of carbon dioxide than

are the waters of cold-temperate and sub-arctic environments. Recent data on the chemistries of some Canadian spring waters as well as additional reliable published data cast doubt on the validity of the relationships proposed by Harmon et al. for  $\text{Ca}^{2+}$ ,  $\text{HCO}_3^-$  and  $\text{Si}_c$  but strongly support a positive linear relationship between  $\log \text{PCO}_2$  in spring waters and water temperature.

The present analysis of variations in spring water chemistry with spring water temperature is essentially a reworking of the topic covered by the three Harmon et al. papers. Substantial use has been made of data collected by these writers.<sup>1</sup> Some regional data sets such as those for Missouri, Kentucky, Pennsylvania and Virginia and West Virginia have been used directly while others have been variously modified and added to. In addition, new chemistry data for springs in the Nahanni<sup>2</sup> and Bruce Peninsula<sup>3</sup> carbonate regions of Canada have been included in the analysis along with published information on some spring waters in New York.<sup>4</sup> Spring temperature and chemistry means for the El Abra region of Mexico, for Texas and for the southern Canadian Rockies have been re-calculated.

---

<sup>1</sup>Data were made available by Russel S. Harmon, Department of Geology, Michigan State University, U.S.A.

<sup>2</sup>Only springs that collect water from limestone areas were considered. Springs discharging groundwater that had first percolated through shales are thought to be 'hydrogeologically unusual.'

<sup>3</sup>Data were collected by D. W. Cowell, McMaster University, Canada.

<sup>4</sup>Jacobson & Langmuir (1972). Both 'open' and 'flooded' spring data were utilized because data from other regions cannot be similarly categorized. It is recognized that strictly speaking only 'flooded' spring data should have been used in calculation of regional spring characteristics for New York.

The data set of the El Abra region of Mexico was modified by eliminating spring waters with a very high sulphate ion content and also by removing some spring analyses with obvious errors (Harmon 1971, 1972; Fish & Russell 1972). Data for the Choy, a large spring emerging at the base of the eastern flank of the El Abra Range were extracted, for instance, because these spring waters have an average sulphate ion concentration of 424 p.p.m.<sup>1</sup> The Canada data set as used in Harmon et al. (1975) was subdivided on the basis of climate and environmental differences into two regional data sets, one representing conditions in the Crows Nest Pass area and one conditions in the Castleguard area of the southern Canadian Rockies.<sup>2</sup> Chemistry-temperature means for Texas were re-calculated using additional data extracted from Texas Water Development Board reports.<sup>3</sup> A number of difficulties were encountered in use of this published material. First, in many instances water temperature measurements are not listed and it was therefore necessary to assume for the purpose of calculating  $SI_C$  and  $\log PCO_2$  that spring waters in this area are at the mean annual air temperature for their location. Secondly these data do not always include reliable field pH determinations; many measurements were made

---

<sup>1</sup>Data for the El Abra region of Mexico were revised by John Fish. Department of Geology, University of Indiana.

<sup>2</sup>Data were collected by D. C. Ford, McMaster University, Canada.

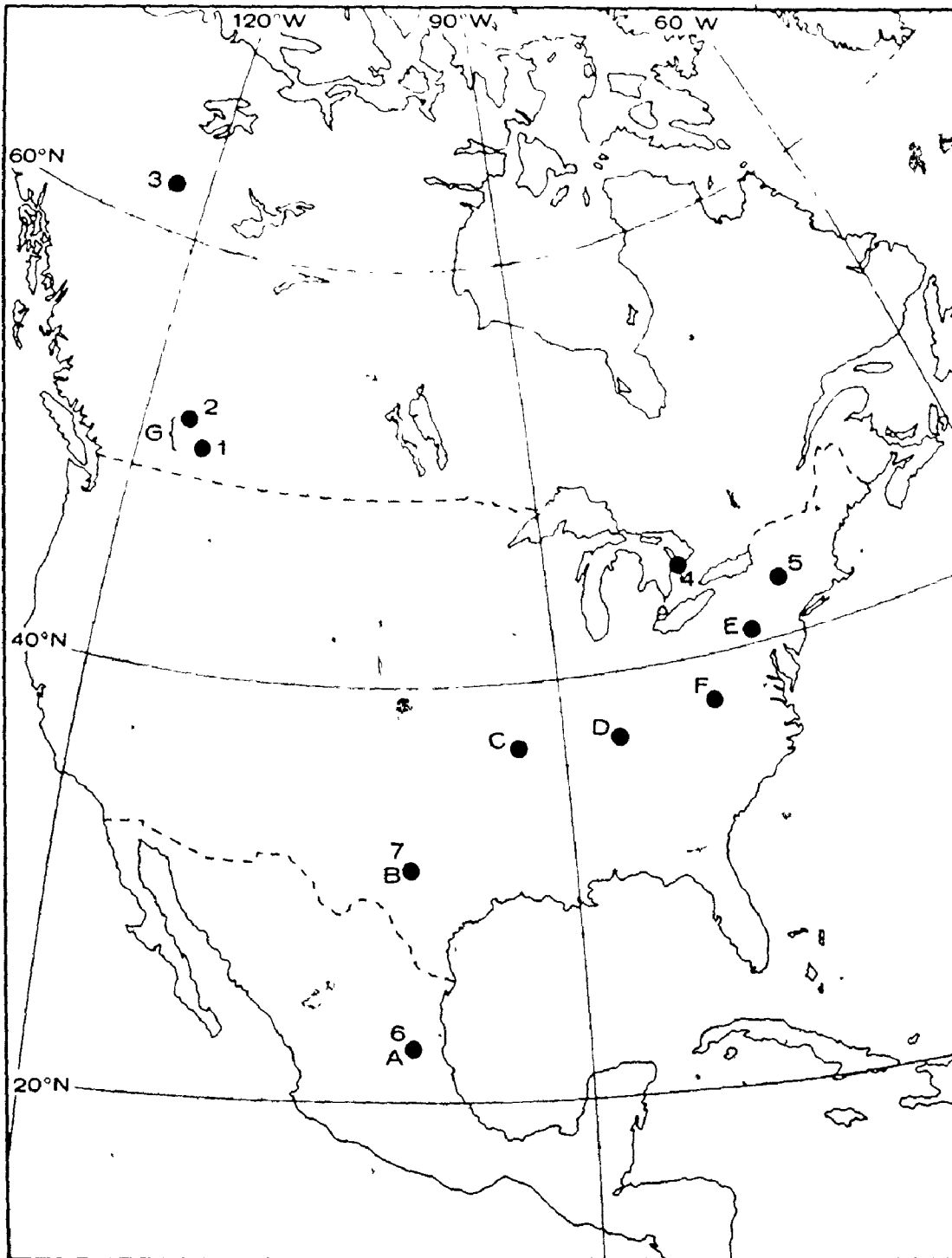
<sup>3</sup>Data for springs in Texas were obtained from Alexander & Patman (1969), Follett (1973), Reeves (1967 & 1969), Reeves & Small (1973) and Sandeen (1972).

in the laboratory. Although it is doubtful if large errors are induced into the calculated values of  $SI_C$  and  $\log PCO_2$  by assuming a water temperature the same cannot be said with certainty of the pH measurements. The Texas data were collected with care and they presented here to show the differences that were found between our data for this area and that accumulated in a similar manner by Harmon et al. (1973, 1975). Whatever the accuracy of the calculated chemical variables in this data set, it is certain that measured  $Ca^{2+}$  and  $HCO_3^-$  ion concentrations are reliable. The locations of areas considered in this reappraisal of the evidence are shown in Figure 5.12.

Harmon et al. (1973, 1975) proposed the following linear relationship between regional mean  $Ca^{2+}$  ion concentration and water temperature for springs in North and Central America.

$$Ca^{2+} \text{ (p.p.m.)} = 5.7 (T^\circ C) - 11.25 \quad (r = 0.90)$$

This proposed relationship and the data that were used in its determination are illustrated in Figure 5.13 along with the additional and modified data being considered in the present analysis. A number of points are of significance. First, the mean  $Ca^{2+}$  ion concentration of Mexican springs as used by Harmon et al. is misleading for it was calculated partly from springs with a large sulphate content. As Figure 5.13 shows, elimination of sulphate-rich waters lowers the mean  $Ca^{2+}$  ion concentration considerably to the El Abra figure. High  $Ca^{2+}$  ion concentrations are to be expected where calcium sulphate has been dissolved for this mineral is far more soluble in water than either



- |      |   |                        |   |                               |
|------|---|------------------------|---|-------------------------------|
| KEY: | A | Mexico                 | 1 | Crows Nest, Canadian Rockies  |
|      | B | Texas                  | 2 | Castleguard, Canadian Rockies |
|      | C | Missouri               | 3 | Nahanni, N.W.T., Canada       |
|      | D | Kentucky               | 4 | Bruce Peninsula, Canada       |
|      | E | Pennsylvania           | 5 | New York, USA                 |
|      | F | Virginia & W. Virginia | 6 | Sierra de El Abra, Mexico     |
|      | G | Canada                 | 7 | Texas, USA                    |

Figure 5.12. Locations of Regions Discussed in the Text.

limestone or dolomite. Furthermore, as the solubility of calcium sulphate is temperature dependent, it increases with increasing temperature; higher  $\text{Ca}^{2+}$  ion concentrations are to be expected in warm as opposed to cold sulphate-rich groundwaters.

The additional data presented in Figure 5.13 clearly question the validity of the  $\text{Ca}^{2+}$ -temperature relationship proposed by Harmon et al. which suggests that at  $0^\circ\text{C}$  spring waters should have a negative concentration of calcium ions. Although there is still an apparent general increase in  $\text{Ca}^{2+}$  ion concentration with increase in temperature, closer examination of the data reveals that many colder waters have  $\text{Ca}^{2+}$  ion concentrations considerably in excess of those measured in warmer spring waters. In fact, waters in New York and the Bruce Peninsula, Canada have  $\text{Ca}^{2+}$  contents very similar to those measured in spring waters in Texas and Mexico. It is evident that  $\text{Ca}^{2+}$  ion concentration is not simply a function of water temperature.

Addition of new and revised data to two further diagrams presented in Harmon et al. (1973) demonstrates that there is no relationship between the  $\text{HCO}_3^-$  ion concentration of a spring water and the water temperature (Figure 5.14) and that warmer waters are not necessarily more saturated with respect to calcite than are colder waters (Figure 5.15).

The strong relationship found by Harmon et al. (1973, 1975) between  $\log \text{PCO}_2$  and water temperature, however, seems to be a significant one (Figure 5.16) although use of new and revised data suggests slight modification of the linear regression model relating these two parameters (Figure 5.17). The model proposed by these workers for meaned regional data:

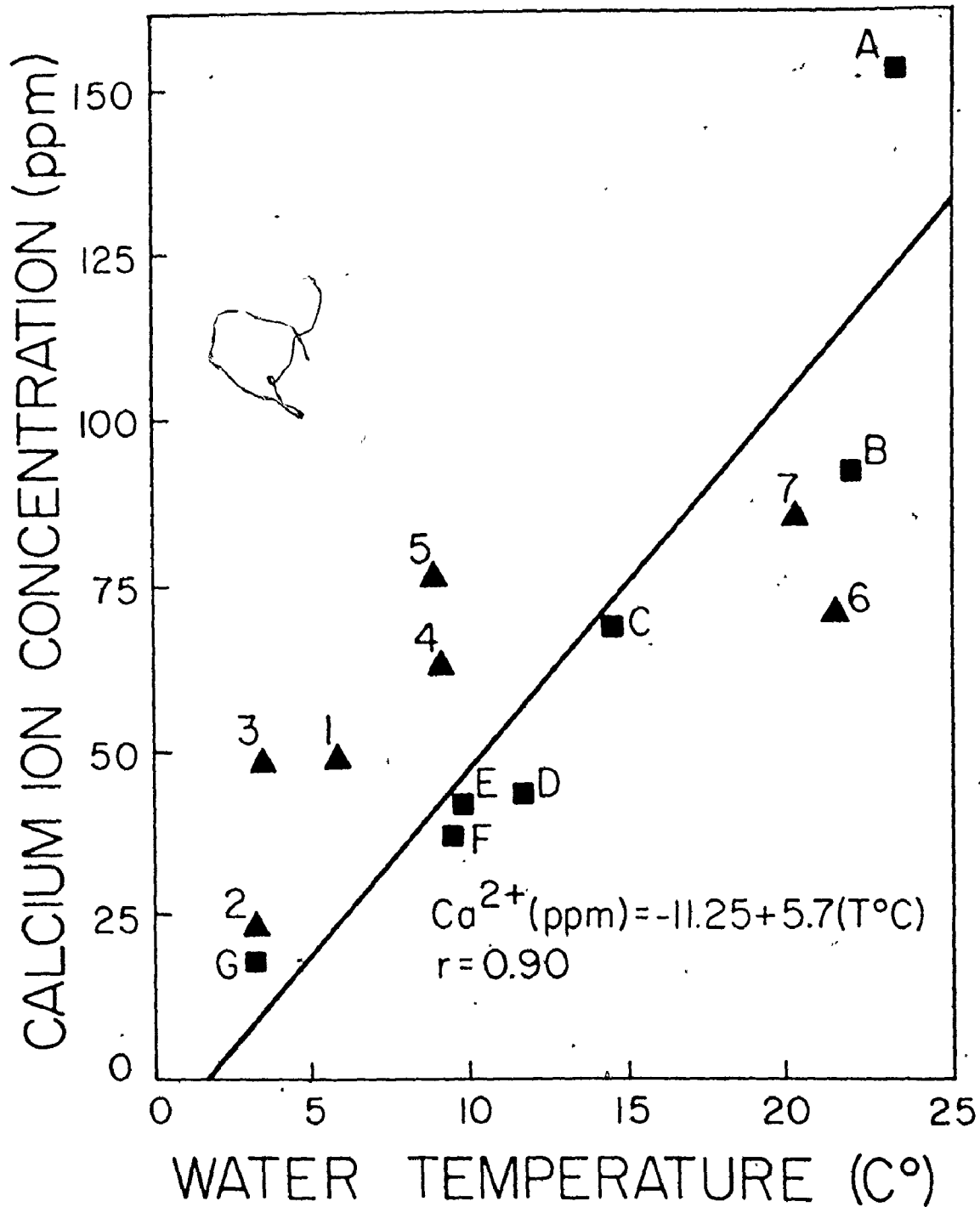


Figure 5.13. Regional Variation in  $Ca^{2+}$  Concentration and Water Temperature. The regression line and equation are for the data used by Harmon *et al.* (1973) and refer to points A to G inclusive.



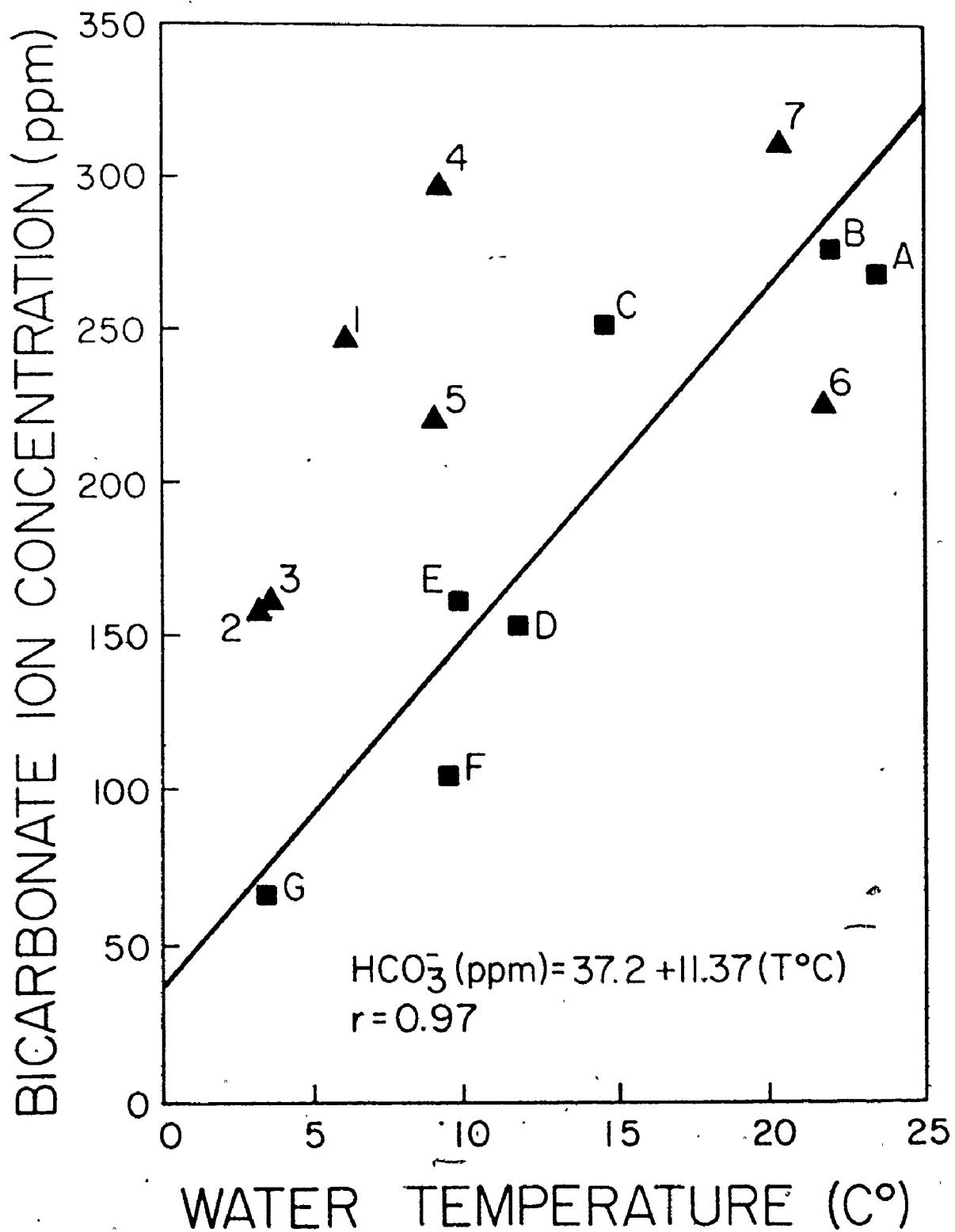


Figure 5.14. Regional Variation in  $\text{HCO}_3^-$  Concentration and Water Temperature. The regression line and equation are for the data used by Harmon *et al.* (1973) and refer to points A to G inclusive.

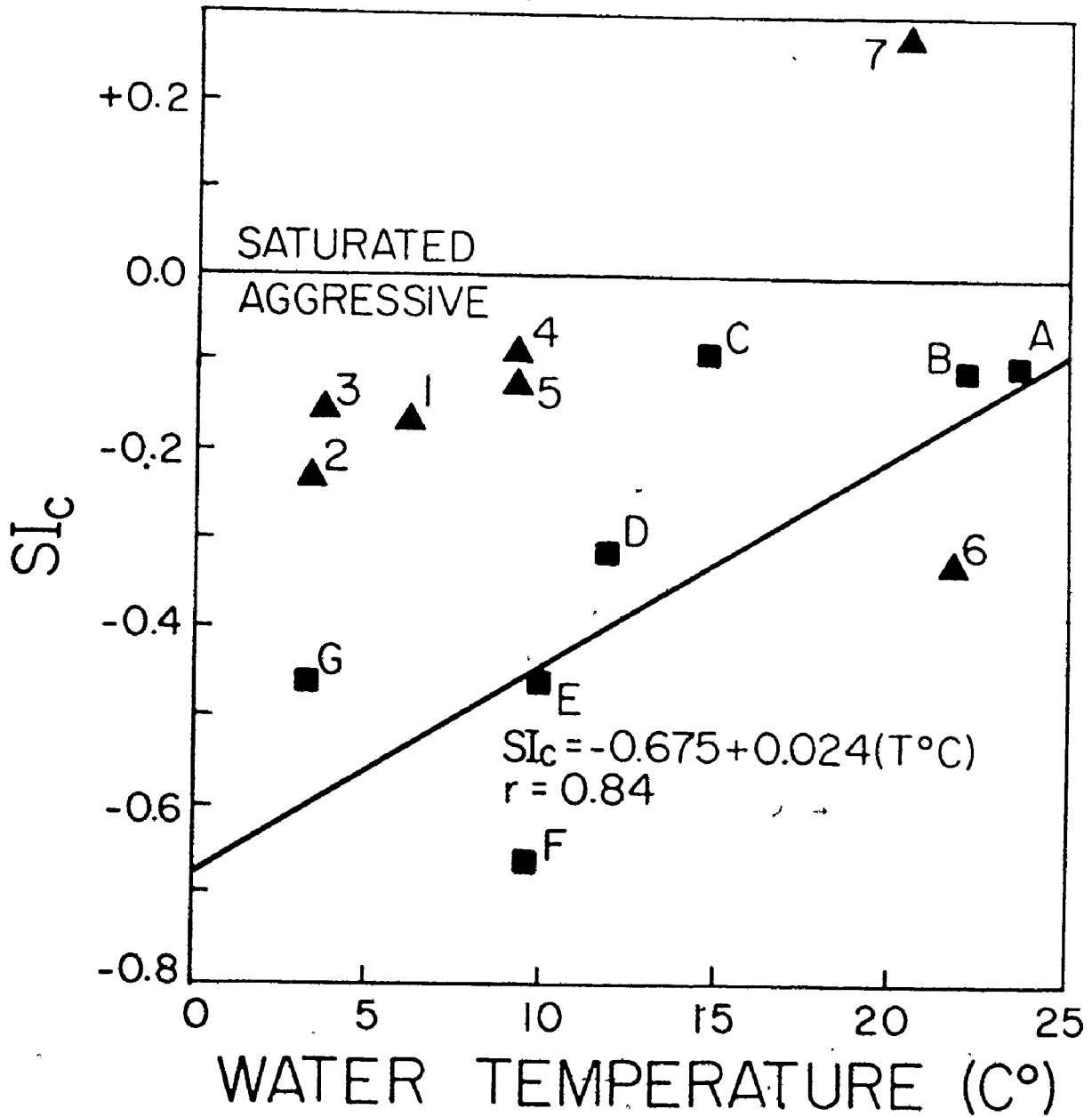


Figure 5.15. Regional Variation in  $SI_c$  and Water Temperature. The regression line and equation are for the data used by Harmon *et al.* (1973) and refer to points A to G inclusive.

$$\log \text{PCO}_2 = -3.33 + 0.08 (\text{T}^\circ\text{C}) \quad (r = 0.96)$$

clearly underestimates levels of carbon dioxide in cold groundwaters and overestimates them in warm waters. Using the total revised data set the following linear relationship is suggested:

$$\log \text{PCO}_2 = -2.93 + 0.05 (\text{T}^\circ\text{C}) \quad (r = 0.85)$$

or if the Texas data is left out for reasons of uncertain accuracy this is modified to:

$$\log \text{PCO}_2 = -3.00 + 0.06 (\text{T}^\circ\text{C}) \quad (r = 0.89)$$

The very strong relationship clearly evident in Figure 5.17 between  $\log \text{PCO}_2$  in spring waters and water temperature indicates that waters in warmer regions have the potential, because of their very high carbon dioxide contents, to dissolve far more limestone per unit volume of water than have waters in colder regions. As we have already seen, Nahanni spring waters derive their  $\text{CO}_2$  from soils in their recharge areas. If the bulk of other springs in north and central America do this also, this implies that  $\text{PCO}_2$ 's in soils are higher in the warmer areas. This would not be a surprising finding in view of the fact that biogenic activity, although related in some degree to soil moisture conditions, is in large part related to soil temperature.

If warmer groundwaters have a greater solution potential than colder ones the question arises as to why  $\text{Ca}^{2+}$  and  $\text{HCO}_3^-$  concentrations do not necessarily increase with increasing water temperature. The answer to this lies in the fact that the solution potential of natural

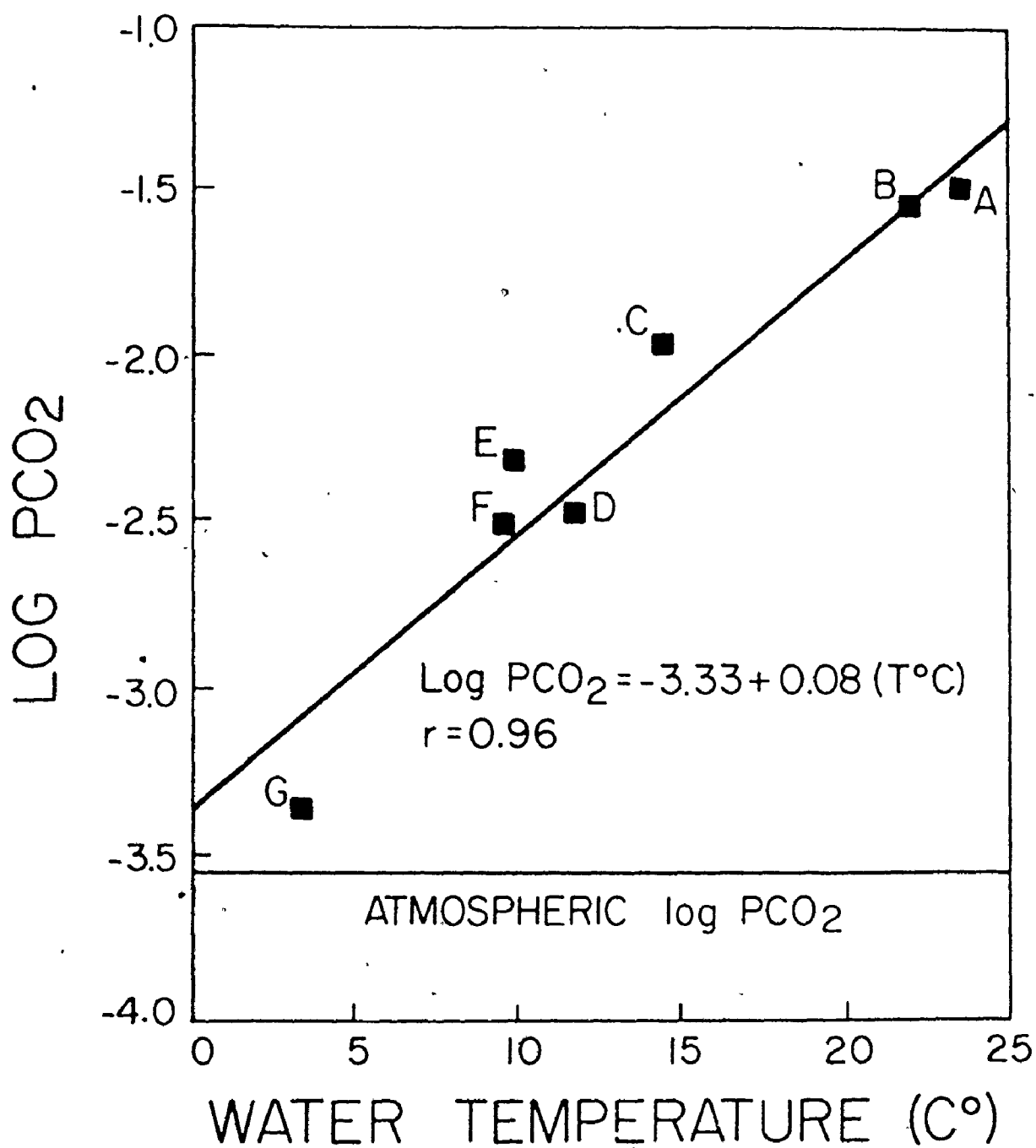


Figure 5.16. Regional Variation in log PCO<sub>2</sub> and Water Temperature (after Harmon et al. (1973, 1975)).

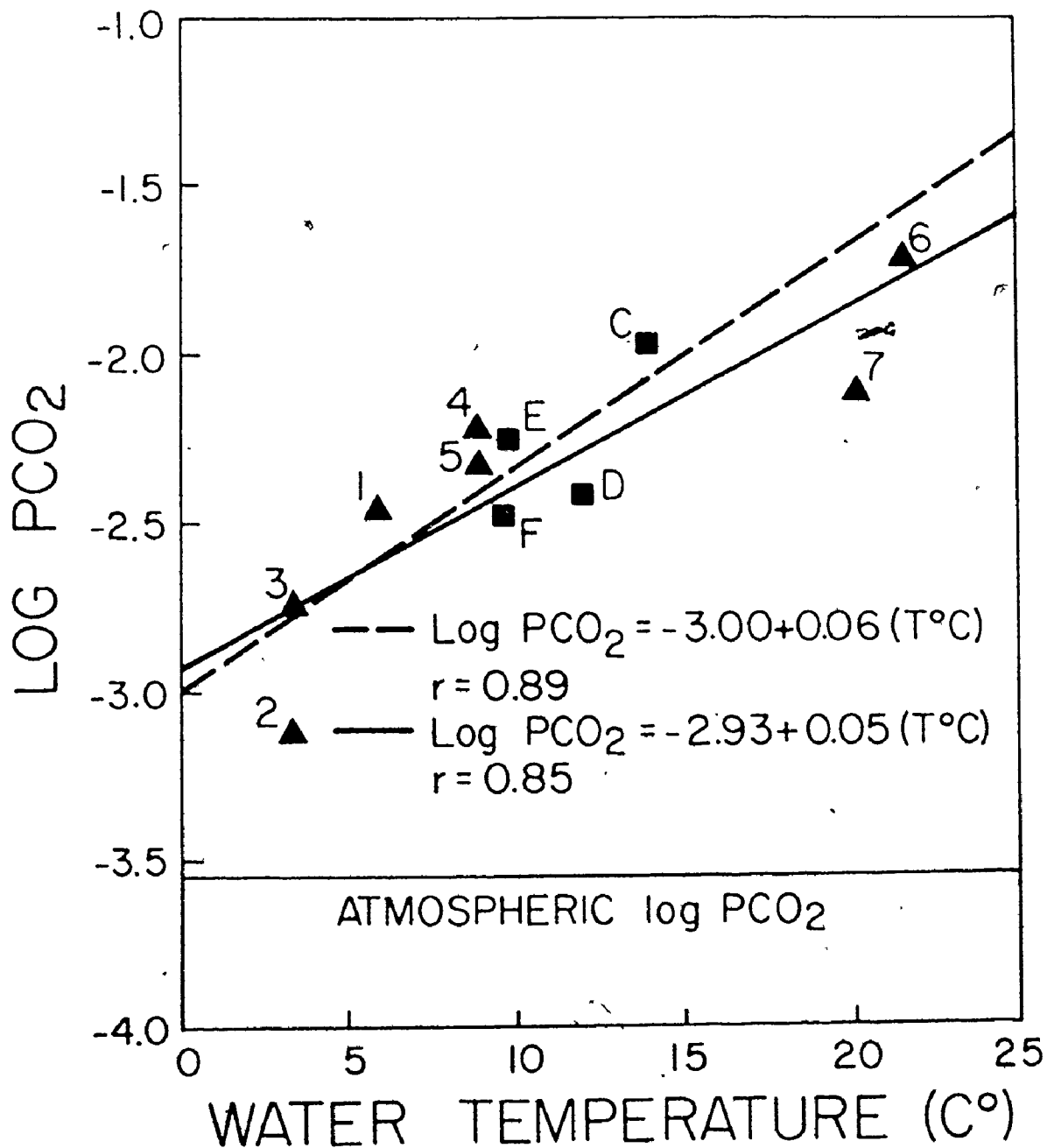


Figure 5.17. Regional Variation in Groundwater Aggressiveness and Water Temperature. The solid regression line was calculated using all of the data shown. The dashed line was calculated using all data except that for Texas (point 7).

waters is not always realized so that solute concentrations in natural waters are strongly controlled by the saturation state of the water. As Figure 5.15 shows, many cold waters are considerably more saturated with respect to calcite than are some warm waters. It is not surprising therefore that  $\text{HCO}_3^-$  concentrations in spring waters in New York State and the Bruce Peninsula, Canada (points 4 & 5) are higher than those in Mexican Springs (point 6) for these waters are much more highly saturated than are the spring waters of Mexico.

The evidence presented here indicates that although the potential for solution by natural waters is greater in warmer regions, the actual solution intensity (measured ionic concentrations) depends upon how much of that potential is utilized, that is upon the degree of saturation reached by the natural waters. As Figures 5.13 and 5.14 show, there is the tendency for actual solution intensity in a given region to increase with temperature but the relationship is by no means a strong one or universal. The cold spring waters of the Nahanni which discharge all water from this area do in fact carry off more material in solution per unit volume of water than do significantly warmer springs in Kentucky, Virginia & W. Virginia and Pennsylvania (Figure 5.13 & 5.14). This is because Nahanni spring waters are more highly saturated with respect to calcite than those other areas (Figure 5.15) and not because they contain more carbon dioxide, for the opposite is the case (Figure 5.17).

The solution potential of natural waters in the Nahanni and the actual intensity of solution in this sub-arctic region have been shown to be far greater than previous work and intuitive assessment would

suggest. In fact the intensity of solution in the Nahanni region appears to be greater than is operating in the extensive and highly developed karst landscapes of Kentucky, Virginia and W. Virginia and Pennsylvania in the United States. As has already been argued, the solution intensity in the Nahanni is related to  $PCO_2$  in soils which in turn is related to hydrogeologic and vegetation densities in this area.

(b) Karst Denudation Rates.

In 1959 Corbel suggested that the annual solutional loss from a limestone terrain is given by the following formula:

$$4 ET (N)/100 = X$$

where E is the runoff in decimeters, T the average  $CaCO_3$  content in the water in ppm., X the amount of limestone solution in  $m^3/km^2/yr.$  or mm/1,000 yrs., and 1/N the proportion of limestone in the drainage basin under consideration. Corbel (1959) used this formula to calculate the amount of limestone lost by solution in karst regions. His estimates based on random isolated observations point to high corrosion rates in alpine and arctic environments and much lower rates in warmer humid areas. Subsequent work has shown that the apparent correlation of high corrosion rates with low temperatures is far too simple and that the factors affecting the solution of limestones are more complex than Corbel originally supposed. More recent estimates of karst denudation rates have generally utilized modified versions of Corbel's original formula for as Drake & Ford (1973) have pointed out, it overestimates the erosion rate for basins in which the stream shows an inverse relationship between

discharge and ionic concentrations. More detailed formulas for the calculation of erosion rates are given in Williams (1963), Douglas (1964) and Drake (1974).

For the Nahanni if we assume an effective precipitation between 31 - 27 cms. (effective precipitation = actual precipitation - evapo-transpiration) and a mean total hardness in waters leaving the karst via the two springs of 144 ppm  $\text{CaCO}_3$ , then substitution in Corbel's formula gives an annual denudation rate of between 17.9 and 27.1  $\text{m}^3/\text{km}^2$  1 yr. or a net surface lowering of 17.9 - 27.1 mm/1,000 yrs. Compared to denudation rates in other parts of the world shown in Table 5.22, it is interesting to note that the upper estimate of denudation is higher than reported in the Southern Canadian Rockies (Drake 1974), in the northern Canadian arctic (Smith 1969), in the Punkva River basin, Czechoslovakia (Stelcl et al. 1969) and in the Mellte River basin, Wales (Groom & Williams 1965).

Although accurate figures are not available there is no doubt, however, that the runoff from the highly developed labyrinth karst - polje belt in the northern portion of the Nahanni karst is much in excess of average estimates for it receives large amounts of allogenic water from surrounding shales. In fact the runoff for this localized area could amount to as much as twice the average for the karst area. If this is the case then this localized region may have a denudation rate somewhere between 35.8 and 54.2  $\text{m}^3/\text{km}^2/\text{yr}$ . with the upper limit slightly lower but comparable to those estimated for Indonesia (Balazs 1968), Jamaica (Versey 1959) and Slovenia, Yugoslavia (Gams 1972) - all very highly developed karst terrains. Such a rate could well



Table 5.22. Calculated Rates of Karst Denudation (largely after Jennings 1970).

SOURCE	KARST AREA	NET DENUDATION RATE $m^3/km^2/yr.$
Smith (1969)	Somerset Island N.W.T., Canada	2
Stelci et al. (1969)	Punkva R., Moravia, Czechoslovakia	25
Williams (1963 & 1970)	Fergus R. & Shannon R., Ireland	51 - 53
Sweeting (1965)	Craven, England	40
Pitty (1968)	Peak District, England	75 - 83
Groom & Williams (1965)	Mellte R., Wales	16
Gams (1962)	Slovenia, Yugoslavia	77 - 80
Balázs (1968)	Indonesia	83
Pigott (1962)	Derbyshire, England	55 - 100
-Versey (1959)	White Limestone, Jamaica	72
Drake (1974)	Athabasca R. & N. Saskatchewan R. Southern Canadian Rockies	24.5 - 28.9

explain the occurrence in this localized belt of an almost 'tropical karst assemblage.'

In summary the evidence presented here on the characteristics of solution in the sub-arctic Nahanni region of Canada has emphasized the role of soil carbon dioxide in determining patterns and intensities of solution in karst terrains. The important part played by bedrock and surficial geology in controlling soil carbon dioxide levels and thus the chemical characteristics of nearby waters has been demonstrated while the significance of acid allogenic waters in karst landform development has been touched upon. The chemical characteristics of Nahanni and other spring waters have suggested revision of concepts on potential- and actual solution-temperature relationships while denudation rates appear to range between those typical of a cool temperate to those typical of a tropical humid region.

Chapter 6. Pleistocene Glaciation in the Southern Mackenzie Mountains,  
N.W.T., Canada.

1. Pleistocene Glaciation of the Western Cordillera, Yukon and N.W.T.:  
An Examination of the Published Evidence.

(a) An Unglaciated Area?

Early investigations of the Mackenzie Mountains led a number of workers to conclude that this area is not one dominated by glacial landforms. After investigating the South Nahanni River region, for instance, Cameron & Warren (1938) noted that "evidence of glaciation is not strongly marked in this area" (p. 17). A possible explanation was introduced by Bostock (1948) who has argued that "during Pleistocene time the Rocky Mountains appear to have been an area of relatively light precipitation, as they are today. In the south, valley glaciation was extensive and the level of the ice was high. Northward the effects of glaciation seem to have been less pronounced, and in some areas north of the Peace River no features attributable to glaciation can be detected in the photographs" (p. 10). In 1958, Wilson et al. summarized the available information and in the first 'Glacial Map of Canada,' delimited two large areas of the Mackenzie Mountains which they labelled 'unglaciated.' In 1967 an updated edition of this map was published, and in this, the most recent summary work available, Prest et al. have delimited an extremely large area of the Mackenzie Mountains which they consider was not glaciated during the last or Classical Wisconsin period. They recognize that parts of this area may not have been glaciated at any time during the Pleistocene.

while other parts may have been covered by ice during one or more of the Pleistocene glacial events. Wilson et al. (1958) consider that the Nahanni karst region was glaciated at some time in the Pleistocene while Prést et al. (1967) suppose that it was last glaciated during the Classical Wisconsin period.

It is apparent that before a worthwhile interpretation of the Nahanni karst landform assemblage can be completed, it is necessary to determine with some degree of certainty whether or not the Nahanni karst region was part of the area of the Mackenzie Mountains that escaped glaciation during one or more of the Pleistocene glacials. The glacial history of the area is, therefore, of some significance and what is known about it will now be outlined.

(b) Laurentide and Cordilleran Ice Sheet Limits and Evidence of Multiple Glaciation in the Western Cordillera, Yukon, British Columbia and N.W.T.

The ice that covered northern Canada during the last glaciation and probably also during earlier glacial periods, is thought to have been made up of three principal ice sheets or glacier complexes that partly coalesced with one another during their maximum stands (Craig & Fyles 1960). "The Laurentide ice sheet was bordered on the west by the Cordilleran ice sheet and on the northeast by a similar glacier complex that occupied Baffin, Devon, Ellesmere and adjoining islands. The eastern ranges of the western Cordillera north of latitude 60°N, may have blocked the westward flow of Laurentide ice so that in this region there may have been only limited and localized contact between the Laurentide and Cordilleran ice sheets.

Aspects of the glacial history of the Selwyn, Mackenzie and Franklin Mountains, the Hyland and Liard Plateaus and the Mackenzie, Great Bear and Great Slave Plains (Figure 1.1) have been discussed by a number of workers including Craig (1965), Gabrielse *et al.* (1965, 1973), Rutter & Boydell (1972), Aitken & Cook (1974) and Ford (1976). Craig (1965) has argued that during the Wisconsin maximum, the eastern ranges of the southern Mackenzie Mountains were covered by Laurentide ice. He points out that an ice surface at between 4,000 and 5,000 ft. elevation would leave only a few peaks exposed and cover the Great Slave Plain with from 2,000 ft. to possibly as much as 4,000 ft. of ice. He found no evidence to indicate that Cordilleran ice from the west had entered the area east of the Mackenzie Mountains. During the early stages of deglaciation, Craig believes that the eastern ranges of the Mackenzie Mountains may have increasingly impeded and eventually stopped the flow of ice to the west diverting it instead to north and south along the mountain front. The ice margin may have remained static against the Nahanni Range while it retreated back from the front ranges to north and south. As overall thinning of the marginal zone of the ice sheet continued, Craig feels that the locus of the margin along the mountain front became independent of the topographic barrier and was determined instead by the regimen of the ice sheet.

Rutter & Boydell (1972) found evidence in the upper Mackenzie River area for two advances of Laurentide ice. The first is recorded by a grey-black stony till which is exposed as the basal unit in many of the tributary valleys of the Mackenzie system - locations where it

is most often preserved, and by glacial erratics on the summit areas of the Mackenzie Mountains up to elevations of approximately 5,000 ft. The second advance is recorded at the surface by a light grey-brown, stony till, separated in section from the lower till by stratified sands and gravels up to 100 ft. thick. The ice of the second advance may have been much thinner than that of the earlier advance, for its flow appears to have been topographically controlled to the extent that a great deal of ice was deflected by the mountains to the south and northwest although tongues of ice were able to penetrate into the west through the gaps in the mountain ranges. The center of deflection appears to have been at the Nahanni Range in the Sibbeston Lake area (Figure 1.1). Rutter and Boydell claim that glacial deposits which relate to the most recent advance are not found above an elevation of about 2,200 ft. and that deglaciation was variable in character and controlled at least in part by topography. In the south, it consisted of a withdrawal of the ice front to the east flanks of the Liard and Nahanni Ranges, beyond which point a uniform thinning of ice took place. The work of Rutter and Boydell (1972) suggests that the deposits laid down by the 'last glacier advance' of Craig (1965) were in fact laid down by two separate advances of ice either during the same glacial period or during different glacial periods:

Gabrielse et al. (1965, 1973) have reported that the Flat River, Glacier Lake and Wrigley Lake map-areas have been glaciated by alpine and valley glaciers and two or more ice sheets. The distribution of glacial erratics and the form of drumlinoid ridges indicate

that a Cordilleran ice sheet moved easterly and northeasterly over the southern part of the Flat River map-area. The ice surface must have been at an elevation of more than 6,415 ft., for a peak five miles southeast of Skinboat Lakes appears to have been completely overridden. Aligned and parallel systems of drainage channels indicate a southwesterly retreat of ice.

A large moraine on the east side of Wrigley Lake which contains boulders of pink and orange-weathering granitic rock characteristic of the Canadian Shield and which is convex to the west, has been interpreted by Gabrielse et al. (1973) as being related to a front of Laurentide ice from the east. The crest of the moraine is at approximately 2,500 ft a.s.l. Erratics also believed to have been derived from the east occur at an elevation of about 4,500 ft. south of North Redstone River opposite the southeast end of Tigonankweine Range, while the minimum upper limit of an ice sheet is well defined by abandoned marginal channels on the northeast slope of Tigonankweine Range at elevations of about 4,500 ft. The slopes of these channels suggest that the Laurentide ice retreated to the south.

Strong evidence of multiple glaciation by Laurentide ice has been found in the South Nahanni River region of the Mackenzie and Selwyn Mountains (Ford 1971c, 1973, 1974, 1976; Brook & Ford 1975). In the most recent summary of the evidence, Ford (1976) recognizes three glacial zones within the South Nahanni River drainage basin. In the west is the 'Cordilleran Glacial Zone' which has been affected by two or more phases of valley glaciation, in the east is the 'Laurentide

Glacial Zone' where there is evidence of three invasions of Laurentide ice and between these is the 'Central Unglaciaded Zone' (Figure 6.1).

In the Laurentide Glacial Zone, the oldest of the three Laurentide ice advances is indicated by the lag of an ancient till up to altitudes of 4,600-5,300 ft. on the east flank of the Nahanni Plateau and everywhere on the Ram Plateau. This must have been emplaced by a Laurentide ice sheet that effectively submerged Nahanni Range, Ram Plateau and Yohin Ridge and came to rest against the east flank of Nahanni Plateau. Ford (1971c) has termed this event the 'First Canyon Glaciation' and has argued that it occurred prior to 300,000 years B.P.

Well-preserved knob and kettle terrain to north and south of the South Nahanni River west of Yohin Ridge, suggests that during the later 'Clausen Glaciation' ice abutted against the lower slopes of the Nahanni and Ram Plateaux and that the ice surface was at or above 2,150 ft. The limits of the most recent Laurentide incursion are marked by a large and complex lateral moraine on the northeast flank of Mattson Mountain which descends the mountain flank from 2,640 ft. to 1,716 ft. Ford believes that during this, the 'Jackfish Glaciation,' ice occupied the steep-walled breach between Mattson Mountain and Twisted Mountain to the north and that west of this, ice thinned rapidly. The Clausen and Jackfish glacial events are tentatively ascribed to the Illinoian and 'Classical' Wisconsin periods respectively (Ford 1976).

Of considerable significance to the problem of interpreting glacial events in the southeastern portion of the Mackenzie Mountains, is work that has been conducted on the surficial geology of the northern Yukon Territory and northwestern district of Mackenzie, N.W.T. (Hughes



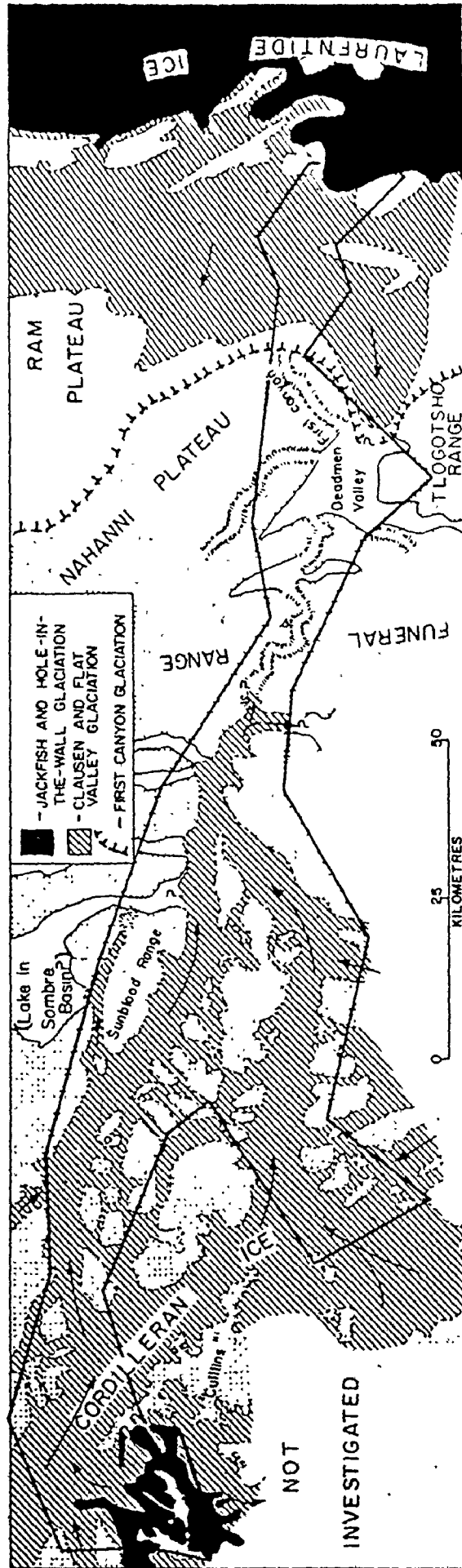


Figure 6.1. Glaciation of the South Nahanni National Park, Mackenzie Mountains, N.W.T., Canada (after Ford 1976).

1969, 1972; Fulton & Klassen 1969). Fulton and Klassen (1969) have found strong evidence of multiple Laurentide glaciation in the north-western district of Mackenzie. They report that Quaternary deposits which pre-date the last glaciation are exposed in several river valleys but that the most complete section discovered, which appears to record much of the Quaternary history of the coastal part of the area, has been exposed by a tributary of the Horton River. This section, which contains at least three tills, lies outside of the moraines built by the last ice advance. Fulton and Klassen consider that sand and gravel at the base of the sequence, which lies between till and bedrock, may possibly be equivalent to the Beaufort Formation, known to be of late Tertiary or early Quaternary age. In addition, they note that a peat bed above the lower two tills and below at least one till, appears to be in the same stratigraphic position as a peat bed in a nearby section dated at older than 38,100 yrs. B.P. The indication is therefore, that this region of the Anderson Plain (Figure 1.1) was covered by ice on at least two separate occasions prior to 38,100 yrs. B.P., and that ice advanced across it a minimum of three or four times during the Quaternary.

Hughes (1972) has noted that extensive invasions of the northern Yukon Territory and northwest district of Mackenzie by Laurentide ice are indicated by widespread drift deposits which contain erratics derived from the Canadian Shield. At its maximum, Laurentide ice covered Peel Plateau, Bonnet Plume Basin, the eastern section of Porcupine Plateau and parts of the Yukon Plain and it may have reached elevations of 3,500 ft. on the east flank of the Richardson Mountains and 4,000 ft. on the north flank of the Mackenzie Mountains (Figure 1.1). In some

areas the maximum limit is defined by subdued moraines and kame terraces or by ice-marginal channels and spillways, while in others it is indicated by the distribution of glacial erratics of granite, gneiss and volcanic material derived from the Canadian Shield. Hughes points out that this limit may represent a composite of two or more separate early advances, but argues from stratigraphic evidence, that in western Peel Plateau and eastern Porcupine Plateau it may have been reached only once during an early glaciation.

On the west side of the Snake River, a tributary of the Peel, a sediment sequence on a bedrock bench about 150 ft. above the river consists of organic silt overlying 10 ft. of boulder gravel and overlain by 55 ft. of gravel. Hughes (1972) notes that wood from the base of the silt has been dated at more than 31,000 yrs. B.P. and concludes that if no erosional disconformity exists above the silt, then it is likely that this locality has not been glaciated during at least the last 31,000 yrs. This indicates, he argues, that the maximum advance of Laurentide ice on to Peel Plateau took place more than 31,000 yrs. ago.

Within the area glaciated by Laurentide ice, landforms appear to be of two or more different ages. Hughes considers that well-preserved landforms in the area to the east of the Richardson Mountains and north of latitude  $66^{\circ}\text{N}$  may be of late-Wisconsin age while more subdued features further west may relate to older Laurentide glaciations in early Wisconsin or pre-Wisconsin time. Flow markings suggest that ice of possible late Wisconsin age moved westwards across southern

Peel Plain and was deflected to the north-northwest parallel to the eastern front of the Richardson Mountains. A minor lobe appears to have extended southwest to about the junction of Peel and Snake Rivers. During retreat, the ice sheet is thought to have developed numerous minor lobes as it did further south (Craig 1965, Rutter & Boydell 1972).

Work in both the northwestern and southwestern districts of Mackenzie has led Rutter (1973) to state that there is evidence in both areas for two Laurentide ice advances. Rutter claims that in the northern area, the 'Classical' Wisconsin limit is marked by well-defined, discontinuous meltwater channels and the earlier limit by the distribution of erratics from the Canadian Shield. Both limits, he says, increase in elevation towards the south. In the Wrigley lake map-area, the 'Classical' Wisconsin limit is at 4,250 ft. and the earlier limit at about 5,000 ft. Rutter notes that although he has not followed the limits southwards through the Dahadinni and Root River map-areas, eastern erratics have been found up to 5,000 ft. in the Sibbeston Lake map-area further south. He points out that "if the elevation of 'Classical' Wisconsin glacial erratics and meltwater channels increases at a constant rate, 5,000 ft. is about the expected elevation for the 'Classical' Wisconsin limit in this area" and therefore concludes that "it may therefore be, that the maximum elevations for 'Classical' Wisconsin and early glacial erratics converge to the south so that both limits lie at about the same elevation (p. 285).

If the published information on Laurentide ice sheet limits in the easternmost ranges of the western Cordillera north of latitude 60°N is reliable, then there have been at least four advances of Laurentide ice into this region (Table 6.1). At its maximum, ice reached up to 4,000 ft. along the northern flank of the Mackenzie Mountains and up to 5,000 ft. along the eastern flank, the limit indicated in most areas, only by the presence of erratic material. The evidence for a second advance that reached up to 4,250-4,500 ft. in the Wrigley Lake area, and 5,000 ft. in the Sibbeston Lake area, is less conclusive. Rutter (1973) has identified it in the Wrigley Lake map-area while in the same area Gabrielse et al. (1973) have identified ice-marginal drainage channels at 4,500 ft. and remark that erratics have been discovered at least up to this elevation. Elsewhere in the Cordillera this limit has not been differentiated. Three separate works (Gabrielse et al., 1973, Ford 1976, Rutter and Boydell 1972) mention an ice limit at 2,150-2,500 ft. in the eastern Mackenzie Mountains that is indicated by reasonably fresh end moraine deposits, while the same limit may be present in the northwestern district of Mackenzie at 1,000-1,500 ft. (Hughes 1973). Finally, Ford (1976) has argued that during one later Laurentide advance, ice was held up by the barrier of the Nahanni Range and did not reach the eastern flank of the Mackenzie Mountains.

As to whether these ice limits represent the maximum positions reached by Laurentide ice during each of four major glaciations, or whether two or more of them were reached during a single glaciation is not clear. All workers regard the oldest of the glacial advances

Table 6.1. Laurentide Ice Sheet Limits in the Eastern Ranges of the Western Cordillera, North of Latitude 60°N.

SOURCE	AREA	LAURENTIDE ICE SHEET LIMITS (ft) AND TENTATIVE CORRELATION BETWEEN AREAS		
Gabrielse et al. (1969, 1973)	Wrigley Lake map- area	>4,500?	4,500	2,500
Ford (1976)	South Nahanni River	4,600- 5,300		2,150   *?
Rutter (1973)	Wrigley Lake map- area	5,000	4,250	
Rutter (1973)	Sibbeston Lake map- area	5,000	5,000?	
Rutter & Boydell (1972)	Southwest District of Mackenzie	5,000		2,200
Hughes (1972)	Northern flank Mackenzie Mts.	4,000		
Hughes (1972)	Eastern flank Richardson Mts.	3,500		1,000- 1,500
Hughes (1972)	Peel Plateau			1,000- 1,500
Aitken & Cook (1974)	Carcajou Canyon map-area	5,000		

\*? Level of ice in Franklin Mts. quoted by Ford is 2,640-1,716 ft.  
This glaciation was less extensive than previous one.

as being of early- or pre-Wisconsin age with Ford (1976) tentatively suggesting that it is of Nebraskan or Kansan age. Rutter (1973) has suggested a 'Classical' Wisconsin age for the second advance while the third advance has been variously ascribed to the Illinoian (Ford 1976) and to minor readvances during 'Classical' Wisconsin deglaciation (Rutter and Boydell 1972). Ford has dated the last glacier advance as being of 'Classical' Wisconsin age. There are, therefore, major disagreements as to the exact glacial history of this area.

(c) Cirque and Valley Glaciation.

Observations on cirque and valley glaciation in the southwestern district of Mackenzie have been made by a number of workers. Gabrielse et al. (1973) have found evidence in the Flat River, Glacier Lake and Wrigley Lake map-areas for at least one period of extensive valley glaciation. Ice is believed to have moved in a southeasterly direction down the valleys of the Flat and South Nahanni Rivers. Gabrielse et al. point out that this valley glaciation may have been a relatively late-stage phenomenon because the upper limit of the ice was lower than the maximum reached by a Cordilleran ice sheet that invaded the area from the southwest.

In the Backbone Ranges of the Mackenzie Mountains (Figure 1.1), valley glaciers are known to have moved towards the north and east. Erratics derived from a westerly or southwesterly source at an elevation of 6,255 ft. on the west side of Thundercloud Range near Little Dal Lake and strongly developed, abandoned lateral drainage channels incised into the eastern slope of a mountain eight miles northwest of

Little Dal Lake up to elevations of 6,500 ft., suggest that the glaciers were of considerable thickness (Gabrielse et al. 1973). Late-stage ice movement from the west is also indicated by the form of prominent grooves at an elevation of more than 4,000 ft. in a valley close to the southeast end of Tigonankweine Range. Gabrielse et al. suggest that this valley glaciation may have obliterated, or greatly subdued evidence of the maximum westerly extent of Laurentide ice in this area.

Ford (1976) considers that there have been two periods of valley glaciation in the 'Cordilleran Glacial Zone' of the South Nahanni River drainage basin (Figure 6.1). He tentatively correlates the earlier and most extensive of these, the 'Flat Valley Glaciation' with the Clausen Laurentide advance and the later 'Hole-In-The-Wall Glaciation' with the Jackfish advance. These events are of possible Illinoian and 'Classical' Wisconsin age respectively.

In the Franklin Mountains, Mackenzie Plain and the eastern ranges of the Mackenzie Mountains, Rutter and Boydell (1972) have found evidence of cirque and valley glaciers at altitudes above 2,000 ft. Late glacial activity, they contend, is also indicated by the presence of cirque moraines in the Liard, Nahanni and McConnell Ranges above elevations of 3,500-4,000 ft. Aitken and Cook (1974) also report cirques and glaciated mountain valleys in the Backbone Ranges of the Carcajou Canyon map-area. In the Canyon Ranges to the east, however, there are only a few poorly developed cirques on the northern exposures of the highest summits.



According to Hughes (1972), valley glaciation in the northern Yukon Territory and northwestern district of Mackenzie occurred mainly in the Mackenzie, Selwyn and Ogilvie Mountains in the southern part of the area. Evidence of multiple valley glaciation is best displayed around the headwaters of Ogilvie River and since this locality lies beyond the western limit of Laurentide ice, inter-relationships of the Laurentide ice sheet and valley glaciers do not complicate interpretation of the glacial features. Deposits left by at least three advances are evident. They include fresh, sharp-ridged moraines which Hughes tentatively correlates with the 'last' glaciation of Vernon and Hughes (1966), moraines that are subdued but still recognizable ('intermediate' glaciation) and patches of till with little or no characteristic moraine ('old' glaciation). Hughes (1972) notes that each successive advance was less extensive than the previous one and that there is no presently available stratigraphic evidence by which the ages of the valley glaciations can be correlated with Laurentide ice sheet advances. The relative freshness of the glacial landforms of the 'last' glaciation, however, and those of the late Wisconsin Laurentide ice advance, suggests that the two glaciations were contemporaneous. Glacial landforms considered as belonging to the 'intermediate' valley glaciation and those near the limit of Laurentide glaciation are all relatively subdued, suggesting an early or pre-Wisconsin age.

Table 6.2 summarises the published information on cirque and valley glaciation in the eastern ranges of the western Cordillera, north of latitude 50°N and presents tentative correlations from one

Table 6.2. Evidence of Cirque and Valley Glaciation in the Eastern Ranges of the Western Cordillera, North of Latitude 60°N.

SOURCE	AREA	VALLEY AND CIRQUE GLACIATIONS AND TENTATIVE CORRELATIONS		
Gabrielse et al. (1969, 1973)	Flat River, Glacier Lake and Wrigley Lake map-areas	*?	Major Valley Glaciation	
Ford (1976)	'Cordilleran Glacial Zone' South Nahanni River drainage basin	*?	Flat Valley Glaciation	Hole-in-the-Wall Glaciation
Hughes (1972)	Northwestern District of Mackenzie	'old' Glaciation	'intermediate' Glaciation	'last' Glaciation
Rutter and Boydell (1972)	Southwestern District of Mackenzie		Cirque and valley glaciers down to 2,000 ft.	Cirques above 3,500-4,000 ft.

\*? Gabrielse et al. report that a period of Cordilleran ice sheet glaciation preceded the period of major valley glaciation. It is possible that this correlates with the 'old' glacial advance of Hughes (1972) and Vernon and Hughes (1966).

area to another. The period of extensive valley glaciation which post-dates the incursion of a Cordilleran ice sheet into the southern portion of the Flat River, Glacier Lake and Wrigley Lake map-areas (Gabrielse et al. 1973), is probably equivalent to the Flat Valley Glaciation of Ford (1976). This suggests that the southern portions of both the Selwyn Mountains and the Backbone Ranges of the Mackenzie Mountains (Figure 1.1) were glaciated on three separate occasions, the first by a Cordilleran ice sheet, the second by extensive valley glaciers and the third by valley glaciers of restricted development. These three glacial periods may well correlate with the three valley glaciations recognized by Hughes (1972) further north (Table 6.2).

In the northwest district of Mackenzie, moraines of the 'intermediate' valley glaciation have not been identified in Wind, Bonnet Plume and Snake valleys, nor anywhere within the limit of Laurentide glaciations along the Mackenzie Mountain front. Hughes (1972) suggests two possible explanations for this: first, that during the 'intermediate' valley glaciation, glaciers extended down Wind, Bonnet Plume and Snake valleys to form piedmont lobes beyond the mountain front, and built terminal moraines that were later destroyed by an advance of Laurentide ice; secondly, that valley glaciers of 'intermediate' age were confluent with the Laurentide ice and, therefore, developed no terminal moraines. Hughes notes that drift containing erratics from the Canadian Shield indicates that during this later advance, Laurentide ice extended up Wind, Bonnet Plume and Snake valleys for several miles south of the northern front of the Mackenzie Mountains. He

points out that if the ice of the valley glaciers was confluent with the Laurentide ice sheet, this must have remained sufficiently thick to extend digitations southward as the valley glaciers retreated.

A similar pattern of glaciation has been suggested by Ford (1976), who believes that in the southern Mackenzie Mountains each glacial period consisted of four major events: i, early and comparatively rapid build up of Cordilleran ice; ii, recession of Cordilleran ice as a consequence of aridity induced by greater ice formation to the west and/or a shifting of storm tracks; iii, arrival of Laurentide ice from the east; iv, general deglaciation.

Hughes (1972) has argued that minimum ages for the 'intermediate' advance at two locations are  $12,550 \pm 190$  yrs. B.P. and  $13,780 \pm 180$  yrs. B.P. respectively. He suggests, however, that in view of a relationship on Peel Plateau where 'intermediate' valley moraines appear to be older than the drift of the Laurentide maximum that has been dated at  $>31,000$  yrs. B.P., these dates are likely much younger than the moraines. Minimum ages for the 'last' glaciation at two locations are  $6,670 \pm 140$  and  $11,550 \pm 160$  yrs. B.P. It may well be, therefore, that the 'last' valley glacier advance occurred during Classical Wisconsin time while the 'intermediate' may be of early or pre-Wisconsin age.

In the Franklin Mountains, Mackenzie Plain and in the easternmost ranges of the Mackenzie Mountains, Rutter and Boydell (1972) and Rutter (1973) have found evidence for two cirque and valley glacier phases and three Laurentide ice incursions (Tables 6.1 and 6.2). Rutter (1973) has stated that Laurentide ice reached up to 4,250 ft.

in the Wrigley Lake area during the 'Classical' Wisconsin period, which suggests that the later Laurentide advance to 2,200 ft. and the two phases of cirque and valley glaciation occurred in post 'Classical' Wisconsin time. This seems highly unlikely. A more realistic interpretation may be that the period of cirque glaciation at between 3,500-4,000 ft. elevation was contemporaneous with the 'last' glaciation of Hughes (1972) and the Hole-In-The-Wall Glaciation of Ford (1976) and that it dates to the 'Classical' Wisconsin. The period of cirque and valley glacier development down to 2,000 ft. may well correlate with the 'intermediate' valley glaciation of Hughes (1972) of possible early Wisconsin age. There is also some evidence to suggest that the Flat Valley Glaciation which Ford (1976) has ascribed to the Illinoian is of the same age (Table 6.2).

(d) Ice-dammed Lakes and Ice-Marginal Drainage in the Easternmost Ranges of the Western Cordillera, Yukon and N.W.T. at the Front of a Laurentide Ice Sheet.

Deposits that indicate the former existence of proglacial, and ice-dammed lakes in the Interior Plains and Cordilleran regions of western Canada, have been identified by a number of workers including Flint (1935), Armstrong and Tipper (1948), Kindle (1952), Craig and Fyles (1960), Wheeler (1961), Craig (1965), Vernon and Hughes (1966), Fulton (1965), Hughes (1967), Muller (1967), Fulton and Klassen (1969), Green (1971), and St.-Onge (1972). Because lakes are known to have been ponded by Laurentide ice moving into the mountains of Labrador-Ungava (Ives 1958, 1960(a), 1960(b); Barnett 1963(b), 1967; Barnett and Peterson 1964), it is to be expected that

they were also ponded at the western margin of the Laurentide ice sheet in the easternmost ranges of the Richardson Mountains, Peel Plateau and Mackenzie Mountains. The published evidence suggests that this was in fact the case.

In the most recent 'Glacial Map of Canada,' Prest et al. (1967) have marked the boundaries of a former ice-dammed lake that occupied the North Redstone River Valley upstream of Wrigley Lake. The lake, which Prest et al. consider to be of Classical Wisconsin age, was ponded by the Laurentide ice sheet that deposited the terminal moraine at the eastern end of Wrigley Lake (Gabrielse et al. 1973). Since the publication of this map, deposits that appear to have been laid down in ice-dammed lakes have been discovered in many of the valley systems that dissect the eastern ranges of the Richardson and Mackenzie Mountains and the Peel Plateau. It now seems likely that many such lakes were ponded all along this mountain front during periods of Laurentide ice incursion.

Rutter and Boydell (1972) have identified glaciolacustrine sands and silts in the valleys of the Netla River, Rabbit Creek and Kotaneelee River west of the Liard valley; in the mountain valleys west of the Liard, Nahanni and Camsell Ranges; in the west part of Willowlake River valley in the Bulmer Lake map-area, and in the upper Blackwater River valley and in the Mackenzie River valley and tributaries in the Wrigley map-area. The glacial lakes are thought to have reached maximum elevations of 1,300 ft. and the drainage out of them, although controlled locally by ice margins and topography, may

ultimately have been to the north. Consistent northward deflections of Carcajou River and other major streams leaving the mountain front in the Carcajou Canyon map-area and the existence of numerous abandoned spillways aligned northwesterly also suggest that during periods of Laurentide glaciation, drainage from the Mackenzie Mountains was diverted to the north along the ice margin (Aitken and Cook 1974).

In the South Nahanni region, Ford (1976) has reported two glaciolacustrine deposits that are geographically and geomorphologically distinct. The first has been identified west of Third Canyon in the South Nahanni valley and also in the Flat River valley, and it appears to have been laid down in a lake with a surface at between 1,694 ft. and 2,145 ft. Ford notes that the sediments, which are locally more than 660 ft. thick, can often be traced up tributary canyons where they terminate at approximately 2,145 ft. a.s.l. in large dissected deltas. The second, has been identified in Deadman valley and in the Mackenzie Plain area immediately east of First Canyon, South Nahanni River, and it appears to have been laid down in a lake with a level at approximately 1,320 ft. a.s.l.

Ford (1976) believes that both lakes were formed when flow out of the South Nahanni River drainage basin was blocked by Laurentide ice (Figure 6.1). He suggests that the older and deeper lake, 'Glacial Lake Nahanni' was impounded by Clausen ice during the Illinoian glacial period and the younger lake, 'Glacial Lake Tetcela' by Jackfish ice during the Classical Wisconsin period. 'Glacial Lake Tetcela' is considered to have overflowed northwards across a low col into the valley of the Tetcela River.

In the northwestern district of Mackenzie, drainage from the Mackenzie and Ogilvie Mountains including the Arctic Red, Snake, Bonnet Plume, Wind and Peel Rivers appears to have been blocked or diverted by Laurentide ice during the last glaciation. Hughes (1972) reports that a glacial lake was impounded in Bonnet Plume basin and that this overflowed through Palmer Lake channel while a major channel about two miles south of 'Taylor Lake' carried the waters of the Arctic Red and Cranswick Rivers westward toward Snake River. On the east flank of the Richardson Mountains, are remnants of a formerly integrated, ice-marginal channel system that not only appears to mark the limit of late Wisconsin Laurentide glaciation in this area but also suggests a northward flow of drainage waters.

Extensive unconsolidated deposits of sand, gravel, silt and peat in Bell, Old Crow and Bluefish Basins, have provided a great deal of information about late Pleistocene events in the northwest district of Mackenzie and northern Yukon. Along the Old Crow River and along Porcupine River below the village of Old Crow, Hughes (1972) reports exposures up to 152 ft. and 190.5 ft. thick respectively but notes that in both areas the sediments extend much below river level. In all three basins the sediments appear to continue below the bedrock thresholds of the depressions, indicating that these are of structural rather than erosional origin. Hughes suggests that the basins may have been formed by warping or faulting in the Tertiary or early Pleistocene.

The stratigraphy of a section of these sediments exposed on the south bank of Porcupine River has been studied by Hughes (1972)



and a palynological analysis has been conducted by Lichti-Federovich (1974). Hughes has interpreted basal Units 1 and 2 of the section as fluvial and deltaic sediments. The presence of logs in Unit 1 is thought to indicate a climate at least as warm as that of today. Unit 3 is believed to be of glaciolacustrine origin, deposited when Laurentide ice advanced westward against the Richardson Mountains and on to Peel Plateau. Eastward drainage was blocked and a vast lake was formed in Old Crow Basin. Following retreat of Laurentide ice, eastward drainage apparently resumed and normal lacustrine, deltaic and fluvial sedimentation (Units 4 and 5) continued in the basins.

A readvance of Laurentide ice re-established the glacial lake which overflowed at 1,180 ft. a.s.l. Unit 6 was laid down in this lake. Hughes believes that well-defined shorelines peripheral to Old Crow and Bluefish Basins at elevations between 1,180 ft. and 1,000 ft., probably relate to this second glaciolacustrine stage and record the gradual downcutting of the outlet. Drainage of the basin lakes was followed by local deposition of fluvial and shallow-water lacustrine sediments and by widespread peat development (Units 7 and 8). Today the Porcupine River is incised as much as 185 ft. below the general level of the Bluefish Basin.

Radiocarbon ages of  $32,400 \pm 770$  yrs.,  $>37,000$  yrs. (mentioned in Lichti-Federovich 1974) and  $>41,000$  yrs. (mentioned in Hughes 1969) for shells and wood in Unit 5, suggest that deposition of this unit began  $>41,000$  yrs. B.P. Deposition of Unit 6, therefore, must have begun  $<32,000$  yrs. B.P. and a radiocarbon age for peat in Unit 7 indicates that it had ceased by, at the latest,  $10,740 \pm 180$  yrs. B.P. From such

evidence, Hughes (1969, 1972) has argued that the glaciolacustrine sediments of Unit 6 were probably laid down during the Classical Wisconsin period while those of Unit 3 were deposited during an early or pre-Wisconsin Laurentide ice advance.

From a palynological analysis of the sediments in the Porcupine River section, Lichti-Federovich (1974) has determined that Units 1 and 2 may have been laid down during the Sangamon Interglacial when the vegetation in the Porcupine River Basin was a spruce-pine boreal forest and the climate may have been broadly similar to that in the southern part of the contemporary boreal forest. Immediately before the early Wisconsin glaciation and the deposition of the Lower Glaciolacustrine unit, this forest zone was replaced by a tundra landscape with abundant grass-sedge-herb communities. The sequence of vegetational changes that occurred between the early and Classical Wisconsin glaciations (Lower and Upper Glaciolacustrine units respectively), suggests a shift from an initial arctic climatic regime to a sub-arctic boreal climate, reverting to an arctic climate again. The post-glacial sediments display a sequence of pollen assemblage types that indicate a zonal succession from an early birch tundra to a spruce forest stage, which was then replaced by the modern forest-tundra. Lichti-Federovich notes that such a sequence has been documented elsewhere and can be interpreted as evidence of postglacial warming and subsequent cooling. That the pollen assemblages in the sediments lack significant amounts of Tertiary pollen has led Lichti-Federovich to suggest that the oldest stratigraphic units are of mid to early Quaternary and not of Tertiary age.

Table 6.3 is a summary of the evidence on former ice-dammed lakes in the eastern ranges of the western Cordillera north of latitude

Table 6.3. Glacial Lakes Poned by Laurentide Ice in the Eastern Ranges of the Western Cordillera North of Latitude 60°N.

SOURCE	AREA	GLACIAL LAKE ELEVATIONS AND TENTATIVE CORRELATIONS	
Rutter and Boydell (1972)	Southwest District of Mackenzie	1,300 ft.	
Ford (1976)	South Nahanni Region	1,320 ft. Glacial Lake Tetcela	2,145 ft. Glacial Lake Nahanni
Hughes (1969, 1972)	Northwest District of Mackenzie/Northern Yukon	1,000-1,180 ft.	*?
Prest <u>et al.</u> (1967)	Wrigley Lake area		+2,000 ft. <sup>1</sup> 'Glacial Lake Wrigley'

\*? Hughes (1972) gives no elevation for a lake older than one at 1,000-1,180 ft. This lake may, however, have been contemporaneous with Glacial Lakes Nahanni and Wrigley.

<sup>1</sup> The name 'Glacial Lake Wrigley' is proposed here. The exact elevation of the lake is not known but is thought to have been close to 2,000 ft. a.s.l.

60°N. Lakes at 1,000-1,320 ft. may well have been formed during the Classical Wisconsin Laurentide advance, while those at 2,000-2,145 ft. in the southwestern district of Mackenzie and a much lower lake reported by Hughes (1969, 1972) in the northwestern district of Mackenzie and northern Yukon, may be of early Wisconsin age. By this interpretation, Glacial Lake Nahanni would be of early Wisconsin rather than of Illinoian age as Ford (1976) has asserted.

The eastern ranges of the western Cordillera north of latitude 60°N have suffered multiple Cordilleran glaciation in the south, several incursions of Laurentide ice in the east and have passed through phases of cirque and valley glacier development. In addition, it is apparent that during at least two Laurentide invasions, lakes were ponded in valleys and basins in the mountains and drainage was diverted to the north. Because the Nahanni karst sits astride the Laurentide ice sheet, valley glacier and ice-dammed lake 'action,' it is pertinent to now examine the evidence of glaciation within this area.

## 2. Evidence of Glaciation in the Nahanni Karst Belt and in Surrounding Areas.

The South Nahanni region of the Mackenzie Mountains appears to have had a complex glacial history. Evidence collected in the field and from aerial photographs is often contradictory as to exact ice limits and thicknesses, but despite this it is clear that the area has suffered multiple glaciation by Laurentide ice and that during at least three of these advances huge ice-dammed lakes were impounded. Although a great deal of information has been collected and the glacial

history of the southern Mackenzie Mountains is better understood than formerly, the outline presented here must still, unfortunately, be considered tentative. There is no doubt that a great deal of additional work will be necessary before the exact glacial history of this area can be outlined with any real degree of certainty.

(a) An Unglaciaded Area?

Detailed examination of the Nahanni Plateau surface between First Canyon, South Nahanni River and Sundog Basin, has revealed no evidence of glaciation above 4,300-4,500 ft. The complete absence of erratic material and the presence of several delicate periglacial tors, indicate that the higher parts of this plateau were not covered by ice of either Cordilleran or Laurentide origin during the Pleistocene period. In the absence of glacial erosion the upland surface is today a felsenmeer of locally-derived, frost-shattered limestone fragments partially sorted and patterned by periglacial processes (Plate 6.1).

(b) Laurentide Ice Sheet Limits.

(i) The First Canyon Glaciation.

The entire upland surface of the Ram Plateau and the eastern slope of the Nahanni Plateau below 4,300 ft., display little of the felsenmeer that is characteristic of apparently unglaciaded areas. Instead, the limestone shows definite evidence of glacial scouring with glaciokarstic limestone pavements ubiquitous, is covered by a thin mantle of till and is strewn with large and small erratic blocks. The largest erratics which are up to 15 ft. in diameter are of locally



Plate 6.1. Patterned ground at 4,800 feet, Nahanni Plateau between Death and Canal Canyons. At this altitude the plateau surface is a felsenmeer of angular, frost-shattered limestone fragments. There is no evidence that ice covered this area at any time during the Pleistocene.

derived limestone, the more massive of them, fresh-looking (Plate 6.2) and those of rubbly bedded limestone in an advanced stage of disintegration (Plate 6.3). The till, which contains igneous and metamorphic pebbles and boulders clearly derived from the Canadian Shield region, was obviously emplaced by westward moving ice.

The glacial deposits on the upland surfaces in the Nahanni region must have been laid down by a Laurentide ice sheet that moved westwards through the Franklin Mountains and finally came to rest against the eastern ranges of the Mackenzie Mountains. This period of glaciation has been called the 'First Canyon Glaciation' by Ford (1973) and at its maximum, ice reached elevations of 4,300-4,500 ft. on the eastern flanks of the Nahanni Plateau (Figure 6.2). This elevation correlates well with observations made by Gabrielse *et al.* (1973) in the Wrigley Lake map-area, where the upper limit of Laurentide glaciation appears to be close to 4,500 ft. (Table 6.1). A slight increase in the elevation of First Canyon ice eastwards from the Mackenzie Mountains could also explain reports of erratic material from the east at elevations of  $\pm 5,000$  ft. in some parts of the southwest district of Mackenzie (Rutter & Boydell 1972, Rutter 1973). The highly weathered nature of material laid down by First Canyon ice and the fact that this appears to be the oldest glacial deposit preserved in the Nahanni region, suggest that the glacial event occurred a very long time ago.

(ii) The Death Canyon Glaciation.

Several of the deep canyons which dissect the eastern flank of the Nahanni Plateau south of Sundog Basin are blocked by huge glacial



Plate 6.2. Fresh limestone erratic at 3,700 feet elevation,  
Nahanni Plateau south of Death Lake.





Plate 6.3. Highly disintegrated limestone erratic at 4,000 feet elevation, Nahanni Plateau north of Canal Canyon.

15

end moraines, some of them more than 400 ft. high (Figure 6.2). The present drainage out of these canyons is via underground routes. Canyons without glacial plugs which are drained entirely by surface streams show distinct evidence that they too were blocked by such deposits at one time. That the canyons downstream of these moraines are choked with glacial debris, while the canyons upstream of them lack such deposits, indicates that they were deposited by ice moving westwards into the mountains and not by ice flowing eastwards out of them.

Some of the moraines, such as that between Moraine and Death Lakes, have irregular surfaces with numerous kettle holes and are built of poorly sorted debris ranging in size from clay to boulders. Igneous and metamorphic erratics are ubiquitous. Other moraines, such as those in Hidden and Ranger Canyons, have extremely flat crests and are composed almost entirely of extremely well-rounded pebbles and boulders clearly of fluvial or fluvio-glacial origins. Although some of these moraines may be composed of glacially reworked stream eroded debris, most are believed to be huge deltas deposited by glacial meltwaters in ice-dammed lakes impounded in the canyons upstream of the ice margin. One such delta in Ranger Canyon, dissected by subsequent stream action, is 300-400 ft. thick and is composed almost entirely of rounded pebbles and boulders of limestone and dolomite with lesser fines (Plate 6.4). Erratics of Canadian Shield origin are present but subsidiary to the more local material.

In Death Canyon, moraines/deltas which block the main canyon and two tributaries have crests at 3,300-3,400 ft. Further south,



Plate 6.4. The remains of a huge delta laid down in an ice-dammed lake, Ranger Canyon, Nahanni Plateau. The upper surface of the delta composed of well-rounded pebbles and boulders is at between 3,500-3,600 feet a.s.l.

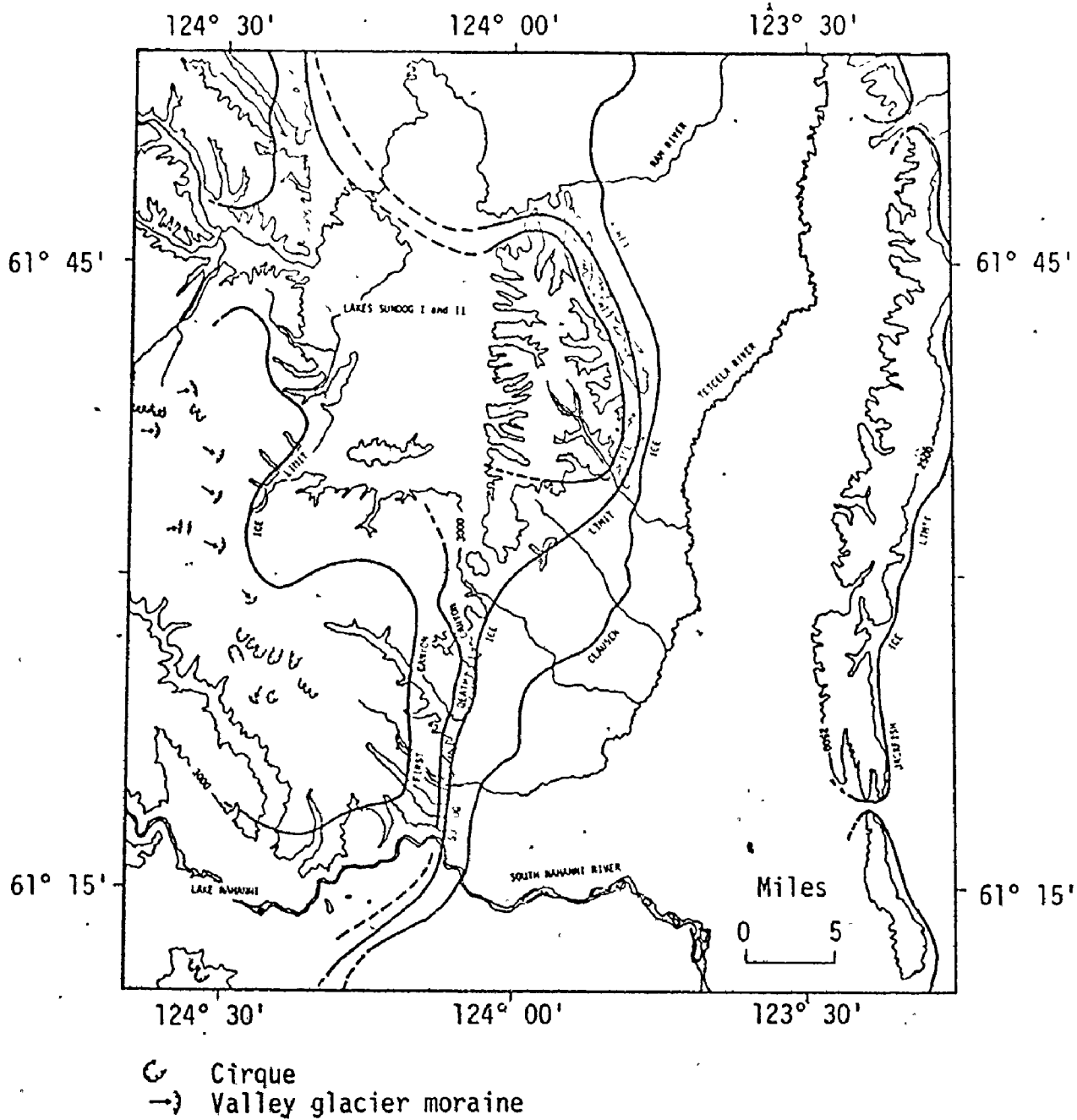


Figure 6.2. Glaciation of the Nahanni karst, N.W.T., Canada.

moraines with crests at 3,300-3,500 ft. are clearly evident in two smaller canyons while the longest and deepest canyon in the area, Canal Canyon, is blocked by an end moraine with a crest at 2,800 ft. In two tributary valleys to the south of Canal Canyon, however, there is evidence to indicate that the ice surface was at approximately 3,500 ft. when this moraine was deposited. Although no evidence of a former end moraine has been found in Lafferty Canyon or in First Canyon, South Nahanni River, parts of a large delta, its upper surface at 3,400-3,500 ft., are preserved in Ranger Canyon just to the north (Plate 6.4).

The end moraines and deltas that block many of the canyons dissecting the eastern flank of the Nahanni Plateau are thought to mark the limits of a Laurentide ice sheet that fingered westwards into the southern Mackenzie Mountains. This ice sheet is believed to have come to rest against the eastern flank of the Nahanni Plateau south of Sundog Basin, its surface at between 3,300 and 3,500 ft. (Figure 6.2). Because the evidence for this glacial phase is best displayed in Death Canyon, the event has been called the 'Death Canyon Glaciation.' The presence of bedded and sorted sands and gravels downvalley of Death Lake, suggests that during retreat, the Death Canyon ice margin may have stood for some considerable time just back from its maximum position, its upper surface at  $\pm 3,000$  ft. Ice-dammed lakes impounded at this time between the ice margin and previously deposited moraines, were filled with fluvio-glacial sands and gravels.

(iii) The Sundog Glaciation.

Bare, often karsted limestone is characteristic of the Nahanni

is overlain by unconsolidated glacial debris. Where Ranger Creek leaves the Nahanni Plateau and flows out on to the Mackenzie Plain, there are terraces 400-500 ft. above river level, their top surfaces at 2,700-2,800 ft. These are clearly all that remain of a former valley fill graded to this elevation. On the Nahanni Plateau remnant between Lafferty Creek and First Canyon, the limestone appears to be mantled by glacial material up to 2,700 ft. That this material is not simply shale of the overlying Fort Simpson Formation, as Douglas and D. K. Norris (1960) contend, is indicated by its presence in the floor of what appears to be a subglacial meltwater channel possibly formed at the time of the Death Canyon or First Canyon Glaciation. Still further south, shallow canyons cut into the extreme southwestern flank of the Nahanni Plateau south of the South Nahanni River, appear choked with sediment up to 2,700 ft. elevation.

The glacial deposits below  $\pm 2,700$  ft. are believed to have been laid down by Laurentide ice, the surface of which came to rest at an elevation of between 2,700-3,000 ft. against the eastern flank of the Nahanni Plateau north of First Canyon (Figure 6.2). This period of glaciation has been called the 'Sundog Glaciation.'

(iv) The Clausen Glaciation.

The advance of Laurentide ice that impounded Lake Nahanni has been called the Clausen Glaciation (Ford 1976). As Ford claims that the surface of Lake Nahanni was at an elevation of close to 2,100 ft., Clausen ice must have reached up to at least this elevation against the eastern flank of the Nahanni Plateau. Depositional terraces at 2,100-2,200 ft. on the extreme southeastern flank of the Nahanni Plateau

west of Clausen Creek may have been deposited at the margin of this ice sheet. Similar terraces are present on the eastern flank of the Ram Plateau. In one case alluviation of a tributary canyon south of the Ram River to 1,900 ft., has resulted in the stream adopting a new drainage route. As Figure 6.3 shows, the stream originally discharged northwards into the Ram River but after the canyon was alluviated it was diverted eastwards in the direction of rock dip cutting a narrow steep-side gorge in the limestone bedrock underlying the alluvial fill. Alluviation of the canyon likely took place during the Clausen Glaciation with the stream developing a new route as it cut down into the sediments after the ice had retreated. The present stream route is, therefore, partially a superposed one.

(v) The Jackfish Glaciation.

The most recent advance of Laurentide ice into the South Nahanni region, occurred during the Jackfish Glaciation which impounded Lake Tetcela at 1,300 ft. in the Mackenzie Plain east and west of Yohin Ridge (Figure 6.4). Further evidence of this glaciation and of Lake Tetcela, is to be found on the eastern flanks of the Ram Plateau where depositional terraces at 1,300 ft. elevation are ubiquitous.

Alluviation of many of the canyons dissecting the eastern flank of the Ram Plateau at the time when Lake Tetcela was impounded by Jackfish ice subsequently caused many streams to change direction after ice retreat. Figure 6.5 illustrates two examples. In one case the valley was filled up to 1,500 ft. and the stream was deflected to the east cutting an extremely narrow, steep-sided gorge through the limestone that originally formed its valley wall (Figure 6.5(a)). In the second

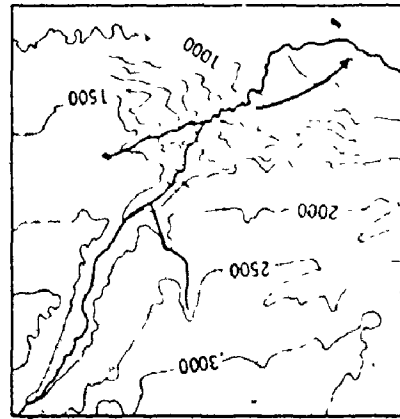
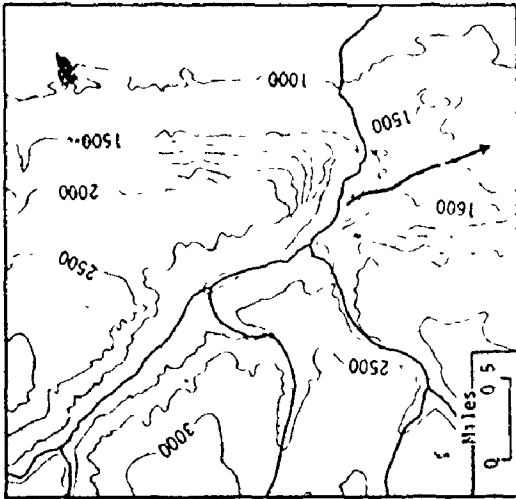


Figure 6.5. Altered stream courses on the eastern edge of Ram Plateau. The old courses of the streams are indicated by arrows.

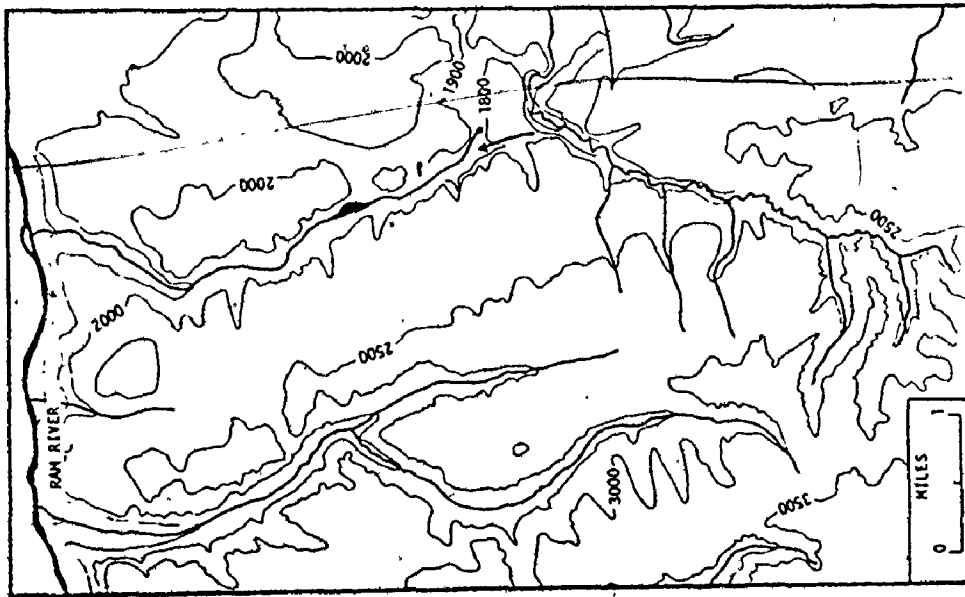


Figure 6.3. Altered stream course, Ram Plateau. The old course of the stream is indicated by the arrow. After alluviation of the canyon during a glacial event the stream adopted a new course cutting a gorge through what had previously been a canyon wall.

b

a



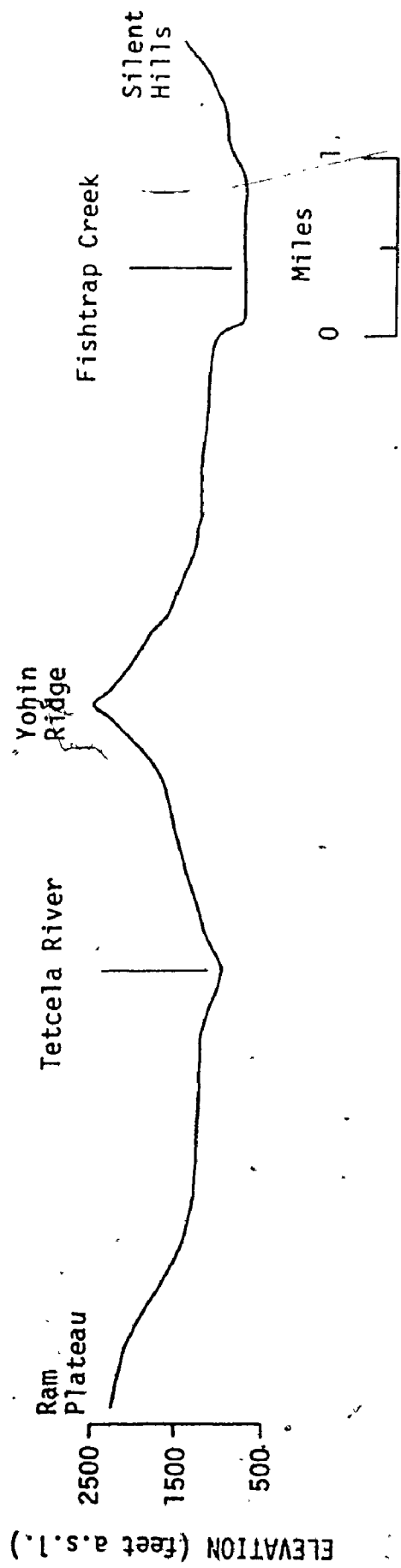


Figure 6.4. Topographic section across Mackenzie Plain showing the bevel on sediments laid down in Lake Tetcela.

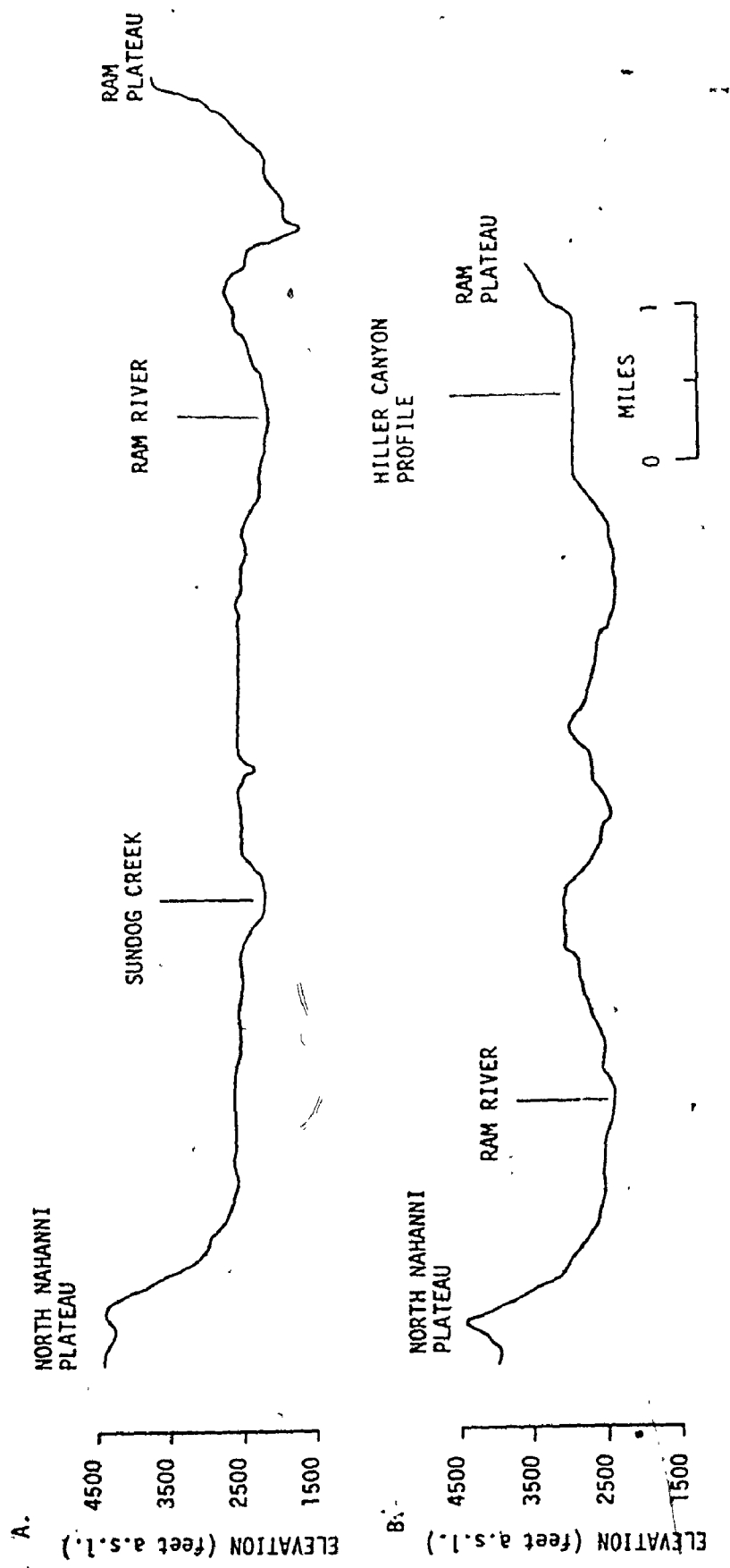


Figure 6.6. East to west topographic sections across Sundog Basin showing bevels on sediments laid down in Lakes Sundog I and II. Section A is in the north of the basin, B in the south.

example (b), the valley was filled to 1,000 ft. elevation and again the stream was deflected eastwards cutting through the walls of its original channel.

(c) Ice-Dammed Lakes.

Ford (1976) has identified sediments within the South Nahanni River drainage basin that indicate the former existence of a lake with a level of approximately 2,000-2,200 ft. and a second lake with a level at 1,300 ft. These lakes he has called Lake Nahanni and Lake Tetcela respectively. In addition to these examples, there can be little doubt that lakes were also impounded in the Sundog Basin during the Pleistocene period.

At present the floor of Sundog Basin - a structural depression between the northern portion of the Nahanni Plateau to the west and the Ram Plateau to the east - is mantled by great thicknesses of unconsolidated sediments (Plate 6.5). The bedrock floors of canyons which dissect the western limb of the Ram Plateau clearly pass beneath this material, indicating that it was deposited when outlets from the basin were blocked by ice and not as the basin was originating as a result of structural deformation.

There can be little doubt that some of the sediment in Sundog Basin - much of it sand and gravel - was emplaced by First Canyon ice in the form of dead ice moraine during glacier retreat. The extreme flatness of the upper surface of the sediment fill today, however, suggests that much of it was laid down in an ice-dammed lake when all low-level outlets from the basin were blocked by Laurentide ice. Elevations of depositional terraces suggest that there were two periods



Plate 6.5. Sundog Basin. Ice-dammed lakes are believed to have occupied this structural depression on at least two occasions during the Pleistocene period. In the most recent inundation, the surface of Glacial Lake Sundog II remained at +2,500 feet for long periods. Sediment deposited in it still covers the floor of the basin today.

when lakes existed in the depression and that these periods were separated by an interval of fluvial erosion in the area.

Many of the canyons which dissect the western flank of Ram Plateau, show distinct evidence that they were at one time alluviated up to 2,600-2,800 ft. elevation. Two canyons in fact, Hiller and Texas, which presently drain underground, are still alluviated to this level. It is clear that alluviation continued out into Sundog Basin, for well-preserved depositional terrace remnants are common all along the lower portions of the western limb of Ram Plateau. That the base level for alluviation in Sundog Basin was at one time  $\pm 2,700$  ft., is further suggested by the fact that all around the basin, unconsolidated sediments are common up to this elevation with bare limestone replacing them at higher levels (Figure 6.6(a)). The base level of sedimentation is believed to have been the surface of an ice-dammed lake - 'Lake Sundog I.' It is clear that the upper surface of the Laurentide ice sheet that impounded this lake was at or above 2,700 ft.

In the extreme southeast portion of the Sundog Basin in the region of the Nahanni poljes, are a series of higher terraces up to 3,100 ft. in elevation. The origin of these is problematical but the most likely explanation of them is that some are dissected sandurs and others kame terraces, both laid down near a glacier that occupied the region around what is now the labyrinth and polje karst belt. Certainly the surficial material of the Sinkhole Plain - a very flat surface at 3,000 ft. west of the Nahanni poljes - appears to be of fluvio-glacial origin for it is poorly sorted with a high content of extremely rounded pebbles. East of First Polje, on the other hand,

is a terrace of sand and gravel - material that may have been deposited at the margins of a glacier tongue.

Lake Sundog I drained when the Laurentide ice impounding it retreated and there followed a period of fluvial erosion during which time much sediment was transported out of the basin. A further advance of Laurentide ice blocked drainage routes out of the basin once more, impounding 'Lake Sundog II' with its surface at 2,400-2,500 ft. elevation (Figure 6.6(b)). The lake was gradually filled with sands and gravels transported into it largely by the Ram River and prior to ice retreat, its volume must have been significantly reduced. Lake Sundog II finally drained following the retreat of the Laurentide ice impounding it and since then, the sediments in the floor of Sundog Basin (Plate 6.5) have been much dissected by stream action.

(d) Cirque and Valley Glaciation.

During the successive advances of Laurentide ice into the southern Mackenzie Mountains, cirque and valley glaciers developed in the heads of canyons dissecting the north and south sections of the Nahanni Plateau and in the Tlogotsho Range (Figure 6.2). It appears that there were two distinct periods of local ice development.

In the earlier period small carapace ice sheets and cirque glaciers developed in the higher parts of the Nahanni Plateau. West of Sundog Basin there is evidence to suggest that valley glaciers extended down some valleys to elevations of 3,200-3,300 ft. but in most to 3,800-3,900 ft. Distinct northeast-facing cirques in the northeastern part of Tlogotsho Range, with moraines at 3,300-3,700, may also relate to this early period. In the Nahanni Plateau south of

of Sundog Basin, there is no evidence of extensive valley glacier development from a high elevation carapace ice mass. Cirques are extremely common, however, in the northeast-facing tributary canyons of the Canal Creek, Lafferty Creek and Prairie Creek basins. At their maximum these cirque glaciers extended down to 3,800-4,000 ft. and this period may correlate with the valley glacier phase further north and the low-elevation cirque phase in the Tlogotsho Range.

A period of high elevation cirque glaciation followed. Cirques in the mountains are common at elevations of 4,000-4,500 ft. and they appear to have retreated in a series of stages. Multiple end moraines are common in many cirques in the headwaters of Canal Canyon. In one case in particular, three moraines are evident in the aerial photographs at elevations of 4,100, 4,350 and 4,400 ft. Others show moraines at 4,300 and 4,500 ft., at 4,100 and 4,400 ft. and at 3,800 and 4,500 ft., respectively. West of Sundog Basin, many valleys display multiple moraines. In one, moraines are evident in the aerial photographs at 3,800, 4,300 and 4,400 ft. in another at 3,900 and 4,500 ft.

The evidence suggests, therefore, that an early period of cirque and valley glaciation with ice extending to 3,800-3,200 ft. was followed by a period of high-level cirque glaciation at 4,100-4,600 ft. During this later stage it is evident that cirque glacier retreat occurred in two or more stages as evidenced by multiple end moraines.

### 3. A Tentative Glacial Chronology for the Southeastern Mackenzie Mountains.

Many fossil caves in the Nahanni karst region contain massive speleothem deposits that were clearly precipitated when the climate was

deposits (Harmon et al. 1975), demonstrate fairly conclusively that there have been at least three periods during which speleothem growth was enhanced by climatic conditions (Table 6.4). These periods, which were probably interglacial phases, occurred at 145,000 years B.P., between 191,000 and 217,000 years B.P., and between 275,000 and >350,000 years B.P. (Table 6.5).

As Table 6.6 shows, there is a close agreement between known periods of high sea level, periods of enhanced speleothem growth in Nahanni caves and peaks in the orbital eccentricity of the earth. This strongly suggests that periods centered at 125,000, 210,000 and 310,000 years B.P. were warm interglacials in the southern Mackenzie Mountains and that these were induced by increases in the eccentricity of the earth's orbit. It also suggests that troughs in the orbital eccentricity curve might correlate with glacial events (Vernekar 1972).

In two fossil caves in the Nahanni, Grotte Valerie and Speleothem Cave, a coarse gravel fill which contains small erratic pebbles clearly derived from the Canadian Shield (the First Clastic Fill of Ford (1973)) is cemented by stalagmite that has been uranium-series dated at older than 350,000 years. The glacial material must have been washed into the caves from the plateau surfaces above them and may be fluvially reworked till deposited by the First Canyon Laurentide ice sheet. If this is the case, then clearly the First Canyon Glaciation must have occurred more than 350,000 years ago and perhaps even 400,000 or 500,000 years ago when the eccentricity of the earth's orbit was very small (Vernekar 1972).



Table 6.4. 230-Th/234-U Age Determinations of Speleothems from Caves in the Nahanni Karst.\*

Sample Number	Cave	Age (yrs. B.P.)	Comments
71016:01	Grotte	>250,000	Oldest layer
71016:02	Valerie	200,000 ± 20,000	Youngest layer
71016:03		217,000 ± 17,000	
71009:05	Cave No. 9	275,000 ± 40,000	
72026:03	Grotte Valerie	145,300 ± 6,000	Oldest layer
72030:07	Grotte	191,000 ± 21,000	Youngest layer
72030:09	Valerie	320,000 ± 26,000	Basal layer
72030:10		280,000 ± 23,000	
72057:02	Grotte Valerie	>350,000	Youngest layer
72066:04	Grotte Valerie	278,000 ± 34,000	Layer near base
72067:04	Cave 12A	301,000 ± 41,000	Youngest layer
72067:05		315,000 ± 24,000	Oldest layer
73051:04	Igloo	>350,000	Oldest layer
73051:05	Cave	>350,000	Youngest layer
73052:06	Ice Curtain Cave	311,100 ± 11,000	Youngest layer
73056:01	Canal Canyon	319,100 ± 28,000	Youngest layer
73056:03	Cave	>350,000	Oldest layer
73057:01	Tower View Cave	346,000 ± 16,000	Oldest layer

\*Speleothems from Grotte Valerie and Cave No. 9 were collected by D. C. Ford, all others by the writer. Age determinations were made by P. Thompson and R. S. Harmon at McMaster University, Canada.

Table 6.5. Interglacial Periods in the Nahanni Region Suggested by  
Periods of Enhanced Speleothem Growth.

Periods of Enhanced Speleothem Growth (years B.P.)	Speleothem Ages (years B.P.)	Locality Collected
	>350,000	Grotte Valerie
	>350,000	Igloo Cave
	>350,000	Igloo Cave
	>350,000	Canal Canyon Cave
	350,000 ± 40,000	Speleothem Cave
>350,000	346,000 ± 16,000	Tower View Cave
to	320,000 ± 26,000	Grotte Valerie
275,000	319,000 ± 28,000	Canal Canyon Cave
	315,000 ± 24,000	Cave 12A
	311,000 ± 11,000	Ice Curtain Cave
	301,000 ± 41,000	Cave 12A
	280,000 ± 23,000	Grotte Valerie
	278,000 ± 34,000	Grotte Valerie
	275,000 ± 40,000	Cave 9
	>250,000	Grotte Valerie
217,000	217,000 ± 17,000	Grotte Valerie
to	200,000 ± 20,000	Grotte Valerie
191,000	191,000 ± 21,000	Grotte Valerie
±145,300	145,300 ± 6,000	Grotte Valerie

Table 6.6. Comparison Between Periods of High Sea Level, Enhanced Speleothem Growth in the Nahanni Karst and Peaks in the Earth's Orbital Eccentricity (years B.P.).

Orbital Eccentricity Peaks	Enhanced Speleothem Growth	Periods of High Sea Level		
		Barbados <sup>1</sup>	Mediterranean <sup>2</sup>	Alaska <sup>3</sup>
				5,000-6,000
			50,000±5,000	33,000-48,000
125,000	145,000	82,000 105,000 125,000	75,000±5,000 125,000±10,000 135,000±15,000	78,000-100,000
210,000	191,000 to 217,000	170,000 230,000		170,000-175,000 210,000-221,000
310,000	275,000 to >350,000			< 300,000±100,000

<sup>1</sup>Mesolella et al. (1969).

<sup>2</sup>Stearns and Thurber (1967).

<sup>3</sup>Karlstrom (1965) and Hopkins et al. (1965).

If it is assumed that the First Canyon Glaciation occurred approximately 400,000 years B.P., and that interglacials occurred 310,000, 210,000 and 125,000 years ago, then it is possible to construct a tentative glacial chronology for the South Nahanni region (Table 6.7). It seems possible that the cirque glaciation above 4,000 ft. occurred approximately at the same time as did the Jackfish Glaciation which impounded Lake Tetcela. Because Jackfish ice seems to have been the last Laurentide ice to enter the southeastern Mackenzie Mountains region and because cirque glacier and ice sheet moraines and lake deposits have a fresh appearance, the two events are considered to correlate with the 'Classical' Wisconsin period. Deposits laid down in Lake Tetcela would, therefore, be of the same age as 'Upper Glaciolacustrine' sediments laid down in an ice-dammed lake that occupied the Porcupine River basin. Such an interpretation would agree with that made by Ford (1976) who has suggested that Lake Tetcela drained across a topographic col at  $\pm 1,300$  ft. in Mackenzie Plain just north of the South Nahanni River.

Ford (1976) has tentatively ascribed the Clausen glacial advance, which impounded Lake Nahanni and which may correlate with a cirque and valley glaciation above 3,500 ft., to the Illinoian period. That sediments laid down in Lake Nahanni are still preserved in the fluvially active South Nahanni River drainage basin, however, may indicate that the Clausen Glaciation was more recent than the Illinoian. It has, therefore, been tentatively ascribed to the early Wisconsin period, suggesting contemporaneity between sediments laid down in Lake Nahanni and the ine the Di

Table 6.7. Tentative Glacial Chronology and Correlations for the Southeastern Mackenzie Mountains.

Continental Correlations	South Nahanni Event	Approximate Age in years B.P.	Ice-Dammed Lakes	Cirque and Valley Glaciation
	Post Glacial	< 10,000		
Classical Wisconsin	Jackfish Glaciation	20,000	Lake Tetcela	Cirque Glaciation above 4,000 ft.
Early Wisconsin	Clausen Glaciation	60,000	Lake Nahanni	Cirque & Valley Glaciation above 3,500 ft.
	Sangamon Interglacial	125,000		
Illinoian	Sundog Glaciation	150,000	Lake Sundog II	
	Grotte Valerie Interglacial II	210,000		
Kansan	Death Canyon Glaciation	260,000	Lake Sundog I	*
	Grotte Valerie Interglacial I	310,000		
Nebraskan	First Canyon Glaciation	400,000		

basin. It is not clear as to the direction of drainage out of Lake Nahanni but there is every reason to believe that it was to the north around the eastern flank of the Ram Plateau.

During the Sundog Glaciation, Laurentide ice appears to have reached to elevations of 2,700-2,800 ft. along the eastern flanks of the Ram Plateau and the southern portion of the Nahanni Plateau. It may have been responsible for the end moraine at >2,500 ft. at the eastern end of Wrigley Lake (Table 6.1), and for Lake Sundog II. In attempting to interrelate the various glacial features that have been identified in the Nahanni region, it was first very tempting to assume that Lakes Nahanni and Sundog II were contemporaneous and that one drained into the other. Unfortunately the situation appears to have been more complex than this. Ford (1976) has demonstrated that the surface of Lake Nahanni was at or slightly above 2,100 ft. implying an ice dam with its upper surface at or slightly above this elevation. Lake Sundog II appears to have had a surface that remained at close to 2,500 ft. for a very long period.

The difference in elevation between Lakes Nahanni and Sundog II is not substantial enough (400 ft.?) to disprove contemporaneity. What is a problem, is that an ice sheet with a surface at or slightly above 2,500 ft. resting against the eastern limb of the Ram Plateau, could not impound a body of water of Lake Sundog II's dimensions. The reason for this is that if easterly drainage routes were blocked by an ice barrier, the Ram River would simply drain northwards across an extremely low topographic col - presently with an elevation of 2,000 ft. - into

the basin of a second tributary of the North Nahanni River. To impound Lake Sundog II, Laurentide ice would also have to block this alternate drainage route. Ice would, therefore, have to pass through the gap between Nahanni and Camsell Ranges, move 20-30 miles up the North Nahanni River valley and then flow southwards towards Sundog Basin. It is doubtful if an ice sheet with an upper surface at 2,200-2,300 ft. could do this.

Lake Sundog II has, therefore, been correlated with the Sundog Glaciation which is believed to have come to rest against the eastern flanks of the Ram Plateau and the Nahanni Plateau south of Sundog Basin at 2,700-2,900 ft. Both events have been tentatively ascribed to the Illinoian period and Lake Sundog II is believed to have drained northwards along the ice margin against the eastern slope of the northern section of the Nahanni Plateau into the North Nahanni River region.

After the retreat of Sundog ice, surface drainage in Sundog Basin was across an even surface of sands and gravels at  $\pm 2,500$  ft. Former drainage channels and the topographic divide between the Ram and North Nahanni Rivers, must have been buried beneath great thicknesses of sediment. The present Ram River drainage pattern must, therefore, be at least partly a superposed one. Certainly the extremely deep and narrow Scimitar Canyon<sup>1</sup> through which the Ram River passes before traversing the Ram Plateau, appears to have been formed by the superposition of the Ram River from overlying sediments onto

---

<sup>1</sup> Scimitar Canyon was first noted by Alan Jackson who gave it its name.

underlying bedrock. There can be little doubt that the Ram River had not cut Scimitar Canyon prior to the Sundog Glaciation - its old channel is probably still partly buried beneath Lake Sundog II sediment.

If the Sundog Glaciation and the impounding of Lake Sundog II occurred during the Illinoian period this implies that the present drainage route of the Ram River across Sundog Basin was initiated in the Wisconsin-Illinoian or Sangamon Interglacial period.

Death Canyon ice may have impounded Lake Sundog I during the Kansan glacial period some 260,000 years ago. Drainage may have been northwards first into the North Nahanni drainage basin and then via Trench Canyon to the Arctic Ocean. The First Canyon Glacial phase certainly occurred more than 350,000 years ago and may correlate with the Nebraskan ice advance that laid down extensive till deposits in the continental U.S.A. and Canada.

There is evidence in the Nahanni karst region of northern Canada of five separate advances of Laurentide ice, of two phases of local cirque and valley glacier development and of four former ice-dammed lakes. The local cirque and valley glacier phases above 3,500 and 4,000 ft. respectively have also been reported by Rutter and Boydell (1972) and probably correlate with the 'last' and 'intermediate' valley glaciations (Table 6.2) of Hughes (1972). Erratics reported by various workers at altitudes ranging from 4,250-5,000 ft. in the Mackenzie Mountains were probably deposited by First Canyon ice possibly of Nebraskan age. Moraines built by Laurentide ice at 2,200 ft. in the southwest district of Mackenzie (Rutter and Boydell,



1972) and at 1,000-1,500 ft. in the Richardson Mountains and Peel Plateau (Hughes 1972) were probably laid down by Clausen ice in the early Wisconsin period (Table 6.1). The moraine at >2,500 ft. east of Wrigley Lake (Gabrielse et al. 1973) may well have been laid down by Sundog ice.

With the evidence available at the present time the chronology outlined in Table 6.7 is the best that can be put together. Further detailed fieldwork will be necessary before the extremely complex ice margin/glacial lake/glacial chronology problems of the Nahanni area can be explained with any real confidence.

An attempt will now be made to synthesize the data that have been presented in Chapters 1 through 6. As it is apparent that one of the most unusual aspects of the sub-arctic Nahanni karst region is the presence there of natural rock labyrinths on a scale not known elsewhere, some discussion of this landform type seems warranted.

1. The Natural Rock Labyrinth Phenomenon.

(a) Labyrinths in Karst Rocks.

Karst streets which are the components of rock labyrinths in soluble rocks, are common in many karst regions of the world but highly developed intersecting networks are relatively rare. As early as 1893 in 'Das Karstphanömen,' Cvijić mentioned the presence of fissures 2-4 meters wide, 1-5 meters deep and a few tens of meters long in the Classical and Dinaric karsts of Yugoslavia. These depressions which Cvijić called 'bogazi' or 'strugas' have also been discussed by Blanc (1958).

Bauer and Zötl (1972) have identified similar landforms in the Austrian Limestone Alps. They note that plateaus that were once covered by Pleistocene glaciers are often characterized by a distinct 'Gassenlandschaft' with more or less straight, narrow ravines which always occur on fault lines and joints and which may be more than 100 meters long and have an average depth of several meters. Because deposits of Augenstein gravel and terra rossa-like soils have been discovered in the bottoms of some of these 'karstgassen,' they are believed to be of

to be derived from the corridor networks. The roofs of the fissure caves collapse and link more and more of the corridors into one system. At the same time the flat floors of the corridors extend both lengthwise and laterally, so that the intervening ridges - which are seen in all stages of destruction - are eliminated. When interconnected by these means, the box valleys retain a completely rectangular joint-controlled branching pattern. The valleys are more continuous and confluent than the streams occupying them which sink into the floors or enter small caves in the valley walls with some frequency. However, the downward gradients of the box valleys are scarcely interrupted by these water-sinks which usually occur in small clay or silt-floored hollows 4-5 ft. deep.

Jennings & Sweeting (1963) note that apart from the karst corridors, enclosed depressions such as conical or basin-shaped dolines typical of temperate karst are rare, nor is anything comparable to the cockpits of tropical humid karst encountered. There are, however, a number of enclosed depressions of rectangular plan, with flat floors and steep or vertical walls. The floors are mainly covered by alluvium or residual soil but rock floors also occur in parts. Stream channels sometimes traverse the floors and disappear into small holes in the alluvium or enter caves in the surrounding walls. The largest of these depressions is about one mile long and has a maximum floor width of 200 yards. The surrounding walls rise 100-150 ft. above the depression floor, and are much broken into ridges and pinnacles by corridor valleys. As Jennings & Sweeting point out, "These depressions do not correspond

well with any of the classical categories of enclosed karst depression, having the dimensions of dolines but, some of the aspect of poljes" (p. 27).

Also present in the Fitzroy Basin are areas of separate towers, pinnacles and narrow ridges scattered over an almost flat rock plain, which is often thinly and patchily veneered by soil and rock debris. In this region of small scale 'tower karst,' towers are a maximum of 150 ft. high and most are much lower. Jennings & Sweeting suggest that as the box valleys, polje-like depressions and marginal amphitheaters enlarge, they intersect to produce the fields of pinnacles and arêtes, noting that every transitional assemblage between the networks of huge karst corridors to the stage of scattered towers is represented in the area.

There can be no doubt as to the marked similarity between the 'dissected karst' of the Limestone Ranges of Western Australia and the 'labyrinth karst' of the Nahanni region of Canada. The karst streets, towers, pinnacles and narrow residual ridges in the Nahanni, although very much bigger than their Fitzroy Basin counterparts, are morphologically similar to the Australian forms. Furthermore, although nothing resembling the 'box valleys' of the Fitzroy have been discovered in northern Canada, the large flat-floored closed depressions of this region, labelled 'miniature poljes' by Jennings & Sweeting (1963), appear to be the tropical semi-arid equivalents of the sub-arctic karst plateaus. Because there is no evidence that they are liable to flooding, they are not thought comparable to the three Nahanni poljes or to poljes elsewhere.

One basic difference between the landforms of these two areas lies in the morphology of depression floors. 'Miniature poljes' and karst streets in the Fitzroy Basin have flat floors which are essentially pediments graded to either the regional or to local base levels. In addition, karst towers, pinnacles and residual limestone ridges project from a pediplain of little relief. Karst streets and platea in the Nahanni, on the other hand, have uneven floors strewn by irregular accumulations of angular frost-shattered collapse debris and walls that invariably exhibit extensively developed screes. It is apparent that these minor variations in morphology relate to differences in both the past and present climates of these regions. In the Fitzroy Basin, tropical semi-arid processes coupled with the action of solution have produced flat-floored, vertical-walled depressions in which there is little rock debris. In the Nahanni, solution has been accompanied by periglacial conditions so that there is an abundance of frost-shattered debris in the floors of enclosed depressions and screes commonly flank the bounding walls.

Karst streets have been discovered under climates ranging from sub-arctic, through Alpine (Bauer & Zötl 1972, Croce 1964), warm temperate (Cvijić 1893, Blanc 1958, Waltham 1970) and tropical semi-arid (Tricart & Da Silva 1960, Jennings & Sweeting 1963, Cooke 1973) to humid tropical (Pannekoek 1948, Sunartadirdja & Lehmann 1960, Jennings & Bik 1962, Wilford & Wall 1965, Verstappen 1964, 1969, Monroe 1964). That almost identical karst landform assemblages can be produced under both tropical semi-arid and sub-arctic climatic conditions suggests that

climatic effects are subordinate in producing karst streets and platea.

Jennings & Sweeting (1963) support the claim made by Tricart & Da Silva (1960) that "there is a new variety of karst to be recognized in the tropical semi-arid climate, differing substantially from the 'classical' tropical karst of more humid conditions, but which is more closely related to that karst style than to any other" (p. 50). In fact the wide distribution of karst street networks with platea, towers and pinnacles, suggests that 'labyrinth karst' should be recognized as a distinctive karst type that like doline karst is not the product of one set of climatic conditions but can be formed under a wide range of climates.

Natural rock labyrinths in karst regions are generally considered to be of solutional origin with other processes playing a 'cosmetic' role. Karst streets are regarded as little more than solutionally enlarged fissures in bedrock, widened by waters moving from the surface underground. Once formed these depressions may be self perpetuating. In arctic and alpine regions, for instance, windblown snow accumulated in them during winter may enhance solution in their floors in spring. In bare karst terrains under all climatic conditions, shallow karst streets also represent soil traps and tend to support a denser vegetation than the surrounding bare limestone. Waters are, therefore, acidified by biogenic carbon dioxide as they percolate underground via these depressions (Monroe 1964). Karst streets in colder regions may have been partially moulded by frost action (Croce 1964) and it seems likely

that the gravitational collapse of street walls, sometimes as a result of solutional undercutting, may have been important in all areas regardless of climate. The processes that produce rock debris, however, can not form karst streets, they can only modify them. Solution is necessary to remove mechanical debris, for without its action, depressions would simply fill up with this material.

Although natural rock labyrinths in karst regions appear to be produced by solutional processes, it is difficult to explain similar forms in less soluble rock types in this way. The question must be asked that if rock labyrinths can form by a process or processes other than solution, could the Nahanni labyrinths have been produced by similar means? To help answer this question, consideration will now be given to rock labyrinths in non-karstic regions and possible origins.

(b) Labyrinths in Non-karst Rocks.

(i) The Wright Dry Valley Labyrinth.

At the head of Wright Dry Valley in Victoria Land, Antarctica, immediately in front of Upper Wright Glacier, is an area of approximately 30 square kilometers<sup>1</sup> that is characterized by a labyrinthine network of erratic, interconnecting channels deeply entrenched in the strongly jointed rock of a thick horizontal dolerite sill 200 meters thick. Smith (1965) reports that channel width ranges from less than 100 meters to more than 300 meters and depth from a few tens of meters to more than 100 meters. Selby and Wilson (1971) note that a few of

---

<sup>1</sup>Selby & Wilson (1971) quote an area of 30 km<sup>2</sup>, Smith (1965) an area of 18 km<sup>2</sup>.

the channels or 'troughs' are virtually through valleys extending west to east across the labyrinth but that most are part of an irregular anastomosing pattern with junctions at a variety of angles, and with many enclosed blind ends and completely enclosed basins. The troughs have highly irregular long profiles and there are many basins within them. Cross profiles are also irregular; where the upper walls are high they are composed of columns of dolerite blocks and are nearly vertical. Where trough walls are lower the walls are stepped and strewn with boulders. Areas between troughs are variously shaped into knob, butte, mesa and ridge forms with approximately accordant summit levels. Rounded rock basins up to 10 meters deep and a few tens of meters in width occur in places on the flatter upper surfaces resembling oversized potholes. Smith (1965) points out that up-valley, "the channeled terrain passes under the ice of Upper Wright Glacier to continue for an undetermined distance" (p. 941).

The Wright Dry Valley Labyrinth has been variously interpreted as being the result of: (1) catastrophic fluvial erosion, possibly during interglacial melting of the ice cap (Smith 1965); (2) a catastrophic flood similar to the jökulhlaup of Iceland caused by a volcanic eruption (Warren 1965); (3) glacial erosion (Cotton 1966); (4) selective salt weathering working along major joints and in areas of close jointing (Selby & Wilson 1971).

Selby & Wilson (1971) have criticized the catastrophic flood hypotheses on the grounds that there is no sign of the debris that should have been deposited lower down the Wright Valley. They also



note that neither Smith (1965) nor Warren (1965) offer an explanation as to how massive fluvial erosion can cut channels 100 meters deep in very resistant dolerite, especially where many of these channels are of highly irregular depth and in some cases form closed basins. Hypotheses requiring glacial or sub-glacial erosion can be objected to on several grounds. First, as Selby and Wilson point out, the landforms of the Labyrinth are quite unlike those known to have been produced by glacial erosion elsewhere. Secondly, they note that contemporary ice in the Upper Wright Valley is too cold at  $-20^{\circ}\text{C}$  to erode and to do so would have to be much thicker and faster moving to reach the pressure melting-point before abrasion could occur. This happened during the last advance of the Wright Glacier to the Ross Sea which may well have been 2.7 million years B.P. As Selby & Wilson rightly argue, it seems highly unlikely that the ice should scour a classic U-shaped valley east of the Dais and produce labyrinth forms west of it leading to the conclusion that the Labyrinth was formed since the retreat of the through glacier. Finally they contend that subglacial erosion either by streams of ice or meltwater is impossible to conceive of at the low temperatures which have prevailed in the Wright Valley for at least the duration of the Quaternary.

Selby & Wilson (1971) suggest that after the upper surface of the dolerite sill was denuded by earlier glacial erosion, salt weathering was concentrated in the major joints and in heavily jointed areas. Deepening depended partly upon the supply of salt from ablated snow and partly upon removal of sand from the hollows by wind. These

workers envisage that the Wright Valley Labyrinth evolved in precisely the manner depicted for the Nahanni labyrinths (Figure 3.41) except that instead of material being removed in solution it is broken down by salt weathering and transported out of the area by the action of the wind.

(ii) The Channeled Scablands of Eastern Washington.

During each Quaternary glaciation, the Cordilleran Ice sheet pushed southward from Canada into the conterminous United States, covering much of the northern Rocky Mountains west of the continental divide and locally encroaching onto the Columbia Plateau. The Columbia Plateau of eastern Washington is underlain by vast flows of Miocene and Pliocene (?) Columbia River basalt. At the eastern margin of the plateau, these flows intertongue with lake beds of the Latch Formation and rest unconformably on deeply dissected granitic terrain. The surface of the plateau is covered extensively by intermittently accumulated Quaternary loess including that of the Palouse Formation; its western part is also covered by the older predominantly lacustrine and alluvial sediments of the Ringold Formation.

Near the maximum of each glacial advance, ice dammed the Clark Fork River at Lake Pend Oreille to form Glacial Lake Missoula, and blocked the Columbia River at Grand Coulee to form Glacial Lake Columbia. At times, it also blocked the Spokane River east and west of Spokane, forming Glacial Lakes Coeur d'Alene and Spokane (Richmond *et al.* 1965). The ice dam that impounded Lake Missoula collapsed at least three times, releasing catastrophic floods of enormous magnitude, which swept through

the Spokane area and southwestwards across the Columbia Plateau. The last of these floods followed the early maximum of the last or Pinedale Glaciation.

The youngest catastrophic flood from Glacial Lake Missoula, first recognized and described by Bretz (1923) scoured moraines and other deposits of early Pinedale age. Its deposits overlies early Pinedale glacial and lake deposits and are themselves overlain by moraines and other deposits of middle Pinedale age. From the mouth of the Clark Fork River to Spokane, water released by collapse of the early Pinedale ice dam reshaped or destroyed all earlier deposits in its path. No older flood deposits have been found here, though such floods could have found no other outlet.

Flood-water traversed the Columbia Plateau along two great tracts from which the Palouse Formation was stripped, and the basalt scoured to form channels and cataracts. Drainage divides were indiscriminantly crossed and recrossed, and the margins of the flood tracts were strewn with debris. When the flood subsided, the coulees were left free of drainage.

The remarkable network of anastomosing channels comprising the 'channeled scablands' region of eastern Washington is thought to have been eroded during this catastrophic flood (e.g. Bretz 1923, 1928, 1932; Bretz, Smith & Neff 1956; Richmond et al. 1965) for which there is conclusive evidence. Joint-controlled plucking and quarrying of basalt by water of great depth and velocity eroded linear tracts as wide as 30 km. in places, occupying drainage divides 300 to 400 ft.

above adjacent valley floors (Bretz 1924). Empty bedrock basins 30 meters or more deep are found on the crests of such divides, and closed depressions twice as deep occur in the floors of narrow coulees. Differential erosion of weakly resistant basalt flows has left benches and butte-like remnants of basalt along many tracts.

Debris left by the flood consists of poorly sorted bouldery gravel forming deltas below cataracts and constructional bars in mid-channels (Bretz 1932). Bars were also built along canyon walls and across the mouths of tributary canyons. Exposures show torrential foreset bedding dipping down-current and up the mouths of tributary canyons. Giant ripple marks constructed of coarse gravel mark the surfaces of many bars.

Some 500 cubic miles of water may have crossed the 'channeled scabland' region at a rate of 9.5 cubic miles per hour on each occasion that the ice barrier holding back Glacial Lake Missoula was breached. This flow rate is about 10 times the combined flow of all of the world's rivers today.

(iii) Vallons de Gélivation.

A number of valleys incised into the west face of Dolly Ridge some 3 miles from Schefferville, Labrador-Ungava, have attracted a great deal of interest. Twidale (1956) has described these valleys, which are cut in argillites dipping at 35-40°, as having an alcove-like morphology with vertical backwalls and irregular long profiles due to the outcropping of resistant strata. At the outlets of these valleys, the largest of which is 90 meters long, 8 meters wide and 8 meters

deep are accumulations of pro-talus moraine ~~80~~ cm. high. Twidale has argued that the valleys were produced by freeze-thaw processes acting along the major fracture lines which are at right angles to the strike of the argillites. Expansion of the valleys into the ridge is considered to have been caused by the freezing of meltwater trickling down the rock-snow interface in spring with the frost-riven material removed by solifluction.

Andrews (1961) has argued that the post-glacial, periglacial theory of the origin of the valleys proposed by Twidale can not explain the valley forms. He does admit, however, that under the present climate, joints in Dolly Ridge are being widened by freeze-thaw processes into incipient valleys which are today choked with debris. Andrews contends that the 'vallons' of Twidale were modified to their present size and morphology during the final stages of deglaciation in the Schefferville area and are little more than a variety of sub-glacial meltwater channel. He presents a considerable body of evidence to support this claim.

Linear fissures of considerable length and depth have been identified in a variety of well-jointed non-karst rocks including dolerite, basalt, argillite and sandstone. Suggested origins include glacier, subglacial meltwater and fluvial erosion, erosion by drainage waters from ice-dammed lakes, salt weathering and freeze-thaw action. If floodwaters from Glacial Lake Missoula did produce the labyrinthine channel network in eastern Washington and if the Labyrinth of the Wright

Dry Valley was formed by either glacial erosion or glacial meltwater erosion, could not the Nahanni labyrinths have been produced either directly or indirectly by glacier action? If they were not, is there any possibility that these features are the result of freeze-thaw processes? To provide answers to these questions relationships between karst landforms in the Nahanni region and glacial events will now be discussed.

## 2. The Age and Origin of Nahanni Karst Landforms and Relationships Between Their Development and Glacial and Periglacial Events.

### (a) The Onset of Karstification: An Age Estimate.

The oldest solutional features in the Nahanni region are the fossil cave fragments that are commonly found in the walls of fluvial canyons and surface depression. These fragments which must once have been part of an extensive underground drainage network are virtually all dominated by features indicative of formation under conditions of phreatic groundwater flow. Their occurrence high in the walls of fluvial canyons and enclosed depressions is strong evidence that this ancient drainage system was in operation long before the surface landforms in the Nahanni region reached their present dimensions.

Some speleothems in these caves have been radiometrically dated at older than 350,000 years, indicating that the caves themselves are at least this age and likely very much older. In both Grotte Valerie and Speleothem Cave, stalagmites of this age rest on the remains of a coarse gravel fill that contains erratic material of Canadian Shield

derivation. This material has been interpreted as fluvially reworked glacial till that was laid down on the upland surface of the Nahanni Plateau south of Sundog Basin by First Canyon ice. As the First Canyon Glaciation has been tentatively correlated with the Nebraskan Glacial event of continental North America (Table 6.7), this suggests that karst development in the southern Mackenzie Mountains may have been well under way prior to the onset of the Pleistocene glacial period.

The now fossil drainage network that once functioned to drain water from the Nahanni region, had fully formed and had drained before speleothem deposition began at some time prior to 350,000 years B.P. This evidence indicates that karstification began in the Nahanni at least 500,000 years B.P. and possibly as much as 1 million years B.P.

(b) Surface Karst Landforms: Their Age and Relationships to Glacial and Periglacial Events.

(i) Surface Karst Development and Periods of Glacial Erosion.

For reasons already outlined by Selby and Wilson (1971), there is little doubt that the natural rock labyrinths of the Nahanni are not forms of glacial erosion. However, glacial erratics up to 10 ft. in diameter and clearly derived from the Canadian Shield region, have been discovered jammed into cracks in the upper surfaces of residual ridges in the labyrinth and in the floors of karst streets and plateaus. If these were not laid down in these locations by an eroding ice sheet, this implies that the region was covered by Laurentide ice on at least one occasion prior to the development of the surface karst landforms.

and that erratic material was either washed into enclosed depressions after they had fully developed, or was gradually lowered into them as they developed.

In the southern sections of the North karst labyrinths, are a series of fluvial valley systems which show distinct evidence of glacial erosion in their upper walls and which are upwards of two thirds filled with what appears to be fluvially reworked glacial debris. Immediately east of Insel Tower, one tributary valley is crossed by a karst street that clearly post-dates both the period of stream incision that initiated the valley network and the glacial erosion that modified it. Many instances of this relative age relationship between glaciated limestone surfaces and karst depressions have been discovered, and in no case is there any sign in the solutional depressions of the glaciated rock surfaces and fluvially reworked glacial debris that are characteristic of nearby valley networks. It can only be concluded that surface karst development did not begin in earnest until the last ice had finally retreated from the area.

Evidence from caves suggests that the labyrinth region may have been glaciated on not one but on two separate occasions, thus providing additional information as to the length of time that has been available for surface karst landform development in this region. Winnowings of till in Speleothem Cave in the north wall of Stal Gorge are thought to record one of these glacial incursions, while erratic boulders and pebbles up to 18 inches in diameter in several other caves are thought to record a second submergence by a Laurentide ice sheet. The erratic



material in Speleothem Cave, which is older than stalagmites dated at greater than 350,000 years B.P., is believed to be reworked till laid down by First Canyon ice. The coarser erratic debris which clearly post-dates the same speleothem deposits, may well be fluviually reworked material laid down by Death Canyon ice that is believed to have invaded the Southern Mackenzie Mountains 260,000 years ago. It is possible, of course, that both cave fills were derived from the same glacial deposit and were washed into the caves at different times, but this is thought unlikely.

(ii) Relationships Between Ice-dammed Lakes in the Sundog Basin and the Development of the North Karst Labyrinth.

If Glacial Lake Sundog I, which is believed to have reached an elevation of 2,800-3,000 ft. during the Death Canyon Glaciation, had extended southwards into the labyrinth karst and polje belt of the Nahanni North karst, glacial lake sediments similar to those further north in Sundog Basin should be preserved west of Mosquito Lake. The absence of such sediments suggests that during the Death Canyon glacial phase, a tongue of ice may have extended northwards across this region towards Lake Sundog I (Figure 6.2). Whatever the truth, there can be no doubt that had the poljes and natural rock labyrinths existed at the time of Lake Sundog I and had the waters of this lake submerged them, the deep enclosed depressions of this region should not be as free of sediment as they are.

It is clear that surface karst landforms in the Nahanni are younger than Lake Sundog I which may have been impounded by Death

Canyon ice some 260,000 years ago. Further ice-dammed lake evidence indicates that surface karst landforms south of Sundog Basin may have reached an advanced stage of development in the  $\pm 100,000$  years before the onset of the Sundog Glaciation which is thought to have occurred 150,000 years B.P.

The bedrock floors of many depressions in the Nahanni North karst including those of Second and Third Poljes and Raven Canyon, are at lower elevations than is Bubbling Spring. As this spring presents the present base level for groundwater flow in this region, this fact implies that during a long period of surface karst development depressions were eroded to a lower base level and subsequently the base level was raised. It is evident that this could have been achieved when Sundog ice impounded Lake Sundog II. The surface of this lake is thought to have been at 2,300-2,500 ft. which means that it probably extended southwards across the northern section of the labyrinth region. This lake was virtually filled with sediments before it drained and it may have been at this time that the three most northerly karst plateaus in the Nahanni became poljes, as streams dumped sediment into the quiet lakes occupying them. The Nahanni poljes may not have been transformed from karst plateaus in this manner but it is possible that they were, and that at the same time alluviation in Sundog Basin raised the groundwater base level in this region.

There is some evidence to suggest, therefore, that a considerable amount of surface karst development took place during the Grotte Valerie II Interglacial which may have been an interval of very much warmer

climate than exists in the Southern Mackenzie Mountains at the present time.

(iii) Surface Karst Development and Phases of Intense Periglacial Climate.

Twidale (1956) has argued that shallow valleys in bedrock can be produced by a combination of freeze-thaw and solifluction action. Frost-shattering has certainly played a part in shaping the karst streets and platea of the Nahanni but there is no evidence to suggest that this process even in combination with solifluction is capable of producing such forms. In fact, without solution to remove frost-shattered debris, it is likely that shallow depressions in the region would quickly become choked with angular fragments of rock (Andrews 1961).

Although periglacial processes could not have produced the Nahanni labyrinths, huge talus aprons and cones against the flanking walls of streets and platea attest to the present or former importance of freeze-thaw action in moulding these landforms. Because many of the screes are heavily vegetated and clearly inactive under present climatic conditions, it is apparent that periglacial processes have been more productive in the past. If the rock labyrinths of the Nahanni have not been ice-covered during the past  $\pm 200,000$  years as the glacial evidence suggests, it seems likely that during the Illinoian and Wisconsin periods, ideal conditions existed for freeze-thaw breakdown to take place in this region. Periglacial debris accumulated during the Sundog glacial period may have been partly removed in solution during the

following Sangamon Interglacial when the climate was warmer than it is at present. The inactive scree in the labyrinths today were most likely generated during the Wisconsin glacial/periglacial phase. It is possible that they are presently being reduced in size as material is funnelled underground in solution.

(c) The Karst-Glacial Meltwater Problem.

That natural rock labyrinths can be produced by processes other than solution has raised the possibility of a direct or indirect glacial origin for the Nahanni forms. An origin by glacier erosion can be discounted on good grounds (Selby & Wilson 1971) but it is difficult to dispute the argument presented by Bretz which has been outlined in a series of articles, that the rock labyrinths of eastern Washington - the 'channeled scablands' - were formed by a series of catastrophic floods by repeated failure of the ice barrier impounding Glacial Lake Missoula. Certainly several ice-dammed lakes are known to have existed in the Southern Mackenzie Mountains during the Pleistocene but there is no evidence to suggest that any of these drained catastrophically across what is now the Nahanni labyrinth region. In any case, had the labyrinths been formed by such a flow of water they should contain sediments deposited in them at this time. That few depressions have sediment in them suggests that they were formed by some other means.

It is much more difficult to assess the role played by ice-dammed lake overflow waters and ice-marginal meltwaters in the formation of the North karst labyrinths. The question is not whether such

waters have influenced karst landform development in the Nahanni, for there can be little doubt that they have, but rather to what degree have they influenced this development. This is no easy question to answer when it is realized that landforms morphologically similar to some in the Nahanni karst have been interpreted by other workers to be of direct or indirect glacial origin. For instance Andersen (1965) believes that the Jutulhogget Canyon in Norway was eroded by overflow waters from Lake Glåmsjö, an ice-dammed lake. The morphology of this channel, a photograph of which is included as Andersen's Figure 12, is strikingly similar to several of the larger isolated karst streets which cross drainage divides in the Nahanni region. Could these also represent former ice-dammed lake overflow routes?

To further complicate matters, Lundquist (1965) has interpreted intersecting networks of shallow linear channels on the slopes of Mount Fulufjället in Sweden as lateral drainage channels. A photograph of these channels which is included as Lundquist's Figure 7, shows them to be almost identical to the shallow karst street networks that are common on the Nahanni Plateau surface south of Sundog Basin above 3,000 ft. Could these karst street networks be ice-marginal drainage channels cut along weak fracture zones in the limestone?

Streets cut in the surface of the Nahanni Plateau up to elevations of  $\pm 4,000$  ft. are clearly well within the range of the First Canyon ice sheet and therefore, could have been formed by ice-marginal or sub-glacial meltwaters. Quite deep karst street networks that have been discovered in aerial photographs of the northern portion of Funeral

Ränge, however, are at an elevation of +5,000 ft. and are therefore beyond the limits of First Canyon ice. Although this area may have been covered on one or more occasions by local valley glacier ice, the existence of karst streets at this elevation implies that these features do not necessarily require glacial meltwaters for their formation.

Furthermore, the evidence suggests that purely karstic processes had produced an extensive, reasonably well integrated underground drainage system in the Nahanni region prior to the onset of Pleistocene glaciation. That a considerable volume of water was draining underground more than 500,000 years B.P., suggests that shallow surface karst depressions - subsequently destroyed by glacial erosion - may have existed at this time. The implication is that glacial meltwater is not necessary for the development of surface karst landforms in the South Nahanni area.

Any explanation of the surface karst landform assemblage of the Nahanni area in terms of ice-marginal or ice-dammed lake overflow drainage, must be able to account for two facts. First, that in the North karst, street networks, plateaus, dolines and poljes display a low level of interconnection at the surface. This is typical of landscapes formed by purely karstic processes where water is rapidly funnelled underground, but is not to be expected even in a soluble rock terrain that has been moulded by surface drainage waters. Secondly, it is difficult to envisage the North karst labyrinths being formed by surface waters without a great volume of fine sand and silt accumulating in the

steep-walled depressions, particularly in view of the abundance of such material in nearby regions such as Death Canyon and Sundog Basin. Except for the sediment that mantles the floors of the Nahanni poljes, which is derived from adjacent shales and glacial deposits, insoluble debris in the deep karst depressions of the North karst is noticeable by its absence.

The evidence suggests that although glacial meltwaters must have influenced karst development in the Nahanni to some degree and may even have been responsible for isolated landforms, their effect may have been subordinate to the purely karstic processes that modified the glacially scoured limestone surfaces following retreat of the last ice sheet to cover the area. Perhaps the most convincing piece of evidence for a predominantly karstic origin for the landforms of the Nahanni region is that which points to a post-Death Canyon Glaciation age for the North karst labyrinths. Had the networks of karst streets been eroded by glacial meltwaters or by ice-dammed lake drainage waters, the glaciated valleys with their partial fill of fluvially reworked glacial debris, should also have been modified by this action with the washing of some of the debris into the developing karst streets. Clearly this did not happen, presumably because the karst streets did not form until after ice retreat and then by purely karstic processes.

(d) A Unique Sub-Arctic Karst?

If the natural rock labyrinths and poljes in the Nahanni did not begin to form until after the Death Canyon ice sheet had finally retreated from the area, this implies that these features have had

more than 200,000 years to reach their present dimensions. At present rates of solutional denudation, which for the whole karst area have been conservatively estimated at 18-27 m<sup>3</sup>/km<sup>2</sup>/yr., between 3,600,000 and 5,400,000 cubic meters of limestone could have been removed from every square kilometer of the karst belt in the last 200,000 years. That is, 5.2-10.8 kilometers of karst streets 50 meters wide and 10 meters deep could have been generated in every square kilometer of terrain. The labyrinth karst and polje belt, which receives large amounts of allogenic water from bounding shales, may have a denudation rate as much as twice the average for the karst area meaning that 20 kilometers of karst streets 50 meters wide and 10 meters deep, could have been generated here in the last 200,000 years.

These statistics demonstrate that the karst landforms of the Nahanni could have been produced during the last ±200,000 years, a glacier-free period. There is therefore no need to invoke catastrophic events to explain this remarkable sub-arctic carbonate terrain which the hydrologic events of July 1972 showed to be anything but a relict landscape.

The sub-arctic Nahanni karst is the most complex and accentuated high-latitude karst known anywhere in the world. It exists in the Southern Mackenzie Mountains of northern Canada in a region of heavily fractured bedrock that allowed easy movement of water underground, in a region that has been recently uplifted giving the available relief necessary for vertical karst development but most importantly in a region that may not have been glaciated for more than 200,000 years.



Other high-latitude, sub-arctic carbonate regions of the world were invariably covered by ice during the Wisconsin glacial period which lasted until  $\pm 10,000$  years B.P. There has, therefore, been only a very short time for the development of surface karst landforms in these regions. The Nahanni karst could well be the only high-latitude karst in existence, that has had sufficient time to develop fully.

### 3. A Tentative Denudation Chronology for the Nahanni Karst Region.

Enough information has now been obtained from the Nahanni area of northern Canada, to allow the construction of a denudational chronology for the region. The outline to be presented, however, must nevertheless be considered tentative for it will certainly be revised and amplified as further studies are made. Fifteen significant and distinct events or periods of landform sculpture are recognized (Table 7.1), ten of these occurring within the last  $\pm 400,000$  years, the other five covering the period 1 million to 150 million years B.P. That the first five phases of landscape evolution cover such a vast interval of time is due to the decreasing amount of evidence that is preserved about ancient events. It is often only possible because of this to broadly generalize what happened over long periods of time. More recent events, on the other hand, are better documented especially when these can be directly or indirectly dated by radiometric or other means.

#### (a) Events 1 through 3 - The Columbian and Laramide Orogenies and the Cretaceous Surface of Erosion.

During the Columbian Orogeny which lasted from the late Jurassic to the earliest upper Cretaceous, the arcuate Selwyn Fold Belt and the

Table 7.1. A Tentative Denudation Chronology for the Nahanni Region.

No	EVENT DESCRIPTION	Age (years B.P.)	CORRELATION
15	Post Glacial	< 10,000	Post Glacial
14	Jackfish Glaciation	20,000	Classical Wisconsin
13	Wisconsin Interstadial	40,000	Middle Wisconsin
12	Clausen Glaciation	60,000	Early Wisconsin
11	Sangamon Interglacial	125,000	
10	Sundog Glaciation	150,000	Illinoian
9	Grotte Valerie Interglacial II	210,000	
8	Death Canyon Glaciation	260,000	Kansan
7	Grotte Valerie Interglacial I	310,000	
6	First Canyon Glaciation	400,000	Nebraskan
5	Cavern Genesis	1-5 million	Miocene to Pliocene
4	Structural Deformation (Cascadian Orogeny?)	1-5 million	Miocene to Pliocene
3	Laramide Orogeny	35-80 million	Late Cretaceous to Early Oligocene
2	Cretaceous Planation	70-135 million	Cretaceous Period
1	Columbian Orogeny	135-150 million	Late Jurassic to Early Cretaceous

western portion of the Mackenzie Fold Belt were created. Subsequent erosion of these upland masses during the Cretaceous and perhaps even in the early Tertiary may have produced a widespread 'planation surface' of subdued relief (Bostock 1970). In the early Tertiary this old surface of erosion was uplifted and warped during the Laramide Orogeny the effects of which were felt in the western Cordillera from the late Cretaceous to early Oligocene time.

Ford (1974) has presented strong evidence to suggest that following the Laramide, mountain ranges may have been sustained only west of Arnica Range and that to the east was an erosional plain of little relief. He notes that the Tlogotsho tableland may have stood as a low plateau to the southeast and that Nahanni Range may have existed although possessing lower relief than it does today. On the plain east of Arnica Range the South Nahanni and Ram Rivers are thought to have meandered eastwards along courses similar to those they take at the present time. Both streams likely had significantly lower gradients than they do today.

(b) Events 4 and 6 - The Cascadian Orogeny (?) and Early Cavern Genesis.

Hughes (1972) has stated that "The Pleistocene sediments in Old Crow and Bluefish Basins, and probably those in Bell Basin, extend below the bedrock thresholds of the respective basins. The basins, therefore, cannot be entirely erosional, and Tertiary and or early Pleistocene warping or faulting must have contributed to their origin" (p. 6-7). As sediments in Sundog Basin bear a similar relationship to the floor

of this structural depression there is also evidence in the Nahanni of deformation and of intense localized faulting in relatively recent times (see Ford 1973). This phase of deformation which has been little discussed in the literature, may correlate with the Cascadian Orogeny (Dott and Batten 1971, p. 413) that is believed to have affected the western Cordillera of North America intermittently during the Miocene to Recent period culminating approximately 3 million years ago.

Warping in the Nahanni region produced the structural domes of Nahanni and Ram Plateaus and the depression of Sundog Basin, it was likely also accompanied by intense fracturing and the Nahanni Fracture Belt may have originated or have been enhanced at this time. Warping must have been gradual for the South Nahanni and Ram Rivers were able to cut antecedent canyons with entrenched meanders in the uprising masses. It also introduced a degree of relief that was absent in this region during earlier periods, with the result that surface water percolated into the limestone via the newly formed fractures and generated an extensive underground drainage network that channelized groundwater to a few springs in the floors of the developing canyons. The caves were formed by solution under conditions of phreatic groundwater flow and they are known to have been fully developed more than 350,000 years ago. Shallow surface karst depressions were probably also developed at this time by waters percolating underground into the limestone aquifer.

Ford (1974) has noted that in the vicinity of First Canyon, fragments of this ancient cave network are several hundreds of feet above present river levels. This is also true of similar remnants in canyons further north (see for instance Plate 2.1) and implies that these caves are either all perched on high-level resistant rock strata, or that they were all formerly graded to a much higher base level than exists in the region at present. The latter of these two possibilities seems the most likely and may indicate that there was a virtual still-stand in the deformation of the Nahanni region during Cascadian times. Two cutoff meanders (Ford 1973) in First Canyon, which indicate river elevations of at least 2,600 ft. and 2,100 ft. respectively at the time of their abandonment, closely correspond in altitude with Grotte Valerie in the north wall of First Canyon at  $\pm 2,300$  ft. a.s.l., and together may suggest a former base level at what is now 2,100-2,600 ft. a.s.l. It is possible that Grotte Valerie functioned as a spring at this time, discharging water into the South Nahanni River just as White Spray does today.

After this still stand, Cascadian deformation continued. The major rivers cut deep canyons in the uprising Nahanni and Ram Plateau landmasses and dissected the underground drainage network that had developed in early Cascadian times. This became fossil as groundwater worked towards the new lower base level of erosion and fragments of it were left 'high and dry' in the walls of the rapidly developing fluvial canyons.

(c) Events 6 and 7 - The First Canyon Glaciation and the Grotte Valerie Interglacial I Period.

Deformation of the Nahanni region may have been complete and fluvial canyons may have cut more deeply into the Nahanni and Ram Plateaus than their present dimensions suggest, by the time the first (?) ice sheet from the east advanced into the southern Mackenzie Mountains. The First Canyon ice mass submerged Nahanni Range and Ram Plateau, and came to rest against the eastern flank of the Nahanni Plateau, its surface at approximately 4,200-4,500 ft. a.s.l. It deposited a till on both uplands and lowlands and scoured the limestone, destroying most of the surface karst depressions produced during Event 5. Ford (1974) has rightly argued, that "Judging from later events, the glacier must have impounded the South Nahanni River, creating an ice-dammed lake in Deadman Valley and to the west of it" (p. 172), but no trace of an early lake has yet been found. During the maximum stand of First Canyon ice or in the early stages of retreat, meltwaters washed poorly sorted glacial debris into the fossil caves filling many passages almost to the ceiling.

Following the First Canyon Glaciation was a long period when the climate both above and below ground was warmer than it is today. Water was able to percolate into the fossil caves from the plateau surfaces above them and deposit stalactites and stalagmites, some of the latter on the coarse gravel fill deposited earlier. Today, there is restricted speleothem deposition for air temperatures in most cave passages are well below freezing. Massive speleothem deposition during the 'Grotte'

Valerie Interglacial I' period (Ford 1976), is known to have begun prior to 350,000 years B.P. and to have continued until at least 275,000 years B.P. The important implications are that the interglacial event was a long one in which there was both surface and underground karst development, and that the First Canyon Glaciation is older than 350,000 years B.P.

(d) Events 8 and 9 - The Death Canyon Glaciation and the Grotte Valerie Interglacial II Period.

Approximately 260,000 years B.P., Laurentide ice again invaded the southern Mackenzie Mountains during the Death Canyon Glaciation. Ice advanced into the canyons dissecting the eastern slopes of the Ram and Nahanni Plateaus east and south of Sundog Basin, respectively. The ice reached elevations of 3,000-3,500 ft. against the eastern flanks of these uplands and covered what is now the labyrinth karst and polje belt. Limestone surfaces were scoured smooth and as ice retreated valleys and shallow depressions were filled with fluvially reworked glacial debris.

At the peak of glaciation, possible Ram River drainage routes to east and north were blocked and an ice-dammed lake - Lake Sundog I' - its surface at  $\pm 2,800$  ft. a.s.l. was created in Sundog Basin. This lake fingered into the canyons cutting through the western flank of Ram Plateau which became filled with debris up to the lake level. It probably overflowed to the north. The South Nahanni River may also have been impounded, but no evidence of a former high-elevation lake that existed west of First Canyon has yet been found. During the Death

Canyon phase, snow or glacier meltwater was discharged into the fossil caves during the summer months and this carried away much of the coarse gravel fill and stalagmite that had been laid down during Events 6 and 7. Dissection probably occurred under conditions of vadose flow.

Speleothem deposition in caves, which had been halted during the Death Canyon Glaciation, began again approximately 217,000 years G.P. at the beginning of the Grotte Valerie Interglacial II period, which may have ended 191,000 years B.P. This interglacial, therefore, appears to have been somewhat shorter than the previous one, and may also have been slightly cooler although conditions were still likely warmer than they are today.

After the retreat of Death Canyon ice, many canyons were blocked by end moraines which prevented direct surface flow out of them. Some subsequently developed surface drainage routes and the outlet streams quickly removed the terminal moraine debris. The drainage waters in a few, however, began to seep underground and where such outlets developed to the extent that they could absorb all of the drainage into the canyons, these remain closed today and often contain lakes.

Surface drainage was quickly re-established in canyons on the west flank of the Ram Plateau which were filled up to  $\pm 2,800$  ft. by sediment deposited in Lake Sundog I. In most cases, streams entrenched this sediment so that little of it is preserved today. However, in one or two canyons the surface streams began to sink underground and in these networks, the sediment fill is better preserved although in one instance enough of it has been funnelled underground from above the main stream sinks that a natural depression has been created. The base



level of erosion in Sundog Basin may well have been at a slightly lower elevation than it is today.

It was during the Grotte Valerie Interglacial II phase that surface karst landform development in the Nahanni began in earnest. Waters percolating underground via open faults and joints in the limestone, solutionally etched the glaciated limestone terrain left by Death Canyon ice. First to form, were vertical-walled solution dolines in the major fractures and as these enlarged and coalesced karst streets and ultimately karst plateaus were developed. In bare limestone terrains, the pattern of surface karst landform development was almost everywhere the same, although there was great areal variation in solutional denudation rates and in the size of karst landforms. Denudation was particularly rapid in the densely fractured structural col separating the Nahanni Plateau south of Sundog Basin from the Ram Plateau. This region was, and still is the locus for acid allogenic stream waters from the surrounding shales. Solution rates here, particularly at the shale-limestone junctions must have been at least twice as great as those elsewhere in the karst - explaining why this region displays the most spectacular karst landform assemblage in the Nahanni region today.

In areas such as the Sinkhole Plain, which had been mantled by glacial deposits laid down during the Death Canyon Glaciation, solution acted on the underlying soluble rocks with the result that subsidence and suffosion dolines developed in the surficial unconsolidated material. In regions where limestone was only thinly covered by insoluble shale, subjacent karst forms resulted. There can be little doubt that by the end of the Grotte Valerie Interglacial II period, which likely lasted

for several tens of thousands of years, the Nahanni region contained a complex set of surface karst landforms.

(e) Events 10 and 11 - The Sundog Glaciation and the Sangamon Interglacial.

During the Sundog Glaciation, Laurentide ice again advanced into the southern Mackenzie Mountains. It could not submerge Nahanni Range as it had done during the First Canyon Glaciation and to a lesser degree during the Death Canyon Glaciation, but it poured through breaches in this barrier into the Mackenzie Plain. It finally came to rest against the eastern flanks of Nahanni and Ram Plateaus, its surface at approximately 2,800 ft. a.s.l. The karst belt was not covered by ice but was influenced by a phase of intense periglacial activity. A great volume of rock accumulated in the floors of the karst depressions and in the large forms, sizeable talus cones and aprons were constructed. During the summer months, some of this material may have been removed in solution by snowmelt and rain waters but it is almost certain that this did not keep pace with the supply of angular frost-shattered debris. ~~Run~~ning water may also have washed loess material, deposited on the upland surfaces, into the underlying fossil caves. Many of these caves are today characterized by such a fill and it is clear that there has been little speleothem deposition since it was laid down.

Easterly drainage routes were blocked by the Sundog ice sheet and a large ice-dammed lake - Lake Sundog II - its surface at 2,400-2,500 ft. for long periods, formed in Sundog Basin. A lake may also have been formed west of First Canyon in the South Nahanni basin but

no evidence of this has been discovered although a delta at 3,500 ft. in the head of Ranger Canyon to the north, may be suggestive of it. Depressions in the northern section of the labyrinth karst and polje belt, their floors below the level of Lake Sundog II, were likely also flooded. Alluviation of what are now the three Nahanni poljes may have begun at this time and the level of the outlet spring into Sundog Basin may have been raised.

The Sundog Glacial incursion was followed by the Sangamon Interglacial which may have culminated approximately 125,000 years ago. The climate of the Nahanni may have been very similar during this phase to that existing today for there was only restricted speleothem deposition. The Ram River developed a new path across Sundog Basin and this was gradually superposed upon underlying bedrock. Screens likely became inactive as solutational processes continued to shape the landscape. Underground drainage in the North karst was restricted because the system had been alluviated during the Sundog Glaciation, and it is likely that sediment continued to accumulate in what were by now the three Nahanni poljes.

(f) Events 12 and 13 - The Clausen Glaciation and the Wisconsin Interstadial.

In early Wisconsin time, ice poured through gaps in the Nahanni Range, spread westwards across Mackenzie Plain and came to rest against the eastern edges of the Nahanni and Ram Plateaus at an altitude of a little more than 2,000 ft. a.s.l. As Ford (1976) has pointed out, Clausen ice impounded the South Nahanni River and created Glacial Lake Nahanni, the water rising to a maximum level of 2,000 ft. before

overflowing possibly to the north along the margins of the Clausen glacier. The lake must have remained at this height for a long period because very extensive lake floor deposits accumulated to this level upstream of Third Canyon.

Clausen ice must also have impounded the Ram River with the formation of a small lake that occupied Ram Canyon and fingered westwards along river valleys into the Sundog Basin. This lake, which probably drained northwards along the margin of the ice sheet, may have filled rapidly with sediment to be replaced by braided streamflow at a high elevation in the Ram Canyon region. Intense periglacial conditions existed in the karst area and talus accumulations that had lain inactive and had been partially denuded in Sangamon times, began to develop once more. Karst processes were probably active during the summer months - in the northern area controlled by the higher base level in Sundog Basin induced by sediment deposition during Event 10.

Clausen ice withdrew from the Southern Mackenzie Mountains at some time prior to 40,000 years B.P. and there followed the Wisconsin Interstadial Event when the climate in the region was somewhat colder than it is at the present time. The major streams entrenched the deposits that had been laid down in ice-dammed lakes. There were many cases of both small and large streams whose valleys had been buried by lake sediments in Clausen times, being superposed onto the underlying bedrock. As the Sangamon and pre-Clausen paths did not always correspond, sections of the pre-Clausen valley systems remain buried today. Periglacial conditions prevailed throughout the Wisconsin Interstadial and

karst landforms continued to be moulded by solution processes in conjunction with mechanical breakdown.

(g) Events 14 and 15 - The Jackfish Glaciation and the Post Glacial Period.


In the Classical Wisconsin period, Laurentide ice again advanced across the Great Slave Plain during the Jackfish Glaciation. The ice sheet was not as extensive as that of Clausen times, coming to rest against the eastern slopes of Nahanni and Camsell Ranges of Franklin Mountains. Jackfish ice impounded the South Nahanni River and created Glacial Lake Tetcela east of Nahanni Plateau (Ford 1976). The lake is believed to have risen to 1,300 ft. a.s.l. and discharged to the north. The karst underwent a third period of intense periglacial climate and deposits laid down during Clausen and Sundog times were further dissected and eroded by stream and soliflual action.

Ford (1974) has argued that the lowering of Glacial Lake Tetcela may have commenced as early as 14,000 years B.P. and that the lake had almost certainly fully drained by 8,000 years B.P., indicating that the Post Glacial period has been at least this long. Under the present interglacial climatic conditions, many periglacial forms are inactive although frost shattering is still important at higher elevations. Hydrologic activity, particularly in the labyrinth karst and polje belt is considerable, especially during the summer months when recharge to the aquifer occurs. Solutional denudation is rapid particularly in the North karst region where acid allogenic stream waters from thickly soil covered and densely vegetated shale areas sink in bare limestone

terrain. There can be no doubt that the karst landscape is still evolving today.

4. Significance of the Nahanni Karst Landform Assemblage to the Morphoclimatic Theory of Karst Landform Development.

The influence of climate on karst landform development was first stressed by H. Lehmann in 1936, who became convinced that conical limestone hills like those of the Sewu Mountains in Java originate in the very beginning of karst development - provided that a humid tropical climate prevails. Where 'humid tropical' karst forms have been identified outside of present-day humid tropical limits, they have usually been interpreted as fossil landforms that were produced under the warmer and wetter conditions of some past geologic period.



Pokorny (1963) for example, has interpreted 'monadnocks' in the southern part of the Cracow Upland in Poland, which he describes as domes, cones, ridges and pinnacles or spires up to 30 meters high, as 'tropical mogotes.' The top surfaces of these residual limestone hills are crossed by widened fissures. He argues that the 'mogotes' in Poland are built of massive reef limestone which is more resistant to solution than the surrounding stratified limestones, and that they began to form in the Paleogene under hot humid climatic conditions. Karst development may have lasted until the end of the Tertiary when it was halted by a worsening climate. Similarly Marker (1971) has identified what she believes to be the remnants of karst cones and towers in the semi-arid eastern Transvaal of South Africa. These have

been interpreted as tropical forms that developed under climatic conditions more humid, if not necessarily warmer than those existing in this region today.

Silar (1965) has argued that, "Tower karst occurs in areas situated at low latitudes with prevailing tropical or subtropical climates" (p. 39), but notes that in China it reaches farther to the north. Because "the climate is a decisive agent in its development" (p. 40) he regards much of the tower karst as having been produced in an earlier period noting that "if in the Tertiary the area of tropical climate extended farther to the north it is not surprising that the tower karst in southern China occurs at higher latitudes" (p. 40).

In all three cases residual limestone towers have been interpreted as tropical forms exotic to the climates under which they now reside and yet, as we have already seen, residual rock towers have been identified in two tropical semi-arid climates (Tricart and Da Silva 1960, Jennings and Sweeting 1963) and in the Nahanni, where such features have developed under sub-arctic climatic conditions. Because karst towers up to 150 ft. high can form under climates ranging from humid tropical to sub-arctic, it is incorrect to interpret them in purely climatic terms for something other than climate influences their development.

The Nahanni karst landscape as a whole, with its dense assemblage of dolines, karst streets and platea - all developed on a large scale - and its three small poljes which are the most northerly examples known, appears exotic to a cold, bare, sub-arctic terrain. This complex and

highly accentuated karst, which is considered to have formed by 'normal' karstic processes during the last 200,000 years and is still actively developing today, is more typical of present humid tropical karsts than it is of other sub-arctic or even warm-temperate carbonate regions.

Corbel (1959) has argued that cold-temperate karsts have in most cases had little time for their development because of interruption during Pleistocene glaciation, whereas tropical 'kegelkarsts' have had a much longer period available for their evolution. That the Nahanni region may not have been covered by ice during the last 200,000 years, is certainly one reason why this karst is so highly developed in relation to other high-latitude karsts. Another reason may be that if solutional denudation rates in the past have been as high as they are at present, they may in restricted areas have been of similar magnitude to those typical of humid tropical regions today.

There can be little doubt that the very existence of the Nahanni karst questions the validity of the widely held view that karst landform morphology is largely a function of climate. If this complex landform assemblage suggests modification of the morphoclimatic concept, landform characteristics point to a possible alternative model that is not entirely climate-dependent. This will now be outlined.

##### 5. A Structural-Lithological Model of Karst Landform Development.

In Jamaica, kegelkarst is restricted to areas of hard, highly fissile White Limestone and is not characteristic of the more chalky and less fissured Montpelier beds (Sweeting 1958). In Puerto Rico, Monroe (1964) has found that each lithologic type of limestone has



given rise to a specific group of solution phenomena and few karst features seem to be common to all lithologies. The structural and lithological properties of limestones are also considered to have influenced the development of karst types in Cuba. Panos and Stelci (1968), for instance, have argued that in this region the climate influences the intensity and speed of processes that act upon a landscape but that the limestones themselves give rise to basic fundamental forms.

Verstappen (1964) feels that "neither age sequence, nor climatological differences alone can . . . satisfactorily explain all phenomena observed and a third factor . . . the lithology of the limestones, . . . including their water absorbing capacity, and their porosity deserves more attention than it usually gets. Only the combination of all three factors can lead towards a better understanding of the origin and development of the diversified karst phenomena" (p. 40-41). Wilford and Wall (1965) contend that it is the low primary porosity of most Sarawak limestones that accounts for the lack of conical karst development in this region. Similar arguments in favor of structural and lithologic control upon karst landform development have been made by, among others, Cooke (1973) and Jennings and Sweeting (1963).

As with the karst landforms in most other areas, those in the Nahanni reflect the structural and lithological properties of the host limestone. The abundance of sub-vertical open fractures in a massively-bedded limestone with few open bedding planes, has left the

solutionally widened fracture - the karst street, the most common landform in this region. If structure and lithology can so dominate the morphology of forms in this area, then they must play at least some part in moulding landscapes elsewhere.

Many workers have attested to the fact that solution proceeds most rapidly along lines of secondary permeability - namely along faults and master joints. When solution attacks a limestone mass, therefore, it will etch out these lines of weakness so that the fracture lines will become depressions and the resistant blocks between hills. The depressions will not all have the same shape for this will likely depend upon the characteristics of the host limestone. Tija (1969) has argued, for instance, that slopes in tropical regions are governed by the spacing of vertical joints and faults and horizontal bedding planes, for these control the rates of solution in these directions. He notes that mogotes develop where the horizontal planes of weakness are unimportant, while karst cones, which have much more gentle slopes, form in limestones which possess definite horizontal planes of weakness.

Tija (1969) has emphasized the role of structure, but lithology must also play a part in controlling slopes in carbonate regions. Consider the slopes that might be typical of the end members of a series of possible structural/lithological limestone types. At one extreme is a crystalline, non-porous, massively-bedded and heavily faulted limestone. It has a low primary permeability and bedding partings are so tightly closed that they permit virtually no groundwater movement along them. The karst landforms that would be expected in such a

limestone, would have a marked vertical component. Walls would tend to be steep to vertical because of fault control and because the rock is massive enough to retain vertical cliffs. Nahanni Formation limestones have such properties, and here a labyrinth karst assemblage developed.

At the other extreme, is a porous, heavily faulted, thinly-bedded limestone with a multitude of minor open joint systems. It has a relatively high primary permeability and water can move easily along the bedding planes. It is unlikely that vertical-walled solutional landforms would develop in such a rock, first because it is not mechanically strong enough to support vertical walls for long, and secondly because the more even distribution of solution as waters percolate into the numerous small cracks, would favor the formation of shallow, rounded karst forms rather than steep, sharp ones. There can be little doubt that the structural and lithological properties of a limestone influence the morphologies of surface landforms. Depending upon the limestone, the slopes of karst depressions and hills might be expected to vary between almost vertical to almost horizontal.

A newly-uplifted, horizontally-bedded limestone, which is crossed by intersecting networks of faults, has a built-in susceptibility to solution. The fractures themselves represent the weakest portions of the limestone mass, so that these will be the zones of most intense solution. Away from each fracture, the limestone is considered to be less and less susceptible to solution. The fractures are etched out in a manner that is controlled by the properties of

the limestone. Three possibilities are shown in Figure 7.1 along with simple waveforms which simulate the hypothetical landscape profiles. In the first case, the rock is massive so that solution is concentrated in the fractures. The bedrock in the second case is medium-bedded and the bedding planes reasonably well developed, so that the slopes of depressions are of lower gradient and the depressions more extensive. In the final example, the limestone is porous and thinly bedded so that depressions are broad and shallow.

A three-dimensional model of the solutional susceptibility of a hypothetical limestone mass crossed by one set of equally-spaced fractures etched out in the manner depicted in Figure 7.1(a), is a simple sine wave surface with the wavelength equal to the spacing of the fractures (Figure 7.2). In a slightly more realistic situation, of a limestone terrain that is crossed by two sets of equally-spaced fractures intersecting at right angles, a picture of the susceptibility to solution is obtained by adding the effects of the two sets of fractures - that is by superimposing two wave surfaces (Figure 7.3). The model of what this hypothetical limestone terrain should look like after solution has acted upon it for a considerable time, strongly resembles mogote karst (Plate 7.1). This suggests that the assumptions made in transforming an initially flat limestone surface crossed by networks of fractures, into a karst terrain model on the basis of the structural and lithological characteristics of the limestone, are reasonably sound.

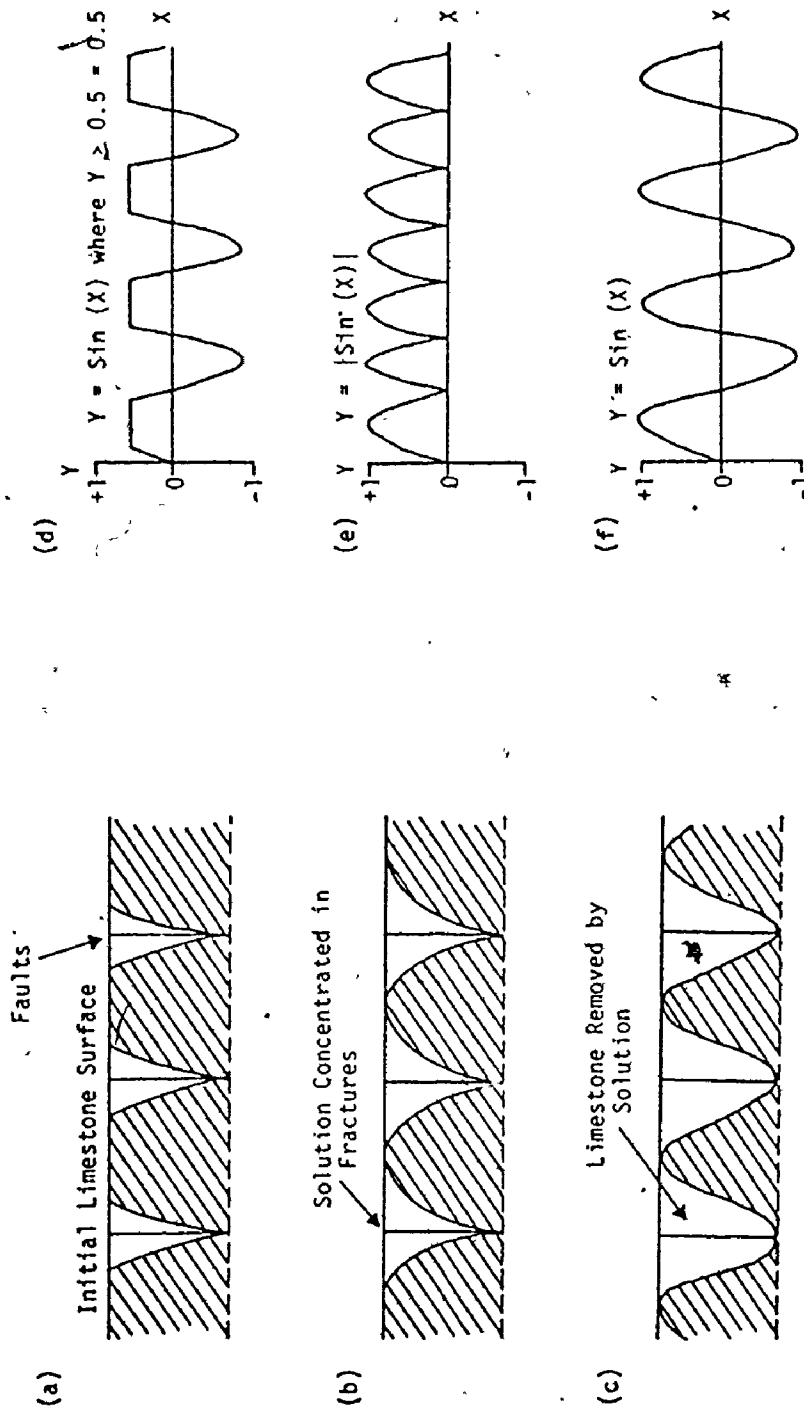


Figure 7.1. Three ways in which fractures in a limestone mass can be etched out by solution (a,b,c) and simple waveforms which simulate the resulting landscape profiles (d,e,f).

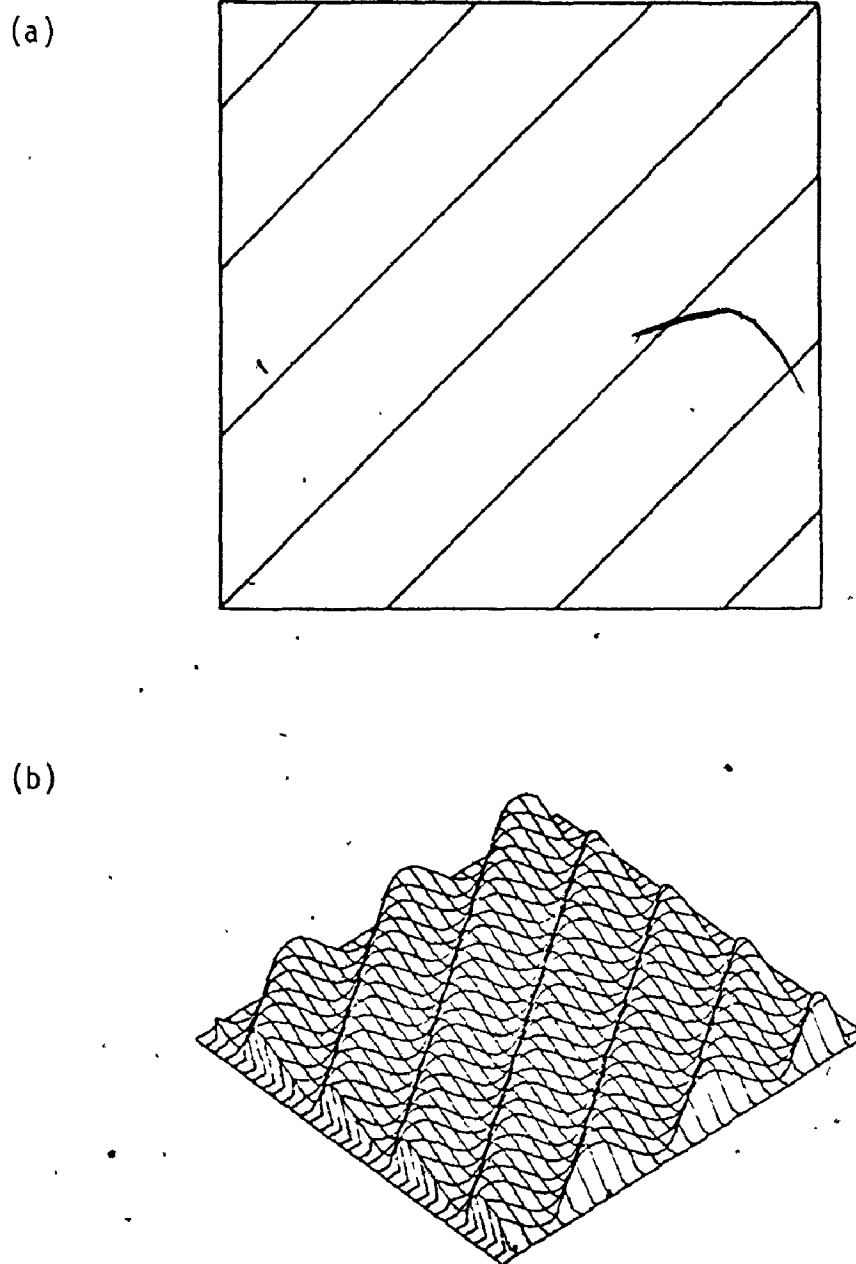


Figure 7.2. A model of the susceptibility to solution (b) of a limestone mass crossed by one set of equally-spaced fractures (a).



Plate 7.1. Karst cockpit and mogotes, Puerto Rico.

Even more realistic karst landscape models are obtained if the limestone is assumed to be crossed by three sets of equally-spaced fractures - two of these at right angles and the other intersecting at  $45^\circ$  instead of simply two. In the simplest case, the model, (produced by superimposing three sine wave surfaces), is a very realistic simulation of many tropical cone and mogote karst terrains with hill summits and depression floors distributed in a spatially irregular fashion, and at a variety of elevations.

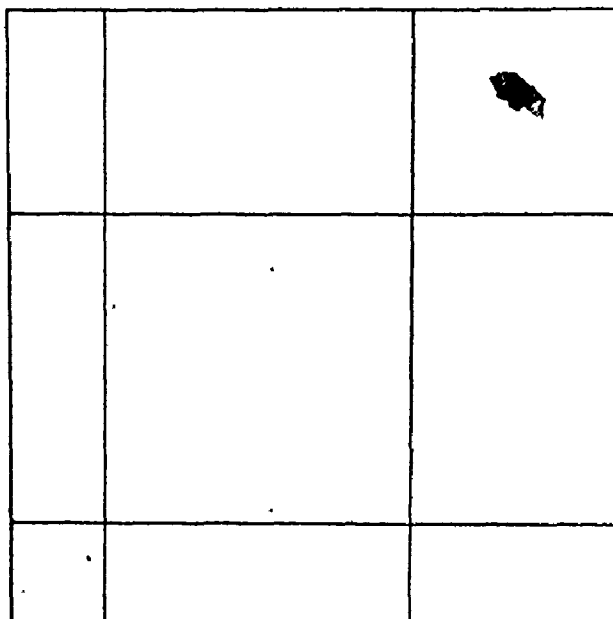
Although a great deal more work is necessary, preliminary results indicate that the simple structural-lithological model of karst landform development just outlined, is a viable alternative to the morphoclimatic theory. That is not to say that climate does not play a part in the moulding of karst landforms, for there can be no doubt that it does, but only that in many instances it may be less significant than the properties of the host limestone. In the Nahanni, this has certainly been the case, and it may well have been the case in many other carbonate areas also.

#### 6. Summary Remarks.

The sub-arctic Nahanni karst of northern Canada is an important discovery: Because it may not have been glaciated during the last 200,000 years, it could well represent one of the few high-latitude carbonate terrains in the world that has had time to develop fully. Its very existence questions the validity of the morphoclimatic theory of karst landform development as it now stands and instead, points towards



(a)



(b)

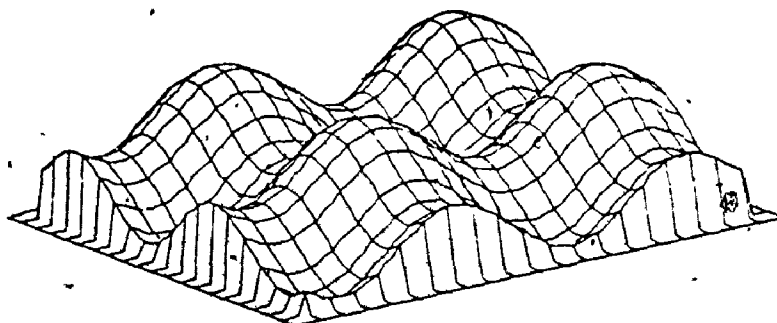


Figure 7.3. A model of the susceptibility to solution (b) of a limestone mass crossed by two sets of equally-spaced fractures which intersect at right angles (a).

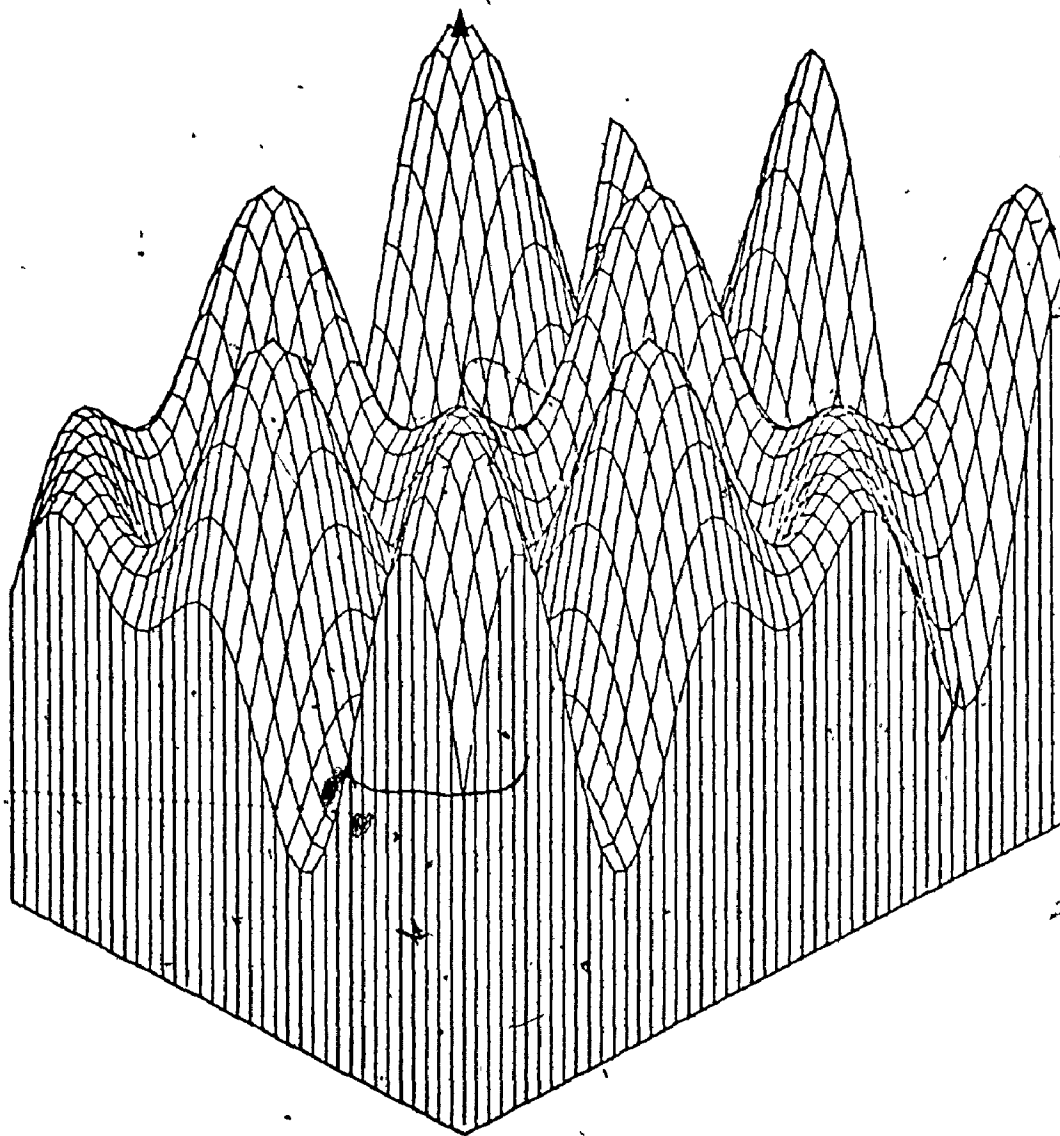


Figure 7.4. A three-dimensional model of the susceptibility to solution of a limestone mass crossed by three sets of fractures.

variations in the structural and lithological properties of the host limestone as the major controlling factors of karst landform morphology.

APPENDIX I

Selected Glossary of Karst Terms<sup>1</sup>

- ANASTOMOSIS. A network of tubular passages or holes in a cave or in a solution sculptured rock such as a limestone pavement.
- BARE KARST. Karst topography having much exposed bedrock.
- BLIND VALLEY. A valley that ends suddenly at the point where its stream disappears underground.
- CENOTE. Steep-walled natural well that extends below the water table; generally caused by collapse of a cave roof. Term used only for features in Yucatan, Mexico.
- CLINT. Slabs of limestone parallel to the bedding forming a pavement. Other name Flachkarren.
- CLOSED DEPRESSION. A general term for an enclosed topographic basin having no external drainage regardless of origin or size.
- CLOSED FLUVIAL CANYON. A large canyon that is no longer drained by surface streams, water instead passing underground. May be a larger version of the blind valley but many have been produced by glacial action.
- COCKPIT KARST. Tropical karst topography containing many closed depressions surrounded by conical hills. Several types are differentiated depending upon the shapes of the hills; these include Kegelkarst, mogote karst and tower karst (Turmkarst).
- COLLAPSE DOLINE. A closed depression formed by the collapse of the roof of a cave.
- COVERED KARST. A terrain of karst features resulting from the development of solution features in limestone covered by unconsolidated superficial sediment.
- GRIKE. A vertical or subvertical fissure in a limestone pavement developed by solution along a joint. Other name Kluftkarren.
- HUM. Residual hill of limestone in the floor of a polje.
- JOINT HOLLOW. A shallow depression on a limestone pavement formed by the coalescence of several grikes. Similar to a karst platea but much smaller.

<sup>1</sup>Based largely on a glossary prepared by Monroe (1970).

- KAMENITZA.** Shallow solution basin formed on bare limestone; generally characterized by a flat bottom and overhanging sides.
- KARREN.** Channels or furrows caused by solution on massive bare limestone surfaces.
- KARST PLATEAU.** Irregularly-shaped closed depression formed by the coalescence of several karst streets. These features often have residual limestone ridges and towers projecting from their floors.
- KARST STREET.** A solutionally-widened fracture in limestone. It is a long, narrow chasm. Other names, Bogaz, Corridor, Karstgassen, Struga, Zanjon.
- LABYRINTH KARST.** An intricate irregular network of karst streets formed by the solutional widening of closely spaced fractures.
- LIMESTONE PAVEMENT.** A bare plane surface of limestone parallel to the bedding which is often divided into blocks (clints) by solutionally-widened joints (grikes).
- LOG PARTIAL PRESSURE CARBON DIOXIDE.** This is a hypothetical value. It essentially refers to the gas phase that would be in equilibrium with a solution if the solution were in equilibrium with a gas phase. A water that has had contact only with atmospheric  $\text{CO}_2$  levels (0.03% by volume) would be in equilibrium with a  $\log \text{PCO}_2$  of -3.52. Lower percentages of  $\text{CO}_2$  give lower  $\log \text{PCO}_2$  values (0.01% gives a  $\log \text{PCO}_2$  of -4.0), higher percentages higher  $\log \text{PCO}_2$ 's (1.0% gives a  $\log \text{PCO}_2$  of -2.0).
- POLJE.** A very large closed depression having a flat floor either of bare limestone or covered by alluvium and generally surrounded by steep walls of limestone. Many are liable to extensive flooding.
- PONOR.** Hole in the bottom or side of a closed depression through which water passes to an underground channel.
- SATURATION INDEX ( $\text{SI}_C$ ,  $\text{SI}_D$ ).** Water completely saturated with respect to calcite and dolomite will have  $\text{SI}_C$  and  $\text{SI}_D$  values close to zero. For supersaturated waters  $\text{SI}_C$  and  $\text{SI}_D$  would be positive (eg + 0.25), for undersaturated waters negative (eg - 0.32).
- SEMI-BLIND VALLEY.** Blind valley in which the stream overflows in flood-time when the sink can not accept all of the water.
- SINKHOLE PLAIN.** Plain on which most of the local relief is due to closed depressions and nearly all drainage is subterranean.
- SOIL CARBON DIOXIDE.** Carbon dioxide in the soil atmosphere produced largely by biogenic processes.

SPELEOTHEM. A secondary mineral deposit formed in caves. Examples are stalagmites and stalactites.

STRUGA. A karst street or corridor formed along a bedding plane.

SUBJACENT KARST. Karst landscape in non-carbonate rocks due to the presence of karstified rocks beneath the surface formation or formations.

SUFFOSION DOLINE. A funnel-shaped enclosed depression in superficial material overlying carbonate rock. It is produced as fines are washed into cavities in the underlying bedrock.

TOWER KARST (TURMKARST). Karst topography characterized by isolated limestone hills. Towers are generally steep-sided; many have flat tops.

TUFA. A mineral precipitate deposited by a spring either hot or cold. Generally composed of calcium carbonate but may contain aragonite.

UVALA. Large closed depression formed by the coalescence of two or more dolines.

VEGETATION HOLLOW. Shallow irregular basin on a pavement surface. Formed by enhanced solution of limestone beneath a vegetation hummock.

APPENDIX IITHE CALCULATION OF SATURATION INDICES AND LOG PCO<sub>2</sub>

The program used in this study was originally written by J.J. Drake at McMaster University and was later expanded and improved by Wigley (1972), who gives a listing and a description of the FORTRAN IV source. The basic steps are:

- 1) Compute the ionic strength of the water sample from the analytical report, assuming in the first instance that all activity coefficients are unity.
- 2) Estimate the activity coefficients for all species from the Debye-Huckel equation.
- 3) Re-evaluate the ionic strength and iterate steps 2 and 3 until a pre-set error criterion is satisfied.
- 4) Compute the values of the various equilibrium constants at the temperature of the water sample from the temperature dependent forms described by Wigley (1972).
- 5) Compute  $SI_c$ ,  $SI_d$ ,  $SI_g$ , and  $P_{CO_2}$ .

## BIBLIOGRAPHY

- Abbott, P. L., 1975. On the hydrology of the Edwards Limestone, south central Texas. J. Hydrol., 24, pp. 251-269.
- Adams, C. S. and Swinnerton, A. C., 1937. The solubility of limestone. Trans. Amer. Geophys. Union, 18, pp. 504-508.
- Aitken, J. D. and Cook, D. G., 1974. Carcajou Canyon map-area, district of Mackenzie, Northwest Territories. Geol. Surv. Canada Pap., 74-13.
- Alexander, W. H. and Patman, J. H., 1969. Groundwater resources of Kimble County, Texas. Texas Water Dev. Board Rept., 95, 93 pp.
- Andersen, B. G., 1965. The Quaternary of Norway, pp. 91-138 in The Geologic Systems: The Quaternary-Volume 1, (ed. K. Rankama), Interscience.
- Anderson, J. C., 1973. Mackenzie basin water balance study, pp. 23-31 in Hydrological Aspects of Northern Pipeline Development, Canada. Environmental-Social Committee Northern Pipelines, Task Force on Northern Oil Development Rpt., 73-3.
- Andrews, J. T., 1961. "Vallons de gélivation" in central Labrador-Ungava. A reappraisal. Canadian Geogr., 5 (4), pp. 1-9.
- Armstrong, J. E. and Tipper, H. W., 1948. Glaciation in north-central British Columbia. Am. J. Sci., 246, pp. 283-310.
- Balázs, D., 1968. Karst regions in Indonesia. Karszt-és Barlangkutató, 1963-67, pp. 325-399.
- Barnes, I., 1965. Geochemistry of Birch Creek, Inyo County, Calif., a travertine depository creek in an arid climate. Geochim. Cosmochim. Acta, 29, pp. 85-112.
- Barnett, D. M., 1963a. Snow depth and distribution in relation to frozen ground in the Ferriman Mine and Denault Lake areas, Schefferville. McGill Sub-Arctic Res. Papers, 13, pp. 72-85.
- Barnett, D. M., 1963b. Former proglacial lake shorelines as indicators of the pattern of deglaciation of the Labrador-Ungava Peninsula. McGill Sub-Arctic Res. Papers, 15, pp. 23-33.
- Barnett, D. M., 1967. Glacial Lake McLean and its relationships with Glacial Lake Naskaupi. Geogr. Bull., 9 (2), pp. 96-101.



- Barnett, D. M and Peterson, J. A., 1964. The significance of Glacial Lake Naskaupi 2 in the deglaciation of Labrador-Ungava. Can. Geogr., 8 (4), pp. 173-181.
- Barrère, P., 1964. Le relief karstique dans l'ouest des Pyrénées centrales. Rev. Belge Géogr., pp. 9-62 in Karst et Climats Froids, Ed. Soc. Roy. Belge Géogr. Spec. Publ., 88 (1-2).
- Bauer, F. and Zötl, J., 1972. Karst of Austria, pp. 225-265 in Karst: Important Karst Regions of the Northern Hemisphere (ed. M. Herak and V. T. Stringfield), Elsevier, 551 pp.
- Bedinger, M. S., 1966. Electric-analog study of cave formation. Bull. Natl. Speleol. Soc., 28 (3), pp. 127-132.
- Billings, M. P., 1972. Structural Geology. Prentice Hall, 606 pp.
- Bird, J. B., 1966. Limestone terrains in southern arctic Canada, pp. 115-121 in Proc. Permafrost Intern. Conf. Indiana (1963), NAS-NRC, Publication 1287.
- Biro, P., 1954. Problèmes de morphologie karstique. Ann. de Géogr., 63, pp. 161-192.
- Blanc, A., 1958. Répertoire bibliographique critique des études de relief karstique en Yougoslavie depuis Jovan Cvijić. Centre de Doc. Cart. et Geogr. Mem. et Doc., 6, pp. 135-228.
- Bostock, H. S., 1948. Physiography of the Canadian Cordillera, with special reference to the area north of the fifty-fifth parallel. Geol. Surv. Canada Mem., 247.
- Bostock, H. S., 1970. Physiographic subdivisions of Canada, pp. 9-30 in Geology and Economic Minerals of Canada (ed. R. J. W. Douglas), Geol. Surv. Canada, 838 pp.
- Bowkett, F. R., 1974. Heavy rainfalls - district of Mackenzie, two case studies. Technical Memoranda 812, Atmos. Environ. Service, Environ. Canada., 19 pp.
- Brandon, L. V., 1963. Groundwater in the permafrost regions of the Yukon, North Cordillera and Mackenzie District. Proc. 1st Canadian Conf. Perm., pp. 131-139.
- Bretz, J. H., 1923. Glacial drainage on the Columbia Plateau. Bull. Geol. Soc. Amer., 34, pp. 573-608.
- Bretz, J. H., 1924. The age of the Spokane glaciation. Am. J. Sci., 5th ser., 8, pp. 336-342.

- Bretz, J. H., 1928. The channeled scabland of eastern Washington. Geogr. Rev., 18, pp. 446-477.
- Bretz, J. H., 1932. The Grand Coulee. American Geogr. Soc. Special Publ., 15, 89 pp.
- Bretz, J. H., Smith, H. T. U. and Neff, G. E., 1956. Channeled scabland of Washington: new data and interpretations. Bull. Geol. Soc. Amer., 67, pp. 957-1049.
- Brook, G. A., Cowell, D. W. and Ford, D. C., 1975. Climate and the chemistry of groundwater in carbonate terrains. Paper given at Can. Assoc. Geogr., Ont. Div. Ann. Conf. Ottawa.
- Brook, G. A. and Ford, D. C., 1974. The Karst Lands of the South Nahanni Region, N.W.T., Contract Report, National and Historic Parks Branch, 501 pp.
- Brown, M. C., 1972. Karst hydrogeology and infrared imagery: an example. Bull. Geol. Soc. Amer., 83, pp. 3151-3154.
- Brown, M. C. and Ford, D. C., 1971. Quantitative tracer methods for investigation of karst hydrologic systems. Trans. Cave Res. Group Gt. Brit., 13 (1), pp. 37-51.
- Brown, R. J. E., 1970. Permafrost in Canada - Its Influence on Northern Development. Univ. of Toronto Press, 234 pp.
- Burns, B. M., 1973. The climate of the Mackenzie Valley - Beaufort Sea, Volume I. Environment Canada, Climatological Studies, 24, 227 pp.
- Burns, B. M., 1974. The climate of the Mackenzie Valley - Beaufort Sea, Volume II. Environment Canada, Climatological Studies, 24, 239 pp.
- Cameron, A. E. and Warren, P. S., 1938. Geology of South Nahanni River, N.W.T. The Canadian Field Naturalist, 52 (2), pp. 15-21.
- Chung, Y. S. and Reinelt, E. R., 1972. On cyclogenesis in the lee of the Canadian Rocky Mountains. Dept. Geogr., Meteor. Sect. Univ. Alta., Edmonton, 32 pp.
- Clayton, K. M., 1966. The origin of the landforms of the Malham area. Field Studies, 2, pp. 359-384.
- Cogley, J. G., 1975. Properties of surface runoff in the high arctic. Unpubl. Ph.D. thesis, McMaster University, 358 pp.
- Cooke, H. J., 1973. A tropical karst in north east Tanzania. Z. Geomorph., 17, pp. 443-459.

- Corbel, J., 1952. Les phénomènes karstiques en Suède. Geografiska Annaler, 3-4, pp. 203-237.
- Corbel, J., 1959. Erosion en terrain calcaire. Ann. Géogr., 68, pp. 97-116.
- Cottón, C. A., 1966. Antarctic scablands. N.Z. J. Geol. and Geophys., 9, pp. 130-132.
- Craig, B. G., 1960. Surficial geology of north-central District of Mackenzie, Northwest Territories. Geol. Surv. Canada Pap., 60-18.
- Craig, B. G. and Fyles, J. G., 1960. Pleistocene geology of Arctic Canada. Geol. Surv. Canada Pap., 60-10.
- Craig, B. G., 1965. Glacial Lake McConnell and the surficial geology of parts of Slave River and Redstone River map-areas, District of Mackenzie. Geol. Surv. Canada, Bull., 122.
- Croce, D., 1964. Cryonival phenomena and karst phenomena in the plateau of the Sella group. Erdkunde, 18 (2), pp. 146-148.
- Cvijić, J., 1893. Das karstphänomen. Geogr. Abhandl., 5 (3), 218-329.
- Cvijić, J., 1901. Morphologische und glaziale Studien aus Bosnien, der Hercegovina und Montenegro, 2, Die Karstpoljen, Abhandl. Geograph. Ges., 3 (2), pp. 1-85.
- Cvijić, J., 1918. Hydrographie souterraine et évolution morphologique du karst. Rec. Trav. Inst. Géograph. Alpine, 6 (4), pp. 376-420.
- Cvijić, J., 1960. La géographie des terrains calcaires. Académie serbe des Sciences et des Arts Monographies, 141.
- Davies, W. E., 1960. Origin of caves in folded limestone. Bull. Natl. Speleol. Soc., 22, pp. 5-18.
- Daviš, J. E., 1973. Statistics and Data Analysis in Geology. Wiley, 550 pp.
- Davis, W. M., 1901. An excursion in Bosnia, Hercegovina and Dalmatia. Bull. Geograph. Soc., 3 (2), pp. 47-50.
- Davis, W. M., 1930. Origin of limestone caverns. Bull. Geol. Soc. Amer., 41, pp. 475-628.
- De Sitter, L. U., 1964. Structural Geology. McGraw-Hill, 551 pp.
- Dixon, W. J., 1972 (ed.). BMD - Biomedical Computer Programs, X-series supplement, Univ. Calif. Publ. in Automatic Computing No. 3, Univ. Calif. Press, Berkeley, pp. 198-224.

- Doornkamp, J. C., 1972. Trend-surface analysis of planation surfaces with an East African case study, pp. 247-281 in Spatial Analysis in Geomorphology (ed. R. J. Chorley), Methuen, 303 pp.
- Dott, R. H. and Batten, R. L., 1971. Evolution of the Earth. McGraw-Hill, 649 pp.
- Douglas, I., 1964. Intensity and periodicity in denudation processes with special reference to the removal of material in solution by rivers. Z. Geomorph., 8, pp. 453-473.
- Douglas, R. J. W., Gabrielse, H., Wheeler, J. O., Stott, D. F. and Belyea, H. R., 1970. Geology of Western Canada, pp. 365-488 in Geology and Economic Minerals of Canada (ed., R. J. W. Douglas), Geol. Surv. Canada, 838 pp.
- Douglas, R. J. W. and Norris, D. K., 1960. Virginia Falls and Sibbeston Lake map-areas, Northwest Territories. Geol. Surv. Canada Pap., 60-19.
- Douglas, R. J. W. and Norris, D. K., 1961. Camsell Bend and Root River map-areas, district of Mackenzie, Northwest Territories. Geol. Surv. Canada Pap., 61-13.
- Douglas, R. J. W. and Norris, D. K., 1962. Dahadinni and Wrigley map-areas, district of Mackenzie, Northwest Territories. Geol. Surv. Canada Pap., 62-33.
- Drake, J. J., 1974. Hydrology and karst solution in the southern Canadian Rockies. Unpubl. Ph.D. thesis, McMaster Univ., 222 pp.
- Drake, J. J., and Ford, D. C., 1973. The dissolved solids regime and hydrology of two mountain rivers. Proc. 5th Internat. Speleological Congress, Olomouc, in press.
- Drake, J. J., and Harmon, R. S., 1973. Hydrochemical environments of carbonate terrains. Water Res. Research, 9 (4), pp. 949-957.
- Drake, J. J. and Wigley, T. M. L., 1975. The effect of climate on the chemistry of carbonate groundwater. Water Res. Research, 11 (6), pp. 958-962.
- Drew, D. P., 1969. A study of the limestone hydrology of the St. Dunstan's well and Ashwick drainage basins, eastern Mendip, Somerset. Proc. Univ. Bristol Speleol. Soc., 11 (3), pp. 257-276.
- Dublenskij, V. N., 1963. On the role of snow in the karstification and the alimentation of karst waters. Izvest. Akad. Nauk S.S.S.R., Ser. Geogr., 2, pp. 69-74. Trans. Nittany Grotto News (1968), 2, pp. 69-74.

- Ek, C., 1969. L'effet de la loi de Henry sur la dissolution du CO<sub>2</sub> dans les eaux naturelles. pp. 53-55 in Problems of the Karst Denudation (ed., O. Stelcl), Brno.
- Enoch, H. and Dasberg, S., 1971. The occurrence of high CO<sub>2</sub> concentrations in soil air. Geoderma, 6 (1), pp. 17-21.
- Fish, J. and Russell, W., 1972. Preliminary results on the groundwater geochemistry of the Sierra de El Abra region, north central Mexico. Bull. Nat. Speleol. Soc., 34 (3), pp. 111-112.
- Flint, R. F., 1935. White silt deposits in the Okanagan Valley, British Columbia, Trans. Roy. Soc. Canada, 34, Section IV, pp. 107-114.
- Follett, C. R., 1973. Ground-water resources of Blanco County, Texas. Texas Water Dev. Board Rept., 1974, 95 pp.
- Ford, D. C., 1971a. Characteristics of limestone solution in the southern Rocky Mountains and Selkirk Mountains, Alberta and British Columbia. Can. J. Earth Sciences, 8 (6), pp. 585-609.
- Ford, D. C., 1971b. Alpine karst in the Mt. Castleguard - Columbia Icefield area, Canadian Rocky Mountains. Arctic Alpine Res., 3 (3), pp. 239-252.
- Ford, D. C., 1971c. Final report upon cavern and allied researches in the First Canyon area, S. Nahanni River, N.W.T., Contract Report, National and Historic Parks Branch, 115 pp.
- Ford, D. C., 1973. Development of the canyons of the South Nahanni River, N.W.T. Can. J. Earth Sciences, 10 (3), 366-378.
- Ford, D. C., 1974. Final report on the geomorphology of South Nahanni National Park, N.W.T., Contract Report, National and Historic Parks Branch, 186 pp.
- Ford, D. C., 1976. Evidence of multiple glaciation in South Nahanni National Park, Mackenzie Mountains, N.W.T. Canadian J. Earth Sciences, in press.
- Ford, D. C. and Quinlan, J. F., 1973. Theme and resource inventory study of the karst regions of Canada, Contract Report, National and Historic Parks Branch, 112 pp.
- Foster, M. D., 1942. Chemistry of ground water, pp. 646-655 in Hydrology (ed., O. E. Meinzer), Dover.
- Fulton, R. J., 1965. Silt deposition in late-glacial lakes of southern British Columbia. Am. J. Sci., 263, pp. 553-570.

- Fulton, R. J. and Klassen, R. W., 1969. Quaternary geology, northwest district of Mackenzie. Geol. Surv. Canada Report of Activities, Pap. 69-1, Part A, pp. 193-194.
- Gabrielse, H., Blusson, S. L. and Roddick, J. A., 1965. Flat River, Glacier Lake and Wrigley Lake map-areas, district of Mackenzie and Yukon Territory. Geol. Surv. Canada Pap. 64-52, 30 pp.
- Gabrielse, H., Blusson, S. L. and Roddick, J. A., 1973. Geology of Flat River, Glacier Lake, and Wrigley Lake map-areas, district of Mackenzie and Yukon Territory. Geol. Surv. Canada Mem. 366, 152 pp.
- Gams, I., 1962. Meritve korozijske intenzitete v sloveniji. Geogr. Vestnik, 34, pp. 3-16.
- Gams, I., 1969. Some morphological characteristics of the Dinaric karst. Geogr. J., 135, pp. 563-572.
- Gardner, J., 1964. Snow studies at Schefferville, Quebec: Winter 1963-64. McGill Sub-Arctic Res. Papers, 19, pp. 1-15.
- Garrels, R. M., and Christ, C. L., 1965. Solutions, Minerals and Equilibria. Harper and Row, New York, 450 pp.
- Gavrilović, D., 1969. Kegelkarst - Elemente in Relief des Gebirges Beljanica, Jugoslavien, pp. 159-166 in Problems of the Karst Denudation (ed., O. Stelcl), Brno.
- Gèze, B., 1965. La spéléologie scientifique. Paris.
- Gray, D. M., 1970. Precipitation, pp. 2.1-2.111 in Handbook on the Principles of Hydrology (ed., D. M. Gray).
- Green, L. H., 1971. Geology of Mayo Lake, Scougale Creek and McQuesten Lake map-areas, Yukon Territory. Geol. Surv. Canada Mem., 357.
- Groom, G. E. and Williams, V. H., 1965. The solution of limestone in South Wales. Geogr. J., 131, pp. 37-41.
- Grund, A., 1903. Die karsthydrographie, Studien aus Westbosnien. Geogr. Abhand., 7 (3), pp. 103-200.
- Grund, A., 1914. Der geographische Zyklus im Karst. Z. Ges. Erdkunde, 52, pp. 621-640.
- Gvozdeckij, N. A., 1965. Types of karst in the U.S.S.R. Prob. Speleol. Res. (Prague), pp. 47-54.
- Hare, F. K. and Hay, J. E., 1971. Anomalies in the large-scale annual water balance over northern North America. Can. Geogr., 15 (2), pp. 70-93.

- Harmon, R. S., 1971. Preliminary results on the groundwater geochemistry of the Sierra de El Abra region, north-central Mexico. Bull. Nat. Speleol. Soc., 33 (2), pp. 73-85.
- Harmon, R. S., 1972. Preliminary results on the groundwater geochemistry of the Sierra de El Abra region, north-central Mexico. (Reply). Bull. Nat. Speleol. Soc., 34 (3), p. 113.
- Harmon, R. S., Drake, J. J., Hess, J. W., Jacobson, R. L., Ford, D. C., White, W. B., Fish, J., Coward, J., Ewers, R. and Quinlan, J. F., 1973. Geochemistry of karst waters in North America. Proc. 6th Internat. Speleol. Congress, Olomouc, in press.
- Harmon, R. S., Hess, J. W., Jacobson, R. W., Shuster, E. T., Haygood, C. and White, W. B., 1972. Chemistry of carbonate denudation in North America. Trans. Cave Res. Grp. Gt. Brit., 14 (2), pp. 96-103.
- Harmon, R. S., Thompson, P.; Schwarcz, H. P. and Ford D. C., 1975. Uranium-series dating of speleothems. Bull. Nat. Speleol. Soc., 37 (2), pp. 21-33.
- Harmon, R. S., White, W. B., Drake, J. J. and Hess, J. W., 1975. Regional hydrochemistry of North American carbonate terrains. Water Res. Research, 11 (6), pp. 963-967.
- Harris, S. F., Taylor, G. L. and Walper, J. J., 1960. Relation of deformational fractures in sedimentary rocks to regional and local structures. Bull. Amer. Assoc. Petrol. Geologists., 44 (12), pp. 1853-1873.
- Harrison, D. A., 1963. The snow survey in the Schefferville Vale, Winter 1961-62. McGill Sub-Arctic Res. Papers, 15, pp. 61-71.
- Henoch, W. E. S., 1960. Geographical survey of the lower Mackenzie and Arctic Red River area. Arctic Circular, 13 (1).
- Hoffmann, E. and Hoffmann, G., 1962. The origin and movement of CO<sub>2</sub> in soil. Z. Pfl. Ernähr Düng, 97, pp. 97-100.
- Hopkins, D. M., MacNeil, F. S., Merklin, R. L. and Petrov, O. M., 1965. Quaternary correlations across Bering Strait. Science, 147, pp. 1107-1114.
- Howard, A. D., 1963. The development of karst features. Bull. Natl. Speleol. Soc., 25 (2), pp. 45-65.
- Hughes, O. L., 1969. Pleistocene stratigraphy, Porcupine and Old Crow Rivers, Yukon Territory. Geol. Surv. Canada Report of Activities Pap., 69-1, Part A, pp. 209-212.

- Hughes, O. L., 1972. Surficial geology of northern Yukon Territory and northwestern district of Mackenzie, Northwest Territories. Geol. Surv. Canada Pap., 69-36.
- Ives, J. D., 1958. Glacial geomorphology of the Torngat Mountains, northern Labrador. Geogr. Bull., 12, pp. 47-75.
- Ives, J. D., 1960a. The deglaciation of Labrador-Ungava: an outline. Cahiers Geog. Québec, 4 (8), pp. 323-343.
- Ives, J. D., 1960b. Former ice-dammed lakes Labrador-Ungava. Geogr. Bull., 14, pp. 44-69.
- Jacobson, R. L. and Langmuir, D., 1972. An accurate method for calculating saturation levels of groundwaters with respect to calcite and dolomite. Trans. Cave Research Group of Great Britain, 14 (2), pp. 104-108.
- Jenko, F., 1959. Hidrologija in vodno gospodarstvo kras (Ljubljana).
- Jennings, J. N., 1969. Karst of the seasonally humid tropics in Australia, pp. 149-158 in Problems of the Karst Denudation (ed., O. Stelcl), Brno.
- Jennings, J. N., 1970. Karst. M.I.T. Press, 241 pp.
- Jennings, J. N. and Bik, M. J., 1962. Karst morphology in Australian New Guinea. Nature, 194, pp. 1036-1038.
- Jennings, J. N. and Sweeting, M. M., 1963. The Limestone Ranges of the Fitzroy Basin, Western Australia; a tropical semi-arid karst. Bonner Geogr. Abhand., 32, 60 pp.
- Jones, R. J., 1965. Aspects of the biological weathering of limestone pavements. Proc. Geol. Assoc., 76, pp. 421-433.
- Karlstrom, T. N.V., 1965. The Quaternary time scale - a current problem of correlation and radiometric dating, pp. 121-150 in Means of Correlation of Quaternary Successions (eds., B. Morrison and H. E. Wright, Jr.), INQUA, 8.
- Katzer, F., 1909. Karst und karsthydrographie, Zur Kunde der Balkanhalbinsel, 8 (Sarajevo).
- Kiersch, G. A. and Hughes, P. W., 1952. Structural localization of groundwater in limestones - "Big Bend District," Texas-Mexico. Econ. Geol., 47, 794-806.
- Kindle, E. D., 1952. Dezadeash map-area, Yukon Territory, Geol. Surv. Can. Mem., 268.



- King, C. A. M., 1969. Trend-surface analysis of central Pennine erosion surfaces. Trans. Inst. Brit. Geographers, 47, pp. 47-59.
- King, L. J., 1969. Statistical Analysis in Geography. Prentice Hall, 288 pp.
- Klein, W. H., 1957. Principal tracks and mean frequencies of cyclones and anticyclones in the Northern Hemisphere. U.S. Dept. Comm., Weather Bur., Res. Pap. 40, 60 pp.
- Kosonen, M., 1968. The relation between the carbon dioxide-production in the soil and the vegetation of a dry meadow. Oikos, 19, pp. 242-249.
- Kurlykova, M. V., 1962. Changes in the composition of soil gases in peat swampy soils of the Yakhroma River Valley. Dokl. S-kh. Akad. Timiryazeva, 76, pp. 63-68.
- Kuzmin, P. P., 1960. Snow cover and snow reserves. Gidrometeor. Izdatel'sko, Leningrad, Trans. Nat. Sci. Foundation, 1963, pp. 1-84 (140) pp.
- Langmuir, D., 1971. The geochemistry of some carbonate waters in central Pennsylvania. Geochim. Cosmochim. Acta, 35 (10), pp. 1023-1045.
- Lattman, L. H. and Parizek, R. R., 1964. Relationship between fracture traces and the occurrence of groundwater in carbonate rocks. J. Hydrol., 2, pp. 73-91.
- Law, J., 1971. Regional Devonian geology and oil and gas possibilities, Upper Mackenzie River area. Bull. Canadian Petrol. Geol., 19 (2), pp. 437-486.
- Lehmann, H., 1936. Morphologische Studien auf Java. Engelhorn, 114 pp.
- Lehmann, H., 1953. Der tropische Kegelkarst in Westindien. Verh. dt. Geogr. Tags., 29, pp. 126-131.
- Lehmann, H., 1956. Der Einfluss des Klimas auf die morphologische Entwicklung des Karstes, in I.G.U. Report of the Commission on Karst Phenomena, 3-7.
- Lehmann, H., 1959. Studien über Poljen in den venaziaschen Voralpen und im Hochapennin. Erdkunde, 12, pp. 258-289.
- Lehmann, O., 1932. Die Hydrographie des Karstes. Leipzig.
- Lichti-Federovich, S., 1974. Palynology of two sections of late Quaternary sediments from the Porcupine River, Yukon Territory. Geol. Surv. Canada Pap., 74-23.

- Lundquist, J., 1965. The Quaternary of Sweden, pp. 139-198 in The Geologic Systems: The Quaternary Volume 1, (ed., K. Rankama), Interscience.
- Mackay, D. K., Fogarasi, S. and Spitzer, M., 1973. Documentation of an extreme summer storm in the Mackenzie Mountains, N.W.T., pp. 191-222 in Hydrological Aspects of Northern Pipeline Development, Canada. Environmental-Social Committee Northern Pipelines, Task Force on Northern Oil Development, Rpt. 73-3.
- Marker, M. E., 1970. Some problems of a karst area in the eastern Transvaal, South Africa. Trans. Inst. Brit. Geogr. 50, pp. 73-85.
- Marker, M. E., 1971. Karst landforms of the northeastern Transvaal. Unpubl. Ph.D. thesis, Univ. of Witwatersrand, 261 pp.
- Martel, E., 1910. La théorie de la 'Grundwasser' et les eaux souterraines du karst. Géographie, 21, pp. 126-130.
- Martel, E., 1921. Nouveau traité des eaux souterraines. Paris.
- Matskevich, V. B., 1957. CO<sub>2</sub> regime in soil air of the steppe and semi-desert under tree and herbaceous coenoses. Vopr. agron. Fiz., pp. 264-275.
- McKay, G. A., 1970. Problems of measuring and evaluating snowcover, pp. 49-62, in Snow Hydrology, Proc. Worksh. Seminar, Can. Nat. Comm. for the Intern. Hydrol., Dec. (1968).
- Meinman, J. R., 1970. Snow accumulation related to elevation, aspect and forest canopy, pp. 34-47 in Snow Hydrology, Proc. Worksh. Seminar, Can. Nat. Comm. for the Intern. Hydrol., Dec. (1968).
- Mesolella, K. J., Matthews, R. K., Broeker, W. S. and Thurber, D. L., 1969. The astronomical theory of climatic change: Barbados data. J. Geol., 77, pp. 250-274.
- Milojević, S. M., 1936. Les brachyclases et leur rôle dans les relations hydrographiques et le relief du karst. Posebna izdanja Srp. Kralj. Akad., 21.
- Milojević, S. M., 1938. Phénomènes et problèmes du karst. Étude dans le karst dinarique et de serbie orientale. Posebna izdanja Srp. kralj. Akad., 36.
- Miotke, F. D., 1972. Die Messung des CO<sub>2</sub> - Gehaltes der Bodenluft mit dem Dräger-Gerät und die beschleunigte kalklösung durch höhere Fliessgeschwindigkeiten. Z. Geomorph., 16, pp. 93-102.
- Monroe, W. H., 1964. The zanjón, a solution feature of karst topography in Puerto Rico. U.S. Geol. Survey Prof. Paper, 501-B, pp. B126-B129.

- Monroe, W. H., 1968. The karst features of northern Puerto Rico. Bull. Nat. Speleol. Soc., 30 (3), pp. 75-86.
- Monroe, W. H., 1970. A glossary of karst terminology. U.S. Geol. Surv. Water-supply Pap., 1899-K, 26 pp.
- Moore, G. K., Burchett, C. R. and Bingham, R. H., 1969. Limestone hydrology in the upper Stones River basin, Central Tennessee. Tennessee Dept. Conservation Div. of Water Res., 58 pp.
- Morozova, R. M. and Bogdanova, G. I., 1965. Problems of biological activity of forest soils. Plodorodie Pochv. Karelii. Akad. Nank S.S.R. Karel'sk. Filial, pp. 56-70.
- Muller, J. E., 1967. Kluane Lake map-area, Yukon Territory. Geol. Surv. Canada Mem., 340.
- Noble, J. P. A. and Ferguson, R. D., 1971. Facies and faunal relations at edge of early mid-Devonian carbonate shelf South Nahanni River area, N.W.T. Bull. Canadian Petrol. Geol., 19 (3), pp. 570-588.
- Palmer, A. N., 1969. A hydrologic study of the Indiana karst. Unpubl. Ph.D. thesis, Indiana Univ., 181 pp.
- Pannekoek, A. J., 1948. Enige Karstterreinen in Indonesie. Tijdschr. K. Ned. Aardrijksk. Genoot., 65, pp. 209-213.
- Panos, V. and Stelcl, O., 1968. Physiographic and geologic control in development of Cuban mogotes. Z. Geomorph., 12, pp. 117-165.
- Parry, J. T., 1960. Limestone pavements of north-western England. Can. Geogr., 16, pp. 14-21.
- Penck, A., 1900. Geomorphologische Studien aus der Hercegovina. Z. Deut. Österreich. Alpenver., 31, pp. 25-41.
- Petrik, M., 1967. Lakes in the Croatian limestone region. Hydrology of Fractured Rocks II. Proc. Dubrovnik Symposium (1965), pp. 565-589.
- Pigott, C. D., 1962. Soil formation and development on the Carboniferous limestone of Derbyshire: parent materials. J. Ecol., 50, pp. 145-156.
- Pitty, A. F., 1968. The scale and significance of solutional loss from the limestone tract of the southern Pennines. Proc. Geol. Assoc., 79, pp. 153-178.
- Pluhar, A. and Ford, D. C., 1970. Dolomite karren of the Niagara Escarpment, Ontario, Canada. Z. Geomorph., 14, pp. 392-410.

- Pokorny, J., 1963. The development of Mogotes in the southern part of the Cracow upland. Bull. de L'Acad. Polonaise des Sciences. Série des Sci. Géol. et Geogr., 11 (3), pp. 169-175.
- Prest, V. K., Grant, D. R., and Rampton, V. N., 1967. Glacial Map of Canada, Geol. Surv. Can. Dept. Energy Mines Resources Map 1253A.
- Price, N. J., 1969. A dynamic mechanism for the development of second-order faults and related structures, pp. 49-71 in Proceedings, Conference on Research in Tectonics (ed., A. J. Baer and D. K. Norris), Geol. Surv. Canada Pap. 68-52.
- Rauch, H. W., and White, W. B., 1970. Lithologic controls on the development of solution porosity in carbonate aquifers. Water Res. Research, 6 (4), pp. 1175-1192.
- Reeves, R. D., 1967. Ground water resources of Kimble County, Texas. Texas Water Devel. Board Rept., 60, 100 pp.
- Reeves, R. D., 1969. Ground water resources of Kerr County, Texas. Texas Water Devel. Board Rept., 102, 58 pp.
- Reeves, R. D. and Small, T. A., 1973. Ground-water resources of Val Verde County, Texas. Texas Water Devel. Board Rept., 172, 144 pp.
- Richmond, G. M., Fryxell, R., Neff, G. E. and Weis, P. L., 1965. The Cordilleran ice sheet of the northern Rocky Mountains, and related Quaternary history of the Columbia Plateau, pp. 231-242 in The Quaternary of the United States (ed., H. E. Wright, Jr. and D. G. Frey), Princeton Univ. Press.
- Rodda, J. C., 1970. A trend-surface analysis trial for the planation surfaces of north Cardiganshire. Trans. Inst. Brit. Geographers, 50, pp. 107-114.
- Roglić, J., 1965. The depth of the fissure circulation of water and the evolution of subterranean cavities in the Dinaric karst, pp. 25-36 in Problems of the Speleological Research (ed., O. Stelcl), Prague.
- Roglić, J., 1972. Historical review of morphologic concepts, pp. 1-18 in Karst: Important Karst Regions of the Northern Hemisphere (ed., M. Herak and V. T. Stringfield), Elsevier, 551 pp.
- Rutter, N. W., 1973. Surficial geology and land classification, Mackenzie Valley transportation corridor (85D, E, 95A, B, G, H, I, J, K, N, O). Geol. Surv. Canada Report of Activities Pap. 74-1, Part A, p. 102.
- Sandeen, W. M., 1972. Ground-water resources of Washington County, Texas. Texas Water Devel. Board Rept., 162, 105 pp.

- Sunartadirdja, M. A. and Lehmann, H., 1960. Der tropische karst von Maros und Nord-Bone in S.W. Celebes. Z. Geomorph., Suppl., 2, pp. 49-65.
- Sweeting, M. M., 1958. The karst lands of Jamaica. Geogr. J., 124, pp. 184-199.
- Sweeting, M. M., 1964. Some factors in the absolute denudation of limestone terrains. Erdkunde, 18 (2), pp. 92-95.
- Sweeting, M. M., 1965. Denudation in limestone regions. Geogr. J., 131, pp. 34-37.
- Sweeting, M. M., 1966. The weathering of limestones. With particular reference to the Carboniferous Limestone of northern England, pp. 177-210 in Essays in Geomorphology (ed., G. H. Dury).
- Sweeting, M. M., 1972. Karst Landforms. Macmillan, 362 pp.
- Swinnerton, A. C., 1942. Hydrology of limestone terrains, pp. 656-677 in Hydrology (ed., O. E. Meinzer), Dover.
- Tamm, E. and Krzysch, G., 1963. The effect of soil temperature and moisture on CO<sub>2</sub> production in a loamy sand. Z. Acker- u Pfl Bau, 117, pp. 359-378.
- Thomas, T. M., 1970. The limestone pavements of the north crop of the South Wales coalfield with special reference to solution rates and processes. Trans. Inst. Brit. Geogr., 50, pp. 87-105.
- Thompson, P., Schwarcz, H. P. and Ford, D. C., 1974. Continental Pleistocene climatic variations from speleothem age and isotopic data. Science, 184, pp. 893-895.
- Thornes, J. B. and Jones, D. K. C., 1969. Regional and local components in the physiography of the Sussex Weald. Area, 1 (2), pp. 13-19.
- Tija, H. D., 1969. Slope development in tropical karst. Z. Geomorph., 13, pp. 260-266.
- Tricart, J. and da Silva, T. C., 1960. Un exemple d'évolution karstique en milieu tropical sec; le morne de Bom de Jesus Lapa, Bahia, Brésil. Z. Geomorph., 4, pp. 29-42.
- Ture, L., 1954. Le bilan d'eau des sols: relations entre les précipitations, l'évaporation et l'écoulement. Ann. Agronomiques, 5, Serie A., pp. 491-595.
- Twidale, C. R., 1956. Vallons de gélivation dans le centre du Labrador. Rev. Géom. Dyn., 7, pp. 17-23.

- gnartadirdja, M. A. and Lehmann, H., 1960. Der tropische karst von Maros und Nord-Bone in S.W. Celebes. Z. Geomorph., Suppl., 2, pp. 49-65.
- veeting, M. M., 1958. The karst lands of Jamaica. Geogr. J., 124, pp. 184-199.
- veeting, M. M., 1964. Some factors in the absolute denudation of limestone terrains. Erdkunde, 18 (2), pp. 92-95.
- veeting, M. M., 1965. Denudation in limestone regions. Geogr. J., 131, pp. 34-37.
- veeting, M. M., 1966. The weathering of limestones. With particular reference to the Carboniferous Limestone of northern England, pp. 177-210 in Essays in Geomorphology (ed., G. H. Dury).
- veeting, M. M., 1972. Karst Landforms. Macmillan, 362 pp.
- innerton, A. C., 1942. Hydrology of limestone terrains, pp. 656-677 in Hydrology (ed., O. E. Meinzer), Dover.
- mm, E. and Krzysch, G., 1963. The effect of soil temperature and moisture on CO<sub>2</sub> production in a loamy sand. Z. Acker- u Pfl Bau, 117, pp. 359-378.
- omas, T. M., 1970. The limestone pavements of the north crop of the South Wales coalfield with special reference to solution rates and processes. Trans. Inst. Brit. Geogr., 50, pp. 87-105.
- ompson, P., Schwarcz, H. P. and Ford, D. C., 1974. Continental Pleistocene climatic variations from speleothem age and isotopic data. Science, 184, pp. 893-895.
- orhes, J. B. and Jones, D. K. C., 1969. Regional and local components in the physiography of the Sussex Weald. Area, 1 (2), pp. 13-19.
- ja, H. D., 1969. Slope development in tropical karst. Z. Geomorph., 13, pp. 260-266.
- icart, J. and da Silva, T. C., 1960. Un exemple d'évolution karstique en milieu tropical sec; le morne de Bom de Jesus Lapa, Bahia, Brésil. Z. Geomorph., 4, pp. 29-42.
- re, L., 1954. Le bilan d'eau des sols: relations entre les précipitations, l'évaporation et l'écoulement. Ann. Agronomiques, 5, Serie A., pp. 491-595.
- idale, C. R., 1956. Vallons de gélivation dans le centre du Labrador. Rev. Géom. Dyn., 7, pp. 17-23.

- Williams, P. W., 1963. An initial estimate of the speed of limestone solution in County Clare. Irish Geogr. 4, pp. 432-441.
- Williams, P. W., 1966. Limestone pavements with special reference to Northern Ireland. Trans. Inst. Brit. Geogr., 40, pp. 155-172.
- Williams, P. W., 1970. Limestone morphology in Ireland. Ch. 7 in Irish Geographical Studies, (ed., R. Glasscock and N. Stephens), Belfast.
- Williams, P. W., 1972. Morphometric analysis of polygonal karst in New Guinea. Bull. Geol. Soc. Amer., 83, pp. 761-796.
- Wilson, J. T., Falconer, G., Mathews, W. H. and Prest, V. K., 1958. Glacial Map of Canada. Geol. Assoc. Canada.
- Witkamp, M., 1969. Cycles of temperature and carbon dioxide evolution from litter and soil. Ecology, 50, pp. 922-924.
- Wolfe, T. E., 1964. Cavern development in the Greenbriar Series, W. Virginia, Bull. Natl. Speleol. Soc., 26, pp. 37-60.
- Yamaguchi, M., Flocker, W. J. and Howard, F. D., 1967. Soil atmosphere as influenced by temperature and moisture. Soil Sci. Amer. Proc., 31, pp. 164-167.
- Zakke, I., 1961. Conditions of O<sub>2</sub> and CO<sub>2</sub> circulation in the air of the arable layer of certain Latvia soils. Augsne un Raza, 11, pp. 43-66.
- Zonn, S. V. and Li, C. K., 1960. Characteristics of the energy relations of biological processes in tropical forest soils. Pochvovedenie, 12, pp. 1-15.
- Zötl, J., 1957. Neue Ergebnisse der Karsthydrologie. Erdkunde, 11, pp. 107-117.
- Zötl, J., 1965. Tasks and results of karst hydrology, pp. 141-145 in Problems of the Speleological Research, (ed., O. Stelcl), Prague.